CANADA

MANITOBA

MANITOBA
DEPARTMENT OF ENERGY AND MINES

MINERAL RESOURCES DIVISION

ECONOMIC GEOLOGY REPORT ER80-1

THE CAT LAKE-WINNIPEG RIVER AND THE WEKUSKO LAKE PEGMATITE FIELDS, MANITOBA

By
P. Černý, D.L. Trueman, D.V. Ziehlke,
B.E. Goad and B.J. Paul
Centre for Precambrian Studies
University of Manitoba
1981

Funding for this program was provided under the Canada/Manitoba Sub-Agreement on Mineral Exploration and Development by the Manitoba Department of Mines, Resources and Environmental Management, and Canada Department of Regional Economic Expansion. The study was carried out under contract by the Centre for Precambrian Studies, University of Manitoba.

88-05003/

Errata to Economic Geology Report ER80-1

"The Cat Lake-Winnipeg River and the
Wekusko Lake Pegmatite Fields, Manitoba"

By P. Černý, D.L. Trueman, D.V. Ziehlke,
B.E. Goad and B.J. Paul

Page 8	Column 1, line 10	...	"have been replaced"
	should read	...	"have been placed"
Page 10	Column 1, line 22	...	"Table 1"
	should read	...	"Table 5"
Page 75	Table 24, line 13	...	"Beryl Tourmaline group (BET) Be"
	should read	...	"Beryl Tourmaline group (BET) Be, B"
Page 85	Figure 78, r.h.s.	...	"APPROX. MARGIN OF TIN LAKE"
	should read	...	"APPROX. MARGIN OF TIN LAKE PEGMATITIC GRANITE"
Page 120	Figure 105, caption	...	"et al.) triangle"
	should read	...	"et al.) triangle (wt. % ratios)"
Page 139	Column 2, line 12	...	"The *quartz diorites* of the English River Gneissic Belt were"
	should read	...	"The *quartz diorites* resemble closely those described"
Page 145	Column 1, line 48	...	"their relatively high Hree contents"
	should read	...	"their relatively high HREE contents"
Page 171	Figure 143, r.h.s.	...	"PW-13-1"
	should read	...	"PW-13-2"

CANADA

MANITOBA

MANITOBA
DEPARTMENT OF ENERGY AND MINES

HON. DONALD W. CRAIK
Minister

PAUL E. JARVIS
Deputy Minister

MINERAL RESOURCES DIVISION
Ian Haugh
Executive Director

ECONOMIC GEOLOGY REPORT
ER80-1

THE CAT LAKE-WINNIPEG RIVER AND THE WEKUSKO LAKE PEGMATITE FIELDS, MANITOBA

By
P. Černý, D.L. Trueman, D.V. Ziehlke
B.E. Goad and B.J. Paul
Centre for Precambrian Studies
University of Manitoba

1981

To our wives, fiancées,
and girlfriends,
who suffer most by our
rocky addiction.

TABLE OF CONTENTS

INTRODUCTION 1
Background 1
Objectives and methods 1
Terminology 2
Analytical procedures 4
Acknowledgements 7

THE CAT LAKE-WINNIPEG RIVER FIELD 7
Introduction 7
Location, access and topography 7
Map coverage 7
Previous work and economic development 7
Present study 8
GENERAL GEOLOGY 8
Regional setting 8
Stratigraphy, intrusive rocks, age relationships 8
Bird River Greenstone Belt 10
Manigotagan Gneiss Belt 10
Winnipeg River Batholithic Belt 10
Age relationships 10
Metavolcanic, metasedimentary and related synvolcanic intrusive rocks: Bird River Greenstone Belt 10
Eaglenest Lake Formation (1) 11
Lamprey Falls Formation (2) 12
Peterson Creek Formation (4) 14
Bernic Lake Formation (5) 19
Flanders Lake Formation (7) 20
Booster Lake Formation (8) 23
Synvolcanic intrusive rocks (3,6) 27
Early to syn-tectonic intrusive and metamorphic rocks 27
Paragneiss (9) 27
Great Falls quartz diorite (10) 32
Migmatite complex (11) 32
Gneissic tonalite (12) 35
Syn- to late-tectonic intrusive and metasomatic rocks 35
Granodiorite (13) 35
Black River suite (14) 35
Inconnu granite (15) 42
Monzogranite, microgranite, and associated pegmatite (16) 42
Lac du Bonnet granite (17) 49
Pegmatitic granites and pegmatites (18) 50
PEGMATITIC GRANITES 50
Structural location and intrusive style 50
Internal composition 61
Accessory minerals 63
Reaction with wall rocks 63
Petrochemistry 73
Mineral compositions 73
Fractionation trends within individual intrusions 74
The Axial pegmatitic granite 75
PEGMATITES 75
Shatford Lake pegmatite group (SHL) 78
Lac du Bonnet pegmatite group (LdB) 79
Greer Lake pegmatite group (GL) 80
Eaglenest Lake pegmatite group (ENL) 83
Axial pegmatite group (AX) 83
Birse Lake pegmatite group (BIS) 85
Rush Lake pegmatite group (RL) 87
Bernic Lake pegmatite group (BL) 93
Eagle-Irgon pegmatite group (EAI) 95
Beryl-Tourmaline pegmatite group (BET) 95
Cat Lake pegmatite group (CAT) .....

Central Claim pegmatite group (CC) 97
Maskwa Lake pegmatite series (MWL) 97
Mineralogy of the pegmatites 100
Potassium feldspars 100
Plagioclase 101
Quartz 101
Holmquistite 101
Biotite and phlogopite 101
Muscovite and lepidolite 102
Spodumene 105
Petalite 106
Eucryptite 106
Pollucite 107
Epidote 108
Chlorite 108
Cordierite 108
Garnet 109
Tourmaline 109
Topaz 111
Gahnite 111
Beryl 111
Chrysoberyl 112
Titanite 112
Allanite 112
Gadolinite 112
Zircon 112
Thorite 116
Uraninite 116
Magnetite 116
Ilmenite 116
Niobian and tantalian rutile 116
Aeschynite (?) 116
Fersmite 116
Euxenite 116
Yttrotantalite 116
Cassiterite 116
Columbite-tantalite group 116
Microlite 119
Tapiolite 122
Wodginite 122
Stibiotantalite 122
Apatite 122
Monazite 123
Xenotime 123
Triphylite-lithiophilite series 123
Amblygonite-montebrasite series 123
Native elements, alloys, sulphides and sulphosalts 124
STRUCTURAL GEOLOGY AND METAMORPHISM 128
Structural geology of the Bird River Greenstone Belt 128
Subarea 1 128
Subarea 2 129
Subarea 3 130
Subarea 4 131
Subarea 5 133
Faulting 133
Metamorphism of the Bird River Greenstone Belt 135
M_1, M_2 assemblages 135
A1.1 quartz-albite-muscovite-biotite-chlorite subfacies 135
A1.2 quartz-andalusite-plagioclase-chlorite subfacies 136
A2.1 andalusite-cordierite-muscovite subfacies 136
A2.2 sillimanite-cordierite-muscovite-almandine subfacies 136
Orthopyroxene-hornblende subfacies 136
M_3, M_4 assemblages 137
Structural geology of the Manigotagan-Ear Falls Gneiss Belt 137
Metamorphism of the Manigotagan-Ear Falls Gneiss Belt 137

Structural geology of the Winnipeg River Batholithic Belt 138
Metamorphism of the Winnipeg River Batholithic Belt 138
GENETIC RELATIONSHIPS 139
Introduction 139
The Winnipeg River district 139
The batholiths 139
The pegmatitic granites 144
The pegmatites 147
Conclusions 150
The Cat Lake-Maskwa Lake district 150
The batholiths 150
The pegmatitic granites 151
The pegmatites 151
Conclusions 151
ECONOMIC CONSIDERATIONS 152
Introduction 152
Geochemical potential of the field 152
The Winnipeg River district 152
The Cat Lake-Maskwa Lake district 152
Exploration target areas 152
The Winnipeg River district 152
The Cat Lake-Maskwa Lake district 153
THE WEKUSKO LAKE FIELD 155
Introduction 155
Location, access and topography 155
Map coverage 155
Previous work and economic development 155
Present study 155
GENERAL GEOLOGY 156
Regional setting 156
Stratigraphy, intrusive rocks, age relationships 157
Amisk Group 157
Amisk metasediments (A) 158
Amisk metavolcanics (B) 158
Missi Group 158
Missi metasediments (C) 158
Missi metavolcanics (D) 160
Andesites and dacites (E) 160
Dion Lake area 160
Granodioritic gneiss (F,G) 160
Paragneiss (H) 160
Synvolcanic intrusions 160
Biotite dacite (J) 160
Dacite to rhyodacite porphyry (K) 162
Syntectonic intrusions 162
Broad Bay granitoids (L) 162
Crowduck Bay and Herb Bay gneissic quartz diorites (M) 162
Crowduck Bay gneissic dome (N,O) 162
Late-tectonic intrusions 162
Rex Lake plutonic complex (P,Q,R,S) 171
Stuart Lake pluton (T) 172
Wekusko and Tramping Lake granites (U,V) 172
Pegmatitic granites and pegmatites (W) 177
PEGMATITIC GRANITES 177
Structural location and intrusive style 177
Internal composition 181
Accessory minerals 181
Reaction with wall rocks 181
Petrochemistry 184
Mineral compositions 185
PEGMATITE GROUPS 185
Sherritt Gordon group (SG) 185
Violet-Thompson group (VT) 185
Green Bay group (GB) 191
Mineralogy

Other occurrences 191
STRUCTURAL GEOLOGY 194
Introduction 194
Interpretation of regional structural history 194
Deformation observed in the Wekusko Lake area relatable to the regional structure 194
Plutonic and associated rocks in the structural development at Wekusko Lake 194
Syntectonic units 194
Late-tectonic intrusions 195
METAMORPHISM 197
Regional metamorphic setting 197
Metamorphic isograds 197
Isograd irregularities 197
Metamorphic history and deformation 197
Position of intrusive rocks in metamorphic framework 198
Syntectonic intrusions 198
Late-tectonic intrusions 198
GENETIC RELATIONSHIPS 199
Introduction 199
The batholiths 199
The pegmatitic granites 199
The pegmatites 201
Conclusions 201
ECONOMIC CONSIDERATIONS 202
Geochemical potential of the field 202
Exploration target areas 202

CONCLUDING REMARKS 203
Introduction 203
Exploration methods 203
Identification of parental granitoids 203
Dispersion aureoles of the pegmatite bodies 203
Preliminary pegmatite evaluation 204
Recommendations for future research 205

REFERENCES 206

FIGURES

Figure 1: Location map of the Cat Lake-Winnipeg River and Herb Lake pegmatite fields in Manitoba XVIII

Figure 2: Location of the Cat Lake-Winnipeg River pegmatite field map area in the English River subprovince 6

Figure 3: Stratigraphic subdivision of the metavolcanic and metasedimentary rocks of the Bird River Greenstone Belt 10

Figure 4: Pillowed metabasalt in the Lamprey Falls Formation 11

Figure 5: AFM variation diagram for the flow rocks and for the synvolcanic intrusive rocks of the Bernic Lake, Peterson Creek, and Lamprey Falls Formation 13

Figure 6: Lapillistone in the Peterson Creek Formation 14

Figure 7: Rb vs. Sr and Rb vs. Ba plots for the metarhyolites of the Peterson Creek Formation, polymictic metaconglomerates of the Bernic Lake Formation, lithic meta-arenites of the Flanders Lake Formation, and for the metagreywacke and metapelite components of the Booster Lake Formation turbidites 16

Figure 8: REE abundances in rhyolitic lava flows, ash flows and tuffs of the Peterson Creek Formation, and in the clastic metasediments and metapelites of the Flanders Lake and Booster Lake Formations 17

Figure 9: Subvertically dipping oligomict metaconglomerate in the Bernic Lake Formation 17

Figure 10: Bedding in metaconglomerate in the Bernic Lake Formation 18

Figure 11: Banded iron formation in the Bernic Lake Formation 19

Figure 12: Granitic lit intercalated in meta-arenite of the Flanders Lake Formation 21

Figure 13: Metaconglomerate in the Flanders Lake Formation 21

Figure 14: Cross-bedded metamorphosed greywacke-mudstone in the Booster Lake Formation 23

Figure 15: Composite section through the Bird River Sill 25

Figure 16: Glomeroporphyritic metagabbro at Bernic Lake 26

Figure 17: Selected compositional and normative characteristics of the Maskwa Lake batholith quartz diorites, granodiorites and granites 29

Figure 18: Rb vs. Sr and Rb vs. Ba plots of the Maskwa Lake batholith quartz diorites, granodiorites and granites 30

Figure 19: REE abundances in the Maskwa Lake batholith granites and quartz diorites 31

Figure 20: Selected compositional and normative characteristics of the Marijane Lake batholith: northern quartz diorites, main body granites and northern granite 32

Figure 21: Rb vs. Sr and Rb vs. Ba in rocks of the Marijane Lake batholith: northern quartz diorites, main body granites and northern granite 34

Figure 22: REE abundances in the rocks of the Marijane Lake batholith: main body granites and northern quartz diorites 35

Figure 23: Compositional characteristics of the gneisses and banded migmatites to massive granites of the migmatite complex . 39

Figure 24: Selected compositional and normative characteristics of the gneissic tonalites, intermediate biotitic derivatives and granitic rocks of the gneissic tonalite "schollen"-zone 39

Figure 25: Rb vs. Sr relationships in the tonalitic gneiss, intermediate biotite derivatives and granitic rocks, and REE abundances in the gneissic tonalites of the gneissic tonalite "schollen"-zone 40

Figure 26: Felsic ternary plots of the Black River suite porphyroblastic gneissic granitoids and massive granites and the Inconnu batholith gneissic porphyroblastic members, massive biotite granite and massive leucocratic granite 40

Figure 27: Rb vs. Sr relationships, and REE abundances in the rocks of the Inconnu batholith 42

Figure 28: Distribution of the different rock types in the Lac du Bonnet batholith 43

Figure 29: Location map of the chemically analyzed samples of the Lac du Bonnet batholith 43

Figure 30: Ternary relationships in the Lac du Bonnet batholith spotted quartz diorite, hornblende granodiorite, biotite granite and leucogranite 45

Figure 31: Rb vs. Sr and Rb vs. Ba relationships in rocks of the Lac du Bonnet batholith: spotted quartz diorite, hornblende granodiorite, biotite granite and leucogranite 45

Figure 32: Al vs. Ga and Y vs. Ca relationships in rocks of the Lac du Bonnet batholith 46

Figure 33: REE abundances in the spotted quartz diorite phase of the Lac du Bonnet batholith 46

Figure 34: Leucogranite, Lac du Bonnet batholith; sections subparallel and normal to lineation 47

Figure 35: Typical textures of sheared and partly recrystallized Lac du Bonnet leucogranite, primary igneous Lac du Bonnet biotite granite, fine grained leucogranite of the pegmatitic granites, and aplitic phase of the pegmatitic granites 48

Figure 36: SiO_2 frequencies in the leucogranite and biotite granite of the Lac du Bonnet batholith 49

Figure 37: REE abundances in the leucogranite and biotite granite of the Lac du Bonnet batholith 50

Figure 38: Geology and sampling locations of the Greer Lake pegmatite granite 51

Figure 39: Geology and sampling locations of the Eaglenest Lake pegmatitic granite 52

Figure 40: Geology and sampling locations of the Tin Lake pegmatitic granite 53

Figure 41: Geology and sampling locations of the Osis Lake pegmatitic granite and its central biotite granite plug 54

Figure 42: Warping and contortion of metapelites in the southeastern tip of the Osis Lake pegmatitic granite 55

Figure 43: The Osis Lake pegmatitic granite filling-in dilation fractures in metapelites of the Booster Lake Formation 55

Figure 44: Ptygmatic folding of pegmatitic granite stringers in the western Osis Lake intrusion 56

Figure 45: Pegmatitic leucogranite, Osis Lake body; light-coloured subhedral K-feldspar with graphic quartz in a groundmass of albite, quartz, muscovite ±garnet and tourmaline 56

Figure 46: Plumose aggregate of muscovite +quartz in the albitic matrix of pegmatitic leucogranite in the Osis Lake body, radial around a garnet grain 57

Figure 47: Plumose muscovite + quartz aggregates in white albite + quartz matrix with large K-feldspars; pegmatitic leucogranite phase of the Osis Lake intrusion 57

Figure 48: A thin, largely tourmalinized screen of metapelitic schist serving as a substrate for oriented growth of club-shaped megacrysts of partly graphic K-feldspar. Pegmatitic leucogranite phase of the Osis Lake intrusion 58

Figure 49: Fine grained leucogranite, Eaglenest Lake pegmatitic granite intrusion: faint banding crosscut by a string of pegmatitic K-feldspars 58

Figure 50: Banded garnetiferous sodic aplite overlain by megacrystic K-feldspar and quartz of the potassic pegmatite phase; Eaglenest Lake pegmatitic granite intrusion 59

Figure 51: Gahnite enclosed in, and corroded by muscovite, with opaque blades of possible Nb, Ta-oxide minerals; Greer Lake pegmatitic granite intrusion 59

Figure 52: Sharp contacts between banded garnetiferous aplite and potassic pegmatite, Greer Lake pegmatitic granite intrusion 60

Figure 53: Anhedral block of altered triphylite in quartz, K-feldspar and platy muscovite of a potassic pegmatite stringer; Osis Lake pegmatitic granite intrusion 60

Figure 54: Gradual transition from pegmatitic leucogranite into potassic pegmatite; Osis Lake pegmatitic granite intrusion 61

Figure 55: Bands of garnetiferous aplite broken and cemented by an impure potassic pegmatite; Greer Lake pegmatitic granite intrusion 62

Figure 56: A thin screen of largely tourmalinized metapelitic schist separating aplitic and pegmatitic crystallization regimes in the Osis Lake pegmatitic granite 62

Figure 57: Beryl and columbite-tantalite compositions from the Greer Lake pegmatitic granite 63

Figure 58: Gradual transition from pegmatitic leucogranite into the mineralized pegmatitic pod A.C. #2; Greer Lake pegmatitic granite intrusion 65

Figure 59: Columnar spodumene + quartz pseudomorphs after petalite in a groundmass of albite, quartz and lithian muscovite; Silverleaf pegmatite offshoots of the Greer Lake pegmatitic granite intrusion 65

Figure 60: Tourmalinization along the edges and in thin fragments of a metapelitc raft, in the western part of the Osis Lake intrusion of pegmatitic granite 66

Figure 61: Symmetrical zoning of a pegmatite layer confined by tourmalinized schist screens; Osis Lake pegmatitic granite intrusion 66

Figure 62: Normative Ab-Or-Qtz and Ab-Or-An plots of fine grained leucogranites, sodic aplites, and pegmatitic leucogranites of the pegmatitic granite intrusions 69

Figure 63: K/Rb vs. Rb plot of the fine grained and pegmatitic leucogranites from pegmatitic granite intrusions 69

Figure 64: Rb vs. Sr plot of the fine grained and pegmatitic leucogranties from pegmatitic granite intrusions 69

Figure 65: Mg/Li vs. Li plot of the fine grained and pegmatitic leucogranites from pegmatitic granite intrusions 70

Figure 66: Al vs. Ga plot of the fine grained and pegmatitic leucogranites from pegmatitic granite intrusions 70

Figure 67: Al/Ga vs. Ga plot of the fine grained and pegmatitic leucogranites from pegmatitic granite intrusions 70

Figure 68: REE abundances in the fine grained leucogranite and pegmatitic leucogranite phases of the four pegmatitic granite intrusions, and in the biotite granite of the Osis Lake body 71

Figure 69: Selected major and trace element relationships in blocky K-feldspars and platy muscovites from the potassic pegmatite phases of the four pegmatitic granite intrusions 72

Figure 70: Obliquity of blocky K-feldspars from the potassic pegmatite phases of the four intrusions of pegmatitic granite 73

Figure 71: Chemical composition of garnet from the pegmatitic leucogranite phase of the four intrusions of pegmatitic granite, in ternary subsystems 73

Figure 72: Molecular percentages of spessartine, and weight percentages of MgO and CaO, of garnets from various assemblages in the four intrusions of pegmatitic granites 73

Figure 73: Fractionation directions in the four pegmatitic granites based on whole-rock K/Rb, blocky K-feldspar K/Rb and K/Cs, muscovite K/Rb, Mg/Li, and Be, and garnet (Mn x 100)/(Mn + Fe) 74

Figure 74: Location map of the Shatford Lake pegmatite group 76

Figure 75: Location map of the Lac du Bonnet pegmatite group 79

Figure 76: Location map of the Greer Lake pegmatite group 79

Figure 77: Location map of the Axial pegmatite group 83

Figure 78: Location map of the Birse Lake pegmatite group 85

Figure 79: Location map of the Rush Lake pegmatite group 85

Figure 80: Location map of the Bernic Lake pegmatite group 90

Figure 81: Location map of the Eagle-Irgon, Beryl-Tourmaline, Cat Lake and Central Claim pegmatite groups 93

Figure 82: Location map of the Maskwa pegmatite series 98

Figure 83: K/Rb vs Cs plot of blocky K-feldspars from pegmatites of the Cat Lake-Winnipeg River pegmatite field 101

Figure 84: K/Rb vs. Cs plot of micas from pegmatites of the Cat Lake-Winnipeg River pegmatite field 103

Figure 85: K/Rb vs. Li plot of micas from pegmatites of the Cat Lake-Winnipeg River pegmatite field 103

Figure 86: Iron content of spodumene from the Cat Lake-Winnipeg River pegmatite field, classified according to the paragenetic plus compositional scheme of Heinrich (1975) 105

Figure 87: Spodumene-quartz intergrowth pseudomorphous after petalite from the Tanco pegmatite 105

Figure 88: Schematic generalized sequence of alteration products replacing spodumene in granitic pegmatites 106

Figure 89: Schematic generalized sequence of alteration products replacing petalite in granitic pegmatites 107

Figure 90: Sericitic muscovite ±spodumene veining pollucite from the Tanco deposit 108

Figure 91: Schematic generalized sequence of alteration products replacing pollucite in granitic pegmatites 108

Figure 92: Aggregate of altered cordierite crystal with fine grained ghost zones and scattered large crystals of garnet, surrounded by blocky K-feldspar and quartz; GL-8W pegmatite, Greer Lake group 110

Figure 93: Altered cordierite from the Greer Lake pegmatites in thin sections normal to its basal parting 110

Figure 94: Composition of garnet from the Cat Lake-Winnipeg River pegmatite field in the Fe0-Mn0-Ca0x10 and Fe0-Mn0-Mg0x10 triangles 111

Figure 95: Tourmaline and beryl filling shear fractures in the CATB pegmatite 111

Figure 96: Unit cell dimensions of tourmalines from selected pegmatites of the Cat Lake-Winnipeg River pegmatite field 111

Figure 97: Cesian beryl along the front of albitization invading quartz core in the Tanco pegmatite 112

Figure 98: Na/Li vs. Cs plot of late beryl generations from the Cat Lake-Winnipeg River pegmatite field 113

Figure 99: Multigeneration beryl sequences from some pegmatite bodies of the Cat Lake-Winnipeg River pegmatite fields. 113

Figure 100: Radial aggregate of fibrous allanite, largely altered into bastnaesite and associated with yttrotantalite; SHL-2, Shatford Lake group 115

Figure 101: Metamict decay and hydrothermal alteration of hafnian zircon from the Tanco pegmatite in thin section 115

Figure 102: Fersmite replacing a platy crystal of columbite in twinned albite of the Huron Claim pegmatite 118

Figure 103: Variations in crystal shape of the columbite-tantalite minerals 118

Figure 104: Columbite-tantalite minerals of the Cat Lake-Winnipeg River pegmatite field in the $FeNb_2O_6$-$FeTa_2O_6$-$MnNb_2O_6$-$MnTa_2O_6$ diagram 120

Figure 105: Columbite-tantalite and related minerals of the Cat Lake-Winnipeg River pegmatite field in the (Fe0 + Mn0)-(Ta_2O_5 +Nb_2O_5)-(TiO_2 +SnO_2 +Sc_2O_3 et al.) triangle 120

Figure 106: Columbite-tantalite minerals of selected pegmatite groups from the Cat Lake-Winnipeg River field plotted in the *a*-*c* unit cell dimensions diagram 122

Figure 107: Skeletal wodginite in a matrix of albite and quartz from the Tanco pegmatite 122

Figure 108: Simpsonite partly replaced along crystal surfaces by microlite and manganotantalite in an albite +quartz +muscovite matrix from the Tanco pegmatite 126

Figure 109: Amblygonite-montebrasite in the Tanco pegmatite: blocky crystals along the quartz-pollucite boundary, and veinlet of secondary montebrasite in primary amblygonite 126

Figure 110: Subdivision of the Bird River Greenstone Belt into structural subareas 128

Figure 111: Structural subarea 1 129

Figure 112: Layering in structural subarea 2 129

Figure 113: Foliation in structural subarea 2 130

Figure 114: Poles to bedding S_0 and foliation S_1 in subarea 3a 130

Figure 115: Poles to bedding S_0 and foliation S_1 in the subarea 3b 131

Figure 116: Outcrops of metaconglomerate in the Flanders Lake Formation compared to ideal type III interference fold pattern ... 132

Figure 117: Poles to bedding S_0 and foliation S_1 in structural subarea 4 132

Figure 118: Poles to schistosity S_2 in the structural subarea 4 133

Figure 119: Poles to bedding S_0 and schistosity S_2 in structural subarea 5 133

Figure 120: Air photo lineaments and faults in the major part of the Cat Lake-Winnipeg River pegmatite field 134

Figure 121: Subdivision of the Bird River Greenstone Belt into metamorphic facies segments 135

Figure 122: K/Rb vs. Rb and K/Ba vs. Ba diagrams for granitic components and quartz diorites of the Maskwa, Marijane and Lac du Bonnet batholiths. 140

Figure 123: Zr/Hf vs. Hf plots of quartz diorites and biotite granites from the Maskwa Lake, Marijane Lake, and Lac du Bonnet batholiths 140

Figure 124: REE abundance fields of biotite granites of the Maskwa Lake, Marijane Lake and Lac du Bonnet batholiths; Lac du Bonnet biotite granite and leucogranite; fine grained leucogranites of pegmatitic granite intrusions and Bird River Greenstone Belt metasediments; and metarhyolites of the Peterson Creek Formation, Lac du Bonnet leucogranite, and the fine grained leucogranite phase of pegmatitic granites 141

Figure 125: Oxygen isotope ratios in selected rock types of the Lac du Bonnet batholith, pegmatitic granite intrusions, and of the Bird River Greenstone Belt 142

Figure 126: Ab-Or-Qtz mesonormative compositions in the Anderson and Cullers (1978) grids: initial melt composition of the Lac du Bonnet biotite granite, crystallization level composition of the Lac du Bonnet leucogranite and fine grained leucogranites of the pegmatitic granite intrusions 143

Figure 127: Rb vs. Ba, Y vs. Ca and Rb vs. Sr plots of the Peterson Creek Formation metarhyolites, Lac du Bonnet leucogranites, and fine grained leucogranites from the pegmatitic granite intrusions 146

Figure 128: Disposition of the Lac du Bonnet batholith, pegmatitic granites and pegmatite groups along the east-west fault system in the Winnipeg River pegmatite district 148

Figure 129: K/Rb vs. Cs in blocky K-feldspars from three major intrusions of pegmatitic granites, and from the pegmatite swarms accompanying them 149

Figure 130: Cross section through the Bernic Lake pegmatite group 149

Figure 131: Ternary normative composition fields for the granitoid rocks of the migmatite complex, the Black River suite and the Inconnu granite 150

Figure 132: Rb vs. Sr and Rb vs. Ba in the migmatite complex, the Black River suite and in the Inconnu granite 150

Figure 133: K vs. Rb in the Inconnu granite compared to the fields covered by the Lac du Bonnet, Marijane Lake, and Maskwa Lake biotite granites and their respective quartz diorites 151

Figure 134: Structural setting of the Tanco pegmatite as an example of a pressure-shadow trap in an anticlinal fold axis at the nose of subvolcanic intrusive unit (6) enveloped in schistose rocks of the Bernic Lake Formation 153

Figure 135: Location of the Wekusko Lake pegmatite field at the southeast boundary of the Churchill Province 156

Figure 136: Compositional characteristics of the Missi, Amisk and Dion Lake gneissic metasediments 158

Figure 137: Compositional characteristics of the Crowduck Bay gneiss dome 165

Figure 138: Selected major and trace element contents of the Crowduck Bay gneiss dome plotted against SiO_2 166

Figure 139: Selected major and trace element contents of the Crowduck Bay gneiss dome 167

Figure 140: Compositional characteristics of the Rex Lake plutonic complex 168

Figure 141: Compositional characteristics of the Rex Lake plutonic complex 170

Figure 142: Selected compositional characteristics of the Rex Lake plutonic complex 171

Figure 143: REE abundances in the gabbros, diorites, granodiorites and granites of the Rex Lake plutonic complex 171

Figure 144: Compositional characteristics of the Wekusko and Tramping Lake granites 173

Figure 145: Selected compositional characteristics of the Wekusko and Tramping Lake granites stressing the internal homogeneity of each 174

Figure 146: REE abundances in the Wekusko and Tramping Lake granites 175

Figure 147: Location of pegmatitic granites and lithium pegmatite deposits in the Wekusko Lake pegmatite field 176

Figure 148: Inclusions of metasediments in fine grained leucogranite of the Osborne Lake pegmatitic granite 177

Figure 149: Schlieren-type layering by digested metasedimentary screens in the fine grained leucogranite phase of the Osborne Lake pegmatitic granites 178

Figure 150: Layered alternation of fine grained leucogranite and pegmatitic leucogranite; Osborne Lake pegmatitic granite intrusion 178

Figure 151: A fracture-filling pegmatite vein in a dilation structure in the gneissic Dion-Hat Lakes terrain 179

Figure 152: A schist screen in a lenticular pegmatitic granite body, in Crowduck Bay 179

Figure 153: Incipient boudinage of a pegmatite dyke, west of Godkin Lake 180

Figure 154: Advanced boudinage of a pegmatite sill in Crowduck Bay 180

Figure 155: Proportions of normative felsic components of the fine grained leucogranite phase and of the pegmatitic leucogranite phase of pegmatitic granites 181

Figure 156: Selected major and trace-element characteristics of the fine grained leucogranites and pegmatitic leucogranites 183

Figure 157: Cs vs. Rb/Sr in the fine grained leucogranites and pegmatitic granites 184

Figure 158: REE abundances in the fine grained leucogranite phase of the pegmatitic granites from Crowduck Bay and from the Osborne Lake body 184

Figure 159: K/Rb ratio vs. Cs in blocky K-feldspars of pegmatitic granites and small pegmatites east of Crowduck Bay 184

Figure 160: The Sherritt Gordon eastern dyke SG-1 186

Figure 161: The Sherritt Gordon western dyke SG-2 187

Figure 162: The Violet-Thompson pegmatite 188

Figure 163: Schematic illustration of the preferred orientation of spodumene (and K-feldspar) in the Violet-Thompson pegmatite dyke 189

Figure 164: The westernmost Green Bay pegmatite dyke, GBA 189

Figure 165: Compositional characteristics of pegmatite minerals from the SG, VT, and GB groups; blocky K-feldspar, muscovite, beryl, and spodumene 193

Figure 166: Folds of the F_4 event, with NE-striking axial planes, in the Crowduck Bay gneiss dome 195

Figure 167: REE abundance relationships: Wekusko and Tramping Lake granites vs. Rex Lake complex granite, and Wekusko and Tramping Lake granites vs. Osborne Lake pegmatitic granite 199

Figure 168: Ab-Or-Qtz mesonormative compositions in the Anderson and Cullers (1978) grids: Wekusko granite, Tramping Lake granite and the main cluster of the fine grained leucogranites of the pegmatitic granite intrusions 200

TABLES

Table 1: Standards used for whole rock and mineral analyses 2

Table 2: Methods, precision and accuracy of chemical analyses of silicate rocks 3

Table 3: Accuracy of replicate INAA determinations of rare earth elements 4

Table 4: Standards used for electron microprobe mineral analyses 5

Table 5: Stratigraphy of the Cat Lake-Winnipeg River pegmatite field 9

Table 6: Representative chemical analyses of the metabasalts, Lamprey Falls Formation (2) 12

Table 7: Representative chemical analyses of the metarhyolites, Peterson Creek Formation (4) 15

Table 8: Representative chemical analyses of the metavolcanics, Bernic Lake Formation (5) 20

Table 9: Representative chemical analyses of lithic arenites, Flanders Lake Formation (7) 22

Table 10: Representative chemical analyses of the metaturbidites, Booster Lake Formation (8) 24

Table 11: Representative chemical analyses of the synvolcanic intrusions (3,6) 25

Table 12: Representative chemical analyses of the Maskwa Lake quartz diorite complex (9) 28

Table 13: Representative chemical analyses of the Marijane Lake quartz diorite complex (10) 33

Table 14: Representative chemical analyses of the migmatite complex (11) 36

Table 15: Representative chemical analyses of the tonalite gneiss "schollen"-zone (12) 37

Table 16: Representative chemical analyses of the Black River suite (14) 38

Table 17: Representative chemical analyses of the Inconnu granite (15) 41

Table 18: Representative chemical analyses of the Lac du Bonnet batholith (17) 44

Table 19: Accessory minerals in the four major intrusions of pegmatitic granites 63

Table 20: Paragenesis of the potassic pegmatite bands and pods in the southwestern part of the Greer Lake pegmatitic granite 64

Table 21: Representative chemical analyses of the pegmatitic granites (18) 67

Table 22: Selected major and trace element relationships in fine grained leucogranites of the four major intrusions of pegmatitic granites 68

Table 23: Arithmetic means of contents (wt.%) and ratios of geochemically significant elements in blocky K-feldspars from potassic pegmatite bands of the four major intrusions of pegmatitic granites 72

Table 24: Subdivision of the Cat Lake-Winnipeg River pegmatite field, and rare elements typical of the different pegmatite groups 75

Table 25: Paragenesis of the Shatford Lake pegmatite group 77

Table 26: Compositional characteristics of selected minerals from the Shatford Lake pegmatite group 78

Table 27: Paragenesis of the Lac du Bonnet pegmatite group 79

Table 28: Compositional characteristics of selected minerals of the Lac du Bonnet pegmatite group 80

Table 29: Paragenesis of the Greer Lake and Eaglenest Lake pegmatite groups 81
Table 30: Compositional characteristics of selected minerals of the Greer Lake pegmatite group 82
Table 31: Compositional characteristics of selected minerals of the Eaglenest pegmatite group 82
Table 32: Paragenesis of the Axial pegmatite group 84
Table 33: Compositional characteristics of selected minerals of the Axial pegmatite group 83
Table 34: Paragenesis of the Birse Lake pegmatite group 86
Table 35: Compositional characteristics of selected minerals of the Birse Lake pegmatite group 87
Table 36: Paragenesis of the Rush Lake pegmatite group 88
Table 37: Compositional characteristics of selected minerals of the Rush Lake pegmatite group 89
Table 38: Schematic vertical zoning sequence in the Tanco pegmatite; modified after Crouse et al. (1979) 90
Table 39: Schematic cross sections through two separate parts of the Buck Claim pegmatite, partly after Lenton (1979) 91
Table 40: Paragenesis of the Bernic Lake pegmatite group 92
Table 41: Compositional characteristics of selected minerals of the Bernic Lake pegmatite group 93
Table 42: Paragenesis of the Eagle-Irgon, Beryl-Tourmaline, Cat Lake, and Central Claim pegmatite groups 94
Table 43: Compositional characteristics of selected minerals of the Eagle-Irgon pegmatite group 95
Table 44: Compositional characteristics of selected minerals of the Beryl-Tourmaline pegmatite group 96
Table 45: Compositional characteristics of selected minerals of the Cat Lake pegmatite group 96
Table 46: Compositional characteristics of selected minerals of the Central Claim pegmatite 98
Table 47: Paragenesis of the Maskwa Lake pegmatite series 99
Table 48: Compositional characteristics of selected minerals of the Maskwa Lake pegmatite series 100
Table 49: Na_2O contents of blocky microcline-perthite 100
Table 50: Partial chemical analyses of trioctahedral micas 102
Table 51: Partial chemical analyses of spodumene and spodumene spodumene +quartz pseudomorphs after petalite 104
Table 52: Chemical composition of petalite 106
Table 53: Chemical composition of eucryptite 107
Table 54: Chemical composition of pollucite and cesian analcime 107
Table 55: Chemical composition of epidote and chlorite 109
Table 56: Chemical composition of beryl 114
Table 57: Chemical composition of zircon 114
Table 58: Chemical composition of ilmenite, niobian and tantalian rutile 117
Table 59: Chemical composition of fersmite 117
Table 60: Chemical composition of cassiterite 119
Table 61: Chemical composition of columbite-tantalite minerals 121

Table 62: Chemical composition of microlite 123

Table 63: Chemical composition of wodginite, tapiolite and stibiotantalite 125

Table 64: Chemical composition of amblygonite-montebrasite 127

Table 65: Native elements, alloys, sulphides and sulphosalts in the Tanco pegmatite 127

Table 66: Lithostratigraphic correlation of subareas 2a and 2b 131

Table 67: Correlation of the major structural events and sedimentation in the Rice Lake-Manigotagan Gneiss Belt-Bird Lake areas 137

Table 68: Compositional characteristics of the Peterson Creek Formation metarhyolites, Lac du Bonnet leucogranites, and fine grained leucogranites of the pegmatitic granite intrusions 146

Table 69: Geochemical indicators of Beus and Sitnin (1968) and Beus et al. (1968) compared to the characteristics of granitic rocks of the Cat Lake-Winnipeg River pegmatite field 147

Table 70: Correlation of accessory mineral content of major pegmatitic-granitic intrusions and their pegmatite aureoles 148

Table 71: Stratigraphy of the Wekusko Lake pegmatite field 157

Table 72: Representative chemical analyses of the metasediments and gneisses (A,B,C,D,F,G,H,) 159

Table 73: Representative chemical analyses of the synvolcanic intrusions (J,K) 161

Table 74: Representative chemical analyses of the gneissic quartz diorite (M) 163

Table 75: Representative chemical analyses of the Crowduck Bay gneiss dome (N,O) 164

Table 76: Representative chemical analyses of the Rex Lake plutonic complex (P,Q,R,S) 169

Table 77: Representative chemical analyses of the Wekusko and Tramping Lake granites (U,V) 172

Table 78: Representative chemical analyses of the pegmatitic granites (W) 182

Table 79: Paragenesis of the Wekusko Lake pegmatite field 190

Table 80: Compositional characteristics of selected minerals of the Sherritt Gordon pegmatites 191

Table 81: Compositional characteristics of selected minerals of the Violet-Thompson pegmatite 192

Table 82: Compositional characteristics of selected minerals of the Green Bay pegmatite group 192

Table 83: Geochemical indicators of Beus and Sitnin (1968) and Beus et al. (1968) compared to the characteristics of granitic rocks of the Wekusko Lake pegmatite field 200

Table 84: Pegmatite types and diagnostic elements in their positive primary dispersion aureoles 204

Table 85: Elements characteristic for primary geochemical dispersion aureoles around pegmatite bodies 204

MAPS

Map 1: Geology of the Cat Lake-Winnipeg River pegmatite field, 1:100 000 ..... (in pocket)

Map 2: Location of the chemically analyzed whole rock samples from the Cat Lake-Winnipeg River pegmatite field, 1:100 000 (in pocket)

Map 3: Structural geology of the Winnipeg River pegmatite district, 1:50 000 ..... (in pocket)

Map 4: Geology of the Wekusko Lake pegmatite field, 1:100 000 ..... (in pocket)

Map 5: Location of the chemically analyzed whole rock samples from the Wekusko Lake pegmatite field, 1:100 000 ..... (in pocket)

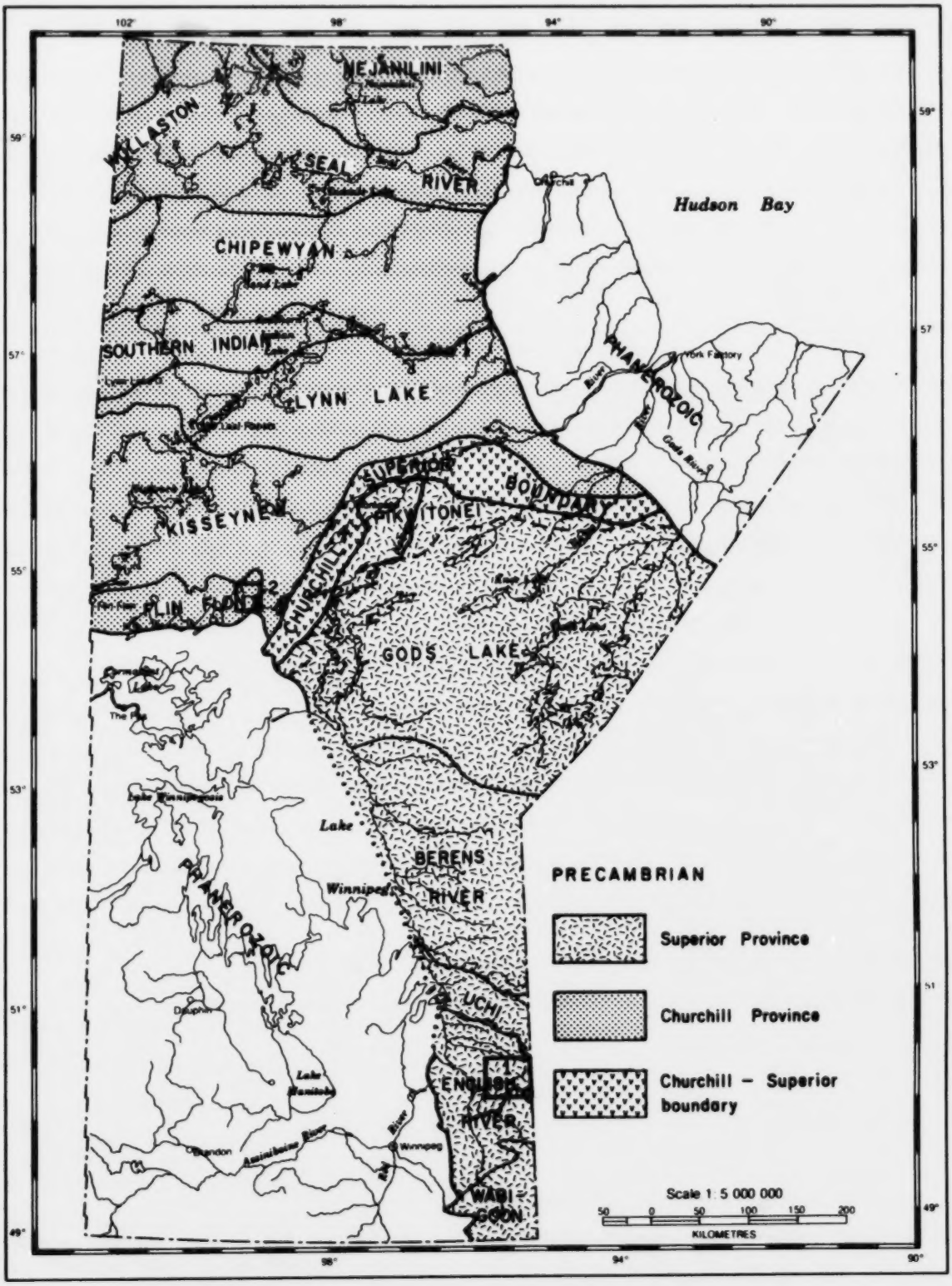

Figure 1: Location map of the Cat Lake-Winnipeg River (1) and Herb Lake (2) pegmatite fields in Manitoba; schematized from the Geological Map of Manitoba, Map 79-2

INTRODUCTION

BACKGROUND

The southwestern margin of the Canadian Shield in Manitoba and adjacent Ontario contains some of the largest rare-element pegmatite fields in the world. Some of their pegmatites contain exceptionally high concentrations of tantalum and cesium, and sizable reserves of lithium, beryllium, rubidium and gallium. They also represent a considerable resource of industrial minerals — micas, feldspars, and quartz. Some granitic bodies in these fields, possibly parental to certain pegmatite types, have a strong radioactive background along their margins, suggesting possible occurrences of U, Th-enriched pegmatites, and of low-grade dispersed radioactive mineralization in the granites themselves.

Past studies of the geology, mineralogy, and geochemistry of these pegmatites have been fragmented, sporadic, and incomplete. The genetic relationship between granites and pegmatites, and the distribution patterns of economically interesting pegmatite types have been guessed at but not systematically studied. No specific exploration guidelines could have been developed from the available information, which is a serious hindrance to prospecting at a time of increasing interest in "pegmatitic" rare elements. Most of these have numerous applications in modern technology, particularly related to energy production, storage and conservation, and consumption rates of these elements are generally increasing.

This report presents the results of the Pegmatite Mineral Evaluation Project which was aimed at rectifying the above situation. It was contracted to the Centre of Precambrian Studies, Department of Earth Sciences, University of Manitoba by the Manitoba Department of Mines, Resources and Environmental Management under the Canada-Manitoba Subsidiary Agreement on Mineral Exploration and Development in Manitoba, supervised by the Canada Department of Regional Economic Expansion.

OBJECTIVES AND METHODS

The main objective of the project was to establish a scientific basis for the appraisal of the economic potential of the two major and most promising pegmatite fields in Manitoba, the Cat Lake-Winnipeg River and Wekusko Lake fields (Fig. 1) with identification of exploration targets of economic interest. More specifically, the purpose was to document the character of pegmatites and their geological setting, and thereby provide a basis for directing further exploration activities that may lead to discovery of new pegmatite deposits of rare elements and industrial minerals.

The only approach capable of yielding realistic guidance to exploration is solving the structural and petrogenetic affiliation of pegmatites and granitic intrusions within the framework of the general geological evolution of the pegmatite-bearing regions. Formidable as this task may be in complex terranes, it cannot be circumvented by any indirect routes. Recognition of the nature of the pegmatite-generating process, identification of parental granitoids (if any), and allocation of the process to a specific time and space in the regional structural and metamorphic history — these are the necessary steps in investigating such a problem.

Consequently, the present research conducted in the two pegmatite fields consisted of the following five studies:

(i) Review of the regional geological history of the pegmatite fields, and of the geochemistry of metamorphic rock suites containing them;

(ii) Distribution, structural setting, mineralogy, geochemistry, and petrogenetic history of granitic bodies;

(iii) Distribution, structural setting, mineralogy, geochemistry, and internal evolution of pegmatites;

(iv) Spatial, temporal, and genetic relationship between the granitic bodies, the pegmatites, and the structures in which the pegmatites occur;

(v) Qualitative appraisal of the economic potential of different pegmatite types, and definition of target areas for exploration.

Due to the unexpectedly high number of granitic and pegmatitic bodies in both pegmatite fields, discovered in part during the Project, and due to the expansion of the investigated area at Wekusko Lake, dictated by regional geology, geochemical studies had to cover more granitic and pegmatitic bodies than anticipated. Consequently, because of limited time and funds, the geochemistry of metamorphic rock suites had to be restricted, being relatively most expendable in terms of the principal objectives of the Project.

The treatment of the two pegmatite fields in this report is considerably unbalanced, mainly because of the different levels of understanding the regional geology and evolutionary history of the areas involved. For example, principal features of regional evolution have been published, or recently deciphered, in the Cat Lake-Winnipeg River field (McRitchie 1971, Trueman 1980) but in the Wekusko Lake area some of the fundamental characteristics of different stratigraphic units and intrusions, and their relative chronology, are reported here for the first time.

TERMINOLOGY

Three categories of terms used in the study of pegmatites deserve clarification: those concerning the geology of pegmatite occurrences, the internal structure of individual pegmatite bodies, and the mineral content of pegmatites and their internal units.

Geology of pegmatite occurrences

The terms designating pegmatite populations as related to geological units of different orders of magnitude, and to diversified igneous complexes that have different ages, structural affiliations and compositions, are only vaguely defined in the literature. The following nomenclature, tailored to the needs of the present study, is adapted mainly from Kuzmenko (1977) using terms common in anglophone literature. It is not proposed for general usage, although it may be developed in future into a universally applicable system encompassing parallel sequences of genetic and descriptive terms.

(i) Pegmatite province — a large-scale geological unit (e.g. segments of Precambrian shields) characterized by widespread and geochemically diversified pegmatite occurrences (e.g., western Superior and Slave Provinces of the Canadian Shield; Rhodesian craton; Pilbara and Yilgarn pegmatite provinces of western Australia).

(ii) Pegmatite belt — a structural unit (structural block, gneissic belt, orogenic zone, etc.) within a pegmatite province with conspicuous concentration of pegmatite occurrences related to one or more stages of igneous activity (e.g., English River and Quetico belts in the western Superior Province; Kings Mountain pegmatite belt in the Carolinas, Kesler 1979).

(iii) Pegmatite field — a large-scale association of diversified granitoids and related pegmatites within a pegmatite province or belt, frequently hosted by a single lithological unit and generated during a single tectonomagmatic stage, and spatially separated from other fields (e.g. Cat Lake-Winnipeg River and Wekusko Lake pegmatite fields in Manitoba; the southeast Leinster pegmatite field, Steiger and Knorring 1975).

(iv) Pegmatite district — a small-scale cluster of structurally and genetically related granitoids and their pegmatite aureoles within a pegmatite field, commonly with distinct geochemical specialization (e.g. Winnipeg River pegmatite district in southeastern Manitoba; Preissac-Lacorne

TABLE 1 STANDARDS USED FOR WHOLE ROCK AND MINERAL ANALYSES

Whole Rocks			
SiO_2, TiO_2, Al_2O_3, Fe, K_2O	X R F	USGS NBS CCRMP ANRT	AGV, GSP 70A, 99, 99A SY2, SY3 GA, GH, GR
Na_2O, K_2O, MgO, MnO, CaO, FeO, P_2O_5, CO_2	A A S	USGS CCRMP ANRT	GSP-1, BCR B1, B2, SY2, SY3 GA, GH, GR
Rb		USGS CCRMP ANRT	BCR, GSP B1, SY2, SY3 GA; GH, GR
Sr		USGS CCRMP ANRT	BCR B1, SY2, SY3 GA, GH, GR
Li		CCRMP ANRT	B1, SY2, SY3 GA, GH, GR
Whole Rocks			
Be		CCRMP ANRT	SY1, SY2, SY3 GA, GH, GR
Pb		NBS CCRMP ANRT	70a, 99a SY2, SY3 GA, GH
Cs		USGS CCRMP ANRT	BCR SY3 GR
K-feldspar		NBS	70a
Beryl		USGS NBS CCRMP	BCR, AGV 27e, 70a, 181, 183 B1, B2, SY2, SY3
Micas		USGS NBS CCRMP ANRT	AGV, GSP-1, BCR 27e, 70a, 181, 183 B2, SY1, SY2, SY3 GA

pegmatite district in western Quebec; Black Hills pegmatite district in South Dakota; the Eräjärvi pegmatite district in Finland, Lahti 1975; north Mtoko pegmatite district in Zimbabwe-Rhodesia, Hornung and Knorring 1962).

(v) Pegmatite group — a swarm of pegmatite bodies, fairly homogeneous to distinctly fractionated in composition, related to a single granitic intrusion within a pegmatite district or field (e.g., Greer Lake group in the Winnipeg River district; Redout-Ross Lakes pegmatite group in the Slave province, Hutchinson 1955).

(vi) Pegmatite series — a provisional term for diversified pegmatite clusters whose subdivision and assignation to specific parent intrusions is not feasible (or known).

Internal structure of pegmatite bodies

This nomenclature is standardized in North American literature, based on the paper by Cameron et al. (1949).

(i) Pegmatite zones are units of primary crystallization, usually disposed as concentric shell-like envelopes, rarely as sheet-like layers. From contacts with enclosing rocks inwards, the border, wall, intermediate (outer, inner) and central (core) zones are distinguished.

(ii) Replacement bodies are units of irregular distribution but commonly following zone contacts; they are of late origin, generated by replacement of pre-existing zones.

(iii) Fracture fillings are units penetrating into open fractures of pre-existing units without noticeable replacement along the fracture walls.

Mineral content

No rules have been established for describing different categories of mineral populations. The present authors find the following hierarchy convenient:

(i) Mineral paragenesis — the total mineral content of a given pegmatite body (some authors would exclude the species generated by supergene alteration).

(ii) Mineral assemblage — the mineral composition of a given zone, replacement body, or fracture filling.

(iii) Mineral association — a close association of species in terms of spatial distribution and, commonly, origin, distinguishable within a broader assemblage of the parent pegmatite units.

The frequently used terms, 'primary and secondary minerals' (or 'crystallization'), should be understandable in the particular context of individual discussions. For example, metasomatic albitization is secondary with respect to a K-feldspar + quartz zone which it is replacing, but low-temperature hydrothermal alteration of beryl into bavenite + chlorite is secondary with respect to the albitization assemblage the beryl belongs to.

ANALYTICAL PROCEDURES

Chemical analyses

Standard rock and mineral analyses have been performed using X-ray fluorescence spectrometry (Si, Al, Ti, total Fe, K), l atomic absorption spectrophotometry (flame - Li, Na, K, Rb, Cs, Ca, Mn, Mg, Be, Sr, Pb; flameless — low Cs, Pb), combustion (H_2O), combustion plus acid digestion (CO_2), titration (FeO), and spectrophotometry (P). Table 1 lists the standards utilized in analyzing the major and trace elements in granitic and metamorphic rocks and pegmatite minerals, and Table 2 presents precision and accuracy data demonstrated for specified concentrations of the relevant oxides and elements in whole-rock analyses as quoted by Ramlal (1979).

TABLE 2. METHODS, PRECISION AND ACCURACY OF CHEMICAL ANALYSES OF SILICATE ROCKS

Constituent	Method(s) Primary	Alternate	Concentration	Instrument precision, σ	Accuracy of replicates, σ
SiO_2	XRF		59.60 wt.%	.12	.20
Al_2O_3	XRF		9.34	.05	.13
Fe_2O_3*	XRF	AAS	10.08	.017	.03
MgO	AAS		4.04	.04	.10
CaO	AAS	XRF	10.22	.02	.07
K_2O	XRF	AAS	2.69	.01	.01
MnO	AAS	XRF	.41	.01	.01
TiO_2	XRF		.48	.02	.02
Na_2O	AAS		4.20	.01	.05
H_2O*	combustion		1.60	.03	.06
CO_2	combustion; acid digestion		1.15	.05	.12
P_2O_5	spectrophotometry		0.20	.01	.01
FeO	titration		10.92	-	0.04
Cs	AAS		820 ppm	5.0	13.0
Cs	AAS flameless		0.95	0.02	0.04
Co	AAS		53	1.0	2.0
Li	AAS		10	.04	.05
Ni	AAS		77	1.0	3.0
Pb	AAS		34	2.0	3.0
Pb	AAS flameless		8	0.2	0.1
Rb	AAS		228	1.0	2.0
Sr	AAS		260	5.0	6.0
Ba	XRF		100		10.0
Y	XRF		100		1.0
Zr	XRF		100		2.0
Sn	XRF		100		1.0
U	XRF		100		1.0
Th	XRF		100		1.5
Ga	XRF		100		2.0

* = total σ = one std. deviation

X-ray fluorescence spectrophotometry has been applied to the determination of additional trace elements by Bondar, Clegg and Co. Ltd. in Ottawa (Ba, Zr, Y, Sn, U, Th, Ga). Accuracy of replicate analyses claimed for samples with < 100 ppm of the above elements is given in Table 2.

The bulk of the whole-rock and mineral analyses has been deposited with, and may be obtained at a nominal charge from, the Depository of Unpublished Data, CISTI, National Science and Engineering Research Council of Canada, Ottawa, Ontario K1A 0S2.

The whole-rock compositions have been normalized using the classic CIPW system which does not calculate biotite, to obtain corundum values comparable to those quoted in the literature (cf. Chappell and White 1974). For ternary feldspar and alkali granite diagrams, Barth's mesonorm was used as modified by H. Ambach in the MESO / I program: apatite, titanite, ilmenite, albite, K-feldspar, riebeckite, magnetite, anorthite, corundum, biotite, diopside, and hornblende. For pegmatitic granites, essentially biotite-free but carrying garnet and muscovite, garnet with sliding Fe/Mn ratio was calculated instead of biotite, and the remainder of Al_2O_3 was assigned to muscovite. However, separate runs with all K_2O assigned to K-feldspar were used for plotting in ternary systems.

Rare earth elements

Table 3 summarizes the accuracy data for the rare earth element determinations performed by Dr. R.V.G. Hancock by neutron activation analysis at the Department of Chemical Engineering and Applied Chemistry, SLOWPOKE Reactor Facility of the University of Toronto. Further details of the analytical technique are given by Hancock (1976). The REE data have been normalized to the Leedey chondrite (Masuda et al. 1973, Masuda 1975, Chou 1977).

Concentrations of some low-abundance REE's have been found below the quantitative detection limits in several samples. In plotting the chondrite-normalized values, the maximum possible content was used but marked by a downward-pointing arrow to indicate the uncertainty. Because of difficulties encountered in determining Tb, Gd values were interpolated between Eu and Dy by the conventional graphic approximation, to emphasize the form of the Eu anomalies. This procedure is also acceptable for the pegmatitic assemblages, as proved by separate analyses run by Dr. B.J. Fryer at the Memorial University for La, Ce, Nd, Sm, Eu, Gd, Dy, and Lu.

TABLE 3. ACCURACY OF REPLICATE INAA DETERMINATIONS OF RARE EARTH ELEMENTS AND HAFNIUM

Element	Concentration ppm	Accuracy σ
La	9.8	0.7
	45	1
	82	2
Ce	20	2
	80	4
	140	10
Nd	7	2
	20	3
	60	6
Sm	1.6	0.2
	6.4	0.2
	12.0	0.6
Eu	0.30	0.04
	1.3	0.05
	2.5	0.4
Dy	0.57	0.08
	4.4	0.3
Yb	1.0	0.2
	3.0	0.3
	7.5	0.6
Lu	0.14	0.02
	0.42	0.04
	0.8	0.1
Hf	1	0.1
	6.5	0.5
	9	0.6

Oxygen isotopes

The analysis of oxygen isotope ratios was performed by Dr. F.J. Longstaffe in Dr. K. Muehlenbach's laboratory at the Department of Geology, University of Aberta, (Longstaffe et al. 1981). Details of the analytical procedure are given in Clayton and Mayeda (1963).

Electron microprobe analyses

The MAC-5 electron microprobe operating in the wavelength dispersive mode has been used mainly for analyzing garnets and complex Nb, Ta-oxide minerals, mostly with an acceleration voltage of 20 kV and a sample current of 0.04 μ amps. Dr. F.C. Hawthorne of the Department of Earth Sciences, University of Manitoba used the standards listed in Table 4. Data reduction was done with the EMPADR VII program (Rucklidge and Gasparrini 1969).

Physical properties

Standard optical methods have been applied to the study of rock-forming and pegmatite minerals: thin sections on fixed and universal stages, sodium light source and Abbe refractometer for determination of refraction indices in liquid immersion.

Density has been determined by aid of a Berman torsion balance, using toluene as the displacement liquid. Several grains have been repeatedly measured to ensure reliable averages.

X-Ray diffraction methods

Standard X-ray powder diffraction techniques have been used for mineral identification: fast-scan goniometer chart records, powder camera and Gandolfi camera films. Unit cell dimensions have been refined from goniometer chart records, calibrated with internal standards admixed to the examined mineral, using the least-squares self-indexing program by Evans et al. (1963).

ACKNOWLEDGEMENTS

A major part of the study in the Cat Lake-Winnipeg River field, and all the investigations of the Wekusko Lake field were supported by the Canada-Manitoba Subsidiary Agreement on Mineral Exploration and Development in Manitoba, under the auspices of the Department of Regional Economic Expansion. However, a large proportion of data collected on pegmatites and granites in the Cat Lake-Winnipeg River field was accumulated while the Principal Investigator was a Post-doctoral Fellow sponsored by National Science and Engineering Research Council of Canada Operating Grants to R.B. Ferguson and A.C. Turnock, and the University of Manitoba in 1968-1971. Substantial proportions of the N.S.E.R.C. Operating Grants awarded to the Principal Investigator in 1971-1974, 1974-1977 and 1977-1980 also contributed, as well as the Department of Energy, Mines and Resources Research Agreements in 1971-1975. The M.Sc. and Ph.D. theses of D.L. Trueman, which contributed most of the geology of the Bird River Greenstone Belt, were financed from the N.S.E.R.C. Operating Grants to A.C. Turnock, and by regional mapping programs of the Manitoba Department of Mines, Resources and Environmental Management.

The authors wish to thank their colleagues and teachers L.D. Ayres, G.P. Beakhouse, W.C. Brisbin, G.S. Clark, R.B. Ferguson and F.C. Hawthorne for their interest and stimulating discussions. W.C. Brisbin and D.H. Hall, former and present Heads of

TABLE 4. STANDARDS USED FOR ELECTRON MICROPROBE ANALYSES

Ta, Nb-oxide minerals

Nb	Manganotantalite, stibiotantalite, $Ba_2NaNb_5O_{15}$
Ta	manganotantalite, stibiotantalite
Mn	manganotantalite
Fe	chromite, olivine
Zr	zircon
Hf	zircon, baddeleyite
Sn	cassiterite
Ti	titanite, benitoite
Ca	titanite, $CaWO_4$
Al	titanite, chromite
Y	REE glass, YAG
Ce	CeO_2, REE glass
La	LaB_6, REE glass
Sc	metallic Sc
Sb	stibiotantalite
Th	ThO_2
U	metallic U
Mg	chromite
Na	albite

Garnets

Mn	spessartine
Fe	chromite, olivine
Al	spessartine
Si	spessartine
Ca	pyrope
Mg	chromite, olivine
Ti	titanite
Sc	metallic Sc
Zr	zircon
Y	YAG

REE glasses from Dr. D. F. Weill, University of Oregon (Drake & Weill, 1972). Metallic U from the Whiteshell Nuclear Research Establishment, AECL, Pinawa. All other standards from Charles M. Taylor Co., Stanford.

the Department of Earth Sciences, encouraged and supported the Project wholeheartedly during their respective terms in office. Most of the microprobe work was expertly handled by F.C. Hawthorne, as well as computer processing of rock and mineral chemistry. Iva Černý took care of organizing the chemical analyses and their statistical processing, and of the worn-out principal investigator during trying times. Field and laboratory assistance was provided by A. Agwu-Jones, J.L. Barber, S. Černý, D.P. Henderson, W.C. Hood, C. Nahnybida, and W. Rennie whose help with mineral separations was priceless. The staff of the chemical laboratory, K. Ramlal, P. Beaudoin, R.J. Chapman, R.A. Gordon, R.M. Hill, and P. Jones carried the burden of monotonous analyzing. Administrative personnel and support staff in offices and technical services also contributed in their respective fields.

Special thanks are due to B.B. Bannatyne, and to F.J. Elbers and J.F. Stephenson from the Department of Mines, Resources and Environmental Management who supervised the progress of the Project. B.B. Bannatyne provided us with valuable information and samples collected during a previous pegmatite study. D.A. Janes from that Department provided much of his field and geochemical experience, and his unpublished geological maps covering parts of the Cat Lake-Winnipeg River area. J.J. Macek was of considerable help in optical studies. W.D. McRitchie, B.B. Bannatyne and A.H. Bailes have edited the manuscript with patient care.

Fruitful cooperation was established with H.Y. Tammemagi (Atomic Energy of Canada Ltd., Whiteshell Nuclear Research Establishment) and his group investigating the Lac du Bonnet pluton, thereby avoiding duplication and enriching the understanding of the intrusion by both parties.

The management and personnel of the Tantalum Mining Corporation of Canada Ltd. at Bernic Lake, C.T. Williams, R.A. Crouse, S. Pataran, J.C. Hayward, and D.L. Trueman, provided considerable help with lodging and transportation of field crews, and made the results of their work available for the project.

Last but not least, the authors greatly benefited from discussions and/or joint field trips to the Project areas and other pegmatite fields with R. Alviola, S. Lahti, and O. Nykänen (Geological Survey of Finland), A.A. Beus (United Nations Organisation, New York), F.W. Breaks (Ontario Geological Survey), D.B. Burt (University of Arizona), R. Capdevila (University of Rennes), E.E.Foord and J.J. Norton (U.S. Geological Survey Denver), C.L.C. Chou and R.W.G. Hancock (University of Toronto), W.L. Roberts, J. Honert and Dr. J.A. Redden (South Dakota School of Mines and Technology), and F.J. Longstaffe whose oxygen isotope study is continuing in K. Muehlenbach's laboratory at the Department of Geology, University of Alberta in Edmonton.

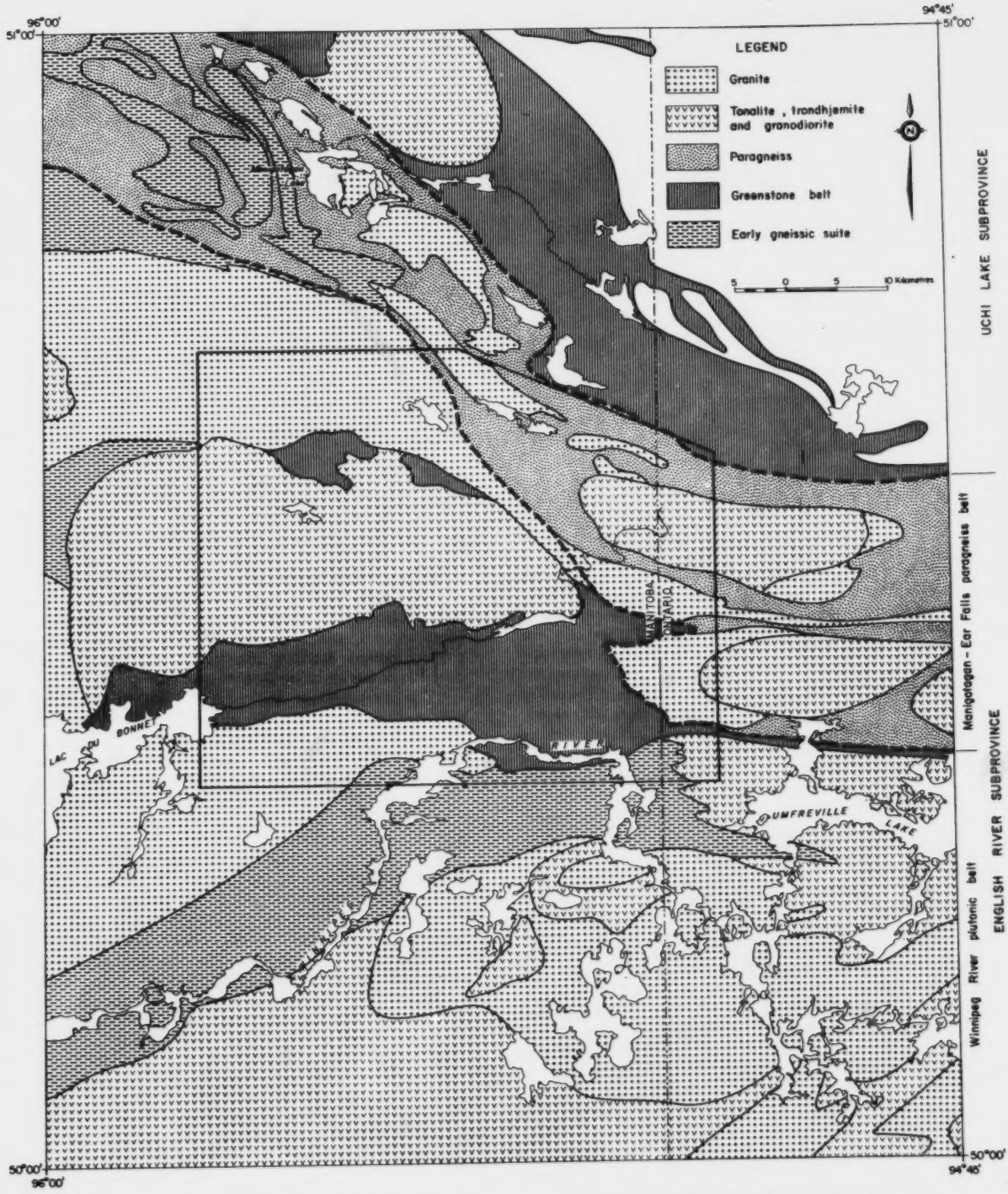

Figure 2: Location of the Cat Lake-Winnipeg River pegmatite field map area in the English River subprovince; schematized from the Geological Map of Manitoba, Map 79-2, and Beakhouse (in prep.)

THE CAT LAKE-WINNIPEG RIVER FIELD

INTRODUCTION

LOCATION, ACCESS, AND TOPOGRAPHY

The Cat Lake-Winnipeg River pegmatite field is situated in the Archean Superior Province of the Canadian Shield in southeastern Manitoba (Figs. 1, 2).

The approximate centre of the area lies about 200 km northeast of Winnipeg, and in general the area is accessible by roads through Bissett, Pointe du Bois, or Lac du Bonnet. Internal access through much of the area can be achieved by most modes of transportation.

The topography and physiography of the area is typical of much of the Canadian Shield and consists of low (< 25 m) rock outcrop mantled by swamp, muskeg, or tree-covered ground.

MAP COVERAGE

National Topographic Series maps are available in both 1:250 000 and 1:50 000 scales from the Map Distribution Office, Ottawa or from the Surveys Branch of the Manitoba Department of Natural Resources, 1007 Century Street, Winnipeg. Aeromagnetic maps also are available from these sources, as well as an airborne radiometric map covering the pegmatite field, Geophysical Series Map P. 1320, at 1:250 000.

Claim maps of the area are available at the Mining Recording Office, 993 Century Street, Winnipeg.

Geological maps accompany most of the Manitoba Mines Branch reports listed in the following review of previous work. At present, a new 1:100 000 geological map is being prepared by D.A. Janes, C.F. Lamb and D.L. Trueman.

Vertical air photo coverage for the area is available in both 1 inch = 1 mile (1:63 360) and 1 inch = 1/4 mile (1:15 840) scales from the National Air Photo Library, 601 Booth Street, Ottawa. Good quality copies of air photos can be obtained from the Air Photo Library of the Manitoba Department of Natural Resources.

PREVIOUS WORK AND ECONOMIC DEVELOPMENT

The first systematic geological investigation in the present study area was conducted by Tyrrell (1900). Moore (1913) proposed the first stratigraphic divisions and correlations of rocks of the area with those of the Rice Lake Group at Bissett.

The discovery of Ni-Cu sulphides in the Cat Lake area prompted extensive investigations of much of the area in the early 1920s by Colony (1920, 1921), McCann (1921), Cooke (1922) and later by Wright (1926, 1932). This work undoubtedly prompted prospecting that led to the discovery of the rare-metal bearing pegmatites of the area, and in the late 1920s and early 1930s attempts were made at Bernic and Shatford Lakes to undertake economic tin production.

In 1942 the discovery of chromite in the area prompted further studies of the region with attendant wartime investigation of some of the Sn-mineralized pegmatites in the area. Subsequent regional mapping was undertaken by Springer (1949, 1950) and Davies (1952, 1955, 1956, 1957), much of this work coinciding with increased interest in the lithium-bearing pegmatites in the area.

The most recent mapping, of regional nature, in the area of concern has been conducted by McRitchie (1971), Trueman (1980), and Janes (in prep.).

In previous years the study area has hosted Ni-Cu production at the Dumbarton Mine, but presently only tantalum is being produced at the Tanco pegmatite at Bernic Lake.

Numerous pegmatite bodies in the field were checked for molybdenum during the First World War (Bruce 1917, DeLury 1926, 1930, Bateman 1943). The first detailed descriptions of Li-bearing localities, and the first attempts at generalization, were published by Derry (1931), Wright (1932) and Stockwell (1933). The great age of the Superior Province was first established on uraninite from the Huron Claim pegmatite (DeLury and Ellsworth 1931, Ellsworth 1932), for which a description of columbite and beryl also was published (Walker 1931).

A second major series of publications dealing with the field appeared in the fifties (Springer 1950, 1952, Davies 1952, 1954, 1955, 1956a, b, 1957, 1958, Rowe 1956, Davies et al. 1962), based on detailed geological mapping of the area; Mulligan's (1957, 1961, 2965, 1968, 1975) reports are based partly on this work.

The recent studies follow Hutchinson's (1959) first description of the Tanco (Montgary, Chemalloy) pegmatite, which established (largely from drill cores) most of the zoning pattern as we know it today. Various aspects of this unique deposit have been dealt with in papers by Nickel (1961), Nickel et al. (1963), Wright (1963), Armstrong (1969), Crouse and Černý (1972), Černá et al. (1972), Černý (1972a, b), Černý and Ferguson (1972), Černý and Macek (1972), Grice et al. (1972), Marshall (1972), Rinaldi et al. (1972), Černý and Simpson (1977, 1978), Černý and Harris (1978), Crouse et al. (1979), and Černý and Siivola (1980). Other pegmatites in the area have been described, mainly from the mineralogical viewpoint, by Černý and Turnock (1971a, 1975), Černý and Bristol (1972), Černý and Harris 1973a, b), and Černý (1978). The first attempt at a detailed pegmatite classification in the area was published by Černý and Turnock (1971b), and the geological framework of their occurrences and possible genetic relationships were discussed by Černý and Trueman (1977, 1978).

PRESENT STUDY

Regional geological background was obtained mainly from the concurrent thesis work of Trueman (1980) and broader regional mapping conducted by D.A. Janes (1976, 1978, in prep.) Field work was oriented mainly toward geochemical sampling of intermediate and acid plutonic rocks and their metamorphic hosts, and detailed documentation of pegmatitic granite intrusions and pegmatites. The station location Map 2 indicates the extent of plutonic and metamorphic rock sampling. The present report also incorporates previous studies of the area by Černý and others, by Trueman, and a multiplicity of descriptions of both regional geology and pegmatitic rocks provided by federal, provincial, and university-related geologists, and also by mining companies that are, or were, actively engaged in pegmatite examination. Two M.Sc. theses based on segments of the present study are almost completed: on pegmatitic granites (B.E.G.) and on the Huron Claim pegmatite (B.J.P.).

GENERAL GEOLOGY

REGIONAL SETTING

The Winnipeg River-Cat Lake pegmatite field covers portions of three major lithostratigraphic-tectonic entities which collectively form the westernmost exposed portions of the English River Gneissic Belt of Wilson (1972). From north to south, these are respectively the Manigotagan-Ear Falls Gneiss Belt, the Bird River Greenstone Belt, and the Winnipeg River Batholithic Belt (Fig. 2). These three entities have been described in detail by McRitchie (1971), Trueman (1980), and Janes (in prep.) respectively, and have been replaced in their regional contexts by Hall (1971), Wilson (1972), Trueman et al. (1976), Beakhouse (1977), Wilson et al. (1977), and Breaks et al. (1978).

STRATIGRAPHY, INTRUSIVE ROCKS, AGE RELATIONSHIPS

Metavolcanic, metasedimentary, and related synvolcanic intrusive rocks: Bird River Greenstone Belt.

The Bird River Greenstone Belt comprises metavolcanic and metasedimentary rocks of the Rice Lake Group which, in the map area, are interpreted as forming a broad anticlinorium-synclinorium pair. Rocks of the Rice Lake Group are divisible into six formations which, in order of age from oldest to youngest, are termed the Eaglenest Lake Formation, the Lamprey Falls Formation, the Flanders Lake Formation, and the Booster Lake Formation (Map #1). A detailed discussion of age relationships is given by Trueman (1980).

The Eaglenest Lake Formation comprises fine to coarse clastic metasediments of volcanic derivation, which exhibit polydeformational structural character and greenschist facies metamorphic grade. These rocks, by their relative stratigraphic position, appear to form the oldest recognizable part of the greenstone belt.

The Lamprey Falls Formation comprises mainly metabasalts and correlative intrusive rocks which include the chromite-enriched Bird River Sill. Associated subordinate rocks include tuffaceous intercalations, hyaloclastites, and extensive iron formations. These rocks are disposed as the enveloping keel-like base to the synclinorium, are of simple deformational style, and display metamorphic assemblages of both hornfelsic and greenschist facies.

The Peterson Creek Formation comprises a mixture of metarhyolite, volcanoclastic, and epiclastic derivatives. These rocks are located in the core area of the synclinorium, are intimately infolded and polydeformed together with a portion of the younger Bernic Lake Formation, and exhibit greenschist and amphibolite facies grades of metamorphic assemblages.

The Bernic Lake Formation rests unconformably above the Eaglenest, Lamprey Falls, and Peterson Creek Formations. It forms a complex of clastic metasedimentary rocks and iron formation interlayered with metabasalt, meta-andesite, metadacite, and metarhyolite, and was intruded by composite stocks of basic to acidic composition. The main part of the Bernic Lake Formation occupies the core of the synclinorium formed by the greenstone belt, and to a lesser extent, is infolded with rocks of the Peterson Creek Formation. The deformational attributes of the Bernic Lake Formation are varied; multiple deformation is evident where these rocks are infolded with the Peterson Creek Formation, but is not defined clearly in the core area of these rocks in the synclinorium. Metamorphic grades in the Bernic Lake Formation are greenschist and amphibolite facies grades.

The Flanders Lake Formation lies in unconformable contact in the eastern extremeties of the greenstone belt, and consists mainly of lithic and pebbly meta-arenites interbedded with metaconglomerate. These rocks exhibit multiple periods of deformation developed with infolding of the rocks of the Peterson Creek and Bernic Lake Formations, and exhibit metamorphic grades of the amphibolite facies.

The Booster Lake Formation comprises metamorphosed greywacke-mudstone turbidites in part interlayered with iron formation. These rocks are disposed along the core of the synclinorium, exhibit one folding event, and are fault-bound along contacts forming a monoclinal sequence. Metamorphic assemblages are of lower amphibolite facies grades.

Synvolcanic intrusive rocks of the area include the chromite-enriched Bird River Sill, high-alumina metagabbro, and composite stocks of gabbroic, tonalitic, and granodioritic composition. Less abundant are dykes and sills of hypabyssal metagabbro, glomeroporphyritic metagabbro, and quartz porphyry.

The age relationships of the rock groups within the Bird River Greenstone Belt have been established on the basis of facing directions in metasedimentary rocks, intrusive relationships, magmatic sequences, unique sedimentary detritus, and basement-cover structural relations.

Accordingly, the Eaglenest Lake Formation forms the oldest recognizable part of the greenstone belt, because it underlies the north-facing Lamprey Falls Formation in the Eaglenest Lake area.

Facing directions in the Lamprey Falls Formation are evident in pillow structures in lavas, inter-flow relationships, and the differentiation sequence of the lavas. In addition, the Bird River Sill, which is intrusive into the Lamprey Falls Formation, confirms through its igneous differentiation sequence the facing directions noted in the lavas.

The oldest possible relative age for the Peterson Creek Formation is not clear. Where these rocks lie in faulted contact with the Lamprey Falls Formation, top directions face both into and away from the Lamprey Falls Formation as a result of the polydeformational history of the Peterson Creek rocks. A minimum relative age for the Peterson Creek Formation, with respect to the greenstone assemblages, can be assigned by the presence of metarhyolite detritus observed in the Bernic Lake Formation and their mutual facing directions.

A maximum relative age for the Bernic Lake Formation is indicated by the presence of Peterson Creek metarhyolite detritus in the Bernic Lake Formation and in addition by the occurrence in these rocks of detritus from the Bird River Sill. A minimum relative age for the Bernic Lake Formation can be assigned on the basis of the occurrence of detritus derived from the Bernic Lake Formation which is found in the younger unconformable Flanders Lake Formation (Posehn 1975).

The relative age of the Flanders Lake Formation can be assigned on the basis of facing directions in these rocks, and by the presence of detritus from the Bernic Lake Formation. In addition, these rocks lie across the boundary of the Peterson Creek and Bernic Lake Formations in angular unconformity.

The relative age of the Booster Lake Formation is uncertain. The absence in this formation of M_1 metamorphic structures suggests the formation post-dates that event, and hence is younger than M_1. However, the preponderance of detritus from a rhyolitic source area, rather than a mix of detritus as would be expected from a metamorphosed (M_1) source area, tends to suggest a possible equivalence of the Booster Lake Formation with, e.g., the Peterson Creek Formation as a source of the felsic material. However, geochemical arguments favor the first interpretation (see Trueman, 1980 for further discussion).

These age relationships form the basis of Table 5.

TABLE 5. STRATIGRAPHY OF THE CAT LAKE-WINNIPEG RIVER PEGMATITE FIELD

	Formation	Dominant lithology	Intrusive rocks	Metamorphic rocks	Metamorphism	Deformation	Structure	Planar fabric
ARCHEAN			pegm. granites, pegmatites (18)					
			Lac du Bonnet (17)					
			monzogranite (16)				F_4^{++}	
			Inconnu granite (15)		M_3	D_3	F_3^{++}	
			Black River Suite (14)					
			granodiorite (13)					
			tonalite (12)					
				migmatite-complex (11)				
			Great Falls QD(10)	paragneiss* (9)	M_2	D_2	F_2^+	S_2
RICE LAKE GROUP	Booster Lake (8)**	metamorphosed greywacke-mudstone						
			UNCONFORMITY					
	Flanders Lake (7)	lithic meta-arenite metaconglomerate			M_1	D_1	F_1^+	S_1
			UNCONFORMITY					
	Bernic Lake (5)	clastic derivatives metarhyolite metadacite meta-andesite metabasalt	metamorphosed: gabbro diorite quartz-feldspar porphyries granodiorite	(6)				
			UNCONFORMITY					
	Peterson Creek (4)	metarhyolite, clastic equivalents						
	Lamprey Falls (2)	metabasalts	Bird River Sill, metagabbro (3)					S_0 (bedding)
	Eaglenest Lake (1)	metamorphosed volcanic wacke						

*in part equivalent to map unit (7)

$^+F_1, F_2$ folding, $^{++}F_3, F_4$ episodic faulting

**possibly equivalent to unit (4); see text for details

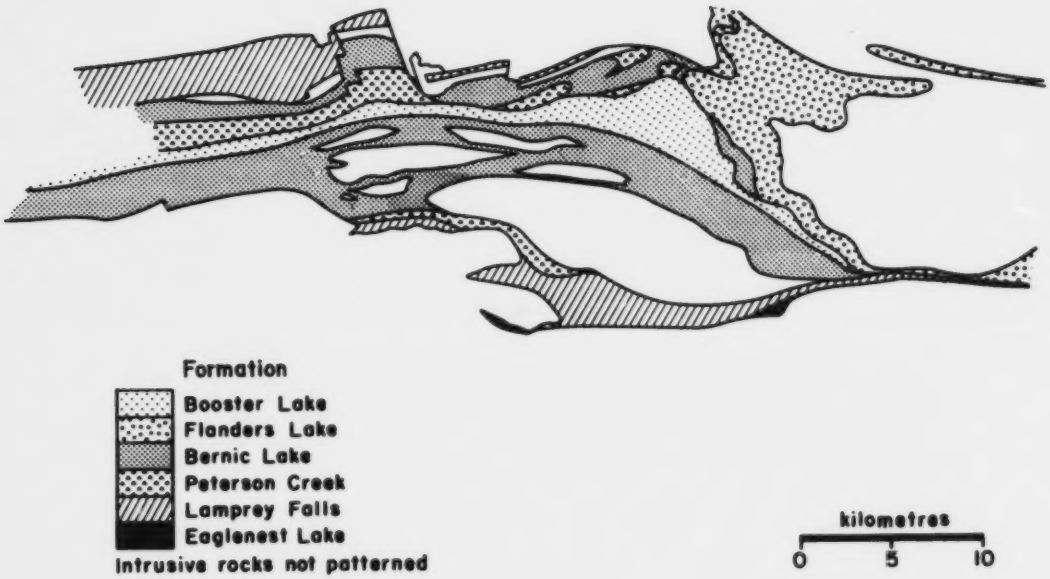

Figure 3: Stratigraphic subdivision of the metavolcanic and metasedimentary rocks of the Bird River Greenstone Belt

The Manigotagan Gneiss Belt

Essential rock types of the Manigotagan Gneiss Belt include paragneisses, and early, syn-, and late-tectonic intrusive rocks and correspondingly developed metasomatites.

Of these, the paragneisses have been documented by Campbell (1971) as being equivalent to the Edmunds Lake Formation of the Rice Lake Group which lies on the north flank of the Manigotagan Gneiss Belt. A similar correlation of gneisses in the Manigotagan Gneiss Belt was reported by Trueman et al. (1976), in which an equivalence of the gneisses with the Flanders Lake Formation was established; this implies, in turn, the equivalence of the Flanders Lake Formation with the Edmunds Lake Formation. This was the proposal first put forth by Moore (1913) which led to the application of the term Rice Lake Group to those rocks of the Bird River Greenstone Belt.

The aforementioned correlation (Trueman et al. 1976) is supported by the correlation of structures and metamorphism at Rice Lake, the features of which have been documented by McRitchie (1971). Accordingly, the deformational and intrusive history in the Manigotagan Gneiss Belt can be ordered chronologically with respect to the Bird River Greenstone Belt, as shown in Table 1.

The Winnipeg River Batholithic Belt

The Winnipeg River Batholithic Belt in the study area comprises quartz-feldspar-biotite gneisses of varied mineral proportions which host enclaves and schlieren of older and more mafic gneisses in what has been termed a schollen zone by Janes (1978). At Greer Lake these gneisses are intruded by pegmatite dikes considered equivalent in age to the pegmatites at Bird River.

The relative ages of the gneissic rocks of the Winnipeg River Batholithic Belt are uncertain. At Eaglenest and Greer Lakes, the Bird River Greenstone Belt lies in intrusive and faulted contact, respectively, with the Winnipeg RiverBatholithic Belt, which confirms the observations of Beakhouse (1977) further to the east. Breaks and Bond (1977) suggest that the gneissic rocks of this area may have served as basement to the Bird River Greenstone Belt, a concept which is lent support by Ermanovics et al. (1979) but which cannot be considered definitive.

The rocks of the Winnipeg River Batholithic Belt are assigned tentatively to the position indicated in Table 5 on the basis of their common fault boundary with the Bird River Greenstone Belt, and their common intrusive history. This assignment is not intended to exclude the possibility that these rocks are older or equivalent in age to those of the Bird River Greenstone Belt.

Age relationships

Absolute ages of regional metamorphism and plutonic intrusions in the area place them into the Kenoran orogeny, 2.70-2.55 Ga (Farquharson and Clark 1971, Penner and Clark 1971, Turek 1971, Turek and Peterman 1971, Farquharson 1975). Most of the data is statistically indistinguishable, indicating a relatively short period of regional evolution:

Volcanics of the Bird River Greenstone Belt: 2.650 ± 0.035 Ga,
Ri = 0.7015 ± 0.0015 (Penner and Clark 1971).
Maskwa Lake quartz diorite: 2.640 ± 0.135 Ga,
Ri = 0.7014 ± 0.0021 (Penner and Clark 1971).
Lac du Bonnet biotite granite: 2.680 ± 0.091 Ga,
Ri = 0.6998 ± 0.0032 (Farquaharson 1975).

In the following sections, systematic description is given of all the geological units quoted above, and of the late pegmatitic suites, in the suggested chronological order.

METAVOLCANIC, METASEDIMENTARY, AND RELATED SYNVOLCANIC INTRUSIVE ROCKS: BIRD RIVER GREENSTONE BELT

The Eaglenest Lake Formation (1)

The rocks of the Eaglenest Lake Formation crop out extensively on the shores and islands of Eaglenest Lake which forms a part of Winnipeg River (Map 1, Fig. 3). These rocks are intruded along their south contact by rocks of the Winnipeg River Batholithic Belt

Figure 4: Pillowed metabasalt in the Lamprey Falls Formation, northwest of the junction of Provincial Roads 314 and 315

(Beakhouse 1977) and form a part of the agmatitic and schollen zone of Janes (1976). To the north the Eaglenest Lake formation lies in fault contact with metabasalts of the Lamprey Falls formation.

Rock types of the Eaglenest Lake Formation include metamorphosed volcanic and pebbly wackes, and volcanic sandstone. Less abundant are biotite schists and amphibolites of uncertain origin which occur between lit of tonalitic and dioritic intrusive materials in the south contact zone. Banded iron formation occurs near the northern fault boundary of the Formation.

The rocks of the Eaglenest Lake Formation form near-vertically dipping limbs of an east-trending fold, are typically dark grey to buff weathering, fine- to coarse-grained, and moderately to strongly schistose. The volcanic wackes and pebbly variants are poorly bedded, lack sorting, and consist chiefly of quartz, albite, chlorite, actinolite, biotite, zoisite, and helicitic and euhedral garnet. Matrix-supported pebble-size lithic fragments variously consist of metabasalt, fine- to medium-grained gabbros, and more felsic volcanic sandstone clasts, all of which are strongly deformed and flattened parallel to the schistosity.

Volcanic sandstones interbedded with the wackes are grey to buff weathering, fine- to medium-grained, show a degree of sorting, and consists essentially of quartz and feldspar detritus, minor biotite, chlorite, and sericite.

Biotite schists and amphibolites are gradational with the above rocks, and appear only to have suffered a more extensive recrystallization with emplacement of intrusive lit from the batholithic complex to the south. Boudinage of beds is common, and ultimately these rocks pass into a dismembered zone of agmatite with porphyroblastic tonalitic and dioritic material.

The iron formation forms a thick (approximately 6 m) unit near the north boundary of the Eaglenest Formation and consists essentially of pyrrhotite, magnetite, pyrite, and interlayered chert laminae. In outcrop the iron formation is badly weathered, forming rubbly gossans from which traces of chalcopyrite have been reported by Davies (1957).

The Lamprey Falls Formation (2)

The Lamprey Falls Formation (Map 1, Fig. 3) crops out extensively in the Winnipeg River area and north of Bird River. In these two locales the Lamprey Falls Formation consists mainly of mafic metavolcanic and related hypabyssal intrusive rocks which in both areas are marked by both fault and intrusive contacts.

Rock types of the Lamprey Falls Formation include metamorphosed pillow basalts, tuffs, hyaloclastites, aquagene breccias, megacrystic basalts, porphyritic and amygdaloidal metabasalts, and iron formation. Related intrusive rocks include numerous hypabyssal metagabbro sills, descriptions of which are presented elsewhere.

Pillow metabasalt (Fig. 4) is the dominant rock type of the Lamprey Falls Formation. This rock is typically dark grey-black to green weathering, fine- to medium-grained, massive to weakly schistose, and is characterized by well defined selvaged pillow structures. The degree of preservation of pillows is generally good, and top determinations are decisive. Elsewhere, a more strongly developed schistosity yields a moderate stretching of pillows.

South of the Winnipeg River, pillow metabasalt is essentially as described above except that these rocks are more commonly marked by the occurrence of small (< 0.5 cm) quartz and quartz-carbonate filled amygdules, and to a lesser extent by the occurrence of small

TABLE 6. REPRESENTATIVE CHEMICAL ANALYSES OF THE METABASALTS, LAMPREY FALLS FORMATION (2)

	72-112	72-110	72-105	6	75-498	75-497	75-496	75-482
SiO_2, wt %	50.35	49.30	50.15	51.65	51.75	50.65	53.00	52.20
Al_2O_3	15.10	14.35	14.95	14.53	19.00	17.45	16.10	18.00
TiO_2	0.97	0.48	0.75	0.93	0.84	0.76	1.17	0.75
Fe_2O_3	1.85	2.43	1.60	3.24	1.65	1.11	1.58	1.79
FeO	10.85	12.76	10.19	8.94	6.47	6.93	7.60	7.48
MnO	0.16	0.21	0.29	0.19	0.24	0.23	0.28	0.29
MgO	6.63	5.97	7.92	7.30	3.99	6.70	5.27	3.92
CaO	9.96	9.63	9.83	7.82	12.30	13.60	11.40	11.20
Na_2O	2.87	2.38	2.49	3.22	2.77	1.65	2.34	2.93
K_2O	0.22	0.35	0.64	0.70	0.25	0.14	0.20	0.14
P_2O_5	0.09	0.08	0.08	0.10	0.06	0.07	0.12	0.05
CO_2	0.20	0.15	0.25		0.02		0.05	0.12
H_2O	0.68	1.00	1.16	1.58	0.58	0.77	0.82	0.59
S	0.06	0.02	0.05		0.06			0.57
Cr_2O_3	0.04	0.03	0.03		0.06	0.06	0.04	0.06
NiO	0.01	0.01	0.02	0.02	0.03	0.03	0.02	0.03
CuO	0.01		0.01					
CoO	0.01	0.01	0.01					
ZnO				0.02				
	100.06	99.21	100.42	100.22	100.07	100.17	99.97	99.91

(< 2 mm) plagioclase (anorthite) phenocrysts.

Metacrystic metabasalts occur in isolated horizons, one approximately 100 m north of the north contact of the Bird River Sill, and one north-west of Greer Lake (see accompanying Geologic Map 1). These metabasalts are marked by an abundance of coarse, single crystal and glomeroporphyritic aggregates of calcic (An79-An85) plagioclase which range in size from 1 to 10 cm. The matrix to these megacrysts is black to green weathering, fine- to medium-grained, and massive, and generally retains dismembered selvaged pillow margins which are in part perforated by the megacrysts.

Mafic tuffs are disposed as thin (< 3 m) intercalations in metabasalt and have little (< 100 m) lateral persistence. These rocks are generally greenish weathering, medium-grained, and moderately to strongly schistose. Lapilli-size (Fisher 1966) fragments are commonly present but never constitute more than 10 per cent of the rock.

A mixed zone of hyaloclastite and pillow metabasalt crops out north of the Bird River. This rock comprises irregularly shaped pillow structures of metabasalt, which give the appearance of floating in a voluminous matrix of fine to coarse shards of clastic quench material. Similar hyaloclastites and aquagene breccias occur at the top of the Lamprey Falls Formation close to its contact with the Peterson Creek Formation along the Winnipeg River.

In thin section all of the above rock types consist of plagioclase (albite-labradorite), tremolite-actinolite, chlorite, biotite, zoisite, leucoxene-ilmenite, local garnet, quartz, and carbonate. Texturally, these rocks vary from lepidoblastic chlorite-rich to massive or nematoblastic amphibole-rich types.

Iron formation occurs intercalated with the mafic metavolcanic rocks of the Lamprey Falls Formation, as two prominent bands in the Winnipeg River area, and as a single band in the area north of Bird River. These features, exposed as rubbly gossans, contain magnetite-chert and iron sulphide assemblages, which at the Dumbarton Mine have been termed Algoman type (Juhas 1973).

Chemical analyses representative of the Lamprey Falls metabasalts are shown in Table 6 and Figure 5, indicating a tholeiitic character of these rocks. Discussion of the metabasalt petrochemistry is given by Trueman (1980).

The Peterson Creek Formation

The Peterson Creek Formation consists of felsic flows and clastic metavolcanic rocks which crop out along Peterson Creek, at Shatford Lake, south of Bird Lake, and east of Tulabi Lake (Fig. 3). Rock types include flow-banded metarhyolite (quartz porphyry), rhyolite breccia, rhyolite tuffs, and epiclastic sandstone derivatives.

Metarhyolite flows are present in the western and central parts of the Bird River area (Map 1). These rocks are present as moderately thick flows (6-20 m) intercalated with clastic equivalents. They are buff to greenish weathering, porphyritic, aphanitic to fine-grained, flow banded, and weakly schistose. Quartz forms the dominant phenocryst in these rocks; feldspars (albite-oligoclase) are less abundant. Phenocryst size ranges up to 0.5 cm, and these are set in a fine-grained matrix of quartz, feldspar, and sericite.

The clastic felsic metavolcanic rocks of the Peterson Creek Formation can be subdivided into tuff, lapillistone, and pyroclastic breccia, according to Fisher (1966). Of these, pyroclastic breccia and lapillistone predominate in the western and central map area (Map 1) and pass eastwards into lapillistone, tuffaceous rocks and ultimately into the derived epiclastic counterparts.

Pyroclastic breccia occurs only in the western part of the map area. These rocks are present in moderately thick beds (< 100 m),

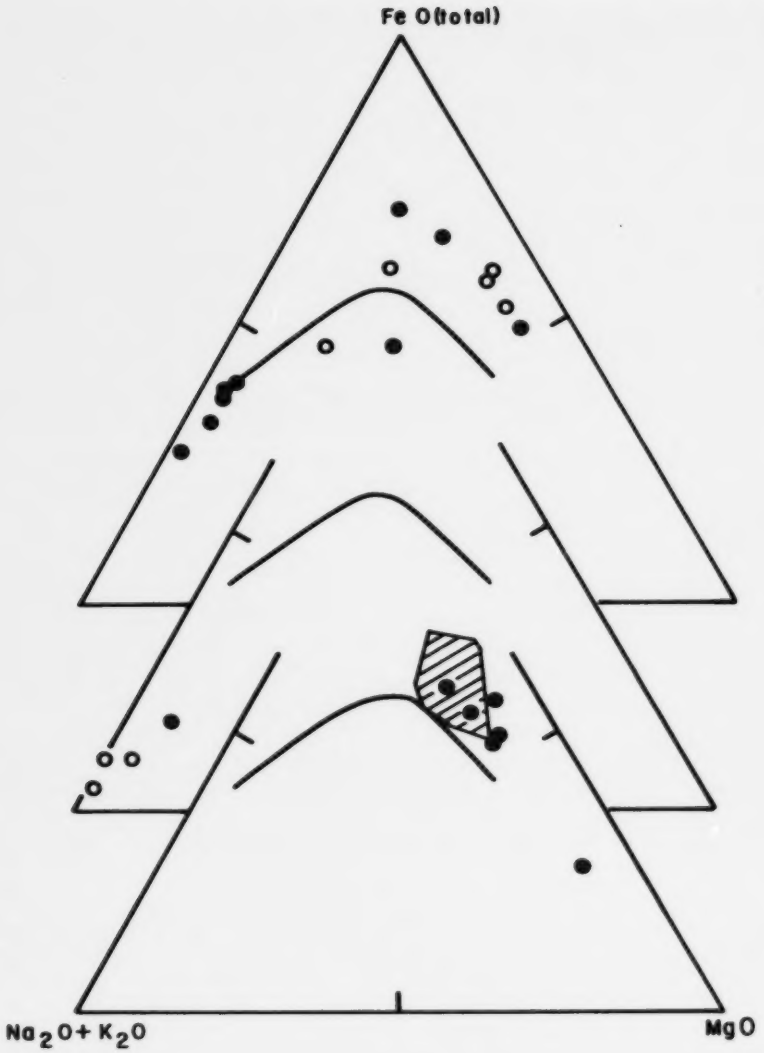

Figure 5: AFM variation diagram for the flow rocks (open circles and ruled field) and for the synvolcanic intrusive rocks (solid dots) of the Bernic Lake (top), Peterson Creek (centre), and Lamprey Falls (bottom) Formations. The solid line separates the tholeiitic and calcalkaline fields after Irvine and Baragar (1971)

are buff-weathering, and schistose. Clasts range from lapilli and tuff sizes up to 8 m, and are aphanitic to fine-grained, commonly porphyritic (quartz phenocrysts), and moderately stretched parallel to schistosity. Matrix material of these breccias consists mainly of brownish to green sericite, and includes finely comminuted quartz and feldspar crystal fragments.

Lapillistone and lapilli tuffs are ubiquitous, but proportionately most abundant in the western and central portions of the Peterson Creek Formation. Lapillistone and lapilli tuff strongly resemble pyroclastic breccia, with which it is interbedded, the principal difference being one of the nomenclature (Fisher 1966). The lapillistone (Fig. 6) and lapilli tuffs are typically brownish to buff or green weathering, carry up to 60 per cent lapilli-size clasts, are thinly bedded ($<$ 6 m), unsorted, and moderately schistose, and lack internal bedding. Clasts exhibit moderate flattening and extension. Long axes of clasts pitch steeply in foliation surfaces.

Rhyolite tuff is abundant in the central portions of the Peterson Creek Formation. These rocks are generally fine-grained, buff to white weathering, moderately schistose and marked by an abundance of quartz, feldspar, and lithic fragments. The thickness of bedding in these rocks varies from 1 to 50 m, and sorting is generally absent.

Volcanic sandstones are abundant in the eastern parts of the Peterson Creek Formation, and these rocks occur, in part, interlayered with minor tuffaceous equivalents. The volcanic sandstones are well bedded and typically buff to white-weathering. The consist of well sorted quartz and feldspar detritus, lack the sericite abundance common to their progenitors, and they are fine grained and moderately schistose. Locally these grade into thin beds of polymictic, felsic, pebble conglomerates which differ from the sandstones only by the occurrence of these epiclasts.

Analyses of representative metarhyolite rocks are shown in

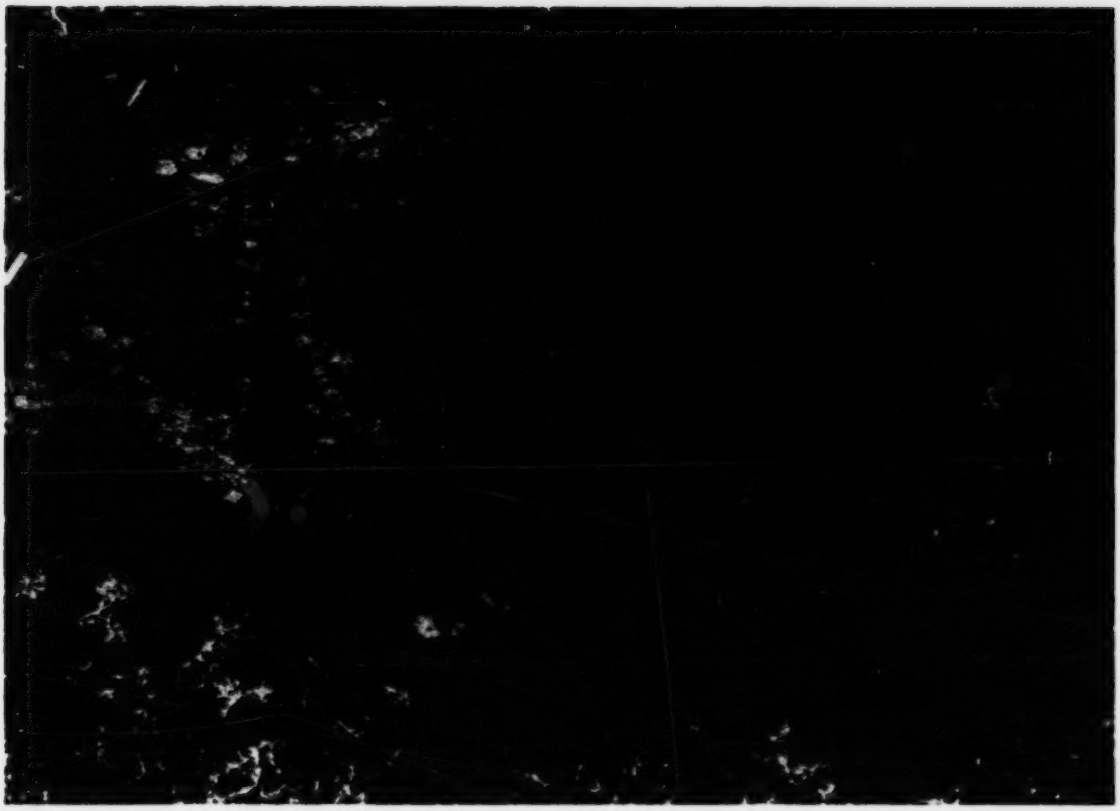

Figure 6: Lapillistone in the Peterson Creek Formation, southwest of the junction of Provincial Roads 314 and 315

Table 7. Most of the samples cannot be used for petrochemical assessment of unmetamorphosed volcanics because of their pyroclastic nature (Fig. 6). Out of the three rhyolite flows, two fall inside the low-T trough in the ternary feldspar diagram (the third being on the K-enriched side), and all three are close to the Ab-Or-Qtz minimum at <500 bars. In general, they display a high igneous-granitic fractionation in terms of Na/Ca, K/Rb, Ca/Sr and Zr/Hf, but they exhibit somewhat scattered Ba, K/Ba, Ga, and Al/Ga values (Fig. 7). All REE patterns shown in Figure 8a are characterized by a moderate total content, a relatively high and subhorizontal HREE side, and a very pronounced negative Eu anomaly. The patterns are of the same type for both rhyolite flows and rhyolite pyroclastics, and both types cover a relatively narrow spread of normalized values. This type of pattern seems to be rather uncommon among rhyolites in Archean greenstone belts (Condie and Baragar 1974). Oxygen isotope values for both lava flows and pyroclastics are high and variable: $\delta\,^{18}O = 9.7\text{-}15.8$ (Longstaffe et al. 1981).

The Bernic Lake Formation (5)

Rock types present in the Bernic Lake Formation include metamorphosed basalt, andesite, dacite, rhyolite, iron formation, polymictic and oligomictic conglomerates, volcanic wackes and sandstones. Of these, metabasalt and iron formation form the only units which display a persistent lateral continuity. The volcanic sandstones are less continuous and the meta-andesite, metadacite, and metarhyolite crop out only intermittently in thin flows of short lateral extent. Polymict and oligomict metaconglomerate are the dominant rocks of the formation, and these are chaotically interlayered with each other, and the other rock types.

Metabasalt is the most abundant of the flow rocks of the Bernic Lake Formation and forms two prominent units: one in the Bernic Lake area and one immediately south of Bird River in the central part of the belt. Elsewhere, metabasalt is present as thin laterally persistent flows, intercalated with clastic rocks.

The metabasalts typically occur as pillowed flows, are greyish-black weathering and are marked by moderate to strongly developed schistosity. Pillow selvages are generally well preserved as in the Bernic Lake area and are suitable for top determinations. Elsewhere, particularly in thin flows, pillow structures may be largely obliterated and flattened by superposition of the schistosity. A flow or succession of flows north of the junction of Provincial Roads 314 and 315 is not characterized by pillow structures, but is marked by the occurrence of narrow 0.5 to 1.5 mm bands of quartz and amygdules filled with quartz and carbonate.

All of the metabasalts consist largely of nematoblastic tremolite-actinolite, chlorite, albite, and zoisite with minor amounts of biotite, leucoxene, and secondary quartz and carbonate.

Meta-andesite is present as thin (<10m) flows in the Bernic Lake Formation. These rocks are almost identical to metabasalt in outcrop, but differ by a tendency to a greyish-white weathering, and display thick prominent selvages. In general, however, the pillow structures are badly deformed and foliated and facing directions are unreliable. The meta-andesites consist chiefly of fine- to medium-grained lepidoblastic biotite, chlorite, tremolite-actinolite, albite and zoisite, with lesser leucoxene, carbonate, and granular secondary quartz.

Metadacite forms thin (<10 m) flows, of limited lateral extent, in the Osis Lake area (Map 1). These rocks, buff to grey-white

TABLE 7. REPRESENTATIVE CHEMICAL ANALYSES OF THE METARHYOLITES, PETERSON CREEK FORMATION (4)

	Rhyolite flow			Reworked tuff	Tuff		Ash flow
	BRGB 5	74-8	74-19	BRGB 6	74-96	75-237	72-15-1
SiO_2, wt.%	77.15	79.55	79.60	66.90	87.50	78.60	79.80
Al_2O_3	12.88	11.26	11.52	16.02	7.73	11.50	10.85
TiO_2	0.02	0.06	0.13	0.06	0.05	0.08	0.09
Fe_2O_3	0.48	0.26	0.31	0.11	0.39	0.22	0.20
FeO	0.40	0.12	0.08	0.52		0.08	0.58
MnO	0.02			0.03	0.01		0.02
MgO	0.32	0.03	0.10	0.43	0.01	0.11	
CaO	0.22	0.13	0.23	0.88	0.53	0.06	
Na_2O	2.95	1.99	3.05	1.25	1.95	0.20	3.82
K_2O	4.89	5.54	4.30	10.65	2.28	8.19	3.50
P_2O_5	0.01		0.01	0.01		0.08	
CO_2	0.13	0.03	0.06	0.45	0.07	0.04	0.18
H_2O	0.65	0.39	0.33	0.51	0.15	0.60	0.34
	100.11	99.40	99.72	99.82	100.67	99.74	99.36
Li, ppm	19	25	15	16	5	15	
Rb	243	264	142	200	75	215	
Cs	2.9	1.2	1.2	0.7	0.8	0.9	
Be	1.9	2.2	0.8	0.9	0.8	1.0	
Sr	13	27	65	68	54	27	
Ba	nd	21	549	649	184	529	
Pb	17	18	8	12	7	4	
Ga	32	5	nd	31	nd	11	
U	nd*	13	9	10	3	22	
Th	30	40	26	18	19	36	
Zr	121	103	103	144	82	109	
Hf	6.05	4.7	3.85	6.2	3.05	4.9	
Sn	9	2	nd	3	3	nd	
K/Rb	167	174	254	442	252	316	
K/(Cs x 100)	140	383	300	1282	236	756	
K/Ba	-	219	65.6	136	103	128.5	
Ba/Rb	-	0.08	3.9	3.2	2.5	2.5	
Ba/Sr	-	0.8	8.4	9.5	3.4	19.6	
Rb/Sr	18.7	9.8	2.2	2.9	1.4	8	
Mg/Li	100	11.2	40	163	12	46.7	
Zr/Sn	13.4	51.5	-	48	27.3	-	
Zr/Hf	20	21.9	26.7	23.2	26.9	22.2	
Al/Ga	2128	11920	-	2735	-	5527	
La, ppm	14.2	6.2	18.7	21.35	14.15	4.35	
Ce	43	20	41.5	57.5	28	14.5	
Nd	29.5	14	18	31	14.5	12	
Sm	5.9	2.83	2.05	5.27	2.29	2.60	
Eu	< 0.07	< 0.06	0.23	0.27	0.17	< 0.06	
Dy	9.85	5.75	2.65	4.8	3.7	6.3	
Yb	4.35	2.45	1.55	4.0	1.85	3.2	
Lu	0.62	0.32	0.19	0.52	0.21	0.38	

*not detected

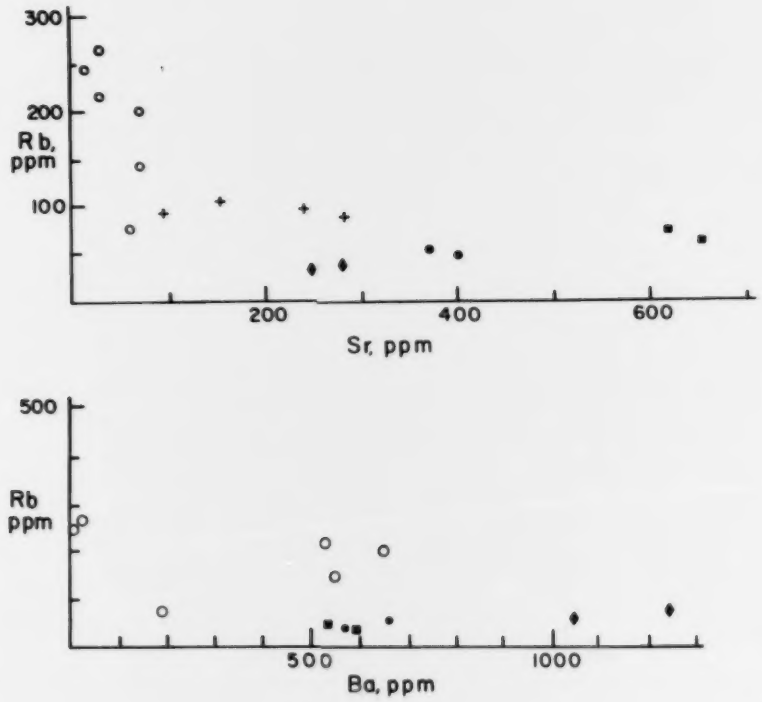

Figure 7: Rb vs. Sr and Rb vs. Ba plots for the metarhyolites of the Peterson Creek Formation (circles), polymictic metaconglomerates of the Bernic Lake Formation (diamonds), lithic meta-arenites (squares) of the Flanders Lake Formation, and for the metagreywacke (dots) and metapelite (crosses) components of the Booster Lake Formation turbidites

weathering, are typically pillowed with thick selvages, and exhibit a strong degree of stretching in a pronounced schistosity. The metadacite is composed largely of granular quartz and albite, set in a matrix of biotite, tremolite-actinolite, chlorite, and zoisite, and locally is marked by the occurrence of small (< 2 mm) phenocrysts of altered plagioclase.

Metarhyolite is not abundant in the Bernic Lake Formation, and was only observed in an area west of Bernic Lake (Map 1). In this locale, the metarhyolite forms a thin (< 10 m), translucent greenish to buff weathering unit marked by a weak schistosity and small (< 1 mm) quartz phenocrysts. The rock is composed essentially of quartz, feldspar, sericite, and secondary quartz and carbonate veining. Contacts of this unit were not observed, and the rock lacks primary structures diagnostic of an extrusive origin suggesting therefore, the possibility that this unit is a sill.

Polymict metaconglomerate is the most abundant rock type in the Bernic Lake Formation. These rocks are typically dark grey to black weathering, and, for the most part, outcrop surfaces do not reveal diagnostic features. Locally, however, clasts weather in considerable relief over matrix and the rocks are otherwise characterized by fine- to coarse-grained biotite+amphibole-rich quartz+feldspar assemblages with a strong lineation imparted down-dip of the schistosity by the elongation of clasts. In some exposures bedding is in evidence, resulting either from variation in clast content, or size, or variation in matrix composition.

The polymict metaconglomerates further exhibit considerable areal variation in composition. In the western part of the map area the metaconglomerate consists of a mix of pebble to boulder (< 2 m) detritus variously derived from mafic and felsic metavolcanic sources, hypabyssal metagabbro, and the Bird River Sill. Detritus from the Bird River Sill includes anorthosite, anorthositic gabbro, chromite, and small chromite-rich chlorite blebs which may represent original lherzolite detritus.

In the area east of the Dumbarton Mine, polymict metaconglomerate is similar to that described above, but the dominant phase is marked by pebbles and cobbles of quartz porphyry, sericite schist, and hypabyssal metagabbro. Anorthositic gabbro clasts from the Bird River Sill are rare. These rocks are further transitional into a dominantly felsic breccia which forms a cap over massive felsic intrusive rocks.

Oligomict metaconglomerate (Fig. 9) is dominant in the southern part of the Bernic Lake formation. These rocks, greyish weathering and fine-to coarse-grained, are marked by pebble-to boulder-size materials set in a grey to black strongly schistose

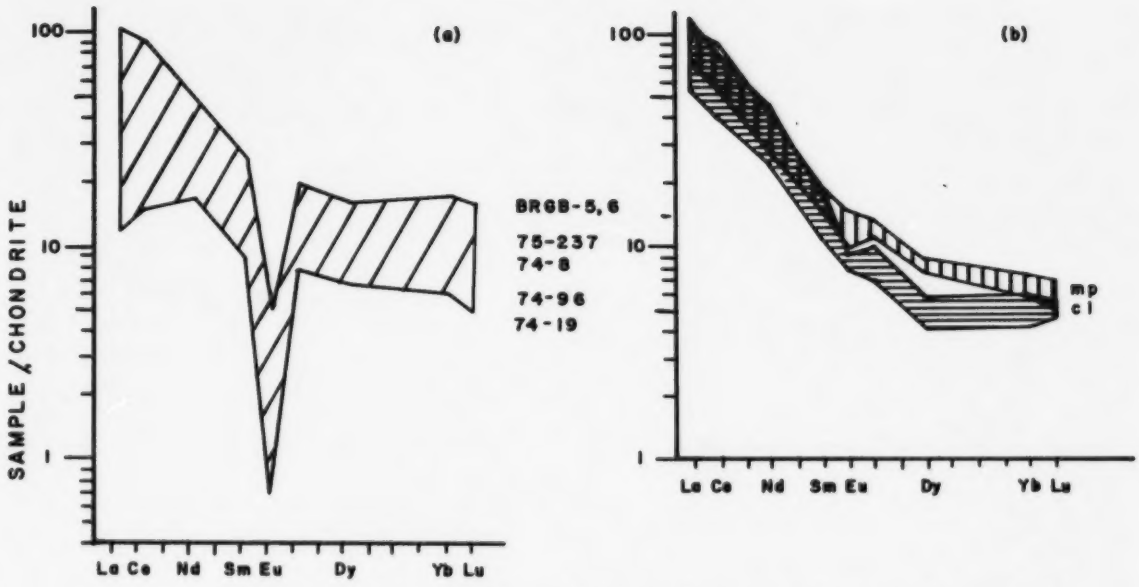

Figure 8: REE abundance in rhyolitic lava flows, ash flows, and tuffs of the Peterson Creek Formation (a), and in the clastic metasediments (cl) and metapelites (mp) of the Flanders Lake and Booster Lake Formations (b)

Figure 9: Subvertically dipping oligomict metaconglomerate in the Bernic Lake Formation, southeast of Poplar Bay, Lac du Bonnet

Figure 10: Bedding in metaconglomerate in the Bernic Lake Formation, north of Birse Lake

matrix. Clasts are chiefly of intermediate or felsic composition, are greyish or buff weathering, and are strongly deformed and locally folded with schistosity. Continuous bedding is in evidence only locally (Fig. 10) and the rocks are otherwise of chaotically intercalated lensoid distribution.

Metamorphosed volcanic wackes and volcanic sandstones occur interlayered with the polymict and oligomict metaconglomerates throughout the Bernic Lake Formation. The volcanic wackes are fine- to medium-grained, greyish-weathering, thin (< 1 cm) to thick (< 5 m), moderately well bedded schists composed mainly of detrital quartz and feldspar with varied proportions of biotite, actinolite-tremolite, and chlorite. In higher metamorphic grade equivalents diopside, cordierite, anthophyllite, and garnet are locally developed, and these rocks may also be marked by the occurrence of fine laminae of cherty or tuffaceous material. In the western, central and southern parts of the Bernic Lake Formation, the volcanic wackes are interlayered with pebbly variants. These rocks are identical with the volcanic wackes, except for the presence of from 5 to 30 per cent pebble-size material of quartzofeldspathic composition.

Metamorphosed volcanic sandstones are buff to white weathering rocks characterized by abundant detrital quartz, thin (< 3 cm) bedding, and good sorting. Schistosity is weak in these rocks and is imparted by minor sericite which forms matrix to granular quartz and feldspar, minor biotite, amphibole, hematite, and quartz and carbonate.

Iron formations are interlayered throughout the Bernic Lake Formation as thin laterally persistent bands which crop out extensively, and are also marked as laterally persistent AEM conductors. Their distribution on the accompanying geologic map is based on both outcrop occurrence and geophysical data (data from Manitoba Mineral Resources Open File, non-confidential assessment report 90008, LYNX area, sheet 4).

The iron formations occur as thin to thick (< 10 m) moderately schistose gossans of both ferruginous metasediments and convoluted bands with interlayered chert (Fig. 11). Both oxide (magnetite) and sulphide (pyrrhotite-pyrite) assemblages are present, and as both of these assemblages are commonly present in the same unit they form typical Algoman-type iron formation.

On one location, north of PR 314 and 3.2 km east from the PR 314-315 junction, are several outcrops of a clastic rock which has attributes of a reworked crystal tuff. The lateral extent of this rock type is uncertain but in thickness it is of the order of less than 50 m. This rock is marked by an abundance of plagioclase (An-65) crystals of equant or elongate euhedral or broken form set in a matrix of actinolite-tremolite, chlorite, quartz and feldspars. In addition the rock carries fragments of equivalent composition up to 10 cm in size, and is further marked by an abundance of rounded (< 2.5 cm) blebs of quartz and carbonate which bear resemblance to pebbles or possibly amygdules from a lava. These blebs are strongly rounded in a moderately developed schistosity, the development of which apparently had little or no effect on the plagioclase crystals.

In three locations within the Bernic Lake Formation unusual metamorphic mineral assemblages are formed at the expense of their protoliths. These include cordierite-anthophyllite-garnet-diopside assemblages, garnet-biotite assemblages, and garnetiferous felsic breccia, all of which occupy the same approximate stratigraphic position near the base of the formation.

Figure 11: Banded iron formation in the Bernic Lake Formation, south of Bird Lake

The cordierite-anthophyllite-garnet-diopside schists are developed along Bird River, south of the Dumbarton Mine and can be traced for approximately 5 km along strike in association with polymict metaconglomerate and volcanic wackes. At a location 2.4 km east of the Dumbarton Mine, these rocks are spatially ordered; diopside-rich beds occur in proximity to the Maskwa Lake batholith, and cordierite-anthophyllite-garnet assemblages lie adjacent to and south of these. The different assemblages are restricted in occurrence to individual pre-metamorphic beds, forming, for example, cordierite-rich beds alternating with anthophyllite-rich beds. Of these assemblages, diopside, anthophyllite, and garnet form randomly oriented euhedral porphyroblasts, and cordierite forms slightly ellipsoidal sericitized porphyroblasts which are locally perforated by the anthophyllite.

Garnet-biotite schists crop out intermittently along strike eastwards from the above cordierite-anthophyllite rocks and pass further along strike into graphite schist and iron formation. Associated rocks include polymict metaconglomerate, and this same association persists on the south side of the greenstone belt in the Shatford Lake-Winnipeg River area. The garnet-biotite schist consists predominantly of euhedral to slightly rounded and fractured garnet which forms up to 70 per cent of the rock, and idioblastic biotite with lesser amounts of quartz, carbonate, magnetite, and limonite.

The garnetiferous felsic breccias occur south of Bird Lake in stratigraphic continuity with garnet-biotite schist, graphite schist, and iron formation. These rocks consist largely of flow-banded quartz-porphyry clasts which are in turn skeined by anastomosing garnet-biotite schist stringers. These rocks change gradationally downward into a more massive greyish weathering garnetiferous quartz porphyry, the nature of this boundary being marked by a decrease in fragmental material and a decrease of garnet+biotite-filled fractures into the massive porphyry.

Representative analyses of metabasalts and a sample of metadacite (75-8-1) are presented in Table 8, and discussed by Trueman (1980). Fig. 5 shows their largely tholeiitic character.

The Flanders Lake Formation (7)

The Flanders Lake Formation crops out extensively in the Flanders Lake-Ryerson Lake-Starr Lake-Reynar Lakes area (Map 1, Fig. 3). The rocks of the Flanders Lake Formation include polymict metaconglomerate and related meta-arenites which are best exposed in the intervening area between Flanders and Booster Lakes. Descriptions of these rocks have been presented by Posehn (1976), and their continuity into the Manigotagan Gneiss Belt has been described by Trueman et al. (1976).

Meta-arenite is the dominant rock type in the Flanders Lake Formation. These rocks are typically greyish weathering, are moderately well bedded and sorted, and display a foliation which develops from a schistosity into a gneissosity in proximity to flanking intrusive rocks. The bedding in meta-arenite forms a span of 1-2 cm up to 2 m, and is marked principally by variation in biotite content. Graded bedding occurs locally, as does cross-bedding, but in general both features are rare.

In composition the meta-arenites are subordinate, comprised mainly of quartz and feldspar detritus, now recrystallized, with subordinate biotite, amphibole, muscovite, magnetite, and hematite. Sillimanite, andalusite, cordierite, and tourmaline occur locally, and

TABLE 8. REPRESENTATIVE CHEMICAL ANALYSES OF THE METAVOLCANICS, BERNIC LAKE FORMATION (5)

	Metabasalt					Metadacite
	75-568	75-507	75-735	75-578	BRGB9	75-8-1
SiO_2, wt %	49.85	54.45	53.00	49.45	49.60	68.90
Al_2O_3	15.47	16.40	14.70	15.60	15.44	13.50
TiO_2	0.70	0.74	1.80	0.70	0.67	1.37
Fe_2O_3	1.25	1.18	2.49	1.74	3.58	0.47
FeO	10.21	7.47	10.76	9.14	10.38	3.90
MnO	0.23	0.17	0.20	0.19	0.30	0.12
MgO	6.75	5.29	3.99	8.33	5.35	1.48
CaO	12.75	12.30	6.30	11.80	10.65	5.24
Na_2O	0.98	1.17	2.42	1.57	1.55	3.34
K_2O	0.16	0.13	2.52	0.13	0.12	0.41
P_2O_5	0.04	0.05	0.40	0.06	0.09	0.21
CO_2	0.23	0.40	0.05	0.17	0.49	0.36
H_2O	1.33	0.77	1.22	1.20	1.69	0.53
S		0.09	0.01	0.02	0.20	0.07
Cr_2O_3		0.09	0.01	0.07	0.20	0.02
NiO		0.03	0.01	0.02	0.015	Tr.*
	99.96	100.69	99.88	100.18	99.92	99.92

* traces

the rocks may also be modified by the occurrence of sparsely distributed clasts of pebble-size felsic metavolcanic or tonalitic detritus. In proximity to the intrusive rocks, the meta-arenites are commonly further modified by lit of intrusive material (Fig. 12), and along the eastern margin of the map area they appear to have undergone partial anatexis with generation of a leucosomal phase.

Metaconglomerate crops out extensively in the Ryerson-Booster-Starr-Davidson Lakes area where these rocks form fold-repeated units.

The metaconglomerate is distinctive (Fig. 13) and is characterized by abundant pebble- and cobble-sized stretched clasts of differing composition (Posehn 1976). These include metatonalite, metabasalt, metagabbro, metarhyolite, felsic sandstones, tourmaline-rich sandstone, and iron formation clasts. The clasts are varied in absolute and relative abundance giving rise locally to ortho-conglomerates and paraconglomerates, although the former are predominant. Matrices are varied accordingly, and in thin section appear identical to the previously described meta-arenites with which the metaconglomerate is interbedded.

Primary bedding features are locally preserved in the meta-conglomerate, and include poorly sorted beds, graded and inverse graded beds, cross-bedding, scour-and-fill structures, and lamination, most of which permit reliable top or facing-direction determination and indicate deposition through turbidity and debris flow mechanisms with subsequent reworking in a fluviatile regime (Posehn 1976).

Representative chemical analyses of lithic arenites are shown in Table 9; their REE abundances are very close to those of the Flanders Lake and Booster Lake Formations clastic metasediments. The meta-arenites are rather low in O^{18}: $\delta^{18}O = 7.7\text{-}9.0$ (Longstaffe et al. 1981).

The Booster Lake Formation (8)

The Booster Lake Formation consists predominantly of greywacke-mudstone turbidites (Fig. 14) which occur in an easterly-trending belt between Poplar Bay and Lac du Bonnet and the Ontario-Manitoba interprovincial boundary (Map 1). The formation includes also minor iron formation, and fault-bounded slices of greywacke-mudstones which occur in the Bernic Lake Formation at Ryerson Lake, Booster Lake, Rush Lake, and intermittently along the western reach of Bird River (Map 1, Fig. 3).

The greywacke-mudstones are everywhere well exposed in the map area. These rocks, interbedded on all scales up to 2 m, are typically buff weathering, well bedded, fine- to coarse-grained, and moderately schistose. In composition, the greywacke component consists principally of felsic metavolcanic detritus which exhibits considerable clast size range up to and including cobble-size material in conglomeratic phases. The mudstone component is largely metamorphosed to assemblages with biotite and cordierite throughout the formation.

Primary structures are abundant in the turbidites and include the classical Bouma sequences with graded bedding, laminated bedding, and ripple cross-bedding. Secondary or diagenetic structures observed are flame structures developed through loading, as well as less clearly evident dewatering cusps. The distribution of these features within the formation, and of interbedded disorganized conglomerates, indicates that the turbidites were deposited as a fan in the area, with a proximal facies in the west, and a more distal facies to the east. The disposition of the sequences also indicates a

Figure 12: Granitic lit intercalated in meta-arenite of the Flanders Lake Formation, southwest of Reynar Lake

Figure 13: Metaconglomerate in the Flanders Lake Formation, south of Starr Lake

TABLE 9. REPRESENTATIVE CHEMICAL ANALYSES OF LITHIC ARENITES, FLANDERS LAKE FORMATION (7)

	Lithic arenite	
	BRGB 1	BRGB 2
SiO_2, wt %	61.40	61.40
Al_2O_3	15.78	17.04
TiO_2	0.44	0.58
Fe_2O_3	1.98	1.40
FeO	3.56	3.64
MnO	0.10	0.10
MgO	4.15	3.00
CaO	5.63	4.95
Na_2O	3.16	3.23
K_2O	1.93	1.93
P_2O_5	0.22	0.22
CO_2	0.14	0.02
H_2O	1.07	0.92
	99.56	98.43
Li, ppm	19	40
Rb	62	78
Cs	1	1.9
Be	1.2	1.2
Sr	655	620
Ba	1046	1254
Pb		
Ga	21	24
U	nd*	nd
Th	2	nd
Zr	259	209
Hf	6.2	6.2
Sn	nd	5
K/Rb	258	205
K/(Cs x 100)	160	84
K/Ba	15.3	12.8
Ba/Rb	16.9	16
Ba/Sr	1.6	2
Rb/Sr	0.09	0.12
Mg/Li	1316	452
Zr/Sn		41.8
Zr/Hf	41.8	33.7
Al/Ga	3976	3758
La, ppm	44.65	
Ce	80.5.	
Nd	33	
Sm	3.98	
Eu	0.66	
Dy	2.2	
Yb	1.0	
Lu	0.18	

* not detected

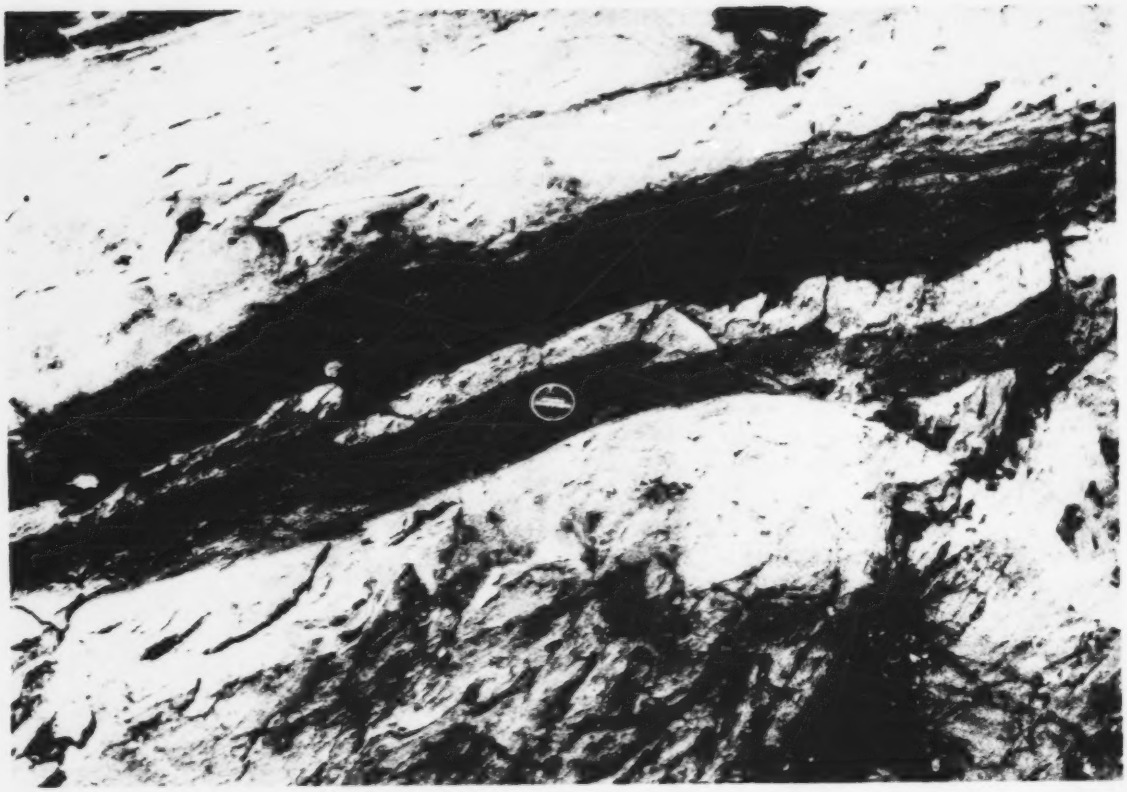

Figure 14: Cross-bedded metamorphosed greywacke-mudstone (light and dark respectively) in the Booster Lake Formation, east of the junction of Provicial Road 315 with the Tanco mine road

regressing source area, as evidenced by the upward (south) increase in mudstone components of the turbidite pairs and the disappearance of the higher-energy sequences coincident with the increased mud fractions.

Iron formation associated with the greywacke-mudstone sequence crops out only in the western part of the map area near Lac du Bonnet in association with conglomerate phases. In this locale the iron formation consists essentially of massive iron sulphides interlayered with chert.

Chemical analyses of the metagreywackes and metapelites are presented in Table 10. Both rock types are higher in SiO_2 and Al_2O_3 than the "average" greywackes and mudstones of Pettijohn (1963) and Wedepohl (1968) but otherwise they are comparable. As expected, the metapelites are enriched in Al_2O_3, TiO_2, Fe, MgO, K_2O, P_2O_5, H_2O, Li, Rb and Cs and depleted in SiO_2, CaO, Na_2O and SrO relative to the metagreywackes. Except for higher Ce, the REE abundances of the metagreywackes (Fig. 8b) fall between the values of "average" greywackes of Haskin (1966) and the Knife Lake Group greywacke-mudstone of Arth and Hanson (1975). The metagreywacke data closely overlap those of the clastic metasediments of the Booster Lake Formation; however, the metapelites are somewhat enriched in HREE (Fig. 8b). The oxygen isotopic composition of the sediments is within expectable limits: $\delta^{18}O = 10.1\text{-}13.0$ (Longstaffe 1981).

Synvolcanic intrusive rocks (3, 6)

Rock types described in this section occur in different units of the Bird River Greenstone Belt (Table 5) but are treated here under a common heading for simplicity. Representative analyses of most types are given in Table 11, and AFM diagrams are shown in Figure 5.

Hypabyssal metagabbro sills are ubiquitous in metabasalts of the Lamprey Falls and Bernic Lake Formations. These sills are generally less than 20 m in thickness, and persist along strike for less than 150 m. Contacts of these bodies are sharp, exhibit finer grain size, and tend to be slightly sheared. Inclusion material is rare.

Typical hypabyssal metagabbro is a dark grey-green weathering fine- to medium-grained, massive to weakly schistose rock, and is comprised essentially of saussuritized plagioclase in a matrix of tremolite-actinolite with lesser magnetite, leucoxene, and secondary quartz and quartz-carbonate veining.

The Bird River Sill is a layered ultramafic to gabbroic body formed through gravitational settling and accumulation of olivine, chromite, and plagioclase (Trueman 1971, 1980). A composite section of this body is shown in Figure 15. From Figure 15, it is evident that the Bird River Sill can be subdivided into five principal units. These are: a feeder dyke, the layered ultramafic cumulates, a picrite layer, layered gabbroic cumulates, and a granophyre.

The feeder dyke to the Bird River Sill is confined to the area enclosing the Bird River Mines Ltd. property through to the east end of the Dumbarton Mines Ltd. property. Rock types of the feeder dykes are disposed in a poorly concentric (and later fault-segmented) pattern; central lherzolite is enveloped by pyroxenite, and this in turn by picrite (Trueman, 1980). These rocks are in general severely altered, and consist variously of assemblages of serpentine, talc, carbonate, tremolite, cummingtonite, and magnetite which almost completely replace original assemblages of olivine, clinopyroxene, and plagioclase.

TABLE 10. REPRESENTATIVE CHEMICAL ANALYSES OF THE METATURBIDITES, BOOSTER LAKE FORMATION (8)

	Metagreywacke		Metapelite	
	BRGB 7	BRGB 8	PG-420	DT-374
SiO_2, wt. %	70.35	72.10	64.85	63.15
Al_2O_3	14.91	14.58	16.37	16.48
TiO_2	0.34	0.30	0.56	0.67
Fe_2O_3	0.54	0.92	1.65	1.97
FeO	2.76	1.76	3.93	4.82
MnO	0.06	0.04	0.07	0.08
MgO	1.15	0.98	2.24	2.59
CaO	2.33	2.05	1.29	1.93
Na_2O	3.90	4.30	1.96	2.92
K_2O	2.20	1.60	4.02	2.76
P_2O_5	0.07	0.05	0.17	0.18
CO_2	0.64	0.42	0.77	0.39
H_2O	0.98	0.86	2.10	2.32
	99.05	99.96	100.28	99.95
Li, ppm	24	19	48	91
Rb	54	48	105	97
Cs	0.4	0.6	3.0	6.2
Be	0.9	0.8	1.3	1.1
Sr	370	400	150	243
Ba	658	566		
Pb		9	4	2
Ga	29	25		
U	3	nd*		
Th	nd	nd		
Zr	174	163		
Hf	3.75	3.75		
Sn	3	3		
K/Rb	311	277	318	236
K/(Cs x 100)	420	222	111	37
K/Ba	25.5	5.8		
Ba/Rb	12.2	11.8		
Ba/Sr	1.8	1.4		
Rb/Sr	0.14	0.12	0.70	0.40
Mg/Li	288	310	281	171
Zr/Sn	58	54.3		
Zr/Hf	46.4	43.5		
Al/Ga	2721	3084		
La, ppm	28.3	28.3	27.0	28.2
Ce	45	45	54	71
Nd	22	22	20	28
Sm	3.2	3.2	3.4	3.7
Eu	0.79	0.79	0.87	1.20
Dy	1.55	1.55	3.1	2.9
Yb	1.4	1.4	1.4	1.7
Lu	0.21	0.21	0.19	0.26

* not detected

TABLE 11. REPRESENTATIVE CHEMICAL ANALYSES OF THE SYNVOLCANIC INTRUSIONS (3, 6; SEE TEXT FOR LOCATIONS)

	Metagabbros				Meta-diorite	Quartz diorite	Grano-diorite
	BRS (CHM)	1096	111	75-514	75-522	75-753	75-738
SiO_2, wt.%	45.27	48.40	49.30	46.50	58.50	71.05	74.75
Al_2O_3	17.91	17.50	14.70	15.90	15.55	13.78	12.76
TiO_2		0.44	0.77	2.28	0.72	0.56	0.42
Fe_2O_3		0.82	1.53	3.14	2.28	1.61	1.31
FeO	5.59	8.21	11.00	11.60	5.44	3.08	1.52
MnO		0.17	0.20	0.20	0.17	0.08	0.06
MgO	14.53	8.55	8.09	5.20	4.25	0.45	0.19
CaO	7.25	9.80	11.09	9.85	6.70	2.34	1.00
Na_2O	1.52	2.01	1.75	2.30	3.54	3.84	4.50
K_2O	0.59	1.50	0.13	0.28	1.24	2.65	2.76
P_2O_5		0.04	0.05	0.19	0.25	0.02	0.07
CO_2	tr	0.40	0.15	0.16	0.05	0.06	0.13
H_2O	3.67	1.93	1.35	1.81	1.11	0.58	0.56
S		0.01	0.20				
Cr_2O_3	0.09	0.05	0.03				
NiO		0.02	0.02				
CoO			0.01				
	99.49	99.85	100.02	99.41	99.80	100.10	100.03

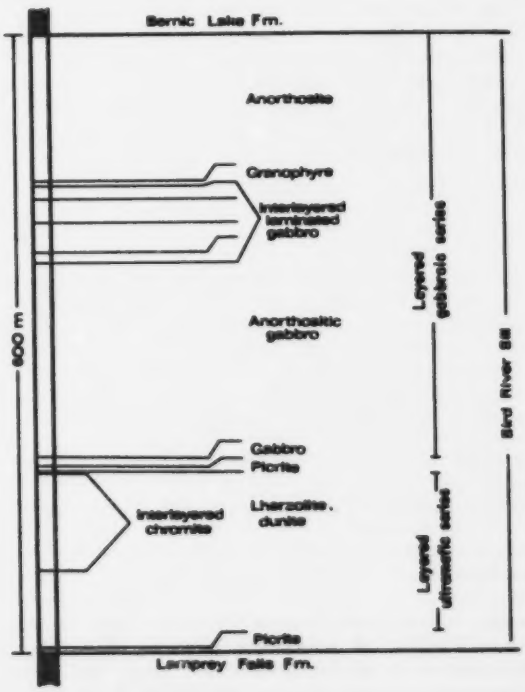

Figure 15: Composite section through the Bird River Sill

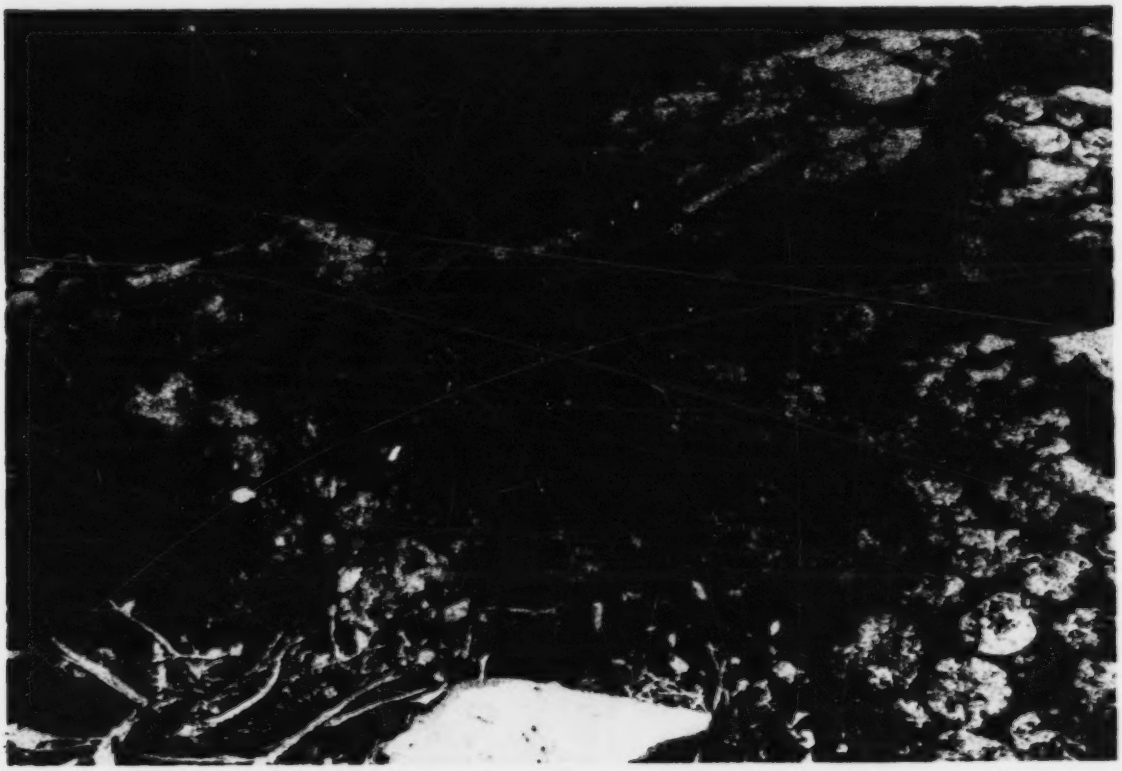

Figure 16: Glomeroporphyritic metagabbro, north shore of Bernic Lake

The layered ultramafic series of rocks comprises interlayered dunites, lherzolites, and feldspathic and chromiferous variants of these. These rocks although texturally well preserved consist mainly of serpentine pseudomorphous after intercumulus clinopyroxene and plagioclase, and chromite. The chromite, generally mantled by chlorite, exhibits a magnetite-enriched rim (Gait 1964) formed through deuteric alteration.

Primary structures are abundant in the layered ultramafic rocks, and include features such as bifurcation and disruption of chromite layers, graded bedding, and flame structures (Trueman 1971, 1980).

Picrite lies in sharp, phase-layered (Jackson 1967) contact above the layered ultramafic rocks. The picrite is marked by an abrupt disappearance of the original olivine, which is now pseudomorphed by serpentine, and by the first appearance of cumulus plagioclase. The plagioclase, extensively pseudomorphed by clinozoisite, is poikilitically enclosed by tremolite in turn pseudomorphous after original intercumulus clinopyroxene.

The layered gabbroic series of rocks, dominated by anorthositic gabbro and northosite, lies in gradational contact above the picrite, and developed as plagioclase formed to the near exclusion of other phases. Cryptic variation of the plagioclase anorthite content indicates that crystal accumulation proceeded from the floor of the magma chamber upwards, and from the roof downwards (Trueman 1971).

The equant plagioclase is mantled by coarse blades of actinolite formed at the expense of an original clinopyroxene. In addition, the plagioclase commonly exhibits resorption textures, concomitant with increases of clinopyroxene (actinolite) contents and gives rise to more mafic and igneous laminated variants.

The granophyre in the Bird River Sill, approximately 6 m in thickness, occupies an intermediate position in the gabbro layers, that was controlled by the upward and downward accumulation of the gabbros. The granophyre consists mainly of granophyric intergrowths of albite-oligoclase and quartz, mantled by fibrous actinolite and extensively saussuritized laths of plagioclase (Trueman 1971).

The composition of the chilled margin of the Bird River Sill, presumable representative of the bulk of the sill, is shown in Table 11 (#BRS(CHM)).

Metagabbro occurs as stocks and sills west of the Dumbarton Mine in the Lamprey Falls formation, and as a sill in the same rocks in the Winnipeg River area (Map 1). This metagabbro is typically mottled, greyish-green weathering, coarse grained, and massive. Near contacts the rock becomes finer-grained, and schistosity becomes pronounced. The rock typically consists of varied amounts of actinolite, plagioclase (An_{60-35}), biotite, zoisite, chlorite, carbonate, ilmenite-leucoxene, hematite, pyrite, and secondary quartz. Inclusion material of volcanogenic metasediments occurs locally in patches, and in one location several large inclusions of tonalitic material of unknown origin were noted. A representative analysis (sample 1096) is presented in Table 11.

Glomeroporphyritic metagabbro occurs as discrete lenses in the Bird River Sill, and as sills in metabasalt in the Bernic Lake area (Map 1). These rocks are characterized by large ovoids of plagioclase crystals (An_{60}) set in a matrix of fine-to coarse-grained metagabbro, or bladed actinolite (Fig. 16). Detailed descriptions of these rocks have been presented by Bond (1974), and by Trueman (1971); a typical analysis is given in Table 11 (sample 111).

A small dyke of *quartz porphyry* crops out at the northeastern end of the Dumbarton Mine, where it transects the ore zone (B. Weir, pers. comm.), and has been described by Juhas (1974). In outcrop the quartz porphyry is a white weathering, inequigranular, strongly foliated rock which strikes northerly and dips vertically. In thin section the quartz porphyry is best termed a cataclasite, and is marked by rolled and crushed quartz phenocrysts streamlined in a finely comminuted matrix of quartz, albite, and sericite.

Synvolcanic intrusive rocks in the Bernic Lake and Lamprey Falls Formations occur as composite parts of ellipsoidal stock-like bodies and as thin sills which show mutually intrusive relationships and differentiation from gabbro to diorite, quartz and feldspar porphyry, and granodiorite.

Metagabbro forms the earliest intrusive phase of the composite stocks in the Bernic Lake Formation, and is present in three of these bodies (Map 1). The metagabbro is typically grey to black weathering, medium- to coarse-grained, and moderately to strongly schistose. At Osis Lake the metagabbro exhibits large metacrysts of amphibole which poikilitically enclose small plagioclase crystals, but elsewhere, the metagabbro is both ophitic and/or coarsely equigranular. The metagabbro at Bernic Lake (footwall amphibolite of Crouse and Černý,1971) displays a normal ophitic texture and also a faint banding of plagioclase-enriched layers which give rise to phase-layering (Jackson 1967) on a 1 to 10 cm scale parallel to the intrusion boundaries. A typical composition of this metagabbro is demonstrated by sample 75-514 in Table 11.

Metadiorite is present as the principal phase of the northeastern-most of the intrusive stocks in the Bernic Lake Formation and is also present as thin sills in the area north and east of Osis Lake. The metadiorite is grey weathering, medium- to coarse-grained equigranular, and moderately schistose. Within core areas of this body is a comagmatic phase otherwise identical to the above, but marked by the occurrence of 1 to 4 mm phenocrysts of hornblende. In composition the metadiorite consists of varied proportions of tremolite-actinolite, biotite, and chlorite set in a granular mosaic of saussuritized plagioclase. Leucoxene, after ilmenite, is the only accessory mineral in evidence. The contacts of the metadiorite are characterized by a thin (<10m) zone of dyking, and the proximity to the boundary is marked by an abundance of schlieren of volcanic and volcaniclastic inclusions. Representative chemical composition is given in Table 11 (sample 75-522).

Quartz-feldspar porphyry (tonalite) and non-porphyritic equivalents form the dominant part of the large stock centered near Birse Lake, and also thin sills in the Greer Lake, Winnipeg River, and Bernic Lake areas. The quartz-feldspar porphyry is a grey-weathering, inequigranular porphyritic, massive to strongly schistose rock. Phenocryst material is prominent along margins of these bodies, but decrease into core areas giving rise to equigranular coarse grained phases. Similarly, the contact border zones exhibit strong schistosity which decreases inwards to the core areas. Inclusion material is rare and contacts are sharp. In composition these rocks consist chiefly of granular plagioclase and quartz set in a matrix of biotite, chlorite, and amphibole, all of which mantle large (> 8 mm) augen of the quartz and plagioclase (albite) phenocrysts. Accessory minerals include minor leucoxene after ilmenite, and minor tourmaline. Zoisite group minerals are ubiquitous, formed after plagioclase in both the matrix and phenocrysts. Sample 75-753 shows a typical composition of this rock type (Table 11).

Granodiorite forms the youngest recognized phase of the composite stocks, and is limited in occurrence to the western ends of the stocks in which it occurs. Granodiorite is the only phase in evidence in the two bodies near Sarap Lake. The granodiorite is a grey-white to pink weathering rock marked by equigranular texture, and a moderate to weak schistosity. In composition, the rock consists of coarse grained subhedral albite-oligoclase and microcline feldspars, in part saussuritized and granulated along crystal boundaries. Biotite and sericite are ubiquitous; chlorite, leucoxene, magnetite, and carbonate are interspersed throughout. The contacts of granodiorite are in general sharp, and these rocks are marked by minor inclusion material of metagabbro and metadiorite. The chemical composition of the granodiorite is exemplified by the analysis of sample 75-738 (Table 11).

EARLY TO SYN-TECTONIC INTRUSIVE AND METAMORPHIC ROCKS

Paragneiss (9)

These rocks consist largely of quartz-biotite and quartz-hornblende bearing schists and gneisses, the layering in which is described by McRitchie (1971) as inherited from pre-existing bedding. Metamorphic grades vary from upper to lower amphibolite facies, and the rocks are marked by interbanding of, or lit of, granodioritic, granitic, and pegmatitic material.

Due to the compositional complexity and large extent of the Manigotagan-Ear Falls Gneiss Belt, we did not attempt a detailed study of this suite. The reader is referred to the papers by McRitchie (1971), Freund and Turnock (1971), and Breaks et al. (1978) for lithologic and petrographic descriptions, and for the basic compositional characteristics.

Great Falls quartz diorite (10)

The Great Falls quartz diorite in the study area encompasses two bodies of batholithic proportion centered on Maskwa Lake (Maskwa Lake quartz diorite) and east of Marijane Lake (Marijane Lake quartz diorite). The emplacement of these bodies has been interpreted as essentially coeval with the M_2 metamorphic event displayed in the metavolcanic and metasedimentary rocks of the Rice Lake Group (Trueman, 1980).

Two dominant rock types are evident in the *Maskwa Lake batholith*. These are a coarse grained, equigranular to quartz-porphyritic, massive, locally gneissic, dark grey to buff quartz diorite, and an equigranular, medium- to coarse-grained, massive buff to pink granite with minor granodiorite. Of these, the granite appears the younger, being present as dykes in the quartz diorite, and hosting inclusions of the same.

The petrography of the Great Falls quartz diorite has been described by McRitchie (1971) as:

> "The characteristic phase of the intrusion is a white-grey automorphic to hypidiomorphic, equigranular, leuco-mesocratic, hornblende-biotite-quartz diorite. Contained minerals include strongly zoned tabular and subhedral plagioclase, deep green, granular and tabular subhedral hornblende, dull brown biotite, and quartz with accessory apatite and magnetite and secondary sphene, epidote, sericite, and chlorite. The plagioclases consist of idiomorphic inner zones and xenomorphic margins indicating prolonged recrystallization. They are twinned on Carlsbad, albite and pericline laws, the individual twins being short and discontinuous. Zoning is patchy and much affected by late strain and kink bands. The amphibole also has patchy extinction and pleochroism with pale green cores and deep green margins. The ferromagnesian minerals are generally clustered and in the more foliated zones rimmed by epidote. Saussuritization and clouding concentrated in the cores of the feldspars, chloritization of the biotite, and sphene coronas around the opaques are typical retrograde reactions."

The plagioclase varies between about An_{28} and An_{30}.

The granitoids display a typical subsolvus granitic structure of subhedral plagioclase (An_{10} to An_{20} in different samples, in places with thin albitic rim An_5) and anhedral quartz and perthitic microcline. Biotite and opaque minerals are partly replaced by chlorite and titanite; epidote and sericite attack the plagioclase. Strain and recrystallization are mostly absent, but some granites are distinctly gneissic in outcrop texture.

TABLE 12. REPRESENTATIVE CHEMICAL ANALYSES OF THE MASKWA LAKE QUARTZ DIORITE COMPLEX (10)

	Quartz diorite		Trondh-jemite	Granite	
	PG 77-1	PG 50	PG 47	PG 150	PG 82
SiO_2, wt. %	65.65	67.95	72.10	72.10	76.90
Al_2O_3	16.56	14.44	14.14	13.45	12.14
TiO_2	0.32	0.45	0.34	0.23	0.10
Fe_2O_3	0.82	2.26	1.10	1.37	0.71
FeO	2.16	2.44	1.64	1.30	0.72
MnO	0.05	0.09	0.04	0.04	0.04
MgO	2.33	1.69	1.04	0.98	0.14
CaO	4.20	3.92	1.96	2.14	0.61
Na_2O	4.66	4.06	4.22	3.45	3.62
K_2O	1.56	1.62	1.65	3.81	4.28
P_2O_5	0.10	0.13	0.09	0.06	0.02
CO_2	0.82	0.10	0.09	0.03	0.03
H_2O	0.06	0.73	0.86	0.78	0.47
	99.29	99.88	99.29	99.74	99.78
Li, ppm	51	54	22	29	32
Rb	42	101	34	144	168
Cs	1.6	2.1	3.5	2.7	2.3
Be	2	3	2	1	3
Sr	448	190	130	138	46
Ba	432	353	549	658	652
Pb	3	9	6	8	21
Ga					
U	nd*	4	1	nd	5
Th	nd	nd	nd	nd	13
Zr	79	179	151	140	148
Hf	2.3	4.7	4.1	4.3	4.6
Sn	nd	2	3	2	4
K/Rb	307	133	403	219	211
K/(Cs x 100)	80	63	39	117	154
K/Ba	29.9	38	24.9	48	54.4
Ba/Rb	10.3	3.5	16.1	4.6	3.9
Ba/Sr	0.96	1.86	4.2	4.8	14.2
Rb/Sr	0.09	0.53	0.26	1.04	3.65
Mg/Li	274	189	286	203	25
Zr/Sn	-	89.5	50.3	70	37
Zr/Hf	34.3		36.8	32.6	32.2
Al/Ga					
La, ppm	6.2	15.05	31.3	28.85	30.8
Ce	14	39	63.5	58.5	72
Nd	7	19.5	24	20	29.5
Sm	1.69	4.14	3.03	2.77	3.83
Eu	0.46	0.81	0.66	0.51	0.38
Dy	1.35	4.8	2.7	1.95	2.95
Yb	0.7	4.8	6.35	1.45	2.05
Lu	0.08	0.62	0.24	0.18	0.28

* not detected

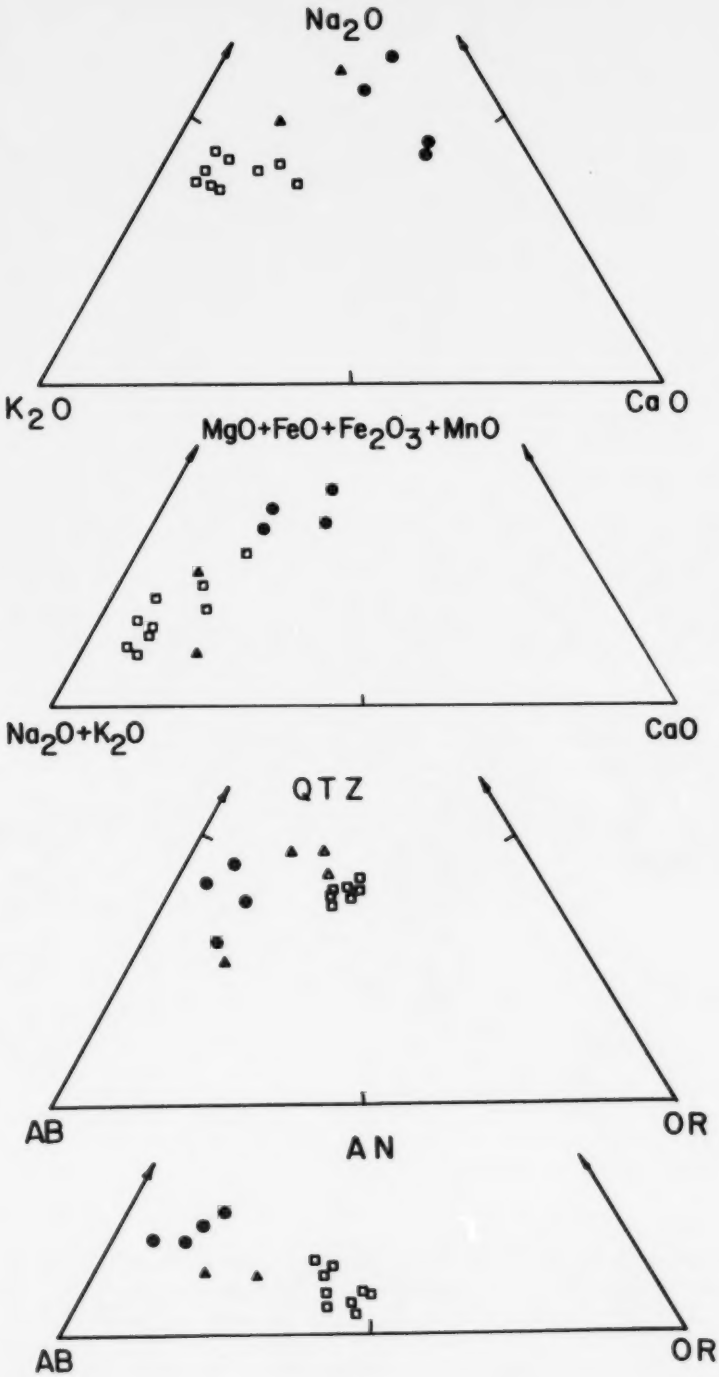

Figure 17: Selected compositional and normative characteristics of the Maskwa Lake batholith: quartz diorites (dots), granodiorites (triangles) and granites (squares)

Chemical composition of both rock types is demonstrated in Table 12 and in Figures 17, 18, and 19. Quartz diorites vary from quartz-poor tonalites to trondhjemitic types; granites also are variable but mostly silica-rich. The majority of their norms places them into the plagioclase-rich side of the low-T through (Fig. 17). Ba contents are highly variable in both rock types but Rb contents separate the quartz diorite and granite trends (Fig. 18).

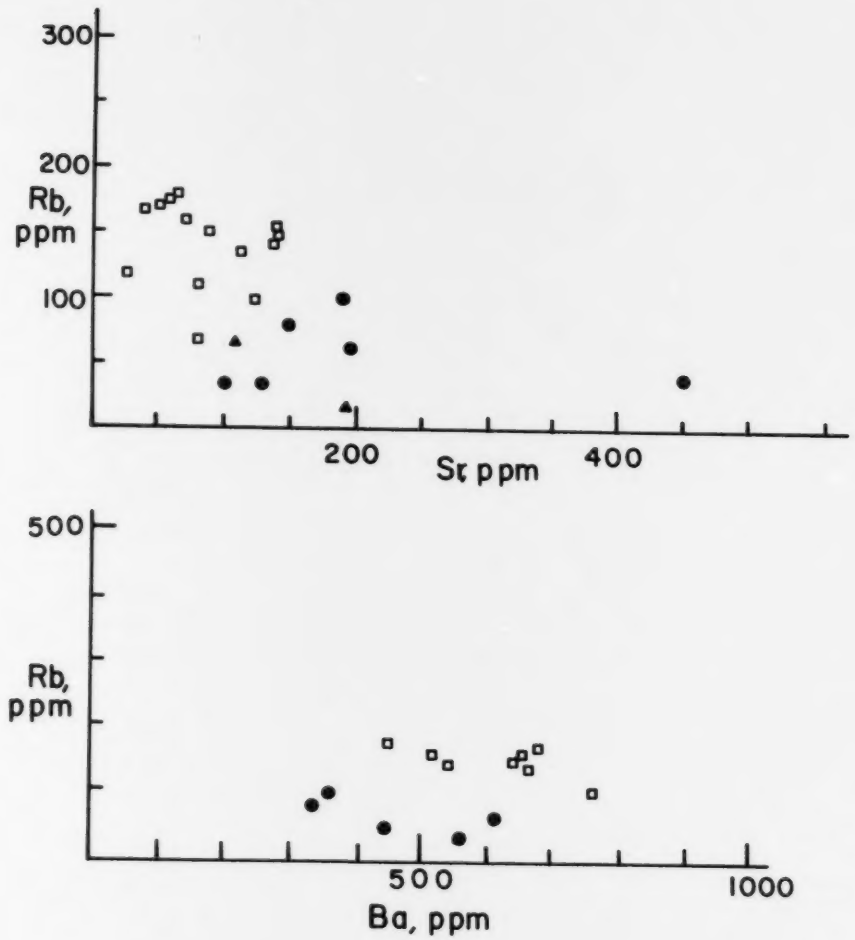

Figure 18: Rb vs. Sr and Rb vs. Ba plots of the Maskwa Lake batholith: quartz diorites (dots), granodiorites (triangles) and granites (squares)

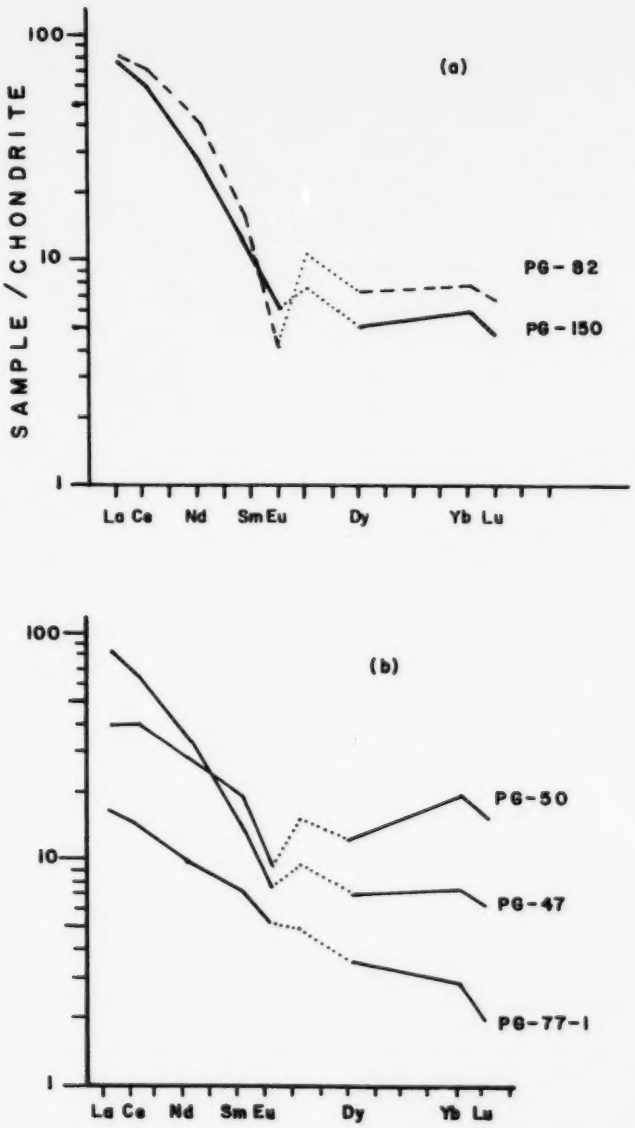

Figure 19: REE abundances in the Maskwa Lake batholith: granites (a) and quartz diorites (b)

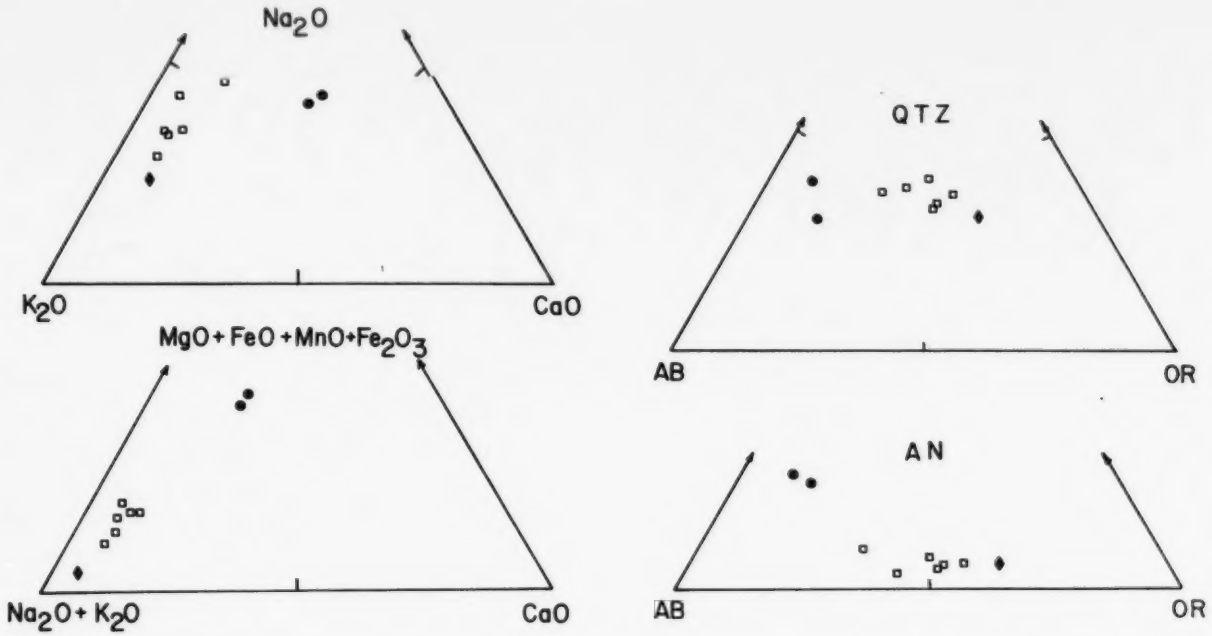

Figure 20: Selected compositional and normative characteristics of the Marijane Lake batholith: northern quartz diorites (dots), main body granites (squares) and northern granite (diamonds)

REE patterns are variable in quartz diorites (Fig. 19b), and their negative Eu anomalies are not readily correlatable with any other patterns published for this rock type.

In the area of Map 1, the *Marijane Lake batholith* consists of a single rock type, a weakly foliated, equigranular, medium- to coarse-grained buff granite. East of the area, however, Carlson (1958) has mapped an extensive area of dioritic rocks within the same intrusive body, which were not examined in the present study. The diorites to quartz diorites discussed below belong to a body north of the main intrusion, mapped as connected by McRitchie (1971) and Beakhouse (1977).

The quartz diorites from this northern occurrence barely fit the definition because the quartz (and also K-feldspar) contents are very low. They are melanocratic and biotite-rich, with weak and patchy zoning in heavily clouded plagioclase An_{30-32}. Otherwise, their microscopic study reveals the same assemblage and alterations as those described for the Maskwa Lake quartz diorite. Granites of the main intrusion also correspond to their Maskwa Lake counterpart, with plagioclase mostly between An_{15} and An_{20}.

Bulk compositions of the quartz diorites listed in Table 13 and illustrated in Figure 20 do not differ greatly from those of the Maskwa Lake members, except for lower SiO_2 and higher K_2O due to higher proportion of biotite. They are, however, enriched in Sr and Ba (Fig. 21). This is also characteristic of the single "granitic" sample from the northern area, which seems to be a K-enriched internal porphyroblasitc mobilizate derived from the quartz diorites rather than an exogenic intrusion. The REE patterns of the quartz diorites (Fig. 22b) are mostly extremely fractionated (in terms of Ce_N/Yb_N), with slight positive (if any) Eu anomalies, and resemble those of the tonalitic gneisses of type 1 from the Eastern Lac Seul area (Chou 1978).

Granite compositions match those from the Maskwa Lake batholith rather closely in terms of both bulk composition and trace elements (Table 13, Figs. 20 and 21). The REE abundances also are very similar (Fig. 22a).

Migmatite complex (11)

Rocks of the migmatite complex are described by Springer (1949) as being dominated by quartz, albite-oligoclase, microcline, biotite, and muscovite-bearing assemblages containing abundant inclusions of quartz-biotite schist. In addition, McRitchie (1971) notes the occurrence in these rocks of cordierite, almandine, sillimanite, and K-feldspars representative of upper amphibolite facies grades of metamorphism. Our observations confirm the above mineral assemblages.

Representative chemical analyses of those rocks are shown in Table 14, and selected data are plotted in Figure 23. Granitic compositions are characterized by high Al_2O_3 contents and normative corundum in the range 1.3 to 2.1% (CIPW), reflecting the presence of garnet and cordierite; high Ba and Sr contents and low Rb, Cs, Be, and Li concentrations are also conspicuous.

Gneissic tonalite unit (12)

Immediately south of the southern boundary of the Bird River Greenstone Belt and of the Lac du Bonnet batholith is the "schollen-textured gneissic tonalite" of Janes (in prep.) which forms the major part of the Winnipeg River Batholithic Belt (cf. also Breaks et al. 1978, "gneissic granitoid suite"). Another sizable area underlain by this unit is located east of Cole Lake (Map 1).

The dominant rock type of this unit is a grey, gneissic, medium- to coarse-grained (porphyritic) tonalite which, in proximity to the Bird River Belt, forms thin sills intercalated with metavolcanic rocks, and rapidly becomes more abundant southwards. These rocks are generally disposed against the greenstones in faulted contact, and are marked by a northeasterly trending steeply-dipping gneissosity.

Large tracts of the gneissic tonalite, however, are highly inhomogeneous internally, as well as having been injected and transected by a great variety of melanocratic-biotitic up to granitoid rocks.

> "The Gneissic Granitoid Suite, composed of a medley of assemblages including predominantly plutonic and subsidiary phases of possible supracrustal origin,

TABLE 13. REPRESENTATIVE CHEMICAL ANALYSES OF THE MARIJANE LAKE QUARTZ DIORITE COMPLEX (10)

	Quartz diorite (N)		Granite (N)	Granites (S)		
	PG 84	PG 85	PG 87-2	PG 71	PG 73	PG 31
SiO_2, wt. %	64.65	63.55	72.80	72.45	73.90	74.90
Al_2O_3	15.36	15.89	13.89	14.40	14.07	13.44
TiO_2	0.66	0.60	0.12	0.26	0.14	0.19
Fe_2O_3	1.90	2.00	0.52	0.53	0.45	0.82
FeO	3.04	2.56	0.64	1.10	0.52	0.76
MnO	0.06	0.07	0.01	0.02	0.01	0.02
MgO	2.54	2.94	0.52	0.35	0.20	0.38
CaO	3.23	3.41	1.00	0.73	0.79	0.94
Na_2O	3.92	4.24	2.46	3.26	3.18	3.04
K_2O	2.32	2.96	7.11	5.67	5.63	4.89
P_2O_5	0.29	0.33	0.16	0.14	0.08	0.08
CO_2	0.29	0.17	0.16	0.08	0.04	0.09
H_2O	0.92	0.80	0.46	0.54	0.38	0.42
	99.18	99.52	99.87	99.62	99.39	99.97
Li, ppm	28	24	13	31	24	20
Rb	92	69	108	237	156	146
Cs	1.7	1.7	0.7	12	3.8	2.8
Be	4	4	3	3	2	1
Sr	973	1319	698	105	135	140
Ba	960	1283	2232	519	523	741
Pb	9	15	34	29	37	33
Ga						
U	nd*	nd	nd	9	12	12
Th	nd	nd	nd	15	nd	13
Zr	200	95	68	179	111	197
Hf	6.2	3.35			2.65	5.25
Sn	4	2	3	4	5	4
K/Rb	209	356	546	199	299	278
K/(Cs x 100)	112	144	842	39	122	145
K/Ba	20	19.17	26.4	90.8	89.3	54.8
Ba/Rb	10.4	18.6	20.7	2.2	3.4	5.07
Ba/Sr	0.99	0.97	3.2	4.9	3.9	5.3
Rb/Sr	0.09	0.05	0.15	2.3	1.1	1.04
Mg/Li	546	737	238	67.7	50	115
Zr/Sn	50	47.5	22.7	44.8	22.2	49.2
Zr/Hf	32.2	28.4			41.9	37.5
Al/Ga						
La, ppm	95.5	23.35			16.1	34.35
Ce	191	57.5			34.5	77
Nd	66.5	30.5			13	29.5
Sm	6.05	4.59			3.12	5.29
Eu	1.5	1.55			0.45	0.53
Dy	2.05	1.85			0.95	2.2
Yb	0.07	<0.75			0.45	0.85
Lu	0.06	0.07			0.06	0.14

* not detected

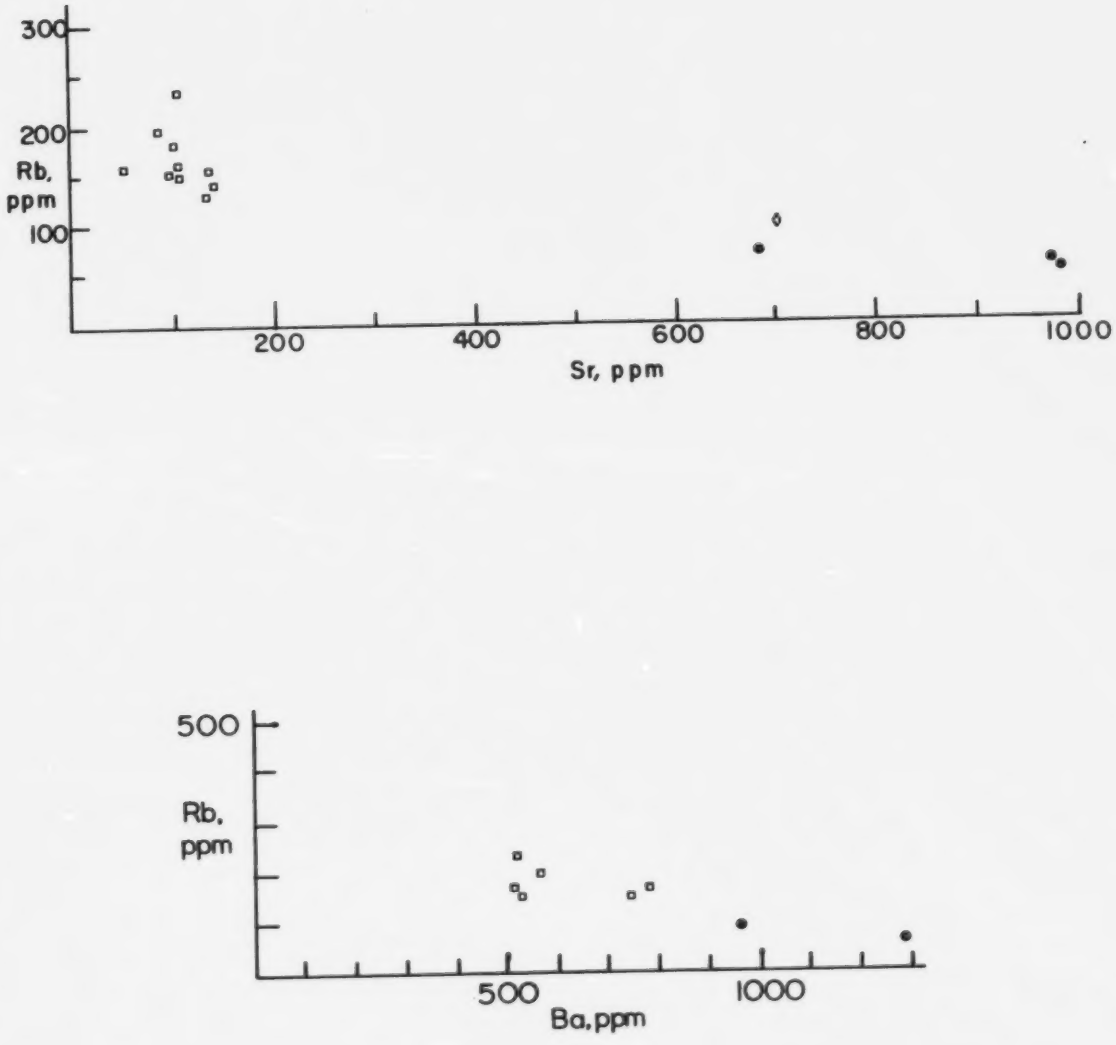

Figure 21: Rb vs. Sr and Rb vs. Ba in rocks of the Marijane Lake batholith: northern quartz diorites (dots), main body granites (squares), and northern granites (diamond)

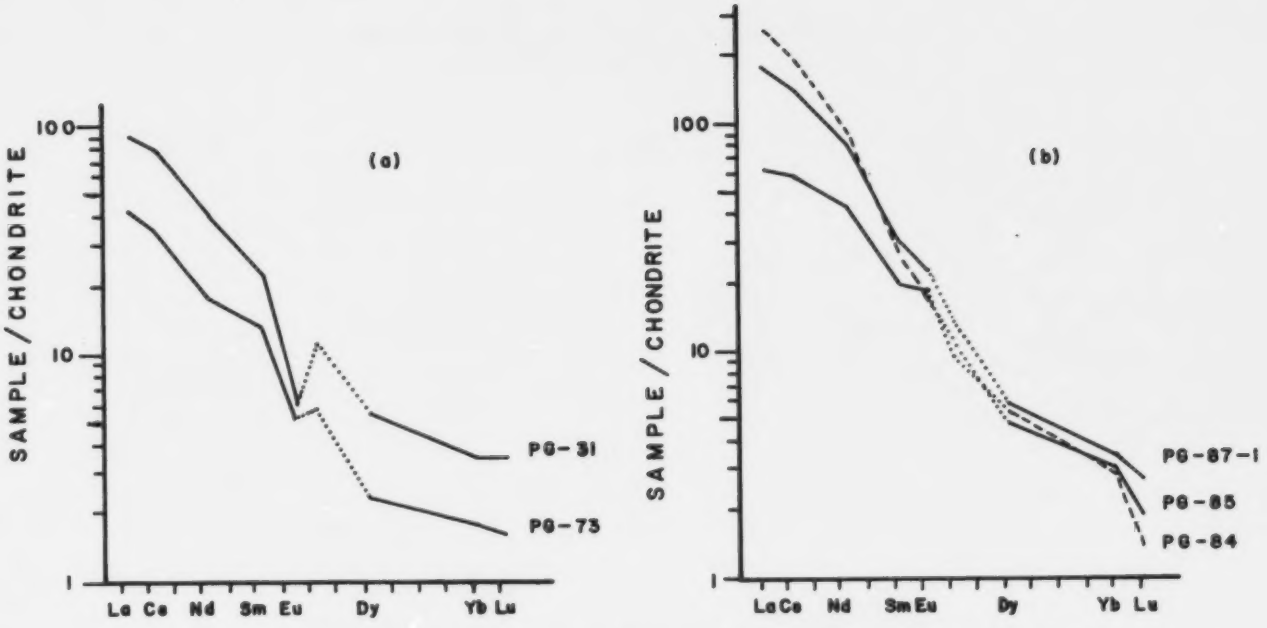

Figure 22: REE abundance in the rocks of the Marijane Lake batholith: main body granites (a) and northern quartz diorites (b)

characteristically displays a layered or gneissic fabric. Heterogeneity within the suite is influenced by the numerous, polycyclic, complexly intermixed, intrusive phases and by changes in fabric produced by chaotic differences in the following: (1) degree of development of layering or foliation; (2) continuity of layering; (3) thickness of layering; (4) percentages of complementary mafic and felsic components" (Breaks et al. 1978).

Representative chemical analyses of the extreme "end members" of this rock suite, gneissic tonalites and the most felsic granitic types, are shown in Table 15 and Figures 24 and 25. The tonalite gneisses form tight clusters in most ternary diagrams, tailed by bands of intermediate members reaching to granitic compositions. However, the compositional characteristics are more diversified than suggested by the bulk data shown in the ternary diagrams and by the samples selected for Table 11. Extreme differences in most trace element contents emphasize the heterogeneity of this unit (cf. also Fig. 25a). In general, the gneissic tonalites resemble the compositional characteristics of the quartz diorites in the northern part of Marijane Lake body.

The REE pattern of the gneissic tonalites (Fig. 25b) are similar to the type 1 of Chou (1978), except sample PG 61 with a prominent positive Eu anomaly. Low $\delta^{18}O$ values are characteristic of this rock type, 7.0-7.5 (Longstaffe et al. 1981).

SYN- TO LATE-TECTONIC INTRUSIVE AND METASOMATIC ROCKS

Granodiorite (13)

A lenticular body of grey, non-porphyritic granodiorite crops out immediately south of the Eaglenest Lake Formation on the east shore of Eaglenest Lake. This body, not studied by the present writers, is further cut by veins and dykes of pink inequigranular biotite- and hornblende-bearing monzogranite (according to Janes, in prep.).

Black River suite (14)

In the accompanying Map 1, the extent of this unit was substantially reduced as compared to McRitchie's (1971) compilation. The formal boundary of this unit with the Inconnu granite (15) as shown in Map 1 is rather arbitrary (D.A. Janes, pers. comm. 1979), as the two units show a gradual transition. The northern segment of the Black River suite shown in Map 1 is characterized by McRitchie (1971) as "predominantly pink, coarse, massive, equigranular biotite-quartz monzonite with infrequent layered concentrations of microcline poikiloblasts". Farther to the east and southeast, he describes this unit as "predominantly pale pink inequigranular biotite-quartz monzonite with occasional large microcline and plagioclase porphyroblasts".

Contacts with adjacent paragneiss (1) are generally sharp, but the suite shows a gradual transition, according to McRitchie, into tonalitic gneisses of unit 5, northwest of present study area, by porphyroblastesis.

Because of their small extent in the present study area, no attempt was made to investigate the porphyroblastic members of this suite. Table 16 shows selected compositions, and Figure 26 illustrates the relationships among the gneissic to granitic specimens which were collected in areas originally designated as the Black River suite by McRitchie (1971) (some of which are within the boundaries of the Inconnu pluton; Map 1, this report, and D.A. Janes, in prep.). Generally, the bulk composition as well as trace element behavior are rather indistinguishable from those given below for the Inconnu granite.

Inconnu granite (15)

The Inconnu batholith lies in close proximity to the southern boundary of the Manigotagan Gneiss Belt in the east, and of the Black River suite in the west; it is separated locally from rocks of the Bird River Greenstone Belt by screens of grey quartz diorite to granodiorite closely resembling phases of the Maskwa Lake batholith.

The dominant rock type of the Inconnu batholith is a weakly gneissic, buff to pink, medium- to coarse-grained biotite± muscovite bearing monzogranite. In general the body is weakly porphyritic, distinctly gneissic, and finer-grained on the north side; it becomes coarser-grained equigranular on the south. It also loses most of the gneissosity along the southern margin. In addition, the southern

TABLE 14. REPRESENTATIVE CHEMICAL ANALYSES OF THE MIGMATITE COMPLEX (11)

	Gneisses		Migmatites		Granite
	PG 107-1	PG 119-1	PG 104-2	PG 96-2	PG 94
SiO_2, wt.%	70.40	62.05	71.60	72.05	78.35
Al_2O_3	14.03	16.08	15.19	15.03	14.48
TiO_2	0.34	0.41	0.20	0.10	0.01
Fe_2O_3	1.41	1.67	0.59	0.65	0.27
FeO	2.68	3.74	1.08	0.68	0.28
MnO	0.05	0.09	0.03	0.02	0.02
MgO	1.34	3.29	0.78	0.44	0.15
CaO	3.45	6.45	2.26	0.98	0.78
Na_2O	2.85	3.85	4.14	3.02	2.96
K_2O	1.73	1.13	3.01	6.09	6.58
P_2O_5	0.11	0.04	0.06	0.15	0.12
CO_2	0.37	0.00	0.11	0.06	0.09
H_2O	0.99	0.97	0.60	0.52	0.40
	99.98	99.81	99.03	99.79	99.99
Li, ppm	27	20	14	14	10
Rb	56	60	123	123	119
Cs	1.7	1.3	0.9	1.9	2.0
Be	1.1	0.8	2	2	2
Sr	441	198	470	189	175
Ba			1207	1014	824
Pb	7	6	24	41	34
Ga					
U			nd*	17	2
Th			2	nd	nd
Zr			159	111	91
Hf	3.8	2.6			
Sn			1	2	4
K/Rb	257	157	203	411	459
K/(Cs x 100)	85	72	167	266	273
K/Ba			20.7	49.8	66.3
Ba/Rb			9.8	8.2	6.9
Ba/Sr			2.6	5.4	4.7
Rb/Sr	0.13	0.30	0.26	0.65	0.68
Mg/Li	300	990	336	186	90
Zr/Sn			159	56	23
Zr/Hf					
Al/Ga					
La, ppm	27.1	12.0			
Ce	54.5	24.5			
Nd	23	9			
Sm	3.35	1.52			
Eu	0.89	0.59			
Dy	1.9	1.25			
Yb	0.85	0.7			
Lu	0.12	0.09			

* not detected

TABLE 15. REPRESENTATIVE CHEMICAL ANALYSES OF THE TONALITE GNEISS "SCHOLLEN"-ZONE (12)

	Gneiss		Granitoids	
	PG 2	PG 61	PG145	PG 68-2
SiO_2, wt. %	69.50	68.15	75.25	76.40
Al_2O_3	15.20	15.36	13.05	12.56
TiO_2	0.36	0.44	0.06	0.12
Fe_2O_3	1.56	1.14	0.75	0.58
FeO	1.96	2.44	0.46	0.40
MnO	0.07	0.06	0.02	0.01
MgO	1.00	1.30	0.18	0.26
CaO	3.09	3.69	1.03	0.19
Na_2O	4.18	4.06	2.90	2.96
K_2O	1.55	1.68	5.94	5.42
P_2O_5	0.16	0.10	0.02	0.02
CO_2	0.07	0.10	0.03	0.06
H_2O	0.67	0.75	0.31	0.44
	99.37	99.27	100.00	99.42
Li, ppm	85	41	19	5
Rb	66	30	154	74
Cs	5.5	0.8	6.1	0.6
Be	2	2	1	2
Sr	222	268	90	48
Ba	376	731	1401	485
Pb	9	9	21	29
Ga				
U	nd*	nd	nd	2
Th	nd	nd	19	24
Zr	233	118	148	135
Hf		3.8		
Sn	9	nd	nd	3
K/Rb	194	463	320	608
K/(Cs x 100)	23	174	81	750
K/Ba	34	19	35	93
Ba/Rb	5.7	24.4	9.1	6.6
Ba/Sr	1.7	2.6	15.6	10.1
Rb/Sr	0.3	0.1	1.7	1.5
Mg/Li	71	190	58	320
Zr/Sn	25.9			45
Zr/Hf		31.1		
Al/Ga				
La, ppm	44.05	25.65		
Ce	107	48.5		
Nd	44.5	17.5		
Sm	5.85	1.77		
Eu	1.51	0.75		
Dy	2.6	0.95		
Yb	1.35	1.15		
Lu	0.22	0.11		

* not detected

TABLE 16. REPRESENTATIVE CHEMICAL ANALYSES OF THE BLACK RIVER SUITE (14)

	Granitoids				
	PG 89	PG 20	PG 99	PG 42	PG44
SiO_2, wt. %	74.50	73.95	71.15	71.15	73.70
Al_2O_3	13.61	12.26	15.19	14.98	14.22
TiO_2	0.13	0.39	0.10	0.19	0.19
Fe_2O_3	0.57	1.24	0.81	1.16	0.77
FeO	0.72	1.24	0.72	0.84	0.72
MnO	0.10	0.05	0.02	0.02	0.02
MgO	0.35	0.51	0.54	0.69	0.47
CaO	1.13	1.18	1.24	1.96	1.14
Na_2O	3.40	2.96	3.92	4.13	3.32
K_2O	4.69	4.86	5.06	3.38	4.54
P_2O_5	0.07	0.14	0.14	0.13	0.07
CO_2	0.11	0.06	0.13	0.15	0.06
H_2O	0.49	0.34	0.47	0.48	0.46
	99.88	99.18	99.49	99.26	99.68
Li, ppm	24	37	39	19	20
Rb	112	239	111	81	120
Cs	2.6	0.9	1.2	0.9	1.7
Be	2	3	2	1	2
Sr	98	153	560	650	259
Ba	554	568	1750	888	746
Pb	28	28	22	22	32
Ga					
U	nd*	9	nd	nd	2
Th	3	104	nd	nd	32
Zr	139	297	151	207	239
Hf					
Sn	3	5	2	6	7
K/Rb	347	169	378	346	314
K/(Cs x 100)	149	448	350	311	222
K/Ba	70.2	70.9	24	31.5	50.5
Ba/Rb	4.9	2.4	16	11	6.2
Ba/Sr	5.7	3.7	3.1	1.4	2.9
Rb/Sr	1.14	1.56	0.2	0.12	0.46
Mg/Li	87.5	84	82	221	140
Zr/Sn	46.3	59.4	75.5	34.5	34.1

* not detected

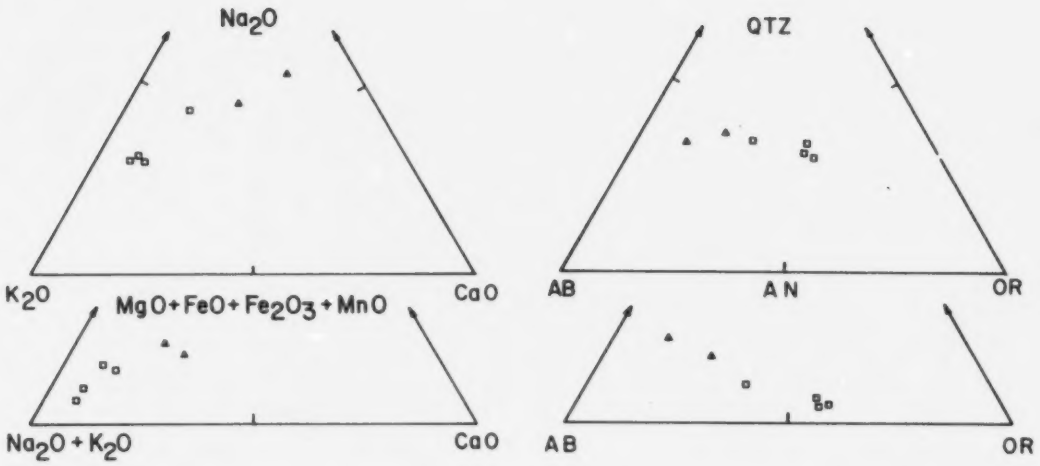

Figure 23: Compositional characteristics of the gneisses (triangles) and banded migmatites to massive granites (squares) of the migmatite complex

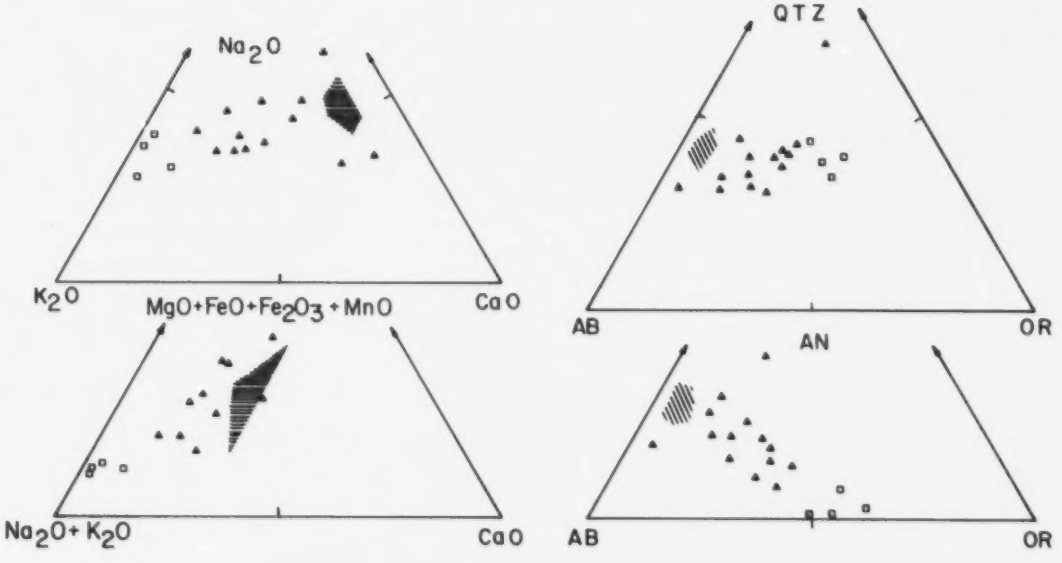

Figure 24: Selected compositional and normative characteristics of the gneissic tonalites (ruled field), intermediate biotitic derivatives (triangles) and granitic rocks (squares) of the gneissic tonalite "schollen"-zone

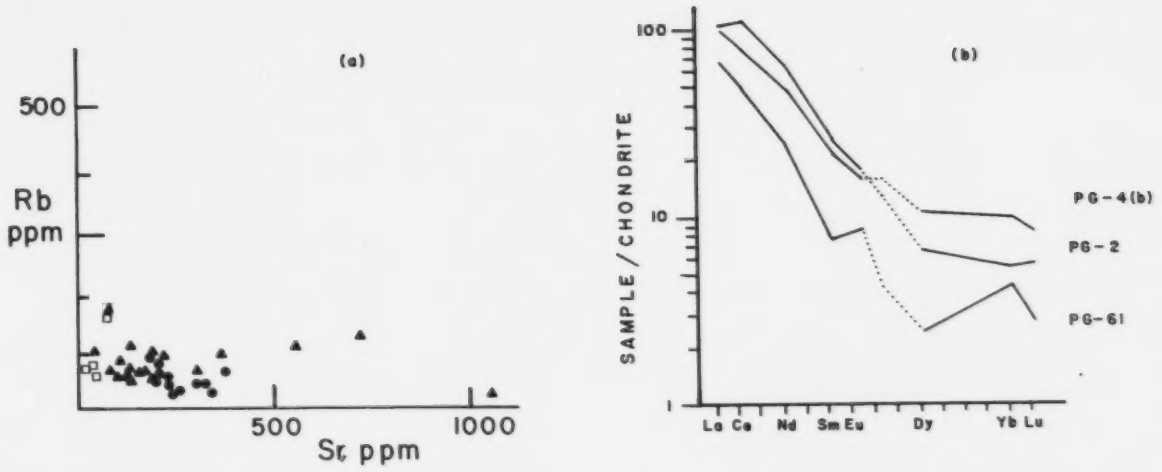

Figure 25: *(a) Rb vs. Sr relationships in the tonalitic gneiss (dots), intermediate biotitic derivatives (triangles) and granitic rocks (squares), and (b) REE abundances in the gneissic tonalites of the gneissic tonalite "schollen"-zone*

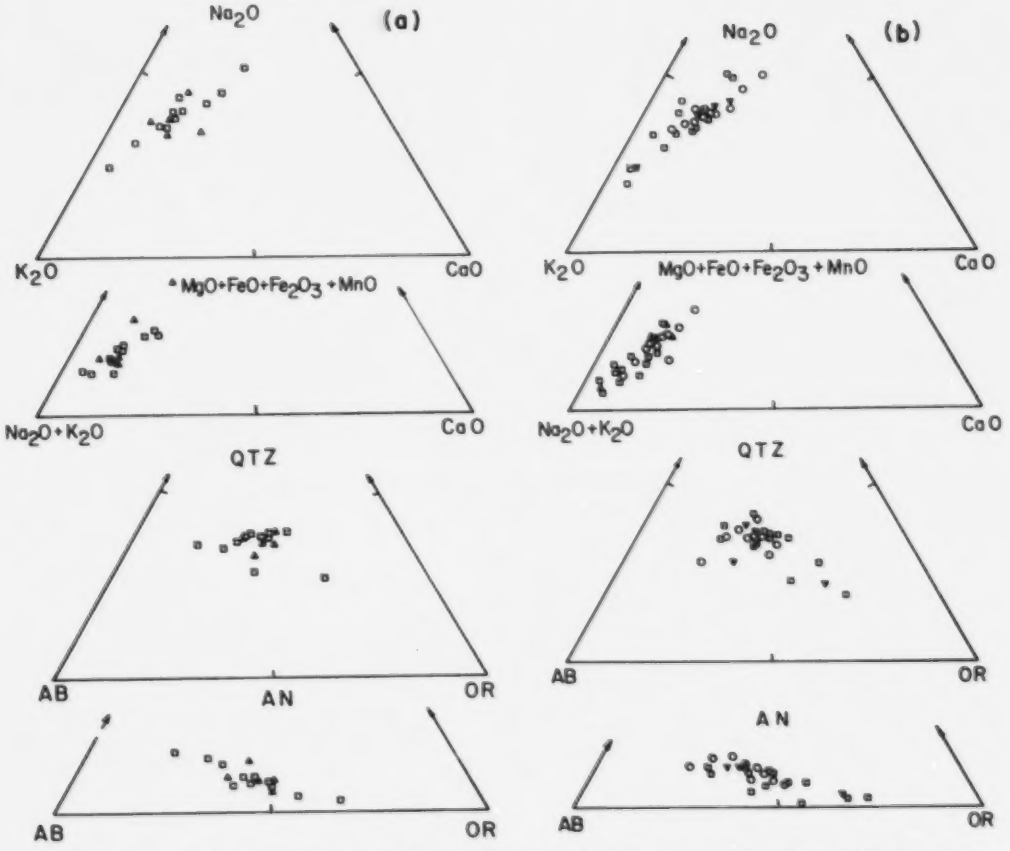

Figure 26: *Felsic ternary plots of (a) the Black River suite: porphyroblastic gneissic granitoids (triangles) and massive granites (squares); (b) the Inconnu batholith: gneissic porphyroblastic members (triangles), massive biotite granite (circles) and massive leucocratic granite (squares)*

TABLE 17. REPRESENTATIVE CHEMICAL ANALYSES OF THE INCONNU GRANITE (15)

	Gneissic porphyroblastic		Massive equigranular		Potassic coarse-grained	
	SR19	Pg160B	PG162A	53-8-2409	SR11	SR15-1
SiO_2, wt. %	69.90	71.40	74.50	72.20	73.30	68.85
Al_2O_3	15.44	15.28	14.04	14.42	14.56	15.91
TiO_2	0.15	0.00	0.00	0.22	0.03	0.12
Fe_2O_3	1.29	0.27	0.34	0.82	0.56	0.94
FeO	0.72	0.28	0.60	1.00	0.12	0.38
MnO	0.03	0.01	0.08	0.02	0.02	0.01
MgO	0.62	0.23	0.15	0.59	0.18	0.40
CaO	1.95	0.59	0.69	1.58	0.43	0.71
Na_2O	4.38	2.79	4.04	3.68	2.55	2.35
K_2O	4.11	8.49	4.86	4.22	7.96	9.42
P_2O_5	0.301	0.07	0.05	0.13	0.04	0.25
CO_2	0.25	0.05	0.03	0.07	0.10	0.03
H_2O	0.67	0.29	0.63	0.59	0.32	0.45
	99.81	99.75	100.01	99.55	100.16	99.82
Li, ppm	10	7	33	39	10	11
Rb	91	179	193	153	161	183
Cs	1.8	0.8	4	1.2	2.3	2.2
Be	0.8	<1	1	1.5	0.5	0.4
Sr	360	448	60	213	189	325
Ba	914	2076	322	784		
Pb	17	41	25	23	32	38
Ga	31	19	28	29		
U	nd*	nd	5	1		
Th	1	5	9	7		
Zr	221	32	101	189		
Hf		1.1	2.8			
Sn	2	nd	3	13		
K/Rb	375	394	209	229	410	427
K/(Cs x 100)	189	881	100	29	287	355
K/Ba	37.3	33.9	125	44.6		
Ba/Rb	10	11.6	1.7	5.1		
Ba/Sr	2.5	4.6	5.4	3.7		
Rb/Sr	0.25	0.4	3.22	0.7	0.85	0.56
Mg/Li	374	200	27.3	92.3	108	219
Zr/Sn	110.5	-	33.7	14.5		
Zr/Hf	-	29	36.1			
Al/Ga	2635	4253	2654	2631		
La, ppm		51.75	16.45			
Ce		117.5	37.5			
Nd		56	17.5			
Sm		7.645	2.415			
Eu		1.115	0.225			
Dy		2.45	1.35			
Yb		0.6	2.0			
Lu		<0.02	0.205			

* not detected

portions are commonly marked by abundant pods of pegmatitic phases, irregular in shape and distribution. Also, the northern contacts are distinctly intrusive whereas in the north they have a gradational character.

This generalized pattern holds on a regional scale but in detail the batholith consists of an irregular sequence of alternating (and gradually transitional) bands of buff-coloured "igneous" massive granite and grey gneissic or migmatitic rocks, streaked along the gneissosity by pink feldspar porphyroblasts. Increasing percentage of porphyroblasts, progressively destroying gneissic fabric and gradually merging into a granitic texture, characterize the transitions. Considerable differences in the structure and content of mafic components penetrated by porphyroblasts suggests that the metamorphic suite intruded and metasomatized by the Inconnu granite was inhomogeneous.

Microscopically, the massive samples with typical granitic texture show subhedral to euhedral plagioclase with An content variable from 4 to 20 in different samples, anhedral quartz, and late microcline which frequently replaces plagioclase. Biotite is partly chloritized. Muscovite, when present, is mostly a late alteration product. Apatite, zircon, and locally tourmaline belong to accessory phases.

Selected chemical analyses of different textural varieties are given in Table 17. They indicate compositions irregularly variable among the different types, which is confirmed in the plots illustrated in Figure 26: different textural varieties show about equal compositional ranges. The ternary feldspar diagram demonstrates, besides variable Ab/An, a considerable spread along the alkali feldspar join but with not too many compositions in the low-T trough. Four analyses show an extraordinary enrichment in K-feldspar, confirming the field and microscopic indications of late mobility and local accumulation of the K-feldspar component. Figure 27a displays broad ranges in the Rb, Sr, and Ba contents in the pluton. The data in Table 17 show that with increasing K, the K/Rb ratio also increases, despite the concomitant increase in Rb. The REE patterns illustrated in Figure 27b show a high variability in shape and individual abundances, reflecting the diversity in other compositional parameters and, possibly, in the character and amount of incorporated metamorphic substrate. A systematic change can be observed from the rather straight and steep pattern of the sample PG 160(b), most enriched in Ce and with the highest Ce_N/Yb_N ratio, to the Ce-poorest specimens with pronounced depletion of the intermediate REE's. All samples are marked by a conspicuous drop in Lu.

Monzogranite, microgranite, and associated pegmatite

These rocks are present in the study area as a stock-like intrusion located midway between Pointe du Bois and Greer Lake. The body is described by Janes (in prep.) as a "medium-grained pink biotite monzogranite with dykes of microgranite and simple pegmatite". The body was not investigated during the present study and the reader is referred to Janes (in prep.) for more details.

Lac du Bonnet granite (17)

The Lac du Bonnet composite intrusion, of batholithic proportions, crops out extensively in the study area between Lamprey Falls on the Winnipeg River in the east, and the Phanerozoic cover in the west. Geophysical data suggest a considerable westward continuation of the body under the Phanerozoic sediments.

The southern boundary of the batholith is gradational, being intercalated or interlayered with gneissic rocks of the Winnipeg River Batholithic belt. The northern boundary, however, is varied: sharp where in contact with mafic metavolcanic rocks of the Bird River Greenstone Belt, and diffuse where it injects clastic rocks as lit or stopes the host rocks. A gravity profile across the batholith by Brisbin (1979) was designed to study the dips of the pluton contacts. The density contrast between the batholithic and host rocks were found too low to model these contacts with any degree of confidence.

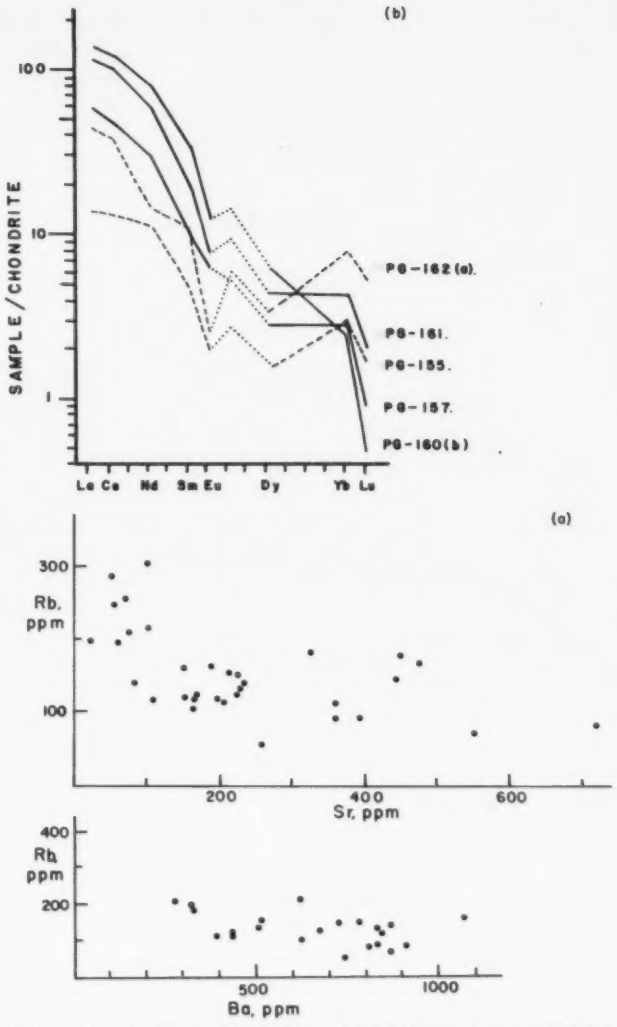

Figure 27: (a) Rb vs. Sr and Rb vs. Ba relationships, and (b) REE abundances in the rocks of the Inconnu batholith

However, the above study and a magnetic profile by Coles (1973) across the batholith indicate the presence of a high density mass with higher than usual levels of magnetization underlying the northern part of the batholith at a depth of approximately 4 km. This mass could be quartz-dioritic, or alternatively, could be composed of rocks of the Bird River Greenstone Belt.

Numerous outcrops of quartz diorite are scattered throughout the granitic batholith, and at Key Lake and to the west from it, central to the batholith, large areas carry inclusions closely resembling flow and clastic rocks of the Bernic Lake Formation.

The fault which separates the Winnipeg River Batholithic Belt from the Bird River Greenstone Belt appears to form the south boundary of the Lac du Bonnet batholith at, and east of, Lamprey Falls. West of Lamprey Falls the fault is not apparent, and the south boundary of the batholith has an intrusive character.

Deformation attendant with emplacement of the main phase of the Lac du Bonnet batholith appears to be confined largely to reorientation of both layering and foliation of rocks of the Bird River belt which envelop the intrusion. No tectonic fabric is imposed by the intrusion on the hosts.

Hornfelsic textures appear locally in the host Bird River

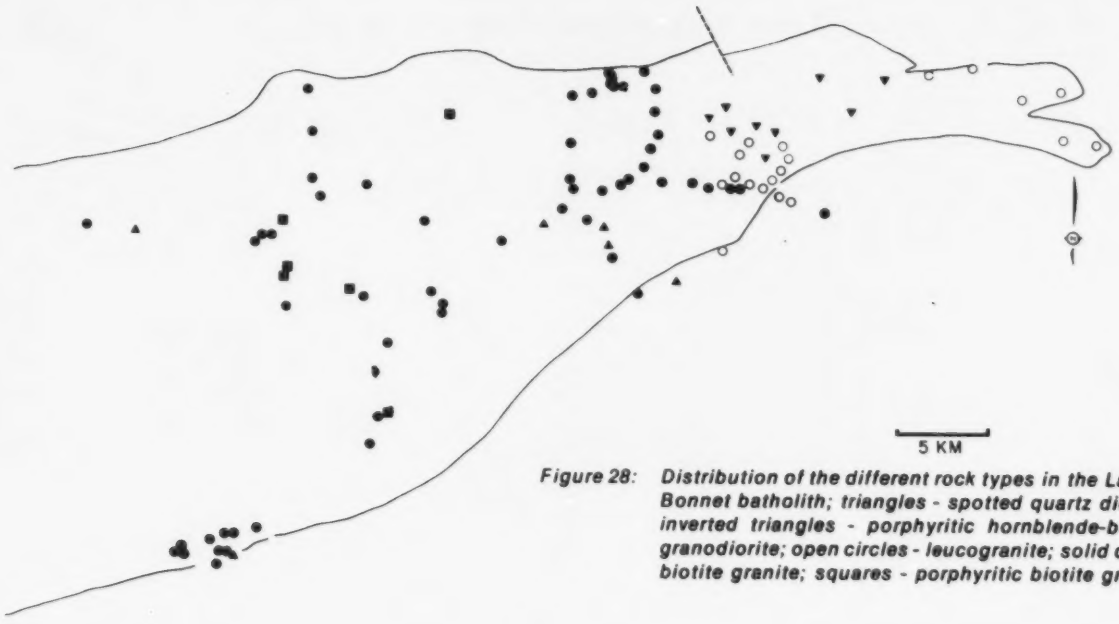

Figure 28: Distribution of the different rock types in the Lac du Bonnet batholith; triangles - spotted quartz diorite; inverted triangles - porphyritic hornblende-biotite granodiorite; open circles - leucogranite; solid dots - biotite granite; squares - porphyritic biotite granite

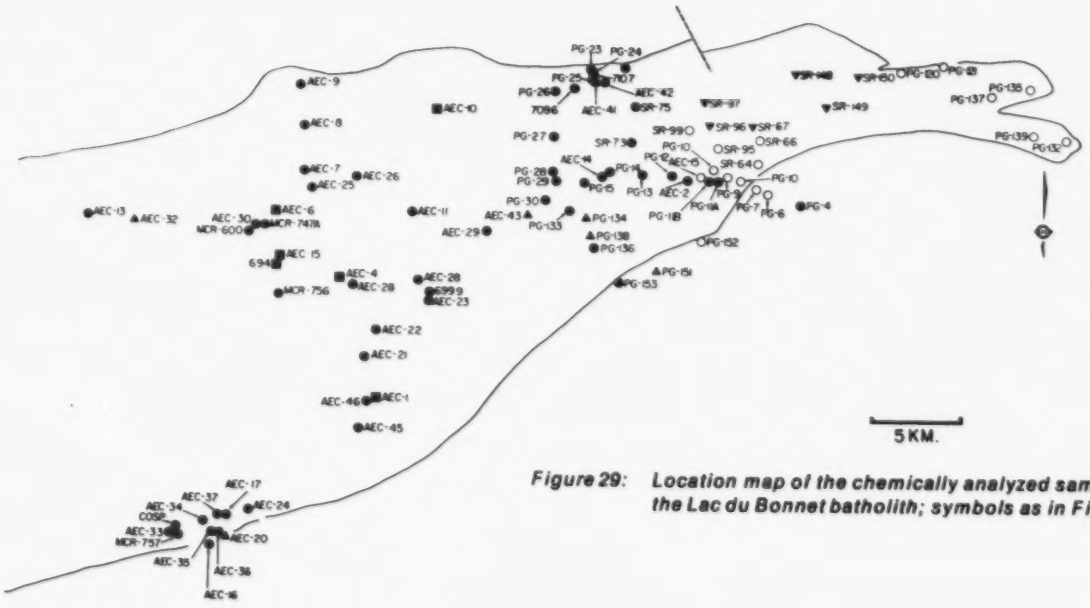

Figure 29: Location map of the chemically analyzed samples of the Lac du Bonnet batholith; symbols as in Figure 28

greenstones around the north and east margins of the Lac du Bonnet batholith, but corresponding metamorphic assemblages are uncertain as both the M_2 assemblages and hornfels assemblages would be of a similar P-T regime.

Internally, the batholith is a composite body consisting of islands of quartz diorite enclosed in two types of granite (Figs. 28 and 29).

Spotted quartz diorite, a mesocratic equigranular gneissic rock with mafic minerals mostly concentrated in isolated small (5-10 mm) lenticular aggregates, constitutes small bodies and isolated outcrops mainly in the southeastern part of the batholith (Fig. 28). Plagioclase (An_{26} to An_{34}) and quartz predominate over subordinate K-feldspar; the ratio of hornblende to biotite is variable but the latter usually predominates. Mineralogy, texture, and chemical composition (Table 18, Figs. 30, 31, 32) including the REE abundances (Fig. 33) are close to the Maskwa Lake quartz diorite and to the tonalitic gneiss of units (9) and (12) respectively. The relatively high $\delta^{18}O$, 8.1 and 8.3, is also distinctive (Longstaffe et al. 1981).

TABLE 18. REPRESENTATIVE CHEMICAL ANALYSES OF THE LAC DU BONNET GRANITE COMPLEX (17)

	Spotted quartz diorite		Porph. hb-bi granodiorite	Leucogranite		Porphyritic biotite granite		Biotite granite	
	AEC-43	PG 151	SR149	SR 95	PG 137	AEC 10	AEC4	AEC 21	PG133
SiO_2, wt. %	68.30	69.60	69.05	76.30	77.75	72.60	73.85	72.65	73.40
Al_2O_3	15.14	16.82	13.96	12.10	11.53	14.92	14.76	14.46	13.62
TiO_2	0.42	0.11	0.53	0.10	0.06	0.16	0.17	0.17	0.11
Fe_2O_3	1.50	0.92	2.26	0.96	0.92	0.78	0.74	0.76	0.97
FeO	2.32	1.40	1.60	0.76	0.52	0.40	0.22	0.76	0.72
MnO	0.09	0.07	0.06	0.05	0.01	0.02	0.01	0.03	0.03
MgO	1.84	0.50	1.43	0.04	0.05	0.43	0.28	0.40	0.45
CaO	2.84	3.13	2.45	0.32	0.34	0.88	0.97	1.01	1.06
Na_2O	4.85	5.43	3.33	3.48	3.66	3.00	3.15	3.65	3.56
K_2O	1.66	1.66	3.98	5.17	4.94	5.79	5.47	5.02	5.63
P_2O_5	0.20	0.13	0.17	0.03	0.02	0.09	0.11	0.09	0.08
CO_2	0.12	0.06	0.09	0.08	0.03	0.21	0.19	0.09	0.04
H_2O	0.68	0.39	0.78	0.24	0.21	0.72	0.56	0.51	0.35
	99.96	100.20	99.69	99.62	100.04	100.00	99.90	99.60	100.02
Li, ppm	148	46	33	72	10	43	17	49	57
Rb	179	65	96	370	154	180	117	224	231
Cs	4.2	1.6	1.3	2.7	2	0.9	0.4	2.6	4.9
Be	5.0	1.9	1.4	2.2	2	1.8	0.8	2.5	2
Sr	208	136	363	2	28	169	169	150	225
Ba	94	967	1065	52	145	707	614	675	926
Pb	5	10	14	15	12	22	19	26	22
Ga	38		20	34	30	23	27	33	28
U	2	8	4	14	6	5	nd	26	2
Th	6	nd	21	40	15	28	40	24	16
Zr	134	406	204	142	217	182	152	217	212
Hf	3.65	11.75		7.75	6.75	6.15		6.15	6.0
Sn	10	4	4	11	12	9	13	4	5
K/Rb	77	212	344	115	266	267	388	186	202
K/(Cs x 100)	32	86	253	158	205	533	1135	160	95
K/Ba	147	14.25	31	825	289	68	73.9	61.8	50
Ba/Rb	0.52	14.9	11.1	0.14	0.94	3.9	5.25	3.0	4
Ba/Sr	0.45	7.1	2.9	26	5.2	4.2	3.6	4.5	4.12
Rb/Sr	0.86	0.48	0.3	185	5.5	1.1	0.7	1.5	1.03
Mg/Li	75	65.6	261	2.9	30	60.5	100	49	47.4
Zr/Sn	13.4	101.5	51	12.9	18.1	20.2	11.7	54.2	42.4
Zr/Hf	36.7	34.6			32.1	29.6			35.3
Al/Ga	2108		3695	1882	2033	3430	2893	2318	2574
La, ppm	55.2	30.6		35.85	39.9	43		41.4	87.1
Ce	105	61.5		97	76	91		87.5	153
Nd	39.5	25.5		44	39	29		33.5	78
Sm	5.60	3.82		9.59	6.79	3.84		5.48	5.94
Eu	0.76	1.7		0.18	0.25	0.59		0.51	0.69
Dy	2.95	2.45		12.05	6.3	1.4		2.2	1.2
Yb	1.7	1.9		7.5	4.95	0.7		1.25	1.25
Lu	0.16	0.24		0.92	0.59	0.08		0.20	0.13

* not detected

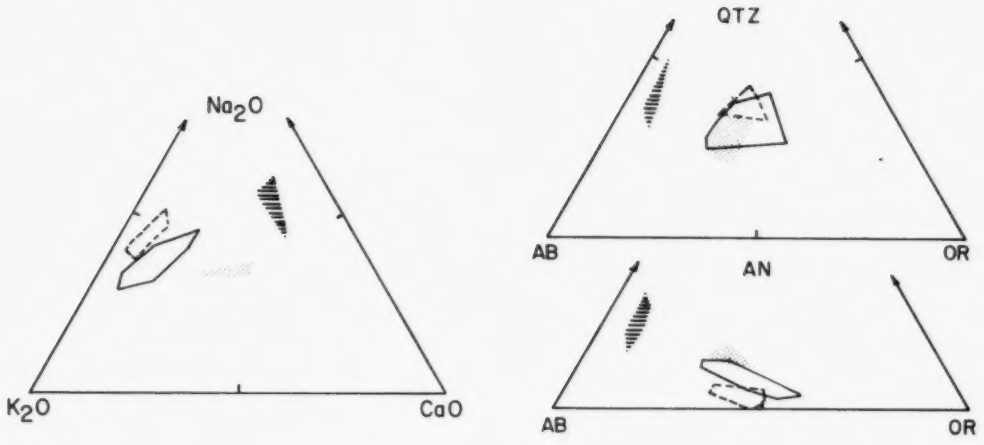

Figure 30: Ternary relationships in the Lac du Bonnet batholith: spotted quartz diorite (ruled field), hornblende-biotite granodiorite (dotted field), biotite granite (solid outline) and leucogranite (dashed outline)

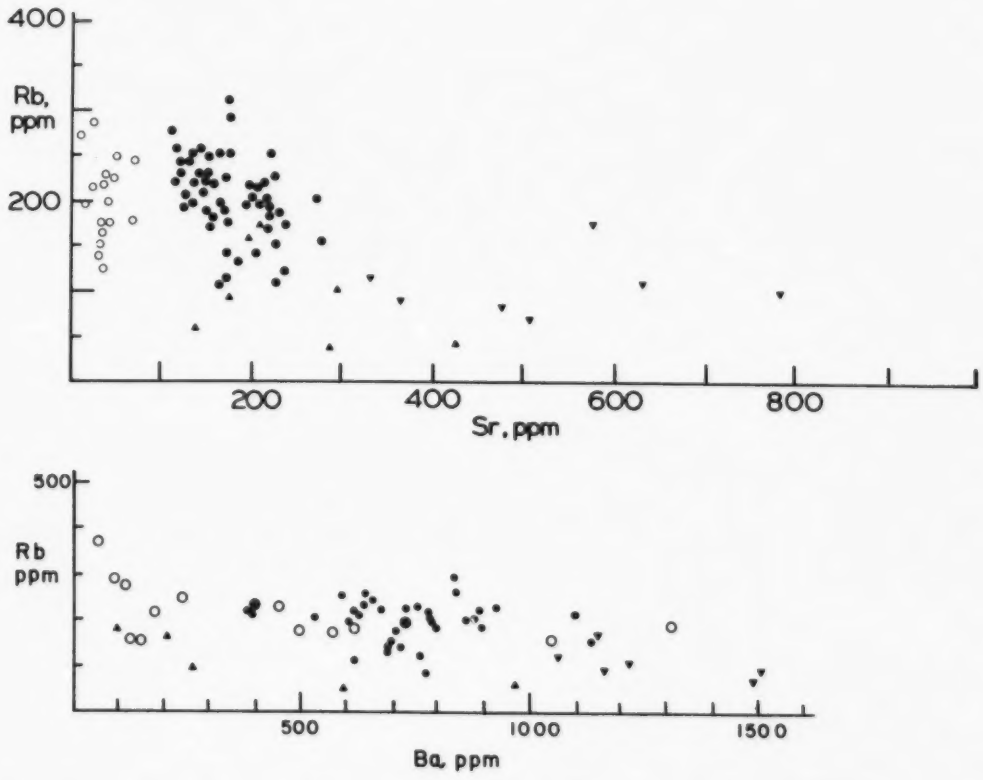

Figure 31: Rb vs. Sr and Rb vs. Ba relationships in rocks of the Lac du Bonnet batholith: spotted quartz diorite (triangles), hornblende-biotite granodiorite (inverted triangles), biotite granite (solid dots) and leucogranite (open circles)

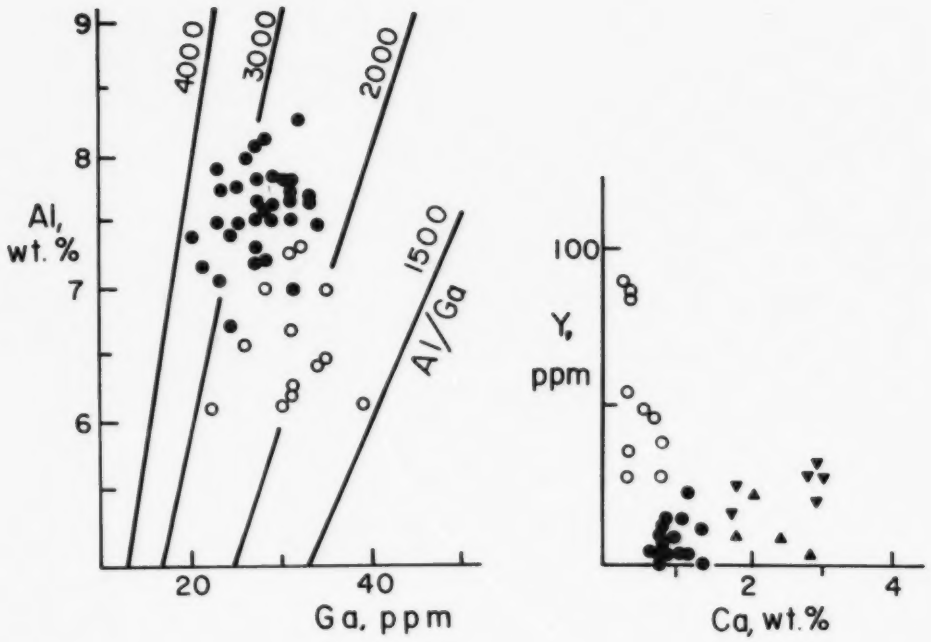

Figure 32: Al vs. Ga and Y vs. Ca relationships in rocks of the Lac du Bonnet batholith. Symbols as in Fig. 31

Porphyritic hornblende-biotite granodiorite is a gneissic, mesocratic greenish-grey rock with abundant white to pink feldspar phenocrysts (5 to 25 mm), rather uniformly oriented subparallel to foliation. It comprises isolated outcrops in a predominantly swamp-covered terrain close to the eastern tip of the batholith (Figs. 28, 29). Plagioclase (clouded with patchy zoning, An_{38} to An_{32}) and K-feldspar are subhedral to euhedral, surrounded by a fine grained assemblage of green hornblende, mostly green biotite, opaque minerals replaced by titanite and magnetite, and subordinate quartz. Bulk composition (Table 18. Fig. 30) of this granodiorite differs from that of the spotted quartz diorite mainly by considerably increased K-feldspar content and somewhat lower quartz percentage. In terms of trace elements, very high Ba and Sr are characteristic. REE abundances show considerable fractionation Ce_N/Yb_N averaging at 30.5), and only faint negative Eu anomalies (Table 18, Fig. 33). Two samples analyzed for oxygen isotopic composition show $\delta\ ^{18}O$ values 7.4 and 7.8 (Longstaffe et al. 1981).

Leucogranite composes the eastern extremity of the batholith, and is also widespread in the area northwest of Pointe du Bois (Map 1, Figs. 28, 29). In the latter area, it exhibits strong subvertical lineation marked by rod-shaped aggregates of biotite and K-feldspar (Fig. 34), locally grading into foliation. In the eastern tip of the intrusion, no preferred orientation of mineral constituents can be observed; the rock is massive, with grains of smoky quartz somewhat larger than the other minerals, but pervasively deformed.

The lineated type exhibits banded granulation and recrystallization of most of its components (Fig. 35) whereas the massive variety shows a typical igneous granitic texture. Plagioclase is very acid, between An_5 and An_3. Locally, mucovite seems to be a primary constituent in very subordinate amounts. Biotite is usually accompanied by apatite and zircon; allanite is rare. Garnet was identified in only one specimen.

Scattered pegmatite schlieren and veinlets cross-cutting the leucogranite carry accessory biotite, garnet, and allanite.

High silica content, very low CaO, and high Fe/Mg ratio are the most conspicuous characteristics of the bulk composition (Table 18, Figs. 30 and 36). Among trace elements, extremely low Sr, low Al/Ga and Mg/Li ratios, and high Y are typical compared to other phases of the intrusion. Ba is variable in a rather erratic manner; the range shown by Rb is also relatively broad but densely populated throughout (Figs. 31, 32). The REE patterns show very pronounced negative Eu anomalies and high HREE contents (Fig. 37). The average normative corundum (CIPW) is 0.27%, and the low $\delta\ ^{18}O$ values are clustered between 7.4 and 8.3 (Longstaffe et al. 1981).

In general, the leucogranite shows a very advanced degree of fractionation, except for the scatter of high Ba values and relatively intermediate Rb concentration; it differs substantially from the granitic rocks of the Maskwa Lake, Marijane Lake, and Inconnu batholiths.

Biotite granite composes the bulk of the central and western parts of the intrusion and is predominant over the total of all other phases in the batholith. Most of the biotite granite is rusty pink, equigranular, fine- to medium-grained, with a low content of randomly oriented biotite; faint foliation is developed only along contacts with the enclosing Bird River greenstones, and with the leucogranite which is older, crosscut, and in brecciated portions cemented by the biotite granite. In the central parts of the batholith, the biotite granite is porphyritic carrying K-feldspar phenocrysts up to 3 cm in size.

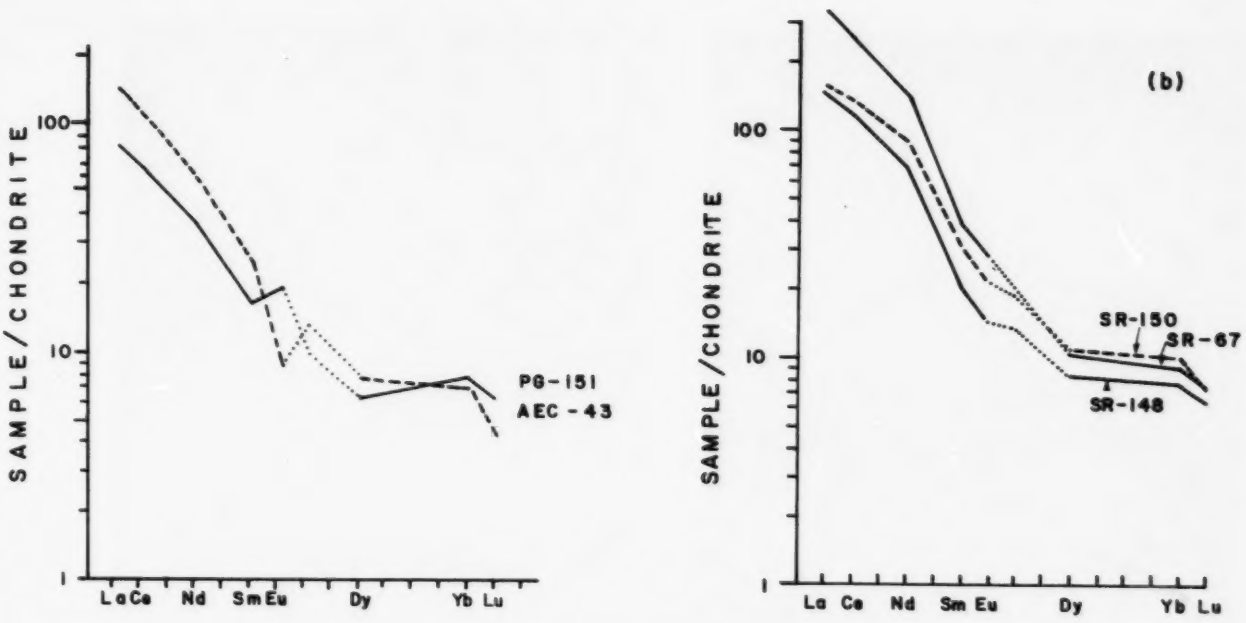

Figure 33: REE abundances in the (a) spotted quartz diorite and (b) hornblende-biotite granodiorite of the Lac du Bonnet batholith

Figure 34: Leucogranite, Lac du Bonnet batholith; sections subparallel (top) and normal (bottom) to lineation

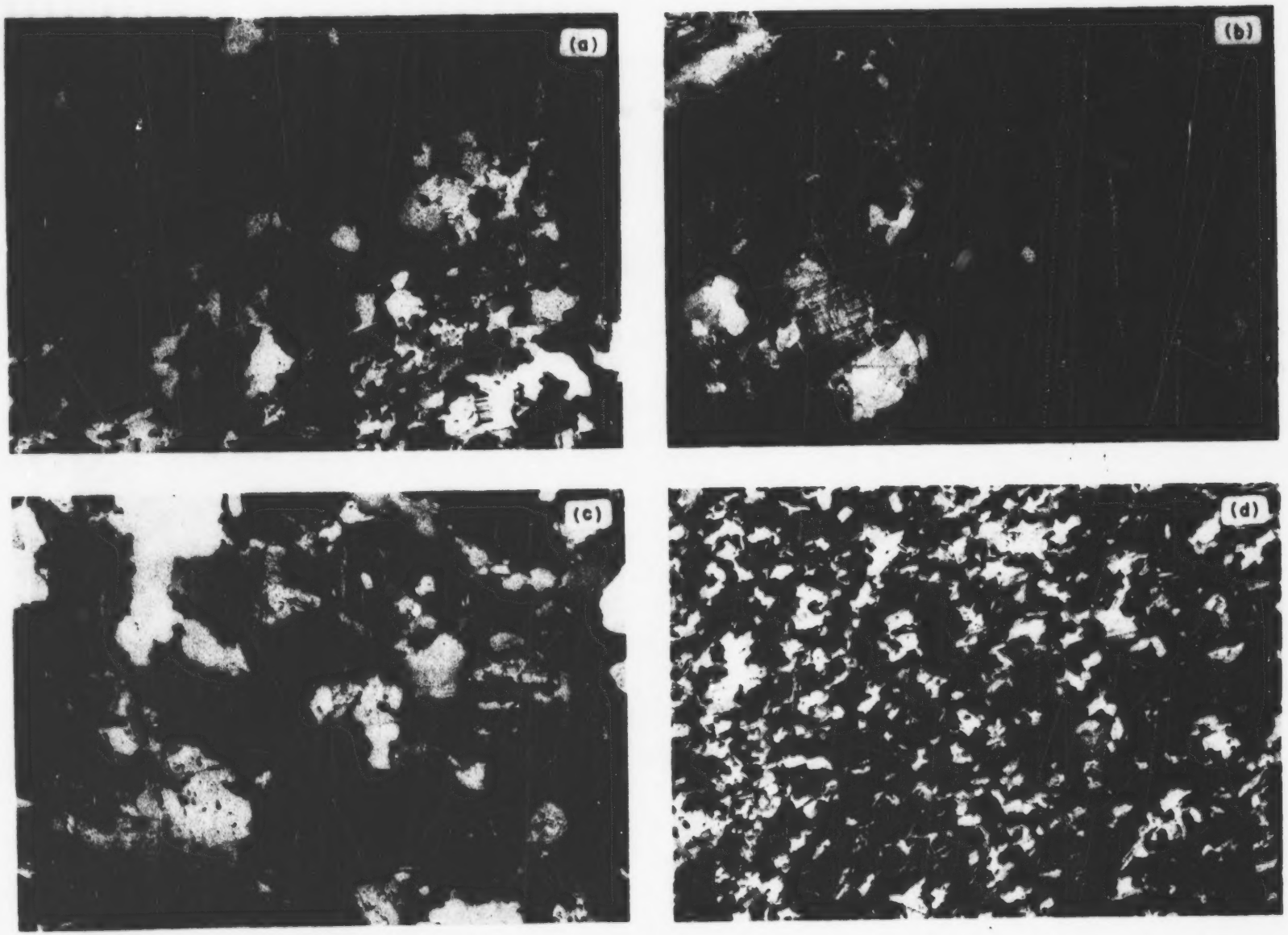

Figure 35: Typical textures of (a) sheared and partly recrystallized Lac du Bonnet leucogranite, (b) primary igneous Lac du Bonnet biotite granite, (c) fine grained leucogranite of the pegmatitic granites, and (d) aplitic phase of the pegmatitic granites

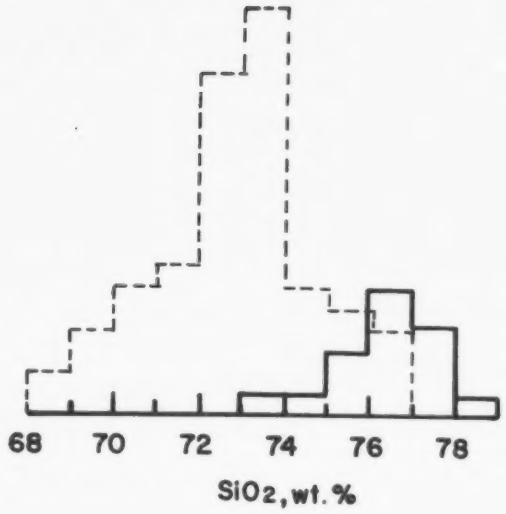

Figure 36: SiO_2 frequencies in the leucogranite (solid outline) and biotite granite (dashed outline) of the Lac du Bonnet batholith; the height of the shortest column corresponds to a single sample

Pegmatite pods and veins contain biotite and allanite as their main accessory species.

Microscopically, the biotite granite exhibits a typical hypidiomorphic granular texture (Fig. 35). Subhedral to euhedral plagioclase (An_{15} to An_{20}) is rimmed by a clear zone of albite, and myrmekite occurs along contacts with mostly anhedral perthitic K-feldspar. Biotite is frequently partly chloritized, and associated with magnetite, apatite and zircon. Hornblende occurs only rarely as a relict mineral from digested fragments of quartz diorite. Further details are provided by McRitchie (1971).

Compared to the leucogranite, the biotite granite is much less fractionated (Table 18, Figs. 30 to 32). Lower SiO_2, Fe/Mg, Pb, Be, Y, and Mg/Li, and higher CaO, Al_2O_3, MgO, TiO_2, Sr and Al/Ga separate it from the former; FeO, Fe_2O_3, Na_2O, K_2O, MnO, Sn, Rb, and Cs remain about the same in both types. Ba is again widely scattered over a range of 380-1140 ppm; it seems to be affected by digestion of quartz diorite which is mostly Ba-rich. The REE abundances (Fig. 37) closely resemble those of the granitic components in the Maskwa Lake and Marijane Lake batholiths, with moderate to small negative Eu anomalies and low concentration levels of the HREE. The average normative corundum content (CIPW) is 0.81%, and the oxygen isotopic composition is within $\delta^{18}O = 7.5 - 9.6$ (Longstaffe et al. 1981).

In general, the biotite granite is less fractionated than the early leucogranite, and the two rock types cannot be related by any simple igneous differentiation or incremental partial melting mechanism. In contrast, the composition of the Lac du Bonnet biotite granite closely resembles the granitic phases of the Maskwa Lake and Marijane Lake batholiths.

Pegmatitic granites and pegmatites (18)

Pegmatitic granites and pegmatites represent the latest intrusions formed in the area, postdating all sedimentary, metamorphic and intrusive events preceding and marking the Kenoran orogeny. Detailed treatment of both rock types is given in the following two sections.

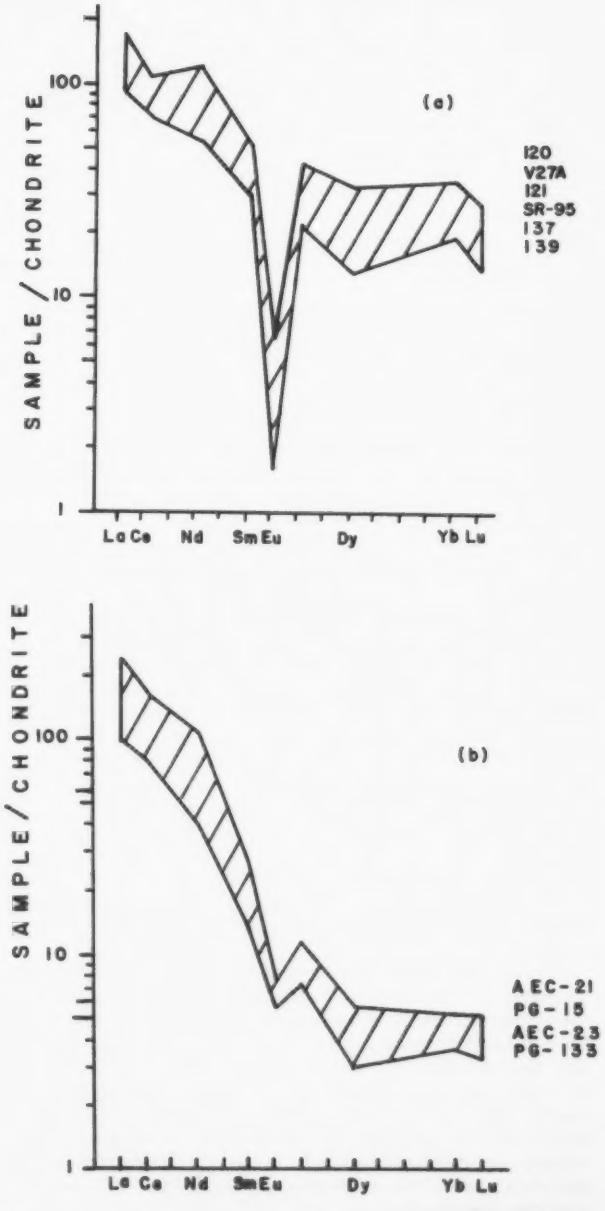

Figure 37: REE abundances in the leucogranite (a) and biotite granite (b) of the Lac du Bonnet batholith

PEGMATITIC GRANITES

Major pegmatitic granite bodies are centred north of Greer Lake, west of Eaglenest Lake, at Tin Lake, and east-northeast of Osis Lake (Map 1, Figs. 38 to 41). They have been named accordingly. A small occurrence of pegmatitic granite, the Axial intrusion, is located southeast of Tin Lake (Map 1); it was examined in much less detail than the four bodies quoted above. To avoid repetition and to emphasize similarities and differences among the major intrusions, individual characteristics are given below jointly for all four major bodies.

Structural location and intrusive style

Several features common to the structural setting of all four pegmatitic granites can be identified. All were intruded along, or flank, early subvertical faults and shear zones which give the greenstone belt its present fault-slice configuration (Map 1). Intrusion took place along dilation zones and was combined with stoping; the latter is not directly observable in the Greer Lake and Eaglenest Lake bodies but can be assumed from the character of the contacts. Evidence of forceful injection is scarce and restricted to the eastern part of the Osis Lake body.

The pegmatitic granite at Greer Lake is hosted largely by metabasalt, with which it displays sharp contact. At the east and west extremities of the Greer Lake body and at the Silverloaf offshoot, the intrusion's contacts trend north at a high angle to the layering and foliation of the metabasalts. These contacts are knife-sharp, truncating both layering and foliation with no evident deformation. Internal dykes are almost absent, as is inclusion material in the pegmatitic granite (except angular blocks of metabasalt in the Silverleaf offshoot).

A fault, striking west-northwest and transecting the Greer Lake body, appears to display predominantly vertical movement separating the body into two zones. This finds additional confirmation in geochemical parameters across the two zones (as discussed below). The fault is marked by the presence of a banded iron formation which extends through the stratigraphy to the west of the body, and which otherwise lies undisturbed in the pegmatitic granite. The iron formation also appears correlative with a unit of iron formation south of the Eaglenest Lake pegmatitic granite. It further appears likely that the pegmatitic granite is also truncated under Greer Lake by the fault marking the boundary between the Bird River Greenstone Belt and the Winnipeg River Batholithic Belt.

The Eaglenest Lake pegmatitic granite lies in the same approximate stratigraphic level as the Greer Lake body but, in contrast to the other pegmatitic granite bodies, can be considered distinctly elongated along both the layering and foliation of its metabasalt host. The body is otherwise identical to that at Greer Lake in that it contains only rare inclusions and its western extremity is sharply truncated against the layering and foliation in the relatively undeformed host rocks. The eastern end, however, displays predominantly a *lit-par-lit* fingering-out pattern in a pronouncedly foliated host.

The Tin Lake pegmatitic granite is a roughly circular stock or plug, separated into two lobes by a cataclastic shear zone which follows the northern boundary of the subvolcanic intrusion centred at Birse Lake. Smaller irregular bodies of pegmatitic granite extend west-northwest and east-southeast from the northern lobe mainly north of the shear zone; they appear to be mostly concordant sills in the clastic volcanic and intrusive rocks of the Bernic Lake Formation which hosts all members of the intrusion. The northern lobe is virtually free of host inclusions but in the southern part they are very abundant, giving the pegmatitic granite a local appearance of agmatitic injection breccia.

The Osis Lake body is located north of the boundary fault separating structural subareas 4 and 5, except for several dyke-like offshoots in its southwestern extremity that transgress to the south. It is hosted by the metaturbidites of the Booster Lake Formation. From east-central parts to the west, the intrusion grades from a more or less homogeneous inclusion-poor body, through an area with abundant subparallel and subvertical rafts and screens of host rocks, into a fingering-out system of mutually parallel dykes which range from several tens of metres to several centimetres in thickness. Though varied in orientation the dykes and masses separating the rafts and screens are mainly concordant, and follow both the layering and foliation of the host turbidites in the limbs of a major conical fold (cf. structural subarea 5, p.).

In its southeastern extremity, the Osis Lake body gives the impression of forceful intrusion (Fig. 42); in the western part, dilation and brittle fragmentation of the host rock is evident (Fig. 43) but plastic behavior is also documented by localized ptygmatic structures (Fig. 44).

Internal composition

The pegmatitic granite intrusions are heterogeneous; all contain bodies of pegmatitic leucogranite, patches of fine grained leucogranite transitional into commonly banded sodic aplite, and lenticular to pod-shaped potassic pegmatite.

Pegmatitic leucogranite is always a substantial, and mostly dominant phase of the pegmatitic granites. Its most conspicuous component is megacrystic K-feldspar (5-100 cm in size) intergrown with graphic quartz, suspended in a medium- to coarse-grained groundmass of albite plagioclase+quartz+muscovite, ± garnet and/or tourmaline (Fig. 45).

The K-feldspar megacrysts may be perfectly euhedral or corroded to various but usually moderate degrees by the groundmass. The groundmass locally contains patches of a plumose muscovite+quartz intergrowth (Fig. 46), which is evenly distributed but locally resembles a late replacement assemblage (Fig. 47).

Along contacts with country rock xenoliths, the graphic K-feldspars tend to grow from the xenolithic substrate into the pegmatitic granite mass (Fig. 48).

Fine grained leucogranite is an equigranular phase consisting of perthitic microcline, quartz, albitic plagioclase, and muscovite; biotite is abundant only in the Tin Lake intrusion, rare in the others. Accessory minerals are represented mainly by garnet, zircon, and apatite. The rock is mostly massive and homogeneous in mineral distribution but faint banding of micas and garnet is evident locally (Fig. 49).

The transition from fine grained leucogranite into *sodic aplite*, which commonly exhibits banded texture (Fig. 50), is marked by an increase in muscovite, albitic plagioclase (which attains platy habit) and garnet, and gradual disappearance of K-feldspar. The composition is typically albitic plagioclase, quartz, muscovite, garnet, and accessory apatite, gahnite, monazite, and possibly Nb-Ta oxide minerals (in order of decreasing abundance; Fig. 51).

Sodic aplite bands are mostly paired or alternating with *potassic pegmatite* bands (Figs. 50, 52). The boundary may be gradual or, more typically, sharp, and it indicates a directed growth of the pegmatitic assemblage normal to the aplite surface. The potassic pegmatite consists of blocky (or partly graphic) K-feldspars and quartz, commonly in concentric zoned patterns, with or without coarse platy muscovite and granular or cleavelandite-type albite. Beryl, columbite-tantalite, triphylite, and arsenopyrite appear sporadically in central parts of the pegmatite bands (Fig. 53).

The potassic pegmatite phase also develops as lenticular bands and pods inside pegmatitic leucogranites, by gradual disappearance of graphic quartz from K-feldspar megacrysts and by their accumulation, at the expense of the albite+quartz+muscovite matrix, around lenses of quartz (Fig. 54).

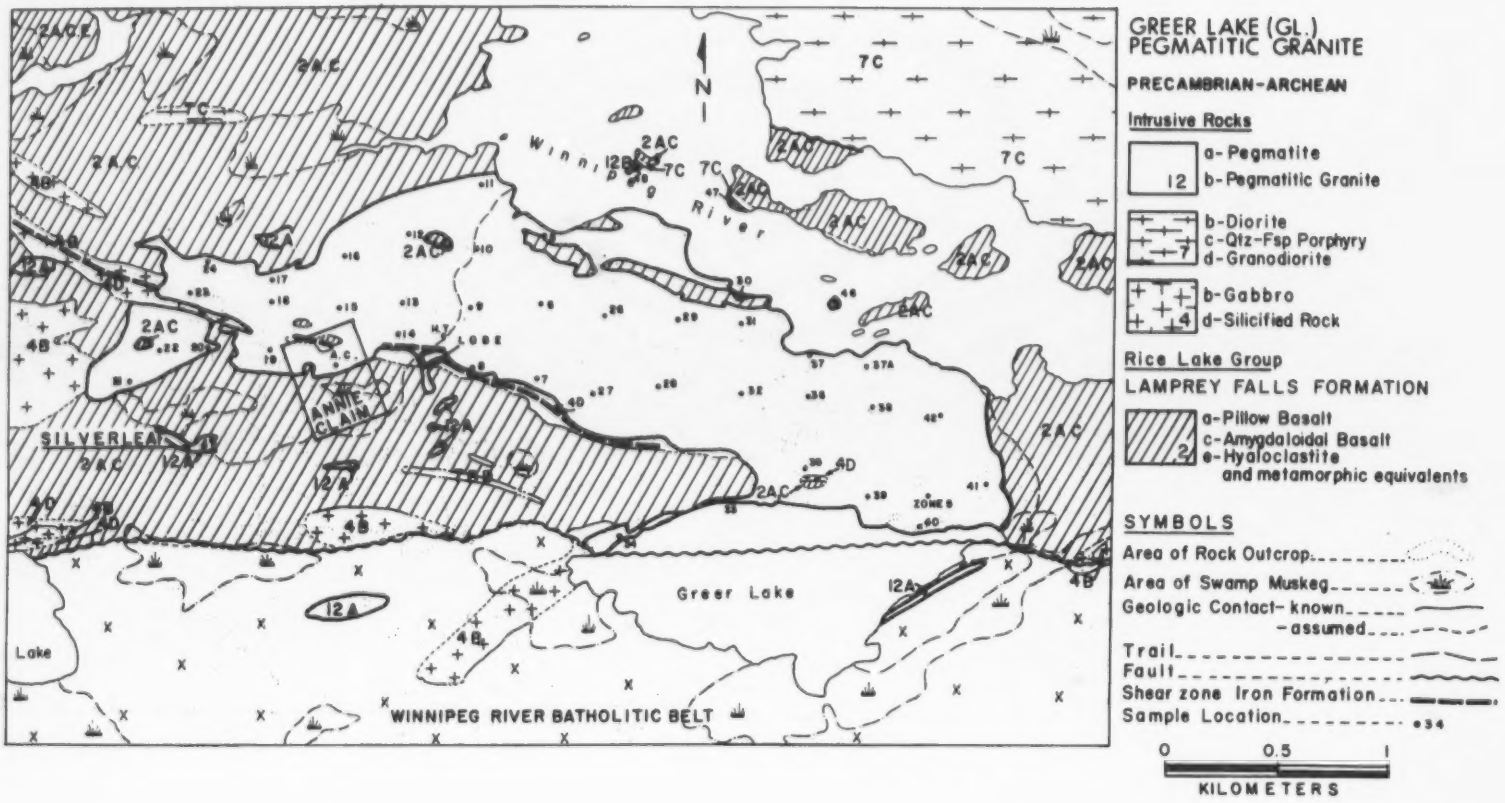

Figure 38: Geology and sampling locations of the Greer Lake pegmatitic granite. Geology after Davies (1955, 1957) and Trueman (1980). From Goad (in prep.)

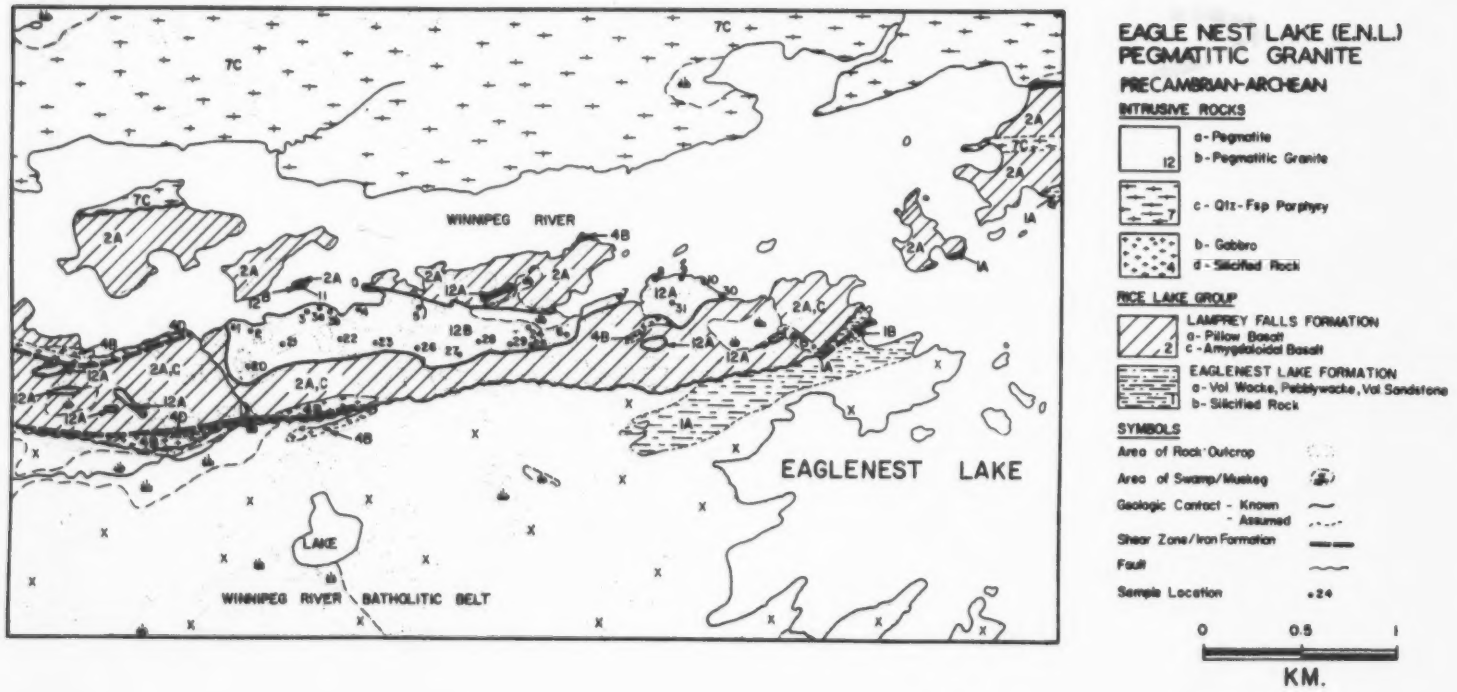

Figure 39: Geology and sampling locations of the Eaglenest Lake pegmatite granite. Geology after Davies (1955, 1957) and Trueman (1980). From Goad (in prep.)

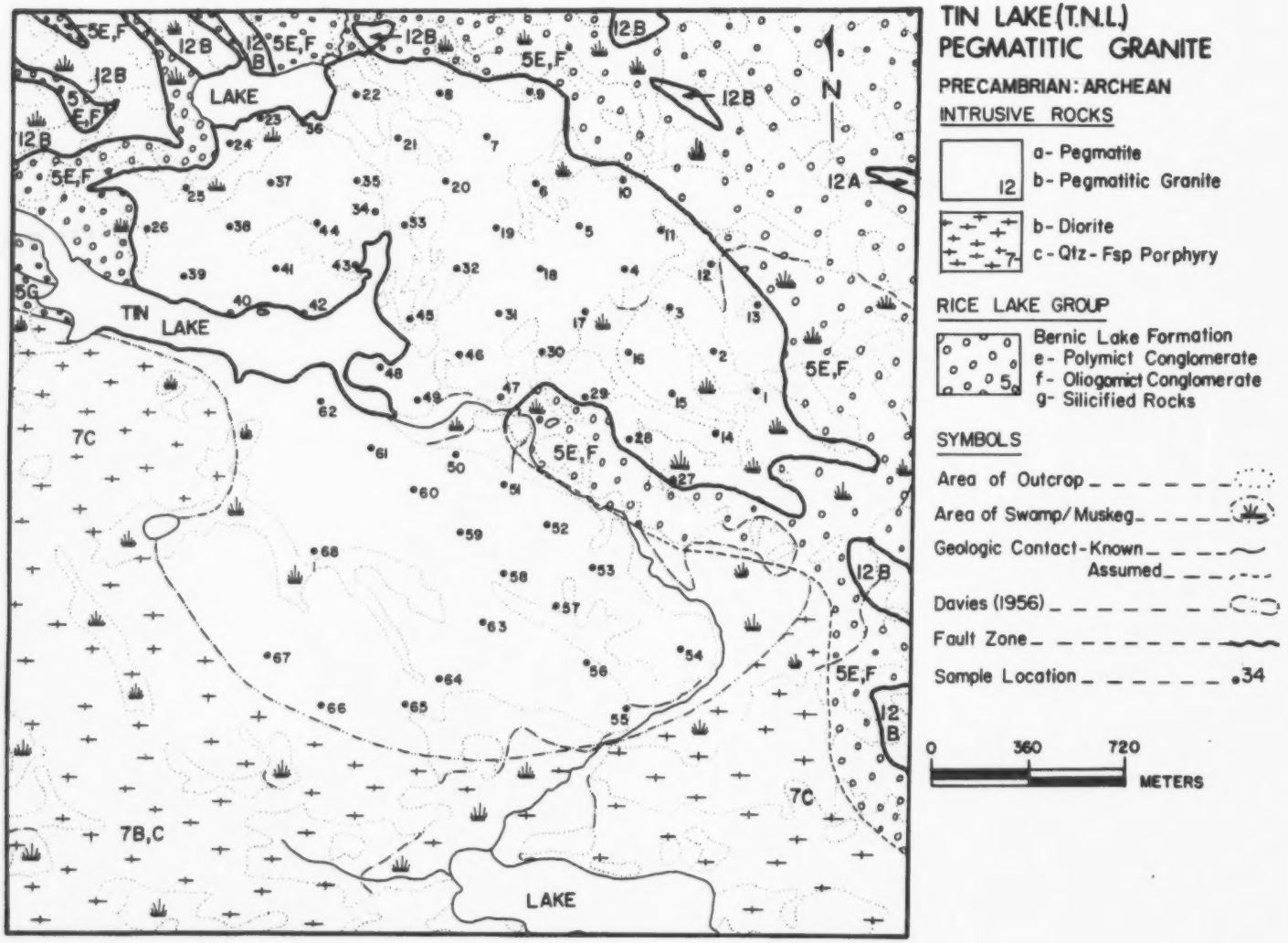

Figure 40: Geology and sampling locations of the Tin Lake pegmatitic granite. Geology after Davies (1955, 1957) and Trueman (1980). From Goad (in prep.)

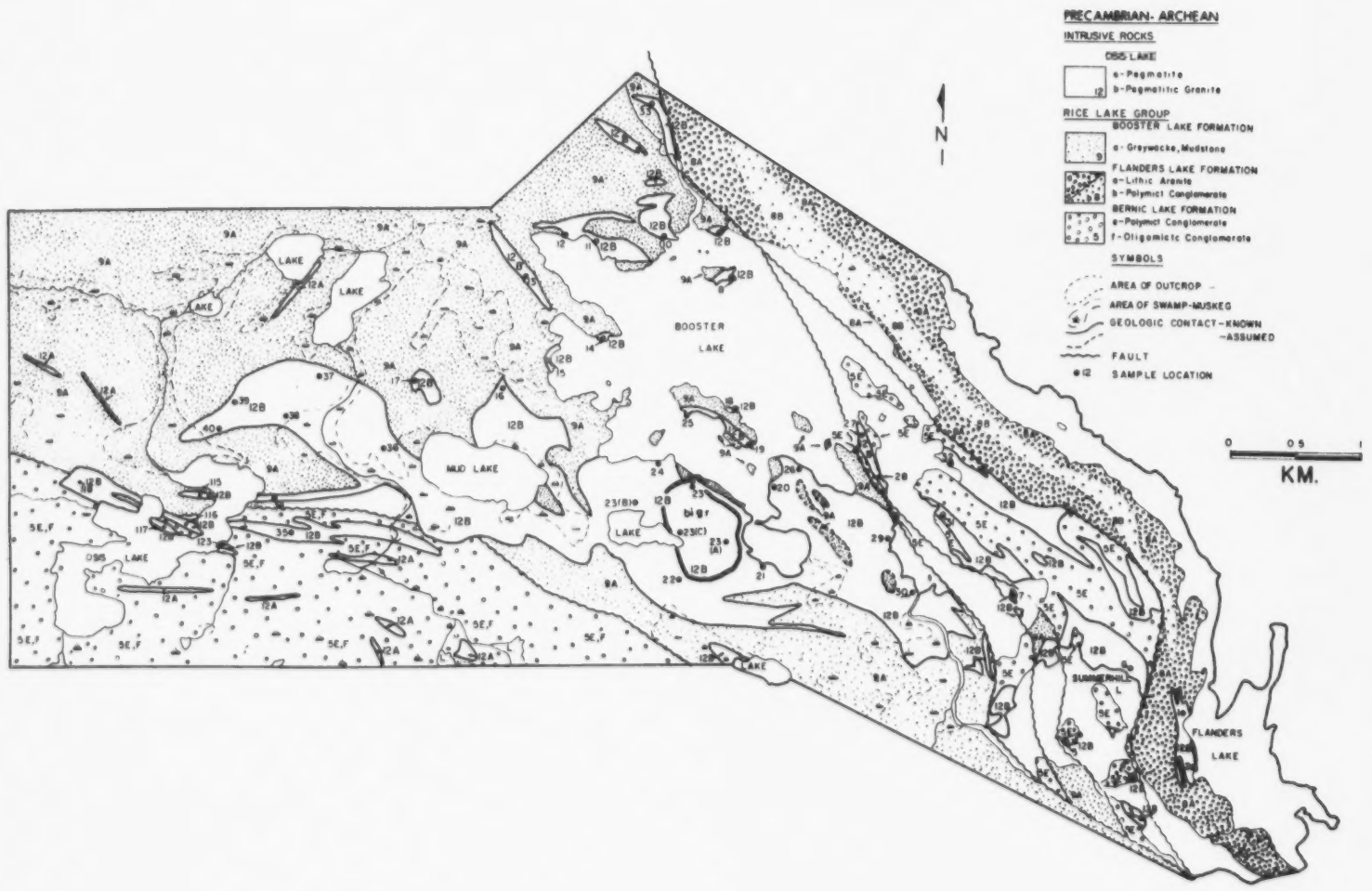

Figure 41: Geology and sampling locations of the Osis Lake pegmatite granite and its central biotite granite plug. Geology after Davies (1955, 1957) and Trueman (1980). From Goad (in prep.)

Figure 42: Warping and contortion of metapelites in the southeastern tip of the Osis Lake pegmatitic granite, suggestive of forcible intrusion of the latter; the vertical edge of the photo is approximately 70 cm long

Figure 43: The Osis Lake pegmatitic granite filling-in dilation fractures in metapelites of the Booster Lake Formation, characteristic of the western part of the intrusion; note the almost perfect match of the metapelitic slab boundaries

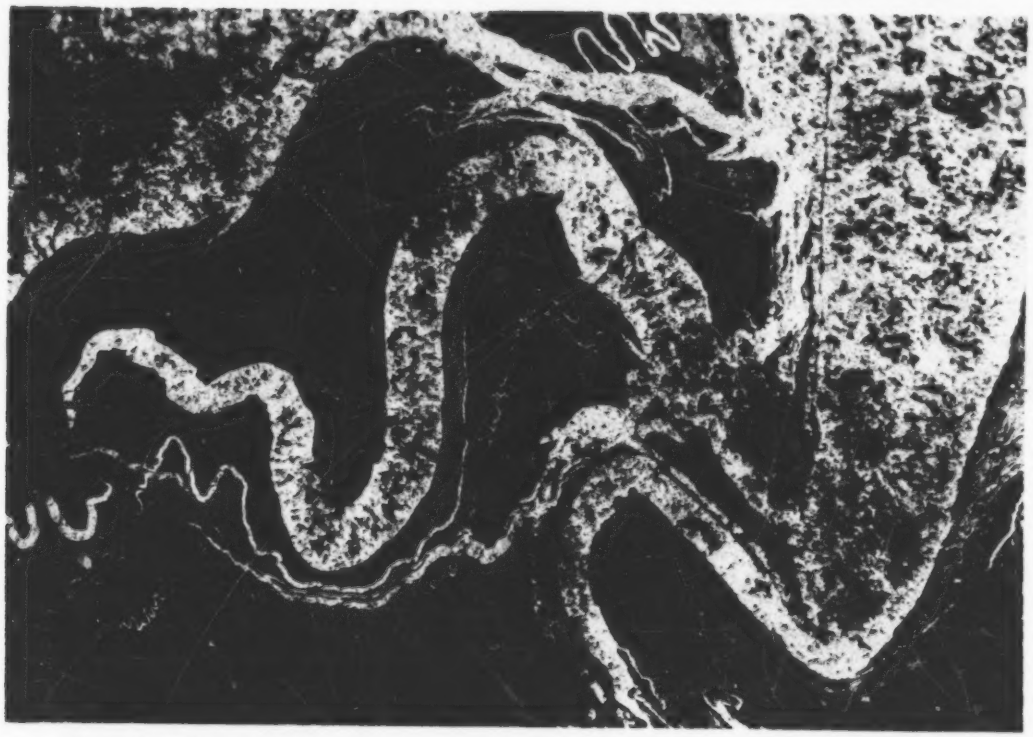

Figure 44: Ptygmatic folding of pegmatitic granite stringers typical of some metapelitic rafts in the western extremity of the Osis Lake intrusion

Figure 45: Pegmatitic leucogranite, Osis Lake body; light-coloured subhedral K-feldspar with graphic quartz in a groundmass of albite, quartz, muscovite, + garnet and tourmaline

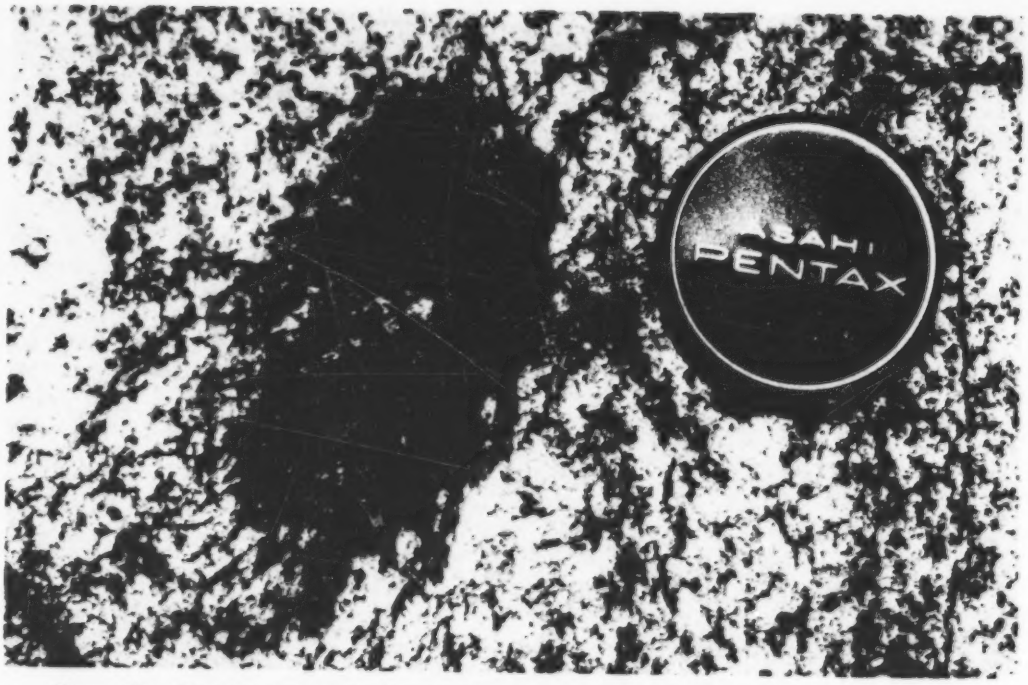

Figure 46: Plumose aggregate of muscovite + quartz in the albitic matrix of pegmatitic leucogranite in the Osis Lake body, radial around a garnet grain

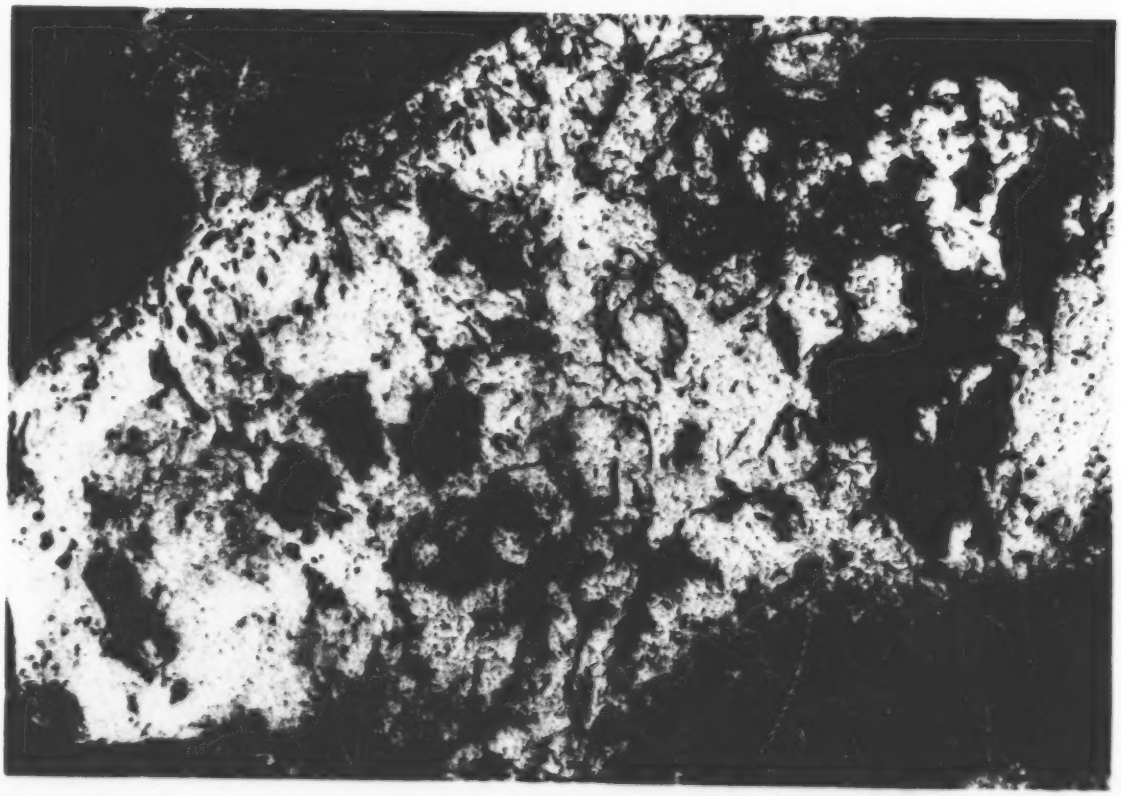

Figure 47: Plumose muscovite + quartz aggregates (dark patches) in white albite + quartz matrix with large K-feldspars (grey); pegmatitic leucogranite phase of the Osis Lake intrusion

Figure 48: A thin, largely tourmalinized screen of metapelitic schist serving as a substrate for oriented growth of club-shaped megacrysts of partly graphic K-feldspar (contoured in ink); note the accumulation of muscovite (dark grains and plates) along the screen. Pegmatitic leucogranite phase of the Osis Lake intrusion

Figure 49: Fine grained leucogranite, Eaglenest Lake pegmatitic granite intrusion: faint banding crosscut by a string of pegmatitic K-feldspars

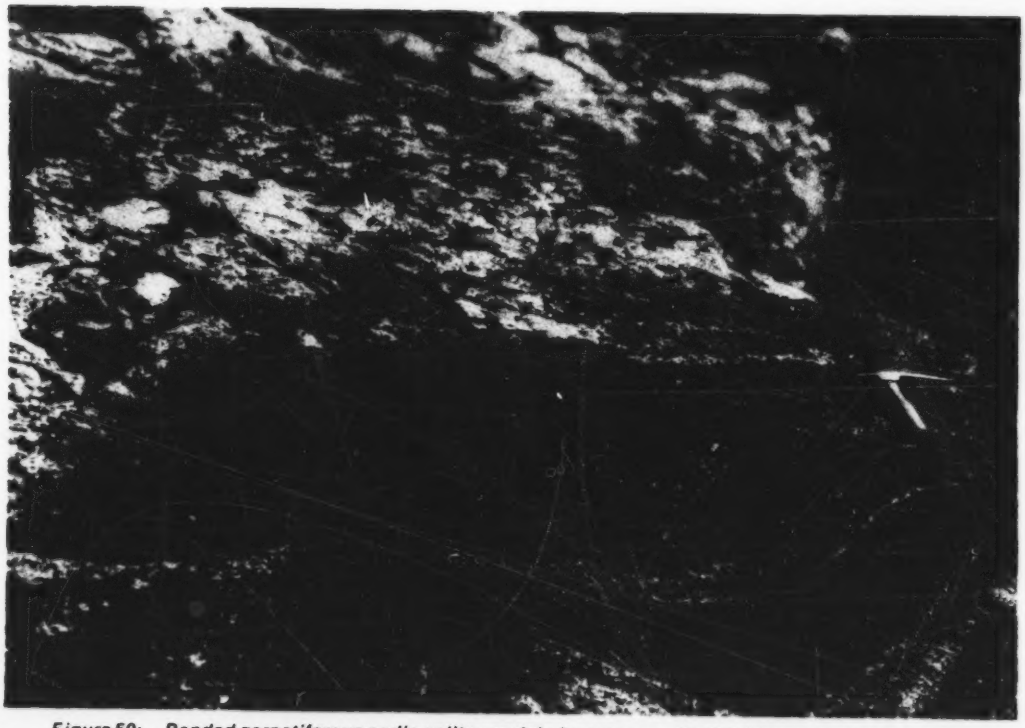

Figure 50: Banded garnetiferous sodic aplite overlain by megacrystic K-feldspar and quartz of the potassic pegmatite phase; Eaglenest Lake pegmatitic granite intrusion

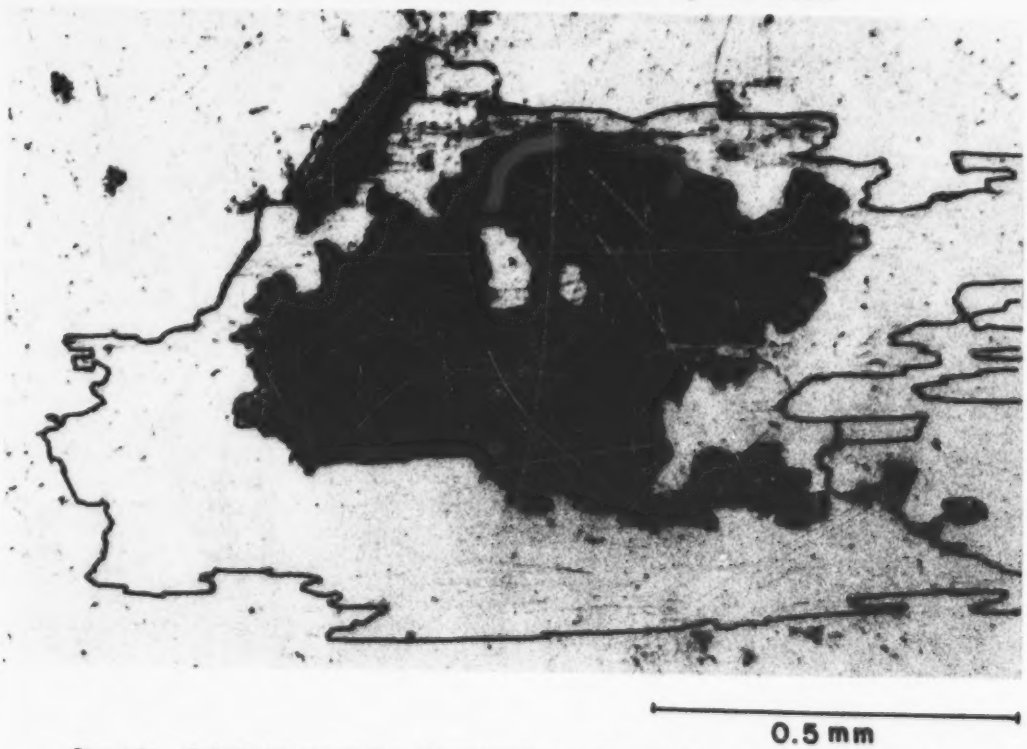

Figure 51: Gahnite (centre, high relief) enclosed in, and corroded by muscovite (outlined in ink) with opaque blades of possible Nb, Ta-oxide minerals; thin section of sodic aplite, Greer Lake pegmatitic granite intrusion

Figure 52: Sharp contacts between banded garnetiferous aplite and potassic pegmatite, Greer Lake pegmatitic granite intrusion: note the growth fabric in the K-feldspar + quartz + muscovite assemblage normal to the boundary

Figure 53: Anhedral block of altered triphylite (6 cm in size, dark in centre) in quartz, K-feldspar and platy muscovite of a potassic pegmatite stringer; Osis Lake pegmatitic granite intrusion

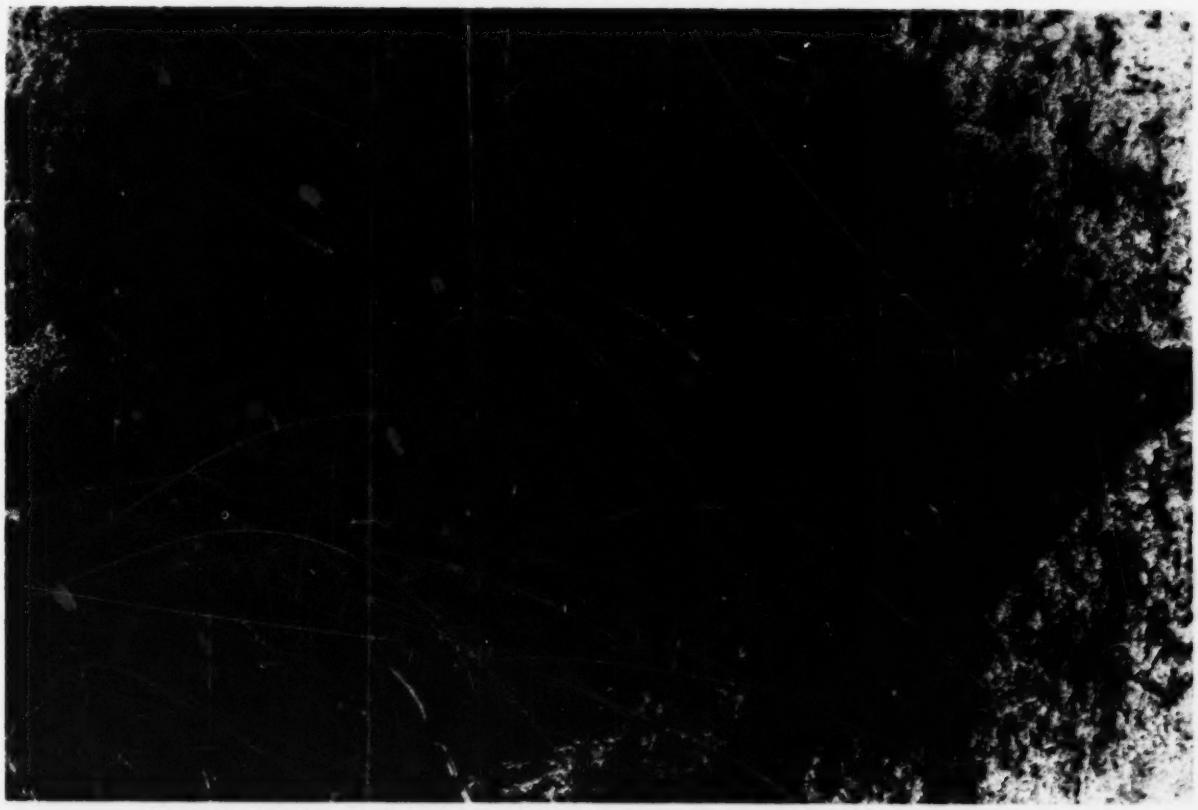

Figure 54: Gradual transition from pegmatitic leucogranite (top and bottom; graphic K-feldspar megacrysts in albite + quartz + muscovite matrix) into potassic pegmatite (blocky K-feldspar and quartz); Osis Lake pegmatitic granite intrusion

Pegmatitic assemblages are the only ones which locally display cross-cutting relationship to the other phases of the pegmatitic granites, indicating that they were the last to solidify (Fig. 55). Stringers and trains of porphyroblastic K-feldspar, transecting textural patterns of fine grained leucogranites and sodic aplites, probably also belong to the late potassic phase (Fig. 49).

Greer Lake and Eaglenest Lake bodies have a good representation of all four phases, with the banded aplitic assemblages oriented roughly parallel to the intrusion margins along the contact but rather chaotic in the interior. The Tin Lake intrusion is exclusively fine grained and leucogranitic in the southern lobe; in the north, pegmatitic material increases in abundance towards the west-northwest, but larger segments of sodic aplite are unusual in all parts of the body. The Osis Lake pegmatitic granite has a good representation of all four phases, in places separated by screens of host rocks (Figs. 48 and 56). In addition, it contains a centrally located subcircular plug of biotitic granite with a classic subsolvus granite texture and random orientation of all minerals. The contacts with the surrounding pegmatitic granite are eroded and covered by soil and vegetation, but they seem to be gradational and show signs of mild shearings.

Accessory minerals

Accessory minerals typical of the four pegmatitic granites are summarized in Table 19. It is evident that garnet is ubiquitous but the Greer Lake and Eaglenest Lake bodies lack tourmaline which is characteristic, in variable quantities, for the two northern intrusions. In terms of the typically pegmatitic accessory minerals, the Greer Lake pegmatitic granite is the most enriched in species of Be, Nb-Ta, and Li; the Osis Lake body carries abundant minerals of Li, P, and As but Eaglenest Lake and Tin Lake intrusions appear barren in comparison.

On the other hand, the Greer Lake and Eaglenest Lake bodies intruding metabasalts along the Winnipeg River are poor in P and particularly in B whereas the northern two bodies in metaturbidites carry abundant P in apatite and triphylite, and they also contain tourmaline which is scarce at Tin Lake but abundant in the Osis Lake body.

Two occurrences of mineralized pods in the Greer Lake intrusion deserve particular notice because of their high fractionation and concentration of rare elements, in which they differ from the ubiquitous potassic pegmatite phase widespread in all four bodies. These are two pods on the Annie Claim along the southern margin of the intrusion, and the Silverleaf occurrence southwest of the main body (Fig. 38). The latter may be considered a separate pegmatite but it is described here as an offshoot of the main mass of the pegmatitic granite, because of its proximity, subvertical attitude, and abundance of garnetiferous aplite atypical in the Greer Lake pegmatites (cf. p.79). The mineral assemblages of these three localities are listed in Table 20; beryl and columbite-tantalite compositions are shown in Figure 57.

The central Annie Claim occurrence (A.C. #2) is an irregular pegmatitic bleb evolving from the surrounding pegmatitic leucogranite through a gradual change in grain size and mica percentage (Fig. 58). The texture of the transitional zone suggests gradual crystallization from the surrounding rock inwards. The western

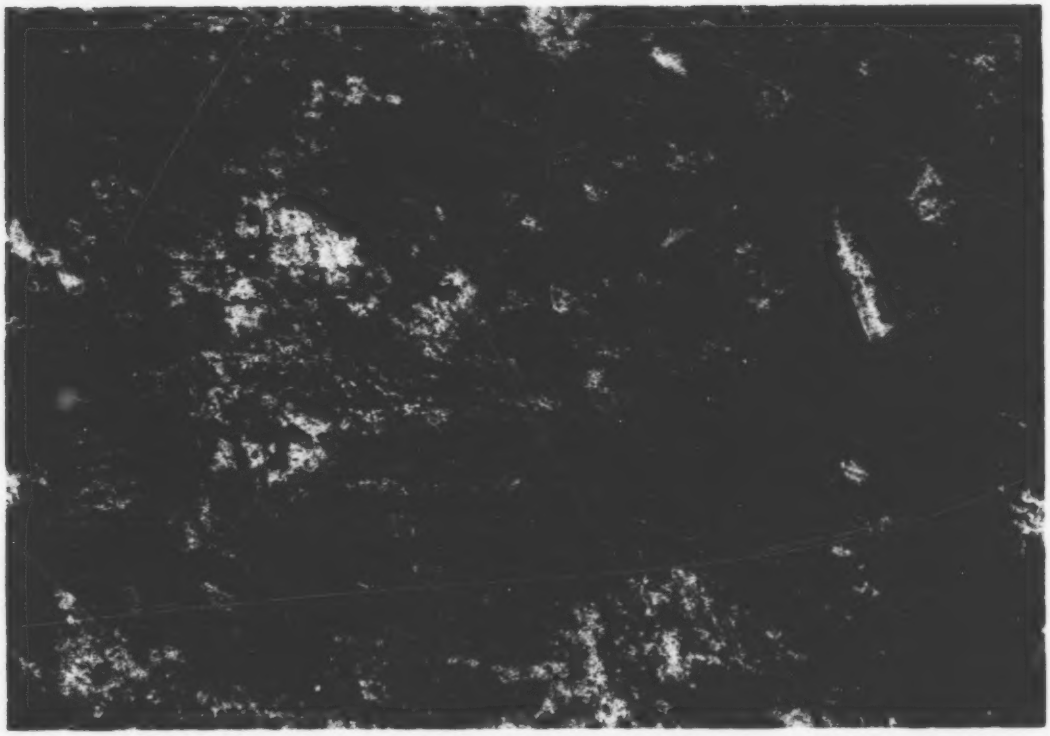

Figure 55: Bands of garnetiferous aplite broken and cemented by an impure potassic pegmatite; Greer Lake pegmatitic granite intrusion

Figure 56: A thin screen of largely tourmalinized metapelitic schist separating aplitic and pegmatitic crystallization regimes in the Osis Lake pegmatitic granite

TABLE 19. ACCESSORY MINERALS IN THE FOUR MAJOR INTRUSIONS OF PEGMATITIC GRANITES

	Greer Lake		Eaglenest Lake	Tin Lake		Osis Lake	
	south*	north		west	east	west	east
biotite				———			
muscovite	———		———	———		———	
garnet	———		———	———		←———	
tourmaline				←·····		←———	
gahnite	– – – – – –		– – – – – – –		·····		·····
cordierite	– – – – – –				– – –		
beryl	– – – – – –						
columbite-tantalite	·····					····	
arsenopyrite	·····		·····				·····
molybdenite				·····			
apatite	·····		·····	———		·····– – →	
triphylite-lithiophilite						←– – –	

common ——— rare – – – – very rare ····· increasing trend ——→

*cf. Table 16 for paragenesis of mineralized pods in the southern part

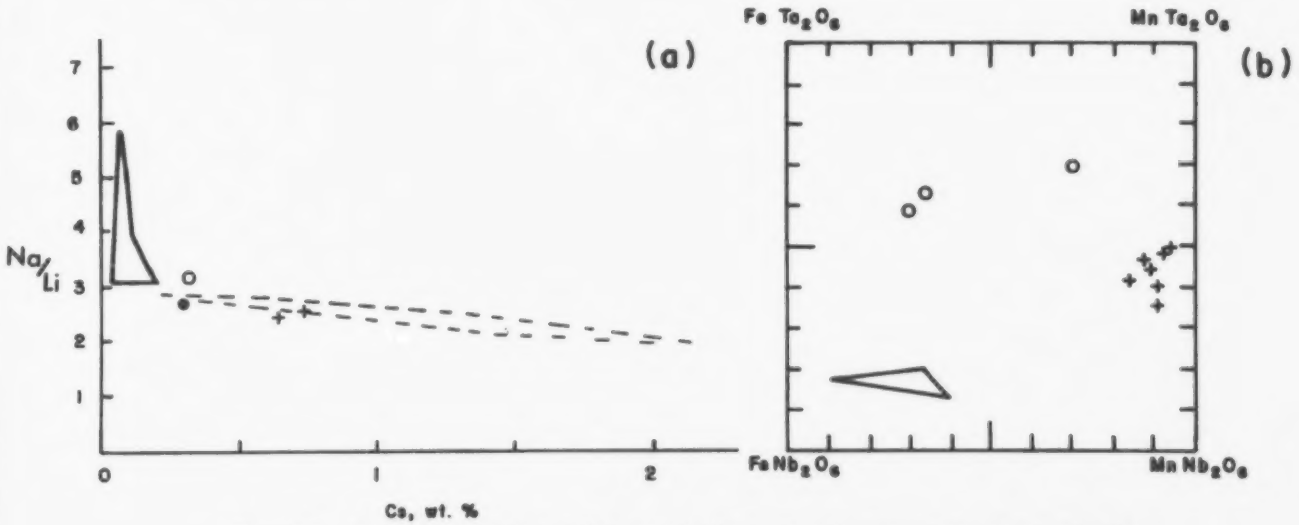

Figure 57: Beryl (a; wt.%) and columbite-tantalite (b; atomic ratios) compositions from the Greer Lake pegmatitic granite: solid outline - potassic pegmatite bands, open circles - A.C. #1, solid dot - A.C. #2, dashed outline A.C. #3, crosses - Silverleaf

Annie Claim locality (A.C. #3) is a subellipsoidal pod with more abrupt but still gradual transition from the surrounding pegmatitic leucogranite, highly enriched in Li, Rb, Cs, Be, and B (Table 20). The Silverleaf offshoot consists largely of garnetiferous aplite with a large rounded pod of the Li, Rb, Mn, Nb-Ta, and Sn-enriched pegmatitic assemblage (Table 20, Fig. 59).

Reaction with wall rocks

Along the meager contact exposures of the Greer Lake and Eaglenest Lake intrusions, reaction with metabasalts is restriced to very limited recrystallization of hornbiende in the metabasalts, and very moderate biotitization. In the southern lobe of the Tin Lake body, small inclusions of the diorites and metavolcanics tend to develop porphyroblastic garnet, and only in the northeastern extremity (not shown in Fig. 40) where the Tin Lake intrusion comes in contact with Booster Lake metaturbidites, is altered cordierite found in fine grained leucogranites.

In contrast, the Osis Lake pegmatitic granite reacts extensively with the metaturbidites of the Booster Lake Formation: tourmalinization of the latter, coupled with growth of albitic plagioclase, is ubiquitous, particularly in thin splinters and screens and on the surface of larger rafts (Fig. 60). Thin screens may become completely digested by the pegmatitic granite (Fig. 61).

Petrochemistry

Representative analyses of the four major bodies are given in

TABLE 20 PARAGENESIS OF THE PEGMATITIC BANDS AND NODULES IN THE SOUTHWESTERN PART OF THE GREER LAKE PEGMATITIC GRANITE

	A.C. #1	A.C. #2	A.C. #3	Silverleaf
Microcline	●	●	X	●
Oligoclase				
Albite	X	●	●	●
Quartz	●	●	●	●
Holmquistite				
Biotite				
Muscovite	X	O	X	X
Li-muscovite		O	●	O
Lepidolite			•	•
Spodumene				X
Petalite				(X)
Eucryptite				
Pollucite				
Epidote				•
Chlorite				
Cordierite				
Garnet	•			X
Schorl			•	
Elbaites			•	•
Topaz				•
Gahnite				•
Beryl	•	•	•	•
Titanite				
Allanite				
Gadolinite				
Zircon				
Thorite				
Uraninite				
Magnetite				
Ilmenite				
Niobian rutile				
Aeschynite				
Fersmite				
Euxenite				
Yttrotantalite				
Cassiterite			•	•
Columbite-tantalite	•	•	•	•
Pseudo-ixiolite				
Microlite				
Tapiolite				
Wodginite				
Simpsonite				
Stibiotantalite				
Apatite		•	•	•
Monazite				•
Xenotime				
Triphylite-lithiophilite				•
Amblygonite-montebrasite				•
Sulphides of Fe, Cu				
As				
Mo				
Zn, Cd			•	
Bi				
Sb				
Pb, Ag				

Hydrothermal alteration produces montebrasite at the expense of amblygonite, and micaceous minerals replace spodumene.
Solid circles - abundant, rock-forming; open circles - subordinate;
x - accessory; dot - rare; ( ) an early phase which is now totally altered; ? - identification questionable.

Figure 58: Gradual transition from pegmatitic leucogranite (lower right) into the mineralized pegmatitic pod A.C. #2 (centre and top); Greer Lake pegmatitic granite intrusion

Figure 59: Columnar spodumene + quartz pseudomorphs after petalite in a darker groundmass of albite, quartz and lithian muscovite; Silverleaf pegmatite offshoot of the Greer Lake pegmatitic granite intrusion

Figure 60: Tourmalinization (almost black) along the edges and in thin fragments of a metapelitic raft, in the western part of the Osis Lake intrusion of pegmatitic granite

Figure 61: Symmetrical zoning of a pegmatite layer confined by tourmalinized schist screens at left, extends to the right where the screens were reduced to barely visible trains of tourmaline; Osis Lake pegmatitic granite intrusion

TABLE 21. REPRESENTATIVE CHEMICAL ANALYSES OF THE PEGMATITIC GRANITES (18)

	F.g. leucogranite		Pegm. leucogranite		Sodic aplite	Potassic pegmatite
	TNL-31	GLW38A	TL1006	GL1003	GLW6aA	GLW6aP
SiO_2, wt. %	77.10	75.90	73.50	75.30	77.50	75.55
Al_2O_3	12.28	13.48	14.40	14.30	12.79	15.01
TiO_2	0.03	0.01	0.03	0.04	0.06	0.04
Fe_2O_3	0.31	0.35	0.47	0.86	0.76	0.56
FeO	0.68	0.26	0.86	0.92	0.80	0.20
MnO	0.01	0.01	0.03	0.06	0.21	0.01
MgO	0.20	0.03	0.09	0.03	0.03	0.05
CaO	0.42	0.31	0.36	0.21	0.40	0.18
Na_2O	3.23	3.66	3.98	5.20	6.22	2.90
K_2O	5.24	5.41	5.63	2.19	0.66	4.65
P_2O_5	0.06	0.06	0.05	0.06	0.04	0.02
CO_2	0.02	0.03	0.09	0.06	0.10	0.22
H_2O	0.52	0.34	0.23	0.55	0.39	1.15
	100.10	99.89	99.74	99.82	99.96	100.54
Li, ppm	42	57	28	76	45	107
Rb	168	340	275	442	138	735
Cs	4	13.7	3.2	2.3	1.5	4.8
Be	1	3	0.5	1.7	2	1.7
Sr	3	20	43	31	5	13
Ba	244	142	50	1	nd*	nd
Pb	30	33	20	11	4	5
Ga	27	45	62	64	51	102
U	36	9	3	8	6	5
Th	15	25	nd	5	12	3
Zr	130	58	5	16	14	2
Hf	4.35	1.2	0.45	1.25	1.8	<0.4
Sn	3	8	13	23	13	20
K/Rb	259	132	170	41.2	39.8	52.5
K/(Cs x 100)	108	32	145	79	36	83
K/Ba	178	318	934	18200	-	-
Ba/Rb	1.45	0.42	0.18	0.002	-	-
Ba/Sr	81.3	7.10	1.16	0.03	-	-
Rb/Sr	56	17	6.4	14.3	27.6	58.5
Mg/Li	28.7	3.2	20	2.7	4.4	2.8
Zr/Sn	43.3	7.2	0.4	0.7	1.1	0.1
Zr/Hf	29.9	48.3	11.1	12.8	7.8	5
Al/Ga	2407	1584	1229	1183	1327	778
La, ppm	19.7	5.5	2.85	7.05	7.36	3
Ce	46	16.5	8	18.5	23	8.5
Nd	5.5	<5	<3.5	8.5	10	<3.5
Sm	7.25	2.95	1.84	4.69	5.3	1.09
Eu	0.18	<0.08	<0.08	<0.05	<0.10	<0.15
Dy	8.9	7.15	2.55	5.85	4.25	0.85
Yb	4.7	3.35	1.3	2.7	2.75	0.8
Lu	0.56	0.32	0.13	0.26	0.45	0.09

* not detected

Table 21, and Figure 62 shows the simplified granitic ternary relationships. Fine grained leucogranites are mostly concentrated around the composition $Ab_{35-5}\ Or_{32-5}\ Qtz_{35}$, and the sodic aplites extend towards the Ab apex by a decrease in the Or component followed by loss of quartz. The plots of pegmatitic granites are scattered in the general area of granitic minima. Difficulties encountered in representative sampling of this coarse grained rock type may be partly responsible for this scatter, but moderate SiO_2 contents and slight predominance of Ab over Or, similar to present results, have been reported from this rock type previously (e.g., Orville 1960, Proctor and El-Etr 1968). In the ternary feldspar system, both fine grained and pegmatitic leucogranites fall mostly into the low-temperature trough but all the sodic aplites are distinctly enriched in Ab. The fine grained leucogranites of the Tin Lake and Osis Lake bodies are somewhat enriched in An.

TABLE 22. SELECTED MAJOR AND TRACE ELEMENT RELATIONSHIPS IN FINE GRAINED LEUCOGRANITES OF THE FOUR MAJOR INTRUSIONS OF PEGMATITIC GRANITES

	Greer Lake	Eaglenest Lake	Tin Lake	Oslo Lake - bio. gr.	Oslo Lake - fg. lgr.
Li, ppm	58* ±20.2 29-86	79.7 ±56.9 27-140	31.83 ±18.30 11-59	71.5 ±11.1 83-87	63.3 ±14.4 47-74
Rb	562 ±309.7 340-1050	536 ±264 293-817	244.75 ±75.3 128-338	187.5 ±9.8 179-196	137.3 ±48.8 103-193
Cs	8.9 ±3.2 5.1-13.7	12.7 ±10.3 3.8-24	7.24 ±3.22 2.9-11.4	15.8 ±3.4 11.8-20	8.4 ±7.4 3.9-17
Be	3.8 ±3.5 1.2-10	5.6 ±6.5 0.7-13	1.98 ±0.66 1-3	0.73 ±0.34 0.3-1	0.77 ±0.45 0.3-1.2
Sr	18.2 ±6.4 11-28	10.3 ± 5.0 5-15	35.42 ±14.33 3-55	83.5 ±22.6 83-105	25.7 ±11.7 13-38
Ba	112.4 ±57.05 12-150	70 ±61 0-110	217.3 ±111.8 31-416	287.3 ± 61.8 203-347	8 ±8.7 3-18
Ga	53 ±18.1 32-73	58.3 ±2 56-60	30 ±7.7 22-46	28 ± 3.2 25-32	46 ±8.2 41-57
U	15 ±9.1 8-30	6 ±2 4-8	26 ±9 13-40	30.2 ± 27.4 12-71	23 ±25.1 8-52
Th	7.4 ±10.4 0-25	7 ±9.6 0-18	10.3 ±8.8 0-30	0	6.7 ±4.6 4-12
Zr	44 ±20.2 11-58	53.3 ±16.6 38-71	103 ±29 61-140	78 ±3.7 73-82	38.3 ±31.1 17-74
Hf	1.2	2.3 ±1.3 0.8-3.4	4.0 ±0.6 3.5-4.6	1.83	3.06
Sn	13.6 ±8.5 5-25	13 ±2 11-15	8.7 ±4.1 0-13	4.75 ±3.1 2-9	13 ±2.6 10-15
K/Rb	87.2 ±34.6 42-132	74.7 ± 33.6 47-112	178.3 ± 67.4 89-327	237 ±16.5 221-260	131.7 ±38 89-158
K/Cs	5108 ±1817 3277-7699	4482 ± 3711 1609-9858	6800 ±4113 3402-15483	2988 ±750 2162-3988	2823 ±1587 1708-4840
K/Ba	767 ±939 215-2425	338 325-351	278.7 ±316.8 75-1258	182.5 ±45.3 136-230	5402 ±4812 507-9687
Ba/Sr	7.4 ±4.5 0.43-12.36	8.2 7.3-9.0	11.7 ±22 1.1-81.3	3.50 ± 0.6 3.0-4.36	0.53 ±0.76 0.083-1.4
Rb/Sr	32.1 ±17.4 17.0-61.8	52.8 ±6.8 45.4-58.6	10.9 ±14.3 3.2-58	2.35 ±0.52 1.87-2.84	6 ±2.5 3.2-7.9
Mg/Li	4.88 ±3.36 1.74-9.36	6 ±5.5 1.7-12.2	48.6 ± 38.5 13.5-127	39.7 ± 6.7 32.03-48.25	11.5 ± 6.7 6.7-18.1
Al/Ga	1526 ± 526 980-2264	1258 ±29 1227-1284	2351 ±,362 1743-2908	2737 ±310 2372-3060	1674 ±189 1530-1885
Zr/Hf	48.3	32.9 ±26.9 14.1-63.7	30.8 ±1.5 29.3-32.6	47.7 48.8-48.7	24.3

* 58: arithmetic mean, ±20.2: 1σ, 29-86: range

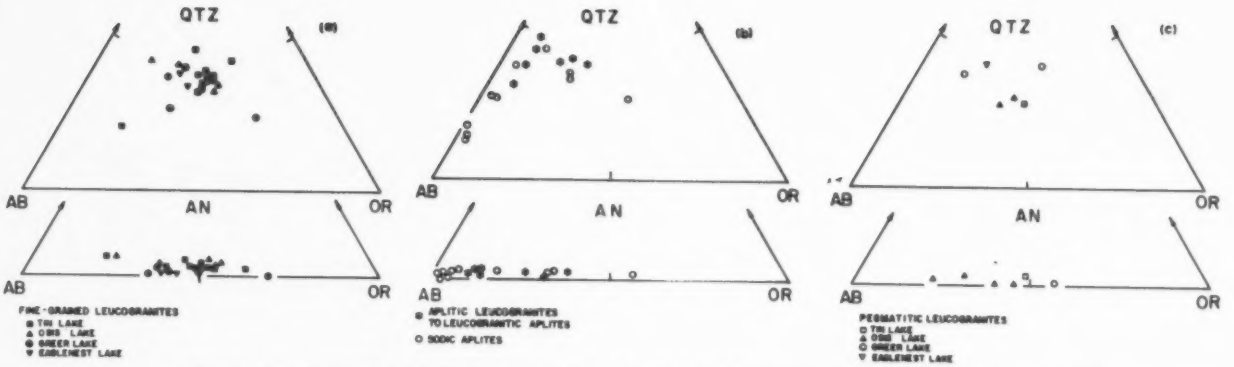

Figure 62: Normative Ab-Or-Qtz and Ab-Or-An plots of fine grained leucogranites (a), sodic aplites (b), and pegmatitic leucogranites (c) of the pegmatitic granite intrusions

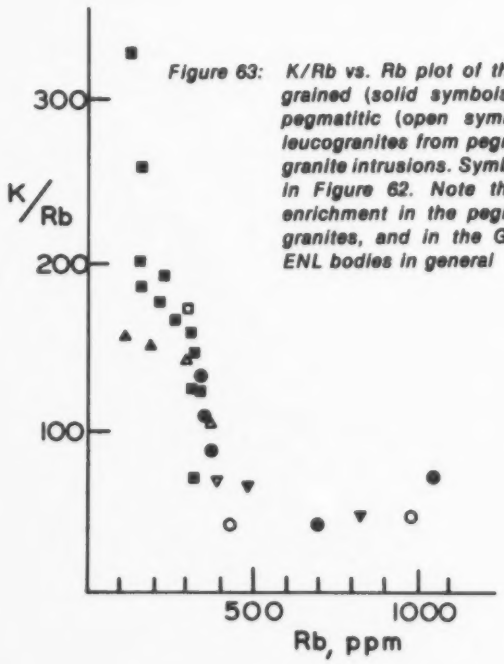

Figure 63: K/Rb vs. Rb plot of the fine grained (solid symbols) and pegmatitic (open symbols) leucogranites from pegmatitic granite intrusions. Symbols as in Figure 62. Note the Rb-enrichment in the pegmatitic granites, and in the GL and ENL bodies in general

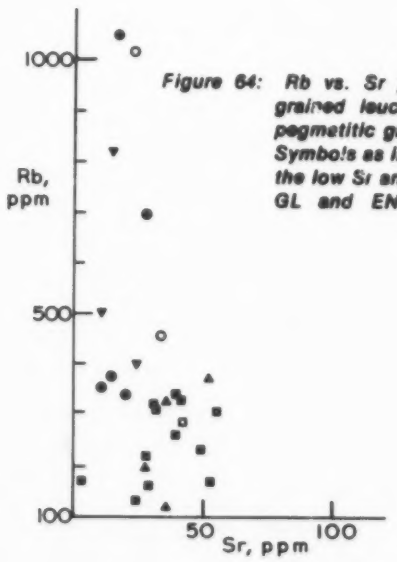

Figure 64: Rb vs. Sr plot of the fine grained leucogranites from pegmatitic granite intrusions. Symbols as in Figure 62. Note the low Sr and high Rb in the GL and ENL bodies

Table 22 summarizes some of the geochemical characteristics of the fine-grained leucogranites (directly comparable to other granitic intrusions in the area) which document the different fractionation levels attained by the individual intrusions Figures 63 to 67 document the wide ranges of fractionation levels and, in most cases, the specific character of the Osis Lake intrusion.

Figure 68 illustrates the REE abundances in the fine-grained leucogranites and pegmatitic leucogranites (usually somewhat lower in the latter phase). In general, the Greer Lake, Eaglenest Lake and Tin Lake bodies show very low abundances, about equal for all REE's except Eu which displays extreme depletion. The abundances decrease in these three bodies with Sr and decreasing K/Rb. In contrast to these three intrusions, the Osis Lake body (including its central plug of biotite granite) exhibits low REE abundances dispite its high K/Rb ratio, moderate Eu anomaly, and relatively high Ce_N/Yb_N.

Oxygen isotopic compositions of the pegmatitic granites are remarkably homogeneous within individual bodies but widely different among them. Most of the data are correlatable with $\delta^{18}O$ values found for enclosing metasedimentary and/or metavolcanic rocks. In the Greer Lake and Eaglenest Lake intrusions seated in O^{18} — low metabasalts, $\delta^{18}O$ = 8.1 - 8.7 and 8.6 - 9.3, respectively. The $\delta^{18}O$ ranges for the Tin Lake and Osis Lake bodies, 10.3 - 10.9 and 11.1 - 12.4, respectively, also closely correspond to those of their metasedimentary hosts. Further discussion of these data follows in the section on Genetic Considerations (p. 142) and is presented in Longstaffe et al. (1981).

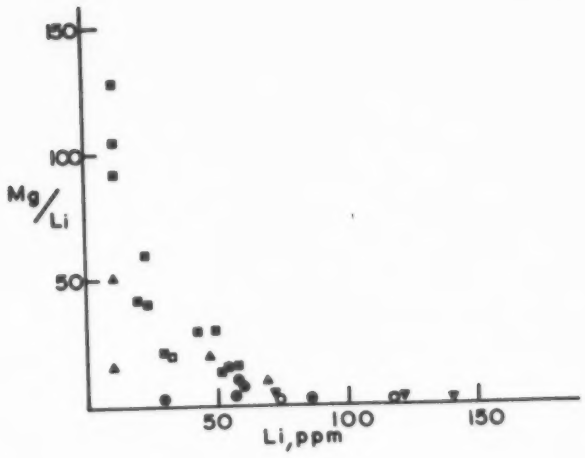

Figure 65: Mg/Li vs. Li plot of the fine grained and pegmatitic leucogranites from pegmatitic granite intrusions. Symbols as in Figure 62. Note the low Mg/Li values in pegmatitic granites, and the Li enrichment in the GL and ENL bodies

Figure 66: Al vs. Ga plot of the fine grained and pegmatitic leucogranites from pegmatitic granite intrusions. Symbols as in Figure 62. Note the high Al and Ga contents of the pegmatitic granites, and the Ga enrichment in the GL and ENL bodies

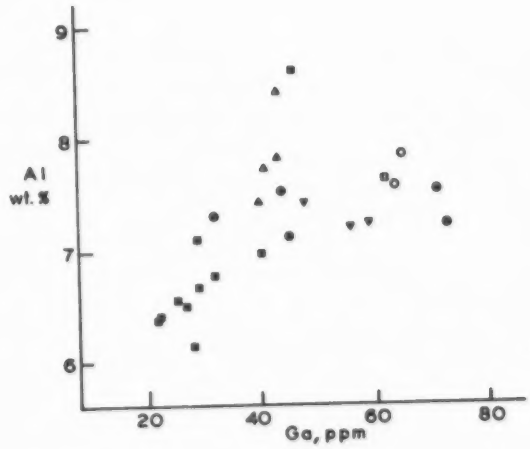

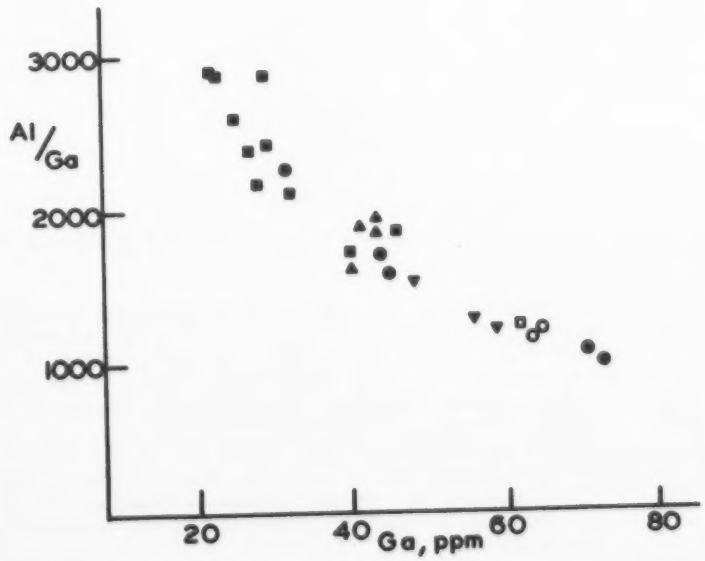

Figure 67: Al/Ga vs. Ga plot of the fine grained and pegmatitic leucogranites from pegmatitic granite intrusions. Symbols as in Figure 62. Note the low Al/Ga ratios of the pegmatitic granites and of the GL and ENL bodies in general

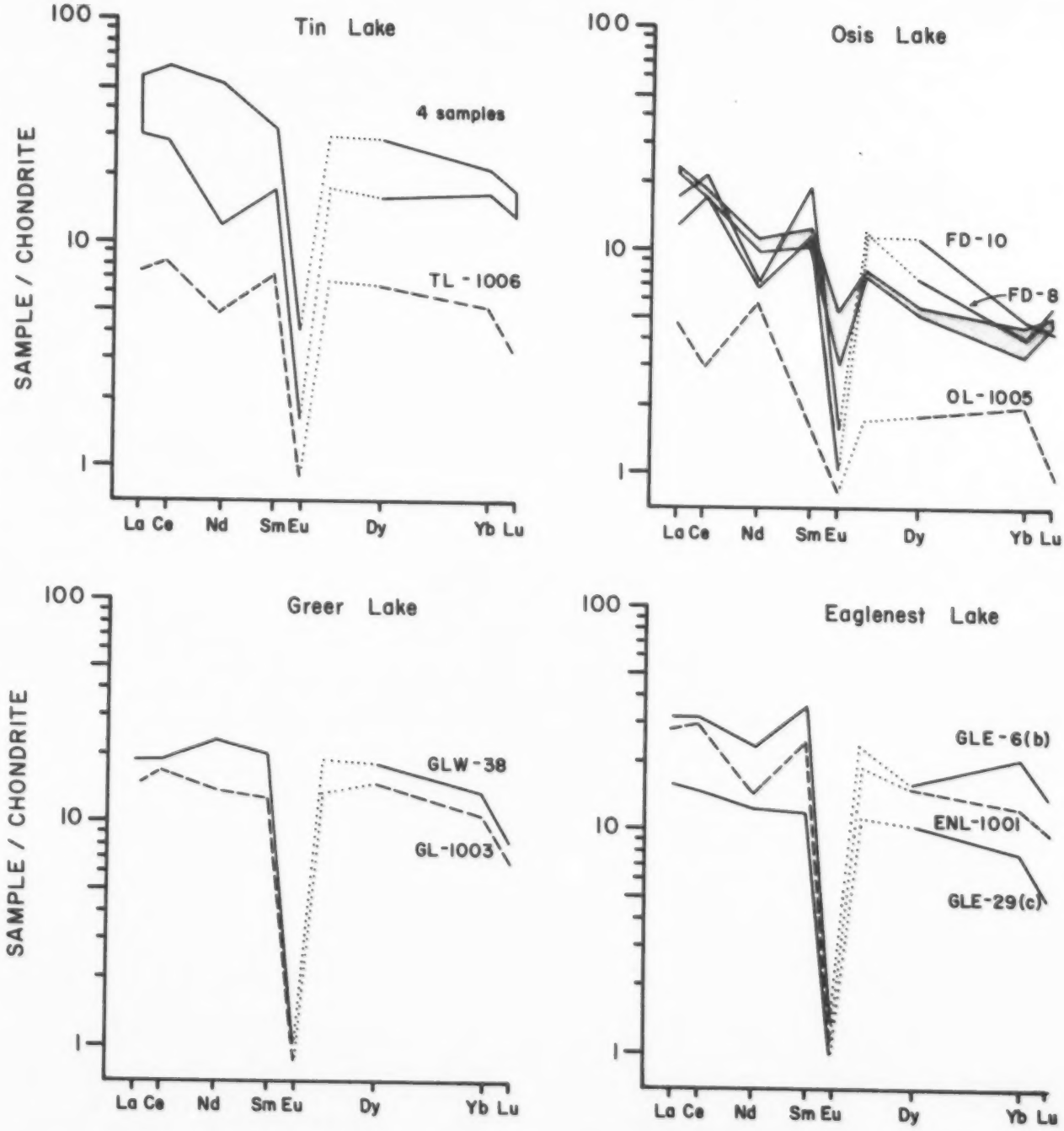

Figure 68: REE abundances in the fine grained leucogranite (solid line and field) and pegmatitic leucogranite (dashed line) phases of the four pegmatitic granite intrusions, and in the biotite granite of the Osis Lake body (dotted field)

TABLE 23. ARITHMETIC MEANS OF CONTENTS (WT.%) AND RATIOS OF GEOCHEMICALLY SIGNIFICANT ELEMENTS IN BLOCKY K-FELDSPARS FROM POTASSIC PEGMATITE BANDS OF THE FOUR MAJOR INTRUSIONS OF PEGMATITIC GRANITES

	K_2O K	Na_2O Na	CaO Ca	Rb_2O Rb	Cs_2O Cs	Li_2O Li	PbO Pb	K/Rb	K/Cs	Rb/Cs
Greer Lake	11.89, wt.%	3.05	.031	.21	.0045	.0058	.0034			
	9.88	2.26	.022	.188	.0042	.0026	.0032	69	4475	68
Eaglenest Lake	12.02	3.13	.059	.221	.0073	.0079	.0039			
	9.98	2.32	.042	.202	.0068	.0037	.0036	56	1982	35
Tin Lake	12.06	2.96	.082	.072	.0025	.0029	.0034			
	10.01	2.20	.059	.066	.0022	.0013	.0032	170	12048	79
Osis Lake	12.15	2.97	.091	.078	.0022	.0036	.0029			
	10.09	2.20	.065	.072	.0020	.0017	.0027	180	8920	52

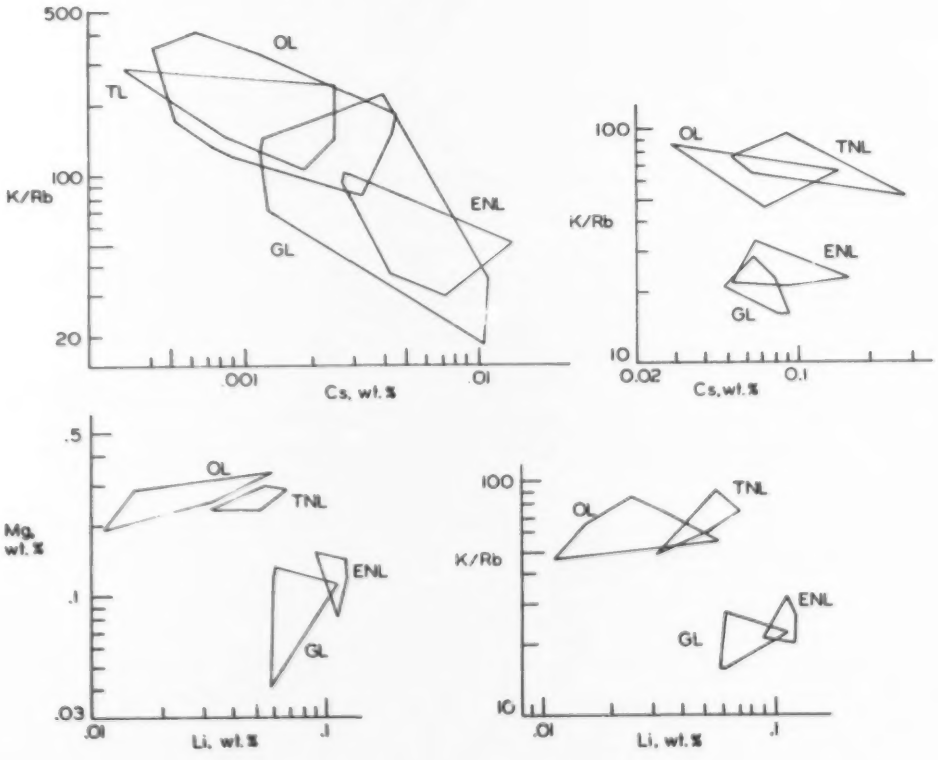

Figure 69: Selected major and trace element relationships in blocky K-feldspars (top left) and platy muscovites from the potassic pegmatite phases of the four pegmatitic granite intrusions

Mineral compositions

Compositional variations in individual minerals also reflect the differences between the Greer Lake-Eaglenest Lake intrusion pair and the Tin and Osis Lakes bodies, and the somewhat special character of the Osis Lake pegmatitic granite.

Figure 69 presents some compositional characteristics of blocky K-feldspars and platy muscovites of the potassic pegmatite phases, documenting the more advanced fractionation of the Greer Lake and Eaglenest Lake intrusions. Numeric data for the blocky K-feldspars are summarized in Table 23. Figure 70 demonstrates the uniform frequency distributions of blocky K-feldspar obliquities in all but the Osis Lake body.

Plagioclase is strongly albitic, covering a range of An_3 to An_6 in the four intrusions. It is somewhat variable in different samples of each individual body, but on the average more albitic in the Greer Lake and Eaglenest Lake intrusions, and slightly more calcic in the other two pegmatitic granites.

Garnet compositions show the lowest Mn-contents in the Tin Lake body somewhat higher in the Greer Lake and Eaglenest intrusions, and highest in the Osis Lake pegmatitic granite (Fig. 71, 72). Within a single intrusion, Mn-enrichment is evident in the garnets from potassic pegmatite bands but the compositions of other paragenetic garnet types largely overlap. The Tin Lake and Osis Lake garnets show distinctly higher CaO and MgO contents than those of garnets from the other two intrusions. Also, the Osis Lake garnets are enriched in P_2O_5 (about 0.23 wt.%), and the Greer Lake and Eaglenest Lake garnets show increased Y_2O_3 contents (0.10 - 0.25 wt.%).

Fractionation trends within individual intrusions

Some fractionation trends are expressed by vectorial changes in accessory mineralogy which can be observed in the field. Such a trend is documented for the Osis Lake and Tin Lake bodies in Table 19, reflecting changes in abundance and mineralogy of B, Li, and P.

Much better evidence is available, of course, from regional variations in different geochemical indicators in whole rock and mineral compositions. Figure 73 shows progressive fractionation trends based on whole-rock K/Rb, blocky K-feldspar K/Rb and K/Cs, muscovite K/Rb, Mg/Li and Be, and garnet Fe/Mn ratios (Goad, in prep.). The best expressed trends are those in the Osis Lake and Greer Lake intrusions; the fractionation in the Tin Lake body embraces a wide range but it is distributed in a random manner.

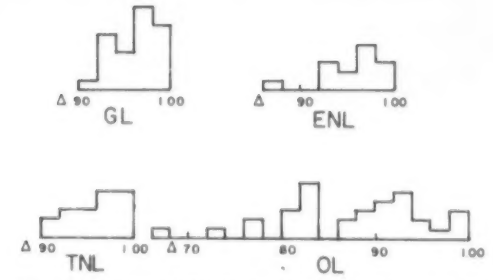

Figure 70: Obliquity of blocky K- feldspars from the potassic pegmatite phases of the four intrusions of pegmatitic granite; the height of the shortest column corresponds to a single sample

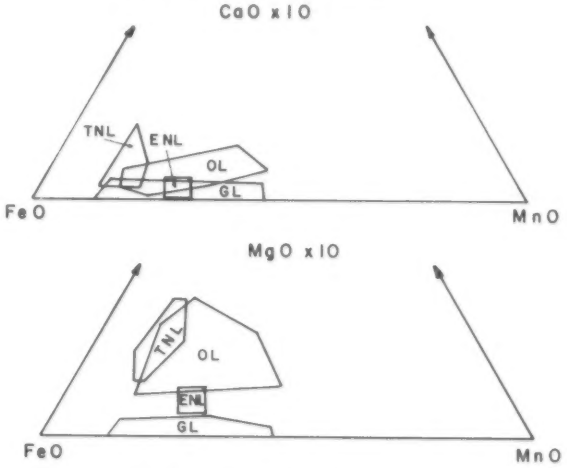

Figure 71: Chemical composition of garnet from the pegmatitic leucogranite phase of the four intrusions of pegmatitic granite, in ternary subsystems (wt.%)

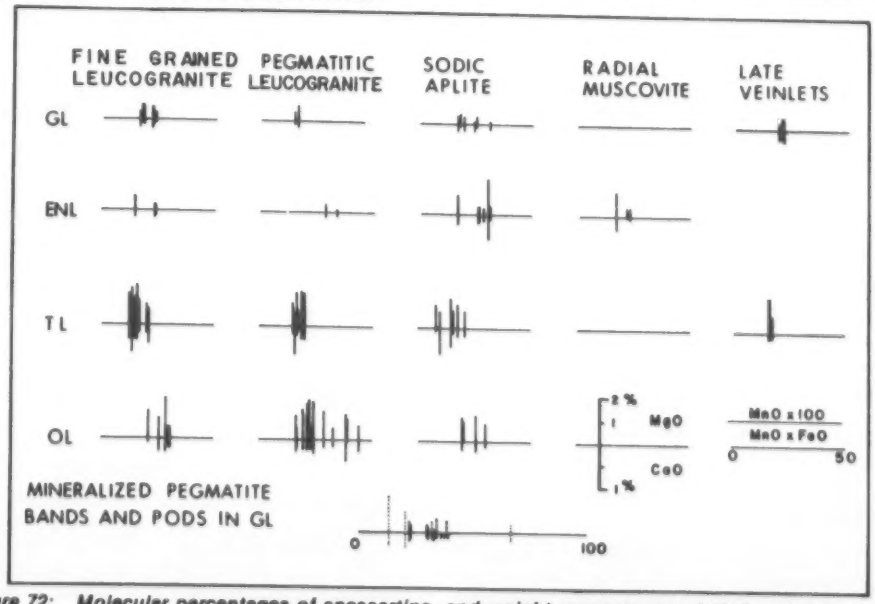

Figure 72: Molecular percentages of spessartine, and weight percentages of MgO and CaO, of garnets from various assemblages in the four intrusions of pegmatitic granites

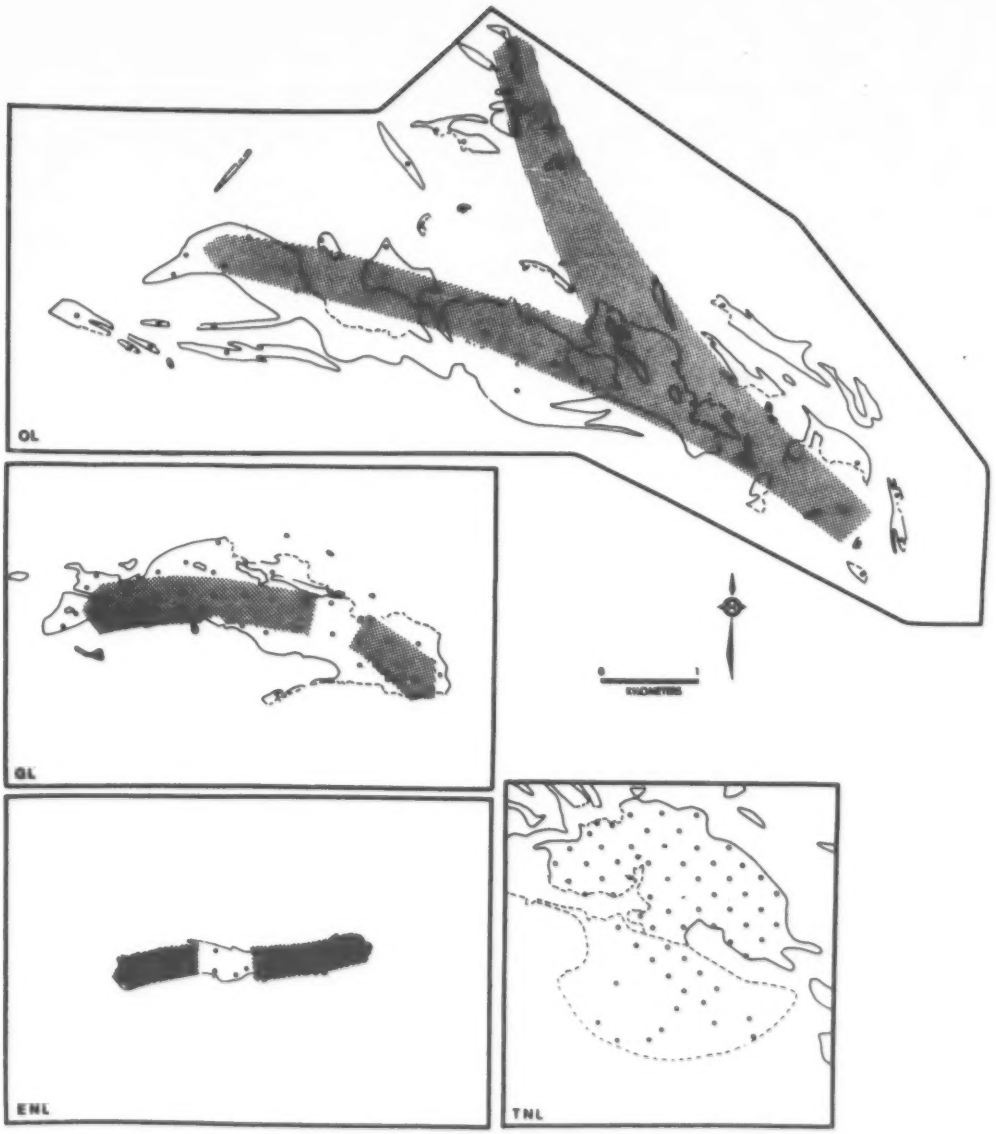

Figure 73: Fractionation directions in the four pegmatitic granites based on whole-rock K/Rb, blocky feldspar K/Rb and K/Cs, muscovite K/Rb, Mg/Li, and Be, and garnet (Mn x 100)/(Mn + Fe)

The Axial pegmatitic granite

This intrusion was not discussed in the preceding section as it occurs in only two or three small patches transitional into the Axial group of pegmatites, and the data base is necessarily very limited. It consists mainly of the pegmatitic leucogranite phase with lenticular bands of potassic pegmatite. Besides two feldspars and quartz, it contains muscovite and minor biotite and garnet. Blocky K-feldspars have a mean K/Rb ratio of 192, and Cs content about 0.0010 wt.%, indicating a very low degree of rare-alkali fractionation; muscovite shows similarly low fractionation. No accessory minerals have been found, except for sporadic garnet.

PEGMATITES

The Cat Lake-Winnipeg River pegmatite field can be subdivided into two pegmatite districts, Winnipeg River in the south and Cat Lake-Maskwa Lake in the north. Within each district, the pegmatites can be separated into groups of spatially, mineralogically, and geochemically related bodies most of which probably also have a common origin. Table 24 presents a list of the pegmatite districts and groups in the order in which they are described below, and some principal geochemical characteristics of individual groups. Locations of the pegmatite groups are shown on Map 1, and individual groups are schematized on location maps accompanying each description; similarly, tables of mineral parageneses and of principal compositional characteristics of important rock-forming and rare-element minerals accompany the text.

In the paragenetic tables accompanying descriptions of individual pegmatite groups, the mineral species are arranged in an unorthodox, geochemical-cum-paragenetic order. Main rock-forming minerals are followed by the only amphibole species represented, micas and Li- and Cs-aluminosilicates; most of the femic and peraluminous minerals with beryl precede silicates of Ti, REE, Zr and Th; the latter are commonly associated with the next group of U, Fe, Ti oxide minerals; Nb, Ta-bearing species are arranged in an approximate geochemical evolutionary sequence, the first of them commonly associated with the two preceding groups and the last ones typical of highly fractionated pegmatites; phosphates, again in geochemical sequence, and sulphides and related species conclude the list. Secondary minerals formed at the expense of pre-existing phases are summarized at the bottom of each paragenetic table. The format of these tables is kept uniform throughout, disregarding abundance or scarcity of mineral species in any given pegmatite group, to maintain identical visual presentation and ease in mutual comparison.

TABLE 24. SUBDIVISION OF THE CAT LAKE-WINNIPEG RIVER PEGMATITE FIELD, AND RARE ELEMENTS TYPICAL OF THE DIFFERENT PEGMATITE GROUPS

Cat Lake-Winnipeg River pegmatite field			
Winnipeg River district	Shatford Lake group (SHL)	Be, Sn, Nb-Ta,Zr,REE,U,Th
	Lac du Bonnet group (LdB)	Li (P)
	Greer Lake group (GL)	Be, Nb-Ta
	Eaglenest Lake group (ENL)	Be
	Axial group (AX)	(Li?)
	Birse Lake group (BIS)	B(Be)
	Rush Lake group (RL)	Li, Rb, Cs, Be, Sn, Ta-Nb, B, P, F
	Bernic Lake group (BL)	Li, Rb, Cs, Be, Sn, Ta-Nb, B, P, F
Cat Lake-Maskwa Lake district	Eagle-Irgon group (EAI)	Li
	Beryl-Tourmaline group (BET)	Be
	Cat Lake group (CAT)	Li, Be
	Central Claim group (CC)	Li, Be, Ta-Nb
	Maskwa Lake series (MWL)	Li;Li,Rb,Cs,Ta-Nb (Be)

Shatford Lake pegmatite group (SHL)

This group is located along the margins of the Lac du Bonnet batholith, in close proximity (up to 800 m) on its northern side and at larger distances (up to 4 km) to the east and southeast. The pegmatites are essentially concordant with layering and foliation in their host rocks, and they show variations in their strike in concert with the layering and foliation enveloping the Lac du Bonnet batholith. Exceptions to this are displayed by the SHCR-1, SHCR-2, SHNW and HC pegmatites which dip at shallow angles or approach the horizontal (Fig. 74).

Individual pegmatites are dyke-like or flat-lenticular in shape, and their dimensions are not known to reach more than 400 m in length and 8 m in thickness (SHS pegmatite). Sharp contacts with the host rocks are characteristic, with negligible biotitization developed in metabasaltic rocks.

Internal structure of the pegmatites is highly variable, ranging from well-developed muscovite+quartz+albite border zone, albite+quartz+K-feldspar (partly graphic)+muscovite intermediate zone, K-feldspar+quartz blocky zone and quartz core in some bodies (e.g., SHEE-2) to coarse grained albite+quartz+muscovite assemblage with megacrysts of graphic and blocky K-feldspar, patches of quartz, and bands of saccharoidal albite+quartz+garnet distributed in a rather haphazard manner (e.g., SHE-2, BB-21, 22). The NUTT pegmatite is also distinct in that it is fine- to medium-grained throughout, apparently unzoned, and sheared parallel with the schistosity of the surrounding metasediments. Post-consolidation tectonic disturbance can be detected in most members of this group; beryl and blocky K-feldspars are particularly vulnerable, and smears of late sericitic mica on slickensided fractures are developed in most mineral assemblages.

Rare-element mineralization is characterized by a relative abundance of Be and Nb-Ta, and minor amounts of Zr-Hf, REE, U, and Th. The mineralogy of rare elements is evident from the paragenetic Table 25. Distribution of rare-element minerals in the pegmatite bodies is irregular. No consistent pattern can be observed but the mineralization is associated mainly with platy albite and along fractures in feldspars and quartz. In reasonably zoned pegmatites, beryl and topaz are concentrated along the boundary of the blocky K-feldspar zone and quartz core.

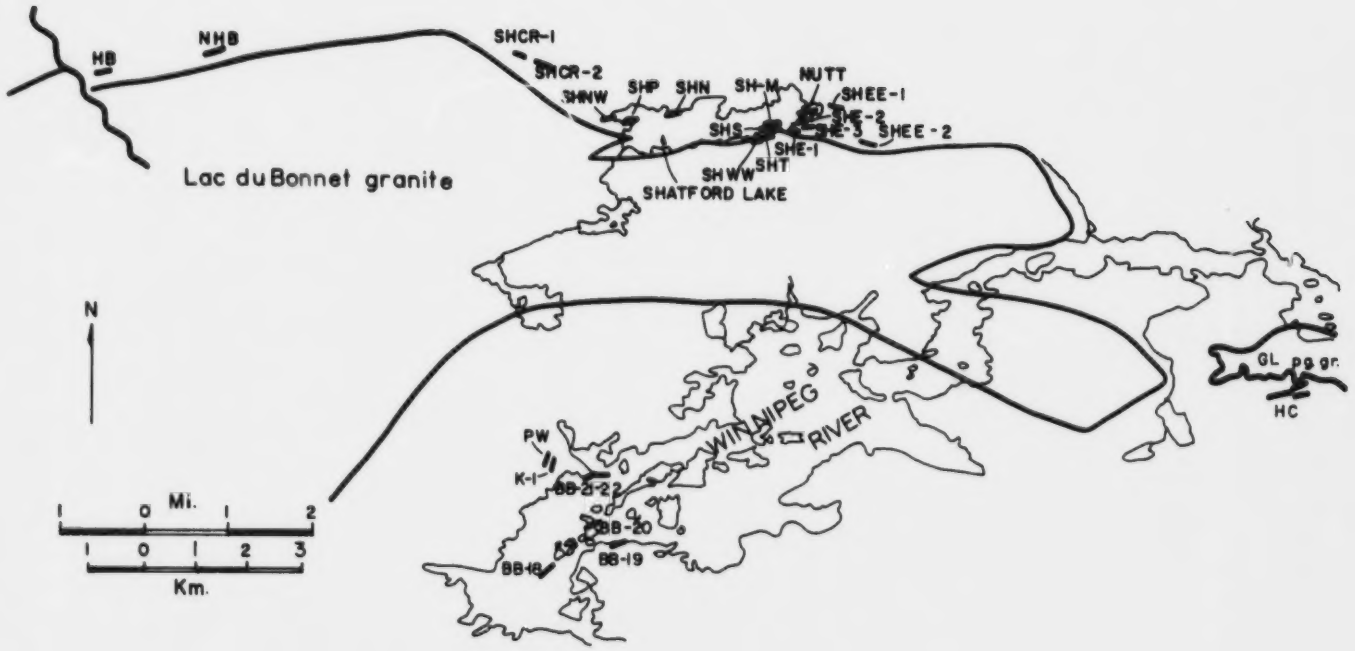

Figure 74: Location map of the Shatford Lake pegmatite group

TABLE 25 PARAGENESIS OF THE SHATFORD LAKE PEGMATITE GROUP, NORTH AND SOUTH

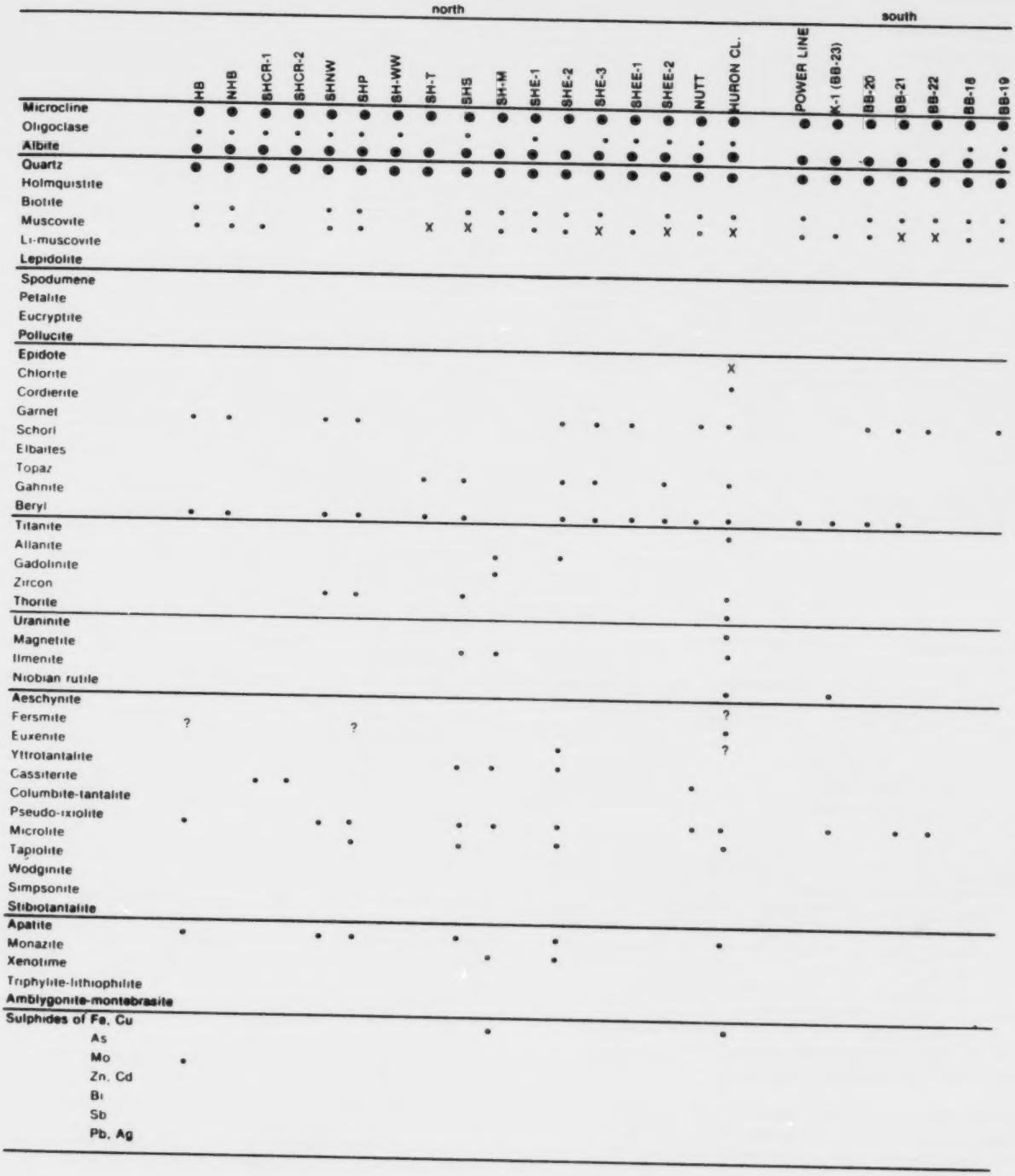

Hydrothermal alteration products include bavenite, bityite, bertrandite, bastnaesite, synchisite, uranophane, sklodowskite, chlorite, calcite, and clay minerals.

Symbols as in Table 20.

TABLE 26. COMPOSITIONAL CHARACTERISTICS OF SELECTED MINERALS FROM THE SHATFORD LAKE PEGMATITE GROUP

		Rb	K/Rb	Cs	
Blocky K-feldspar	arith. mean, wt.%	0.181	66.5	0.0061	
(55 samples)	std. deviation	±0.088	±20.6	±0.0117	
	range	0.094-0.705	14.0-113.0	0.0003-0.0820	
	Li	Rb	K/Rb	Cs	
Core muscovite	0.217	0.465	24.1	0.064	
(11)	±0.201	±0.286	±15.3	±0.158	
	0.021-0.540	0.159-1.09	7.2-53.3	0.0047-0.54	
	Li	Na	Na/Li	Cs	
Late beryl	0.044	0.306	9.36	0.049	
(33)	±0.039	±0.137	±4.3	±0.027	
	0.009-0.19	0.111-0.756	3.97-24.7	0.012-0.163	
	FeO	MnO	(MnO x 100)/ (MnO + FeO)	CaO	MgO
Garnet	20.60	21.72	51.26	0.52	0.19
(6)	±3.97	±4.26	±9.32	±0.33	±0.09
	15.84-26.97	16.95-27.28	38.59-63.26	0.28-1.13	0.07-0.29
	(MnO x 100) / (MnO + FeO)		$(Ta_2O_5 \times 100) / (Ta_2O_5 + Nb_2O_5)$		
Columbite-tantalite	40.57		58.34		
(16)	±17.12		±21.46		
	18.11-69.18		31.84-91.98		

Blocky K-feldspars and muscovites have a wide range of rare-alkali concentrations but they are generally low (Table 26). Muscovite is always Fe-rich, reaching 8.50 wt.% total Fe as Fe_2O_3 in some samples. Beryl is mostly pale-green and frequently sheath-shaped, enveloping cores of neighbouring mineral assemblages (predominantly albite+quartz). Compositionally, beryl from the Shatford Lake pegmatites is a typical representative of sodic beryls extremely poor in Li and Cs (Beus 1960, Černý 1975).

Topaz is a characteristic constituent, in crystals up to 20 cm in length with 18.8 to 19.5 wt.% F_2. In some pegmatites it attains gem quality, being clear and flawless in small fragments and brownish-yellow in color.

Minerals of the columbite group are highly disordered and mostly enriched in Ti and Sn. Their Nb/Ta ratio is quite variable in different pegmatite bodies, and reaches surprisingly low minimum in the SHP pegmatite, although the general fractionation level is more advanced in other members of the group, e.g. the Huron Claim pegmatite. Other minerals carrying Nb and Ta, except possibly microlite, occur only sporadically in several pegmatite bodies (euxenite, yttrotantalite, fersmite, aeschynite, microlite).

Important role of rare-earth elements is evident from the multitude of phosphates, complex oxides, and silicates carrying them (Table 25). It must be noted, however, that with the possible exception of the SHS-M and HC pegmatites, their quantities are very low.

Partly altered uraninite and metamict, sulphide-studded thorite have been found in the Huron Claim pegmatite, but high U and Th contents are characteristic of metamict zircons from other pegmatites as well.

Late hydrothermal alterations are rather typical of the Shatford Lake pegmatites; calcite and chlorite are ubiquitous, muscovite replaces most of the topaz, secondary beryllium silicates form at the expense of beryl, and REE-fluorocarbonates replace monazite and allanite (Table 25).

In general, the Shatford Lake pegmatite group can be classified as the gadolinite-type of beryllium-enriched, partly albitized blocky microcline-biotite pegmatites, according to Beus (1960). Despite the scarcity of gadolinite itself, this pegmatite group displays all the geochemical features of this type: high concentration of Na, Fe, Be, F, and REE, contrasting with negligible role of rare alkalis and B. These relationships are expressed in the mineral paragenesis by abundance of albite and beryl, conspicuous presence of biotite and magnetite, high Fe-content of muscovite, common occurrences of topaz, and the variety of REE-bearing minerals quoted above.

An M.Sc. thesis devoted to the detailed mineralogy and geochemistry of the best mineralized member of the group, the Huron Claim pegmatite, is in progress (Paul, in prep.).

The Lac du Bonnet pegmatite group (LdB)

This group is confined to a relatively small area west of the confluence of Peterson Creek with the Bird River (Map 1, Fig. 75).

The pegmatites strike north-northwest, dip steeply or vertically, and truncate both layering and foliation of their host rocks. The only major structure in evidence in the area parallel to these dykes is a fault which cuts the Lac du Bonnet batholith and the metasediments of the Bernic Lake Formation, displaying a right-lateral strike-slip component. The northern extension of this fault into the Flanders Lake Formation north of Bird River is uncertain.

The pegmatites form flat lenticular bodies up to 40 m in exposed length and not exceeding 3 m in width. Contacts with the wall rock metasediments are sharp, rarely with some muscovite replacing the schists.

The larger of the bodies (C-1, C-2, C-3) are zoned, with aplitic albite+quartz wall zone separated from the K-feldspar+quartz+spodumene core by diffuse bands of fine-flaked muscovite. Altered triphylite-lithiophilite tends to occur in the outer parts of the core assemblage; apatite is more widespread in the aplitic wall zone (Table 27). The core of the pegmatites is texturally rather homogeneous except for a sporadic tendency of the K-feldspars to

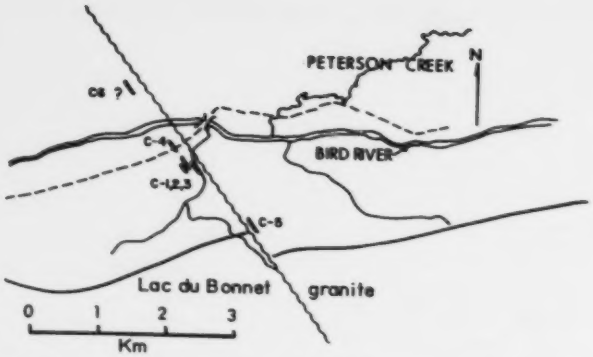

Figure 75: Location map of the Lac du Bonnet pegmatite group

be elongated parallel to the pegmatite contacts. Spodumene is mostly anhedral with respect to the blocky K-feldspar, and locally fills fractures in the latter, together with quartz. The longest individual crystals of spodumene and K-feldspar attain 25 cm in length.

In small pegmatite bodies (C-4, C-5) no zoning is observable, and the veins display a heavily brecciated texture of K-feldspar and spodumene fragments cemented by albite, quartz, and muscovite, al with indications of strong intra- and post-crystallization deformation.

Blocky K-feldspars show low K/Rb and high Cs concentrations, and white spodumene contains high Na_2O but low Fe_2O_3 contents (Table 28). The spodumene corresponds to Heinrich's (1975) class of zonal spodumene, in terms of location as well as composition.

With exception of the fine muscovite penetrating the contacts of the wall zone and core, and the Mn-sicklerite pseudomorphous after triphylite-lithiophilite, no significant hydrothermal or supergene alterations are noticeable.

The Lac du Bonnet pegmatite group belongs to the widespread class of well-differentiated blocky lithium pegmatites with primary zonal spodumene and very subordinate replacement, an almost complete absence of other kinds of mineralization, but with an exceptionally high concentration of Rb and Cs in the K-feldspars. No Ta, Nb-bearing minerals or beryl have been found to date but their occurrence should not be surprising.

The Greer Lake pegmatite group (GL)

This group surrounds the southern part of Greer Lake in the northern-most part of the Whiteshell Provincial Park (Map 1, Fig. 76). (The GLW-30 locality, the paragenesis of which is quoted in Table 29, is of uncertain nature, cropping out as a small island in the Winnipeg River just north of the margin of the main mass of the Greer Lake pegmatitic granite). The pegmatites are dominantly concordant bodies, pinching and swelling within the foliation of the host tonalitic gneisses, both along strike and downdip.

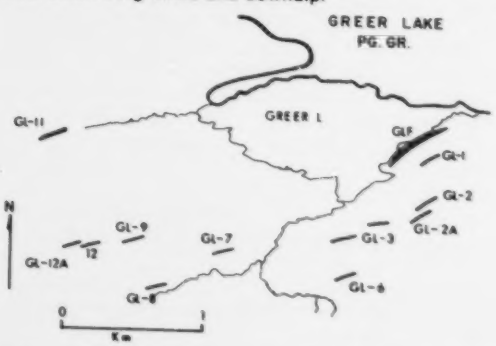

Figure 76: Location map of the Greer Lake pegmatite group

TABLE 27. THE PARAGENESIS OF THE LAC DU BONNET PEGMATITE GROUP

	C1	C2	C3	C4	C5
Microcline	●	●	●	●	●
Oligoclase					
Albite	●	●	●	●	●
Quartz	●	●	●	●	●
Holmquistite					
Biotite					
Muscovite	o	o	o	o	o
Li-muscovite					
Lepidolite					
Spodumene	o	o	o	•	•
Petalite					
Eucryptite					
Pollucite					
Epidote					
Chlorite					
Cordierite					
Garnet					
Schorl					
Elbaites					
Topaz					
Gahnite					
Beryl					
Titanite					
Allanite					
Gadolinite					
Zircon					
Thorite					
Uraninite					
Magnetite					
Ilmenite					
Niobian rutile					
Aeschynite					
Fersmite					
Euxenite					
Yttrotantalite					
Cassiterite					
Columbite-tantalite					
Pseudo-ixiolite					
Microlite					
Tapiolite					
Wodginite					
Simpsonite					
Stibiotantalite					
Apatite	•				
Monazite					
Xenotime					
Triphylite-lithiophilite	•	•	•		
Amblygonite-montebrasite					
Sulphides of Fe, Cu					
As					
Mo					
Zn, Cd					
Bi					
Sb					
Pb, Ag					

Surface oxidation and leaching of the triphylite-lithiophilite produces Mn-sicklerite.

Symbols as in Table 20.

TABLE 28. COMPOSITIONAL CHARACTERISTICS OF SELECTED MINERALS OF THE LAC DU BONNET PEGMATITE GROUP

		Rb	K/Rb	Cs	
Blocky K-feldspar	arith. mean, wt.%	0.825	14.0	0.058	
(7 samples)	std. deviation	±0.117	±1.6	±0.047	
	range	0.710-0.974	12.0-16.0	0.018-0.156	
	Li	Rb	K/Rb	Cs	Be
Core muscovite	0.46	1.12	7.32	0.063	0.002
(2)					
	0.43-0.49	1.06-1.18	7.05-7.58	0.045-0.080	0.0012-0.0028
	Na_2O	Fe as Fe_2O_3			
Spodumene	0.42	0.115			
(3)	±0.3	±0.048			
	0.22-0.76	0.082-0.170			

The largest of the dykes, tabular or lenticular in shape, attain 400 m in length and 15 m in width (GLF). Typically, however, lengths are well under 100 m and widths less than 10 m. Contacts with the country rocks are invariably sharp.

Most of the pegmatites show a regular and rather uniform zoning in an asymmetric concentric manner. A thin but continuous border zone consists of medium grained oligoclase > K-feldspar+quartz. The wall zone consists of large crystals of K-feldspar intergrown with hieroglyphic quartz, imbedded in a coarse-grained assemblage of albite+quartz+biotite (± muscovite); it is considerably thicker than the border zone but rather patchy. The core consists of blocky K-feldspar and quartz, with ubiquitous but usually subordinate cleavelandite and muscovite; only rarely is it separated into a blocky band of K-feldspar+quartz surrounding a lenticular quartz core. Bands and patches of a fine- to medium-grained albite+quartz+muscovite ±garnet are located at the outer margins of the blocky core, and may be classified as a locally developed intermediate zone. Striped bands of garnetiferous albitic aplite, with phenocrysts of coarsely graphic K-feldspar, are exceptional features found in the wall zones of some pegmatites.

The most abundant accessory minerals are garnet, beryl, and altered cordierite. Other minerals listed in Table 29 are rare to exceptional. Most are associated with the albite+quartz+garnet assemblage of the patchy, and largely metasomatic, intermediate zone. Despite the rather simple assemblage of accessory minerals, the pegmatites of the Greer Lake group are conspicuously diversified. They range from bodies carrying predominantly Nb> Ta, Ti and REE (GL-6, GL-8, GL-9) to veins lacking Ti and REE but with Nb=Ta, Li and Cs-rich beryl, and Li-enriched late muscovite (GL-11, 12, 12A). No regular zoning in the distribution of the different pegmatite bodies can be observed except for possible increased fractionation to the northwest and southeast of the GLF, GL-4, GL-7, and GL-8 bodies. The wide range of accessory mineral assemblages is reflected in the broad range of trace-element contents in the rock forming minerals, and in the compositional span covered by the individual accessory minerals (Table 30). Beryl ranges from greenish, Li- and Cs-poor types to milky white Cs-rich varieties, but all types of beryl exhibit high Cs relative to their Na/Li values (Černý 1975 and Černý and Turnock 1975a). The blocky K-feldspars also reach high concentrations of Cs in the more fractionated bodies.

Most of the columbite-tantilite minerals are disordered, with minor Ti and Sn contents, and some are moderately metamict. They are usually fine grained and associated with cleavelandite. Cassiterite and niobian to tantalian rutile are almost indistinguishable from them in hand specimen.

Large crystals of cordierite, altered to muscovite > green biotite > chlorite, are the most conspicuous earmark of the Greer Lake pegmatites, not found so far in any other pegmatite group of the district. They contain ghost zones and scattered crystals of garnet, locally flattened parallel to the basal parting of cordierite. It is not yet clear whether they represent primary inclusions or secondary alteration products formed simultaneously with the micaceous minerals.

Apart from the hydrothermal breakdown of cordierite, the Greer Lake pegmatites did not suffer any hydrothermal alteration or supergene weathering. Beryl is particularly conspicuous by its almost perfect preservation.

The Greer Lake pegmatites can be classified as well-differentiated, albitized, beryl- and columbite-tantalite-bearing blocky muscovite-microcline bodies (Beus 1951, 1960), with an incipient tendency to lithium enrichment only in the most fractionated bodies.

Nb-Ta oxide minerals and beryls from the Greer Lake group have been described in detail by Černý and Turnock (1971a, 1975a).

The Eaglenest pegmatite group (ENL)

This group is represented by a few narrow veins located just southeast of the eastern end of the Eaglenest pegmatitic granite, on the shore of, and on an island in, the Winnipeg River (Map 1). Another dyke occurs isolated on an island north of the pegmatitic granite. Their structural position mostly corresponds to those of the Greer Lake group, but the only mineralized body transects the tonalitic gneiss in a southwest direction with subvertical dip.

The eastern pegmatites are only 10 to 80 cm wide, and the largest body was traced for a length of about 40 m. The northern dyke is about 40 m long in outcrop, and 2 m wide. The fracture-filling bodies are parallel-walled dykes without conspicuous pinch or swell undulations. However, they are locally offset by later transecting faults. Their contacts with the gneissic wall rocks are sharp.

Internally, the dykes are homogeneous or slightly concentrically zoned, with medium grained albite+quartz+K-feldspar along the margins passing gradually into coarse blocky K-feldspar+quartz core. Muscovite, garnet, and beryl are usually found close to the margins; partly oxidized crystals of pyrite occur in the same location (Table 29).

Only one of the Eaglenest dykes, the largest of the eastern

TABLE 29. PARAGENESIS OF THE GREER AND EAGLENEST LAKE PEGMATITE GROUPS

	GL															ENL	
	GI-F	GL-1	GL-2	GL-2A	GL-3	GL-4A	GL-4B	GL-6	GL-7	GL-8	GL-9	GL-11	GL-12	GL-12A	GLW-30	BB-44	1D
Microcline	●	●	●	●	●	●	●	●	●	●	●	●	●	●	●	●	●
Oligoclase		O						O		O	O						
Albite	●	●	●	●	●	●	●	●	●	●	●	●	●	●	●	●	●
Quartz	●	●	●	●	●	●	●	●	●	●	●	●	●	●	●	●	●
Holmquistite																	
Biotite	•	•						•	•		•	•				X	X
Muscovite	X	X	X	X	•	X	X	•	X	X	X	X	X	X	X		
Li-muscovite													X		•		
Lepidolite																	
Spodumene																	
Petalite																	
Eucryptite																	
Pollucite																	
Epidote																	
Chlorite								•		•							
Cordierite		(•)				(•)	(X)			(X)	(•)	(•)	(•)				
Garnet	•	•	•	•	X	•	•	X	X	X	X	•	X	X		X	X
Schorl																	
Elbaites																	
Topaz																	
Gahnite											•		•				
Beryl		•	X	•	•		•	X	•	•	•	•	•	•	•	•	
Titanite																	
Allanite																	
Gadolinite																	
Zircon										•	•						
Thorite																	
Uraninite																	
Magnetite																	
Ilmenite										•							
Niobian rutile										•	•		•x				
Aeschynite																	
Fersmite																	
Euxenite																	
Yttrotantalite																	
Cassiterite										•	•			•			
Columbite-tantalite														•			
Pseudo-ixiolite			•	•	?			•		•	•	•	•				
Microlite			•	•	•			•		•	•	•	•	•			
Tapiolite																	
Wodginite																	
Simpsonite																	
Stibiotantalite																	
Apatite								•		•	•		•				
Monazite								•		•			•				
Xenotime										•							
Triphylite-lithiophilite																	
Amblygonite-montebrasite																	
Sulphides of Fe, Cu	•	•						•									
As																	
Mo																	
Zn, Cd																	
Bi																	
Sb																	
Pb, Ag																	

Hydrothermal alteration products include late muscovite, chlorite, and green biotite formed at the expense of cordierite.

x - tantalian rutile with Ta>Nb.

Symbols as in Table 20.

TABLE 30. COMPOSITIONAL CHARACTERISTICS OF SELECTED MINERALS OF THE GREER LAKE PEGMATITE GROUP

Blocky K-feldspar (36 samples)	arith. mean, wt.%	Rb 0.339	K/Rb 42.3	Cs 0.025	
	std. deviation	±0.223	±23.2	±0.047	
	range	0.102-0.820	13.0-96.0	0.001-0.179	
Core muscovite (11)	Li 0.14	Rb 0.549	K/Rb 15.1	Cs 0.023	
	±0.075	±0.313	±5.6	±0.018	
	0.073-0.322	0.327-1.33	5.6-21.8	0.008-0.058	
Lithian muscovite and lepidolite (1)	Li 1.10	Rb 2.17	K/Rb 3.6	Cs 0.207	
Late beryl (26)	Li 0.120	Na 0.515	Na/Li 6.37	Cs 0.320	
	±0.093	±0.223	±4.9	±0.335	
	0.041-0.343	0.259-0.994	2.5-22.22	0.044-1.179	
Garnet (2)	Fe0 14.68	Mn0 27.63	(Mn0 x 100)/(Mn0 + Fe0) 65.33	Ca0 0.39	Mg0 0.36
	±5.20	±5.08	±12.13	±0.21	±0.26
	4.21-21.95	21.24-36.28	46.79-89.44	0.10-0.87	0.05-0.92
Columbite-tantalite (9)	(Mn0 x 100) / (Mn0 + Fe0) 64.11		$(Ta_2O_5 \times 100)/(Ta_2O_5 + Nb_2O_5)$ 64.72		
	±14.31		±23.23		
	49.37-84.49		23.89-93.48		

TABLE 31. COMPOSITIONAL CHARACTERISTICS OF SELECTED MINERALS OF THE EAGLENEST LAKE PEGMATITE GROUP

Blocky K-feldspar (6 samples)	arith. mean, wt.%	Rb 0.25	K/Rb 40.0	Cs 0.0043
	std. deviation	±0.02	± 3.2	± 0.0036
	range	0.18-0.27	35.0-51.2	0.0009-0.0093
Late beryl (1)	Li 0.031	Na 1.36	Na/Li 43.87	Cs 0.46

group, carries beryl. The other pegmatites are barren at their present erosion surface. The characteristics of blocky K-feldspars are comparable with those of the less-fractionated Greer Lake pegmatites, but the single beryl crystal analyzed shows very exotic parameters (Table 31). A contamination by albite is suspected.

The representation of this poorly exposed pegmatite group is too meager to make any meaningful attempts at classification. Despite the simple and scarce mineralization, the geochemical indicators suggest that it may be similar to the Greer Lake pegmatite group.

TABLE 33. COMPOSITIONAL CHARACTERISTICS OF SELECTED MINERALS FROM THE AXIAL PEGMATITE GROUP

		Rb	K/Rb	Cs	
Blocky K-feldspar (28 samples)	arith. mean, wt.%	0.064	176	0.0014	
	std. deviation	±0.032	±44.2	±0.0015	
	range	0.042-0.207	47.4-247	0.0003-0.0075	
	Li	**Rb**	**K/Rb**	**Cs**	**Be**
Core muscovite (5)	0.031	0.121	65.2	0.012	0.0012
	±0.022	±0.026	±19.7	±0.013	±0.0004
	0.020-0.066	0.086-0.154	45.8-93.5	0.003-0.034	0.0006-0.0015

Axial pegmatite group (AX)

This group is located in the body of subvolcanic Birse Lake quartz diorite, southwest of Tin Lake (Map 1, Fig. 77). The dykes are generally concordant with the S_2 foliation in the quartz diorite stock; they are most abundant along the axis of this body which is interpreted by Trueman (in prep.) as being the axial trace of a D_2-event anticline. Like other concordant pegmatites in the district, they pinch and swell with attendant warping of the foliation.

Individual bodies are flat-lenticular in shape, and they attain maximum length of about 100 m and width of 8 m in outcrop. Contacts with the host rock are sharp.

Internal structure is mostly irregular; medium- to coarse-grained aggregates of albite, quartz+muscovite grade into blocky patches of K-feldspar and quartz.

No rare-element minerals have been observed in this pegmatite group (Table 32) which is somewhat surprising. The geochemical characteristics of K-feldspars and micas do not suggest extensive mineralization but they coincide with the less-fractionated part of the Shatford Lake group, and they partly overlap with the least-fractionated segment of the Greer Lake group (Table 33). More intensive search may lead to finding accessory mineralization.

Spodumene has been reported from a pegmatite situated west of the main group shown in Figure 77 (R.A. Crouse, pers. comm. 1975). The pegmatite could not be located during the present study.

Birse Lake pegmatite group (BIS)

This group extends from Tin Lake to west-northwest to the northern side of Birse Lake and the southeastern part of Osis Lake (Map 1, Fig. 78). In the east, it merges gradationally with the fringes of the Tin Lake pegmatitic granite intrusion, and the boundary shown in Figure 78 is arbitrary. The Birse Lake pegmatites are essentially concordant to the bedding, layering and foliation of their host rocks of the Bernic Lake Formation, but they locally show offsets along joints which cross the strike of foliation at high angles, and in outcrop therefore give rise to local *en echelon* patterns.

Due to local variations in old structures hosting the pegmatites, coupled with late offsets, the shape of the pegmatite bodies tends to be irregular. Contorted lenticular forms predominate in the east, flat lenses and elongate dykes are typical of the western part. Dimensions reach about 1300 m in length (RNW) and 12 in width, but most of the bodies are considerably smaller. Contacts with the country rocks are predominantly sharp; only locally are they diffuse, exhibiting recrystallization of the wall rocks and penetration by felsic components of the pegmatite.

Internal structure of most of the Birse Lake pegmatites is patchy, with no regular relationship to the shapes of the bodies. Main assemblages are fine- to medium-grained albite+quartz±K-feldspar

Figure 77: Location map of the Axial pegmatite group

along the margins, and pods and schlieren of blocky K-feldspar+quartz grading into K-feldspar+tourmaline±quartz in a random manner. Only a few pegmatites (e.g., RQQ and parts of RNW) display concentric patterns of classic zoning: medium grained albite+quartz +muscovite (±K-feldspar) along the margings, grading into an intermediate zone of mainly K-feldspar+quartz+muscovite, which in turn grades into blocky K-feldspar+quartz+tourmaline megacrystals (± book muscovite), surrounding a quartz core. Large patches of quartz (and quartz core where developed) tend to be partly rose in colour.

Garnet and beryl are the only widespread accessory minerals in this pegmatite group (Table 34). Both are associated with medium grained or cleavelandite-like albite but separated from larger masses of the tourmaline+K-feldspar assemblage. Columbite-tantalite and amblygonite-montebrasite were found only in a single pegmatite (RNW), and heavily oxidized grains of triphylite-lithiophilite are also

TABLE 32. PARAGENESIS OF THE AXIAL PEGMATITE GROUP

	AX-1	AX-2	AX-3	AX-4	AX-5	AX-6	AX-7	AX-8	AX-9	AX-10	AX-11	AX-12	AX-13
Microcline	●	●	●	●	●	●	●	●	●	●	●	●	●
Oligoclase													
Albite	●	●	●	●	●	●	●	●	●	●	●	●	●
Quartz	●	●	●	●	●	●	●	●	●	●	●	●	●
Holmquistite													
Biotite													
Muscovite	•		•		X	X	X	•	•				
Li-muscovite												X	
Lepidolite													
Spodumene													
Petalite													
Eucryptite													
Pollucite													
Epidote													
Chlorite													
Cordierite													
Garnet			•			•	•		•				
Schorl													
Elbaites													
Topaz													
Gahnite													
Beryl													
Titanite													
Allanite													
Gadolinite													
Zircon													
Thorite													
Uraninite													
Magnetite													
Ilmenite													
Niobian rutile													
Aeschynite													
Fersmite													
Euxenite													
Yttrotantalite													
Cassiterite													
Columbite-tantalite													
Pseudo-ixiolite													
Microlite													
Tapiolite													
Wodginite													
Simpsonite													
Stibiotantalite													
Apatite													
Monazite													
Xenotime													
Triphylite-lithiophilite													
Amblygonite-montebrasite													
Sulphides of Fe, Cu													
As													
Mo													
Zn, Cd													
Bi													
Sb													
Pb, Ag													

Symbols as in Table 20.

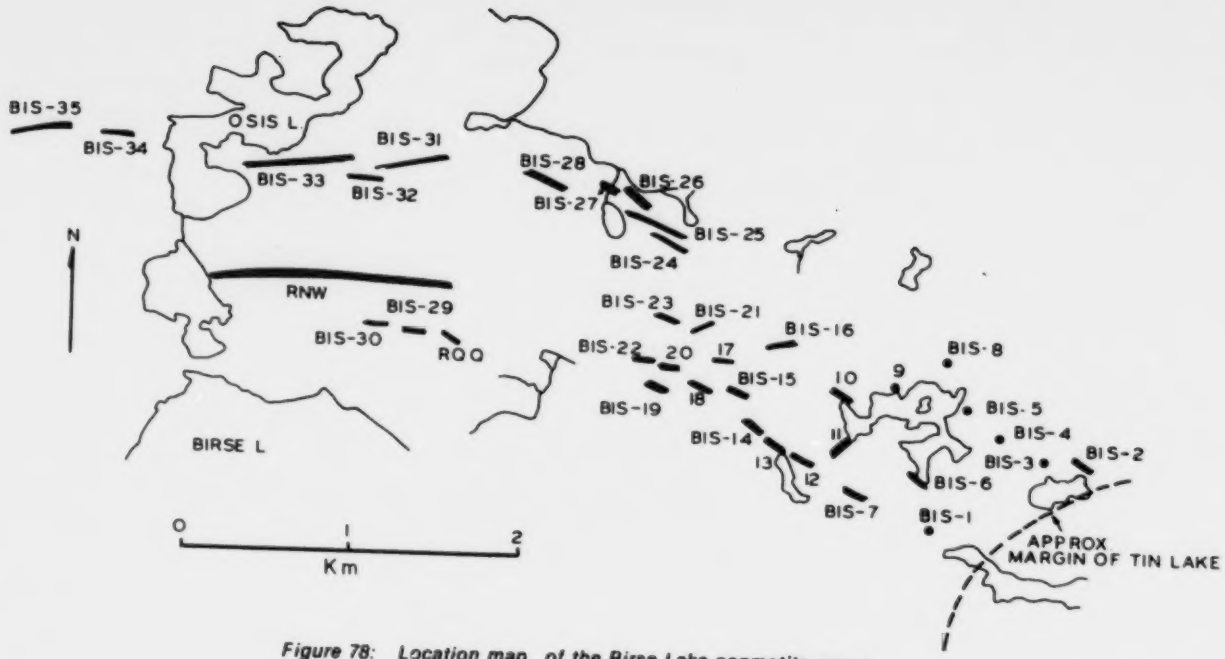

Figure 78: Location map of the Birse Lake pegmatite group

scarce. Thus the predominant mineralization carries Be, with Li (in the form of phosphates) and Nb-Ta being very sporadic.

Geochemical indicators show wide ranges of values (Table 35) that have only a limited regularity in spatial distribution. There is a steady decrease in K/Rb and an increase in Cs and Li in the blocky K-feldspars and muscovite from the east westwards along the southern margin of the group (pegmatites BIS-1 to BIS-23 and the southwestern swarm RNW, ROQ, BIS-29 and BIS-30), whereas the northern sequence of pegmatites (from BIS-24 in the east to BIS-35 in the west) seems to be geochemically separated and much less fractionated (Fig. 78).

Beryl is pale greenish to off-white in all of its occurrences, and it shows rather low Na/Li values but moderate Cs contents. Columbite-tantalite forms thin platy crystals bunched in radiating aggregates. Amblygonite-montebrasite occurs in small elongate grains which are difficult to distinguish from beryl.

Late alterations of pegmatite minerals are negligible. Hydrothermal sericitization of beryl is sporadic but K-feldspars may be heavily decomposed adjacent to the offsetting joints. Surface oxidation of triphylite-lithiophilite produces ill-defined mixtures of mainly sicklerite and heterosite.

The Birse Lake pegmatite group can be classified as mostly incompletely differentiated, weakly albitized, beryl-bearing blocky muscovite-microcline pegmatites (Beus 1951, 1960), with incipient tendency to more diversified mineralization only in the most fractionated bodies.

Rush lake pegmatite group (RL)

This group is located north to west of Rush Lake, west of the extreme fingering-out reaches of the Osis Lake pegmatitic granite (Map 1, Fig. 79). The pegmatites display two prominent controls that dictate their respective morphologies. In general, they are concordant to the layering and foliation of their host rocks, with only minor local discordances at very low angles. Such dykes, however, are, in the cases of the ODD West, ODD-SW-2, RL-2 and RL-1, connected to essentially flat-lying or tabular lobes which themselves carry notable accessory mineralization. Such lobes are seen to dip both northward or eastward at shallow angles, paralleling joint sets

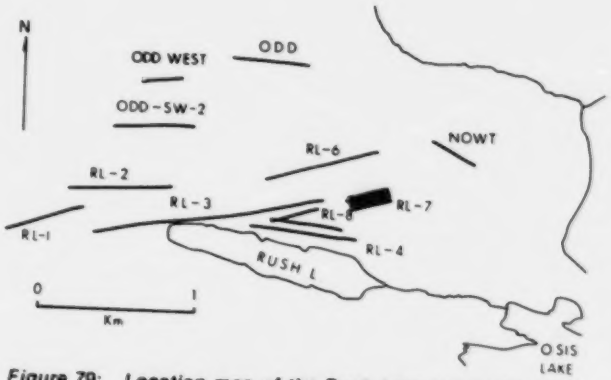

Figure 79: Location map of the Rush Lake pegmatite group

across the foliation in the host rocks. Pinching and swelling of both the near-vertical and near-horizontal components of the dykes is in evidence with attendant gentle warping of the containing surfaces.

A typical pegmatite of this group, such as the RL-1 body, is about 400 m long and reaches a maximum width of about 7 m. The RL-3 pegmatite, if truly continuous as schematized in Figure 79, would be over 1300 m in length, but a swamp covering it at an intersection with a shear zone makes this extent doubtful. Contacts with the country rocks are sharp, but associated with minor biotitization in metavolcanics and some muscovite, penetrating metasedimentary wall rocks.

Two textural and paragenetic types belong to the Rush Lake group. The first is very simple in both respects, unzoned or with a coarsening of grain size inwards (RL-3 to RL-8, ODD-SW-1, ODD-SW-3). The second, complex pegmatite type shows prominent zoning and replacement veining. Medium grained albite+quartz (± muscovite, K-feldspar) +tourmaline wall zones are characteristic, sporadically carrying patches of quartz+muscovite with subordinate verdelite, cassiterite and Ta/Nb oxide minerals. Intermediate zones

TABLE 34. PARAGENESIS OF THE BIRSE LAKE PEGMATITE GROUP

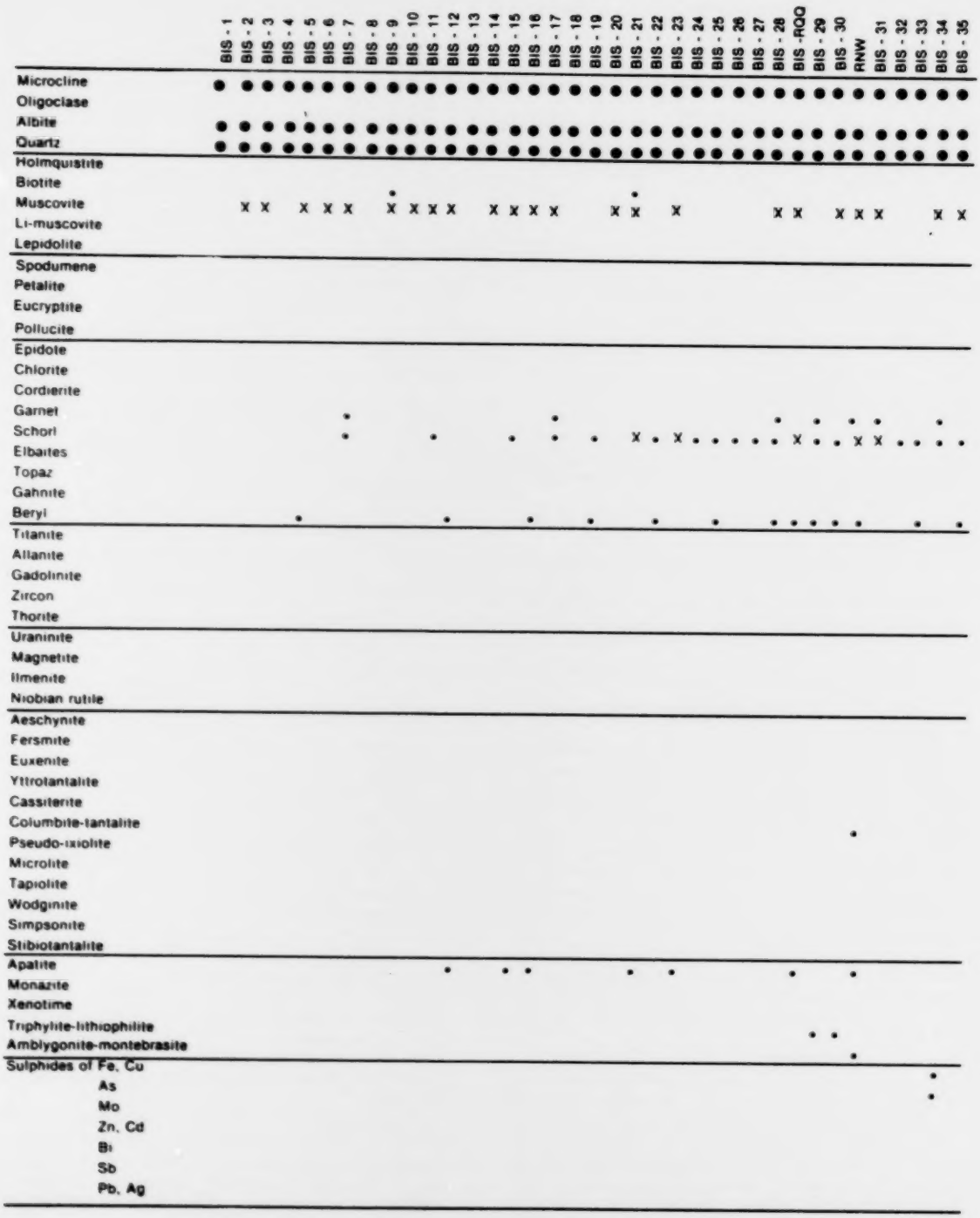

Symbols as in Table 20.

TABLE 35. COMPOSITIONAL CHARACTERISTICS OF SELECTED MINERALS FROM THE BIRSE LAKE PEGMATITE GROUP

		Rb	K/Rb	Cs	
Blocky K-feldspar	arith. mean, wt. %	0.108	118.7	0.0052	
(69 samples)	std. deviation	±0.076	±81.4	±0.0077	
	range	0.015-0.511	21.7-620.	0.0004-0.0411	
	Li	Rb	K/Rb	Cs	Be
Core muscovite	0.095	0.271	40.1	0.0316	0.0015
(21)	±0.133	±0.222	±18.9	± 0.0295	±0.0010
	0.011-0.346	0.099-1.13	8.0-84.6	0.0006-0.114	0.0004-0.0042
	Li	Na	Na/Li	Cs	
Late beryl	0.11	0.44	3.9	0.280	
(7)	±0.05	±0.24	±0.8	±0.085	
	0.057-0.18	0.22-0.90	3.05-5.0	0.179-0.391	
	Fe0	Mn0	(Mn0 x 100) / (Mn0 + Fe0)	Ca0	Mg0
Garnet	32.75	9.28	22.70	0.21	0.47
(5)	±0.50	±0.86	±1.85	± 0.02	± 0.36
	32.20-33.20	7.91-10.10	19.24-23.87	0.19-0.24	0.24-1.11

carry large club-shaped crystals of partly graphic K-feldspar surrounded by a coarse grained matrix of albite and quartz. Central parts of the dykes are occupied by blocky K-feldspar and quartz with either platy spodumene or columnar spodumene+quartz pseudomorphs after petalite; amblygonite-montebrasite and pollucite pods are found there, as well as albitization with other late accessory minerals. Quartz cores have not been observed in any of the outcrops.

Accessory minerals of the unzoned, reddish-colored pegmatite type are represented by biotite and tourmaline. The zoned type, however, exhibits diversified mineralization with substantial quantities of Li, Rb, Cs, Be, Sn, Ta-Nb, B, P, and F (Table 36). Lithium is concentrated mainly in spodumene or pseudomorphs after petalite, besides some amblygonite-montebrasite and triphylite-lithiophilite, but so far no extensive reserves of the Li-aluminosilicates have been found. Rb and Cs are enriched in feldspars and micas, and the OW dyke carries mica and clay pseudomorphs after pollucite pods. Beryl is subordinate, as are the different Ta, Nb-bearing minerals; however, cassiterite is rather abundant in some bodies (ODD, OW). The complex mineralogy of Sn, Ta, Nb, and Sb in these pegmatites is still under study; e.g., the exact nature of Sb-rich microlite (a possible new species), and staringite-like cassiterite rich in Ta, Nb and Fe are yet to be determined. Tourmaline is ubiquitous, and the Li-phosphates and apatite signify a considerable concentration of phosphorus. Fluorine participates in the amblygonite-montebrasite minerals and in micas, particularly the Li-bearing varieties.

Accessory occurrence of native metals and alloys (antimony, stibarsen) and sulphides (arsenopyrite, stibnite, sphalerite) is characteristic of the Rush Lake group; it is not encountered in any of the previously described pegmatite types.

Apart from some cassiterite and Ta-Nb minerals which occur in the inner parts of wall zones, all the rare-element mineralization is located in the central parts of the bodies. Spodumene, petalite, amblygonite-montebrasite, and pollucite belong to the primary components of the central blocky zones. Most of the Sn and Ta-Nb minerals, as well as beryl, Li-muscovite, lepidolite and the native metals and sulphides of Sb, As, Zn, Fe are associated with late albitization and micaceous alteration located in the central blocky zones or in the adjacent parts of intermediate zones.

Table 37 demonstrates the very advanced fractionation attained by the Rush lake pegmatites. The average feldspar and mica values are somewhat misleading because the data include samples from both simple and complex pegmatites belonging to the group.

Beryl is white or waterclear, subhedral to anhedral in shape, and its Na/Li and Cs values are close to the extreme enrichment known in primary beryl (Černý 1975). Partial analyses of platy spodumene, and of spodumene from the pseudomorphs after petalite, show Fe contents which are probably excessive over the true values. The only samples of both spodumene varieties that could be analyzed are somewhat altered, a feature which is always attended by Fe adsorption. Ta, Nb-oxide minerals occur mostly in small irregular grains, indistinguishable from cassiterite in some pegmatites. The mineralogical complexity of their aggregates requires at least X-ray diffraction for reliable identification. Fresh pollucite has not been found yet but pseudomorphous micaceous and clay associations developed at its expense were identified (Černý 1978). This breakdown of pollucite, probably hydrothermal, and the surface weathering of spodumene and triphylite are the most typical alteration processes in this pegmatite group.

In general, the complex pegmatites of the Rush Lake group can be classified as fully differentiated, partly to extensively replaced spodumene-albite-microcline and petalite-albite-microcline pegmatites with or without lepidolite, and with remarkable Cs-enrichment (Beus 1951, 1960).

The Bernic Lake pegmatite group (BL)

Exposures of this group are concentrated at the eastern end of Bernic Lake, the only exception being the Tanco pegmatite at its northwestern extremity (Map 1, Fig. 80). However, the extensive subhorizontal sheets typical of this group underlie most of the area, particularly north of Bernic Lake where additional bodies (eroded or hidden) are suggested by rare-alkali dispersion haloes in the host

TABLE 38. PARAGENESIS OF THE RUSH LAKE PEGMATITE GROUP

	ODD	OW	ODD-SW-2	RL-2	RL-1	ODD-SW-1	ODD-SW-3	RL-3	RL-4	RL-6	RL-7	RL-8	NOWT
Microcline	o	●	●	●	●	●	●	●	●	●	●	●	●
Oligoclase													
Albite	●	●	●	●	o	o	o	o	o	o	o	o	●
Quartz	●	●	●	●	●	●	●	●	●	●	●	●	●
Holmquistite													
Biotite		•	•		•	•	•	•	•	•	•	•	•
Muscovite	•	x	o	x	x	o	x	•	•	•	•	•	o
Li-muscovite		•		•									
Lepidolite		•											
Spodumene		•	x	•									
Petalite			(•)	(•)									
Eucryptite													
Pollucite		(•)											
Epidote													
Chlorite													
Cordierite													
Garnet													
Schorl		x	x	x	x	•	•	•	•	•	•	•	x
Elbaites		•	•	•									
Topaz													
Gahnite													
Beryl		•	•	•									•
Titanite													
Allanite													
Gadolinite													
Zircon													
Thorite													
Uraninite													
Magnetite													
Ilmenite													
Niobian rutile													
Aeschynite													
Fersmite													
Euxenite													
Yttrotantalite													
Cassiterite	x	•	•	•	•				•				
Columbite-tantalite		•											
Pseudo-ixiolite					•				•				
Microlite		•											
Tapiolite		•											
Wodginite					?								
Simpsonite													
Stibiotantalite		•											
Apatite	•	•	•	•	•	•	•						
Monazite													•
Xenotime													
Triphylite-lithiophilite		•			•								
Amblygonite-montebrasite		x	x	•									
Sulphides of Fe, Cu		•			•								
As		•			•								
Mo													
Zn, Cd					•								
Bi													
Sb		•											
Pb, Ag													

Hydrothermal alteration produced sericite at the expense of K-feldspar, spodumene and elbaites, and totally decomposed pollucite.

Symbols as in Table 20.

TABLE 37. COMPOSITIONAL CHARACTERISTICS OF SELECTED MINERALS FROM THE RUSH LAKE PEGMATITE GROUP

Blocky K-feldspar (31 samples)	arith. mean, wt.%	Rb 0.315	K/Rb 50.6	Cs 0.0265	
	std. deviation	±0.209	±28	±0.0261	
	range	0.10-0.881	14.0-108	0.0023-0.0870	
Core muscovite (10)	Li 0.10	Rb 0.35	K/Rb 24.1	Cs 0.053	Be 0.0020
	±0.70	±0.09	±5.3	±0.059	±0.0003
	0.026-0.22	0.22-0.53	16.3-32.9	0.008-0.190	0.0014-0.0024
Lithian muscovite and lepidolite (6)	Li 1.64	Rb 0.94	K/Rb 8.7	Cs 0.57	Be 0.0019
	±0.16	±0.27	±2.2	±0.24	±0.0003
	1.42-1.86	0.62-1.34	6.1-11.5	0.24-0.85	0.0015-0.0022
Late beryl (5)	Li 0.414	Na 0.939	Na/Li 2.4	Cs 2.152	
	±0.141	±0.207	±0.6	±1.115	
	0.171-0.538	0.608-1.179	2.1-3.6	0.235-3.018	
Garnet (1)	FeO 26.78	MnO 16.05	(MnO x 100) / (MnO + FeO) 37.47	CaO 0.24	MgO 0.32
Columbite-tantalite (3)	(MnO x 100) / (MnO + FeO) 42.09		$(Ta_2O_5 \times 100) / (Ta_2O_5 + Nb_2O_5)$ 66.61		
	±12.74		±35.61		
	31.17-56.08		26.77-95.33		
Spodumene (8)	Na_2O 0.335	Fe as Fe_2O_3 0.212			
	±0.323	±0.125			
	0.08-0.90	0.086-0.480			

rocks. All pegmatites belonging to this group are hosted by metavolcanics and associated subvolcanic intrusions of the Bernic Lake Formation.

The Tanco pegmatite is localized in a subhorizontal position across the axial trace of a D_2 anticline (Crouse et al. 1979), where this axis crosses the gabbro (so-called footwall amphibolite)-granodiorite boundary of the synvolcanic stock at the west end of Bernic Lake.

The Buck, Coe, Pegli and associated dykes are somewhat problematic as to their extent and structural affiliation. Two major bodies of this group extend for considerable distances westward, at a shallow dip (cf. below in Genetic Relationships, Fig. 130). However, diamond drilling results west of their outcrop indicate that the pegmatites are associated with a fault which separates metabasalt from clastic rocks north of, and parallel to, the north shore of Bernic Lake (Fig. 80). Individual pegmatite bodies are restricted to one or another side of the fault; none of them cross it. In general, as outlined from diamond drilling, the bodies appear to be parallel (with localized pinching and swelling) to prominent shallow west-dipping joints on Bernic Lake shoreline.

The smaller pegmatites at the east end of Bernic Lake display varied attitudes from east-west to northeast on strike, and subhorizontal to near-vertical in dip.

In summary, most of the Bernic Lake pegmatites (and definitely all large ones) have the form of flat subhorizontal sheets which occupy late fracture systems. The maximum dimensions of the Tanco pegmatite, the contouring of which was concluded recently, are 1400 x 600 x 100 m. The Coe and Pegli dykes are thinner (max. 10 m) but at least 2.5 km long in the east-west direction and open to the west and south. In contrast, bodies with a steeper dip, such as the Coe and BEP pegmatites, are much smaller.

Contacts with the metabasaltic-metagabbroic host rocks are invariably sharp. They are mostly simple and straight for the subhorizontal bodies, but the wall rock is heavily brecciated along the subvertical dykes. Thin metasomatic zones are developed in the wall rock consisting of biotite>tourmaline±holmquistite. Biotite is Li, Rb, Cs-rich; tourmaline is brownish-black and Mg-enriched; holmquistite is mostly dispersed on joints farther away from the contact. The reaction zones at the Tanco pegmatite contain locally abundant arsenopyrite and pyrrhotite with chalcopyrite in minor quantities.

Figure 80: Location map of the Bernic Lake pegmatite group

TABLE 38. SCHEMATIC VERTICAL ZONING SEQUENCE IN THE TANCO PEGMATITE
(Modified after Crouse et al. 1979)

Primary zones		Replacement units	
	←	Border unit (1)	albite, quartz (tourmaline, apatite)
wall zone (2)	albite, quartz, micas (beryl)		
pollucite zone (8)	pollucite (petalite, quartz, micas)		
upper intermediate zone (5)	quartz, spodumene, amblygonite (petalite, pollucite, K-feldspar)		
	←	lepidolite unit (9)	Li-micas, K-feldspar (Ta-Nb,Be,Zr-Hf,Sn minerals)
central intermediate zone (6)	K-feldspar, quartz (muscovite)		
	←	saccharoidal albite unit (3)	albite, quartz, (muscovite, Ta-Nb,Be,Zr-Hf,Sn minerals; sulphides)
quartz zone (7)	quartz		
	←		
wall zone (2)	albite, quartz, micas (beryl)		
	←	border unit (1)	albite, quartz (tourmaline, apatite)

The lower intermediate zone (4) (albite, K-feldspar, quartz, spodumene, amblygonite predominant over micas, triphylite), which is not included in the diagram, occurs alternately in different locations among the bottom four zones.

Location of the quartz zone (7) is also somewhat variable.

TABLE 39. SCHEMATIC CROSS SECTIONS THROUGH THE BUCK CLAIM PEGMATITE
(Partly after Lenton 1979)

D3*			
(W) 85-95 m downdip		Surface trench	(E)
		border zone	albite, quartz, tourmaline
		upper wall zone	tourmaline, albite, quartz, muscovite
		upper intermediate zone	cleavelandite, quartz, beryl, micas, K-feldspar, amblygonite, tantalite
upper intermediate zone	coarse albite, quartz, muscovite	core	quartz (blocky K-feldspar, amblygonite, triphylite, spodumene + quartz)
core	spodumene + quartz	lower intermediate zone	cleavelandite, quartz, beryl, micas, K-feldspar, amblygonite
lower intermediate zone	blocky K-feldspar, quartz	lower wall zone	saccharoidal albite quartz (tourmaline)
wall zone	saccharoidal albite, quartz (tourmaline)		

*The drill hole intersection D3 is 900 metres west of the surface exposure. The wall "zones" in both sections and the border zone in the trench are essentially metasomatic, the intermediate zones in the trench partly so.

Internal zoning is well developed in the large subhorizontal bodies. The Tanco pegmatite consists of a sequence of 9 units, 6 of which are zones of predominantly primary crystallization and 3 are metasomatic replacements (Table 38, modified from Crouse et al. 1979).

In the other subhorizontal pegmatites such as the Buck Claim body, zoning is even more regular but changes considerably along the dip. Table 39 shows the vertical zoning sequence at two widely separated sections of this pegmatite. The updip changes in zoning and mineral content indicate progressive differentiation of the pegmatite and an increasing extent of metasomatic reactions but the transitions are not as simple and gradational as disclosed by diamond drilling. Sizeable patches of petalite or lithium micas, which occupy almost the full width of the pegmatite, occur close to its crest; the significance of these accumulations in the zoning scheme cannot be evaluated unless the shape of the pegmatite is known in their immediate vicinity.

The steep-dipping pegmatites such as the Coe Claim body, retain the zoning sequences described above but they are combined with much more pronounced differences along the dip. For example, the Coe pegmatite is zoned at depth in a manner similar to the surface showing of the Buck body (except generally low K-feldspar content), but on the surface it consists almost solely of petalite, with subordinate quartz, altered triphylite, apatite, and muscovite. In the BEP pegmatite, a quartz core rimmed by albitization predominates at the surface level.

Rare-element mineralization is qualitatively identical with, but quantitatively more abundant than in the Rush Lake group. The same assemblage of elements (Li, Rb, Cs, Be, Sn, Ta-Nb, B, P, F, plus Zr-Hf) composes a more diversified association of minerals carrying them (Table 40). The major differences lie in the predominance of petalite and secondary spodumene+quartz pseudomorphs after it, primary spodumene being extremely rare; in the much broader spectrum of Ta, Nb-bearing species; in the relatively abundant occurrence of hafnian zircon at Tanco; and in an exotic assemblage of native metals, alloys, sulphides and sulphosalts particularly well developed at Tanco. Petalite, amblygonite and pollucite are usually concentrated in the innermost zones of the Bernic Lake pegmatites. Minerals of Ta-Nb, Sn, Be, and Zr-Hf are associated with various forms of albitization which may follow either the contacts with wall rock, or internal zone boundaries, or it may preferably attack K-feldspar-rich zones. Saccharoidal, granular, and platy cleavelanditic albite may all be accompanied by rare-element minerals, in different combinations in different pegmatites.

Geochemical characteristics of the Bernic Lake pegmatites are summarized in Table 41. It is evident that this group reaches the maximum fractionation levels known in granitic pegmatites in most respects (K/Rb, Cs, Fe/Mn, Nb/Ta). White to pink beryl reaches

TABLE 40. PARAGENESIS OF THE BERNIC LAKE PEGMATITE GROUP

	TANCO	LOWER TANCO	BCSE	BEP	BCNW	COE	PEGLI - 1	PEGLI - 2	BCF
Microcline	●	●	●	O	●	O	●	●	●
Oligoclase									
Albite	●	●	●	●	●	●	●	●	●
Quartz	●	●	●	●	●	●	●	●	●
Holmquistite	•		•	•	•	•	•	•	
Biotite	•	•	•	•	•	•	•	•	•
Muscovite	X	X	X	X	X	X	X	X	X
Li-muscovite	X			•	•		•	•	
Lepidolite	•	?			•				
Spodumene	●	●	•	•	X	O	O	O	
Petalite	●	●		(•)	X	●	●	●	
Eucryptite	X								
Pollucite	●				(•)				
Epidote									
Chlorite									
Cordierite									
Garnet	?								
Schorl	X	•	X	X	X	•	•	•	
Elbaites	•				•				
Topaz									
Gahnite	?								
Beryl	•		•	X	•	•		•	
Titanite									
Allanite									
Gadolinite									
Zircon	•								
Thorite	•								
Uraninite	?								
Magnetite									
Ilmenite	•								
Niobian rutile									
Aeschynite									
Fersmite									
Euxenite									
Yttrotantalite									
Cassiterite	•	?		•	•		•	•	
Columbite-tantalite	•	?		•	•		•		
Pseudo-ixiolite	•								
Microlite	•	?							
Tapiolite	•								
Wodginite	•	?							
Simpsonite	•								
Stibiotantalite	?								
Apatite	•	•	•	X	X	X	•	•	
Monazite									
Xenotime									
Triphylite-lithiophilite	•		X		X	X	•	•	
Amblygonite-montebrasite	O	O	•	•	X	X	X	X	
Sulphides of Fe, Cu	•		•		•	•		•	
As	•		•						
Mo	•					•			
Zn, Cd	•								
Bi	•								
Sb	•				•				
Pb, Ag	•								

Hydrothermal alteration of mainly spodumene, petalite, pollucite and phosphates produced adularia, albite, cesian analcime, cookeite, illite, kaolinite, montmorillonite, calcite, rhodochrosite, apatite, lithiophosphate, tancoite, herderite, hurlbutite, overite, fairfieldite, whitlockite and crandallite.

Symbols as in Table 20.

TABLE 41. COMPOSITIONAL CHARACTERISTICS OF SELECTED MINERALS FROM THE BERNIC LAKE PEGMATITE GROUP

Blocky K-feldspar (57 samples)	arith. mean, wt.%	Rb	K/Rb	Cs
	std. deviation	1.476	9.5	0.1262
	range	±0.62	±5.4	±0.0837
		0.388-2.66	4.0-24.3	0.0165-0.286
Core musovite (19)	Li	Rb	K/Rb	Cs
	0.24	1.33	6.4	0.087
	±0.07	±0.44	±2.4	±0.054
	0.14-0.42	0.72-2.05	3.7-10.3	0.028-0.200
Lithian muscovite and lepidolite (25)	Li	Rb	K/Rb	Cs
	1.22	2.33	3.7	0.392
	±0.56	±0.82	±1.9	±0.238
	0.14-2.34	0.96-3.69	1.9-8.4	0.039-0.834
Late beryl (59)	Li	Na	Na/Li	Cs
	0.422	0.987	2.4	1.911
	±0.129	±0.261	±0.5	±1.103
	0.157-0.599	0.445-1.498	1.83-5.11	0.197-3.574
Columbite-tantalite (20)	(MnO x 100) / (MnO + FeO)		$(Ta_2O_5 \times 100) / (Ta_2O_5 + Nb_2O_5)$	
	91.50		73.78	
	±13.82		±12.10	
	48.75-99.32		42.68-95.43	
Spodumene (10)	Na_2O	Fe as Fe_2O_3		
	0.235	0.162		
	±0.157	±0.155		
	0.08-0.51	0.02-0.41		

extreme Cs-enrichment. Oxide minerals of Ta-Nb are Mn- and Ta-rich; they vary in grain size, colour, and other easily observable properties but their identification in field is difficult, particularly in fine grained aggregates. Identification of petalite may also be a problem because its appearance may simulate K-feldspar in some cases and spodumene in others.

Late alterations are common but not extensively developed: hydrothermal action affects mainly spodumene and petalite (albite, muscovite, adularia, cookeite, cesian analcime, rhodochrosite, calcite, clay minerals), and to a lesser degree also amblygonite (montebrasite, muscovite, apatite, cookeite, lithiophosphate, tancoite), triphylite (calcite, apatite), pollucite (micas, clay minerals), and rarely beryl (hurlbutite, herderite). Hydrothermal weathering may be responsible for decomposition of pollucite, and triphylite is usually heavily oxidized in surface exposures.

The Bernic Lake pegmatite group belongs to the fully differentiated, extensively replaced petalite-albite-microcline pegmatites with lepidolite and pollucite (Beus 1951, 1960), and with remarkable enrichment in Be, Sn, Ta, and P.

Publications devoted to the Tanco pegmatite are listed in the section referring to Previous Work. Studies of other mineral groups from this pegmatite and of the geochemistry of Rb, Cs, Tl and Ga are in progress, as is the description of a new phosphate species tancoite (Ramik, in prep.). Of the other pegmatites belonging to the Bernic Lake group, the Buck Claim body was studied by Lenton (1979), and its pollucite alteration was reported by Černý (1978).

The Eagle-Irgon pegmatite group (EAI)

This group is located in the greenstone belt just north of Cat Lake and westwards from there (Map 1, Fig. 81). They are essentially concordant to the tectonic fabric of their host rocks, striking west-northwest to west and dipping nearly vertically. The major bodies appear coincidentally (?) along their mutual strike projections.

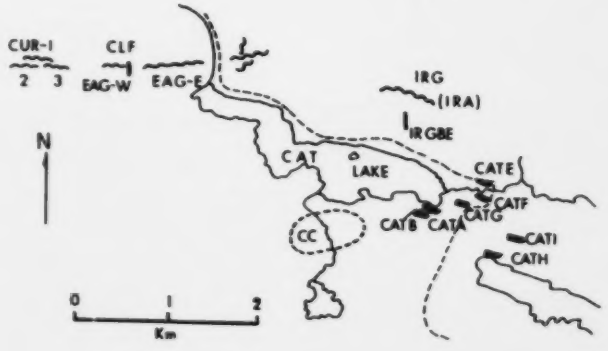

Figure 81: Location map of the Eagle-Irgon, Beryl-Tourmaline, Cat Lake and Central Claim pegmatite groups

TABLE 42. PARAGENESIS OF THE EAGLE-IRGON, BERYL-TOURMALINE, CAT LAKE AND CENTRAL CLAIM PEGMATITE GROUPS

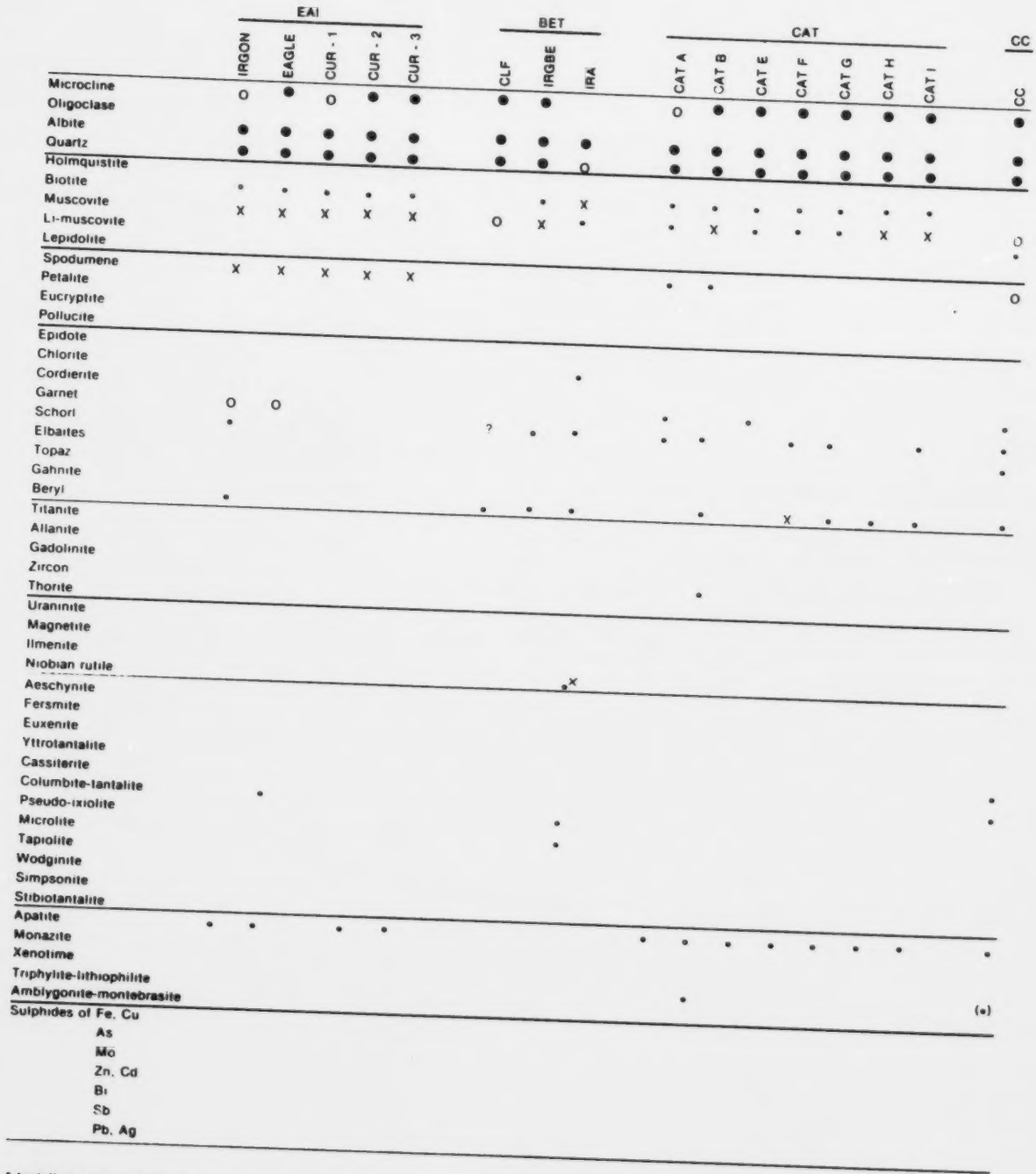

* tantalian rutile with Ta> Nb.

In the CAT group, hydrothermal alteration produces sericitization of spodumene and beryl, and surface weathering leads to oxidation and leaching of triphylite.

In the CC pegmatite, alluaudite and vivianite are alteration products after, probably, triphylite. Chrysoberyl was identified in this pegmatite too late to be included in the Table.

Symbols as in Table 20.

TABLE 43. COMPOSITIONAL CHARACTERISTICS OF SELECTED MINERALS FROM THE EAGLE-IRGON PEGMATITE GROUP

Blocky K-feldspar (18 samples)	arith. mean, wt.%	Rb	K/Rb	Cs	
	std. deviation	0.71	16.8	0.022	
	range	±0.20	±5.4	±0.013	
		0.412-1.21	9.0-28.0	0.008-0.058	
Garnet (2)	FeO	MnO	(MnO x 100) / (MnO + FeO)	CaO	MgO
	15.98	26.50	62.26	0.44	0.47
	12.45-19.50	22.40-30.59	53.46-71.07	0.31-0.58	0.22-0.73
Spodumene (4)	Na_2O	Fe as Fe_2O_3			
	0.162	1.34			
	±0.096	±0.14			
	0.096-0.30	1.14-1.46			

The pegmatite bodies are flat-lenticular with common pinch and swell variations in thickness. Locally they seem to be segmented along strike, and they typically occur in closely spaced pairs. Maximum dimensions are attained by the Eagle dyke which is, if continuous, about 1100 m long; the thickness does not exceed 12 m and mostly is 6 m or less.

Internal structure is rather homogeneous and mostly gneissic in appearance. Only the least-strained sections exhibit blocky K-feldspar in a matrix of quartz, albite, and spodumene, with subordinate garnet. Otherwise, the fabric is gneissic, oriented parallel to the attitude of the pegmatites, with alternating bands of feldspars, spodumene and quartz, and trains of garnet. Small lenticular or ovoidal aggregates of randomly oriented spodumene and quartz are the only features disrupting the banded fabric, but even these are oriented parallel to the attitude of the pegmatites. Cataclastic effects are common both along the margins and in the unstrained blocky parts of the dykes. Biotite flakes occur sporadically along the contacts, muscovite is subordinate to rare in the interior and mainly in the unstrained pegmatites. The overall composition of the dykes is almost anhydrous.

Spodumene is the only rare-element mineral present in conspicuous quantities (Table 42). It belongs to the phenocrystic variety of Heinrich's (1975) classification, although its textural characteristics are not adequate for this term sensu stricto. Garnets are fairly manganoan in composition, with moderate CaO and MgO contents. K-feldspars exhibit, however, advanced fractionation of rare alkalis (Table 43).

Columbite-tantalite was found in the Eagle pegmatite in tiny grains barely sufficient for X-ray diffraction identification. Green beryl also is scarce, and is found only in a peculiar fracture-filling association with black tourmaline in the Irgon dyke (cf. CAT group below, p. 95).

Late alterations are practically non-existent in the Eagle-Irgon group.

This pegmatite group can be classified as replaced spodumene-albite pegmatites of Beus (1951, 1960), almost devoid of any other mineralization but with remarkably low K/Rb and K/Cs ratios.

The Beryl-Tourmaline pegmatite group (BET)

This group is scattered in an east-west direction in close vicinity of the Eagle-Irgon bodies (Map 1, Fig. 81). Members of this group are north-striking and steeply dipping, crosscutting the regional foliation (and the EAI-pegmatite directions parallel to it) at high angles approaching normal. One of them, the Cliff (CLF) pegmatite, crosscuts the western part of the Eagle dyke. Structural controls of the Beryl-Tourmaline pegmatites are uncertain, but it is noted that they lie parallel to a suite of earlier (?) emplaced felsite dykes of the Cat Lake area, and to a strong photo-lineament which runs north-south parallel to Central Creek at the eastern exposure of the Central Claim pegmatite.

The pegmatites of this group are small bodies not exceeding about 15 m in length, and their widths are mostly less than 1 m. The Irgon-Albite (IRA) veinlets have a maximum thickness of about 20 cm.

Internal structure of the BET pegmatites is inhomogeneous and rather patchy in appearance, lacking any definable zonal pattern. Also, it is variable from body to body, dependent upon the different mineral parageneses. If it was not for the attitude and beryl content that are common to all four dykes, it would be very tenuous to assemble them into a single group. The IRA pegmatites differ even in their shape and attitude, forming ptygmatically folded veinlets in metabasalts and volcanogenic metasediments adjacent to the Irgon spodumene dykes.

Table 42 presents the mineral associations of the individual members of this group, and Table 44 illustrates some of the geochemical characteristics. Rare-alkali enrichment is low, as is the Ta and Mn fractionation. All beryl samples analyzed proved to be excessively contaminated by albite and/or muscovite and the results were meaningless. Nevertheless, the green colour of beryl and its low refractive indices suggest low alkali contents, in accord with the feldspar chemistry.

Late alterations are rather limited, except sericitization of beryl and feldspars.

With hesitation, the BET pegmatites may be likened to the not fully differentiated muscovite-blocky microcline class of Beus (1951, 1960); some of the known occurrences, and any possible future finds of new bodies belonging to this group, require additional study. A possible relationship of these pegmatites to the tourmaline-beryl veinlets transecting the EAI and CAT pegmatites (c.f. p.93 and 95) should be examined.

The Cat Lake pegmatite group (CAT)

This group is concentrated in a relatively small area between and around the adjacent extremities of Cat and Euclid Lakes (Map 1, Fig. 81). The pegmatites are largely concordant to the foliation of their host metabasaltic rocks with which they dip in near-vertical attitudes. The only variation to this habit is that of bifurcation of the CATB dyke, which extends in subparallel branches along the foliation.

TABLE 44. COMPOSITIONAL CHARACTERISTICS OF SELECTED MINERALS OF THE BERYL-TOURMALINE PEGMATITE GROUP

		Rb	K/Rb	Cs
Blocky K-feldspar	arith. mean, wt.%	0.315	35.0	0.009
(3 samples)	std. deviation	±0.024	±2.6	±0.003
	range	0.297-0.342	32.0-37.0	0.007-0.012
	$(MnO \times 100) / (MnO + FeO)$	$(Ta_2O_5 \times 100) / (Ta_2O_5 + Nb_2O_5)$		
Columbite-tantalite	28.77	54.40		
(4)	±11.94	±4.94		
	22.31-46.67	48.62-59.42		

TABLE 45. COMPOSITIONAL CHARACTERISTICS OF SELECTED MINERALS OF THE CAT LAKE PEGMATITE GROUP

		Rb	K/Rb	Cs	
Blocky K-feldspar	arith. mean, wt.%	0.41	30.8	0.0187	
(12 samples)	std. deviation	±0.15	±11.8	±0.0100	
	range	0.217-0.65	18.0-51.8	0.0008-0.00053	
	Li	Rb	K/Rb	Cs	Be
Core muscovite	0.11	0.53	17.8	0.034	0.0019
(8)	±0.035	±0.2	±6.7	±0.011	±0.0014
	0.057-0.15	0.28-0.78	10.7-24.2	0.021-0.049	0.0008-0.0053
	Li	Na	Na/Li	Cs	
Late beryl	0.26	0.88	3.37	0.15	
(4)	±0.08	±0.25	±0.23	±0.04	
	0.17-0.35	0.63-1.15	3.18-3.71	0.12-0.20	
	FeO	MnO	$(MnO \times 100)/(MnO + FeO)$	CaO	MgO
Garnet	24.19	18.11	42.79	0.43	0.33
(6)	±2.80	±3.00	±6.92	±0.22	± 0.21
	21.43-29.35	12.47-20.70	29.82-48.71	0.20-0.72	0.0-0.58
	$(MnO \times 100) / (MnO + FeO)$	$(Ta_2O_5 \times 100) / (Ta_2O_5 + Nb_2O_5)$			
Columbite-tantalite	66.38	76.92			
(3)	±12.24	±1.04			
	59.27-80.52	75.79-77.85			
	Na_2O	Fe as Fe_2O_3			
Spodumene	0.138	0.73			
(2)					
	0.075-0.20	0.71-0.74			

In contrast to the preceding group, the CAT pegmatites appear to be smaller with a lower length-to-width ratio. The largest of these lenticular dykes is about 150 m long in outcrop, and the width rarely exceeds 5 m. Contacts with host rocks are sharp, and locally somewhat sheared.

Internally, some of the dykes appear homogeneous, displaying 2-10 cm grain size, random orientation and even distribution of mineral constituents (e.g., CATF). Other dykes show the same texture but with gradual increase in grain size inwards, and with quartz somewhat accumulated in central parts (e.g., CATI). The largest pegmatites, however, are heterogeneous in their texture and mineral assemblage (CATA, CATB). Typical associations are saccharoidal albite+garnet±muscovite; granular albite+quartz+ spodumene; and blocky K-feldspar+quartz+book muscovite. Distribution of these assemblages within individual pegmatite bodies is irregular, and concentric zoning is virtually absent. In some of the bodies, shearing is extensive along margins and pronounced foliation is developed in the narrow portions and pinch-out ends of the pegmatites, similar to the texture predominant in the Eagle-Irgon group.

The paragenesis of this pegmatite group is rather simple (Table 42) and the geochemical characteristics indicate only a modest degree of fractionation (Table 45). Spodumene belongs again to the "phenocrystic" category of Heinrich (1975), being fairly Fe-rich but texturally quite different, mostly fine grained to columnar and not exceeding 6 cm in length. Green to off-white beryl shows low Na/Li ratio but very low Cs contents. Garnets contain about equal Fe0 and Mn0, and the Ca0 and Mg0 percentages are very low. The few grains of Nb/Ta oxide minerals found in the CATB body are complex in phase composition and chemistry, but the main components are Ti-enriched tantalite and manganotantalite.

The CATB body is transected by approximately north-striking subvertical fracture fillings comprised of black tourmaline and beryl, with local open vugs. This assemblage closely resembles the late fracture fillings observed in the Irgon pegmatite (c.f. p. 95).

Late hydrothermal alterations affect spodumene and, to a much lesser degree, beryl; both are commonly sericitized. Surface weathering attacks triphylite-lithiophilite which breaks down into the more oxidized and alkali-poor members of the heterosite and sicklerite groups.

In terms of pegmatite classification of Beus (1951, 1960), the Cat group is best described as an initial transition from fully differentiated, partly albitized blocky K-feldspar+muscovite pegmatites to the replaced spodumene+albite pegmatites. However, the mineralization seems to be more diversified than in the geochemically and "evolutionally" more advanced Eagle-Irgon dykes.

The Central Claim group (CC)

This group is defined as a separate type, although represented by only a single pegmatite, because of its specific character and genetic significance. The Central Claim body is located south of Cat Lake, and it outcrops along the banks of Central Creek (Map 1, Fig. 81).

The pegmatite, as defined by mapping and diamond drilling, is a subhorizontal tabular body averaging about 4 m in thickness (but varying between 1.10 and 7 m) and extending in excess of 500 m and 350 m in the north and east directions, respectively, through the Maskwa Lake quartz diorite. Two "rolls" are evident in the body, the axes of which plunge shallowly westward parallel to the dip direction of the pegmatite. The attitude of the pegmatite does not appear to conform to a recognized regional structural control, the host fracture being unique in this district.

Four features are of significance in attempting to interpret the structural setting: (1) the hanging wall and footwall contacts are both sheared and/or "lined" with schistose biotite; (2) a strong north-south airphoto lineament controlling Central Creek passes through the outcrop area and is parallel to the felsite dykes elsewhere in the neighbourhood; (3) the CATA, CATB pegmatite lineament terminates at the northeast corner of the pegmatite; and (4) a linear lithium anomaly extends westward from the southwest corner of the Central Claim body.

It is suggested therefore (but highly interpretative) that the Central Claim dyke may have been emplaced along a north-striking fault which postdated and offset the CATA and CATB pegmatites in a sinistral direction. However, this interpretation does not account for the shallow nature of the dip of such a fault, especially in view of steep subvertical dips of the parallel-striking felsite dykes.

The biotite zone along the pegmatite contacts, mentioned earlier, contains 0.62% Li_20, 0.54% Rb_20, and 0.57% Cs_20. It seems to be gradational into the wall rock in places, but it is sharply separated from the pegmatite.

The pegmatite is well zoned but most of the primary zoning pattern is obliterated by subsequent metasomatic processes. Three units can be distinguished: (1) upper and lower muscovite+quartz zone with subordinate albite, accessory apatite and garnet, and relictic blocky microcline; (2) central core of platy spodumene and quartz, and (3) a replacement unit of saccharoidal quartz penetrating in an irregular manner both of the preceding units (mainly the core), carrying also beryl, tantalite, tourmaline, apatite, cassiterite, and products of triphylite alteration. Within the upper and lower zones, a substantial part of the muscovite+quartz assemblage may also be metasomatic, as suggested by the highly corroded character of the relictic K-feldspar.

The paragenesis of the pegmatite is summarized in Table 42, and some of the geochemical characteristics of its minerals are given in Table 46. Fractionation of rare alkalis is considerably advanced, as is that of Mn and Ta in oxide minerals of these metals and in garnet (based on preliminary microprobe results). White subhedral to anhedral beryl suggests an unusual trend of Na/Li increasing with Cs-enrichment but this is probably caused by analysis of only a few samples. Chrysoberyl occurs in one of the outcrops, in the absence of beryl. Most of the columbite-tantalite seems to be present in the form of needle-shaped crystals of microscopic size, ingrown in saccharoidal albite. The analyzed sample is one of the very few grains reaching over 2 mm in size. Spodumene belongs to the zonal type of Heinrich (1975) despite the somewhat higher than "regulation" content of Fe. However, at least some of the determined Fe_2O_3 comes from the Fe-hydroxide stain penetrating along cleavage, which could not be avoided in sample separation. No fresh triphylite-lithiophilite was found but alluaudite and vivianite belong to its most frequent alteration products (Moore 1971, 1973).

Secondary alterations are very limited, except for this apparently quantitative decomposition of triphylite-lithiophilite. Micaceous replacement of spodumene is rather exceptional, and only small patches of purplish lithium-bearing mica have been found in intimate intergrowth with saccharoidal albite.

The pegmatite belongs to the class of fully differentiated and replaced spodumene-albite pegmatites of Beus (1951, 1960).

The Maskwa Lake pegmatite series (MWL)

This closely-spaced swarm of pegmatites which show geochemical similarities but paragenetically consist of three types is provisionally grouped into a single series. Two of the types are represented by single pegmatites, and only discoveries of new bodies in the area might lead to a more detailed subdivision into groups. The Maskwa Lake pegmatites are located northwest of Donner Lake (Map 1, Fig. 82).

With the exception of the High-Grade dyke, the Maskwa Lake series strikes northeasterly, and dips subvertically. The pattern of host fractures coincides with orientation of shear and fault zones which cross the Maskwa Lake batholith and extend into the Bird River Greenstone Belt, transecting it at high angles to its internal fabrics. These shears and faults appear to be of peri-anticlinal nature (de Sitter 1956), spreading from an axial or crestal fault zone passing through Maskwa Lake southeast toward the eastern end of Bird Lake (Trueman 1971, 1980; cf Fig. 120).

TABLE 46. COMPOSITIONAL CHARACTERISTICS OF SELECTED MINERALS OF THE CENTRAL CLAIM PEGMATITE

Blocky K-feldspar (10 samples)	arith. mean, wt.%	Rb 0.773	K/Rb 14.5	Cs 0.038	
	std. deviation	±0.078	±0.9	±0.011	
	range	0.59-0.88	13.0-16.0	0.020-0.054	
Core muscovite (2)	Li 0.081	Rb 0.99	K/Rb 8.25	Cs 0.1	Be 0.0019
	0.065-0.097	0.97-1.01	8.05-8.44	0.068-0.133	0.0017-0.002
Late beryl (4)	Li 0.383	Na 1.154	Na/Li 2.99	Cs 0.519	
	±0.067	±0.255	±0.17	±0.128	
	0.283-0.422	0.772-1.305	2.73-3.09	0.33-0.613	
Garnet	FeO	MnO	(MnO x 100) / (MnO + FeO) ~60	CaO	
Spodumene (5)	Na_2O 0.126	Fe as Fe_2O_3 0.155			
	±0.064	±0.057			
	0.077-0.220	0.088-0.225			

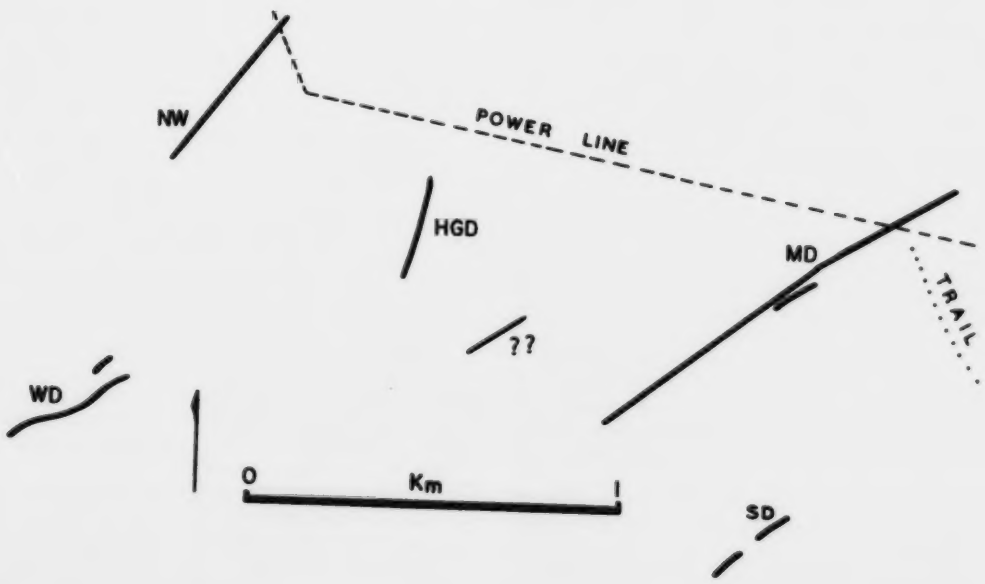

Figure 82: Location map of the Maskwa Lake pegmatite series

The High-Grade dyke strikes north and dips steeply to the west at about 70°. No structural pattern is evident which may control this dyke, although some of the regional airphoto lineaments approach the north-south strike rather closely.

The first and most abundant pegmatite type at Maskwa Lake consists of spodumene-bearing dykes (Main, Western, and Southern, Fig. 82) which form narrow, somewhat pinching and swelling bodies attaining about 550 m in length and between 3 and 5 m in width. The Main dyke consists of at least three closely spaced parallel bodies irregularly overlapping along strike. The contacts with the country rocks are sharp and marked by local patches of holmquistite.

The dykes are rather homogeneous, with local indications of inwardly increasing grain size, and irregular distribution of pods and bands of fine grained albite+quartz± muscovite. The main mineral assemblage consists of columnar K-feldspars (3 to 10 cm in length) in a mass of quartz, albite and spodumene. Other minerals present in this pegmatite type are scarce (Table 47). K-feldspars are considerably enriched in Rb and Cs (Table 48). Spodumene is white but its chemical composition is not known as all attempts at separation from quartz, muscovite and albite failed.

These dykes can be related to the fully differentiated and replaced spodumene+albite type of Beus (1951, 1960), with negligible zoning and no significant mineralization other than Li, but highly fractionated.

The second type in the Maskwa Lake area is represented by the petalite-bearing Northwest dyke which extends for about 250 m, with average thickness of about 5 m; its total extent is not known (Fig. 82). Sharp contacts are rimmed by a thin biotite selvage, and holmquistite is present locally.

The paragenesis of the dyke is rather simple (Table 47), and the geochemical characteristics match closely those of the preceding pegmatite type in the area. However, spodumene in the northwest dyke is secondary after petalite, the original crystals of which attained 15 cm in length. The spodumene+quartz pseudomorphs after them are imbedded, together with columnar K-feldspar, in a matrix of albite+quartz+Li-enriched curvilamellar mica, with random orientation and without any noticeable zoning throughout the thickness of the dyke. The matrix minerals corrode the K-feldspar blocks but the spodumene+quartz pseudomorphs seem to retain the original shape of petalite crystals much better. Chemical analyses of spodumene show rather high Fe content, the majority of which comes from clayey alteration of the mineral. Fresh material was not available for chemical analysis.

The Northwest pegmatite belongs to the group of replaced petalite+albite pegmatites in terms of the Beus (1951, 1960) classification, showing a very high degree of rare alkali fractionation but no appreciable rare-element mineralization, in the preserved part, other than Li.

The last pegmatite type in the Maskwa Lake series is again represented by only a single body, the pollucite-bearing High-Grade dyke (Fig. 82). It has been drilled for 150 m along the strike; its thickness reaches a maximum of 1.80 m and is variable both along strike and downdip. Its lower extremities have not been reached to date. Contacts with the metabasaltic wall rock are mostly sharp, except for a few structurally disturbed spots of feldspar diffusion into the greenstone, and they are sporadically lined with holmquistite.

Internally, the dyke is extremely but patchily differentiated, with superposed metasomatic assemblages. Typical primary assemblages are blocky K-feldspar+quartz, pollucite+quartz, and quartz+spodumene. Albitization is very widespread; replacement units of lepidolite are spotty but extremely rich in this mica, to the exclusion of all other minerals.

The paragenesis of the HGD pegmatite shown in Table 47 is incomplete; exmination of drill cores obtained at the time of writing will probably reveal some additional species. This is expected mainly because of the extremely fractionated geochemical characteristics

TABLE 47. PARAGENESIS OF THE MASKWA LAKE PEGMATITE SERIES

	HGD	NW	MAIN DYKE	WD	SD
Microcline	●	●	●	●	●
Oligoclase					
Albite	●	●	●	●	●
Quartz	●	●	●	●	●
Holmquistite	•		•		
Biotite	•	•	•	•	•
Muscovite	X	X	•	•	X
Li-muscovite		X			
Lepidolite	X				
Spodumene	X	X	X	X	•
Petalite	?	X			
Eucryptite					
Pollucite	•				
Epidote					
Chlorite					
Cordierite					
Garnet	•		•		
Schorl	•	•			
Elbaites	•				
Topaz					
Gahnite					
Beryl	•	•			
Titanite					
Allanite					
Gadolinite					
Zircon					
Thorite					
Uraninite					
Magnetite					
Ilmenite					
Niobian rutile					
Aeschynite					
Fersmite					
Euxenite					
Yttrotantalite					
Cassiterite					
Columbite-tantalite	•		•		
Pseudo-ixiolite					
Microlite	•				
Tapiolite					
Wodginite					
Simpsonite					
Stibiotantalite					
Apatite					
Monazite					
Xenotime					
Triphylite-lithiophilite					
Amblygonite-montebrasite					
Sulphides of Fe, Cu					
As					
Mo					
Zn, Cd					
Bi					
Sb					
Pb, Ag					

Hydrothermal alteration produces late feldspars, micas, and clay minerals at the expense of spodumene and pollucite.

Symbols as in Table 20.

TABLE 48. COMPOSITIONAL CHARACTERISTICS OF SELECTED MINERALS FROM THE MASKWA LAKE PEGMATITE SERIES

Blocky K-feldspar (15 samples)	arith. mean, wt.%	Rb 1.57	K/Rb 7.4	Cs 0.091
	std. deviation	±0.48	±2.0	±0.068
	range	1.19-3.05	3.4-9.7	0.016-0.292
	Li	Rb	K/Rb	Cs
Lithian muscovite and lepidolite (1)	1.50	2.41	2.3	0.7
	Na_2O	Fe as Fe_2O_3		
Spodumene (3)	0.292	0.073		
	±0.045	±0.012		
	0.24-0.32	0.064-0.087		

of the pegmatite, ranging it to the same level in rare-alkali enrichment as the Tanco pegmatite in the Winnipeg River district (Table 48).

Spodumene is white and low in Fe, corresponding to the zonal type as defined by Heinrich (1975). It appears to be entirely primary, as no indications of pseudomorphs after petalite were observed. This is quite surprising in view of the fact that the HGD pegmatite is obviously an open-fracture-filling body with only limited signs of shearing; it contains pollucite which prefers low P environment, and is close to the Northwest dyke which has all of its primary anhydrous Li-aluminosilicate in the form of petalite.

A few crystals of white anhedral beryl were noted in drill cores but they were too small for chemical analysis. Pollucite and spodumene suffer from late hydrothermal alteration, veined by a late adularia-type K-feldspar, albite and micaceous minerals. Some of the clay alteration products may be of supergene origin.

This pegmatite is convincingly a representative of the fully differentiated and replaced albite+spodumene type, with lepidolite and spodumene (Beus 1951, 1960) and, as suggested above, its mineral paragenesis may become more diversified with continuing investigation.

MINERALOGY OF THE PEGMATITES

The following notes on mineral species are restricted mainly to those of their properties which contribute to the paragenetic and geochemical characterization of the parent pegmatite groups. Chemical analyses of petrologically and economically important minerals are also presented where available, and references to published papers are quoted. The individual species are described in the same geochemical-paragenetic sequence as used for tabulations in the chapter on the Pegmatite Groups.

Species discussed below are restricted to the primary phases of pegmatite crystallization, including low-temperature minerals crystallizing in vugs and fissures. Late minerals which are obviously secondary, formed at the expense of a pre-existing species during hydrothermal stages, are quoted as alteration products of the latter in the conclusion of its description.

Potassium feldspars

Microcline-perthite is the only type constituting the primary K-feldspars in all zones of all pegmatite groups. The structural state of the potassic component is always close to low microcline, its

TABLE 49. Na_2O CONTENTS OF BLOCKY MICROCLINE-PERTHITE

Pegmatite group (no. of samples)	$\bar{x}$, wt.%	±1σ	Range	Pegmatite group (no. of samples)	$\bar{x}$, wt.%	±1σ	Range
SHL (47)	2.74	0.45	1.16-3.59	BL* (31)	1.94	0.66	0.72-3.83
LdB (7)	1.76	0.23	1.48-2.08	Tanco (26)	1.30	0.46	0.55-2.28
GL (36)	3.02	0.48	1.78-3.87	EAI (18)	1.84	0.31	1.28-2.40
ENL (6)	3.30	0.31	2.88-3.75	BET (3)	2.44	0.04	2.40-2.48
AX (28)	3.05	0.29	2.24-3.48	CAT (12)	1.81	0.45	1.10-2.74
BIS (66)	3.19	0.57	1.52-4.04	CC (10)	2.02	0.77	0.90-3.90
RL (19)	2.22	0.54	1.11-2.94	MWL (15)	1.58	0.21	1.22-1.95

* except Tanco

obliquity ranging mostly between 0.80 and 0.95. Intermediate microcline is sporadically found in outer zones of pegmatite bodies but K-feldspars from internal blocky zones are invariably within the quoted limits. Slight differences can be detected among pegmatite groups on a statistical basis but they are not specific enough to identify the affiliation of invididual pegmatite veins.

The total Na_2O content, representative of the exsolved perthitic albite plus the albitic component still in solid solution, is moderately variable. In general, it can be said to be inversely proportional to the overall degree of fractionation of the parent pegmatite (Table 49). However, even statistically meaningful series of carefully separated samples fail to distinguish between related pegmatite groups.

Ratios of K/Rb plotted against Cs contents are a convenient measure of fractionation attained by different pegmatites. Figure 83 shows the compositional fields of individual groups. The large areas covered by each of the SHL, BIS, and GL groups reflect their internal diversity. Overlapping fields indicate a general geochemical similarity of several pegmatite groups, particularly the less fractionated ones. However, the highly fractionated parts of the GL and RL groups, the LdB and BL groups, and the conspicuous Rb and Cs enrichment in the Cat Lake-Maskwa Lake district are clearly separated from the other pegmatite types.

Extensive recrystallization of K-feldspars is typical of blocky zones in the most fractionated pegmatite types. Segregation of perthitic albite and increasing obliquity is usually accompanied by coarsening of microcline grid twinning up to its disappearance (Černý and Macek 1972).

The only paragenetic type of K-feldspar other than the rock-forming constituent of primary pegmatite zones encountered is a late secondary generation with typical adularia habit and high-sanidine structural state, found in the Tanco deposit (Černý 1972b), Buck Claim pegmatite (Lenton 1979), HGD pegmatite (Černý 1978), and in the Silverleaf offshoot of the Greer Lake pegmatitic granite. The last occurrence is the only one showing intermediate to low structural states in some specimens.

Plagioclase

The morphological diversity of plagioclase is decidedly broader than its compositional range. Albite- oligoclase An_{10-20} is found in the immediate contacts of some pegmatites with basic wall rocks. Virtually all plagioclase located inside pegmatite bodies belongs to the range of An_{8-0}. Also, all plagioclase samples investigated display a low structural state, differences in composition and assemblage notwithstanding.

Primary plagioclase can be safely recognized only in border and wall zones of a few pegmatite groups, notably SHL and GL. It is characteristically equidimensional or short tabular, and evenly distributed in a homogeneous "granitic" association with K-feldspar and quartz. Most of albite varieties, however, belong to metasomatic assemblages. Platy cleavelandite and fine grained saccharoidal albite are most frequent, and they are commonly associated with minerals of Be, Nb-Ta, Zr-Hf, REE, etc. Not all varieties of albite carry this mineralization. For example, cleavelandite is typically accompanied by Nb-Ta minerals in the GL group but only exceptionally in the BL pegmatites. Saccharoidal albite is the main carrier of Ta-Nb minerals in the Tanco pegmatite but only in the central parts of the body; saccharoidal albitization penetrating along the contacts with enclosing amphibolite carries only negligible quantities of beryl.

Quartz

No mineralogical studies of quartz have been conducted to date. From the paragenetic viewpoint, bluish grey quartz is typical of central parts of the GL pegmatites whereas rose quartz occurs in the same location in the BIS group. In other pegmatites the physical appearance of this species is not diagnostic. Patches of dark smoky quartz frequently develop around grains of Ta-Nb oxide minerals, zircon, thorite, monazite, allanite and other species containing radioactive elements.

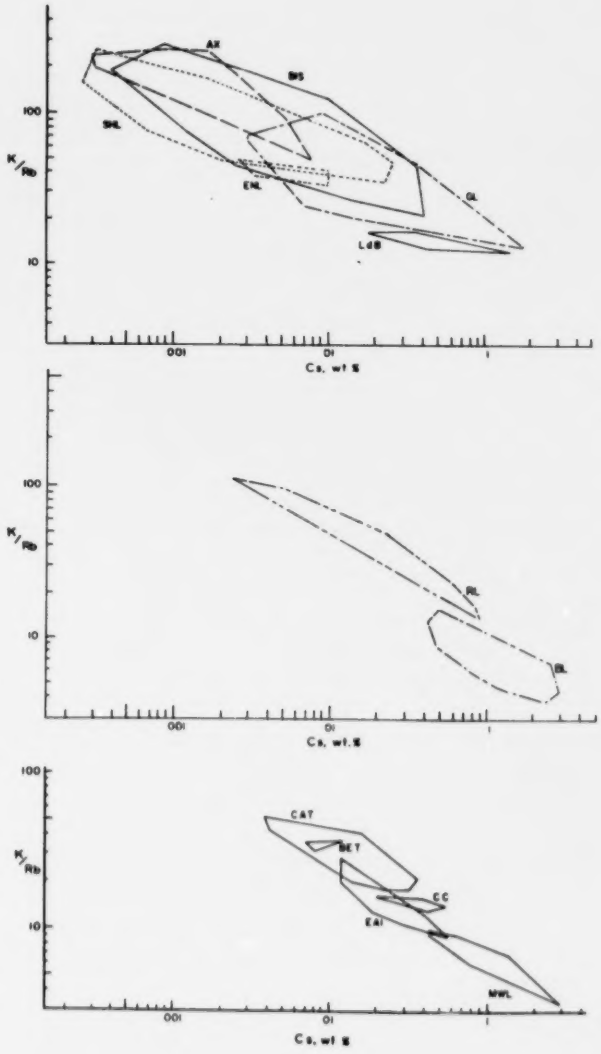

Figure 83: K/Rb vs. Cs plot of blocky K-feldspars from pegmatites of the Cat Lake-Winnipeg River pegmatite field. Letter symbols designate compositional fields of individual pegmatite groups and series

Holmquistite

This purple orthorhombic amphibole is a rather common metasomatic and fracture-filling constituent of alteration haloes surrounding Li-rich pegmatites intruded into metabasalts. Its occurrences are particularly common in the BL group and MWL series. Holmquistite is usually found at some distance from the pegmatite contacts; it has been identified as far as 20 m from them. Thus its appearance in a barren amphibolite terrain may serve as an indicator of possible hidden pegmatite bodies.

Biotite and phlogopite

Two paragenetic types of biotite occur in the examined pegmatites.

An accessory lath-shaped biotite is developed in the outer zones of less differentiated pegmatites; it is particularly typical of the SHL,

TABLE 50. PARTIAL CHEMICAL ANALYSIS OF TRIOCTAHEDRAL MICAS

	Wall zones, SHL group				Contacts with wall rocks				
Sample #	SHS-E-3	SHS-W-1	SHE-1A	SHE-2-5	GL-11-CS	NECC-CS	GL-6-CS	COE-12	BB-43-6
Li_20, wt.%	0.50	0.92	0.80	0.36	0.67	0.62	0.19	2.33	1.89
Na_20	0.52	0.21	0.23	0.19	0.08	0.04	0.28	0.08	0.18
K_20	8.90	10.40	9.30	9.40	9.58	6.79	8.58	8.35	8.99
Rb_20	0.26	0.34	0.31	0.50	0.55	0.54	0.44	1.87	0.46
Cs_20	0.009	0.024	0.014	0.068	0.07	0.57	0.14	0.46	0.66
FeO*	n.d.**	n.d.	n.d.	n.d.	9.78	12.36	22.13	12.74	15.83
CaO	0.003	0.03	n.d.	n.d.	0.16	0.32	0.58	0.92	0.08
MgO	n.d.	n.d.	n.d.	n.d.	14.80	12.40	6.62	5.22	3.20

* total Fe as FeO

** not determined

Analysts, R.M. Hill and R. Chapman

SHS-E-2, SHS-W-1, SHE-1A, SHE-2-5: wall zones of SHL group pegmatites intruded into metabasalts of the Lamprey Falls Formation

GL-11-Cs: pegmatite GL-11 of the GL group; contact with gneissic tonalite

NECC-CS: CC pegmatite; contact with Maskwa Lake quartz diorite

GL-6-CS: pegmatite GL-6 of the GL group; contact with gneissic tonalite

COE-12: Coe Claim pegmatite of the BL group; contact with metabasalt of the Bernic Lake Formation

BB-43-6: pegmatite BB-43, unclassified; contact with metabasalt of the Lamprey Falls Formation

AX, GL, and CAT groups. This biotite is mostly slightly weathered, suffering partial loss of alkalis; for this reason it was not systematically analyzed. Compositions of biotites from the SHL group quoted in Table 50 show the ability of biotite to concentrate relatively high contents of rare alkalis even in pegmatites which are not enriched in them in their bulk composition.

The second type of ferromagnesian mica is a product of reaction between pegmatite veins and metabasaltic host rocks. It is found mainly along contacts of the SHL and BL pegmatites located in amphibolites, but stringers of late mica also occur along and outside pegmatite veins penetrating quartz-dioritic hosts, as in the CC and GL groups. The composition of these micas varies between biotite and phlogopite, judging from the Σ Fe/Mg ratio, and some of them are extremely enriched in rare alkalis, particularly Li and Rb (Table 50).

Muscovite and lepidolite

Among the paragenetic types of muscovites and Li-enriched micas encountered in the pegmatite field, five varieties are widespread and of paragenetic plus geochemical importance. These will be described in more detail below. Other mica types are of secondary origin and quantitatively insignificant, or of restricted local importance only: sericitic phases replacing Li-aluminosilicates and feldspars, and covering open fractures, are the most common.

(1) Platy white, yellowish or greenish muscovite is the most frequent mica type. It has a wide crystallization span from wall zones into blocky assemblages rimming central quartz cores. It is usually most abundant in intermediate zones, where it may belong to quartz-muscovite replacement bodies, but its crystals reach largest dimensions on the blocky-core boundary (up to 50 cm across the plates in GL pegmatites). This mica is allways low in rare alkalis; Li_20 varies between 0.02 and 0.40 wt.% in the less fractionated pegmatite groups and in the 0.20 - 1.08 wt.% range in the geochemically most advanced pegmatites.

A brownish to dark brown muscovite from the SHL pegmatites intruded into metabasalts is a notable exception to the above. This Fe-rich muscovite is mostly curvilamellar, and its total Fe content reaches the equivalent of 8.49 wt.% Fe_20_3. Li_20 contents vary between 0.09 and 1.08 wt.%.

All micas of this type examined to date belong to the common $2M_1$ polytype.

(2) Radial aggregates of lath- or wedge-shaped individuals, brownish to purplish-grey, occur in the BL pegmatites (except Tanco) and in the Silverleaf offshoot of the Greer Lake pegmatitic granite. They usually corrode or mantle K-feldspar in intermediate zones. Rare alkali contents of this mica are distinctly higher than in platy muscovite, as exemplified by the Li_20 range of 1.66 to 2.50 wt.%, but X-ray powder diffraction invariably shows $2M_1$ patterns. Thus the mica may be termed lithian muscovite.

(3) Curvilamellar mica in subparallel or radiating aggregates of crystals elongated parallel to *c* is mostly greyish, dirty brownish or pinkish. It is typically associated with cleavelandite and quartz replacing intermediate and blocky zones of the RL and BL pegmatite groups; rarely, it occurs in the most differentiated GL dykes, but it is rather widespread in the Silverleaf and Annie Claim #2 and #3 pods, and in the NW dyke of the MWL group. In the Tanco pegmatite the Li_20 content is rather low (0.79-2.80 wt.%) compared to ther localities where it rises to the 2.37-3.99 wt.% range. All examined micas of this type consist of $2M_1$+1M polytypes mixed in various proportions, except for a single specimen from Tanco (1.85 wt.% Li_20; $2M_1$). The

phase composition of the curvilamellar mica is evidently lithian muscovite+lepidolite.

(4) Fine-flaked pale-pink to purple micas are known from the RL, BL and MWL groups, and from the Silverleaf offshoot. They constitute small to large and almost monomineralic pods in central parts of pegmatite bodies. In some cases they are metasomatic after microcline-rich zones (as in Tanco; Rinaldi et al. 1972) but small clusters in other bodies may be primary.

Relative to other types, this mica is most enriched in rare alkalis; the overall range of Li_2O for all localities is 3.06-5.04 wt.%. However, the polytypism is fairly erratic. Most samples consist of mixed $2M_1$+ 1M intergrowths, with the 1M component generally more abundant than in the preceding curvilamellar type, but four specimens from as many localities produce pure $2M_1$ powder patterns, with Li_2O contents of 3.23, 3.66, 3.91, and 5.04 wt.%. Thus most of this mica can be classified as mixed lithian muscovite>lepidolite, but some samples may belong to the $2M_1$ trilithionite known as a synthetic phase (Munoz 1968) and from a single natural occurrence (Černý et al. 1970).

(5) Late fine-flaked to sericitic micas, greenish to pale pink, occur in most pegmatite groups but larger accumulations, locally associated with Ta-Nb, Sn, Be and Zr-Hf mineralization are found only in the RL and BL groups. Most of this mica type replaces K-feldspar zones in front of albitization poor in rare alkalis. This is reflected in the low Li_2O contents which range between 0.15 and 0.37 wt.%, and in the structure which is invariably of the $2M_1$ type. The only exceptions are two greenish-brown micas forming small pods in the PEGLI-2 and Buck pegmatites, the origin of which is not

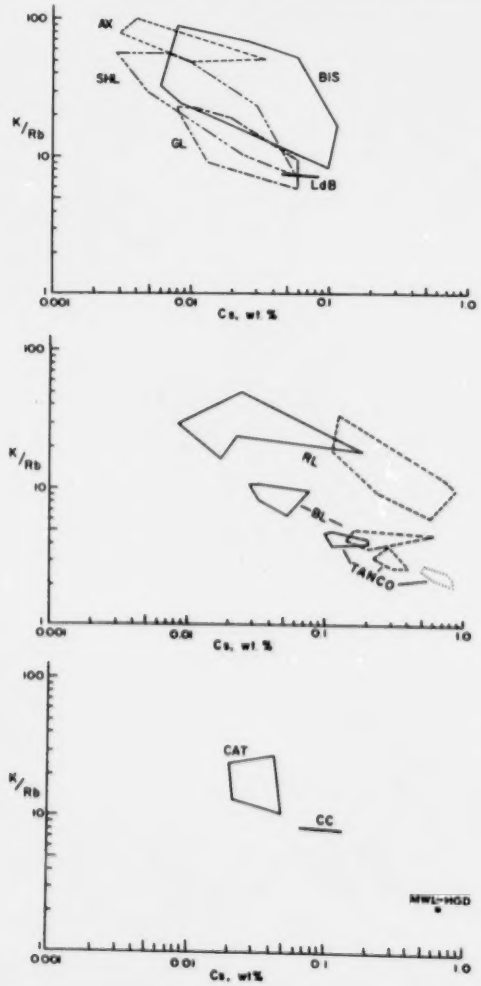

Figure 84: K/Rb vs. Cs plot of micas from pegmatites of the Cat Lake-Winnipeg River pegmatite field. Letter symbols designate compositional fields of individual pegmatite groups and series. Tanco micas are separated from the BL group to emphasize their high fractionation level. Top - muscovite only; centre - muscovite (solid outline), lithian muscovite (dashed outline), and lepidolite (± muscovite) (dotted outline); bottom - muscovite except for the HGD lepidolite (dot)

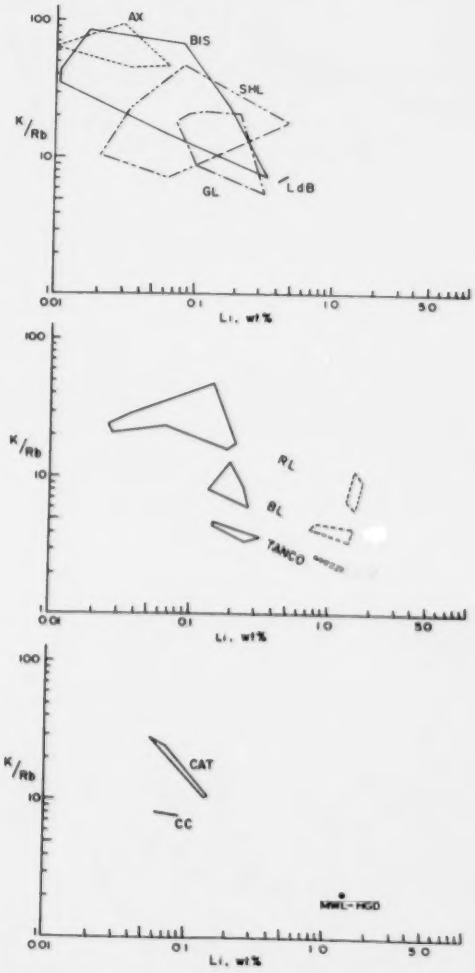

Figure 85: K/Rb vs. Li plot of micas from pegmatites of the Cat Lake- Winnipeg River pegmatite field. Letter symbols designate compositional fields of individual pegmatite groups and series. Tanco micas are separated from the BL group to emphasize their high fractionated level. Top - muscovite only; centre - muscovite (solid outline), lithian muscovite (dashed outline), and lepidolite (± muscovite) (dotted outline); bottom - muscovite except for the HGD lepidolite (dot)

TABLE 51. PARTIAL CHEMICAL ANALYSES OF SPODUMENE AND SPODUMENE + QUARTZ PSEUDOMORPHS AFTER PETALITE

Pegmatite	Group	Sample#	Type*	Na_2O	Fe_2O_3**	Li_2O
C1	LdB	C1(2)	z	0.27 wt.%	0.09 wt.%	7.88 wt.%
C2	LdB	C2-20	z	0.76	0.17	6.80
C2	LdB	C2-21	z	0.22	0.08	7.71
ODD-SW-2	RL	ODD-SW-2	z	0.09	0.21	7.66
ODD-SW-2	RL	ODD-SW-1+Q	z	0.09	0.21	7.32
ODD-SW	RL	ODD-SW-19	z	0.08	0.28	7.45
ODD-SW	RL	ODD-SW-20	z	0.08	0.19	7.54
RL-2	RL	RL-2	z	0.73	0.11	6.95
RL-2	RL	RL-2-20	z	0.31	0.09	7.23
ODD-SW-2	RL	ODD-SW-2-21	ps	0.22	0.30	4.78
RL-2	RL	RL-2-21	ps	0.66	0.10	5.68
COE	BL	COE-17	z	0.08	0.38	8.05
COE	BL	COE-18	z	0.09	0.41	8.05
TANCO	BL	SPD-1	z	0.11	0.05	7.87
TANCO	BL	SPD-1A	z	0.13	0.09	7.80
TANCO	BL	BLM-11	z	0.25	0.15	7.32
TANCO	BL	BLM-12	z	0.21	0.35	7.50
COE	BL	COE-13	ps	0.28	0.04	4.31
BCNW	BL	BCNW-32	ps	n.d.+	n.d.	4.69
BCNW	BL	BCNW-33	ps	n.d.	n.d.	3.96
TANCO	BL	BLM-33	ps	0.22	0.02	4.49
TANCO	BL	BLM-34	ps	0.28	0.03	4.46
EAGLE	EAI	EE		0.10	1.39	7.87
EAGLE	EAI	EW		0.15	1.14	7.19
EAGLE	EAI	EAGLE	ph	0.10	1.46	7.23
IRGON	EAI	IRGON	ph	0.30	1.36	7.06
CATB	CAT	CATB-5	ph	0.20	0.74	7.32
CATB	CAT	CATB-6	ph	0.08	0.71	7.49
CC	CC	CC-50		0.22	0.19	6.37
CC	CC	CC-51	z	0.08	0.09	8.01
CC	CC	CC	z	0.09	0.11	7.90
CC	CC	DH-1-2	z	0.08	0.17	7.49
CC	CC	DH-14-2	z	0.16	0.23	7.41
HGD	MWL	HGD	z	0.32	0.09	7.34
HGD	MWL	HGD-N	z	0.32	0.06	7.23
HGD	MWL	MWL	z	0.24	0.07	7.23
NW	MWL	NW-1	ps	0.32	0.12	4.13
NW	MWL	NW-2	ps	0.34	0.16	4.22

* classification after Heinrich (1975): ph - phenocrystic, z - zonal, ps - pseudomorphs after petalite

** total Fe as Fe_2O_3

+ not determined

Analysts, R.M. Hill and R. Chapman

Tanco data from Černý and Ferguson (1972)

unequivocally established (3.44 and 1.10 wt.% Li_2O, respectively with mixed $2M_1+1M$ polytypes). Muscovite is evidently the vastly predominant species in this category.

Figures 84 and 85 illustrate the relationships among K/Rb, Li, and Cs in some of the most significant mica types. The K/Rb *vs.* Cs plots separate the individual pegmatite groups better than the K/Rb *vs.* Li graph. For a single mica type, separation of compositional fields of different pegmatite groups is evidently due much more to the K/Rb ratio than to the Cs content. However, fractionation sequences of all mica types from a single pegmatite group follow diagonal courses determined by progressive changes in both parameters. The same is also true of the K/Rb *vs.* Li trends.

We may conclude that muscovite, lithian muscovite, and lepidolite are the only species and varieties of Fe,Mg-poor micas positively identified in the Cat Lake-Winnipeg River pegmatite field. Ferroan muscovite is an additional type restricted to the SHL group. Despite earlier reports based on physical appearance, no zinnwaldite has been found to date.

Spodumene

Spodumene is represented in the examined pegmatite field by all three paragenetic varieties recognized by Heinrich (1975).

Iron-rich "phenocrystic" spodumene is typical of the EAI and CAT groups in the Cat Lake-Maskwa Lake district. It is disseminated through most of the volume of these pegmatites, white to greenish in colour, associated with quartz and albite, and it contains up to 1.5 wt.% total Fe as Fe_2O_3 (Table 51, Fig. 86).

Zonal spodumene is widespread in the LdB, CC and MWL groups and it also occurs, although in subordinate quantities, in the RL and BL pegmatites. It is found mostly in central or intermediate zones, associated mainly with quartz, in the form of white columnar crystals up to several metres long. Most of its Fe_2O_3 content is less than 0.25 wt.%, but nevertheless significantly higher than the approximate upper limit quoted for this variety by Heinrich (1975).

The last type of spodumene is pseudomorphous after petalite in fibrous aggregates of mostly parallel spodumene laths intimately intergrown with quartz (Figs. 87a, b). The bulk composition of these intergrowths closely corresponds to that of the original petalite, the isochemical breakdown of the primary phase having been caused by its instability at low temperatures:

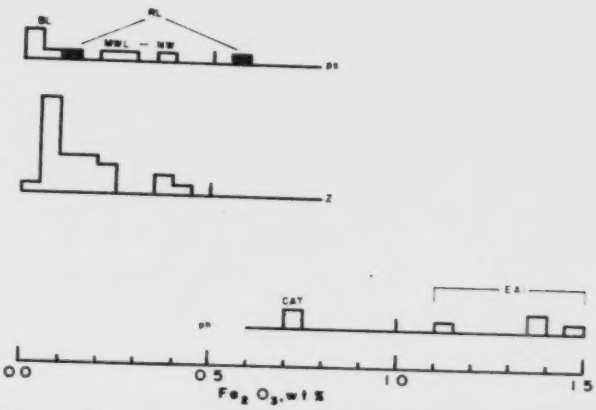

Figure 86: Iron content of spodumene from the Cat Lake-Winnipeg River pegmatite field, classified according to the paragenetic plus compositional scheme of Heinrich (1975): ph - phenocrystic, z-zonal, and ps - pseudomorphous after petalite

$$\text{petalite} \longrightarrow \text{spodumene} + \text{quartz}$$

$$LiAlSi_4O_{10} \longrightarrow LiAlSi_2O_6 + 2\,SiO_2$$

Spodumene is always Fe-poor in these intergrowths, having inherited the Fe-poor composition of the original petalite; Heinrich (1975) places the upper limit of its Fe_2O_3 content at 0.03 wt.%. This is much less than shown by some present analyses (Fig. 86, Table 51), and the reasons may be twofold. The NW and RL specimens available for chemical analysis were slightly altered, and the high Fe_2O_3 contents may come mainly from adsorbed Fe-compounds. Also, some of the primary petalites contain Fe_2O_3 percentages above the usual average, and some of the iron content may be inherited.

Spodumene is very reactive at low temperatures in a hydrothermal environment. Replacement by micas, cookeite, albite, and clay minerals is widespread, and it is frequently extremely difficult to separate a pure phase for chemical analysis. Most of the

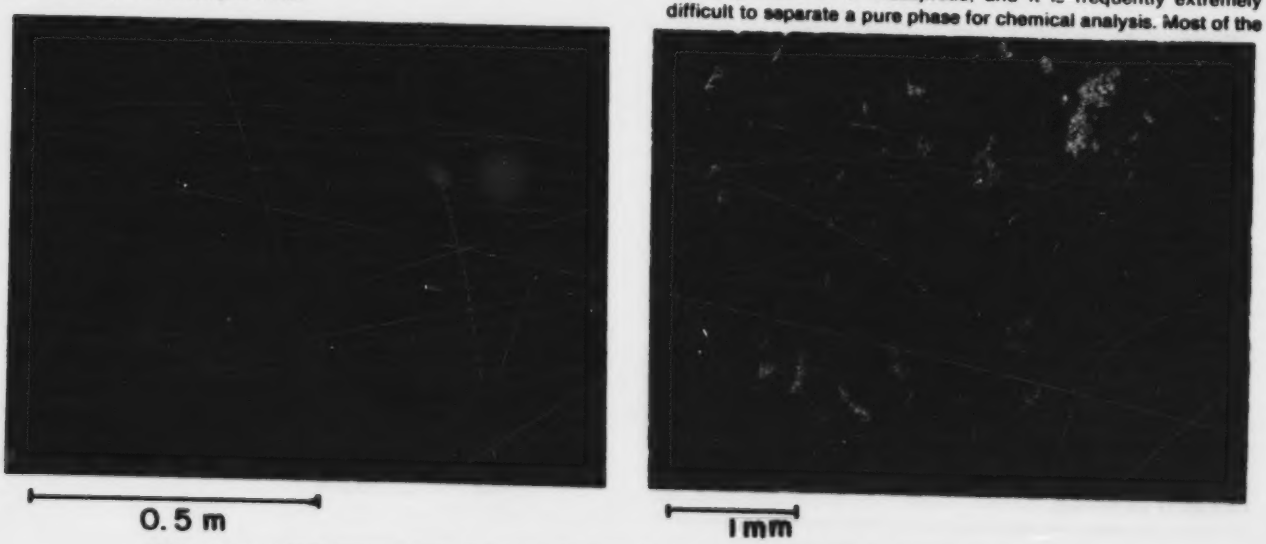

Figure 87: Spodumene-quartz intergrowth pseudomorphous after petalite from the Tanco pegmatite: (a) underground exposure in zone (5) of the pegmatite; (b) microscopic view in thin section, plane-polarized light.

TABLE 52. CHEMICAL COMPOSITION OF PETALITE

Sample #	BLM-50G	BLM-50WH	BLM-51	PET-12	PET-13	PET-14	PET-15	5-190	2-199
SiO_2, wt.%	77.85	77.60	77.66	78.30	77.80	77.85	77.75	n.d.*	n.d.
Al_2O_3	16.60	16.66	17.20	16.84	16.55	16.80	16.69	n.d.	n.d.
Fe_2O_3**	0.05	0.05	0.03	0.05	0.002	0.05	0.01	0.07	0.01
MgO	0.03	0.01	0.02	n.d.	n.d.	0.04	0.01	n.d.	n.d.
CaO	0.01	0.00	0.04	n.d.	n.d.	0.002	0.002	n.d.	n.d.
Li_2O	4.54	4.84	4.41	4.41	4.55	4.32	4.48	4.53	4.57
Na_2O	0.15	0.12	0.24	n.d.	n.d.	0.02	0.08	n.d.	n.d.
K_2O	0.05	0.04	0.29	n.d.	n.d.	0.07	0.03	n.d.	n.d.
H_2O-	0.13	0.11	-	0.09	0.06	0.06	0.03	0.09	0.07
H_2O+	0.37	0.47	-	0.44	0.29	0.33	0.23	0.39	0.36
	99.78	99.90	99.89	100.13	99.25	99.55	99.31	-	-

* not determined

** total Fe as Fe_2O_3

Analysts, K. Ramlal, R.M. Hill and R. Chapman

All samples from the BL pegmatite group

BLM-50G	Tanco zone (5), grey (Černý and Ferguson 1972)
BLM-50WH	Tanco zone (5), white (Černý and Ferguson 1972)
BLM-51	Tanco Zone (5), adjusted for admixture of pollucite (Černý and Ferguson 1972)
PET-12	Tanco zone (5), white
PET-13	Tanco zone (5), grey
PET-14	Coe Claim, grey
PET-15	Coe Claim, grey
5-190	PEGLI pegmatites, drill core sample DDH5-190
2-199	PEGLI pegmatites, drill core sample DDH2-199

high Na_2O contents shown by some analyses in Table 51 come from inseparable albitization pervading spodumene on a microscopic scale. Alteration processes of spodumene are schematized in Figure 88. All the different associations shown in the graph occur in southeastern Manitoba, except albite+eucryptite and zeolite minerals.

Petalite

This lithium aluminosilicate is typical of the RL and BL groups, and it was present also in the NW dyke of the MWL group. However, most of this species broke down into the spodumene+quartz intergrowths described above, and petalite is preserved only in a few localities of the BL group: the Tanco, Coe, and Pegli pegmatites. Table 52 shows its fairly constant composition, and it also demonstrates its low Fe_2O_3 contents. No significant differences can be observed between the grey and white to colourless varieties. However, the Li_2O content decreases and H_2O increases with incipient turbidity caused by alteration.

Hydrothermal alteration of petalite is not so widespread as that of spodumene but where it has occurred it usually has destroyed all of the crystals affected. Quartz, calcite, cookeite and adularia-type K-feldspar are the most common association of alteration products. All of the secondary mineral associations after petalite as shown in Figure 89 have been identified in the BL pegmatites.

Eucryptite

Eucryptite is known from the Tanco pegmatite as very inconspicuous, white, greyish or pinkish masses associated with

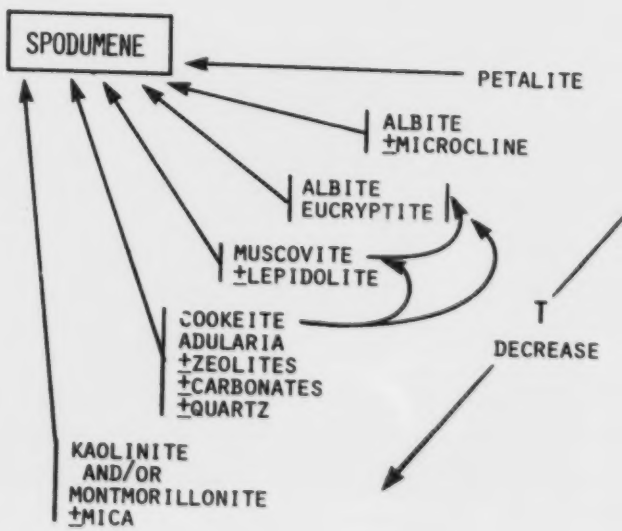

Figure 88: Schematic generalized sequence of alteration products replacing spodumene in granitic pegmatites

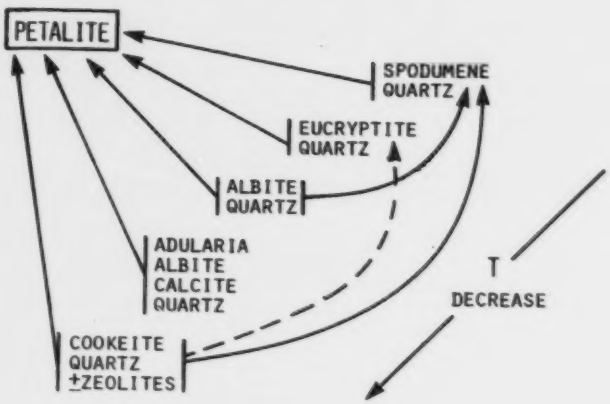

Figure 89: Schematic generalized sequence of alteration products replacing petalite in granitic pegmatites

spodumene+quartz pseudomorphs after petalite and, in some cases, evidently replacing them. Eucryptite is mostly indistinguishable from quartz in hand specimen. Even the usual means of identification, carmine red or blue fluorescence in ultraviolet light, fails in most cases because the Tanco mineral loses this property after mechanical disturbance such as a hammer blow, drilling, or pulverizing. Chemical composition of the Tanco eucryptite is shown in Table 53 (Černý 1972a).

Pollucite

Occurrences of this species are restricted mainly to the petalite-bearing low-pressure pegmatites of the RL and BL groups, and to the HGD dyke of the MWL group. However, in some of these occurrences (BCNW, OW) pollucite was completely destroyed by low-temperature alteration processes (Černý 1978).

The largest accumulation of pollucite is located in the Tanco pegmatite (Černý and Simpson 1978); the other occurrences contain (or contained) much smaller quantities of this mineral, judging from the outcrops and drilling results. Chemistry of the Tanco and HGD pollucites shown in Table 54 falls within the range of most common compositions of this species (70-80 mol.% pollucite, 30-20 mol.% analcime; Černý 1974). However, late low-temperature members of the series discovered at the Tanco pegmatite are predominantly sodic (Table 54; Černý 1972b).

TABLE 53. CHEMICAL COMPOSITION OF EUCRYPTITE
(From Černý 1972a)

Sample #	EUC-2	EUC-3a
SiO_2, wt.%	45.93	44.43
Al_2O_3	42.74	44.84
Li_2O	11.33	10.73
	100.00	100.00

Analysts, K. Ramlal and R. M. Hill

EUC-2 eucryptite Tanco (BL group), recalculated from analysis of material slightly contaminated by cesian analcime

EUC-3a eucryptite Tanco (BL group), as above

TABLE 54. CHEMICAL COMPOSITION OF POLLUCITE AND CESIAN ANALCIME
(From Černý and Simpson 1978, and Černý 1972b)

Species	Pollucite Tanco zone (8)			Cesian analcime Tanco zone (5)		
Sample #	U-39-95.8	B-12-226.2	B-12-207.2	1	2-1**	2
SiO_2, wt.%	47.80	46.09	47.42	54.85	52.93	52.10
Al_2O_3	15.70	16.38	16.02	20.36	19.27	17.60
Fe_2O_3	0.01	0.01	0.01	n.d.*	n.d.	n.d.
MgO	0.003	0.003*	0.01	n.d.	n.d.	n.d.
CaO	0.04	0.01	0.06	0.05	0.06	0.13
Li_2O	0.28	0.43	0.29	n.d.	n.d.	n.d.
Na_2O	1.98	1.74	1.30	10.30	9.29	6.46
K_2O	0.17	0.16	0.10	0.40	0.19	0.19
Rb_2O	0.77	0.74	0.68	0.01	n.d.	0.06
Cs_2O	30.60	32.20	32.57	6.00	10.50	18.00
H_2O-	0.08	0.04	0.04	0.41	-	0.14
H_2O+	2.11	1.73	1.37	7.51	7.76	4.45
	99.54	99.53	99.87	99.89	100.00	99.13

* not determined

** recalculated from analysis of material contaminated by eucryptite

Analysts, K. Ramlal and R. Chapman

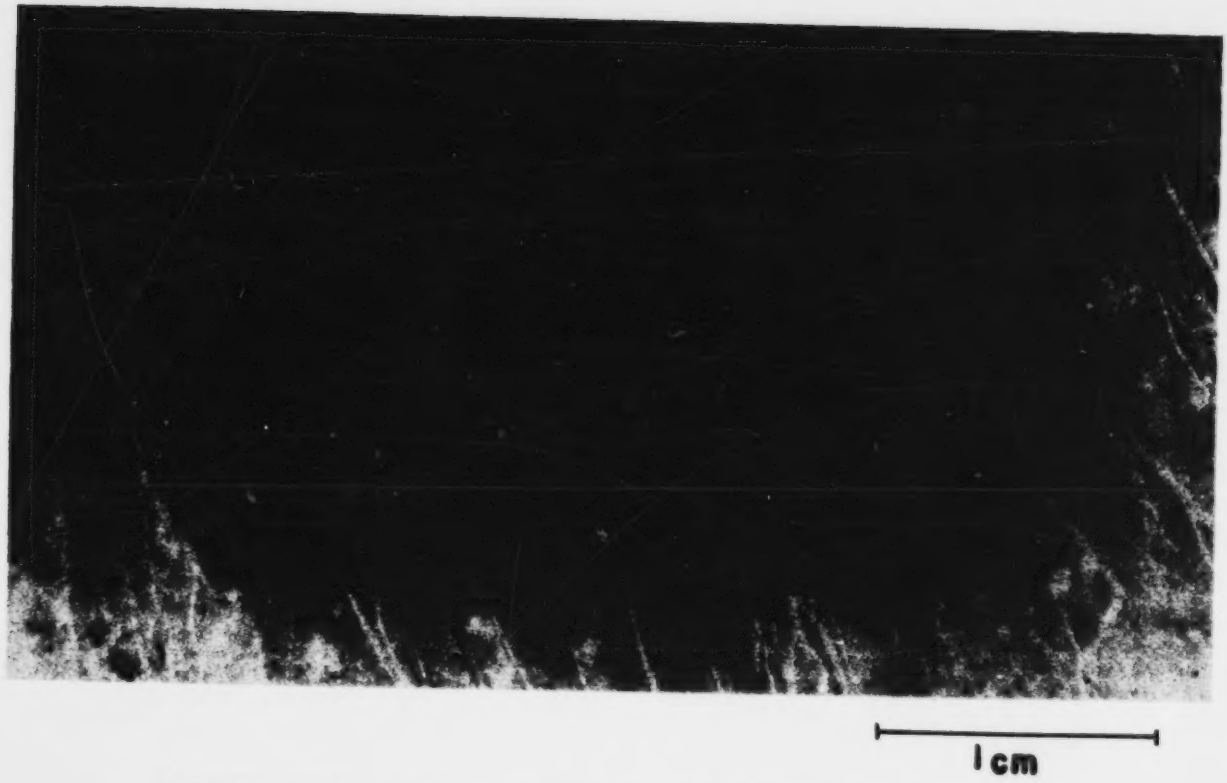

Figure 90: Sericitic muscovite + spodumene veining darker pollucite from the Tanco deposit; polished hand specimen

Veining of pollucite by quartz, non-perthitic microcline, albite and lepidolite represents the first and most widespread stage of its alteration. Fine veining by muscovite, adularia and spodumene follows (Fig. 90), and total breakdown of remaining pollucite usually produces microscopic mixtures of clay minerals, quartz and calcite (Černý 1978). A schematic representation of alteration processes encountered in pollucites from southeastern Manitoba is shown in Figure 91.

Epidote

The Huron Claim pegmatite is the only locality of epidote in the Cat Lake-Winnipeg River pegmatite field. However, epidote is fairly abundant there in the form of late vug- and fracture-fillings. Its colour varies from pale greenish-yellow to dark shades of green, but the difference in chemical composition of extreme colour varieties is rather small (Table 55; Paul, in prep.). Clay minerals commonly replace epidote.

Chlorite

Besides its sporadic occurrence as an alteration product (e.g., after cordierite), chlorite is also found as a late "primary" mineral crystallizing in vugs and open fractures. It is known in this form from the SHL pegmatites, several bodies in the GL group, and from the BET pegmatites in the northern district. Chemical analyses of these chlorites show them to be highly ferruginous (Table 55). In the Huron Claim pegmatite, chlorite also succumbs to local alteration into clay minerals (Paul, in prep.).

Cordierite

Cordierite seems to occur exclusively in the GL pegmatite group. Its stubby columnar crystals reaching 30 cm in length (Fig. 92) have been found, so far, completely altered into muscovite, green biotite, and chlorite (in order of decreasing abundance). However, the crystal shape of the pseudomorphs, and the texture of the

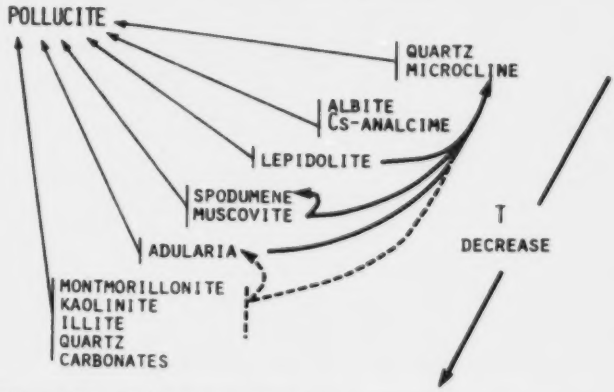

Figure 91: Schematic generalized sequence of alteration products replacing pollucite in granitic pegmatites

alteration products with prominent traces of basal parting (Fig. 93 a, b) leave no reasonable doubt about the nature of the original species.

The role of garnet in the pseudomorphs is uncertain. Concentric envelopes of garnet, resembling ghost surfaces covered by garnet during growth of cordierite crystals, and isolated subhedral crystals randomly scattered throughout the pseudomorphs suggest primary inclusions (Figs. 92, 93a). This is supported by their composition which is close to that of other garnets from their parent pegmatites. Other garnets are, however, located within the basal parting of the original cordierite and flattened parallel to it (Fig. 93b), or on the surface of the pseudomorphs in perfect conformity with cordierite morphology. These textural relationships suggest a secondary

TABLE. 55. CHEMICAL COMPOSITION OF EPIDOTE AND CHLORITE

(After Paul, in prep.)

Species	Epidote		Chlorite			
Sample #	P3-17Y	P3-17DG	P3-83	SHS-C	IRA	GL-6
SiO_2, wt.%	37.80	38.10	23.50	22.25	n.d.*	n.d.
TiO_2	0.00	0.00	0.00	0.00	n.d.	n.d.
Al_2O_3	27.28	25.28	20.40	21.64	n.d.	n.d.
Fe_2O_3	7.95	9.54	7.50	6.48		
FeO	0.28	1.16	23.36	31.56	29.5**	34.9**
MnO	0.33	0.46	0.82	0.86	n.d.	n.d.
CaO	22.90	21.90	0.10	0.10	n.d.	n.d.
MgO	0.10	0.23	12.50	5.44	6.25	7.14
Na_2O	0.06	0.05	0.05	0.06	n.d.	n.d.
K_2O	0.16	0.20	0.05	0.11	n.d.	n.d.
H_2O-	0.11	0.14	0.44	0.21	n.d.	n.d.
H_2O+	2.11	2.19	10.73	10.41	n.d.	n.d.
CO_2	0.04	0.01	0.02	0.06	n.d.	n.d.
P_2O_5	0.49	0.46	0.56	0.48	n.d.	n.d.
	99.61	99.58	100.03	99.72	-	-

* not determined

** total Fe as FeO

Analysts, K. Ramlal and R. Chapman

P3-17Y yellow epidote, Huron Claim pegmatite of the SHL group

P3-17DG dark green epidote, Huron Claim pegmatite of the SHL group

P3-83 chlorite, Huron Claim pegmatite of the SHL group

SHS-C chlorite, SHS pegmatite of the SHL group

IRA chlorite, IRA pegmatite of the BET group

GL-6 chlorite, GL-6 pegmatite of the GL group

origin but chemical composition of this garnet type is again close to other garnet varieties from parent pegmatite bodies.

Garnet

Garnet is most widespread in the SHL, GL, and ENL groups, and in the Irgon and Eagle pegmatites of the EAI group. Smaller amounts of this mineral are present in some pegmatites of the AX, BIS and CAT groups, and the CC and MWL pegmatites carry just a few scattered crystals.

Composition of garnet varies with the general geochemistry of the parent pegmatite group, and with its position in the zoning sequence of its parent pegmatite. However, multiple generations of garnet are rather rare in the examined pegmatites. Most of the garnet occurrences are restricted to medium grained albite+quartz+ muscovite associations of the intermediate zones, or to a saccharoidal albite+quartz in replacement bodies. The latter variety of garnet is always enriched in Mn relative to the former.

Comparing the garnet compositions of different pegmatite groups, the Fe/Mn ratio is the most conspicuous variable. As shown in Figure 94, the range of the Fe/Mn ratio in garnets of individual pegmatite groups is roughly correlatable with their overall degree of fractionation. Ca, Mg and Y contents, although generally very subordinate, also exhibit characteristic differences. An increase in Ca, and a decrease in Mg, is observed with decreasing Fe/Mn ratio in garnets of all well-documented pegmatite groups, except for the EAI group represented by two analyses only.

Tourmaline

In the Winnipeg district, tourmaline occurrences are restricted to, but abundant in the three northern pegmatite groups, BIS, RL and BL.

The BIS group carries schorl largely disseminated throughout each pegmatite body; in a few dykes larger columnar crystals up to 50 x 10 cm in size occur along the margins of quartz cores (RQQ pegmatite). In the RL and BL groups, schorl occurs along contacts with country rocks, verdelite to indigolite in association with muscovite+quartz in the intermediate zones, and verdelite with rubellite in more central locations associated with Li-enriched micas, cleavelandite, and pollucite.

In the Cat Lake-Maskwa Lake district, tourmaline is not particularly abundant in any of the pegmatite groups. Minor amounts are found in the CC, EAI, CAT and some of the BET dykes; a somewhat larger concentration is found in the HGD body of the MWL series.

All colour varieties of tourmaline, including waterclear achroite, are confined to central parts of the HGD pegmatite. In the CC and IRGBE dykes, tourmaline occurrences are restricted to small black or bluish patches in saccharoidal albite. Schorl is the only tourmaline species in the EAI and CAT groups, mostly filling-in late shear fissures in association with greenish beryl (Fig. 95).

Physical properties and unit cell dimensions indicate that tourmalines from both districts belong to the schorl-elbaite series,

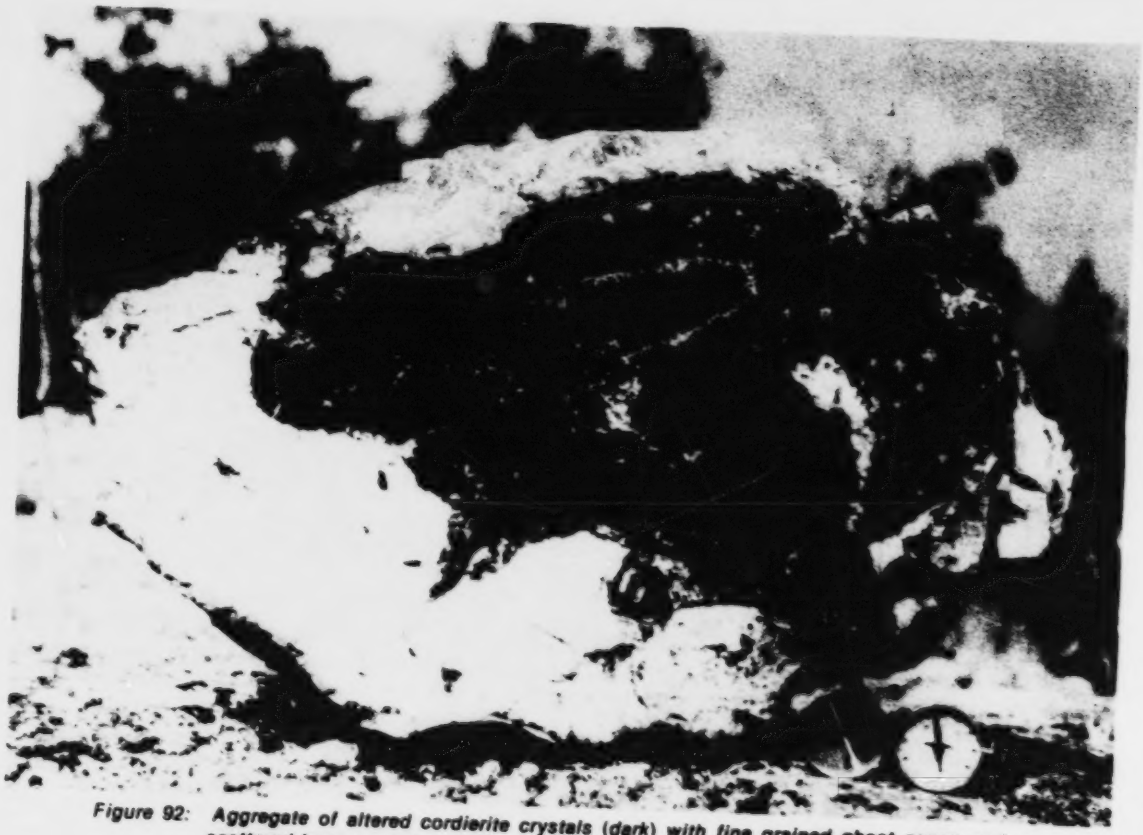

Figure 92: Aggregate of altered cordierite crystals (dark) with fine grained ghost zones and scattered large crystals of garnet (light dots), surrounded by blocky K-feldspar and quartz; GL-8W pegmatite, Greer Lake group

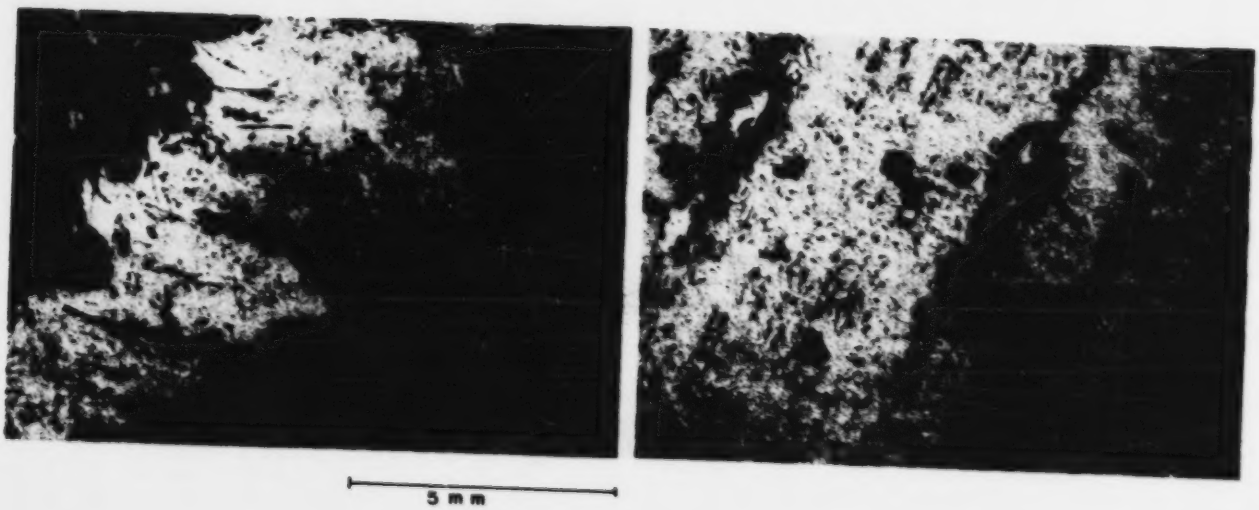

Figure 93: Altered cordierite from the Greer Lake pegmatites in thin sections normal to its basal parting (marked by arrows): (a) with a ghost zone of granular garnet, (b) with platy garnet in the parting planes; plane-polarized light

except for a few brownish-black types adjacent to, or penetrating into amphibolite wall rock which correspond to schorl with a low percentage of the dravite component (Fig. 96).

Topaz

The SHL group is the only one which can be said to carry topaz as a characteristic and widespread accessory mineral. The only other occurrence is that in the Silverleaf offshoot of the Greer Lake pegmatitic granite.

Long- to short-prismatic topaz from the SHL pegmatites ranges from milky to brownish-yellow in colour, the latter type being locally of gem quality (SHT dyke). Replacement by sericitic to coarse-flaked muscovite is widespread.

Optical properties and unit cell dimensions of topaz from the SHL pegmatites and from the Silverleaf claim indicate that the F contents are within the 17.9-19.7 wt.% range for all occurrences.

Gahnite

This mineral is known in octahedral crystals up to 1 cm in size from some of the GL pegmatites, in tiny green grains from the BIS-1 body, and its presence is suspected in the Tanco pegmatite where it could not be positively identified because of lack of separable material. Qualitative tests for Zn and Al, and unit cell edges within a narrow range of 8.07-8.09Å confirm its identity in other occurrences. This species is possibly more widespread, judging by its relative abundance in some of the pegmatitic granites, but it may easily escape attention in the field because of its inconspicuous shape, colour, and common alteration into muscovite.

Figure 95: Tourmaline (black) and beryl (white specks in tourmaline) filling shear fractures in the CATB pegmatite

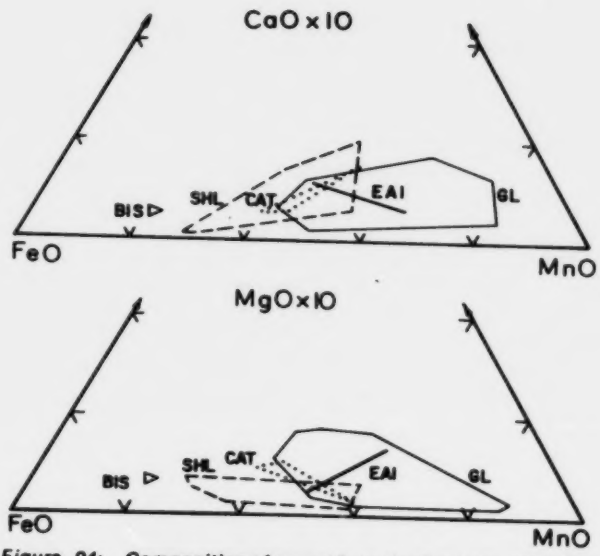

Figure 94: Composition of garnet from the Cat Lake - Winnipeg River pegmatite field in the Fe0-Mn0-Ca0x10 and Fe0-Mn0-Mg0x10 triangles. Letter symbols designate compositional fields of individual pegmatite groups

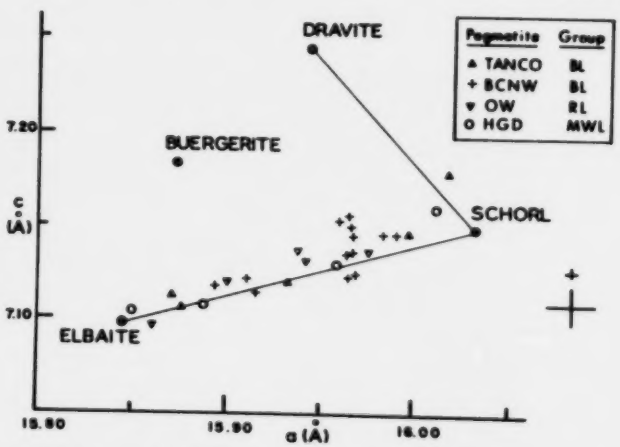

Figure 96: Unit cell dimensions of tourmalines from selected pegmatites of the Cat Lake-Winnipeg River pegmatite field. Crosses designate maximal and minimal one standard deviation

Beryl

Beryl is one of the most widespread accessory minerals in the Cat Lake-Winnipeg River pegmatite field. Only the LdB and AX groups do not carry it in the Winnipeg River area, and the unzoned MWL pegmatites in the northern district.

Alkali substitution in beryl reflects the overall geochemistry of its parent pegmatite, particularly its degree of enrichment in rare alkalis. Na is the first element which enters beryl even in simple pegmatite types. With progressing fractionation Li starts substituting for Be and the Na/Li ratio rapidly decreases. With further rare-alkali enrichment, Cs content starts increasing just when the changes in numeric values of Na/Li become less informative (Beus 1960, Černý 1975). Alkali contents of pegmatitic beryl can be roughly estimated

from its refractive indices (Černý and Hawthorne 1976).

Parallel with the qualitative and quantitative changes in the alkali content, colour and crystal havit of beryl also change. Prismatic, columnar, green sodian and sodian-lithian beryl changes to short-prismatic habit and yellow, bluish and milky colour at low Na/Li values. With incipient increase in Cs, beryl becomes white, colourless or pale-pink, and its crystals are either anhedral or tabular parallel to the basal pinacoid (Fig. 97). Compositional fields of late (or central) beryl varieties from seven pegmatite groups are demonstrated in Figure 98. The distinction between some of the groups is unmistakable but several groups completely or partially overlap, due to their overall geochemical similarity (compare with the K-feldspar and mica graphs in Figs. 83, 84, and 85). Table 56 shows the chemical composition of typical alkali-rich beryl from the Tanco deposit.

Compositional variation of beryl is, however, much broader within each individual pegmatite group, even a single pegmatite body, than it appears to be in Figure 98 which is restricted to late, mutually comparable generations. Multigenerational sequences from individual pegmatites may cover most of the whole range, as illustrated in Figure 99. More detailed information is available in papers by Černý and Turnock (1975a) and Černý and Simpson (1977).

Sericitization of beryl is mostly negligible but very widespread. More complex and extensive alteration of beryl is characteristic of the SHL and BL groups. In the Huron Claim pegmatite, breakdown of beryl yields bityite, bertrandite, and bavenite intimately intergrown with chlorite; a single pseudomorph of muscovite and clay has been found with considerable BeO contents in both alteration products (Paul, in prep.). In the Tanco pegmatite, beryl suffers sporadic corrosion followed by crystallization of apatite and calcite. Herderite and hurlbutite have been identified as buff-coloured coatings on etched fracture surfaces of beryl in the BCSE pegmatite.

Chrysoberyl

This species has been discovered in the northernmost outcrop of the Central Claim pegmatite. Pale yellow-green tabular crystals up to 3 x 20 mm in size occur here, closely associated with granular muscovite, in a fine- to medium-grained assemblage of albite, quartz and platy muscovite.

Titanite

The only occurrence of titanite is known from the Huron Claim pegmatite of the SHL group. Small brown crystals are associated there with albite (Paul, in prep.). Preliminary electron microprobe data indicate high Nb, Ta and Al contents.

Allanite

SHS-M and SHE-2 are the only pegmatites carrying allanite, both members of the SHL group. In both localities, allanite is associated with complex oxide minerals of Fe, Mn, Ca, Nb, Ta, Ti and REE. It is also largely decomposed: hydrated and oxidized into yellow and reddish X-ray amorphous compounds in the first case, and replaced by bastnaesite in the other occurrence. Most of its spectacular radiating fibres consist of this fluorocarbonate of Ca and Ce (Fig. 100).

Gadolinite

This species, reported by Mulligan (1968) from one of the SHL pegmatites on the southern shore of Shatford Lake, has been positively identified at the Geological Survey of Canada in Ottawa.

Zircon

Zircon is typical of the SHL and GL groups and relatively abundant

Figure 97: Cesian beryl along the front of albitization invading quartz core in the Tanco pegmatite; the largest crystals are 20 cm in length

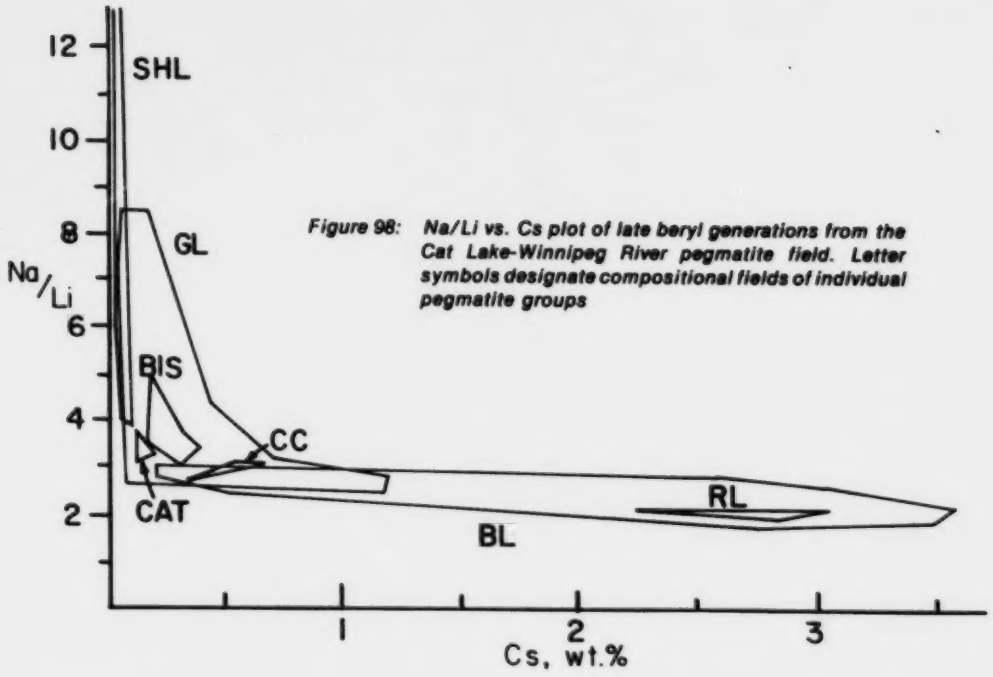

Figure 98: Na/Li vs. Cs plot of late beryl generations from the Cat Lake-Winnipeg River pegmatite field. Letter symbols designate compositional fields of individual pegmatite groups

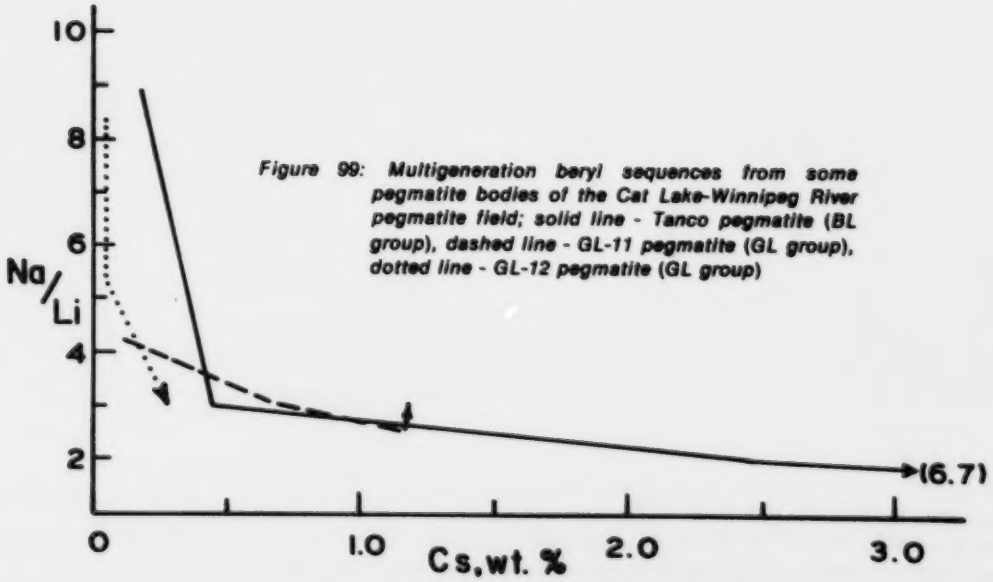

Figure 99: Multigeneration beryl sequences from some pegmatite bodies of the Cat Lake-Winnipeg River pegmatite field; solid line - Tanco pegmatite (BL group), dashed line - GL-11 pegmatite (GL group), dotted line - GL-12 pegmatite (GL group)

TABLE 58. CHEMICAL COMPOSITION OF BERYL
(After Černý and Simpson 1977)

	Tanco zone (6+3)		
Sample #	U-10-11.5	B-188.8	BE-3*
SiO_2, wt.%	62.35	62.00	63.36
Al_2O_3	17.50	17.71	16.77
Fe_2O_3	0.027	0.018	0.073
MnO	0.007	0.004	0.001
CaO	0.007	0.030	0.120
MgO	0.001	0.017	0.003
BeO	11.66	11.32	11.21
Li_2O	0.98	1.13	1.29
Na_2O	1.38	1.68	1.68
K_2O	0.046	0.269	0.089
Rb_2O	0.071	0.109	0.068
Cs_2O	2.47	3.27	2.92
H_2O^+	0.08	0.07	0.05
H_2O^-	1.96	2.06	2.10
	98.54	99.68	99.70

Analysts, K. Ramlal and R. Chapman

* contaminated by about 1% quartz

TABLE 57. CHEMICAL COMPOSITION OF ZIRCON
(After Černý and Silvola 1980)

Sample #	ZH-1		ZH-3/11		ZH-4/17		ZH-5/10	
	S*	C**	S	C	S	C	S	C
SiO_2, wt.%	32.2	31.4	29.4	28.4	28.5	28.5	30.8	32.3
ZrO_2	50.4	38.4	52.8	49.3	53.0	49.4	52.6	47.4
HfO_2	17.4	17.5	17.9	13.3	17.6	14.8	17.3	15.3
Al_2O_3	0.0	0.0	0.0	0.0	0.8	0.8	0.7	0.7
FeO	0.04	0.9	0.1	0.8	0.03	0.5	0.01	0.0
MnO	0.2	1.0	0.6	0.9	0.02	0.3	0.1	0.3
CaO	0.02	2.3	0.3	3.6	0.0	0.4	0.0	0.4
	100.26	91.5	101.1	96.3	99.95	94.7	101.3	96.4

Microprobe analyst, J. Silvola

* fresh surface of crystals

** altered core of crystals

ZH-1 large crystal, zone (5) of th Tanco pegmatite, BL group

ZH-3/11 Sn-enriched lepidolite unit (9) in the western part of the Tanco pegmatite, BL group

ZH-4/17 Sn-enriched albitization (3) in the western central intermediate zone (6) of the Tanco pegmatite, BL group

ZH-5/10 Sn-enriched lepidolite unit (9) in the eastern part of the Tanco pegmatite, BL group

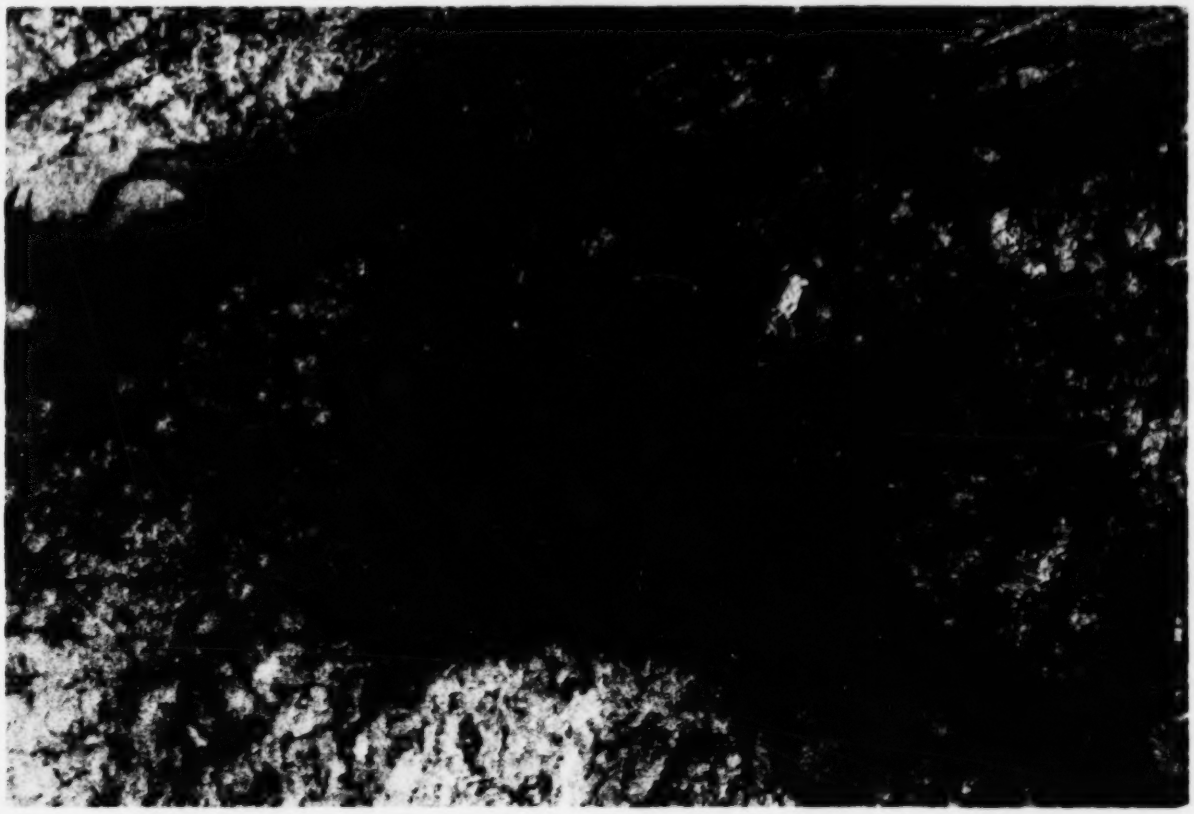

Figure 100: Radial aggregate of fibrous allanite, largely altered into bastnaesite and associated with yttrotantalite (invisible in the photograph); SHL-2 pegmatite, Shatford Lake group

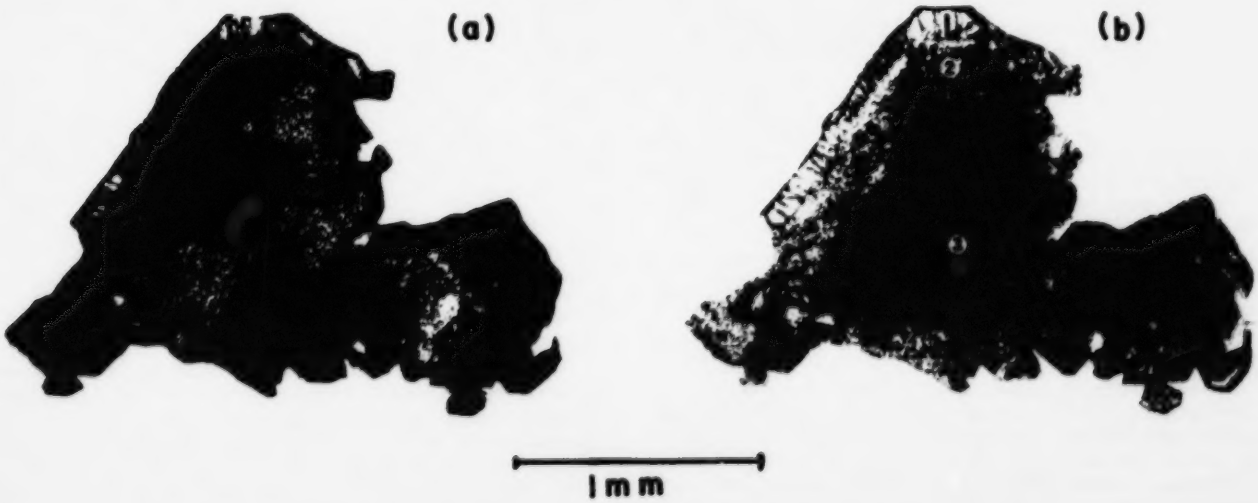

Figure 101: Metamict decay and hydrothermal alteration of hafnian zircon from the Tanco pegmatite in thin section: (a) plane-polarized light, (b) crossed polars; (1) fresh clear crystalline zircon, (2) clouded faintly birefringent zone, (3) isotropic X-ray amorphous core

in the Tanco pegmatite. A single crystal was also found in the CATB dyke. In all occurrences it is partly to completely metamict, and heavily affected by late hydrothermal alteration (Fig. 101). Preliminary data indicate HfO_2 contents in the range of 4.0-6.5 wt.½ for the SHL group, and 3.5-8.0 wt.% for the GL group. These values cannot be taken as geochemically significant because most of them have been collected on heavily altered material. The analyses of fresh, stoichiometric and altered, hydrated and nonstoichiometric portions of single crystals from the Tanco pegmatite clearly indicate that the Zr/Hf ratio is sensitive to hydrothermal leaching (Table 57; Černý and Siivola 1980).

Thorite

This species occurs as black or dark brown rounded grains in the Huron Claim pegmatite (SHL group) and as microscopic inclusions in hafnian zircon from the Tanco deposit. In this latter occurrence, the grains are barely large enough for qualitative identification by electron microprobe.

The Huron Claim thorite is metamict and X-ray amorphous, but recrystallizes upon heating in air. Preliminary results indicate P_2O_5 contents in the range of 3.2-6.0 wt.%, UO_2 up to 17 wt.%, Fe_2O_3 2-15 wt.%, total REE 1-4 wt.%; low totals indicate considerable hydration (Paul, in prep.). Subhedral pyrite inclusions are characteristic of the black variety, and are accumulated to the point of typical poikilitic intergrowth.

Uraninite

Uraninite has been identified in the Huron Claim pegmatite as long as 50 years ago, and it yielded the first absolute age over 2 Ga ever recorded in the Canadian Shield (Ellsworth 1932). Black cubes of uraninite from this locality exhibit some of the highest ThO_2 substitutions known for pegmatite occurrences of this species (14-28 wt.%; DeLury and Ellsworth 1931; Paul, in prep.). Sooty black, yellow and orange alteration products commonly replace large portions of the crystals; uranophane and sklodowskite have been identified by Bristol (1962).

Magnetite

Huron Claim is the only pegmatite in which magnetite has been reported (Bristol 1962). However, no additional specimens of magnetite have been found during recent study of this pegmatite (Paul, in prep.), and examination of the original sample in polished sections revealed the presence of euhedral inclusions of coffinite. This hydrosilicate of uranium and thorium is also known excusively from the magnetite-bearing specimen. This singular occurrence of two species confined to a unique hand specimen casts some doubt on its provenance.

Ilmenite

Three occurrences of ilmenite have been identified in the Winnipeg River district: in thin veinlets of plagioclase, quartz, carbonates and chlorite in close vicinity of the Huron Claim and Silverleaf localities, and in the Tanco pegmatite.

The first two occurrences are marked by low MnO contents; in contrast, the Tanco ilmenite is pronouncedly manganoan (Table 58; Grice et al. 1972). The low total of the Tanco ilmenite may be partly caused by Nb and Ta which were not analyzed for, and by some Fe present in the trivalent state.

Niobian and tantalian rutile

These minerals, also known under varietal names of ilmenorutile and strüverite, respectively, occur in the SHL and GL groups, and in the BET pegmatites. They are found in two forms: as primary grains of microscopic to 1 cm dimensions, and as microscopic skeletal and mossy patches in columbite-tantalite minerals suggesting an exsolution origin. Primary niobian rutile is commonly crisscrossed by flame-like exsolution lamellae of columbite-tantalite whereas tantalian rutile typical of the BET pegmitites is homogeneous. Chemical compositions of the niobian and tantalian rutiles are presented in Table 58. In general, these minerals follow the compositional trends of columbite-tantalite in terms of Nb/Ta fractionation but not in the Fe/Mn ratios. Fe is evidently preferred by the rutile structure.

Aeschynite

Aeschynite-like X-ray powder diffraction patterns are produced, after heating, by some metamict phases associated with columbite-tantalite in the Huron Claim (SHL group) pegmatite (Paul, in prep.).

Fersmite

This species is the most common replacement product after columbite-tantalite in the Huron Claim pegmatite (Fig. 102), and it may be present also in some other dykes of the SHL group, but positive identification has yet to be made.

The Huron Claim fersmite displays quite a range in the Nb/Ta ratio (Table 59) and the presence of rynersonite is suspected from preliminary analyses. However, in terms of large cations it is Ca-based with negligible contents of RE elements.

Euxenite

Several black and highly lustrous grains from the SHL pegmatites, metamict in the natural state, give good euxenite patterns after heating (comparable to heated euxenite data by Lima de Faria 1964). None of these minerals could be mounted for electron microprobe analysis.

Yttrotantalite

Yttrotantalite also occurs in the SHL pegmatites. Metamict in the natural state, it yields X-ray powder diffraction patterns typical of yttrotantalite heating products, after high temperature treatment according to Lima de Faria (1964). Qualitative checks by electron microprobe confirmed its identity.

Cassiterite

The SHL and GL pegmatite groups and the CC body carry some cassiterite but its major concentrations are found in the RL and BL pegmatites. Fine-grained cassiterite occurs disseminated in saccharoidal albite throughout the Odd dyke, and in saccharoidal albite or muscovite associated with Ta, Nb-oxide minerals and hafnian zircon in the Tanco pegmatite. The most conspicuous occurrence is that in the Odd West pegmatite of the RL group, where it forms irregular dark brown crystals up to 6 cm in size, in a muscovite + verdelite + quartz assemblage of the upper intermediate zone.

Chemical composition of cassiterite varies within narrow limits of FeO, MnO, Nb_2O_5 and Ta_2O_5 admixtures (Table 60) However, more complex compositions found in the RL group are still under investigation. They are considerably inhomogeneous and resemble staringite, rich in the oxides quoted above.

Columbite-tantalite group

To date, the LdB and AX groups are the only ones in which columbite-tantalite minerals have not been observed. Most of the occurrences elsewhere are extremely scarce. It is only the SHL, GL, RL and BL groups in the Winnipeg River district that show noticeable contents of columbite-tantalite, and the CC body in the northern district.

Columbite-tantalite minerals vary in size and habit of their crystals rather widely, and commonly so within a single pegmatite body. The size ranges from microscopic to 20 cm, and the habit may be acicular, lath-shaped and platy, columnar, stubby prismatic or equidimensional (Fig. 103). The colour is black, with rare exceptions of brownish-black to reddish-brown manganotantalites. The identity of the mineral and its composition are extremely difficult to judge from its appearance in hand specimen. Four compositional and structural variables serve to distinguish different paragenetic types of columbite-tantalite phases:

TABLE 58. CHEMICAL COMPOSITION OF ILMENITE, NIOBIAN AND TANTALIAN RUTILE

Species	Ilmenite		Niobian rutile			Tantalian rutile	
Sample #	SFTI	TANIL	GL-8W-28	K-1	M17303 A	IRA-15	IRA-16
Ta_2O_5, wt.%	0.0	n.d.*	20.9	3.5	3.4	37.0	40.6
Nb_2O_5	0.0	n.d.*	33.2	3.8	20.7	3.9	5.3
TiO_2	51.8	51.0	22.8	87.8	65.9	47.4	40.5
SnO_2	0.0	n.d.	6.3	0.4	0.9	0.3	0.4
ZrO_2	0.0	n.d.	0.0	1.4	0.0	0.0	0.0
Sb_2O_3	0.0	n.d.	n.d.	0.01	0.0	0.02	0.02
Al_2O_3	0.0	traces	n.d.	0.0	0.1	0.2	0.0
FeO	46.1	36.0	14.2	3.4	9.1	10.6	11.8
MnO	1.4	9.1	2.6	0.2	0.01	0.05	0.03
CaO	0.0	n.d.	n.d.	0.2	0.0	0.0	0.0
MgO	0.0	0.5	0.0	0.0	0.0	0.0	0.0
	99.3	96.6	100.0	100.7	100.1	99.4	98.6

* not determined

SFTI ilmenite Silverleaf Claim, Greer Lake pegmatitc granite; electron microprobe analysis by F.C. Hawthorne

TANIL ilmenite Tanco pegmatite, albitization (3) in central intermediate zone (6) (BL group); a.a. and XRF analysis by J.D. Grice (Grice et al. 1972)

GL-8W-28 niobian rutile with columbite exsolutions, GL-8 pegmatite of the GL group; XRF analysis by K. Ramlal (Černý and Turnock 1971a)

K-1 niobian rutile inclusions in disordered columbite, K-1 pegmatite of the SHL group; electron microprobe analysis by F.C. Hawthorne

M17303 A niobian rutile from a quasi-graphic intergrowth with disordered columbite; Huron Claim pegmatite of the SHL group; electron microprobe analysis by R. Chapman.

IRA-15 tantalian rutile, IRA pegmatite of the BET group; electron microprobe analysis by F.C. Hawthorne

IRA-16 tantalian rutile, IRA pegmatite of the BET group; electron microprobe analysis by F.C. Hawthorne

TABLE 59. CHEMICAL COMPOSITION OF FERSMITE (AFTER PAUL, IN PREP.)

Sample #	GL-10**	P3-47	P3-19	77-3T-C3
Ta_2O_5, wt.%	24.9	24.7	23.9	21.9
Nb_2O_5	54.0	60.4	61.5	62.4
TiO_2	0.4	0.5	0.6	0.6
SnO_2	0.0	0.1	0.0	0.3
Al_2O_3	n.d.*	0.01	0.0	0.0
Sb_2O_3	0.0	0.03	0.0	0.1
FeO	0.1	0.3	0.1	0.1
MnO	0.1	0.2	0.1	0.1
CaO	15.5	14.8	14.4	14.5
	95.0	101.0	100.6	100.0

* not determined

All samples from the HC pegmatite of the SHL group

GL-10 from Foord and Mrose (1978)

Microprobe analysts, E.E. Foord** and F.C. Hawthorne

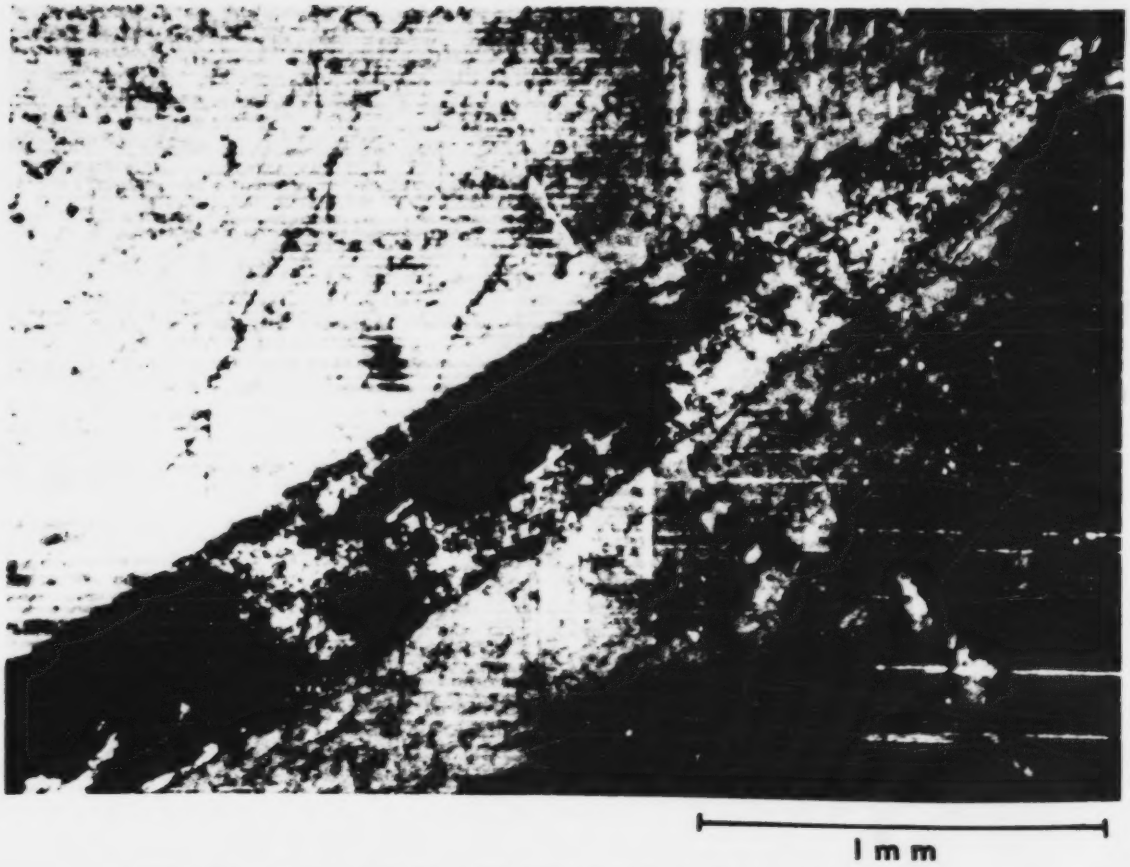

Figure 102: Fersmite (mottled birefringence) replacing a platy crystal of columbite (black) in twinned albite of the Huron Claim pegmatite; thin section between crossed polars

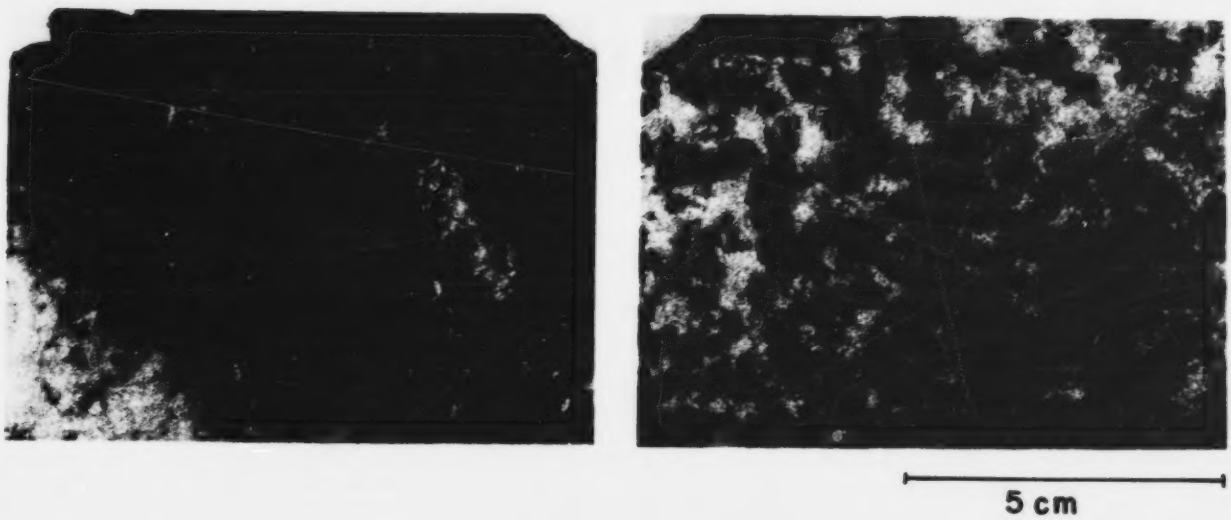

Figure 103: Variations in crystal shape of the columbite-tantalite minerals: (a) platy disordered columbite-tantalite from the GL-2A pegmatite, (b) brick-shaped crystals of disordered tantalite from the Tanco pegmatite

TABLE 60. CHEMICAL COMPOSITION OF CASSITERITE

Sample #	NUTT-1	NUTT-5	L-20	WTA-14+	SF-14	SF-15
Ta_2O_5, wt.%	2.3	4.8	0.5	0.01	4.7	4.9
Nb_2O_5	0.0	2.4	0.0	0.05	0.0	0.0
TiO_2	0.3	0.6	0.1	0.01	0.0	0.0
SnO_2	95.4	89.8	97.3	100.0	94.4	94.0
ZrO_2	0.6	0.0	0.0	n.d.*	0.0	0.0
Sb_2O_3	0.0	0.7	0.0	n.d.	0.0	0.0
FeO	0.1	0.2	0.5	0.01	0.7	1.0
MnO	0.4	0.6	0.02	0.08	0.2	0.1
CaO	0.0	0.1	0.5	0.0	0.0	0.0
	99.1	99.2	99.4**	100.2	100.0	100.0

* not determined

** includes 0.5 MgO

+ Microprobe analysts, E. E. Foord and F.C. Hawthorne

NUTT-1 NUTT pegmatite of the SHL group

NUTT-5 NUTT pegmatite of the SHL group

L-20 RL-4 pegmatite of the RL group

WTA-14 Tanco pegmatite of the BL group, albitization (3) in western zone (6). According to Grice et al. (1972); microprobe analyses of cassiterite from the eastern counterpart of this assemblage contain up to 3% of Ta_2O_5 and/or Nb_2O_5, as well as minor amounts of TiO_2 and FeO

SF-14 Silverleaf claim of the Greer Lake pegmatitic granite

SF-15 Silverleaf claim of the Greer Lake pegmatitic granite

(i) The Fe/Mn ratio decreases with progressive fractionation (Fig. 104). It can be indirectly estimated from unit cell dimensions of ordered phases, notably *a* (Komkov 1970, Černý and Turncock 1971a).

(ii) The Nb/Ta ratio also decreases with progressive fractionation. However, the changes in Fe/Mn and Nb/Ta are not closely interrelated, as shown in Figure 104, and different Fe/Mn vs. Nb/Ta trends appear to be characteristic for individual pegmatite groups and even pegmatite bodies. Komkov (1970) recommends the intensity ratio I_{321}/I_{312} of ordered phases for estimates of the Nb/Ta ratio.

(iii) Substitution of Sn, Ti, Sc, Ca and other cations for Fe, Mn, Nb and Ta is commonly characteristic for certain pegmatite groups, or for specific generations of columbite-tantalite minerals within a single pegmatite body (Fig. 105).

(iv) A cation order-disorder relationship exists in the columbite-tantalite group. (Fe, Mn) and (Nb, Ta) are separated in two kinds of specific sites in an ordered structure, whereas disordered phases have both types of cations randomly distributed over the two sites, and the *a* dimension of the unit cell equal to (*a*/3) of ordered structure (Nickel et al. 1963b). On heating, disordered columbite-tantalite converts into ordered structure ("pseudo-ixiolite" of Nickel et al. 1963b), or it yields wodginite, olovo-tantalite and/or $FeNb_4O_4$-type X-ray diffraction patterns instead of, or in addition to, the ordered columbite-tantalite phases (ixiolite proper). This second case is typical of non-stoichiometric minerals with noticeable substitution of Sn, Ti, Sc, Ca etc., generally when more than 3-5 wt. % of their sum is present.

Figure 106 demonstrates differences in the structural state characteristic of the columbite-tantalite minerals from the Winnipeg River district. GL phases are invariably disordered "pseudo-ixiolites". Huron Claim minerals are structurally intermediate, and manganotantalites from the BL and RL groups are well ordered.

Typical compositions of columbite-tantalite minerals from different pegmatite groups are given in Table 61, and fractionation trends are shown in Figure 104. More detailed information on this mineral group from some pegmatites is available in Černý and Turnock (1971a), Grice et al. (1972), and Paul (in prep.). Columbite-tantalite phases from the pegmatitic granites are described by Goad (in prep.).

Microlite

This species is closely associated with columbite-tantalite minerals in most of their occurrences, thus its general distribution is about the same as quoted above for the columbite-tantalite group. Microlite is inconspicuous in hand specimens, usually fine grained and dispersed, and commonly can be seen and identified only by microscope.

Part of the reason is the mode of its formation. Primary microlite co-existing with other Nb, Ta-bearing mineral as rounded grains or octahedral crystals is relatively rare; it is found in some GL pegmatites (Černý and Turnock 1971a) and in the Tanco deposit (Grice et al. 1971). In most of its occurrences, however, microlite is a secondary phase replacing columbite-tantalite minerals.

Both types of microlite are enriched in Ta, compared to

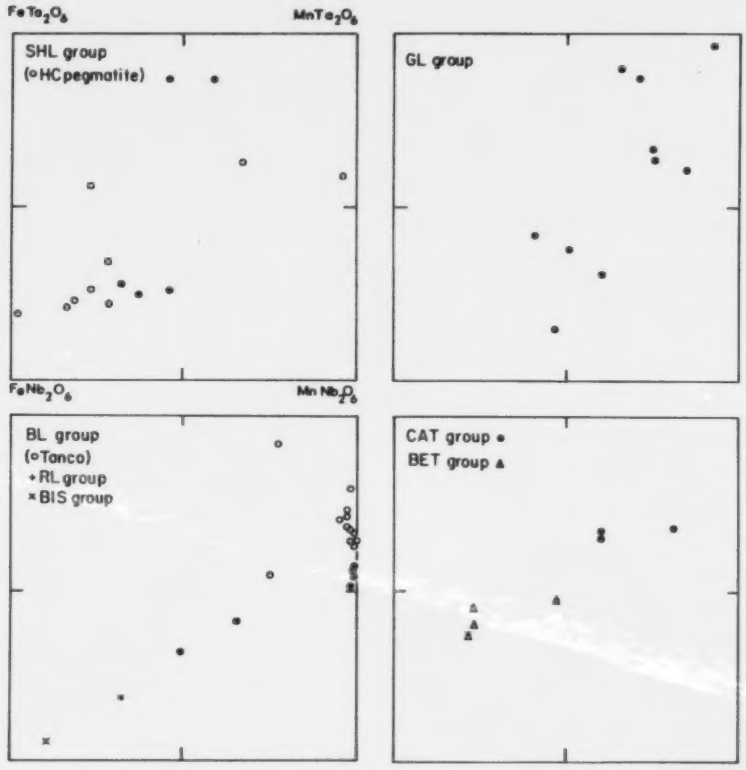

Figure 104: Columbite-tantalite minerals of the Cat Lake-Winnipeg River pegmatite field in the $FeNb_2O_6$-$FeTa_2O_6$-$MnNb_2O_6$-$MnTa_2O_6$ (mol.%) diagram

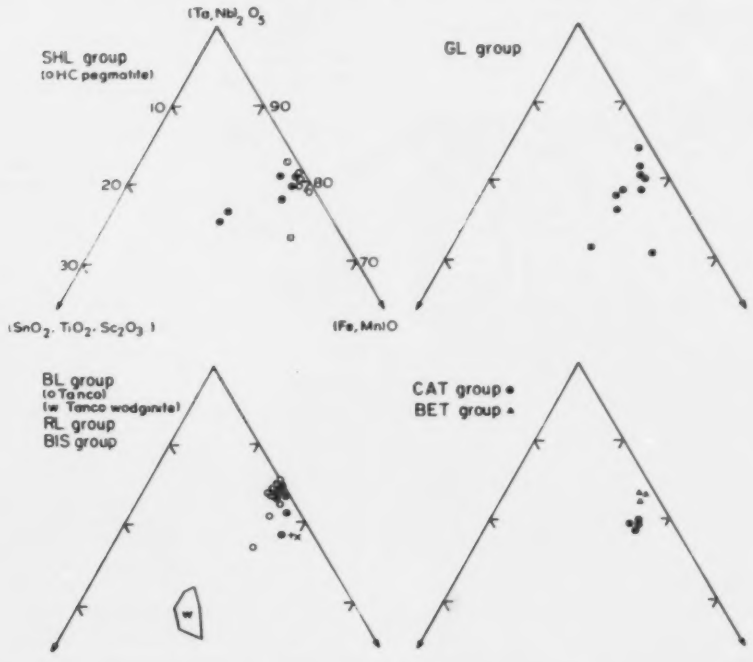

Figure 105: Columbite-tantalite and related minerals of the Cat Lake-Winnipeg River pegmatite field in the $(FeO + MnO)$-$(Ta_2O_5 + Nb_2O_5)$-$(TiO_2 + SnO_2 + Sc_2O_3$ et al.) triangle

TABLE 61. CHEMICAL COMPOSITION OF COLUMBITE-TANTALITE MINERALS

Pegmatite group	SHL					GL		BIS	RL
Sample #	M-57303	HC-2	P2-07	SHP-21	SHP-B2	GL-9-18	GL-12A-2	SR-104	RL-1
Ta_2O_5, wt.%	2.9	37.3	55.8	70.6	68.7	38.0	84.0	7.6	21.1
Nb_2O_5	70.9	42.5	26.3	6.2	6.4	37.1	1.3	69.6	57.7
TiO_2	4.8	0.2	0.7	1.3	1.1	8.8	0.7	1.7	2.0
SnO_2	0.2	n.d.*	0.0	8.3	10.3	3.3	0.2	0.1	0.0
ZrO_2	0.0	n.d.	0.0	0.0	0.01	n.d.	0.0	0.0	0.0
Al_2O_3	0.05	n.d.	0.0	0.3	0.2	n.d.	0.01	0.0	0.3
Sc_2O_3	0.0	n.d.	0.0	0.0	0.0	0.6	0.0	0.0	0.0
Sb_2O_3	0.0	n.d.	0.2	0.3	0.2	0.0	0.0	0.0	0.0
FeO	17.3	16.4	12.4	5.3	5.5	8.0	1.1	17.1	13.1
MnO	3.9	4.5	3.7	7.6	6.9	7.6	13.3	2.0	5.9
CaO	0.1	n.d.	0.1	0.2	0.1	n.d.	0.0	0.02	0.0
MgO	0.2	n.d.	0.0	0.0	0.0	n.d.	0.1	0.0	0.0
	100.3	100.9	99.2	100.1	99.4	103.6	100.7	98.7	100.1

Pegmatite group	BL						BET		CAT
Sample #	BEP-NE	BCNW-84	BCNW-107-1	G-69-31	G-69-52	L-6	IRA-15MH	IRA-16	CATB-25
Ta_2O_5, wt.%	42.9	33.7	64.4	64.0	83.5	72.5	38.1	48.2	64.1
Nb_2O_5	37.6	43.8	20.0	18.0	4.0	11.3	40.3	32.9	19.0
TiO_2	1.1	2.1	0.1	1.7	0.2	0.2	4.1	3.4	1.1
SnO_2	0.2	0.7	0.5	1.8	0.0	0.0	0.2	0.1	0.4
ZrO_2	0.0	0.0	0.0	n.d.	n.d.	0.0	0.0	0.0	0.0
Al_2O_3	0.1	0.1	0.1	n.d.	n.d.	0.0	0.2	0.2	0.0
Sc_2O_3	0.0	0.0	0.0	n.d.	n.d.	0.0	0.0	0.0	0.0
Sb_2O_3	0.06	0.4	0.3	n.d.	n.d.	0.2	0.03	0.02	0.0
FeO	5.9	9.0	0.2	0.5	3.3	0.3	13.0	8.8	6.1
MnO	10.9	8.5	14.6	15.1	11.3	14.4	3.7	7.7	8.9
CaO	0.1	0.04	0.1	n.d.	n.d.	0.1	0.0	0.0	0.1
MgO	0.0	0.0	0.0	n.d.	n.d.	0.0	0.0	0.0	0.0
	98.9	98.3	100.3	101.1	102.3	99.0	99.6	101.3	99.7

* not determined

M-57303	partly disordered ferrocolumbite, Huron Claim pegmatite
HC-2	partly disordered ferrocolumbite, Huron Claim pegmatite; XRF analysis by K. Ramlal (Černý and Turnock 1971a)
P2-07	partly disordered ferrocolumbite-ferrotantalite, Huron Claim pegmatite
SHP-21	disordered stannian tantalite, SHP pegmatite
SHP-B2	disordered stannian tantalite, SHP pegmatite
GI-9-18	disordered titanian columbite, GL-9 pegmatite; electron microprobe analysis by E.E. Foord
GL-12A-2	disordered manganotantalite, GL-12A pegmatite
SR-104	disordered ferrocolumbite, RNW pegmatite
RL-1	disordered ferrocolumbite, RL-1 pegmatite
BEP-NE	disordered manganocolumbite, BEP pegmatite
BCNW-84	manganotantalite, BCNW pegmatite
BCNW-107-1	interior part of a large ordered manganotantalite, BCNW pegmatite
G-69-31	disordered manganotantalite; Tanco pegmatite, albitization (3) of eastern part of zone (6); electron microprobe analysis by S. Jones (Grice et al. 1972).
G-69-52	ordered manganotantalite; Tanco pegmatite, albitization (3) of eastern part of zone (6); electron microprobe analysis by S. Jones (Grice et al. 1972)
L-6	ordered manganotantalite; Tanco pegmatite, albitization (3) of western part of zone (6)
IRA-15MH	disordered titanian ferrocolumbite, IRA pegmatite veins
IRA-16	disordered titanian columbite, IRA pegmatite veins
CATB-25	disordered columbite, CATB pegmatite

If analyst not quoted, electron microprobe analysis by F.C. Hawthorne.

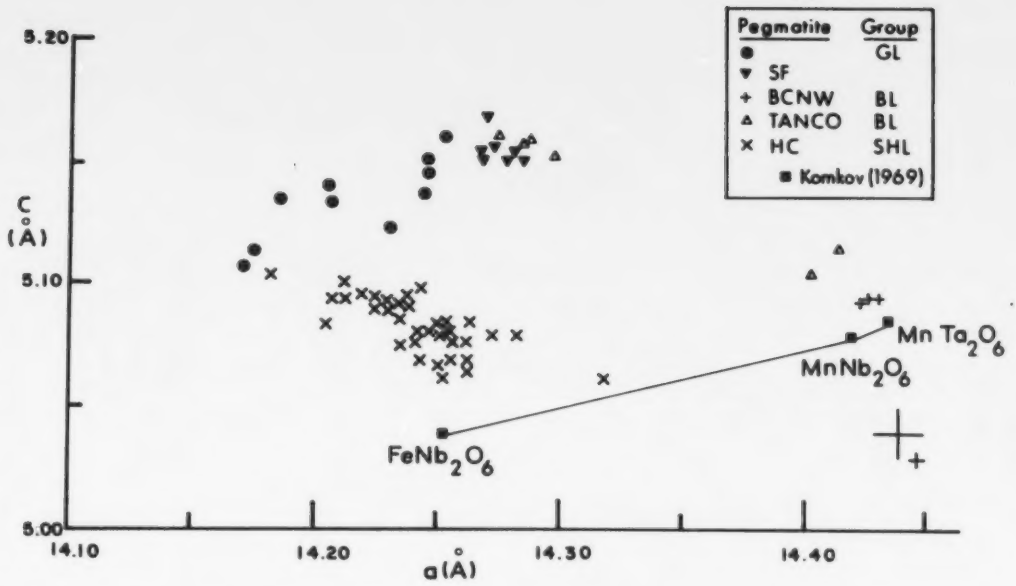

Figure 106: Columbite-tantalite minerals of selected pegmatite groups from the Cat Lake-Winnipeg River field plotted in the a-c unit cell dimension diagram. For disordered phased, a values are multiplied 3x. Crosses indicate minimum and maximum standard errors encountered. Solid squares designate synthetic ordered phases of Komkov (1970)

Figure 107: Skeletal wodginite (diamond-shaped, white) and microlite (faintly greyish, pitted) in a matrix of albite and quartz from the Tanco pegmatite; polished section, plane-polarized light

TABLE 62. CHEMICAL COMPOSITION OF MICROLITE*

Pegmatite group	SHL	GL		RL	BL		
Sample #	SHE-2	GL-6-1	GI-2-2	MOW	G-69-31	WTa-10	WTa-16
Ta_2O_5, wt.%	67.5	54.2	69.0	72.1	74.0	77.3	80.6
Nb_2O_5	7.4	16.4	3.6	5.1	5.5	1.4	0.6
TiO_2	2.0	3.1	2.9	0.0	1.0	0.1	0.1
SnO_2	0.05	1.4	0.5	0.0	0.2	0.1	0.04
ZrO_2	0.0	0.0	0.0	n.d.	n.d.**	n.d.	n.d.
Sb_2O_3	n.d.	n.d.	n.d.	1.6	n.d.	n.d.	n.d.
FeO	1.5	0.6	0.7	1.9	0.5	0.01	0.1
MnO	0.8	0.2	0.3	0.0	0.7	0.02	0.0
CaO	13.1	19.4	13.6	8.3	n.d.	11.2	11.1
Na_2O	2.0	0.7	2.2	n.d.	n.d.	n.d.	n.d.
F_2	1.5	1.5	2.3	n.d.	n.d.	3.9	4.3

*totals not given because H_2O and, partly, Na_2O and F_2 data are not available

**not determined

SHE-2 veins in disordered tantalite, SHE-2 pegmatite; microprobe analysis by E. E. Foord

GL-6-1 co-existing with disordered columbite, GL-6 pegmatite; electron microprobe analysis by E. E. Foord

GL-2-2 replacement of disordered manganotantalite, GL-2 pegmatite; electron microprobe analysis by E. E. Foord

MOW replacing stibiotantalite; OW pegmatite of the RL group; electron microprobe analysis by D. C. Harris (Černý and Harris 1973b)

GL-69-31 replacement of disordered manganotantalite; Tanco pegmatite, zone (4); electron microprobe analysis by S. Jones (Grice et al. 1972)

WTa-10 co-existing with wodginite; Tanco pegmatite, albitization (3) of western part of zone (6); electron microprobe analysis by E. E. Foord

WTa-16 co-existing with wodginite; Tanco pegmatite, albitization (3) of western part of zone (6); electron microprobe analysis by E. E. Foord

co-existing or replaced columbite-tantalite minerals. Table 62 presents examples of typical microlite compositions from different pegmatite groups; totals are low because H_2O and, in most cases, F could not be determined on the electron microprobe.

Tapiolite

Tapiolite is rare, and so far it has been found only in microscopic grains. Its occurrences are restricted to the BL group (Tanco) and RL group (OW pegmatite). The chemical composition given in Table 63 shows a predominance of Fe and Ta over Mn and Nb, typical of the species. Additional information on tapiolite from the Winnipeg River district can be found in Grice et al. (1972) and Černý and Harris (1973a).

Wodginite

This mineral was described as a new species from Wodgina, Australia and from the Tanco pegmatite by Nickel et al. (1963a). The Tanco deposit is, to date, its only locality in southeastern Manitoba. However, wodginite is abundant in that pegmatite and constitutes the main ore mineral of tantalum there. Figure 107 shows the typical diamond-shaped cross-section of its crystals in saccharoidal albite.

Table 63 presents the range of published (Grice et al. 1972) and new compositions of the Tanco wodginite in terms of Fe/Mn, Sn, Ti, and Nb/Ta contents.

Simpsonite

The Tanco pegmatite is the only locality of this mineral in the Cat Lake-Winnipeg River pegmatite field. This is in accord with its other occurrences around the world which are confined to extremely fractionated pegmatites. Simpsonite is white to colourless, associated with wodginite and microlite in the western part of the Tanco deposit, and mostly not recognizable in hand specimens except by aid of UV lamp; it fluoresces bright white, yellowish-white or bluish-white. Larger crystals are commonly replaced by manganotantalite and microlite, along margins (Fig. 108) or in their entirety.

Stibiotantalite

This mineral has been found in the OW pegmatite (RL group), and it probably also occurs in the Tanco deposit. However, it was detected only in an X-ray diffraction pattern (admixed to simpsonite) at Tanco, and conclusive proof is not yet available.

Brown columnar crystals of stibiotantalite in the OW dyke are veined and replaced byantimonian microlite (Černý and Harris 1973a). Chemical composition of this stibiotantalite is given in Table 63.

Apatite

Sparse grains of apatite are found in all pegmatite groups of the examined field. However, the LdB, GL, ENL, AX, BET, and

MWL groups are very poor in this mineral, whereas the RL and BL pegmatites carry it in abundance. In most pegmatite groups, apatite is green, grey or pale bluish in colour; in the RL and BL pegmatites, primary apatite is mostly dark blue.

All primary apatites examined exhibit optical properties close to those of fluorapatite. Partial analyses of the blue apatites from the RL and BL groups show a MnO content up to 2.0 wt.%. Multigeneration apatite sequences which occur in the most fractionate pegmatites (e.g., Tanco and Buck Claim in the BL group) are characterized by alteration of the blue apatites into (OH)-enriched phases, and by late generations of fracture-coating and vug-filling white and brown apatites with increased H_2O and CO_2 contents (Černý 1972b, Lenton 1979).

Monazite

Monazite occurrences are restricted to the SHL and GL pegmatites. Detailed studies of monazite are in progress as its geochemistry may significantly contribute to understanding genetic links between the two pegmatite groups. Unit cell dimensions suggest that most of the samples under study belong to phases intermediate between monazite, cheralite and huttonite.

In the SHE-2 pegmatite, pseudomorphs of synchisite after monazite have been found (Černý and Bristol 1972). Sulphide veining and slight alteration along microscopic fractures is typical of most other occurrences.

Xenotime

This species is known, so far, only from the GL-8 pegmatite. Microscopic crystals of xenotime occur there in association with a columbite-tantalite mineral and zircon. Qualitative test by electron microprobe and optical properties identify the mineral.

Triphylite-lithiophilite series

Minerals of this phosphate series occur as rare accessory phases in the LdB, BIS, CAT, CC, and MWL pegmatites but in much larger quantities in the RL and particularly BL groups. Optical properties and partial chemical analyses indicate that most of the green to beige minerals belong to the Fe-rich triphylite part of the series (e.g., Lenton 1979). The only exceptions seem to be the occurrences in the Tanco pegmatite, where the buff-coloured blocky material approximates an atomic Fe/Mn ratio of 1.0, and an orange-coloured late generation shows Mn in excess over Fe, a lithiophilite composition.

Members of this series commonly succumb to alteration, either hydrothermal (blue apatite + calcite at Tanco, alluaudite in the CC and Buck pegmatites) or supergene (sicklerite and heterosite-type oxidation products widespread in most localities, and vivianite in the CC pegmatite).

Amblygonite- montebrasite series

Negligible amounts of these minerals are known from the most fractionated pegmatites of the BIS and MWL groups. However, their main occurrences are those in the RL and particularly the BL pegmatites. In general, three generations can be distinguished:

(i) Blocky amblygonite-montebrasite in and around quartz cores and, to lesser degree, in the intermediate zones (Fig.109a). It is commonly associated with quartz and blocky K-feldspar. Pinkish, yellowish or white in colour, it has intermediate compositions (7-4 wt.% F_2) and extremely low contents of alkalis other than Li.

(ii) Lath- or rod-shaped crystals of Na-enriched amblygonite-montebrasite associated with metasomatic cleavelandite and Li-bearing micas in the intermediate and blocky zones. This variety is generally white, with typical rusty-reddish surface crusts of secondary apatite. In terms of the (F, OH) contents, this type is also intermediate to (OH)-enriched (3.6-6.6 wt.% F_2), and Na_2O reaches up to 1.0 wt.%.

(iii) Secondary montebrasite is widespread as veining and replacement of the two varieties described above. It is usually grey, brownish or dirty greenish, and always poor in fluorine (1.0-4.0 wt.% F_2). The replacement process is rather complex texturally (Fig. 109b), and it is usually associated with surface alteration and veining.

Chemical analyses of typical representatives of the first and third type of amblygonites-montebrasites are given in Table 64. Further details on mineralogy of this group are provided by Černá et al. (1972) and Lenton (1979).

The most frequent association developing at the expense of amblygonite-montebrasite, on the surface of its crystals and along fractures, is apatite + muscovite ± cookeite ± quartz (Černá et al. 1972). A low-temperature association of lithiophosphate followed by pink apatite (Černý 1972b) is locally covered by tancoite and an unidentified hydrous phosphate of Na (Ramik et al., in prep.) in the Tanco pegmatite. Another association of secondary phosphates has been recently found at Tanco: whitlockite, crandallite, overite and fairfieldite (R.A. Ramik, pers. comm. 1979). It may be a product of amblygonite-montebrasite alteration but no relics of primary phosphates were found with it.

Native elements, alloys, sulphides and sulphosalts

Minerals belonging to these systematic classes are extremely restricted in their distribution and abundance. Most pegmatite groups do not contain any of them. Some occurrences, such as those of pyrite in several SHL pegmatites, come from remobilized sulphidic iron formation rather than from the pegmatite fluids proper. In the GL, BIS and ENL groups, however, trace amounts of pyrite and chalcopyrite do not have an obvious external source.

The most varied association of sulphides and related minerals is found in the most fractionated pegmatites of the RL and BL groups. Pyrite, chalcopyrite, stibarsen intergrown with native Sb, stibnite, sphalerite, and arsenopyrite have been identified in the RL pegmatites, with stibiconite as an oxidation product of stibnite (e.g., Černý and Harris 1973a).

Sphalerite, tetrahedrite, pyrrohotite, chalcopyrite and molybdenite are known from several pegmatites of the BL group but the largest variety of species and, relatively, the greatest abundance is found in the Tanco pegmatite. Detailed description of these minerals, listed in Table 65, is given by Černý and Harris (1978).

TABLE 63. CHEMICAL COMPOSITIONS OF WODGINITE, TAPIOLITE AND STIBIOTANTALITE

Species	Wodginite					Tapiolite				Stibiotantalite
Sample #	G-69-8	G-69-21W	WTa-10	WTa-19W	WTa-14	GL-69-21T	GL-69-52	WTa-19T	TOW	SOW
Ta_2O_5, wt.%	66.9	69.1	68.3	71.0	70.5	85.0	85.0	81.2	79.5	54.5
Nb_2O_5	5.5	2.7	3.3	6.6	2.3	2.4	2.2	1.7	5.8	4.0
TiO_2	3.2	0.2	0.2	0.1	2.5	0.2	0.1	1.4	0.0	n.d.
SnO_2	14.7	17.0	15.6	12.7	14.9	0.2	0.2	2.1	0.0	n.d.
Sb_2O_3	n.d.	n.d.	n.d.	n.d.	n.d.	n.d.	n.d.	n.d.	0.0	41.8
FeO	3.3	5.2	2.9	1.8	0.1	13.5	14.0	12.6	13.7	n.d.
MnO	8.9	8.3	9.3	8.6	11.0	2.1	2.2	1.4	0.5	n.d.
CaO	n.d.	n.d.	n.d.	0.0	0.1	n.d.	n.d.	0.01	0.0	0.1
	102.5	102.5	99.6	100.8	101.4	103.4	103.7	100.4	99.5	100.4

* not determined

G-69-8 Tanco pegmatite of the BL group, albitization (3) in the eastern part of zone (6); electron microprobe analysis by S. Jones (Grice et al. 1972)

G-69-21W Tanco pegmatite, albitization (3) in the eastern part of zone (6); electron microprobe analysis by S. Jones (Grice et al. 1972)

WTa-10 Tanco pegmatite, albitization (3) in the western part of zone (6); electron microprobe analysis by E.E. Foord

WTa-19W Tanco pegmatite, albitization (3) in the western part of zone (6); electron microprobe analysis by E.E. Foord

WTa-14 Tanco pegmatite, albitization (3) in the western part of zone (6); electron microprobe analysis by E.E. Foord

GL-69-21T Tanco pegmatite, albitization (3) in the eastern part of zone (6); electron microprobe analysis by S. Jones (Grice et al. 1972)

GL-69-52 Tanco pegmatite, albitization (3) in the eastern part of zone (6); electron microprobe analysis by S. Jones (Grice et al. 1972)

WTa-19T Tanco pegmatite, albitization (3) in the western part of zone (6); electron microprobe analysis by E.E. Foord

TOW Odd West pegmatite of the RL group; electron microprobe analysis by D.C. Harris (Černý and Harris 1973a)

SOW Odd West pegmatite of the RL group; electron microprobe analysis by D.C. Harris (Černý and Harris 1973a)

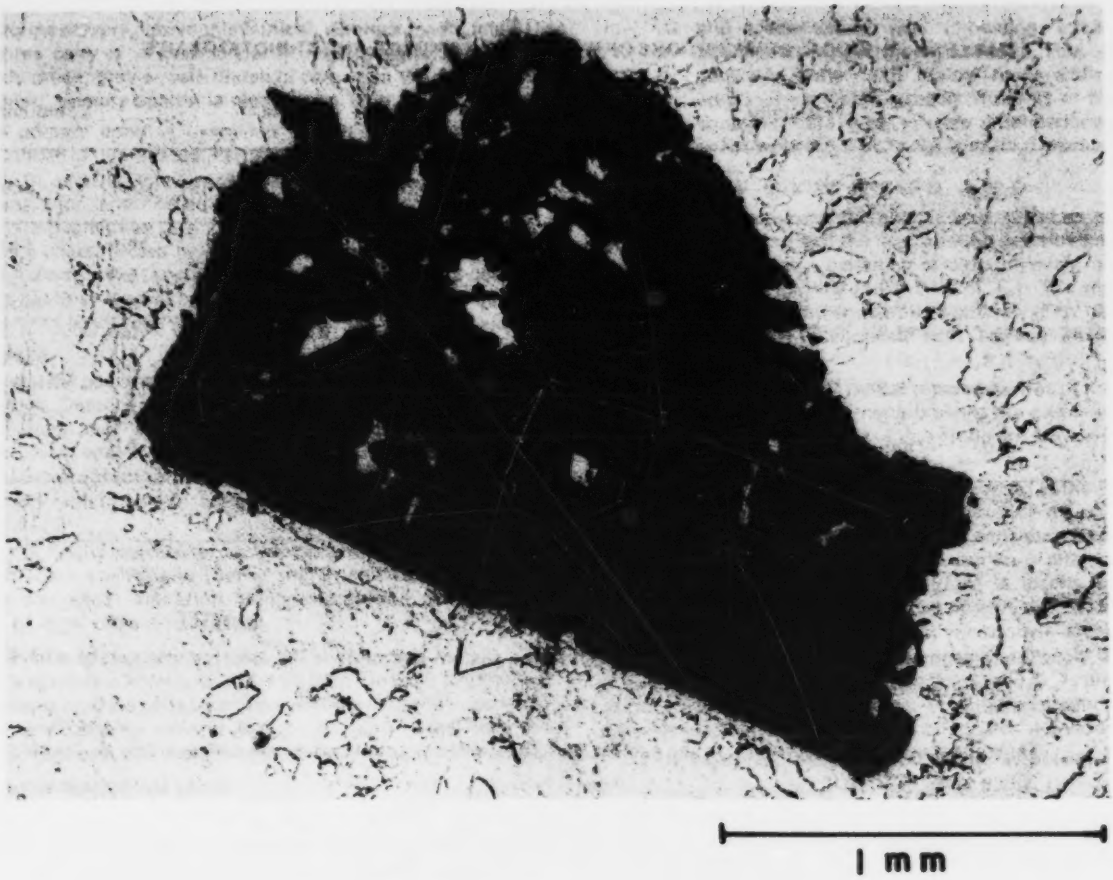

Figure 108: Simpsonite (rectangular crystals with high relief) partly replaced along crystal surfaces by microlite and manganotantalite (near opaque) in an albite + quartz + muscovite matrix from the Tanco pegmatite; thin section, plane polarized light

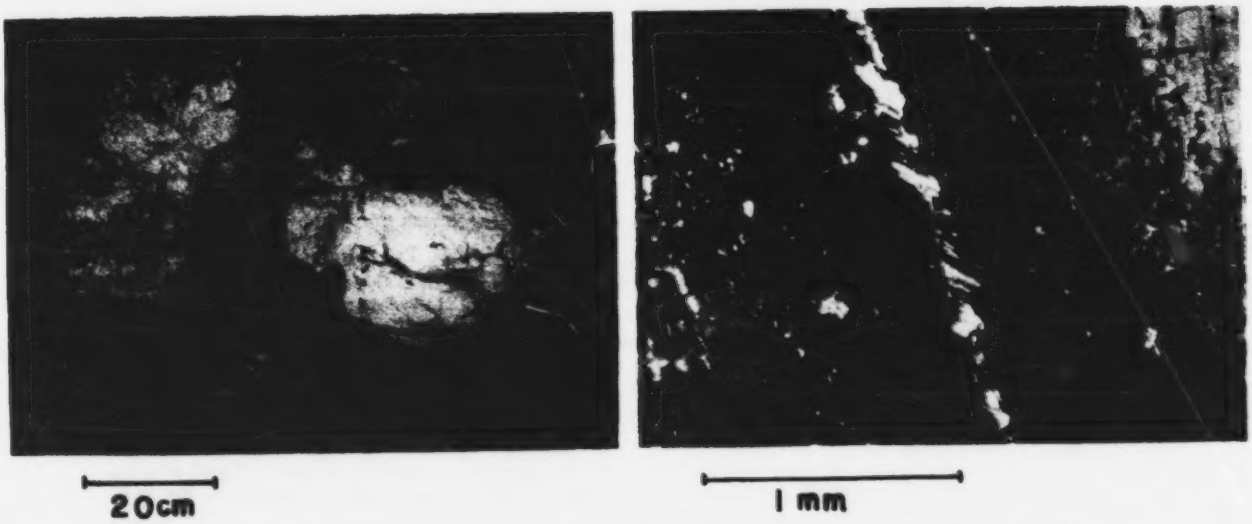

Figure 109: Amblygonite-montebrasite in the Tanco pegmatite: (a) blocky crystals along the quartz-pollucite boundary, and (b) veinlet of secondary montebrasite in primary amblygonite; thin section, crossed polars

TABLE 64. CHEMICAL COMPOSITION OF AMBLYGONITE-MONTEBRASITE (AFTER ČERNÁ ET AL. 1972)

Sample #	A-13	A-1	A-5	A-2	A-22
Al_2O_3, wt.%	34.18	34.53	34.86	34.53	35.10
Fe_2O_3	n.d.*	0.11	0.028	0.11	n.d.
CaO	0.015	0.17	0.074	0.17	0.065
MgO	0.00	0.005	0.002	0.002	0.003
Li_2O	9.52	9.86	10.29	9.86	9.52
Na_2O	0.085	0.054	0.044	0.025	0.139
K_2O	0.005	n.d.	n.d.	n.d.	0.005
P_2O_5	49.11	49.32	49.26	49.21	49.11
H_2O-	0.06	0.10	0.08	0.04	0.07
H_2O+	3.37	3.39	3.30	4.09	5.25
F	6.43	5.56	4.51	3.65	1.40
	102.775	103.099	102.448	101.687	100.682
$-0=2F$	−2.70	−2.341	−1.898	−1.536	−0.59
	100.075	100.758	100.55	100.151	100.092

* not determined

A-13 white, Tanco pegmatite

A-1 pink, Tanco zone (4)

A-5 yellow, Tanco pegmatite

A-2 yellow, Tanco zone (4); outer rim on sample A-1

A-22 brownish secondary, Tanco zone (4)

TABLE 65. NATIVE ELEMENTS, ALLOYS, SULPHIDES AND SULPHOSALTS IN THE TANCO PEGMATITE

LEAD	Pb
COPPER	Cu
BISMUTH	Bi
ARSENIC	As
ANTIMONY	(Sb>> Bi)
STIBARSEN	SbAs
DYSCRASITE	Ag_3Sb
GALENA	PbS
SPHALERITE	(Zn,Cd)S
HAWLEYITE	(Cd,Zn)S
PYRRHOTITE	$Fe_{1-x}S$
PYRITE	FeS_2
MARCASITE	FeS_2
ARSENOPYRITE	FeAsS
MOLYBDENITE	MoS_2
CUBANITE	$CuFe_2S_3$
CHALCOPYRITE	$CuFeS_2$
COSALITE	$PbBiS_2$
GLADITE	$CuPbBi_5S_9$
PEKOITE	$CuPbBi_{11}S_{18}$
GUSTAVITE	$Pb_3Ag_3Bi_{11}S_{24}$
TETRAHEDRITE	$(Cu,Fe,Ag)_{12}Sb_2S_{13}$
FREIBERGITE	$(Ag,Cu,Fe)_{12}Sb_2S_{13}$
BOURNONITE	$PbCuSbS_3$
PYRARGYRITE	Ag_3SbS_3
MIARGYRITE	$AgSbS_2$
STANNITE	Cu_2FeSnS_4
KESTERITE	Cu_2ZnSnS_4
ČERNÝITE	Cu_2CdSnS_4

STRUCTURAL GEOLOGY AND METAMORPHISM

The Cat Lake-Winnipeg River pegmatite field area, as previously mentioned, displays a three-fold subdivision into the Manigotagan-Ear Falls Gneiss Belt, the Bird River Greenstone Belt, and the Winnipeg River Batholithic Belt (Fig. 3). These three units are separated by common fault boundaries, lithologic and metamorphic changes and are dealt with herein as separate structural entities for purposes of description.

STRUCTURAL GEOLOGY OF THE BIRD RIVER GREENSTONE BELT

The six formations and synvolcanic intrusive rocks which form the Bird River Greenstone Belt are disposed in east-trending, nearly vertically dipping attitudes on the flanks and in the core of a synclinorium, the outer limits of which are marked to the north by the Maskwa Lake batholith and to the south by the Lac du Bonnet batholith. All of the rocks within this synclinorium can be grouped into five structural subareas, the boundaries and nomenclature of which are shown in Figure 110. From this figure it is evident that the designated subarea 1 corresponds to the Eaglenest Lake Formation, subarea 2 corresponds to the Lamprey Falls Formation, subarea 3 comprises segments of the Peterson Creek, Bernic Lake, and

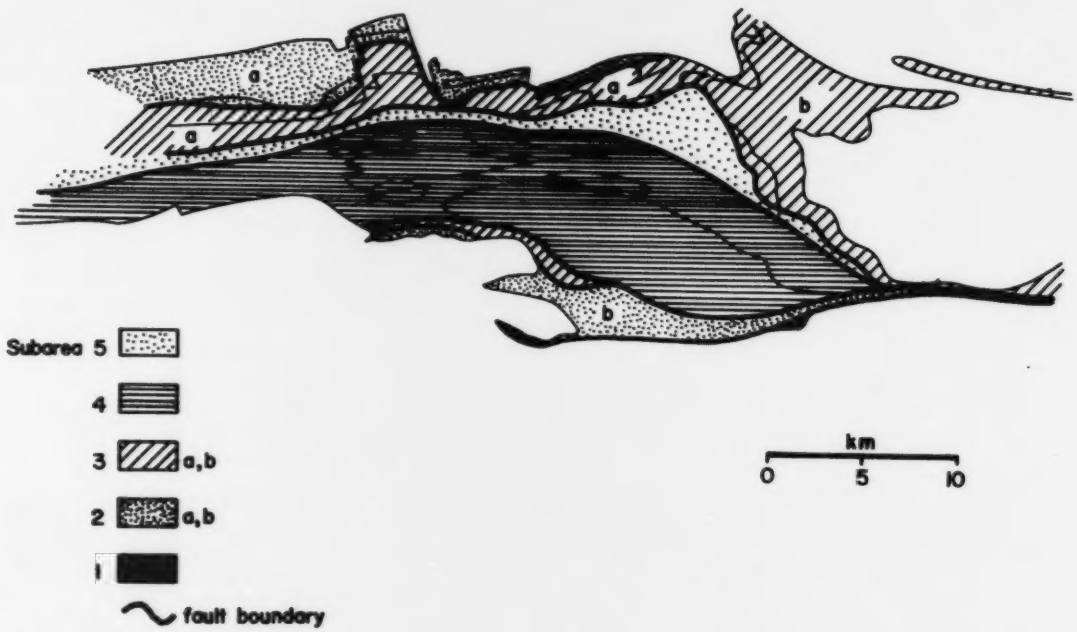

Figure 110: Subdivision of the Bird River Greenstone Belt into structural subareas

Flanders Lake Formations, subarea 4 contains the major part of the Bernic Lake Formation, and subarea 5 comprises the Booster Lake Formation. These subareas have differing structural styles developed during deformation and metamorphism and hence are described separately below. The boundaries of the subareas are faulted, and these faults are described separately below. Detailed structural documentation is presented in Map 3 and accompanying sections.

Subarea 1

Bedding (S_0) is evident in most of the metasedimentary rocks of subarea 1, and includes such features as rip-up structures which according to D.A. Janes (pers. Comm.) in one location define north-facing tops.

Two schistosites are present in the rocks of subarea 1. Of these, the first or oldest (S_1) is everywhere parallel to bedding (S_0). Both of these (S_0 and S_1) are plotted as poles, and contoured in Figure 111. The second, or younger schistosity (S_2) is of a discrete, widely spaced occurrence, and is only recognizable in hinge area of F_2 minor folds where it is parallel to the F_2 axial planes.

Minor folds are present in serveral outcrops of subarea 1. The folds are of type III (Ramsay 1962) interference pattern formed through passive (F_2) refolding on S_2 surfaces of earlier F_1 folds. In Figure 111 axes of minor folds are plotted, and compare favourably with the pole to the girdle defined by the contoured S_0 and S_1 data.

S and Z asymmetries are evident in the minor fold of subarea 1, and serve to locate the axial trace. The orientation of the larger fold so defined, can be approximated from the minor F_2 fold data and from Figure 111, and the fold can be described as a west-plunging (75°) isoclinal synform.

Subarea 2

Structural subarea 2 corresponds to the Lamprey Falls Formation. It is, for purpose of description, subdivided into segments A and B as shown in Figure 110, segment A being the south-facing sequence of rocks north of Bird River, and segment B being the north-facing sequence disposed along Winnipeg River.

Bedding or layering (S_0) in subarea 2 is manifest by continuity of particular lava flows, tuffaceous intercalations, gravity stratification in the Bird River Sill, and by bedding in iron formation. Facing directions in these are indicated by pillow structures in lavas, and in the sequence of differentiation products in the Bird River Sill.

In general, bedding and layering in subarea 2 strike east and dip nearly vertically, or slightly to the south of vertical. These attitudes are shown in Figure 112, from which it is evident that the tendency to south inclination is common to both subarea 2A and 2B.

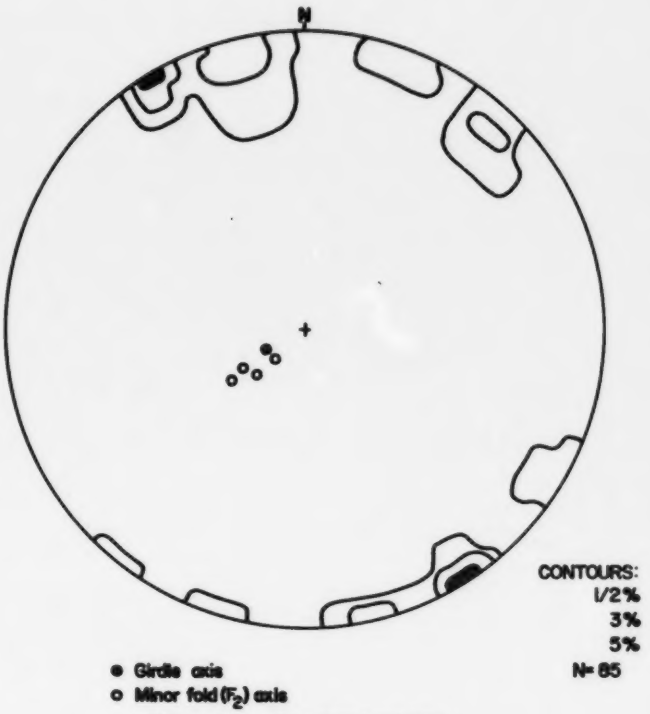

Figure 111: Structural subarea 1

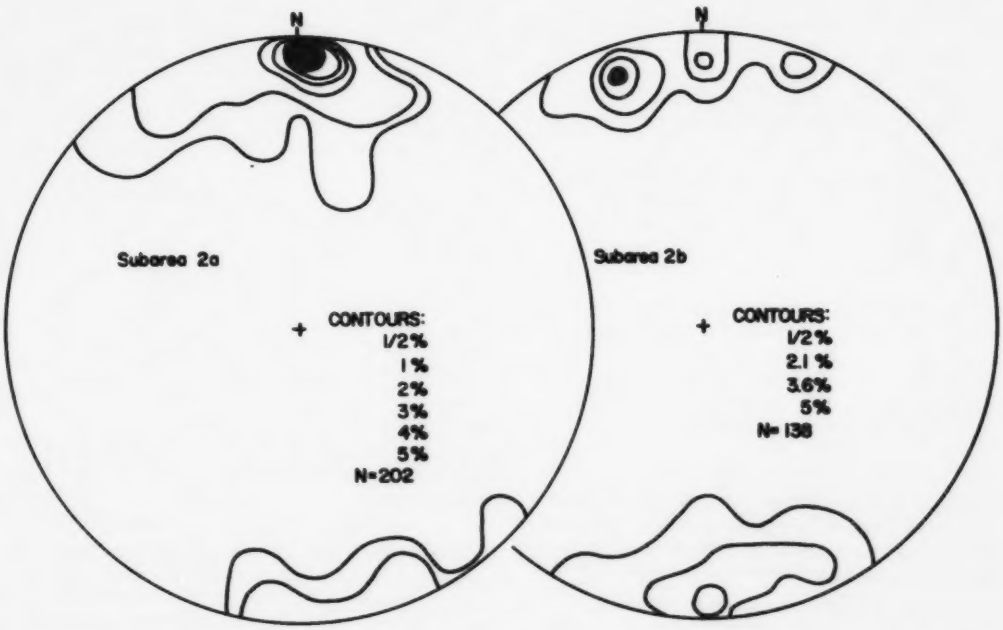

Figure 112: Layering in structural subarea 2

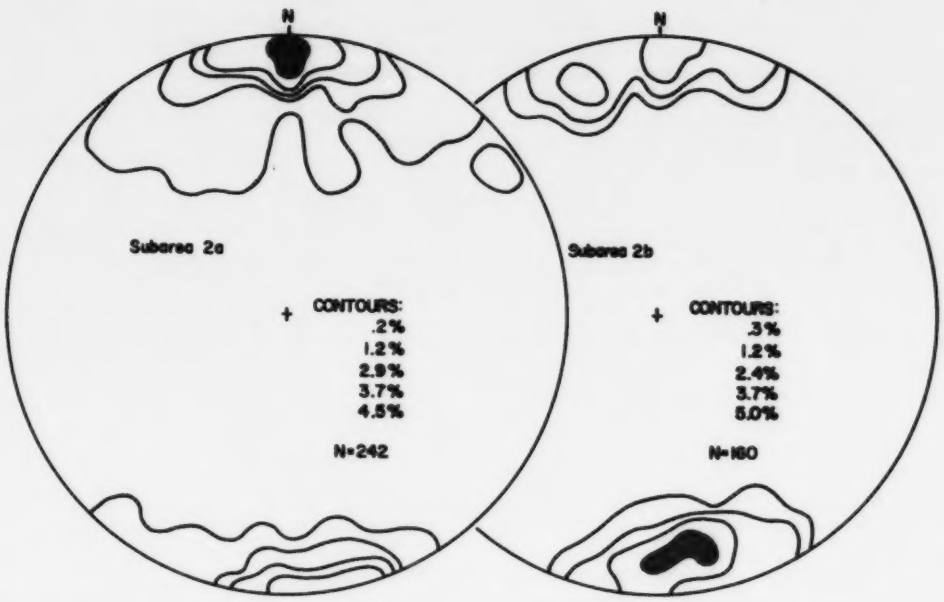

Figure 113: Foliation in structural subarea 2

A single penetrative schistosity is evident in most of the rocks of subarea 2 and in general is very weakly developed. No indications of an older foliation were observed. The schistosity in evidence, however, corresponds in attitude to that identified as S_2 in adjacent areas and for this reason is interpreted as S_2 in these rocks.

Foliation (S_2) data for segments 2A and B are presented in Figure 113 from which it is evident that foliations trend east in strike. Dips in the two areas are slightly convergent; the foliation in segment 2A dips slighly south of vertical, and the foliation in segments 2B dips slightly north of vertical.

Minor fold structures are absent in segments 2A and 2B. The existence of a major synclinal fold structure in the Lamprey Falls Formation can be interpreted on the basis of facing directions in segments 2A and 2B (Map 3). In addition, the existence of a syncline is also supported by a lithostratigraphic correlation of segments 2A and 2B which is shown in Table 66.

Subarea 3

Structural subarea 3 incorporates the Peterson Creek Formation, the Flanders Lake Formation, and the northern segment of the Bernic Lake Formation. This subarea is further subdivided for descriptive purposes as shown in Figure 110.

Bedding (S_0) is evident in most of the rocks of subarea 3, and includes primary sedimentary structures diagnostic of facing directions. They have been described above in the respective formation descriptions.

Two schistosities are evident in subarea 3. The first of these,

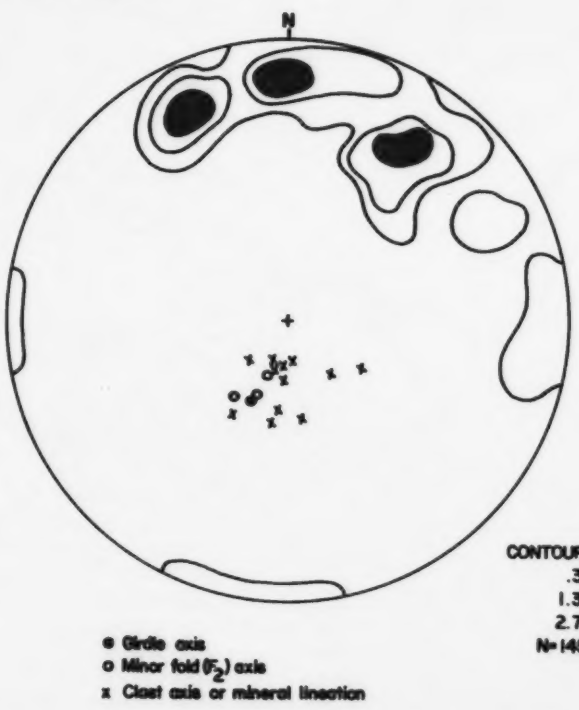

Figure 114: Poles to bedding S_0 and foliation S_1 in subarea 3a

TABLE 66. LITHOSTRATIGRAPHIC CORRELATION OF SUBAREA 2A AND 2B

LAMPREY FALLS FORMATION	
STRUCTURAL SUBAREA 2A	STRUCTURAL SUBAREA 2B
metagabbro	metagabbro
Bird River Sill	
hyaloclastite	aquagene breccia, hyaloclastite
megacrystic metabasalt	
pillow metabasalt tuff hypabyssal metagabbro	pillow metabasalt tuff hypabyssal metagabbro
iron formation	iron formation
pillow metabasalt tuff hypabyssal metagabbro	pillow metabasalt tuff hypabyssal metagabbro
	iron formation
	pillow metabasalt tuff hypabyssal metagabbro

or oldest (S_1) is moderately well developed and is parallel in attitude to the strike and dip of the layering (S_0). For segment 3A poles to S_0 and S_1 are plotted in stereographic projection in Figure 114. For segment 3B, poles to S_0 and S_1 are plotted in Figure 115.

The second, or younger schistosity (S_2) is developed axial planar to the fold structures of subarea 3.

Major cross-fold structures developed by D_2 in segment 3A are displayed by the outcrop distribution of rock types in the area south of Bird Lake. These interference structures, formed by the superposition of F_2 folds on F_1 folds have also resulted in the superposition of an axial planar S_2 fabric on S_0 and S_1. The F_2 fold axes pitch steeply to the south on east-striking south-dipping axial planes, and find a general correlation with mineral elongation, clast elongation, and minor fold axis linear data.

Major cross-folds in segment 3B are shown by the outcrop distribution of metaconglomerate in the Flanders Lake Formation. These folds are shown in Figure 116A in comparison with ideal Type III interference patterns (Fig. 116B), and are seen to display the diagnostic open forms with converging and diverging V-shapes (Ramsay 1962).

The F_2 fold axes in segment 3B are continuous with those of segment 3A, and hence are products of the same D_2 deformational event. The axes of the folds are southwest plunging, oriented on northwest-trending southeast dipping F_2 axial planes (Fig. 115).

Subarea 4

Structural subarea 4 corresponds to the major fault-bound segment of the Bernic Lake Formation, the disposition of which is shown in Figure 110.

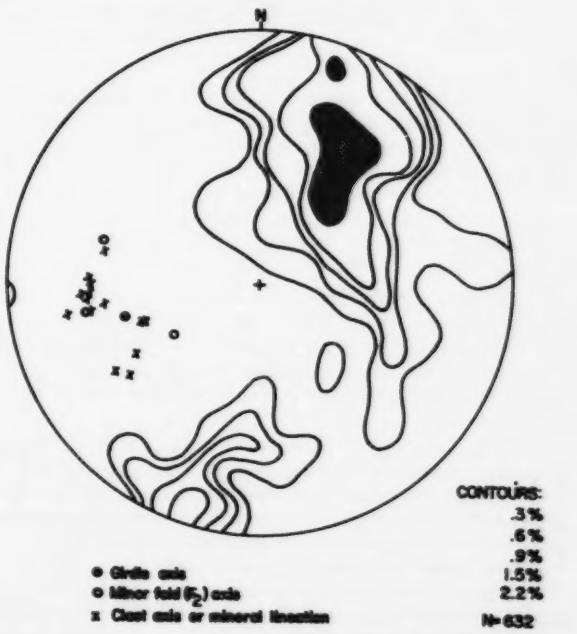

Figure 115: Poles to bedding S_0 and foliation S_1 in the subarea 3B

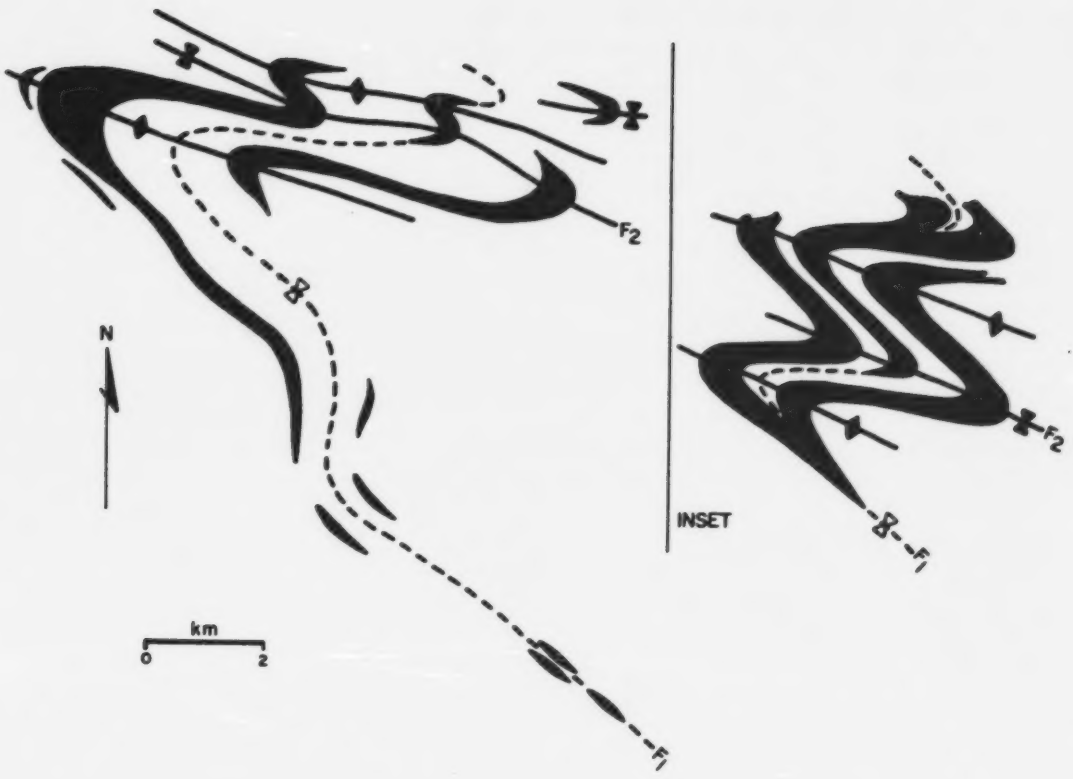

Figure 116: Outcrops of metaconglomerate in the Flanders Lake Formation (a) compared to ideal type III interference fold pattern (b)

Layering (S_0) in subarea 4 is generally poorly defined, and most of the rocks are characterized by thick, chaotic, intercalated beds. Bedding is, however, locally well preserved in zones disposed at the termini of the ellipsoidal synvolcanic intrusive stocks which perforate the subarea. In such areas bedding is oblique to the foliation, and converges inwards parallel to the boundaries of the intrusions. Poles to bedding (S_0) are presented in Figure 117.

Two foliations (schistosities) are evident in the rocks of subarea 4. These are interpreted as S_1 and S_2 respectively.

The S_1 schistosity is rarely evident, and was observed only in the termini of the intrusive bodies. In such cases this fabric is parallel to bedding structures, and locally forms open flexures where cut by S_2.

The S_2 schistosity is pervasive in subarea 4, but is disposed more as a discrete cleavage in termini of the intrusive bodies. For the most part, the fabric trends east and dips at relatively steep angles both north and south, in areas in proximity to the flanks of intrusive bodies. Poles to the S_2 schistosity are shown in Figure 118. Also shown are mineral lineation data.

Folding is not clearly in evidence in subarea 4, and only locally are minor folds noted. Examination of the data of Figures 117 and 118, however, supports a concept of folding in these rocks, and to this end it is possible to inscribe a girdle to the pole data of Figure 117.

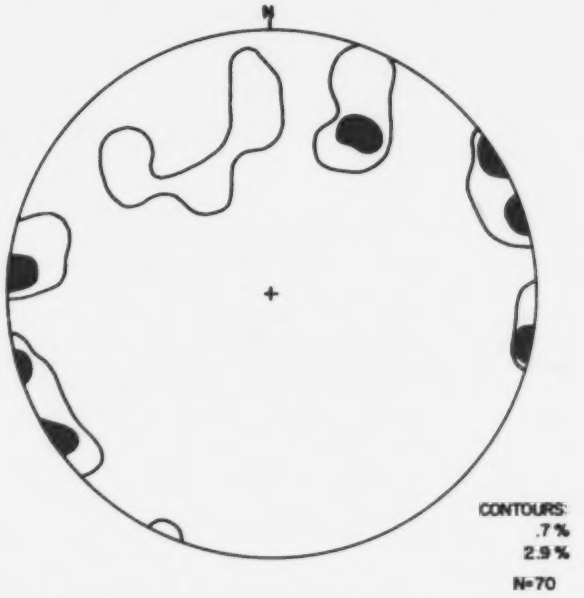

Figure 117: Poles to bedding S_0 and foliation S_1 in structural subarea 4

Subarea 5

Structural subarea 5 corresponds to the major fault segment of the Booster Lake Formation (Fig. 110).

Bedding (S_0) in subarea 5 has been extensively described in a preceding section. Features diagnostic of top directions abound, and it is evident that much of subarea 5 forms an east-trending, south-facing, steeply dipping monoclinal sequence (see Maps 1 and 3).

A strong penetrative tectonic foliation (S_2) is present in all of the rocks of subarea 5. This fabric for the most part is parallel to bedding, but on small scale is seen to refract between the less ductile greywacke and more ductile mudstone components.

Major and minor folds are evident throughout subarea 5. Minor folds display S and Z asymmetry in the west and east areas respectively (Maps 1 and 3), and display varied degrees of closure becoming more tightly closed in the axial area of the major fold south of Bird Lake.

Poles to bedding (S_0) and schistosity (S_2) are presented in Figure 119. Analysis indicates that the folding is conical, the cone axis plunging moderately steeply in a north-northwest direction.

Faulting

The previously described structural subareas are fault-juxtaposed (Maps 1 and 3). In additon, the northern part of subarea 2 (Lamprey Falls Formation) is extensively fault-segmented and , in part, these latter faults are seen to interact with the subarea 2-3 boundary. All of these features are described below, the former as F_3, the latter as F_4 events.

The ***subarea 1-2 boundary fault*** in the Eaglenest Lake area is an extension of the fault which separates subarea 2 from rocks of the Winnipeg River Batholithic Belt in the Greer Lake area. This fault crops out on small island in Eaglenest Lake, and in this locale is marked by a narrow (<2 metre) zone of mylonite which strikes 085 degrees and dips south at approximately 80 degrees. The mylonite appears to be developed at the expense of the poly-deformed Eaglenest Formation rocks. Deformation in Lamprey Falls Formation rocks is negligible.

At Greer Lake this fault is marked by intense deformation, and the affected gneisses south of the fault vary between cataclasite and protomylonite. Attitudes in the zone of shearing at Greer Lake strike 075 degrees and dip vertically. Drag folds with Z asymmetry plunge southwesterly, and slickensides plunge approximately 80 degrees with an azimuth of 225 degrees. These data, in conjunction with cusp development in the slickenside surface, indicate a movement of the south side (Winnipeg River Batholithic Belt) upwards and to the east.

The ***subarea 2-3 boundary*** fault separates rocks of the Lamprey Falls, Peterson Creek-Bernic Lake Formation in the northern map area (Maps 1 and 3). In the southern map area this boundary transgresses the Lamprey Falls-Peterson Creek Formations at Shatford Lake, and becomes the boundary between the intrusive stock centered at Birse Lake and the Lamprey Falls Formation along Winnipeg River. In the northern map area the subarea 2-3 boundary is marked by mylonite, in part, and elsewhere by a gouge of chlorite schist. Along the Winnipeg River, deformation is less extreme and the affected rocks exhibit protoclastic to good cataclastic textures. In both cases the deformed rocks are largely confined to relatively narrow (<8 metre) zones.

Various structural data bearing on the subarea 2-3 boundary are shown in Trueman (1980).

The ***subarea 3-4 boundary*** corresponds to the unconformity

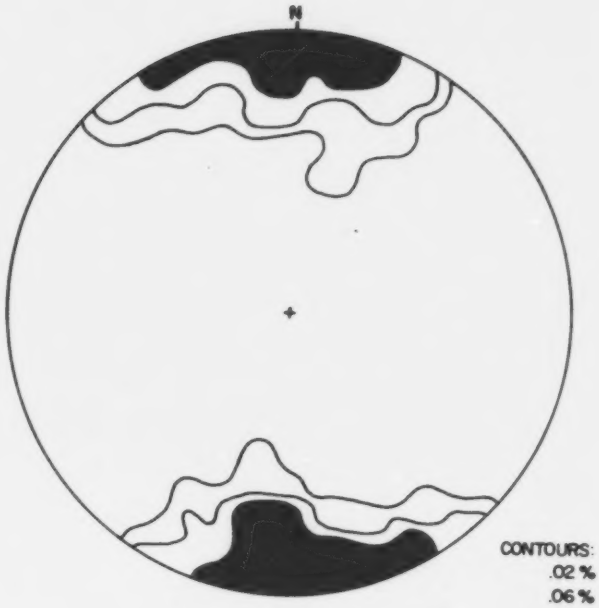

Figure 118: Poles to schistosity S_2 in the structural subarea 4

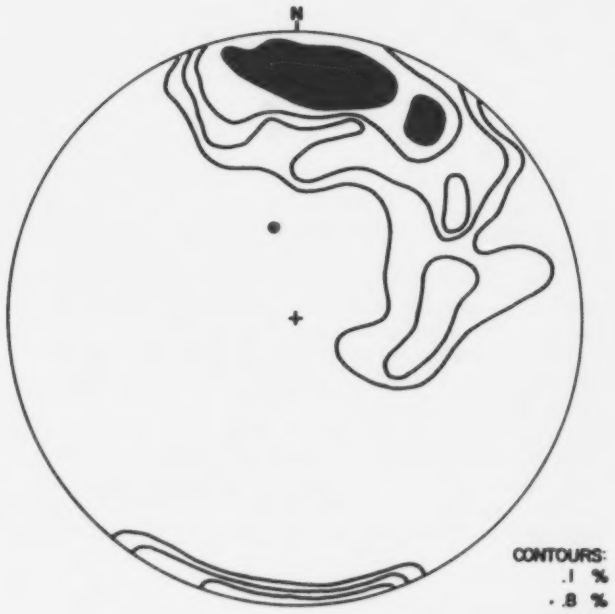

Figure 119: Poles to bedding S_0 and schistosity S_2 in structural subarea 5

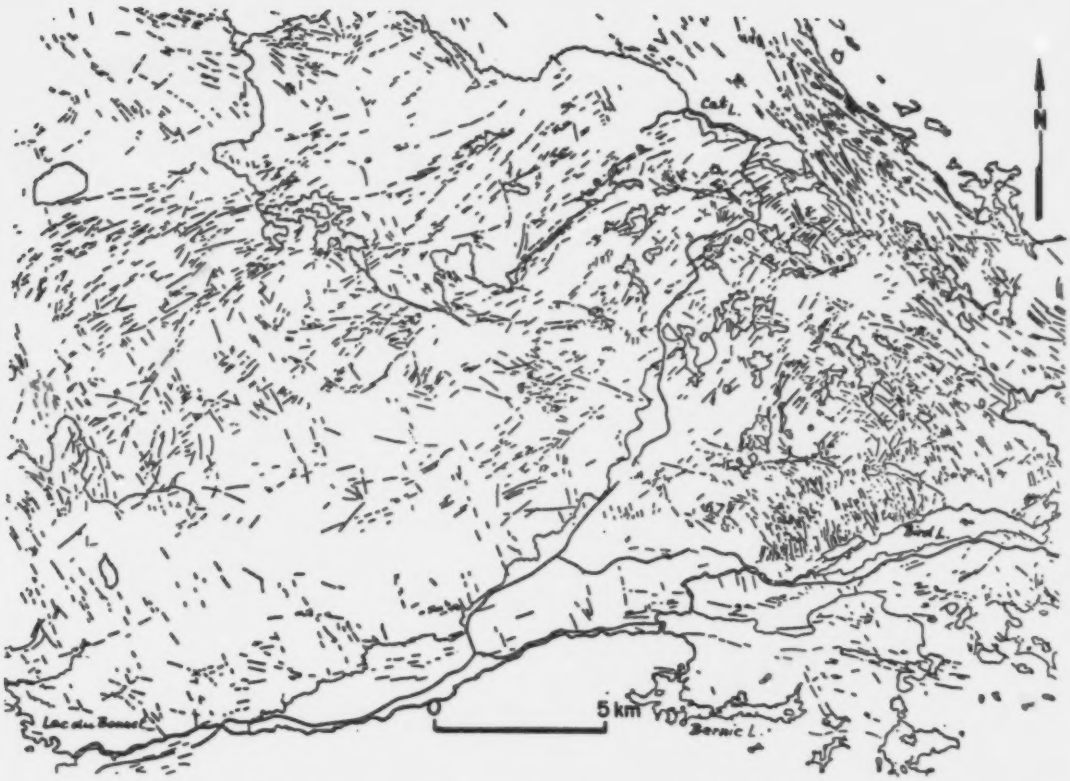

Figure 120: Air photo lineaments and faults in the major part of the Cat Lake-Winnipeg River pegmatite field

which exists between the greywacke-mudstone turbidetes (Booster Lake Formation) and the older metavolcanic and related rocks (Map 1).

In the field there exists little evidence of displacement along the subarea 3-4 boundary. Rather, where this contact is exposed there is minor cataclasis, and prograde regional metamorphic assemblages (e.g. cordierite) are seen to be retrogressed with growth of idioblastic chlorite across foliation surfaces.

The truncation of F_2 fold axes at the Booster Lake Formation boundary also indicates faulting on this boundary. This is in contrast to the expected manifestation of folding of the Booster Lake sequence if this formation had occupied its present position during the F_2 event.

Other evidence of the fault movement on the subarea 3-4 boundary is the occurrence of tectonic intercalation of turbidite material in the Booster Lake-Ryerson Lake areas (Map 1). These intercalations, badly deformed or sheared, maintain a south-facing attitude which could not be expected if their position was the result of folding.

Drag folds, close to the north boundary at Louie Lakes, indicate a horizontal component of left lateral movement along the boundary. Plunges are unknown.

Much of the *subarea 3-5 boundary* which occurs at Shatford Lake is covered by the lake, and elsewhere along the north shore of Shatford Lake is covered by swamp and drift-filled lineaments. One outcrop, close to the powerline east of Shatford Lake (Map 1), is intensely sheared and occupied by a melange of sericite schist (metarhyolite) of the Peterson Creek Formation, tectonic intercalations of polymict metaconglomerate of the Bernic Lake Formation and a cataclasite formed of the composite stock centered on Birse Lake. Strike and dip orientations measured in this area vary from 84 to 106 degrees and 70 to 81 degrees north respectively. 'S' drag folds suggest some left lateral component of movement.

The *subarea 4-5 boundary* is a zone occupied by several faults which anastomose about tectonic intercalations of both the Booster and Bernic Lake Formations (Map 1 and 3).

The major parts of these faults in the 4-5 boundary zone are shown in Trueman (1980) with data bearing on orientations and sense of movement. Accordingly it is evident that two major faults are convergent upwards at angles of 5 to 15 degrees. Dips on these faults are varied, from nearly vertical to 56 degrees south. The smaller faults which mantle the greywacke-mudstone turbidite intercalations converge both up and down dip, as well as along strike.

The sense of movement along the above faults is not clear. Lineations (slickensides) in general pitch steeply in the shear plane. Observed drag folds are of 'S' asymmetry indicating left-lateral movement. In addition, as the older Bernic Lake Formation rocks are juxtaposed above the younger Booster Lake rocks, it is suggested that the fault movement was of reverse nature with the hanging wall (south side) moving upward and easterly.

Faults in the Lamprey Falls Formation, north of Bird River trend northwesterly into the Maskwa Lake batholith. These faults, and corresponding air-photo lineaments are shown in Figure 120. The behavioral patterns (apical-perianticlinal) on these faults have been described by Trueman (1971,1980).

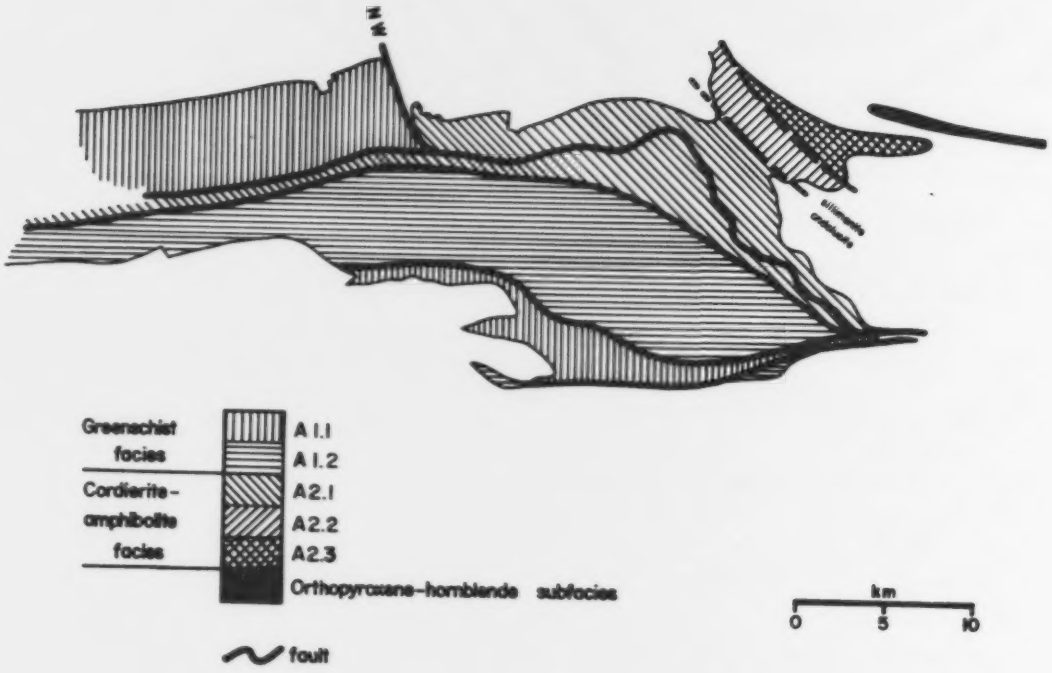

Figure 121: Subdivision of the Bird River Greenstone Belt into metamorphic facies segments

In addition to the above faults a northwesterly-trend fault is apparent 8 km east of Poplar Bay, Lac du Bonnet (Map 1). Although this fault is not evident in outcrop, its presence is indicated by an airphoto lineament. To the east and to the west of this lineament, lithologic units are truncated in the Bernic Lake Formation, and a corresponding change in facing directions of rocks is also noted. There is no evidence that this fault transects the Booster Lake Formation; however, as the fault offset affects the Lac du Bonnet batholith, it must be younger than the batholith.

METAMORPHISM OF THE BIRD RIVER GREENSTONE BELT

The metamorphic history of the Bird River area is complex, and the textures of metamorphic minerals in the schists in all areas of the belt are found aligned in relation to the structures of the two major deformational events, D_1 and D_2. These minerals, and assemblages, are termed M_1 and M_2. In addition, minerals of hydrothermal replacement origin are concentrated near F_3 and F_4 faults. Texturally, these are post-tectonic, replace M_2 minerals, and are interpreted as having formed during the F_3 and F_4 faulting and are called M_3 and M_4 assemblages.

M_1, M_2 assemblages

Little remains of the M_1 metamorphic assemblages in the area; those that are recongnized consist of deformed garnet and biotite which are preserved, and form the relict S_1 schistosity, in crests of F_2 folds.

The assemblages which formed in the pelitic rocks of the Bird River area during the M_2 metamorphic event contain cordierite and/or andalusite which are indicative of a low pressure-high teperature style of metamorphism such as that of the Abukuma Plateau in Japan (Winkler 1967). The M_2 assemblages are therefore examined using the facies concepts, and designations (A1.1,A1.2, A2.1...) of Winkler (1967), and their dispositions are shown in Figure 12

A1.1 quartz-albite-muscovite-biotite-chlorite subfacies

A1.1 subfacies of rocks includes parts of the Lamprey Falls, the Bird River Sill, Peterson Creek, and Bernic Lake Formations (Figs. 110, 121). For those rocks lying north of Bird River, the A1.1 subfacies is bounded on the east side by the fault designated "NW" in Figure 121.

Assemblages of A1.1 subfacies are as follows:

Lamprey Falls Formation metabasalt:

actinolite + epidote + albite ± chlorite ± quartz ±biotite

Bird River Sill ultramafic rocks:

tremolite ± serpentine ± chlorite ± talc ± magnetite ± chlorite

Gabbroic rocks intrusive into the Lamprey Falls Formation:

tremolite + epidote + albite ± chlorite ± biotite

Peterson Creek Formation felsic rocks:

quartz + albite + epidote + sericite ± chlorite ± biotite

Bernic Lake Formation metaconglomerate:

actinolite + epidote + albite ± chlorite ± biotite ± quartz

A1.2 quartz-andalusite-plagioclase-chlorite subfacies

The A1.2 subfacies of rocks is confined to the fault-bounded segment of the Bernic Lake Formation which forms structural subarea 4 (Fig. 110), and the Eaglenest Lake Formation (Figs. 3, 121). Rocks of the A1.2 subfacies carry both actinolite-tremolite and hornblende, the coexistence of which is indicative of this particular subfacies (Winkler 1967).

Assemblages of the A1.2 subfacies are as follows:

Bernic Lake Formation mafic to intermediate metavolcanic rocks:

actinolite + hornblende + epidote + plagioclase ± chlorite ± quartz ± biotite

Bernic Lake Formation felsic rocks:

quartz + chlorite ± biotite ± plagioclase ± sericite ± actinolite

Bernic Lake and Eaglenest Lake Formation metasedimentary rocks:

quartz + chlorite + biotite ± actinolite ± hornblende ± plagioclase ± epidote

From the Bernic Lake area eastward, most of the clastic rocks are characterized by the occurrence of nodular and vermiform calc-silicate concretions of hornblende, plagioclase, and epidote.

A2.1 andalusite-cordierite-muscovite subfacies

The A2.1 subfacies is found in the Booster Lake, Flanders Lake, Bernic Lake, Peterson Creek, and Lamprey Falls Formations, and the Bird River Sill, as far to the northeast as the andalusite-sillimanite isograd (Fig. 121). The andalusite-sillimanite isograd is located in Figure 121 on only one occurrence of andalusite, and one of sillimanite. The extension (dashed projections) is speculative, except for the observation that metamorphic recrystallization and grain size is increased concomitant with obliteration of primary textures on the sillimanite side.

Assemblages of the A2.1 subfacies are as follows:

Lamprey Falls Formation:

hornblende + plagioclase ± garnet

Bird River Sill ultramafic rocks:

olivine ± diopside ± cummingtonite ± plagioclase

(Rocks of the Bird River Sill containing the above assemblages are severely retrogressed, and the M_2 age assigned to these is uncertain. These assemblages have been interpreted by Juhas (1973) and Coats et al. (1979) as prograde metamorphic products, and they are herein assigned to the M_2 event on the basis of their equivalence to M_2, A2.1 assemblages in rocks of the surrounding formations).

Peterson Creek Formation felsic rocks:

quartz + plagioclase + muscovite ± biotite

Bernic Lake Formation pelitic metasediments:

cordierite + garnet + biotite ± hornblende ± plagioclase ± quartz ± anthophyllite ± diopside ± andalusite

In addition, rocks of the Bernic Lake Formation in the A2.1 subfacies are marked by the occurrence of nodular and vermiform calc-silicate concretions of hornblende and plagioclase.

Flanders Lake Formation pelitic metasediments:

quartz + plagioclase + biotite ± hornblende ± andalusite

Booster Lake Formation pelitic metasediments:

quartz + biotite + cordierite ± plagioclase ± garnet

In addition, in the eastern one-half ot the formation nodular calc-silicate concretions of hornblende and plagioclase become abundant.

A2.2 sillimanite-cordierite-muscovite-almandine subfacies

The A2.2 subfacies is shown in Figure 121, bound to the southwest by the sillimanite-andalusite isograd and to the northeast by the A2.3 boundary. Rocks of the A2.2 subfacies include the Flanders Lake Formation, Peterson Creek Formation, and mafic to intermediate rocks of the Bernic Lake Formation.

Assemblages of the A2.2 subfacies are as follows:

Peterson Creek Formation of felsic rocks:

quartz + plagioclase + muscovite + biotite

Bernic Lake Formation:

hornblende + plagioclase + garnet ± biotite

Flanders Lake Formation meta-arenites:

quartz + plagioclase + hornblende ± sillimanite ± muscovite ± biotite ± garnet

A2.3 sillimanite-cordierite-orthoclase-almandine subfacies

The A2.3 subfacies boundary is located in Figure 121 on the basis of the appearance of lit of granitic composition intercalated in the meta-arenites of the Flanders Lake Formation, the disappearance of muscovite, and the appearance of K-feldspar.

Assemblages of the A2.3 subfacies are as follows:

Flanders Lake Formation meta-arenites:

quartz + plagioclase ± hornblende ± biotite ± K-feldspar

Orthopyroxene-hornblende subfacies

Orthopyroxene-bearing rocks are found in the northeastern portion of the study area in an elongate synform of metasedimentary rocks correlative with the Flanders Lake Formation (Trueman et al. 1975); these rocks are considered a part of the Manigotagan Gneiss Belt of McRitchie (1971).

Examination of samples from this particular area revealed the existence of relict orthopyroxene. The noted assemblages include:

quartz + plagioclase + K-feldspar ± orthopyroxene ± diopside ± hornblende ± biotite

M_3, M_4 assemblages

M_3 and M_4 metamorphic assemblages are retrograde, and consist of chlorite, albite, epidote, and actinolite-bearing rocks in proximity to the east-west boundary faults, and the northwesterly striking F_4 faults. In addition, serpentine- talc-carbonate alteration is present in the F_4 faults where these faults transect ultramafic rocks of the Bird River Sill, and these may be in part responsible for wholesale retrogression in that part of the Bird River Sill located in the A2.1 subfacies (Juhas 1973, Coats et al. 1979).

STRUCTURAL GEOLOGY OF THE MANIGOTAGAN-EAR FALLS GNEISS BELT

Within the study area the structural geology of the Manigotagan Gneiss Belt has been extensively described by McRitchie (1971), and correlated with the deformation evident in the Bird River Greenstone Belt by Trueman et al. (1976). This correlation, based largely on sedimentation of the Flanders Lake Formation and Edmunds Lake Formation at Bissett is shown in Table 67, and involves the D_1 and D_2 faulting events documented at Bird River.

TABLE 67. CORRELATION OF THE MAJOR STRUCTURAL EVENTS AND SEDIMENTATION IN THE RICE LAKE-MANIGOTAGAN GNEISS BELT-BIRD LAKE AREAS

EVENT	BIRD LAKE AREA	MANIGOTAGAN GNEISS BELT	RICE LAKE AREA
D_3	local, generative, flexural folding	local	
D_2	regional passive asymmetric S and Z folds, on reclined south dipping axial planes	regional asymmetric Z folds	regional passive asymmetric Z folds on reclined north dipping axial planes
SEDIMENTATION	greywacke/mudstone	?	San Antonio Formation
D_1	major isoclinal flexural folds with axial traces parallel to gneiss belt boundaries, minor folds local and rare	flexural folds	major isoclinal flexural folds with axial traces parralel to gneiss belt boundaries, minor folds locally developed
SEDIMENTATION	greywacke/conglomerate	greywacke (paragneiss)	Edmunds Lake Formation
?	uplift		uplift
	DEPOSITION RICE LAKE GROUP		DEPOSITION RICE LAKE GROUP

The early metamorphic event recognized in the Manigotagan Gneiss Belt is described by McRitchie (1971) as being displayed by "narrow isoclinally folded belts of granodioritized sediment alternating with thin zones of migmatite and pegmatite", most evident southwest of Manigotagan Lake. "The folds plunge shallowly to the west-northwest and east-southeast on steep southwest-dipping or vertical axial planes, and are characterized by a biotite foliation parallel to the layering in the rocks".

The D_2 structural event in the Manigotagan Gneiss Belt was characterized by development of axial planar schistosity striking easterly and dipping vertically, and where superposed on D_1 folds shows development of the Type III interference patterns typifying the D_2 event at Bird River.

The fourth, fifth, and sixth deformational events in the Manigotagan Gneiss Belt involved faulting along easterly trending steeply dipping zones of brecciation and mylonitization. Such faulting tentatively correlated with the episodic faulting within the Bird River Greenstone Belt, yielded local retrogression of metamorphic assemblages, and served to "telescope" the principal metamorphic zones defined in the gneissis and adjacent Rice Lake Greenstone Belt.

METAMORPHISM OF THE MANIGOTAGAN-EAR FALLS GNEISS BELT

McRitchie (1971) defined 7 metamorphic zones extending southward from the Rice Lake area, and attaining the highest metamorphic rank with assemblages forming a sillimanite-cordierite-almandine-orthoclase zone, the north boundary of which lies in the Manigotagan Gneiss Belt north of Black Lake (Map 1).

The development of these assemblages is attributed by McRitchie (1971) to the M_1 metamorphic event in that area and accompanied the D_1 deformational event.

Further to the south, at Euclid Lake, Tulabee Lake and Starr Lake (Butrenchuk 1970, Posehn 1977, Trueman 1980), the grades of metamorphism are reversed; these locales are the southernmost known occurrences of sillimanite and coincide approximately with the arbitrary boundary of the Gneiss Belt (Map 1).

STRUCTURAL GEOLOGY OF THE WINNIPEG RIVER BATHOLITHIC BELT

Within the study area, the chronology of metamorphism and deformation is not clear in the Winnipeg River Batholithic Belt; suffice it to say that the belt lies in fault contact with the Bird River Greenstone Belt.

Most of the rocks of the Winnipeg River Batholithic Belt, within the study area, are characterized by a weak to strongly developed gneissosity which strikes east-northeasterly, and dips nearly vertically. In certain locales, as at Lamprey Falls, this fabric exhibits northwesterly strikes of a regional nature, but does not preclude the possibile occurrence of folding which is otherwise not in evidence.

Within the study area, the only observed fault is that which separates the Winnipeg River Batholithic Belt from the Bird River greenstones to the north.

This fault (described in part above, p. 133) trends mainly parallel to the greenstone belt boundary, as does the foliation within the greenstones, and transects strikes of the gneissic fabric of rocks of the batholithic belt at angles of 10-20 degrees. Dips measured on the fault are nearly vertical, slickensides plunge shallowly east and west, and both sinistral and dextral movements are noted. At Greer Lake, it is also noted that divergent or horsetail faulting presumably connected with the boundary fault, transects pegmatitic granite north and northwest of Greer Lake.

The boundary fault, by its general parallelism to those faults separating structural entities in the greenstone belt, is tentatively correlated with those other features, and it is further suggested as having developed simultaneously with those faults transecting the Manigotagan Gneiss Belt.

Further south, faults and profound air-photo lineaments transect the batholithic belt but in general are parallel to the gneissic foliation of the belt, and not to its north boundary.

METAMORPHISM OF THE WINNIPEG RIVER BATHOLITHIC BELT

The grade of metamorphism of gneissic rocks of the Winnipeg River Batholithic Belt is uncertain, as the noted assemblages of quartz, feldspar, biotite, and hornblende are all stable into the upper amphibolite facies grade. Diagnostic minerals are not in evidence.

GENETIC RELATIONSHIPS

INTRODUCTION

This section reviews the genetic significance of the field observations and laboratory data presented in the preceding chapters, to establish principal constraints on the relationships among the different plutonic bodies, pegmatitic granites, and pegmatite groups.

The interpretation of the pegmatite genesis and distribution presented below is based on the classic theory of igneous differentiation and postmagmatic fractionation. The available evidence supports this concept and no indicatons of other processes (listed by, e.g., Jahns 1955) have been found:

(a) The lack of phenomena suggestive of in situ "sweating-out". The temporal gap between prograde metamorphism and pegmatite injection (that are separated by a period of large-scale faulting), and the generally low metamorphic grade in the western part of the Winnipeg River district (insufficient to initiate local melting at the level of pegmatite emplacement) - all these disqualify generation of pegmatites by a short-range anatectic "lateral secretion" process.

(b) Direct anatectic derivation of highly fractionated pegmatites at greater depth and their ascent to the low-grade schist hosts is also unrealistic. Extremely small percentages of initial partial melts would be necessary to achieve adequate fractionation levels, and high concentration of Li and H_2O in these melts would be difficult to achieve (Holland and Lambert 1972, Fyfe 1973, Fyfe et al. 1978). Segregation of this low-percentage melt into large pegmatite bodies without equilibrating with country rocks is likewise difficult to imagine. For example, rough calculations indicate that the Cs content of the Tanco pegmatite would have to be totally extracted and concentrated from at least 25 km^3 of metasediments and metavolcanic rocks of the Bird River Greenstone Belt, and the source volume would have to be even greater if some Cs were to be left behind.

(c) An aqueous hypothesis which may overcome the fractionation and mobility problems of the preceding mechanism is hampered even more by the aforementioned reactivity with country rocks through which the vapors and/or solutions would pass. This is amply documented by the rare-alkali biotite and holmquistite which form rather narrow haloes around Li-rich pegmatites, and by the more remote occurrences of rare-alkali metasomatites (e.g., Gordiyenko et al. 1975) which are generated by fluids emanating from pegmatites (and their sources) rather than by fluids converging to form them. Also, Luth and Tuttle (1969) have shown that high-temperature fluids capable of precipitating feldspars can originate only in the presence of igneous melts.

Because of marked differences between the Winnipeg River and the Cat Lake-Maskwa Lake districts, in terms of rock type representation and observable relations, they are discussed in separate sections.

THE WINNIPEG RIVER DISTRICT

The pegmatites have been established as the last, late- to post-tectonic intrusive event in the area. Thus the possible parental granitoids should be sought among the latest intrusions recognized, or suspected hidden, in the district. The granitic components of the three major batholiths and the pegmatitic granites are the prime suspects.

The batholiths

All three batholiths - Maskwa Lake, Marijane Lake, and Lac du Bonnet - consist of two principal components. The older one is represented by hornblendic quartz diorites (to granodiorites), largely gneissic and diapiric. Massive biotite granites which crosscut the quartz diorites and/or mantle them compose the younger component.

The quartz diorites of the English River Gneissic Belt were interpreted as melts of lower crustal or upper mantle origin by Ermanovics et al. (1979). The preseht study confirms this interpretation.

The *quartz diorites* of the English River Gneissic Belt were from other parts of the English River and Quetico Gneissic Belts (e.g.. Breaks et al. 1978, Franklin 1978, Mason 1978, Beakhouse, in prep.) in terms of both field relationships and chemistry. Geological position and compositional characteristics are also closely comparable to the rather uniform properties of tonalites and trondhjemites reported from greenstone-granodiorite terranes in the Canadian and other Archean shields as early, pre-granitic (within their tectonomagmatic cycle), pegmatite-free formations of juvenile origin (Anhaeusser 1971, 1973, Condie and Hunter 1976, Glikson 1976, Wilson et al. 1978). Generally high Al_2O_3 (14.5 wt.%) and low Yb_N (<8) agree with Arth's (1979) definition of continental tonalites, as does the overall distribution of REE abundances. These differ among individual bodies but they all show the same near log-linear, HREE-depleted pattern, indicative of a residuum rich in hornblende or garnet; negative Eu anomalies shown by some samples suggest extensive plagioclase removal. Together with oxygen and Rb-Sr isotope data, all these characteristics suggest, compared to recent interpretation by Barker and Arth (1976), Arth(1976,1979) and Arth et al. (1978), an origin by partial melting of amphibolite in lower crust or upper mantle at a depth of less than 60 km, rather than fractional crystallization of gabbroic progenitors.

The *granitic components* of the Maskwa Lake and Marijane Lake batholiths and the late biotite granite of the Lac du Bonnet intrusion belong to a single family with common mineral composition, bulk chemistry, and trace element characteristics. A working hypothisis of partial melting by progressive metamorphism of metasediments was used earlier in the present study (Černy and Trueman 1978), along the lines of Arth and Hanson's (1975) model. Ermanovics et al. (1979) propose differentiation of basaltic magma via calc-alkaline differentiation trends as a process generating these potassic granites.

The biotite granites examined in the present study represent a late igneous phase termed the granodiorite-granite suite (Beakhouse 1977, in prep.) or potassic plutonic suite (Breaks et al. 1978) of the English River Gneissic Belt, comparable to late potassic granites identified in other subprovinces of the Canadian shield (e.g., Goodwin 1972, Schwerdtner et al. 1979), and in other Archean terranes (e.g., Anhaeusser et al. 1969, Anhaeusser 1973, Glikson 1976).

A genetic hiatus between the quartz diorites and the granites of the English River Gneissic Belt pointed out by, e.g., Beakhouse (in prep.) is indicated by structural differences and lack of intergradation in the field, by separated fields of bulk composition, and by trace-element evidence. Figure 122 illustrates separate K/Rb and K/Ba trends with no lateral spread, which is not suggestive of mutual transition. Figure 123 shows intersecting Zr/Hf vs. Hf trends which indicate different fractionation styles between the two elements in the quartz diorites and granites, although the quartz diorite trends are based on very few specimens and their alignment may be somewhat incidental.

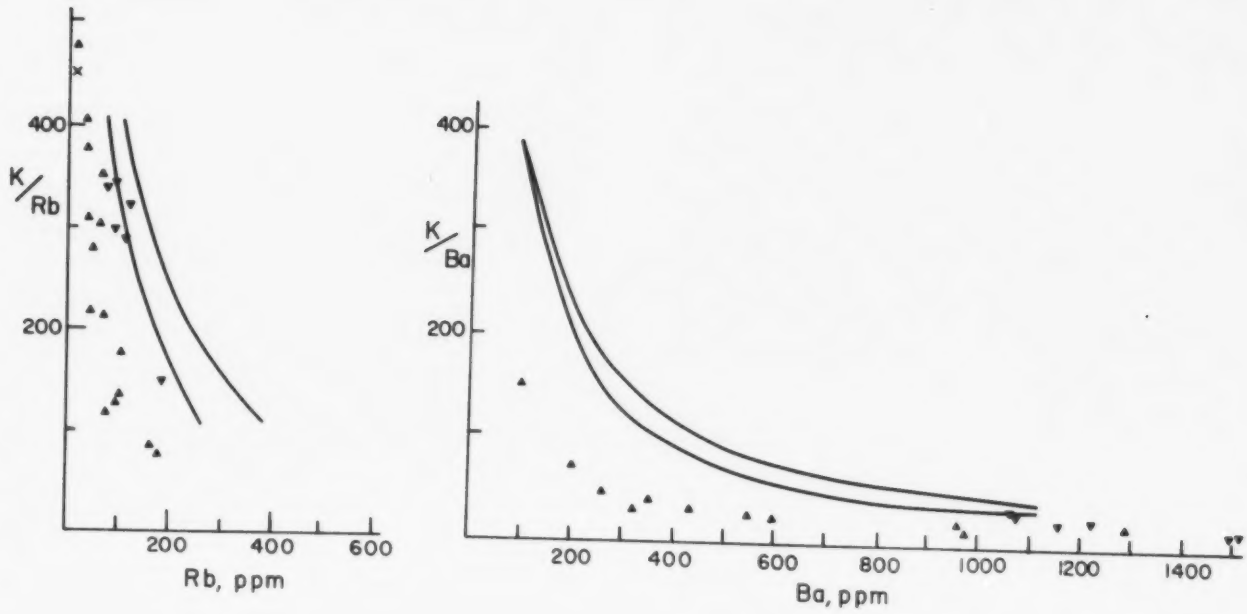

Figure 122: K/Rb vs. Rb and K/Ba vs. Ba diagrams for granitic components (solid outlines) and quartz diorites (triangles) of the Maskwa, Marijane and Lac du Bonnet batholiths. Inverted triangles mark the hornblende-biotite granodiorite from the Lac du Bonnet complex

For the present case of biotite granites examined here, the following lines of evidence delimit genetic conditions: (1) The bulk compositions lie largely away from the Ab-Or-Qtz minima and eutectics, shifted somewhat towards the Or apex. High homogeneity of individual bodies is their most conspicuous feature. None of the granites consist of a fractionated sequence; the compositional data within each individual body tend to bunch together without well-defined linear trends. Also, the fields of individual bodies do not align themselves along differentiation trends, suggesting a separate partial melting history of each. (2) A mutal similarity is, however, underlined by common general ranges of trace element contents and, in particular, by the identical type and overlap of their REE abundances, characterized by considerable HREE depletion and moderate negative Eu anomalies (Fig. 124). These patterns suggest considerable fractionation by hornblende (and/or garnet) and plagioclase removal. (3) Oxygen isotopic composition of the Lac du Bonnet biotite granite quoted earlier in this study (Fig. 125) strongly suggests that ^{18}O-rich supracrustal rocks were unimportant in its genesis, and a low initial $^{87}Sr/^{86}Sr$ ratio (Farquharson 1975) rules out earlier sialic crust as a source. This evidence, combined with other compositional data, suggests derivation from lower crust or mantle.

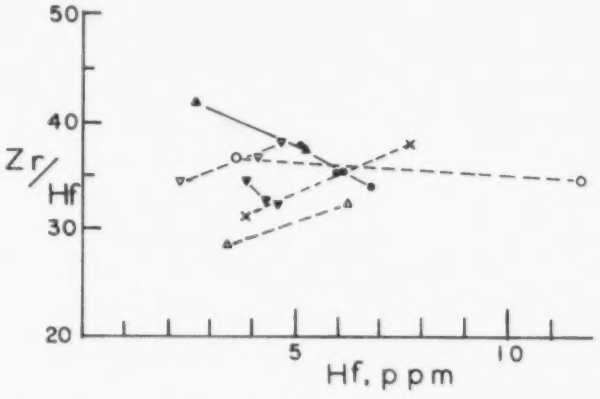

Figure 123: Zr/Hf vs. Hf plots of quartz diorites (open symbols, dashed trend lines) and biotite granites (solid symbols and trend lines) from the Maskwa Lake (inverted triangles), Marijane Lake (triangles), and Lac du Bonnet (circles) batholiths; x designates tonalitic gneisses of unit (12)

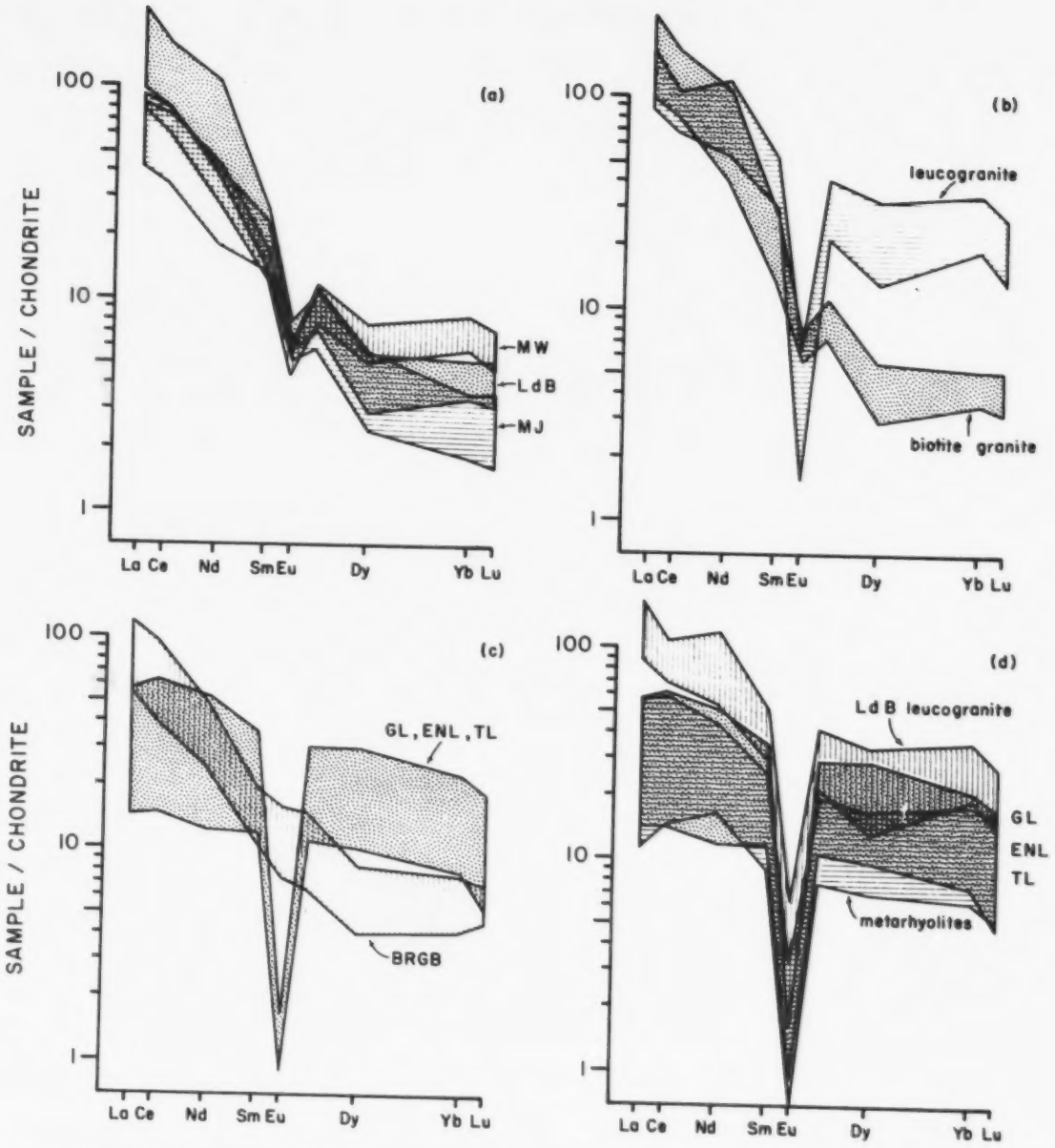

Figure 124: REE abundance fields of (a) biotite granites of the Maskwa Lake, Marijane Lake and Lac du Bonnet batholiths; (b) Lac du Bonnet biotite granite and leucogranite; (c) fine grained leucogranites of pegmatitic granite intrusions and Bird River Greenstone Belt sediments; and (d) metarhyolites of the Peterson Creek Formation, Lac du Bonnet leucogranite, and the fine grained leucogranite phase of three pegmatitic granites

Thus a deep-seated juvenile origin of these granites is indicated, by partial melting of intermediate to mafic sources rather than by igneous differentiation. No significant contamination either by digestion of upper crust or supracrustal sequences, or by mixing with their partial melts, is suggested. However, variation in quartz content among individual intrusions, concomitant with slight differences in overall fractionation levels, suggests some adjustment during the ascent of individual portions of partial melts, mainly in response to decreasing pressure. Some plagioclase fractionation could have taken place during the ascent as well. Taking the composition of the Lac du Bonnet biotite granite (the most primitive and quartz-poor of the three) as possibly representative of the initial melt, the fusion pressure could have been 5-8 kb (20-32 km), with most data clustering about 7 kb (27 km; Fig. 126). This estimate places the source within the uppermost basaltic crust which extends from 21 to 30 km below the present surface in the immediate vicinity of the Lac du Bonnet pluton (Hall and Hajnal 1973, Hall 1974, Beakhouse 1977).

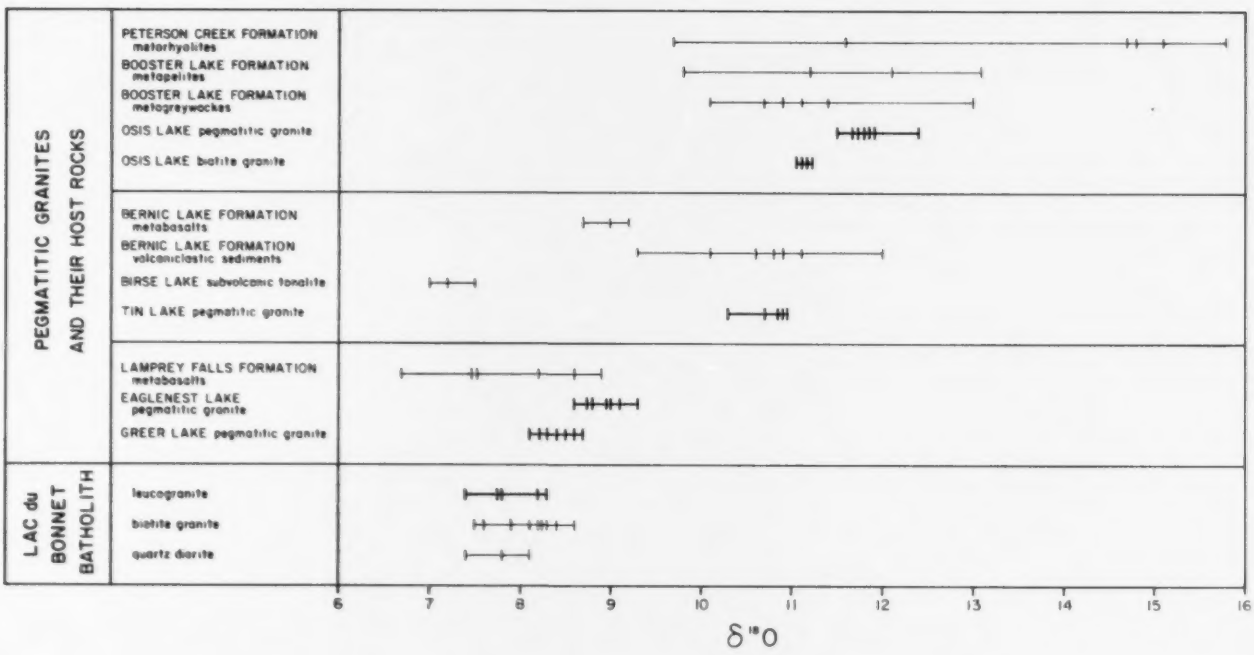

Figure 125: Oxygen isotope ratios in selected rock types of the Lac du Bonnet batholith, pegmatitic granite intrusions, and of the Bird River Greenstone Belt, after Longstaffe et al. (1981)

The biotite granites under discussion are remarkably similar, in most respects, to the biotite granites of the Vermilion and Giants Range batholiths in northeastern Minnesota described by Arth and Hanson (1975). These authors proposed a derivation of these granites by partial melting of short-lived greywacke at crustal depths, leaving a residue predominantly composed of plagioclase, hornblende, garnet and pyroxene or biotite. However, some of the granites in the Winnipeg River district differ in their Rb and Sr contents, and their REE abundances are not correlatable with those of the greenstone-belt metasediments as a possible source. Also, the $\delta^{18}O$ values are not compatible with supracrustal sources unless a thorough exchange with basaltic crust is invoked during deep-seated partial melting. Thus the juvenile origin outlined above is preferred.

The only granite recognized in the batholiths which does not fit the features of the granite family defined above is the ***early but highly fractionated leucogranite from the Lac du Bonnet batholith.*** Not only is the leucogranite much more fractionated in general, but its characteristics are such that a direct genetic link to the late, less fractionated biotite granite seems to be impossible. The relative age difference and the composition are strong evidence against differentiation. Also refuted is fractionation by incremental melting of a common source, as this is not compatible with the sequence of intrusion (cf. Figs. 31 and

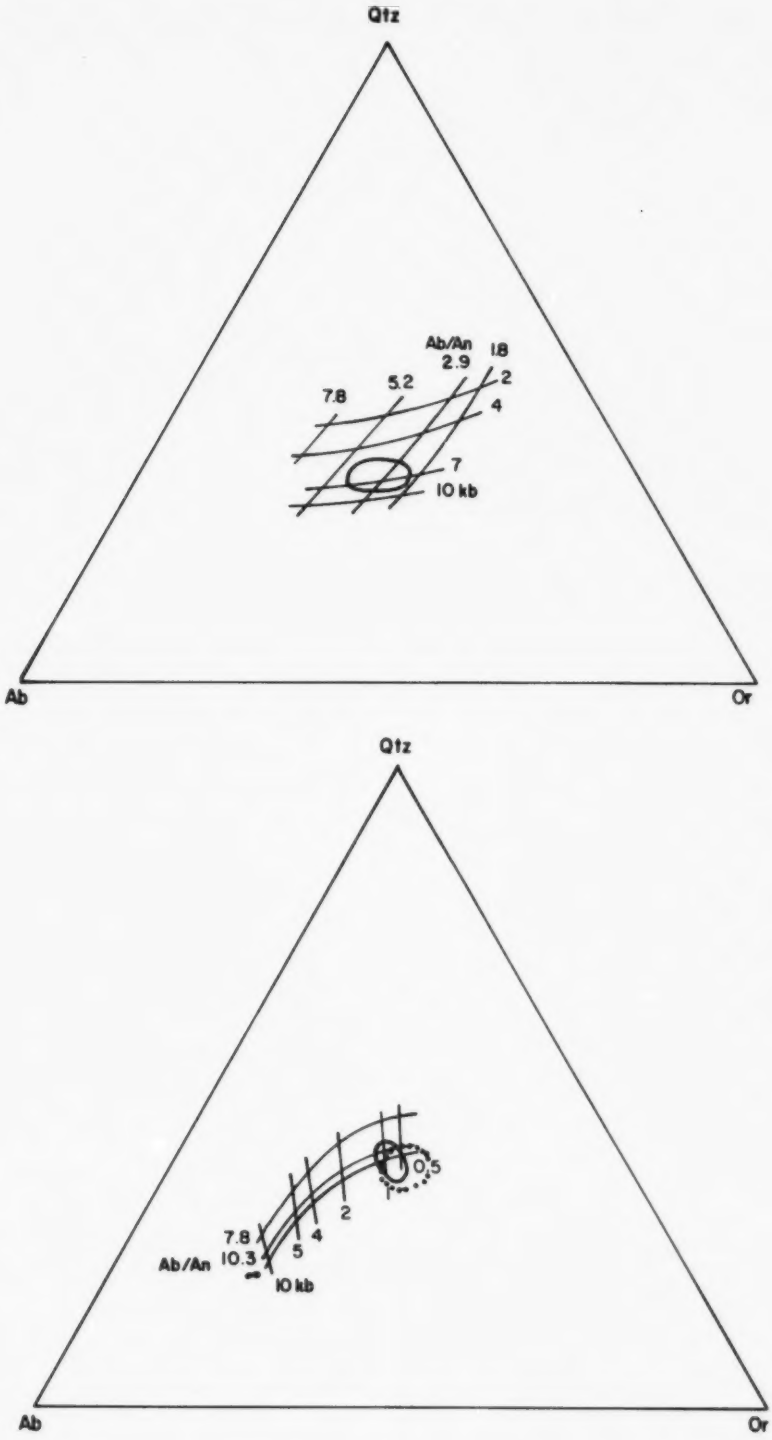

Figure 126: Ab-Or-Qtz mesonormative compositions in the Anderson and Cullers (1978) grids: (a) initial melt composition of the Lac du Bonnet biotite granite, (b) crystallization level composition of the Lac du Bonnet leucogranite (solid outline) and fine grained leucogranites of the pegmatitic granite intrusions (dotted outline)

32). The REE abundances compared in Figure 124 also indicate a fundamentally different origin. The relatively undepleted HREE contents of the leucogranite argue against partial melting which would leave substantial garnet and/or hornblende and/or clinopyroxene in the residuum. The prominent negative Eu anomaly, together with low Ca, Sr and high Rb and Cs, indicates plagioclase removal as the dominant process. Patterns matching closely that of the leucogranite have been attributed to igneous differentiation from granitoid parents with relatively flat log-linear REE abundances (Buma et al. 1971, Emmerman et al. 1975, Condie and Hunter 1976, Thorpe et al, 1977, Anderson and Cullers 1978).

The low range of $\delta\ ^{18}0$ (Fig. 125) suggests a deep-seated juvenile provenance, and the Ab-Or-Qtz composition corresponds to a granitic minimum at about 0.5 to 1 kb (2-4 km; Fig. 126). Thus the composition of the leucogranite reflects conditions of crystallization of a shallow-seated igneous differentiate that could have evolved during ascent from deep-seated juvenile granitoid precursors other than the plutonic granites exposed at the present surface. However, this mode of origin is not exclusive, as indicated by the close relationship of the leucogranite to the pegmatitic granites described below.

The pegmatitic granites

Because of their internal complexity and diversified chemistry, different aspects of the pegmatitic granites will be treated under separate headings.

In terms of ***internal phase composition,*** the four rock types distinguished in all four intrusions show the following relationships:

(1) The fine grained and pegmatitic leucogranite phases have not been found in mutual contact, and the difference between them was probably established below the present surface level, prior to emplacement and solidification. The differences in their bulk chemistry and trace element contents suggest that the fine grained phase crystallized from a ***relatively*** dry melt, whereas the pegmatitic phase originated from a more fractionated and volatile-oversaturated melt, which did not reach a stage of large-scale spatial separation of supercritical fluids from residual magma. According to Jahns and Burnham (1969), graphic K-feldspar + quartz megacrysts may have grown from local concentrations of supercritical fluids which did not coalesce.

(2) Potassic pegmatite bands develop locally by gradual or abrupt change in mineral assemblage and texture of pegmatitic leucogranite (Fig. 54). This corresponds to incipient segregation of supercritical fluids into larger pods, extracting preferentially K, Si and some trace elements. However, this process is not widespread as most of the pegmatitic leucogranite phase is texturally and compositionally homogeneous (Fig. 45).

(3) Fine grained leucogranites (and, rarely, pegmatitic leucogranites) grade into banded assemblages of garnetiferous sodic aplite alternating with potassic pegmatite (Fig. 50). Two interpretations may be applied to this association of aplitic and pegmatitic rock types. One is that advocated and documented by Jahns and Burnham (1969), which considers the quartz-poor sodic aplite to be a crystallizate from residual melt impoverished in silica, potassium and most rare elements by their partitioning into a separated supercritical fluid that gave rise to the pegmatitic bands. The other possibility is a metasomatic origin of the banded garnetiferous aplite asseblage, analogous to saccharoidal albitization fronts in complex pegmatites.

Textural and mineral-compositional characteristics of the banded aplite-pegmatite association favour the first mechanism: (i) the surface of aplitic bands commonly serves as a substrate for crystallization of pegmatitic assemblages (Fig. 52); (ii) pegmatitic assemblages crosscut and cement broken bands of sodic aplite, but reverse cases of sodic aplite penetrating potassic pegmatite are extremely rare (Fig. 55); (iii) the An content of albite in the sodic aplite is, on average, about the same as in the other phases composing pegmatitic granite intrusions whereas metasomatic albite could be expected to be An-poor; (iv) the Mn content of garnets in fine grained and pegmatitic leucogranites; enrichment in Mn could be expected in garnet associated with albitization.

The only aspect of the sodic aplites pointing to an analogy with albitization is the assemblage of accessory minerals, which is close to that of many typical albitized units in pegmatites. However, if the banded aplitic assemblages were generated through sodic metasomatism, then their textural relationships to the pegmatitic assemblages quoted above would indicate total recrystallization of original rock type(s). A thorough examination of this possibility could not be made within the framework of the present study.

An ***estimate of the P, T conditions*** under which the pegmatitic granite intrusions crystallized is hampered by several compositional characteristics of the different rock types. The procedures applied by Castle and Theodore (1972) and Harris (1974) to similar rocks cannot be used rigorously in our case because of compositional complexities introduced by the presence of Li, B and F. Wyllie and Tuttle (1964) proved the fluxing role of Li, and Chorlton and Martin (1978) established the same for B. The profound influence of F on the granitic solidus, depressing it partly by dissolving more H_20, was recognized by Wyllie and Tuttle (1961), Koster van Groos and Wyllie (1968) and Kovalenko (1977), and stressed by Bailey (1977) and Wyllie (1979). Thus any estimates based on simple experimental systems lacking Li, B and F would yield excessively high temperature values, partly due to an unrealistic granite solidus and probably also because of F-induced shifts in the stability field of (OH)-muscovite.

Of the four phases constituting the pegmatitic granite intrusions, the fine grained leucogranite is the most simple and "primitive" rock type. Its composition is probably not exactly representative of the starting melt from which some members of the present suite of phases evolved, and a possible partial loss of some components (e.g., alkalis and Si) into F-bearing supercritical fluids introduces some doubt into comparison with experimental results. Nevertheless, most of the fine grained leucogranite analyses cluster rather tightly at the low-pressure granitic minima, probably representing relatively undisturbed compositions. Plotted in Figure 126, this cluster suggests 0.5-1 kb (2-4 km) during crystallization which is the same pressure range as estimated for the Lac du Bonnet leucogranite. The low pressure (if correct) is misleading as to the depth at which the pegmatitic granites consolidated, but indicative of the conditions prevalent in large-scale dilation zones into which the pegmatitic granites were emplaced.

As to the temperature of crystallization, the available experimental grids are even more difficult to use, as indicated earlier. However, the two-feldspar geothermometer of Whitney and Stormer (1977) suggests a realistic temperature range between 640 and 600° C (for 1 to 2 kb P H_20), and even lower if the K-feldspar equilibrated in partly disordered state.

The ***petrogenesis*** of the pegmatitic granites is a controversial subject. A review of the literature dealing with the

origin of compositionally related granites reveals a split between concepts proposing low-percentage partial melting of supracrustal (or generally sialic metamorphic) sources, and hypotheses advocating advanced igneous fractionation. Dostal (1975) presents an excellent case for the anatectic origin, which is also preferred by Didier and Lameyre (1969), Dickson (1974), Harris (1974) and Mackie (1978), and experimentally supported by Winkler et al. (1974); Hauseux (1977) goes even farther proposing a metasomatic process. On the other hand, Kolbe and Taylor (1966), Proctor and El-Etr (1968), Taylor et al. (1971), McKenzie and Clark (1975), and Anderson and Cullers (1978) provide ample proof for granitic differentiation reaching the bulk composition and trace element fractionation levels attained in the studied pegmatitic granites. Igneous differentiation reaching fractionation levels similar to, and even surpassing, the compositions of the examined pegmatitic granites is also known from some rhyolite units of predominantly juvenile origin. (e.g., Ewart et al. 1977).

Within the framework of the regional lithology and possible deep-seated sources, the following processes should be considered for the origin of the examined pegmatitic granites: differentiation from the potassic biotite granites, partial melting from deep sialic crust, partial melting from the greenstone belt metasediments, and differentiation from juvenile granitoid melts.

(1) Igneous differentiation from the potassic biotite granites, and more specifically from the spatially associated Lac du Bonnet biotite granite, meets with the same difficulties as in the case of the Lac du Bonnet leucogranite (p. 142) which is very closely related to the composition of the pegmatitic granites. Because of the generally higher fractionation of the pegmatitic granites, the genetic incompatibility between the different trace element and REE distributions is even more conspicuous.

(2) Partial melting of deep-level sialic crust is postulated for certain types of Archean as well as younger rhyolite sequences. The notorious Taupo rhyolites of New Zealand (Ewart et al. 1968), Prince Albert Group rhyolites (Fryer and Jenner 1978), the Tobifera silicic volcanics in the southernmost Andes (Bruhn et al. 1978) and the group of undepleted siliceous volcanics of Condie (1976) as a whole are considered partial melts from granulite-facies crust, a concept also applied to a multitude of intrusive granitoids. However, all these igneous formations are characterized by a considerably high Ce_N/Yb_N ratio in their REE abundances, despite their relatively high Hree contents (at least in comparison with Condie's depleted group). The pegmatitic granites examined here have lower Ce_N/Yb_N, higher overall HREE contents, and much more prominent negative Eu anomalies. A single-stage process is therefore unlikely. The REE abundances could possibly be approached only after extensive fractionation of the original anatectic melt at the quartz-feldspar minimum, which would modify earlier trace element characteristics.

Other lines of available evidence are inconclusive because of a wide variety of possible lithologies, trace element abundances and oxygen isotope ratios in the source region. It should be stressed, however, that the anomalous thickness of sialic crust in close neighbourhood of the pegmatitic granite occurrences (Hall and Hajnal 1973, Hall 1974, Beakhouse 1977) indicates a large and diversified volume of possible sources at more than sufficient depth.

(3) A direct derivation by partial melting of metasediments and metavolcanics of the greenstone belt is incompatible with the REE abundances of the pegmatitic granites. Most of the greenstone belt lithologies should produce residual plagioclase with hornblende and/or garnet on partial melting (as documented by Arth and Hanson 1975, on metaturbidites similar to the metasediments most abundant in the Bird River Greenstone Belt). Resulting depletion in HREE's and minimal, if any, Eu anomaly in the melt fraction are the opposite of what is observed in the pegmatitic granites (Fig. 124).

A two-stage process of anatectic melting of suitable lithologies (particularly metapelites and metarhyolitic compositions) followed by igneous fractionation is, however, a distinct possibility. The REE abundances of the initial melts, controlled by residual phases, could have been modified by the magmatic fractionation. Normative corundum contents of 2-5% (CIPW) are typical of S-type granites, and the oxygen isotopic ratios could be interpreted as inherited from metasedimentary protoliths in the Tin Lake and Osis Lake bodies, and modified by exchange with metabasalt hosts in the Greer Lake and Eaglenest Lake intrusions (Fig. 125). The differences in accessory mineral assemblages, and in some aspects of trace element geochemistry, between the Tin Lake and Osis Lake vs. the Greer Lake and Eaglenest Lake intrusions could be explained by differences in source lithologies. The biotite granite plug, central to the Osis Lake pegmatitic granite, could represent a magma close to the initial anatectic melt from which the pegmatitic granites fractionated.

(4) Differentiation from an undisclosed juvenile igneous source of granitoid composition seems to be in accordance with the compositional characteristics of the pegmatitic granites. The same argument applies here as given in the discussion of the closely related Lac du Bonnet leucogranite. The extremely similar geochemistry of this leucogranite and of the leucogranitic phases of the pegmatitic granites is shown by, e.g., the plots of Rb vs. Sr, Rb vs. Ba and Y vs. Ca in Figure 127. These plots also show a close similarity of these two granite types to the metarhyolites of the Peterson Creek Formation, described on p. 13. Table 68 documents a possible fractionation relationship among the three siliceous and potassic rock types, progressive with decreasing age.

A petrogenetic history common to all three rock types, and separate from other intrusions in the area, is also supported by the REE abundances. All phases of the pegmatitic granites have the same REE pattern type as the Peterson Creek metarhyolites and the Lac du Bonnet leucogranite (Fig. 124; the LREE abundances in this last intrusion, higher than in the other two rocks, may be due to its allanite content). These patterns are rather exceptional within the Superior Province as a whole (e.g., Condie and Baragar 1974). They are sharply different from, and genetically incompatible with, any other granitoids in the examined pegmatite field; however, this type of flat pattern with very low Ce_N/Yb_N values is considered typical of differentiation sequences derived from basaltic parents (Ewart et al. 1977, Bruhn et al. 1978).

TABLE 66. COMPOSITIONAL CHARACTERISTICS OF THE PETERSON CREEK FORMATION METARHYOLITES, LAC DU BONNET LEUCOGRANITES, AND FINE GRAINED LEUCOGRANITES OF THE PEGMATITIC GRANITE INTRUSION

	Metarhyolites (3 anal.)	Leucogranites (18 anal., 2 bodies)	Pegm. granites (22anal., 4 bodies)
K/Rb	198* (167-254)	190 ±51 (286-113)	117 ±46 (176-75)
K/Cs	27,433 14,000-38,300)	18,397 ±10,812 (45,375-5,094)	4,798 ±1,645 (6,800-2,823)
K/Ba	142 (65-219)	222 ±221 (27-825)	1,696 ±2,480 (279-5,402)
Rb/Sr	10.2 (18.7-2.2)	17.3 ±42.2 (185-2.76)	25.4 ±21.5 (52.8-6)
Ca/Sr	19.9 (1.9-33.3)	139.1 ±49.1 (86-280)	147.6 ±50.2 (103.7-204.7)
Mg/Li	50.4 (100-11.2)	27.6 ±18.5 (66.7-2.9)	17.7 ±20.8 (48.6-6)
Al/Ga	7,024 (11,920-2,128)	2,156 ±333 (2,764-1,568)	1,695 ±466 (2,351-1,258)
Zr/Hf	22.9 (20-26.7)	27.5 ±5.8 (18.3-34.3)	34 ±10 (24.3-48.3)
Th/U**	4.2	2.6	0.4

* Arithmetic mean, ±1σ, (range)

** ratios of average Th and U contents

Within the group of pegmatitic granites themselves, the overall REE abundances decrease, and the negative Eu anomaly increases with decreasing K/Rb, K/Cs and other indicators of progressive fractionation. The general decrease in REE abundances in the final stages of granitic differentiation was recognized by, e.g., Nagasawa and Schnetzler (1971), Koljonen and Rosenberg (1974), and Emmerman et al. (1975). Plagioclase fractionation is evidently responsible for deepening Eu anomaly, and the concomitant flattening of the pattern (LREE depletion faster than that of HREE) suggests residual biotite and apatite (e.g., Puchelt and Emmerman 1976, Hanson 1978). The abundances of the two latter minerals decrease in the discussed intrusions with decreasing REE abundances.

Other lines of compositional evidence available for the origin of pegmatitic granites do not contradict a juvenile origin, when the highly probable possibility of contamination during the passages through the greenstone belt is considered. Thorough equilibration with the host metasediments in the Tin Lake and Osis Lake intrusions, and just a slight adjustment in the Greer Lake and Eaglenest bodies which intrude metabasalts, can plausibly explain the oxygen isotope abundances (Longstaffe et al. 1981). Extensive hybridization of original melts in the Tin Lake and Osis Lake pegmatitic granites, partly suggested by field observations, may be responsible for their exclusive content of boron and remarkably increased phosphorus concentration. It is the Osis Lake intrusion, displaying the highest B and P contents, which is located closest to the P-enriched Flanders Lake Formation containing tourmaline-bearing clasts (Posehn 1976), and within the P-rich metapelites of the Booster Lake Formation (Tables 9 and 10). Hybridization and a loss of alkalies to the country rocks through fluid phase can account for the corundum-normative compositions, which are not specific for S-type granites (e.g., Cawthorn et al. 1976, Cawthorn and Brown, 1976).

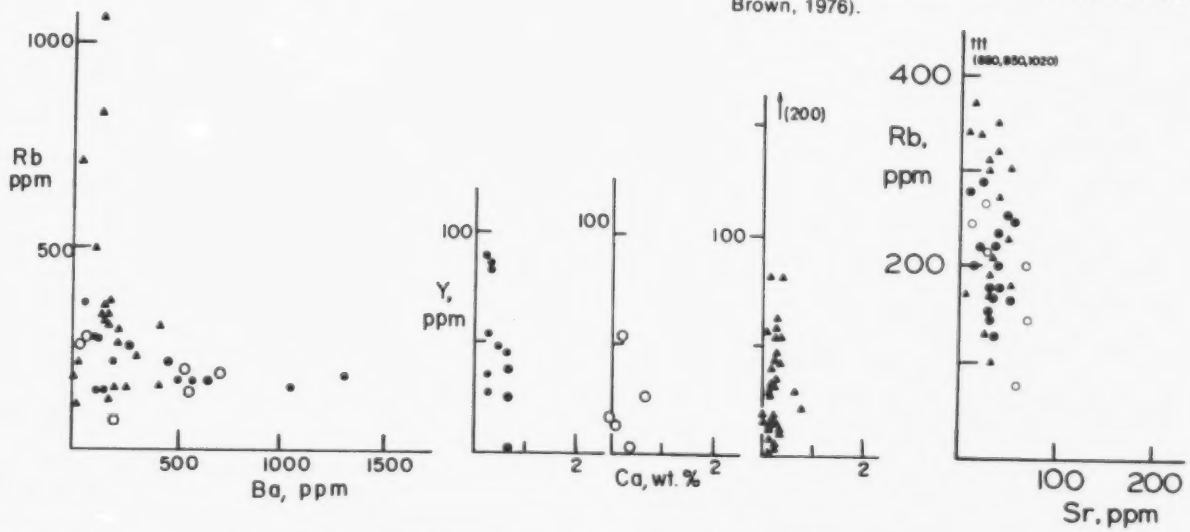

Figure 127: Rb vs. Ba, Y vs. Ca and Rb vs. Sr plots of the Peterson Creek Formation metarhyolites (open circles), Lac du Bonnet leucogranites (solid dots), and fine grained leucogranites from the pegmatitic granite intrusion (triangles)

The above discussion indicates that at the present stage of study, the origin of the pegmatitic granites cannot be unequivocally resolved. The partial melting of greenstone-belt metasediments modified by igneous fractionation is in accord with the interpretation of pegmatitic granites in the eastern continuation of the English River subprovince in Ontario (Breaks et al. 1978), and in the Yellowknife pegmatite field (Drury 1979). It is also supported by the restricted mobility of wet melts and a relative proximity of the pegmatitic granites to an underlying granulite isograd (Fig. 121). On the other hand, the petrochemical relationship of the pegmatitic granites to the metarhyolites of the Peterson Creek Formation and to the Lac du Bonnet leucogranite is undeniable, and an anatectic or igneous juvenile provenance coupled with hybridization in the greenstone belt fits the available data easily. In either case of S-type or I-type granites, the restriction of the Winnipeg River pegmatitic granites to major regional fault systems seems to be significant in their genesis and evolution, as demonstrated recently on leucogranites of Brittany by Strong (1981).

The pegmatites

Several lines of evidence point to derivation of individual pegmatite groups from the different granitic intrusions discussed earlier:

(1) Close spatial relationship exists between individual granites and associated pegmatite groups, as illustrated in Figure 128. It is significant that the pegmatite groups are restricted to the intrusions of differentiated Lac du Bonnet leucogranite and pegmatitic granites; they show no spatial affinity to the plutonic quartz diorites or biotite granites. As shown in Table 69, the leucogranites are the only ones in the district capable of producing highly mineralized pegmatites.

(2) Similarity (up to identity) in accessory mineralization of the granitic intrusions and the adjacent pegmatite groups, is shown semiquantitatively in Table 70. For example, the Greer Lake and Eaglenest Lake pegmatitic granites are virtually free of B-bearing minerals and very

TABLE 69. GEOCHEMICAL INDICATORS OF BEUS AND SITNIN (1968) AND BEUS ET AL. (1968) COMPARED TO THE CHARACTERISTICS OF GRANITIC ROCKS OF THE CAT LAKE-WINNIPEG RIVER PEGMATITE FIELD. FIGURES IN BRACKETS ARE BASED ON LESS THAN 10 SAMPLES

	Li		Rb	Sn	V	Mg/Li		Zr/Sn	
Intrusion type	< 25ppm	> 100ppm	< 150ppm	> 20ppm	> 4ppm	<30	>100	<30	>100
Parental to Ta-bearing apogranites	<1%	64%	<1%	28%	1%	100%	<0.1%	83%	<0.1%
Parental to Ta-bearing pegmatites	<1	41	5	26	1	39	0.4	93	14
Parental to Ta-poor pegmatites	26	27	24	16	1	27	30	87	5
Parental to Ta-free greisens	26	23	30	21	14	44	12	46	70
Barren granites	54	2	43	1	30	<<0.1	98	7	48
LdB biotitic granite	14	7	14	0	-	9.3	14	33.3	13.3
LdB leucogranite	46.7	0	13.3	0	-	60	0	(78)	(0)
TNL fg. leucogranite	46	0	7.7	0	-	46	15.5	92	0
OL fg. leucogranite	(0)	(0)	(16.7)	(0)	-	(33.3)	(0)	(85.3)	(0)
GL and ENL fg. leucogranites	(0)	(14.3)	(0)	(28.6)	-	100	0	100	0
Inconnu granite	52	0	48	0	-	18.5	44.5	67	0
Maskwa L. granites	57	0	50	(0)	-	7	36	(12.5)	(0)
Marijane L. granites	40	0	20	(0)	-	0	30	(20)	(0)

TABLE 70. CORRELATION OF ACCESSORY MINERAL CONTENT OF MAJOR GRANITIC INTRUSIONS AND THEIR PEGMATITE AUREOLES. ADJUSTED AFTER ČERNÝ AND TRUEMAN (1978)

MAJOR INTRUSIONS			ASSOCIATED PEGMATITES		
TYPICAL ACCESSORIES	LOCAL MINERALIZATION	MINOR ELEMENTS	TYPICAL ACCESSORIES	RARE-ELEMENT MINERALIZATION	MINOR ELEMENTS
LAC DU BONNET LEUCOGRANITE			**SHATFORD LAKE GROUP**		
zircon, allanite, monazite, ((garnet))	((Be))	high Th,U; very low Li,Rb,Cs	beryl, garnet, topaz, allanite, monazite, zircon, thorite, uraninite	Be,Nb≥Ta,REE, Zr,U,Th, (Sn)	high U,Th; very low Li,Rb,Cs
GREER AND EAGLENEST LAKE PEGMATITIC GRANITES			**GREER AND EAGLENEST LAKE GROUPS**		
garnet cordierite ((gahnite))	Be,Nb-Ta, (Li,Rb,Cs)	intermediate Li,Rb,Cs	garnet, cordierite, beryl, Nb-Ta oxides, ((gahnite))	Be,Nb≥Ta,(Li) ((Sn))	intermediate Li,Rb,Cs
AXIAL PEGMATITIC GRANITE			**AXIAL GROUP**		
garnet	-	low Li,Rb,Cs	garnet	-	low Li,Rb,Cs
TIN LAKE PEGMATITIC GRANITE			**BIRSE LAKE GROUP**		
garnet ((tourmaline))	((Mo))	very low Li,Rb,Cs	tourmaline, beryl	Be ((Li,Nb > Ta))	very low Li,Rb,Cs
OSIS LAKE PEGMATITIC GRANITE			**RUSH LAKE GROUP**		
garnet tourmaline apatite (triphylite-lithiophilite)	((Li))	intermediate Li,Rb,Cs	tourmaline, beryl, LiAl-silicates, Li-phosphates, Nb<Ta oxides, ((pollucite))	Li,Rb,(Cs),Be, Sn,Nb<Ta	intermediate to very high Li,Rb, Cs; high Be,Sn, Nb<Ta,?,B,F

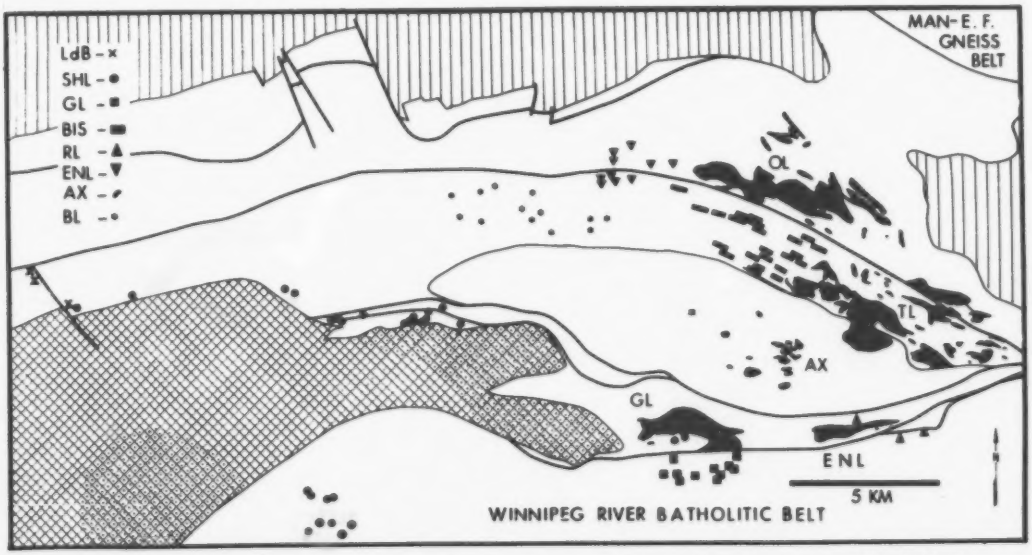

Figure 128: Disposition of the Lac du Bonnet batholith (diamond grid; leucogranite dotted), pegmatitic granites (black, letter symbols) and pegmatite groups (see inset) along the east-west fault systems in the Winnipeg River pegmatite district. Modified after Černý and Trueman (1978)

low in P, and so are their pegmatite aureoles. In contrast, these two elements are enriched in the Tin Lake and particularly Osis Lake intrusions, and this is also reflected in the abundance of tourmaline and phosphates in the adjacent pegmatite groups.

(3) Bands and schlieren of mineralized potassic pegmatite phase inside the pegmatitic granites are commonly indistinguishable from individual bodies of adjacent pegmatite swarms. This is particularly true of the Greer Lake, Eaglenest Lake, and Tin Lake intrusions. The last of them exhibits gradual transition into the Birse Lake pegmatite group in such a manner that the boundary drawn between the pegmatitic granite and pegmatites proper (Fig. 78) is rather arbitrary. Even the most complex pegmatite types of the Bernic Lake and Rush Lake groups have their petrologic and paragenetic analogs inside the pegmatitic granites. The Silverleaf and particularly Annie Claim #3 pegmatitic nodules, enriched in Li, Rb, Cs, Be, Ta and F, represent local gradually evolving lithologic facies in the Greer Lake pegmatitic granite, with mineral assemblages and geochemical characteristics close to those of the above pegmatite groups.

(4) Geochemical relation between rock-forming minerals from the individual major intrusions and from their respective pegmatite aureoles also indicate fractionation relationships. This is illustrated in Figure 129 on the example of blocky K-feldspars from the potassic pegmatite phase of three pegmatitic granites, plotted together with blocky K-feldspars from their adjacent pegmatite groups, in the K/Rb vs. Cs graphs. The same relationships are shown by other fractionation-sensitive elements in K-feldspars and muscovites.

There are only two pegmatite groups in the Winnipeg River district which cannot be assigned to a specific, and exposed, source intrusion. One of them is the above-mentioned Lac du Bonnet group with primary zonal spodumene, injected into shear fractures along a fault displacing the margin of the late biotite-granite phase of the Lac du Bonnet batholith and adjacent metasediments. The source of this group is evidently hidden, and its nature uncertain. However, in view of its advanced fractionation and late relative age, this group may be consanguineous with the Bernic Lake-type pegmatites but intruded into a different tectonic regime affecting its phase petrology.

The other group with no apparent source is the most mineralized and economically important Bernic Lake group. The following evidence would seem to preclude an affiliation with the Osis Lake pegmatitic granite, as a continuation of the Rush Lake group:

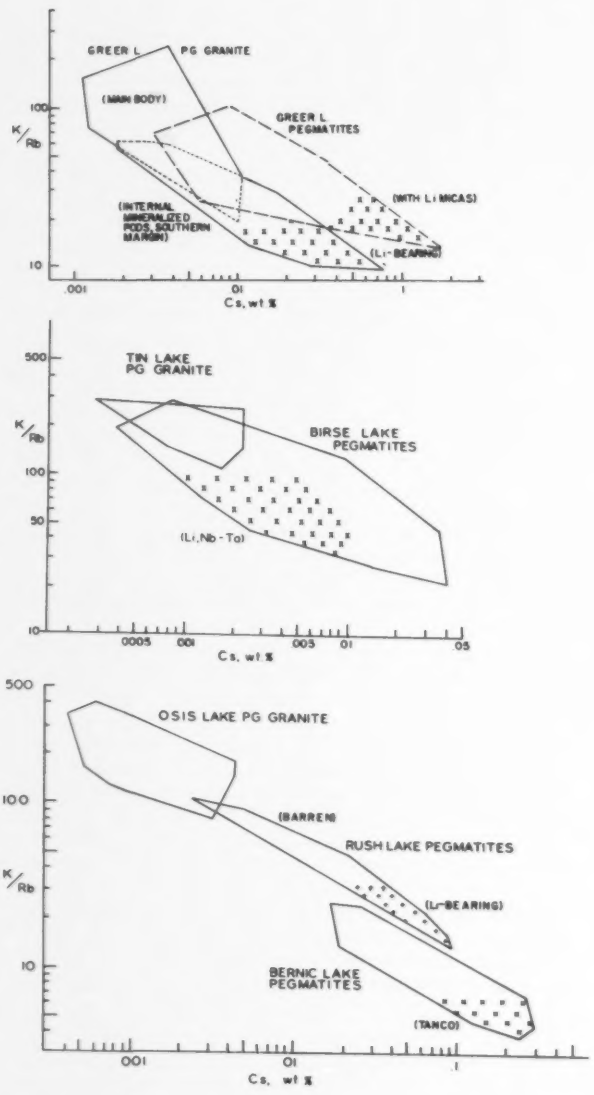

Figure 129: K/Rb vs. Cs in blocky K-feldspars from three major intrusions of pegmatitic granites, and from the pegmatite swarms accompanying them

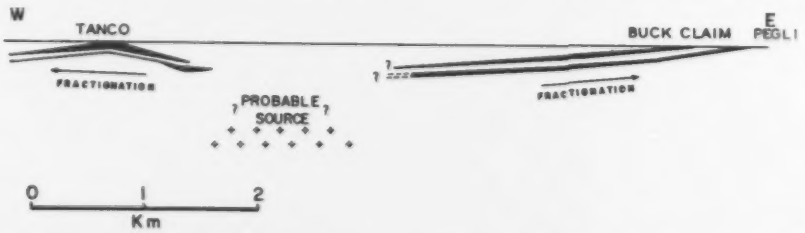

Figure 130: Cross section through the Bernic Lake pegmatite group (only three major and best-explored pegmatites are shown). Trace-element fractionation in the rock-forming minerals in the east, and in the late metasomatic assemblages in the Tanco pegmatite shown by arrows. Since the eastern pegmatites dip WNW, and the Tanco body dips collectively northwards, the hypothetical source is probably north of the section plane

(1) The distance spanned between the Osis Lake pegmatitic granite in the east and the Tanco pegmatite at the western extremity, about 8 km, is much in excess of maximum distances between parental granites and derived pegmatites, about 2 km, established in a variety of geological environments (Beus et al. 1968).

(2) Geochemistry of feldspars (Fig. 129) and micas suggests a parallel but not a sequential fractionation in the Rush Lake and Bernic Lake groups.

(3) Fractionation directions disclosed by the shallow-dipping members of the Bernic Lake group strongly suggest spreading from a source inside the group (or somewhat north of its centre; Fig. 130).

(4) A hidden source in the above location is also in agreement with the maximal fractionation and enrichment in rare elements of the Bernic Lake group. In a 3-dimensional pegmatite aureole flanking and topping a parental intrusion, extreme enrichment in volatile and associated rare elements should be expected in its topmost part.

(5) A pegmatitic granite of the Greer Lake type may be envisaged as a parental body. The Silverleaf and the Annie Claim #3 pods in the Greer Lake intrusion are not as fractionated as the Bernic Lake pegmatites but they exhibit the same low-P assemblage (petalite as the primary Li-aluminosilicate) and similar paragenesis.

Conclusions

Three igneous formations with separate lines of descent can be identified among the intermediate to acid intrusions of the Winnipeg River District: (i) syntectonic diapiric quartz diorites, anatectic from lower crust or mantle; (ii) late-tectonic biotite granites formed in a separate and relatively shallow anatectic event, and possibly from a different source, in the basaltic crust; (iii) pegmatitic granites which may be derived by partial melting of the greenstone-belt lithologies and subsequent igneous fractionation(S-type), or by anatexis and fractionation of juvenile sources hybridized by assimilation and exchange with the greenstone-belt metasediments (I-type). In the latter case, a consanguinity is indicated with silicic rhyolites of the Peterson Creek Formation, and in both cases, with the Lac du Bonnet leucogranite. It is this latter leucogranite and the pegmatitic granites which generated aureoles of pegmatites by continued

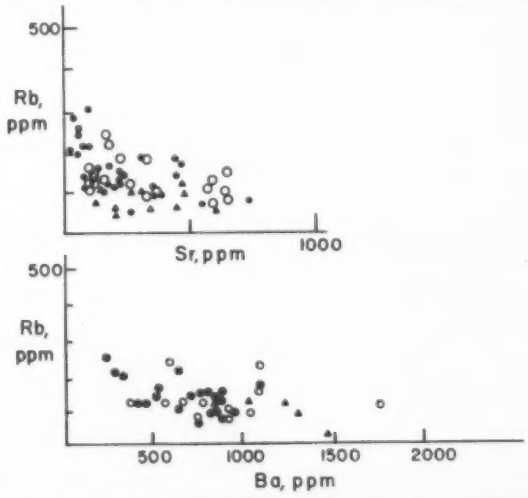

Figure 132: Rb vs. Sr and Rb vs. Ba in the migmatite complex (triangles), the Black River suite (open circles), and the Inconnu granite (solid dots)

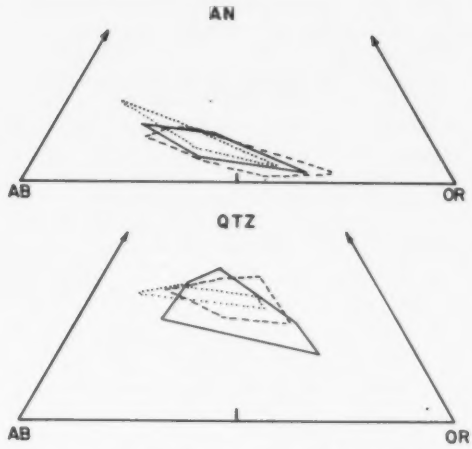

Figure 131: Ternary normative composition fields for the granitoid rocks of the migmatite complex (dotted), the Black River suite (dashed) and the Inconnu granite (solid outline)

igneous differentiation at a quartz-feldspar minimum, coupled with separation of supercritical fluids from volatile-oversaturated residual melts.

While the generation of most pegmatitic groups via igneous plus supercritical fractionation is proven beyond reasonable doubt, the provenance of the silicic igneous parents is not clear. This problem could possibly be unambiguously resolved only by Rb-Sr and U-Pb isotope research which was beyond the scope of the present study.

THE CAT LAKE-MASKWA LAKE DISTRICT

In this district, the variety of exposed granitic rocks is much restricted in comparison with the Winnipeg River area, and the relationships between major intrusions and pegmatites are rather obscure.

The batholiths

Besides the northern part of the Maskwa Lake quartz diorite and its late granitic component, the only other sizeable granitic body in this district is the Inconnu batholith. This granite shows distinctly intrusive boundaries along its southern margin but gradual transition into the porphyroblastic and possibly partly metasomatic Black River suite in the north. The virtual identity of both gneissic and granitic components of these two suites is demonstrated by bulk compositions as well as trace elements. Moreover, the migmatitic-to-granitic members of the migmatite unit 11 do not differ substantially from the Inconnu or Black River compositions (Fig. 131 and 132) except for a highly peraluminous character of the former, shown in CIPW norms and by accessory cordierite and garnet. All three units are probably synchronous anatectic mobilizates activated to a different degree from different source rocks; more specific conclusions cannot be reached without additional evidence.

The Inconnu granite is similar to the biotitic granites of the Winnipeg River district in average bulk composition, and in the general type of the REE pattern, but differs in the wide range of its alkali and trace element contents (Figs. 26, 27, and 133). This variability is caused by relatively late migration of the K-feldspar component observable microscopically. This feature is almost totally missing in the biotitic granites of the Winnipeg River district. Besides explaining the internal compositional variability, the late mobility of K-feldspar also suggests that the porphyroblastic members of the Black River suite may have received their K-feldspar component from the granite.

The pegmatitic granites

Apart from a few patches of pegmatitic material along the southern margin of the Inconnu granite, no rocks resembling pegmatitic granites have been found. At the time of writing this study, tourmaline-bearing dyke-like rocks were found in the southern parts of the Inconnu batholith north and northwest of Cat Lake. No analytical data are available, and the nature of these rocks and their role in the regional igneous evolution is yet to be established.

The pegmatites

Most of the Li-bearing pegmatites in this district carry primary spodumene, suggestive of a relatively high pressure/low temperature mode of crystallization. The only exception is the Northwest Dyke at the northwestern extremity of the district which carries pseudomorphs after petalite; also, the nearby HGD dyke, with the only pollucite occurrences in the district, is suggestive of a low-pressure regime.

Disregarding the predominant high-pressure character of the pegmatites, the degree of rare-alkali enrichment is remarkable; its difference between the most-enriched primary-spodumene types and petalite-bearing bodies is rather negligible (e.g., Fig. 83). Except for the least-fractionated members of the Cat Lake and BET groups, the fractionation levels do not differ greatly among the different groups. This is also reflected in the mineralogy of the spodumene-bearing pegmatite types which is largely uniform. Nevertheless, the different groups of the district (and internal subdivision of the Maskwa Lake series) are distinctive in their characteristics and, judging from the relationships established in the Winnipeg River district, were probably derived from different sources.

The genetic linkage of the pegmatite groups remains undisclosed at present. The granites of the Maskwa Lake diapir and of the Inconnu batholith do not seem to be capable of producing Li-rich pegmatites (Table 69), and the role of the recently discovered pegmatitic granites is so far unknown. However, even if the latter prove to be parental to some pegmatite groups, the source of the others would still have to be sought at depth.

Conclusions

No definite links can be established at present between the pegmatites of the district and outcropping granitoids, and most of the granitic sources are probably hidden below the present erosional surface.

A comparison of the district with that of the Winnipeg River area indicates differences in metamorphic niveau, structural style, granitoid emplacement, and pegmatite type, the only exception being the Maskwa Lake batholith which borders both districts. In the Cat Lake-Maskwa Lake district, the metamorphic grade is uniformly amphibolite facies, and granites mobilized at lower levels have mostly metasomatic contacts with metamorphic rocks. The generally tight structural pattern lacks the dilation features so prominent in the Winnipeg River area. The relatively few structural traps have been active during and after pegmatite emplacement, imparting banded, sheared and foliated fabrics on them. Accordingly, most of the pegmatites are of high pressure/low temperature type with primary spodumene, in contrast to the predominance of the low pressure/high temperature type prominent in the south, and their source rocks are not exposed.

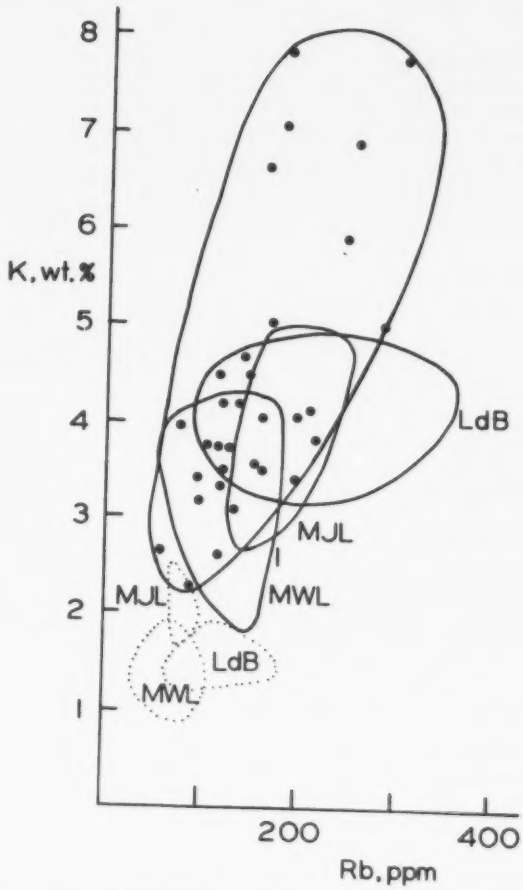

Figure 133: K vs. Rb in the Inconnu granite (solid dots) compared to the fields covered by the Lac du Bonnet, Marijane Lake, and Maskwa Lake biotite (solid outlines) and their respective quartz diorites (dotted outlines)

ECONOMIC CONSIDERATIONS

INTRODUCTION

Two subjects should be considered in evaluating economic potential of any pegmatite-bearing area and specifying prospective exploration targets: the geochemical potential of the known (and, possibly, expectable) pegmatite types, and the main controls on the distribution of pegmatites. Both closely depend on the immediate geological framework hosting the pegmatites; therefore they will be discussed separately for each pegmatite district.

GEOCHEMICAL POTENTIAL OF THE FIELD

The Winnipeg River district

Judging from the accessory mineralization identified in the individual pegmatite groups, from the overall fractionation levels attained by them, and from the characteristics of their granitic sources, the following can be said about the pegmatite groups of the district:

The *Shatford Lake group* is characterized by a Be, Sn, Nb/Ta, Zr, REE, U, Th-bearing asseblage. Beryl is considerably enriched in several dykes (e.g., Huron Claim, K-1, SHE-2) and complex oxides of Nb/Ta reach economically marginal levels in some bodies (for the present market situation a least). Both Be and Nb/Ta can be expected to be accumulated in the most fractionated pegmatites of this group but they seem to be not restricted to them. The high variability of the Nb/Ta ratio typical of this group must be considered in pegmatite evaluation.

The *Lac du Bonnet group* characterized by Li(P) mineralization has considerable Li potential but so far no other rare-element minerals have been found, despite the highly fractionated character of the bodies.

The *Greer Lake group* belongs to the Be, Nb/Ta type, It has been partly explored, and reserves of Be have been identified; at present, Nb/Ta in some recently explored bodies may be marginally economic. As in the case of the Shatford Lake group, the most rare-alkali fractionated pegmatites may have the best mineralization potential in terms of Ta fractionation, but in the known pegmatite dykes Be and Nb/Ta do not seem to have any particular preferences as to the overall degree of fractionation.

The *Eaglenest Lake group* carrying Be mineralization is extremely poorly represented at the present surface but judging from the geochemical characteristics of the parent pegmatitic granite (similar to the Greer Lake body), a Be and possibly Nb/Ta potential can be expected. However, it appears that pegmatites associated with this pegmatitic granite may have been intruded at a high level and have since been eroded.

The *Axial group* seems to be barren in terms of both accessory minerals and overall geochemistry. The occurrence of spodumene-bearing dykes in this group has not been confirmed to date.

The *Birse Lake group* with the B, Be-bearing accessory mineralization is geochemically primitive in its bulk. Quite a few of its members contain beryl, and only some of the most fractionated pegmatites also carry traces of columbite-tantalite and amblygonite. Be is the only element that may be accumulated in economically interesting quantities.

The *Rush Lake group* is, with its Li, Rb, Cs, Be, Sn, Ta-Nb, B, P, F association of rare elements, qualitatively and petrologically close to the Bernic Lake group but so far no economic concentrations of any of the above elements have been found. Nevertheless, the potential for Li, Rb, Cs, Be, (Sn) and Ta-Nb is there, and the attitude of a pegmatite, combined with its vertical location with respect to the erosional surface, may be the crucial factor influencing the rare-element accumulation and size of potential deposits.

The *Bernic Lake group* is qualitatively equal to the Li, Rb, Cs, Be, Sn, Ta-Nb, B, P, F-bearing Rush Lake group but in quantitative terms it has a much better economic potential, as exemplified by the Tanco deposit. Subhorizontal bodies with high-grade accumulation of rare-element mineralization are typical. Li, Rb, Cs, Be, (Sn), and Ta-Nb can be expected to be accumulated in members of this group, together with refractory-ceramic grade of petalite and spodumene.

The Cat Lake-Maskwa Lake district

The *Eagle-Irgon group* is characterized by almost extreme Li accumulation but so far no other mineralization of possible economic significance has been recognized. It is highly probable that Li will ocur in economic quanitites in most members of this group.

The *Beryl-Tourmaline group* has a distinct Be, B geochemical signature but seems to be insignificant in terms of number and size of its members. Be could possibly become interesting if larger bodies of this type are discovered.

The *Cat Lake group* has a Li, Be mineralization with traces of Nb-Ta. Be is the only element that in places is accumulated in larger than trace quantities.

The *Central Claim group* characterized by a Li, Be, Ta-Nb assemblage has, so far, the best potential for Ta-Nb in the district; spodumene and beryl are very subordinate in the only pegmatite known to belong to this type. Unfortunately, as discussed in the following section, the pegmatite has a unique, and so far poorly understood, structural position, and the chances of finding more bodies of this type are rather poor.

The *Maskwa Lake series* consists of a variety of pegmatites with, collectively, a broader assemblage of rare elements: Li, Rb, Cs, Ta-Nb, and (Be). Pegmatite dykes carrying primary spodumene closely resemble the Eagle-Irgon group, and their potential seems to be restricted to Li only. On the other hand, the pegmatite type represented by the HGD and NW bodies closely approaches the Bernic Lake group in the southern district in terms of both mineralization and overall geochemical characteristics. This seems to be the most promising pegmatite type in the northern district for Li, Rb, Cs, Ta-Nb and refractory-grade spodumene; so far, Sn concentration seems to be very low, as is that of Be.

EXPLORATION TARGET AREAS

In any pegmatite district, the spatial distribution of pegmatites is controlled by the location of parent plutonic bodies and structural patterns. These will be considered in the following sections, separately for each district.

The Winnipeg River district

The primary controls on both parental granitic intrusions and pegmatite groups in this district are the east-trending faults that served as channelways for the ascent of major intrusions and also streamlined the spreading of pegmatites from them. This can be observed in Figure 128, and in Maps 1 and 3.

An example of a fault system deserving exploration is the boundary fault separating the Booster Lake and Bernic Lake Formations within structural subareas 4 and 5, particularly the segment from Rush Lake westwards. The area near the faults and the faults themselves, withing reasonable distances from the pegmatitic granites and leucogranites, should be examined.

A minor but locally important fault and shear system different from the above is that transecting the Lac du Bonnet batholith boundary at the inlet of Bird River into Lac du Bonnet. Spodumene-bearing Lac du Bonnet pegmatites are hosted by this structure, which extends rather deeply into the greenstone belt, and may hold more dykes of the Lac du Bonnet type, particularly hidden ones.

Inside the greenstone slabs separated by the boundary

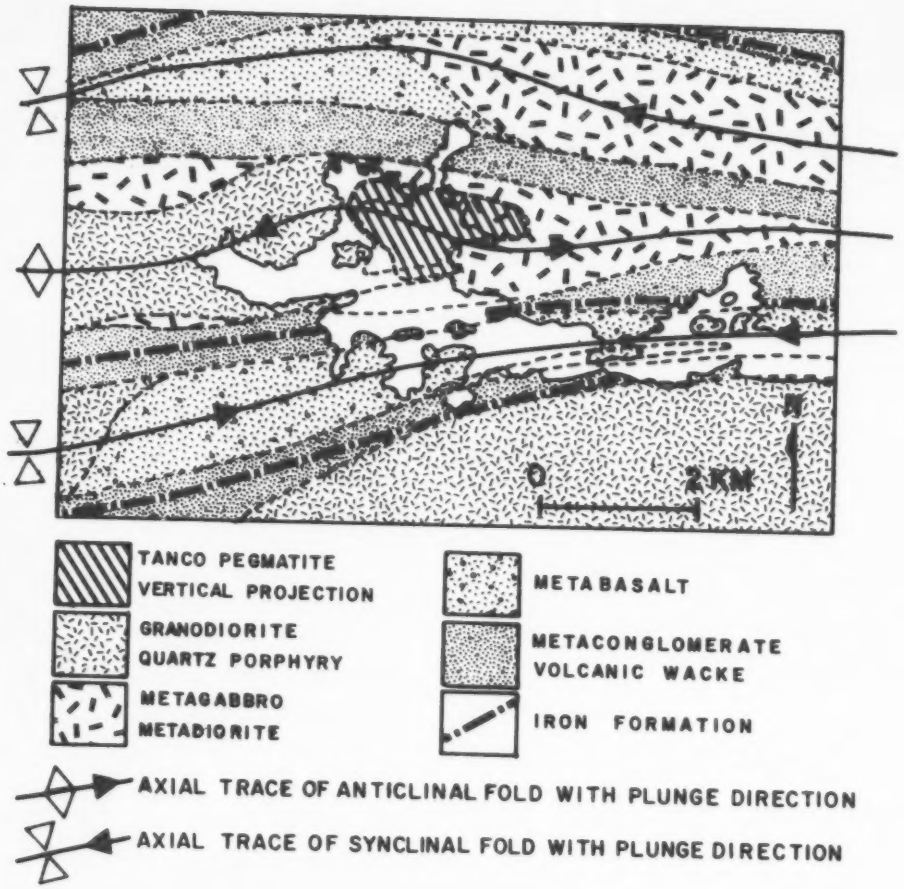

Figure 134: Structural setting of the Tanco pegmatite as an example of a pressure-shadow trap in an anticlinal fold axis at the nose of a subvolcanic intrusive unit (6) enveloped in schistose rocks of the Bernic Lake Formation. From Crouse et al. (1979)

faults, pegmatites are confined to dilated foliation planes and concomitantly opened subhorizontal joint systems. Most pegmatites of the Birse Lake group are an example of foliation-hosted bodies. Bernic Lake group pegmatites penetrate subhorizontal joints subnormal to foliation, and all members of the Rush Lake group that have been drilled in detail consist of both subvertical (foliation-controlled) and subhorizontal (joint-hosted) components.

Particular attention should be paid to the subhorizontal joint systems which host the largest and economic pegmatites of the district, the Bernic Lake group. These joint systems formed, and had the best chance of opening, in pressure shadows developed at major lithological and competency changes along east-trending fold axes, in response to ductility contrast between the adjacent units. Figure 134 shows the Tanco deposit as an example of pegmatite emplacement into this kind of structure.

Thus the areas surrounding eastern and western extremities of the competent subvolcanic intrusions of unit 6 should be examined, both inside and in the enveloping less-competent schists of unit 5 (Maps 1 and 3).

As a concluding note it should be pointed out that the central and western part of the pegmatite district is more promising for exploration than its eastern segment. The eastern area preserved its tight compressed structure without extensive dilation, as shown by rather forceful intrusion of pegmatitic granites. This indicates a lack of structural traps for pegmatites. Furthermore, all pegmatite groups in the district that show asymmetric fractionation trends (shown also by the Osis Lake pegmatitic granite) differentiate westwards, apparently towards lower pressure sites which were not available in the opposite direction. Finally, no significant pegmatite finds have been reported to date from the eastern part of the district.

The Cat Lake-Maskwa Lake district

In this district, major granitic intrusions parental to the pegmatite groups could not be identified and are most probably hidden. Consequently, structural control provides the only guidance for exploration

Two major structures host the pegmatites of the district: the apical-perianticlinal shears and faults which belong to the major fault system related to the Maskwa Lake diapir, and the foliation in the greenstones.

The pegmatites are grouped in two prominent clusters: one of them comprises the pegmatite groups surrounding Cat Lake which intruded along S_2 surfaces; the other is represented by the Maskwa Lake series seated in perianticlinal faults northwest of Donner Lake. Both these clusters are associated with metavolcanics and metasediments of the Rice Lake Group where they are in subvertical contact with the more competent quartz diorites and granites of the Maskwa Lake and Inconnu batholiths. Contrasting ductilities of the greenstones and granitoids may be responsible for strictly localized dilation and consequent clustering of the pegmatites.

On the basis of this information, exploration in this district should be confined to the greenstone belt and to the close vicinity of greenstone-granitoid boundaries. Inside the batholithic bodies, the dilation structures are likely to fade out. Judging from the regional disposition of the greenstones and from the nature of their boundaries with the granitoids, detailed exploration of the known pegmatite clusters and their close surroundings should be recommended rather than other parts of the greenstone belt.

THE WEKUSKO LAKE FIELD

INTRODUCTION

LOCATION, ACCESS, AND TOPOGRAPHY

The Wekusko Lake pegmatite field is located in north-central Manitoba, bounded by latitudes 54°45' north to 54°55' north and longitudes 99°33' west to 99°55' west. The western boundary of the study area lies 6 km east of the town Snow Lake (Map 4).

The area encompasses much of Wekusko Lake through which the Grass River flows, crossing the area from southwest to the northeast. Access to these waterways is provided via paved Provincial Road 392 to Wekusko Falls on the west side of Wekusko Lake, where government-maintained boat launching facilities are located. Access is also provided by float-equipped aircraft which can be chartered at Wabowden 73 km to the east, or at Flin Flon 120 km to the west. An excellent seaplane dock is centrally located at the townsite of Herb Lake on the east side of Wekusko Lake.

Water and swamp cover most of the area. Patchy glacial drift and a thin soil horizon support spruce, jack pine, poplar, alder and isolated stands of birch. Topographic relief ranges to a maximum of 45 metres above the lake level. Outcrop distribution is patchy; best exposures are on long northeast-trending, structurally controlled ridges. The area is drained by the Grass River.

MAP COVERAGE

National Topographic Series maps are available at two scales for the area; 1:250 000 for sheet 63J, and 1:50 000 for sheets 63J/13 and 63J/12. These maps and the accompanying 1:50 000 aeromagnetic maps 2566G and 2565G, are available from either the Map Distribution Office, Ottawa or from the Surveys and Mapping Branch of the Manitoba Department of Natural Resources, 1007 Century Street, Winnipeg.

Claim maps of the area are available at the Mining Recorder's Office in either The Pas or in Winnipeg at 993 Century Street.

Geological maps accompany most of the Geological Survey of Canada and Manitoba Mines Branch reports listed under the "Previous work" section. However, some of the older reports are no longer in print and may not be available.

Vertical airphoto coverage for the entire area is available in both 1 inch = 1 mile (1:63 360) and 1 inch = 1/4 mile (1:15 840) scales. Photos can be obtained from the National Air Photo Library, 601 Booth Street, Ottawa; good quality copies of airphotos can be obtained more rapidly from the Air Photo Library, Surveys and Mapping Branch, Manitoba Department of Natural Resources, 1007 Century Street, Winnipeg.

PREVIOUS WORK AND ECONOMIC DEVELOPMENT

Early regional geological mapping in the area included work by Alcock (1918, 1920) at 1:126 720, Armstrong (1941) at 1:63 360 and Frarey (1950) at 1:63 360. More detailed work included Stockwell's (1937) study on the gold deposits at Herb Lake, and Russell's (1957) structural study of the Snow Lake area which included the eastern part of the present study area. Davies et al. (1962) includes a description of the geology of the area plus a review of the economic development to that time.

Geological reports by Bailes (1971, 1975) on the Snow Lake-Flin Flon-Sherridon area and on the Guay-Wimapedi Lakes area include brief discussions of the regional setting of the Wekusko Lake area. Other reports on the area include work done by Moore and Froese (1972), and a paper delineating metamorphic isograds in the Snow Lake area by Froese and Gasparrini (1975). An unpublished M.Sc. thesis by Shanks (1979), University of Manitoba, describes the Missi Group rocks in the Wekusko Lake area.

To date the economic development of the area has featured the extraction of gold from quartz-filled shear zones in a variety of host rocks. Approximately 60,000 ounces (1 886 018 g) was extracted between 1914 and 1939, mainly from the Laguna (or Rex) Mine (Stockwell 1937, Davies et al. 1962).

Short-term revival of the Ferro Mine property in 1973-74 by Crowduck Bay Mines resulted in the rehabilitation of the 90 tonne mill and some open pit operation.

A small Cu-Ni deposit occurs in gabbro on Rice Island. Other Cu-Ni showings occur in gabbroic rocks in the Wekusko Lake area but to date no production of Cu-Ni has occured.

A number of Cu-Zn type massive sulphide deposits are currently producing in the Snow Lake area a few kilometres west of the present study area. To date no economic massive sulphide discoveries have been made within the study area.

A number of lithium-bearing pegmatite dykes, the Sherritt Gordon, Violet-Thompson and Green Bay dykes, occur within the study area. Although there has been no Li production from these deposits, increased future demand for Li may eventually result in their development.

PRESENT STUDY

No attempt was made to re-map the entire area, in the light of abundant previous regional mapping. Instead, mapping was generally confined to regions of abundant pegmatites. The station location map (Map 5) indicates areas of study, while the geology elsewhere was compiled from earlier workers.

Field mapping and sampling for geochemical analysis was conducted on all pegmatitic granites and their host rocks. In addition, all felsic plutonic rocks were mapped and sampled in an effort to investigate genetic relationships between felsic plutons and pegmatites. These studies led investigators beyond the defined limits of the area but were deemed necessary to develop a realistic understanding of the pegmatite potential of the region.

In addition to general structural observations, detailed 100 feet = 1 inch (1:1 200) maps were produced for the known spodumene-bearing pegmatite dykes; the Sherritt Gordon dykes, the Violet-Thompson dyke, and the largest of the Green Bay dykes.

GENERAL GEOLOGY

REGIONAL SETTING

The Wekusko Lake pegmatite district occurs in the Churchill geological province at the northeastern edge of the Flin Flon Volcanic Belt (Fig. 135). The east-trending Flin Flon Volcanic Belt lies along the southern edge of the 140 km wide, 240 km long, east-trending Kisseynew Sedimentary Gneiss Belt. The Flin Flon Belt, when joined with contiguous volcanic rocks in Saskatchewan and with the northern Lynn Lake Volcanic Belt, is also interpreted as a part of the "circum-Kisseynew volcanic belt" (Sangster 1978). This is believed to be a large volcanic-flanked sedimentary basin feature (Bailes 1975, Sangster 1978).

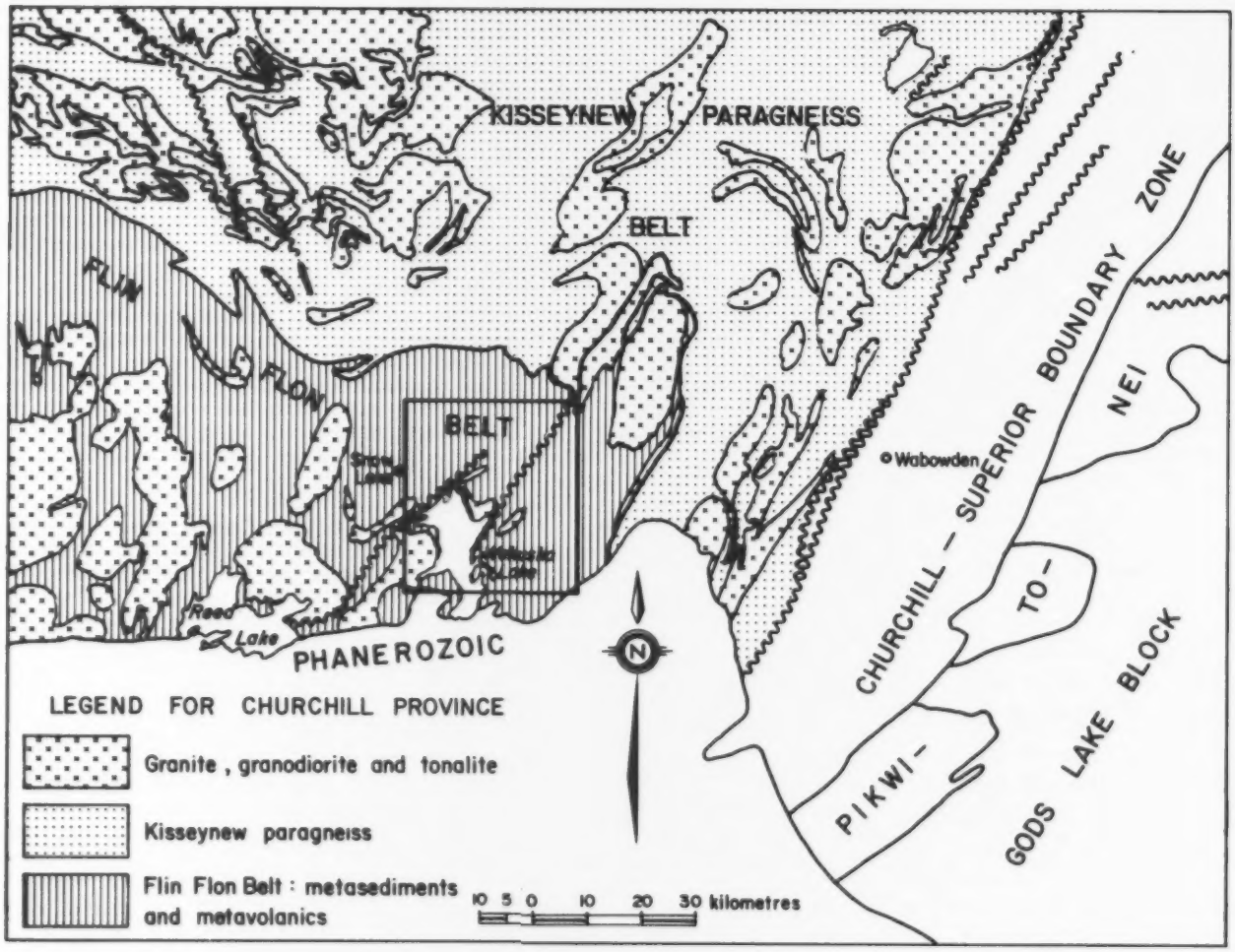

Figure 135: Location of the Wekusko Lake pegmatite field (black rectangle) at the southeast boundary of the Churchill Province. Schematized from the Geological Map of Manitoba, Map 79-2

TABLE 71. STRATIGRAPHY OF THE WEKUSKO LAKE PEGMATITE FIELD

Layered sequence	Intrusive rocks	Metamorphism	Deformation	Structure
	LATE TECTONIC: (W) pegmatitic granites, pegmatites; (U,V) Wekusko and Tramping Lake granites; (T) Stuart Lake plutonic complex; (S) Rex granite; (R) Lake granodiorite; (Q) plutonic diorite; (P) complex: gabbro		D_5	F_5
		M_2	D_4(?)	F_4(?)
			D_3	F_3
	SYNTECTONIC: Crowduck Bay gneiss dome: (O) diatexite to anatexite; (N) migmatitic paragneiss (relative age uncertain)	M_1	(diapirism)	
	(M) Crowduck Bay and Herb Bay gneissic quartz diorite		D_2	F_2
	(L) Broad Bay granite-granodiorite		D_1	F_1
MISSI: (E) mixed dacitic-rhyodacitic fragmentals, brecciated flows; (D) basaltic to andesitic flows, subordinate rhyolite; (C) meta-arkose, metagreywacke, quartzite, metaconglomerate	SYNVOLCANIC: (K) felsic quartz and/or feldspar porphyry, partly extrusive; (J) biotite dacite, subporphyritic feldspar + biotite dacite, felsic biotite schist			
UNCONFORMITY				
AMISK: (B) metabasalt flows and fragmentals, reworked tuffs; (A) metagreywacke, meta-argillite, metasiltstone, tuff				

DION LAKE AREA

(pre- to syntectonic gneisses of uncertain origin, possibly derived from Missi and Amisk groups)

- (H_B) porphyritic gneissic granodiorite
- (H_A) meta-arkose to metagreywacke paragneiss
- (G) quartzofeldspathic grey gneiss
- (F) subporphyritic granodioritic biotite gneiss

A steep metamorphic gradient from greenschist to upper amphibolite facies occurs across the northern edge of the Flin Flon Volcanic Belt with grade increasing towards the Kisseynew Sedimentary Gneiss Belt (Froese and Gasparrini 1975; Bailes and McRitchie 1978).

STRATIGRAPHY, INTRUSIVE ROCKS, AGE RELATIONSHIPS

The history of the development of the stratigraphic succession of the region is not described here, as it is tabled in detail by Russell (1957), Davies et al. (1962), and Bailes (1975). Table 71 presents the general relationships in the study area.

Layered rocks within the Wekusko Lake pegmatite fields consist of three groups: an early mafic volcanic-sedimentary sequence termed the Amisk Group (Frarey 1948), a later sedimentary-volcanic sequence termed the Missi Group, and a paragneissic to migmatitic group at Dion Lake. The names Amisk and Missi were first used by Bruce (1918) for rocks in the Flin Flon district and were used to describe similar rocks in the Snow Lake area by later workers such as Frarey (1949), Bailes (1971, 1975), and Shanks and Bailes (1977). The relationship of the Dion Lake gneisses to the Amisk and Missi Groups is uncertain.

Intrusive rocks comprise synvolcanic intrusions associated with the Missi Group, and several generations of post-volcanic intrusions of varied composition and relative age. Among the post-volcanic intrusions, the Crowduck Bay gneiss dome, three bodies of gneissic quartz diorite, and the Broad Bay granitoids comprise a syntectonic group. The Rex Lake complex, followed by the Wekusko and Tramping Lake granites, are late-tectonic. Among the latest intrusions identified in the area are the pegmatitic granites and pegmatites.

Rb-Sr whole-rock isochron ages ranging from 1.820 to 1.699 Ga have been reported from the Flin Flon and Kisseynew Belts (Anderson 1974, Josse 1974, Clark et al. 1974). Massive sulphide deposits in the Flin Flon Belt also yield an average age of about 1.822 Ga (Sangster 1978).

The following sections describe individual units as observed during the Project, taking into consideration the data of earlier authors. Sequence of units generally follows from the oldest to the youngest.

AMISK GROUP

The Amisk Group rocks occur along the northeast edge of the area of study, around the edges of the Wekusko granite and the

Rex Lake pluton, and north of Herb Bay (Map 4). These rocks are believed to be the oldest in the area (Frarey 1948). They comprise metavolcanic and metasedimentary rocks which exhibit a northerly increase in metamorphic grade (Froese and Gasparrini 1975).

Amisk metasediments (A)

Amisk Group metasedimentary rocks appear to underly the volcanic sequence west of Roberts Lake (Frarey 1949) but to the east, near Snow Lake, they overlie the volcanics in most places (Froese and Moore, pers. comm. 1978).

The metasediments are thought to have been derived from argillite, greywacke and tuff. They are now metamorphosed to fine- to medium-grained (0.5-4 mm) garnetiferous feldspar -biotite schist and minor staurolite-sillimanite schist (Frarey 1950). Sedimentary rocks northeast of Crowduck Bay, between the Amisk volcanics and the Grass River, were originally assigned to the lower Missi Series by Frarey (1950) but were included in the Amisk Group by Bailes (1971) and Shanks and Bailes (1978), as shown on the compilation map accompanying this report (Map 4). These rocks consist of interlayered fine grained (0.2 - 0.8 mm) to medium grained (1 - 3 mm) feldspar + quartz + (muscovite) gneiss and feldspar + quartz + biotite + (garnet) biotite schist, plus very fine grained (0.1 - 0.5 mm) metasediments consisting predominantly of quartz and muscovite. They are interpreted to be metagreywacke, metasiltstone and meta-arkose, and they include some metachert or very fine grained quartzite. These units have been collectively termed turbidites by Bailes (1971).

Amisk metasediments in the Herb Bay region and along the edges of the Rex and Wekusko plutons consist of fine grained (0.1 - 0.7 mm) dark grey metasiltstone, meta-argillite and metagreywacke, some of which may be volcanogenic and contain scattered lapilli-sized fragments. Graded bedding and cross-bedding are often visible in shoreline outcrops with beds 1 cm to 2 metres thick. North of Herb Bay where higher grade metamorphism has occurred (Froese and Gasparrini 1975), these rocks have lost their primary features and have become staurolite-biotite schists or sillimanite-garnet schists and gneisses.

Chemical compositions of Amisk metasediments and gneisses (Table 72, Fig. 136) compared to the mean composition of principal sandstone classes and average sandstone (Pettijohn 1963, Pettijohn et al. 1972) resemble average greywackes most noticeably in their high Al_2O_3 content (12-17.5%). This anomalously high Al_2O_3 content may be due to the high clay content in poorly sorted sediments.

The contents of Sr vary within the range typical of Precambrian greywackes (Peterman et al. 1967) but the Rb contents are distinctly lower (except a single sample) and consequently the K/Rb ratios are high, in the range of 350 to 600.

The Fe^{2+} content is greater than that of Fe^{3+} for all the Amisk metasediments, similar to Pettijohn's average greywacke composition, except for the two samples east of the Grass River (PW136-1 and PW185-1). These two samples are located near the stratigraphic top of the Amisk, close to the Amisk-Missi unconformity (Bailes 1971, Froese and Moore, in press), and may have been exposed to near-surface weathering longer than sediments lower in the section. The total iron oxide content of the Amisk rocks ranges from approximately 5 to 9%.

The mafic layer (PW297-2) in the Amisk gneisses along the western shore of the Crowduck Bay gneiss dome, has a composition very similar to both diabase dykes and olivine basalts (Carmicheal, Turner, and Verhoogen 1974, Tables 9-10, and 9-12).

Amisk metavolcanics (B)

Rocks classified as Amisk metavolcanics occur mainly in the northeastern part of the region, north of Roberts Lake, and in a small patch south of Dion Lake.

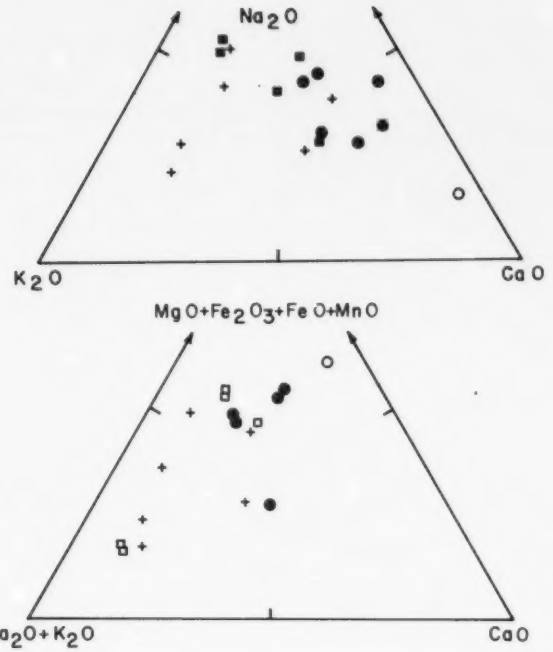

Figure 136: Compositional characteristics of the Missi (squares), Amisk (dots) and Dion Lake gneissic (crosses) metasediments

These rocks consist mainly of dark green to black, fine- to medium-grained pillowed andesitic and basaltic flows with some flow breccia, tuff, and volcaniclastic metasediments. Some mafic flow rocks grade into "coarse grained structureless dioritic bodies of irregular outline" (Frarey 1950).

The mafic volcanic rocks southeast of Dion Lake consist of a heterogeneous assemblage of fine grained black amphibolite and garnetiferous biotite schist with leucocratic stringers and calc-silicate knots. Some outcrops contain layered amphibolite and light grey tuffaceous metasediments.

The pillow structures, which are abundant north of Roberts Lake, suggest a submarine environment whereas the presence of fragmental rocks and volcanogenic metasediments suggest that this marine environment may have been shallow to emerging.

MISSI GROUP

The Missi Group consists of a series of metasedimentary and metavolcanic rocks which unconformably overlie the Amisk Group (Bailes 1971). The unconformity is suggested in the Snow Lake region by the fact that Missi rocks lie on diverse rocks of the Amisk Group (Froese and Moore, pers. comm. 1978), plus the large amount of volcanic detritus in the Missi conglomerate beds (Shanks and Bailes 1977).

Missi metasediments (C)

The lower Missi Group rocks east of Wekusko Lake consist of a thick, monotonous sequence of fine- to medium- and medium- to coarse-grained sandstone, predominantly sub-greywacke in composition with a number of polymictic conglomerate beds (Shanks and Bailes 1977). Crossbedding is the main primary feature preserved in the Missi metasediments.

The metasediments farther to the north, along the eastern shore of Crowduck Bay, are separated from the main body of the Missi sediments by the Missi volcanic sequence. These Missi metasediments, containing abundant pegmatite dykes, consist of more pelitic metasandstone, meta-subarkoses, and meta-greywackes.

TABLE 72. REPRESENTATIVE CHEMICAL ANALYSES OF THE METASEDIMENTS AND GNEISSES (A, B, C, D, F, G, H)

	Amisk		Missi		Dion Lake gneisses			D.L. in situ pgs.	
	136-1	279-1B	210-1	221-1	308-1	344-1A	2151-1	334-1C	350-3
SiO_2, wt.%	73.00	62.55	67.05	73.50	71.90	71.40	70.40	74.70	76.90
Al_2O_3	12.46	17.38	14.48	14.58	13.84	12.10	14.58	12.10	12.68
TiO_2	0.51	0.45	0.53	0.11	0.59	0.50	0.32	0.25	0.02
Fe_2O_3	3.11	0.71	5.21	1.16	0.84	3.30	1.29	2.40	0.33
FeO	1.72	4.92	0.72	0.56	1.36	1.40	1.72	0.48	0.08
MnO	0.07	0.06	0.08	0.02	0.03	0.06	0.05	0.03	0.04
MgO	1.12	2.65	2.59	0.15	0.55	1.93	1.27	0.62	0.07
CaO	2.48	3.02	2.18	1.08	1.38	1.28	2.84	1.04	0.12
Na_2O	3.05	3.73	2.92	4.58	2.53	1.50	3.72	2.20	1.25
K_2O	1.38	2.11	2.22	3.11	5.01	4.32	3.22	4.38	8.08
P_2O_5	0.12	0.15	0.16	0.04	0.12	0.07	0.10	0.01	0.01
CO_2	0.12	0.65	0.36	0.77	0.47	0.24	0.05	0.77	0.07
H_2O	0.61	1.73	1.28	0.69	0.94	1.46	0.60	1.09	0.30
	99.75	100.10	99.78	100.35	99.56	99.56	100.16	100.06	99.94
Li, ppm	35	60	38	18	26	37	44	18	5
Rb	31	36	52	60	80	80	83	72	102
Cs	0.6	1.7	2.1	1.6	0.6	1.1	3.4	0.8	0.8
Be	1.4	0.8	1.3	1.0	1.0	0.7	1.4	1.3	0.3
Sr	321	428	238	125	260	275	181	201	345
Ba	436	903	605	1030	796		832	1458	3047
Pb	3	3	3	6	7	13	5	6	11
Ga					29				13
U	1	nd*	nd	2			1		
Th	nd	nd	nd	nd			nd		
Zr	131	99	134	150	262		187	347	240
Hf									
Sn	nd	1	2	2	3		9	3	9
K/Rb	371	486	354	430	520	449	322	506	658
K/(Cs x 100)	192	103	88	161	693	326	78	455	839
K/Ba	26	19	30	25	52		32	25	22
Ba/Rb	14	25	11.6	17.2	9.9		10	20	30
Ba/Sr	1.4	2.1	2.5	8.2	3.1		4.6	7.3	8.8
Rb/Sr	0.1	0.08	0.2	0.5	0.3	0.3	0.5	0.4	0.3
Mg/Li	194	267	411	50	127	314	175	206	80
Zr/Sn	-	99	67	75	87		21	116	27
Zr/Hf									
Al/Ga					2524				5162

* not detected

Of the six Missi metasediments analyzed chemically, four come from the pegmatite-bearing northern metasediments and two from the Hat Lake region (Table 72, Fig.136). The compositions are similar to the mean composition for greywackes (Pettijohn 1973) but they are more silicic, less aluminous and calcium-poor, particularly in comparison with the Amisk sediments which are relatively alkali- and Mg-poor but iron -rich in comparison. Normal Sr and low Rb contents are characteristic of the Missi sediments, as is the relatively stable K/Ba ratio and variable Mg/Li, Ca/Sr, Ba /Sr and Fe/Mn ratios.

Missi metavolcanics (D)

The volcanic assemblages occupying the syncline between Wekusko Lake and Stuart Lake overlies the surrounding Missi metasediments (Shanks and Bailes 1977). These rocks consist of interlayered mafic to felsic flows, fragmentals, laminated cherts and greywackes. The lack of pillow structures in the flow rocks differs from the older, pillowed Amisk lavas and suggests a subaerial depositional environment for the Missi lavas (Frarey 1950, Shanks and Bailes 1977). A single analysis of a felsic flow rock (PW149-1) yields a rhyolite composition with a high K/Rb ratio of 434.

Andesites and dacites (E)

This unit occurs on the north shore of Puella Bay, on the south shore of Goose Bay, and in a lens northeast of Herb Lake townsite. It consists predominantly of mixed lapilli to block-sized fragmentals, flow breccia and quartz-eye crystal tuff, which are composed of light grey to greenish, biotite-bearing dacite to andesite. These rocks may be in part subvolcanic intrusions, in which case they are transitional with units J or K.

A single chemical analysis from the north shore of Puella Bay, PW131-1, yields a tholeiitic andesite bulk composition (Irvine and Baragar 1971) with typical trace contents.

DION LAKE AREA

Pre- to syn-tectonic gneisses of uncertain age occur outside the defined area of study, and comprise only a few per cent of the total rocks in the Wekusko Lake field. However, they have been included in the present study because of their spatial association to pegmatites in the Dion Lake area, and because of the differences between these gneisses and the surrounding Amisk and Missi metasediments.

Granodioritic gneiss (F,G)

Unit F consists of medium grained (2-5 mm) pink to grey, subporphyritic biotite granodiorite gneiss, and unit G of a medium grained (2-4 mm) quartzo-feldspathic biotite gneiss. Both units look igneous in hand specimen but are layered in outcrop due to subtle compositional and grain size variations in the latter. Unit F occurs interlayered with and in part underlies Amisk metavolcanic rocks south of Dion Lake. Unit G displays similar interlayered relationships to mafic Amisk rocks south of Dion Lake. The high grade metamorphism and coarse recrystallization in the area south and east of Dion Lake has obliterated primary sedimentary features.

The intimate interlayering between these gneisses and metavolcanic rocks suggests a possible volcanogenic origin for the gneisses. This is supported by a single whole rock analysis of unit G (PW308-1; Table 72) sampled immediately south of Dion Lake, which is almost identical to the average compositions of rhyolite (Carmichael et al. 1974 after Nockolds 1954).

Paragneiss (H)

This unit is observed in two separate localities, east of Dion Lake and northwest of Godkin Lake. It has a varied composition. East of Dion Lake it comprises a light pink to greyish, fine- to medium-grained (0.5-4 mm), two feldspars + quartz + biotite + hornblende (+ chlorite + magnetite + garnet) meta-arkosic to metagreywacke paragneiss. Northwest of Godkin Lake it occurs as a reddish-pink, medium grained (1-4 mm), inhomogeneous, slighly porphyritic, two-feldspars + quartz + biotite + hornblende gneissic granodiorite with up to 5% K-feldspar porphyroblasts up to 1 cm across. This porphyroblastic gneissic granodiorite may be the higher metamorphic grade equivalent of the paragneisses east of Dion Lake. Mapping by Bailes and Malyon (1976) indicates that the unit east of Dion Lake trends southwestward (off the Saw Lake sheet) towards Godkin Lake, suggesting a possible continuation.

Whole rock analysis of a single sample from east of Dion Lake (PW344-1A) and of two samples northwest of Godkin Lake (PW2151-1 and PW2152-1a) do not strongly support the above suggestion as the Godkin Lake samples display higher Al_2O_3, Na_2O, and CaO, and slightly lower total Fe (Table 72, Fig. 136). However, considering the distance of separation and the possible higher metamorphic grade of the Godkin Lake rocks, the compositional difference is not prohibitive of a single source for both rocks. On the other hand, the western Godkin Lake porphyritic gneiss may be a separate unit nor related to the paragneiss east of Dion Lake.

In relation to the Amisk and Missi metasediments, the Dion Lake gneisses are more closely related to the Missi Group but they are distinctly more potassic than both Missi and Amisk. On the other hand, the K/Rb, K/Ba, and Ca/Sr ratios remain about the same in all three units.

SYNVOLCANIC INTRUSIONS

Biotite dacite (J)

This unit occurs as an irregular band along the northwest edge of the Missi metavolcanic series (Map 4). Intrusive relations with Missi metasediments were observed by Frarey (1950). The unit comprises a dark grey, fine grained (0.5 - 1.0 mm) feldspar + quartz + biotite + muscovite (+ pyrite) schist which grades into biotite dacite, with 2 - 4 mm pink feldspar crystals comprising <1% to 10% of the rock. The biotite content ranges from 4% to 12% indicating considerable heterogeneity within the unit. Locally up to 50% lithic fragments of crystal tuff were observed near Percy Lake, suggesting a possible extrusive fragmental or intrusive breccia genesis, in part.

A single whole rock analysis PW-239-1 (Table 73) reveals a composition comparable to a tholeiitic dacite (Irvine and Baragar 1971).

Field relations, together with physical and chemical resemblance to volcanic rocks, suggest a subvolcanic genesis for some parts of this unit, whereas other segments appear to be extrusive.

Dacite to rhyodacite porphyry (K)

This unit occurs in two main bodies, one northwest of Lost Frog Lake and another north of McCafferty Lake, and as numerous small dykes and intrusions into Missi rocks east of the Grass River. The rock is a light tan to light grey, very fine grained (0.1 - 0.5 mm) feldspar + quartz dacite porphyry; quartz eyes, ranging from 1 to 7 mm, compose generally 2-5% of the rock, and up to 12% locally.

Feldspar phenocrysts, which are 1-4 mm in size, compose 1-5% of the rock and occur both with and without quartz eyes. Locally biotite composes 8% of the rock, occurring as 1-3 mm-long flakes defining foliation. Along the northeast edge of the main body west of McCafferty Lake the rock consists of light grey subrounded and slightly tectonically flattened quartz eyes in a fine grained dacite matrix.

On the northeastern shore of Lost Frog Lake possible fragments are visible in water-worn outcrops. Minor occurrences such as these suggest that Unit K may be in part extrusive, despite its overall intrusive nature.

Whole rock analysis of five samples from three different bodies of Unit K (Table 73) indicate a composition between average rhyolite and average dacite as reported by Carmichael et

TABLE 73. REPRESENTATIVE CHEMICAL ANALYSES OF THE SYNVOLCANIC INTRUSIONS (J, K)

	Bio. dacite	Dacite to rhyolite porphyry				
	239-1	83-2	86-1	241-1	242-1A	239-2
SiO_2, wt.%	59.25	77.20	73.10	61.50	71.55	73.75
Al_2O_3	15.62	13.40	13.36	14.70	14.34	13.50
TiO_2	0.71	0.20	0.27	0.71	0.26	0.18
Fe_2O_3	1.27	1.04	1.87	1.09	0.53	0.67
FeO	4.10	2.24	1.32	3.46	1.26	0.48
MnO	0.10	0.04	0.04	0.08	0.03	0.04
MgO	2.65	0.50	0.35	2.55	1.00	0.34
CaO	4.62	1.23	1.38	4.35	1.48	1.57
Na_2O	4.75	5.10	3.08	3.42	3.75	5.93
K_2O	2.45	1.41	3.68	2.72	3.49	1.27
P_2O_5	0.31	0.03	0.02	0.31	0.12	0.08
CO_2	2.51	1.64	0.33	3.02	0.87	1.16
H_2O	1.33	0.68	0.74	1.73	1.02	0.56
	99.67	99.71	99.54	99.64	99.70	99.59
Li, ppm	26	18	21	36	15	5
Rb	53	36	86	53	52	19
Cs	1.8	1.4	5.5	1.8	1.1	0.3
Be	1.0	1.2	2.8	1.2	1.3	1.1
Sr	245	201	102	235	169	181
Ba	950	480	954	785	939	664
Pb	7	4	3	3	6	7
Ga						
U	nd*	nd	5	nd	2	3
Th	nd	nd	nd	nd	nd	nd
Zr	182	295	257	173	150	141
Hf		7	7	1	3	nd
Sn	4					
K/Rb	383	325	354	426	558	553
K/(Cs x100)	113	84	55	126	264	350
K/Ba	21	40	4	29	31	16
Ba/Rb	18	13.3	11	15	18	35
Ba/Sr	3.9	2.4	9.4	3.3	5.6	3.7
Rb/Sr	0.2	0.18	0.8	0.2	0.3	0.1
Mg/Li	615	167	100	428	400	420
Zr/Sn	46	42	37	173	50	-

* not detected

al. (1974). All the subvolcanic bodies display the same primitive geochemistry as the associated metavolcanics, except for a single rhyolitic composition (PW-83-2) which shows somewhat advanced fractionation in terms of K/Rb, K/Ba and Ca/Sr.

SYNTECTONIC INTRUSIONS

Broad Bay granitoids (L)

This unit occurs on the east side of Wekusko Lake, along the south shore of Broad Bay. It consists of a fine- to medium-grained plagioclase + K-feldspar (0-10%) + quartz (15-20%) + (biotite + muscovite) (2-14%) granodiorite to granite. Compositional variation is local and related to the amount and type of included material, and to the intensity of alteration (to be discussed in a later section). Unit L displays considerable fracturing and brecciation of early formed igneous plagioclase. Elongation of biotite and quartz varies from moderately to well developed. Inclusions of mafic lava and biotite schist country rocks are abundant in brecciated contact zones, but also occur internally in patches.

Crowduck Bay and Herb Bay gneissic quartz diorites (M)

This unit occurs in three bodies, each up to several kilometres long: one northeast of Crowduck Bay, one southwest of Crowduck Bay and another north of Herb Bay (Map 4). All units are elongate in the northwest direction.

The rock consists of a fine- to medium-grained (0.5-4 mm), inhomogeneous feldspar +quartz (10-20%) + (biotite + hornblende) (7-15%) gneissic quartz diorite. Gneissosity is defined by biotite and hornblende smears, elongate mafic inclusions and grain size variations across foliation.

Thin section study reveals a partly recrystallized igneous granular texture with preserved oscillatory zoning of plagioclase suggesting an igneous origin (Emmons 1953). Optically determined plagioclase compositions indicate normal zoning with compositions An_{38} to An_{35}.

A representative chemical analysis, shown in Table 74, and additional data indicate a fairly homogeneous composition, the main variable being the SiO_2 content. The trace elements also conform to the monotonous pattern of the major elements, displaying low Rb and Sr but high Ba.

Crowduck Bay gneissic dome (N,O)

This unit forms a structural dome, 3 x 15 km in size at the present erosion surface, trending northeast of the study area (Map 4). A strong northeast-trending gneissosity parallel to the elongation of the body suggests an emplacement of the dome during a strong northeast-directed tectonism. The contacts of the dome are everywhere swamp- or drift-covered but the outward-dipping gneissosity and foliation imply that the gneiss dome is structurally underlying Amisk rocks to the northwest.

The dome consists of a quartz-dioritic to granitic gneiss with minor schist layers and widespread, locally abundant clots and stringers of pegmatitic material. A transition into a non-gneissic, intrusive-like granite (unit 0) can be observed towards the centre of the dome.

The main non-migmatitic rock type consists of pinkish tan to greyish-pink, fine- to medium-grained (0.2 - 3 mm), 2-feldspars + quartz (23 - 57%) + biotite + hornblende (+ magnetite + garnet) gneiss with minor biotite + hornblende schist layers. Non-zoned plagioclase ranges from An_{37} to An_{16} in the granitic material but from An_{37} to An_{31} in the hornblende + biotite schist layers. Frequent alterations of garnetiferous and garnet-free layers are observed. The overall textural character of the rock is paragneissic.

In accord with modal analyses, the chemical composition of the gneiss is uniformly high in silica but with peculiar reciprocal variations in Na_2O and K_2O combined with a narrow range of randomly variable CaO (Figs. 137 and 138). Rb/Sr and Ca/Sr decrease with increasing SiO_2; Ba/Rb and K/Ba ratios show rather restricted scatter but the K/Rb ratio displays a wide range of values (Fig. 139). In general, the gneiss has compositions between Pettijohn's (1963) average arkose and average greywacke. The high SiO_2 and low total Fe, CaO, MgO and TiO_2 are close to the arkose, the high Al_2O_3 corresponds better to the greywacke; Na_2O is excessive for both.

The compositional characteristics represented in Table 75 compare closely with the data for unit C3 of Bailes (1975, Table 6) - the pink granitoid oligoclase-quartz-microcline gneiss of the Herblet Lake gneiss dome complex. A comparison of the present data with the composition of some of the Missi volcanogenic metasediments described above (unit C) also supports the possibility of their material identity (Bailes 1975). The trace elements distribution in the two rock groups quantitatively supports such a relationship even more distincly than the bulk compositions. The latter seem to be changing systematically, and slightly, in the gneiss dome but in a haphazard manner over a wider range in the Missi sediments.

As to the nature of the sedimentary material, Bailes (1980) suggests that gneisses of his (1975) type C3 are derived from felsic ash flows. The bulk compositions of the Crowduck Bay gneisses support this interpretation. They are close to calc-alkalic rhyolites (Nockolds 1954) and to a rhyolitic ignimbrite quoted by Pettijohn et al. (1972). The highly variable K/Na ratio, the relatively high Sn and low Zr contents, and U>Th also suggest rhyolitic origin, despite the low degrees of Rb and Cs accumulation which is, as mentioned earlier, characteristic of all rock units in the Wekusko Lake area.

Leucocratic pegmatite material, in concordant bands and diffuse schlieren as well as in crosscutting stringers, is composed of 2 feldspars + quartz + subhedral magnetite (up to 1 cm in size). The orientation of the pegmatitic bands is generally controlled by the northeast-trending fabric in the host gneiss although some penetrate cross-shears. The most common orientation of these local crosscutting veinlets is approximately northwest, with accompanying dextral offset on mafic layers in gneiss. Compositionally, the leucocratic material varies from potassic to sodic in its feldspar composition, and a similar variability is suggested for the intrusive-looking granitoid material in the core of the dome. This range is well within the compositional range of the host gneiss, and the same is true for the trace elements (Figs. 137-139). All this points toward local derivation of the pegmatitic- and granitic-looking components by recrystallization with no appreciable fractionation.

The mafic layers carry hornblende and biotite in variable proportions. Their chemical composition, in terms of both major and trace elements, resembles those of basalts modified to variable extent by alkali metasomatism from the enclosing gneisses. The mafic layers are very similar to analogous units in Amisk gneisses to the northwest, and they may represent lavas or dykes in the original sediments.

LATE-TECTONIC INTRUSIONS

Major late-tectonic intrusions are represented by the Rex Lake and Stuart Lake plutonic complexes, and by the Wekusko and Tramping Lake granites. Pegmatitic granites and pegmatites seem to be the youngest intrusions.

Rex Lake plutonic complex (P, Q, R, S)

The multiphase Rex Lake intrusion is a roughly circular body approximately 8 km in diameter located close to the centre of the study area (Map 4). Contacts with country rocks, Amisk metasediments and metavolcanics are marked by a zone of brecciation with numerous rafts and fragments of the Amisk lithologies enclosed and partly digested. The four units defined in this pluton correspond to individual intrusive phases: gabbro, diorite to quartz-diorite, granodiorite, and granite, respectively.

The earliest phase, unit P, is a black to dark grey, medium- to coarse-grained (3-8 mm) plagioclase (An_{48}-An_{35}) + hornblende + (pyroxene) + biotite + quartz (0-5%) gabbro and porphyritic

TABLE 74. REPRESENTATIVE CHEMICAL ANALYSES OF THE GNEISSIC QUARTZ DIORITE (M)

	106-1	108-1	110-1A
SiO_2, wt.%	66.70	66.50	68.30
Al_2O_3	14.62	14.82	14.84
TiO_2	0.54	0.39	0.42
Fe_2O_3	1.40	1.56	1.02
FeO	4.84	4.40	3.56
MnO	0.09	0.08	0.07
MgO	1.38	1.52	1.22
CaO	3.75	3.78	3.25
Na_2O	2.90	3.22	3.30
K_2O	2.38	2.12	2.68
P_2O_5	0.13	0.13	0.09
CO_2	0.05	0.10	0.17
H_2O	0.94	1.02	0.79
	99.76	99.76	99.71
Li, ppm	50	40	31
Rb	46	42	47
Cs	2.0	1.3	1.0
Be	1.0	1.2	1.0
Sr	158	168	168
Ba	841	944	908
Pb	4	3	3
Ga	14		
U	4	5	1
Th	nd*	nd	nd
Zr	143	135	139
Hf			
Sn	nd	1	nd
K/Rb	430	419	472
K/(Cs x 100)	99	135	222
K/Ba	24	19	24
Ba/Rb	18.3	22	19.3
Ba/Sr	5.3	5.6	5.4
Rb/Sr	0.3	0.25	0.3
Mg/Li	166	230	239
Zr/Sn	-	135	-
Zr/Hf			
Al/Ga	5521		

* not detected

TABLE 75. REPRESENTATIVE CHEMICAL ANALYSES OF THE CROWDUCK BAY GNEISSIC DOME (N, O)

	Gneisses		Leuco-layers		"Granitic" core		Mafic layers	
	79-2a	35-1	28-3	79-2B	293-1B	295-1	152-2	296-1
SiO_2, wt.%	77.50	73.75	73.45	77.80	66.25	77.90	47.35	48.10
Al_2O_3	12.80	14.90	14.52	12.04	15.10	12.14	17.20	14.00
TiO_2	0.08	0.12	0.03	0.10	0.26	0.07	0.88	1.01
Fe_2O_3	1.00	1.00	0.96	1.22	1.26	0.72	2.81	4.43
FeO	0.44	0.40	0.20	0.18	3.80	0.50	8.52	10.70
MnO	0.01	0.02	0.03	0.001	0.12	0.01	0.23	0.28
MgO	0.26	0.28	0.27	0.16	2.75	0.18	6.90	5.15
CaO	2.53	1.58	1.88	2.13	3.40	2.45	8.70	10.74
Na_2O	4.43	4.15	3.45	4.62	3.23	4.00	2.73	2.48
K_2O	0.45	3.15	4.40	0.49	1.72	0.78	2.20	0.50
P_2O_5	0.02	0.02	0.04	0.10	0.07	0.02	0.15	0.22
CO_2	0.02	0.09	0.17	0.07	0.48	0.11	0.26	0.46
H_2O	0.20	0.54	0.48	0.19	1.31	0.39	1.79	1.81
	99.70	100.00	99.87	99.10	99.75	99.18	99.72	99.88
Li, ppm	6	19	14	8	17	7	42	8
Rb	22	72	48	22	28	2	52	2
Cs	0.4	1.4	1.0	0.4	0.6	0.6	0.7	0.4
Be	1.1	0.9	1.3	1.6	0.5	0.8	0.6	0.3
Sr	201	204	204	181	133	158	91	234
Ba	348	1335	1526	399	517	187	515	
Pb	2	5	6	1	5	3	6	6
Ga					17			
U	1	nd*	10	4			nd	
Th	nd	nd	nd	nd			nd	
Zr	137	111	75	157	37	157	81	
Hf								
Sn	4	6	4	1	13	5	nd	
K/Rb	168	363	760	186	511	3250	352	2100
K/(Cs x 100)	92	186	365	102	238	108	261	105
K/Ba	11	20	24	10	28	35	38	
Ba/Rb	15.8	18.5	32	18	18.5	94	9.9	
Ba/Sr	1.7	6.5	7.5	2.2	3.9	1.2	5.7	
Rb/Sr	0.11	0.35	0.23	0.1	0.2	0.01	0.6	0.008
Mg/Li	267	89	114	125	976	157	990	3887
Zr/Sn	34	19	19	157	3	31	-	-
Zr/Hf								
Al/Ga					4700			

* not detected

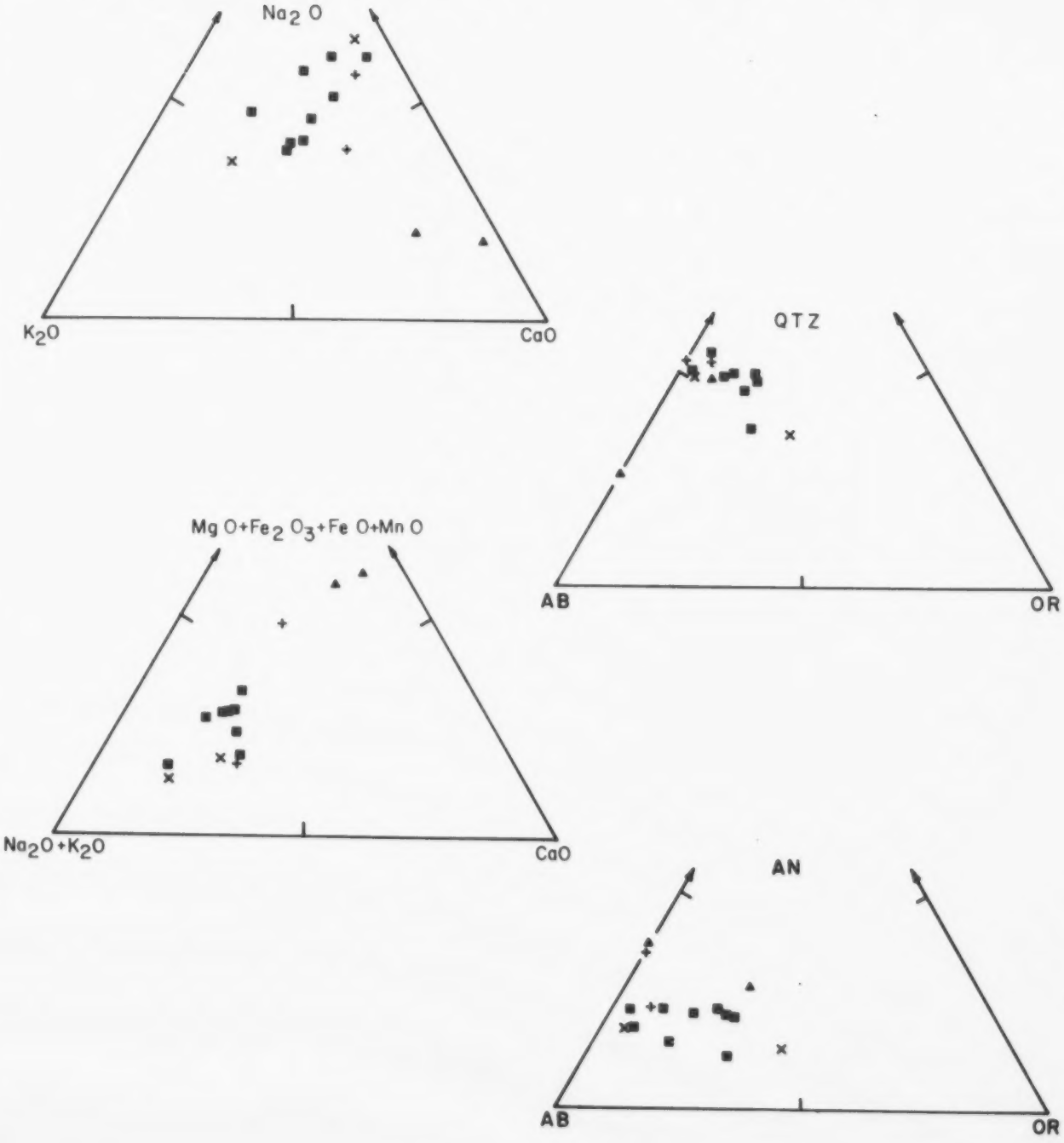

Figure 137: Compositional characteristics of the Crowduck Bay gneiss dome: gneisses (squares), leuco-layers (x), mafic layers (triangles), and granitoid core members (crosses)

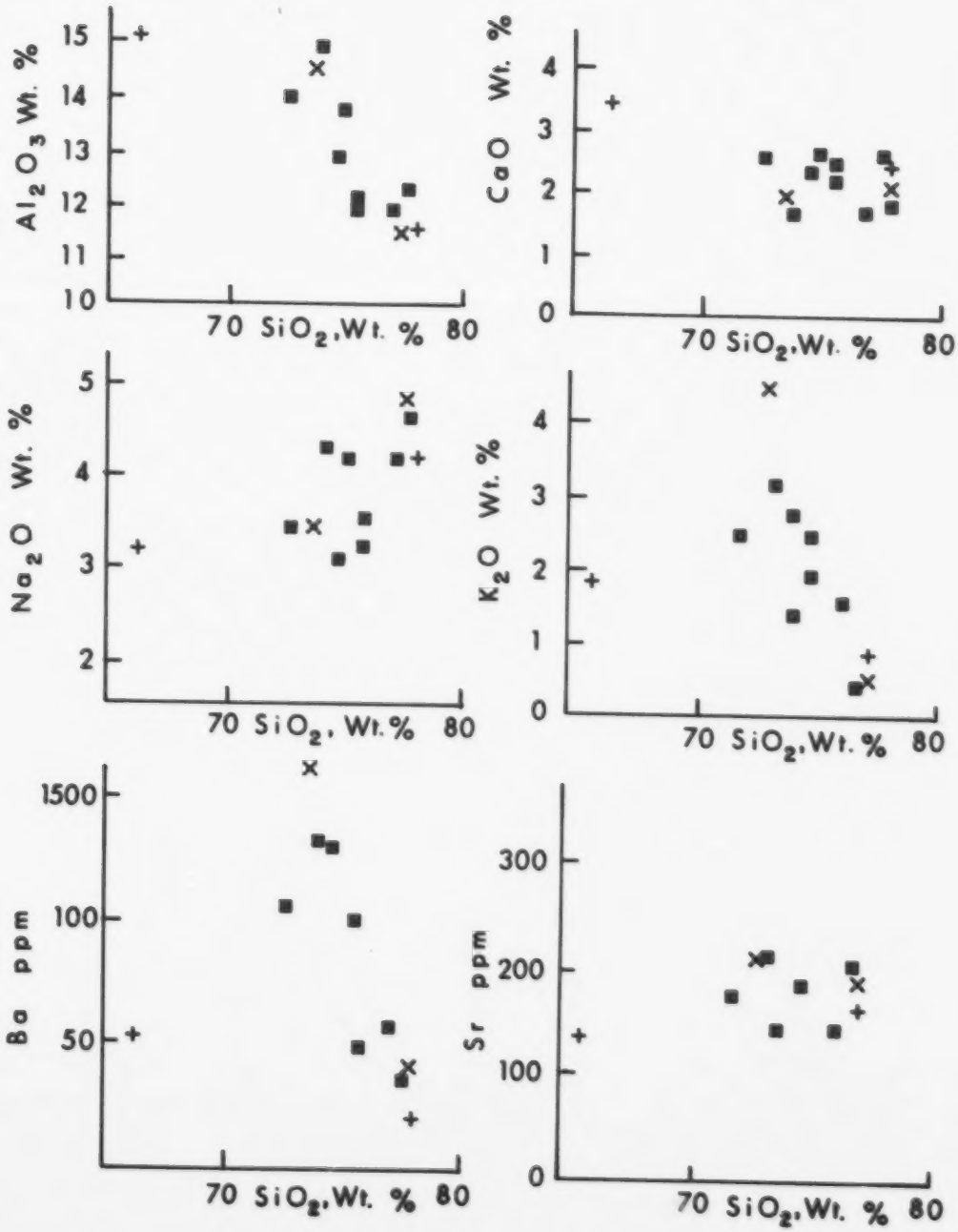

Figure 138: Selected major and trace element contents of the Crowduck Bay gneiss dome plotted against SiO_2. Symbols as in Figure 137

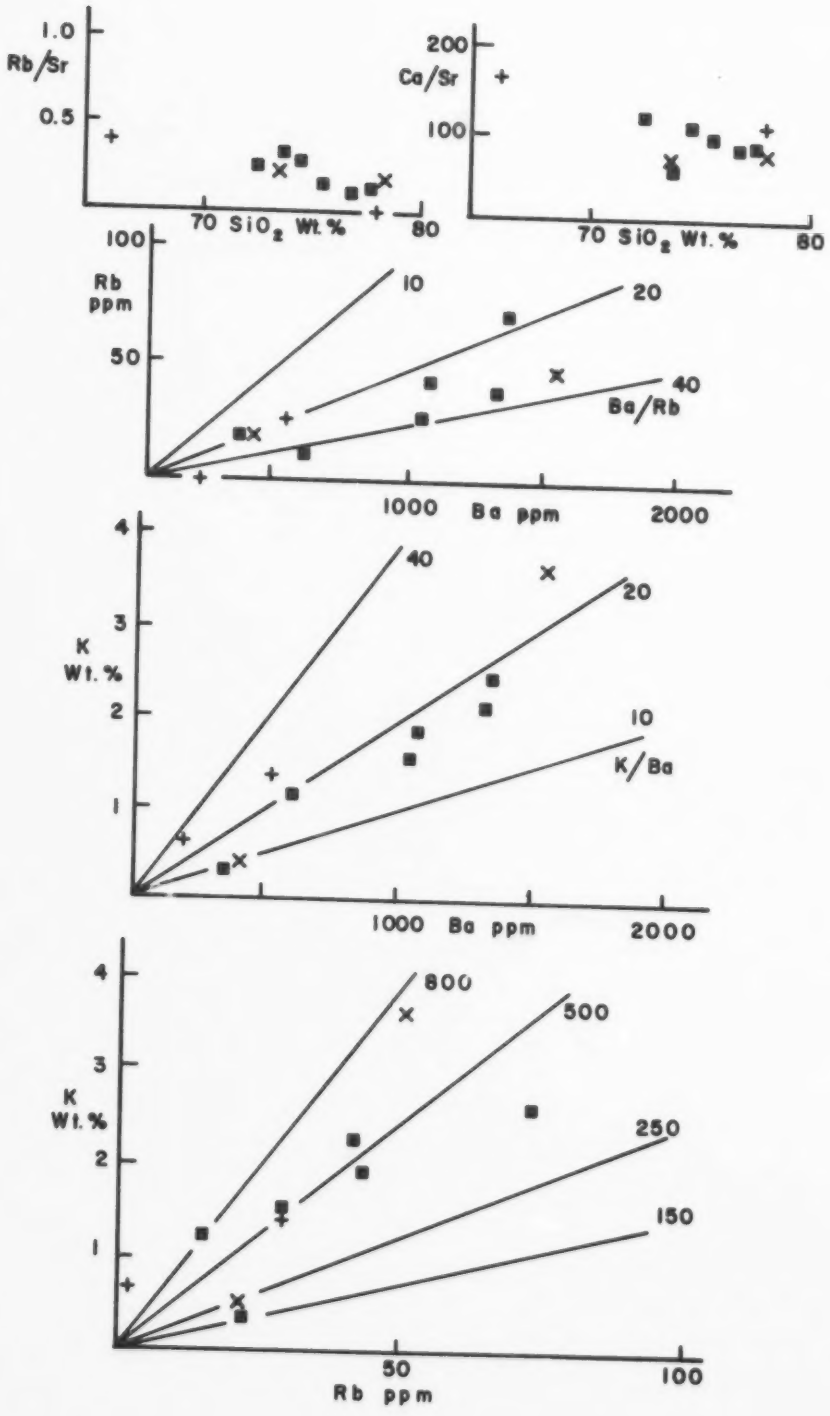

Figure 139: Selected major and trace elements contents of the Crowduck Bay gneiss dome. Symbols as in Figure 137

gabbro, with plagioclase phenocrysts 1-3 cm long comprising 0-70% of the rock. Sporadic patches of cumulate plagioclase are typical for this unit.

Unit Q is a heterogeneous, dark grey, medium grained (2-3 mm), plagioclase ($An_{3\,5}$) +quartz (6-22%) +hornblende (+biotite) (12-20%) diorite to quartz diorite, which intrudes unit P.

Unit R intrudes both preceding rock types. It consists of a light pink to tan medium grained plagioclase (An_{29}-An_{24}) + microcline, quartz (15-25%) + (biotite ≥ hornblende; 6-14%) granodiorite, often characterized by the presence of blue quartz "eyes".

The final intrusive phase of the Rex Lake plutonic complex is unit S, a light buff to grey, fine- to medium-grained (0.5-2.0 mm), plagioclase (An_{25}-An_{20}) + microcline + quartz + (biotite + muscovite; 2-3%) granite, observed in only a few outcrops, intruding unit R. Even the best samples of this unit are considerably contaminated by hornblende-bearing fragments of the granodiorite; thus the true compositions of this granitic phase may be more fractionated than is indicated by available chemical analyses.

Intrusive relationships between individual units are complex, especially near the edges of the batholith where numerous inclusions of Amisk metasediments, often partially digested, locally alter the appearance of the host phase. No regular zoning is observed within the Rex Lake pluton.

In selecting samples for chemical analyses, porphyritic varieties and cumulate plagioclase have been avoided. Compositionally, the Rex Lake multiple intrusion is a mainly subalkalic igneous complex with marked increase in SiO_2 and depletion in absolute iron during its evolution (Table 76, Fig. 140-143). In the AFM diagram, only two samples of diorite cross into the calc-alkalic field, deviating from an overall tholeiitic trend. Some plots of major oxides against silica suggest a continuous differentiation in the sequence but most indicate a segmented evolution, continuous within each of the four rock types but interrupted and shifted in each consecutive magma injection. The same segmented pattern also appears in the distribution of most trace elements. Nevertheless, the principal fractionation trends indicated by the earliest member of the complex remain characteristic of the whole sequence, although in some cases in a highly cyclic and repetitive manner (e.g., Zr/Y and K/Rb).

The increase in the K/Rb ratio is the most interesting feature of the Rex Lake complex. Several examples of similar gabbroic to granodioritic complexes are known in literature which display and increasing trend (e.g., early Archean granodiorite suite in Swaziland; Hunter et al. 1978). However, in these sequences the absolute contents of either Rb alone, or both K and Rb, decrease whereas the Rex Lake pluton shows a segmented but steady increase in both. Fractionation by plagioclase and hornblende is evidently responsible for most of this trend, but its continuation into K-feldspar + biotite-enriched composition is anomalous. The aforementioned contamination of the granitic phase is probably responsible.

The only deviation from the general fractionation patterns occurs at the very end of the series, in the granitic compositions, and only in terms of a few elements (Ba and partly Sr).

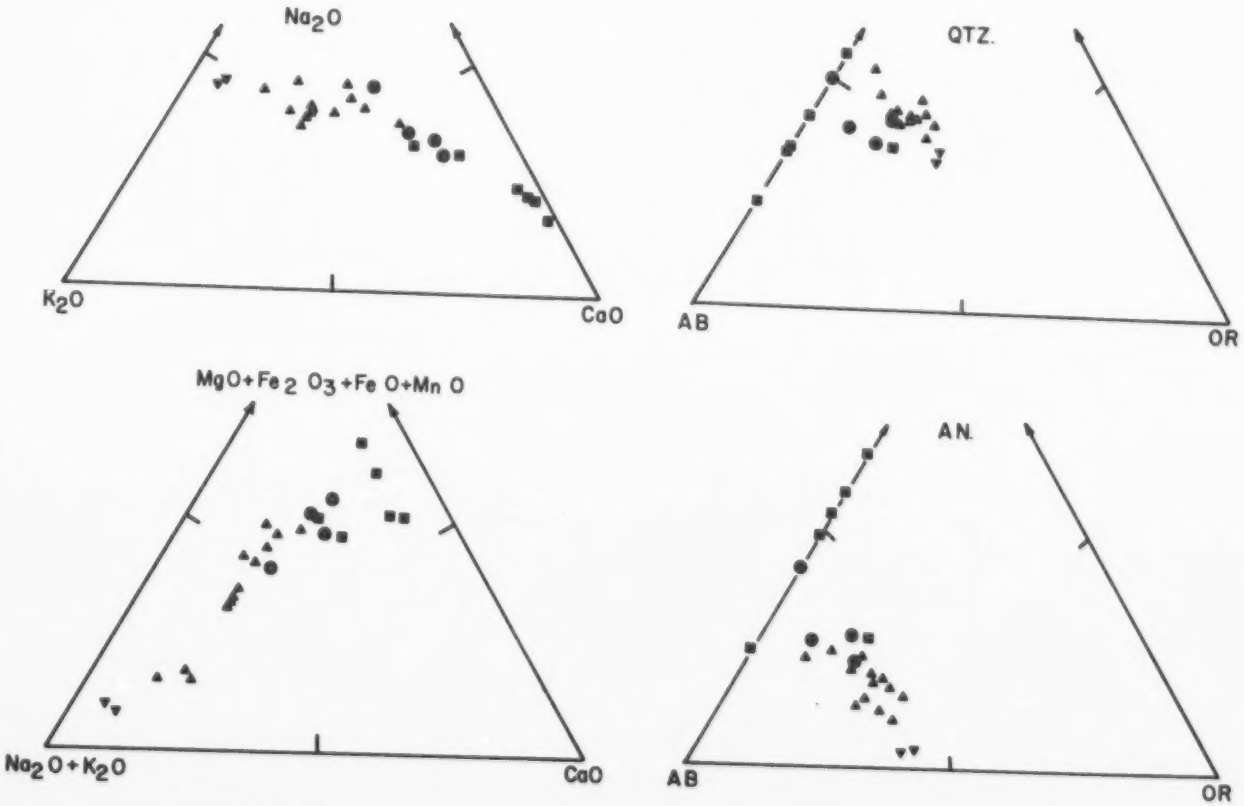

Figure 140: Compositional characteristics of the Rex Lake plutonic complex: gabbros (squares), diorites (dots), granodiorites (triangles) and granites (inverted triangles)

TABLE 76. REPRESENTATIVE CHEMICAL ANALYSES OF THE REX LAKE PLUTONIC COMPLEX (P, Q, R, S)

	Gabbro	Diorite	Granodiorite	Granite
	65-1	248-1	2005-1	13-2
SiO_2, wt.%	49.55	64.45	74.75	75.25
Al_2O_3	19.80	15.18	13.84	13.58
TiO_2	1.18	0.61	0.10	0.08
Fe_2O_3	2.49	0.72	0.21	0.27
FeO	7.26	5.76	1.12	0.30
MnO	0.14	0.12	0.02	0.01
MgO	4.19	2.07	0.42	0.20
CaO	10.30	5.07	1.75	0.68
Na_2O	2.80	3.20	3.82	4.10
K_2O	0.31	1.51	3.01	4.58
P_2O_5	0.18	0.17	0.01	0.06
CO_2	0.20	0.04	0.23	0.36
H_2O	1.26	1.18	0.61	0.40
	99.66	100.08	99.89	99.88
Li, ppm	13	45	39	75
Rb	4	39	64	62
Cs	0.7	2.5		1.1
Be	0.5	1.4		1.7
Sr	266	141		77
Ba	403	833		645
Pb	1	3		6
Ga		21		21
U	2	nd*		nd
Th	nd	nd		nd
Zr	67	113		89
Hf	1.6	3.1		
Sn	nd	nd		4
K/Rb	650	321	391	613
K/(Cs x 100)	37	50		345
K/Ba	6.4	15		59
Ba/Rb	101	21		10.4
Ba/Sr	1.5	5.9		8.4
Rb/Sr	0.01	0.3		0.8
Mg/Li	1948	276	64	16
Zr/Sn	-	-		22
Zr/Hf	42	36.5		
Al/Ga		3824		3419
La, ppm	3.75	10.85	14.0	10.5
Ce	10	23.5	27.0	22.8
Nd	6	17.5	16.0	<7.5
Sm	1.48	2.91	1.82	1.47
Eu	1.2	0.97	0.47	0.24
Dy	2.45	4.95	1.85	1.20
Yb	1.7	3.1	0.95	0.4
Lu	0.24	0.37	0.14	0.07

* not detected

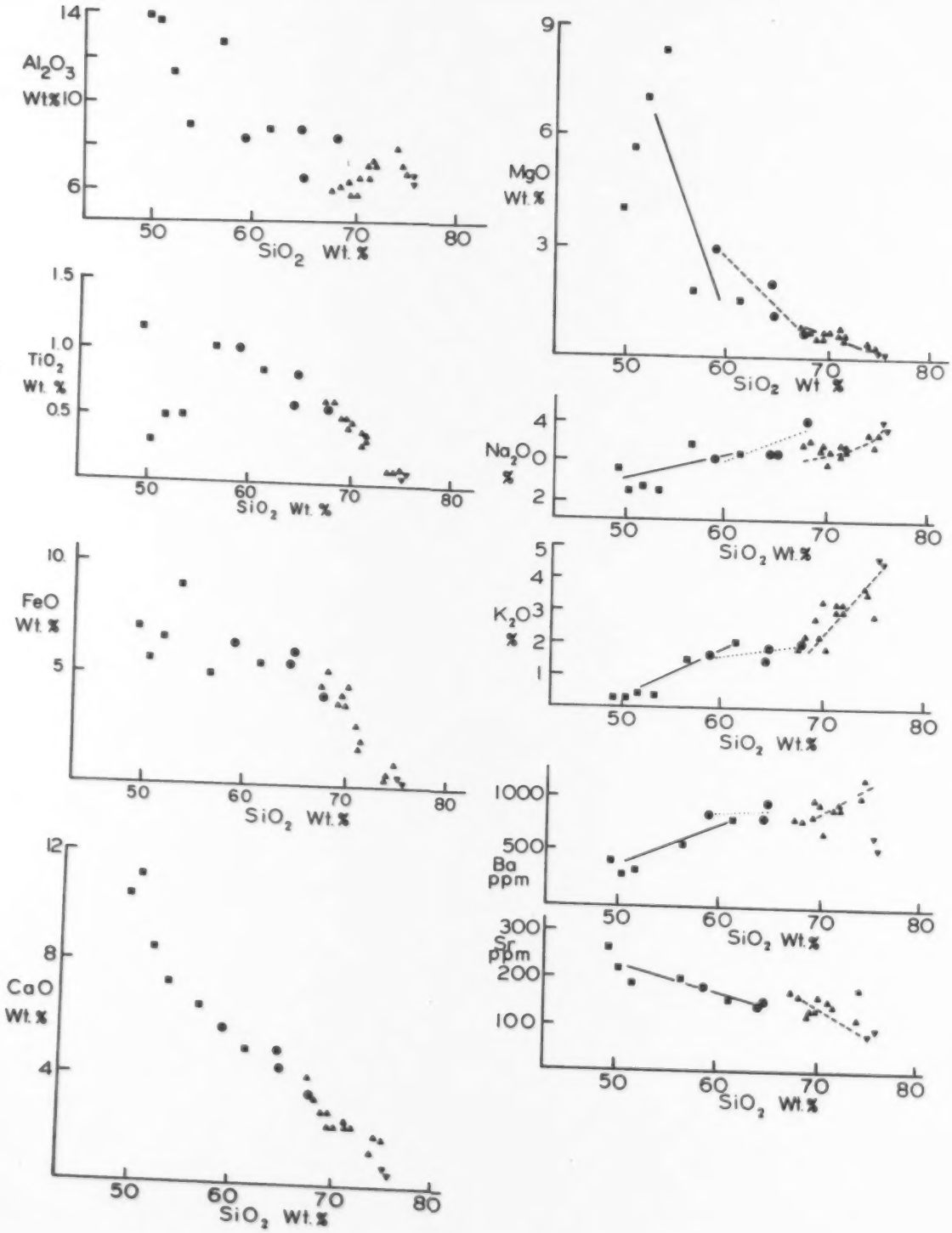

Figure 141: Selected compositional characteristics of the Rex Lake plutonic complex. Symbols as in Figure 140. Note the segmented character of most of the trends

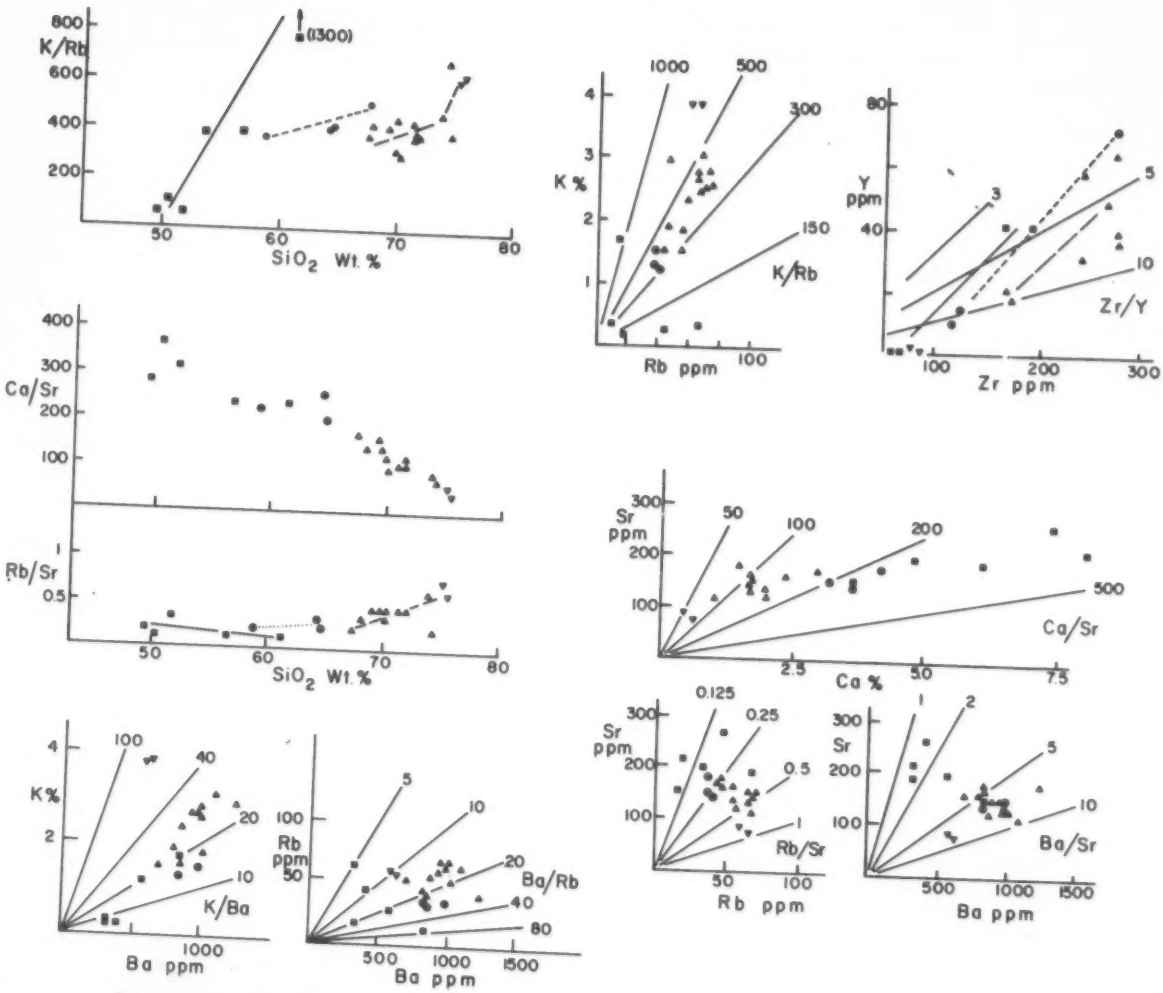

Figure 142: Selected compositional characteristics of the Rex Lake plutonic complex. Symbols as in Figure 140. Note the segmented nature of some of the trends, notably K/Rb vs. SiO_2 and Y vs. Zr, marked by solid, short-dash and long-dash lines for gabbros, diorites and granodiorites, respectively

Rare earth element abundances in samples representing the four rock types of the complex support a consanguineous origin of its phases. Loss of substantial plagioclase explains the overall increase in REE abundances coupled with elimination of the positive Eu anomaly from gabbro to diorite, and continuing loss of plagioclase coupled with a decrease in hornblende can be responsible for the deepening negative Eu anomaly and decreasing HREE abundances in granodiorite and granite (Fig. 143). However, the four data sets cannot be considered sufficient to characterize the whole differentiation sequence, in view of the segmenting shown by other trends.

The Rex Lake pluton is classified as late tectonic because biotite foliations have a tendency to be aligned roughly parallel to the main northeast-trending regional fabric, as though crystallization proceeded under directed stress, strongly interfering with the more usual flow-aligned orientation parallel to the intrusive contacts.

Stuart Lake pluton (T)

This unit consists of a single stock 1 km in diameter at the southwest end of Stuart Lake. The stock is zoned with a thin

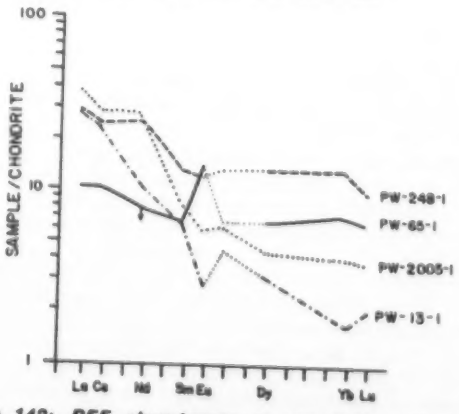

Figure 143: REE abundances in the gabbros (solid line), diorites (dashed line), granodiorites (dotted line) and granites (dash-dot line) of the Rex Lake plutonic complex

(<100 m wide) outer rim and a massive but locally foliated and sheared inner zone. These textural characteristics suggest an intrusive age close to that of the Rex Lake complex.

The outer rim consists of black medium- to coarse-grained (4-12 mm) gabbro containing hornblende (+biotite, up to 65%) + plagioclase + quartz (1-3%) + opaques (mostly sulphides, <1%). The inner zone consists of light pink to greyish pink, fine- to medium-grained (0.2-2.5 mm), 2-feldspar + quartz (15-20%) + (biotite + muscovite + epidote; 8-12%) + opaques (sulphide; < 1%) granodiorite. The inner zone also contains up to 5% tiny mafic clots and blocky inclusions of metasedimentary country rocks.

The few chemical analyses available from this intrusion suggest a close relation to the Rex Lake suite. Two other bodies located farther to the south, one at Monette Lake and the other on the southeast shore of Herb Lake, consist of gabbroic to dioritic multiphase intrusions and are tentatively mapped as similar to the Rex Lake and Stuart Lake plutons.

Wekusko and Tramping Lake granites (U, V)

Wekusko granite forms an oval-shaped body approximately 8 km in diameter, located at the southwest corner of the study area (Map 4); Tramping Lake granite is adjacent to this body along its western and northwestern sides. These two essentially massive and homogeneous rocks have intruded the Amisk metasediments and metavolcanics, although very few inclusions are visible in the granites at the present level of exposure. The lack of a tectonic fabric in these plutonic rocks places them among late-tectonic to post-tectonic intrusions of the region, synchronously emplaced.

The Wekusko granite is a light pink to reddish pink, medium- to coarse-grained (3-8 mm), and commonly porphyritic rock with biotite and rare hornblende (3-7% of the mafic minerals). K-feldspar phenocrysts reach 2 cm in length, and they compose 1 to 15% of the rock. Zircon, allanite, apatite, and magnetite are the accessory minerals. In the examined part of the pluton three phases were observed, exhibiting minor textural differences and mutual intrusive relations, but no compositional differences among them could be established. However, in the western part of the body, which was not investigated in the present study, earlier work revealed the presence of mixed gabbroic to dioritic rocks possibly resembling those of the Rex Lake complex (Stanton 1945).

The Tramping Lake granite is light tan to pink, fairly equigranular (2-4 mm), and contains 2-feldspars + quartz + biotite (chlorite) (3-4%).

In comparison to the Wekusko intrustion, this granite is fine grained and relatively leucocratic. Both intrusions are fairly homogeneous and they lack pegmatitic patches or veinlets inside as well as along contacts.

Compositionally, the Tramping Lake granite is more potassic and less calcic than the Wekusko intrusion, as shown in the ternary diagrams, norms and modes (Figs. 144-145 and in Table 77). An interesting feature of the Wekusko granite is that it falls distinctly outside the low-temperature trough in the Ab-Or-An diagram whereas the Tramping Lake compositions are located at its low-temperature end (Fig. 144). The K/Rb ratio is about the same in both bodies but Sr, Al/Ga and Mg/Li decrease and Rb/Sr plus K/Ba increase in the Tramping Lake body indicating its more fractionated composition. As in most units of the Wekusko Lake area described earlier, the K/Rb ratio ranging between 400 and 600 is much higher than average for granitic rocks in general.

The REE abundances show mutually related and moderately fractionated patterns in both bodies, with subhorizontal distribution of the heavy elements (Fig. 146). The Tramping Lake granite is more fractionated, mainly by loss of plagioclase relative to the Wekusko intrusion.

TABLE 77. REPRESENTATIVE CHEMICAL ANALYSES OF THE WEKUSKO AND TRAMPING LAKE GRANITES (U, V)

	Wekusko		Tramping Lake
	94-1	17-1	197-1
SiO_2, wt.%	73.30	74.25	76.00
Al_2O_3	13.80	12.75	12.72
TiO_2	0.16	0.20	0.15
Fe_2O_3	1.06	1.12	0.48
FeO	1.40	1.36	0.98
MnO	0.04	0.03	0.02
MgO	0.52	0.47	0.23
CaO	1.93	1.48	0.58
Na_2O	3.35	3.13	2.90
K_2O	3.75	4.18	4.92
P_2O_5	0.02	0.04	0.05
CO_2	0.11	0.20	0.30
H_2O	0.49	0.84	0.47
	99.73	99.85	99.78
Li, ppm	36	58	35
Rb	65	78	107
Cs	4.0	2.8	2.4
Be	1.8	1.8	1.6
Sr	114	96	32
Ba	1077	894	841
Pb	7	4	4
Ga		17	
U	nd*	2	5
Th	nd	nd	nd
Zr	208	181	202
Hf		5.25	
Sn	4	nd	11
K/Rb	479	445	381
K/(Ca x 100)	78	124	170
K/Ba	29	39	49
Ba/Rb	16.6	11.5	7.9
Ba/Sr	9.4	9.1	26.3
Rb/Sr	0.6	0.8	3.3
Mg/Li	88	50	40
Zr/Sn	52	-	18
Zr/Hf		34.5	
Al/Ga		3985	
La, ppm		18.25	26.8
Ce		36.5	55.5
Nd		24.5	44.5
Sm		5.14	6.88
Eu		0.76	0.49
Dy		6.25	9.55
Yb		4.7	8.45
Lu		0.56	0.78

* not detected

The Pegmatitic granites and pegmatites (W)

One of the last intrusive events in the Herb Lake area was the intrusion of granitic pegmatitic rocks. Two principal types can be distinguished: (i)stocks, plugs,and lenticular dykes of pegmatitic granites characteristically composed of several textural and compositional phases; their occurrences are concentrated in four locations - near Osborne Lake, along Crowduck Bay, northeast of the Grass River, and in the Dion-Hat Lakes area; (ii) lithium-bearing pegmatite dykes, with the three known occurrences referred to as (a) Sherritt-Gordon 1 and 2, cutting the eastern margin of the Rex Lake plutonic complex, (b) Violet-Thompson dyke located in Misal metamorphics, and (c) Green Bay dykes hosted by the Amisk Group (Fig. 147).

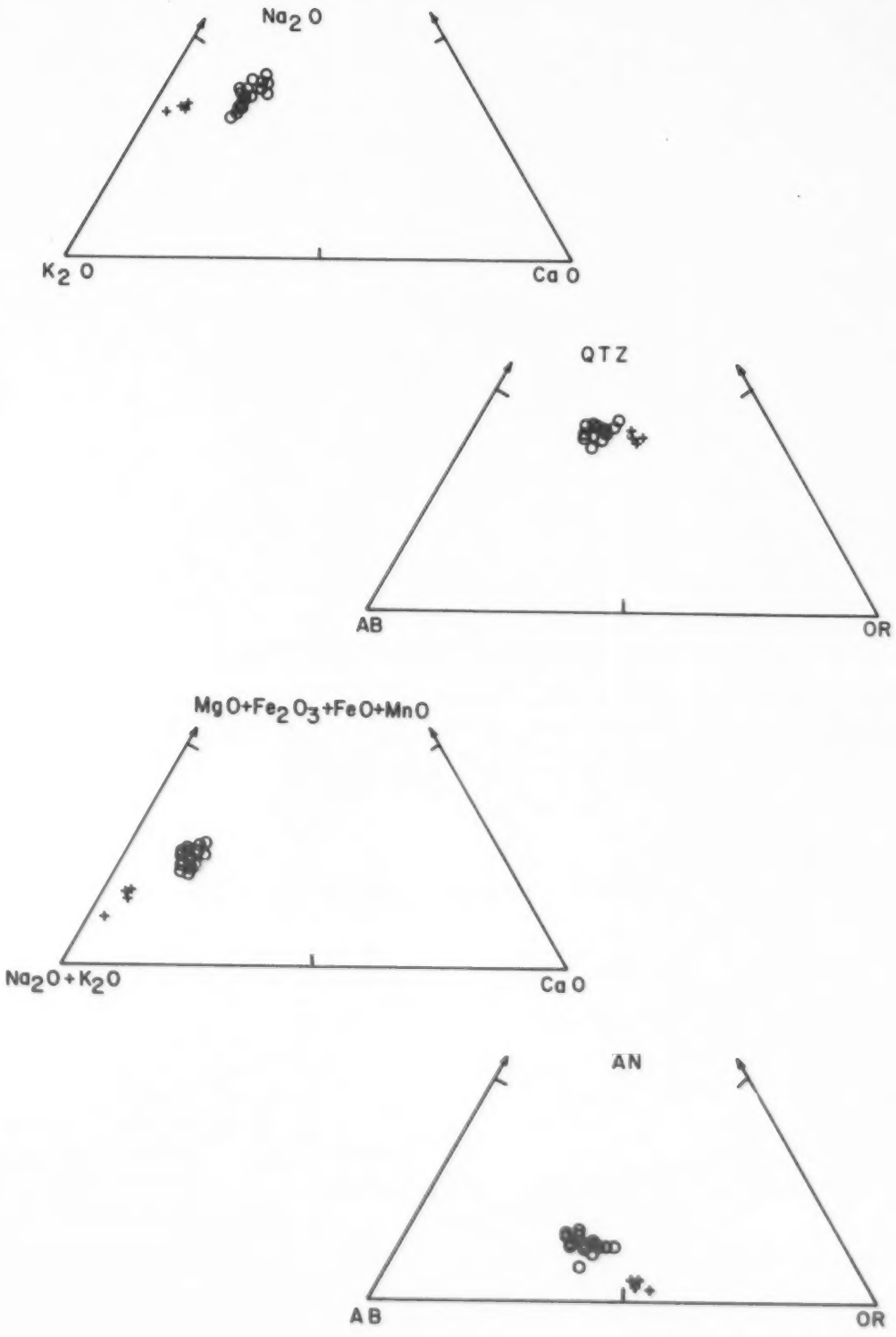

Figure 144: Compositional characteristics of the Wekusko (circles) and Tramping Lake (crosses) granites. Note the tight clustering of data in each body, and their mutual separation

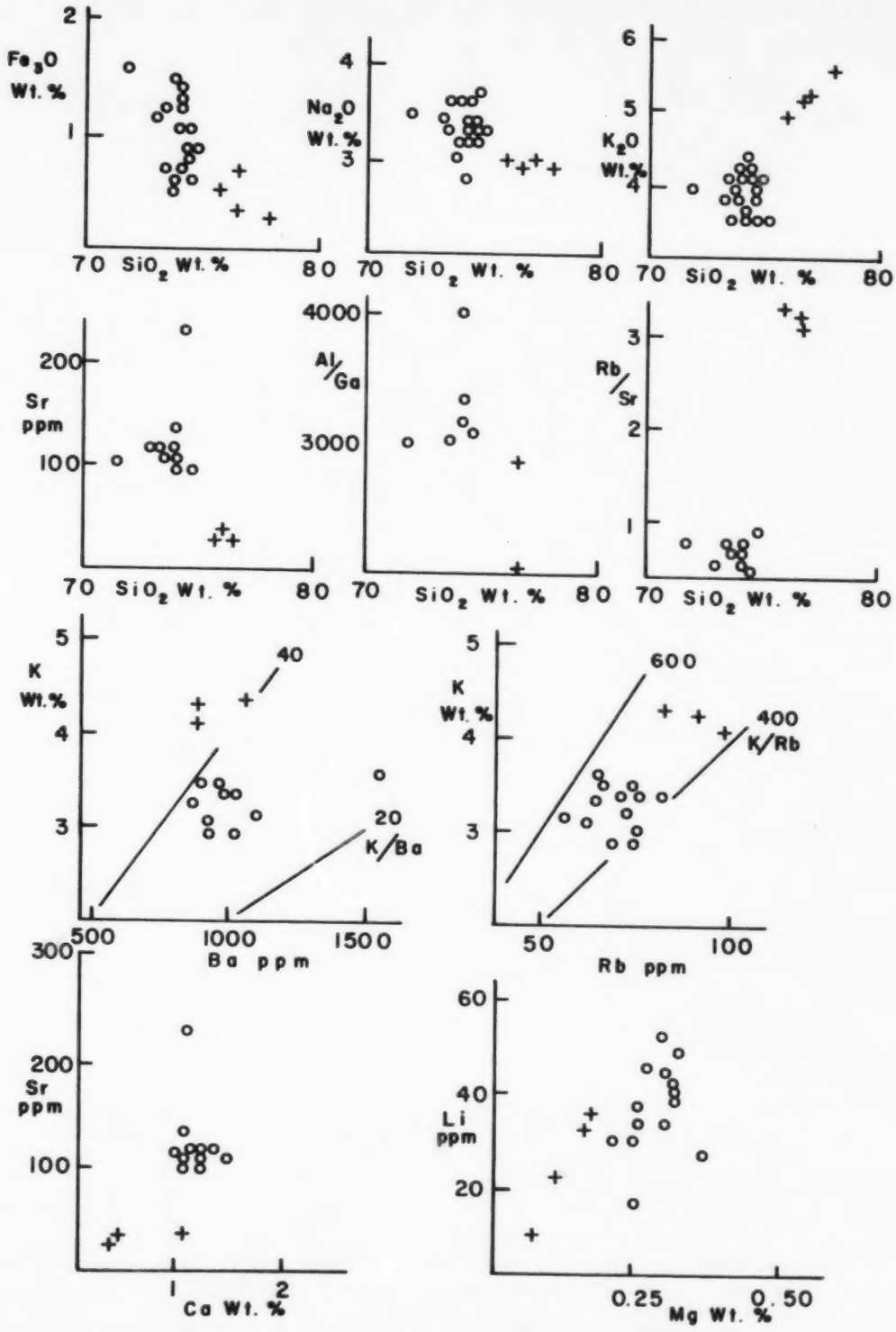

Figure 145: Selected compositional characteristics of the Wekusko (circles) and Tramping Lake (crosses) granites stressing the internal homogeneity of each, and the non-gradational relationship of the two bodies

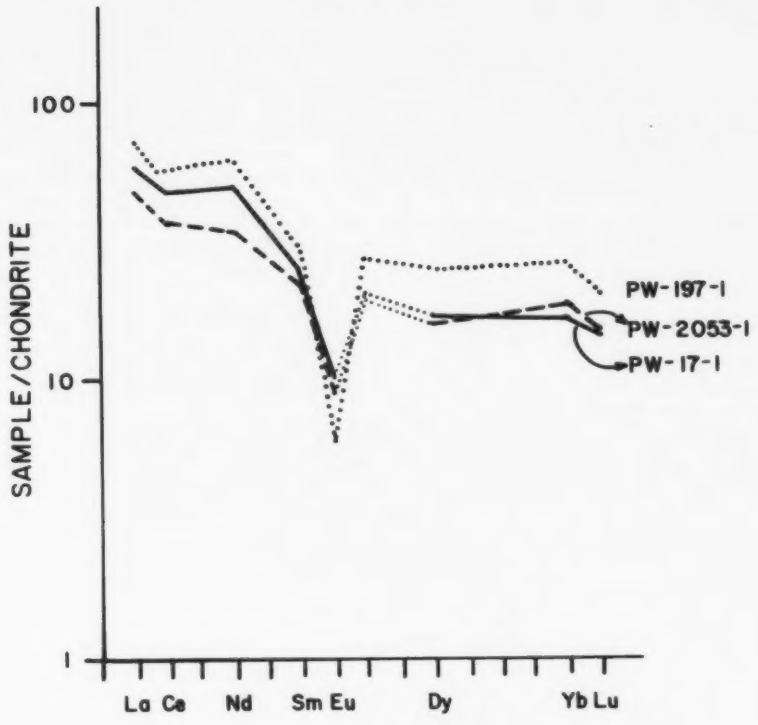

Figure 146: REE abundances in the Wekusko (solid and dashed lines) and Tramping Lake (dotted) granites

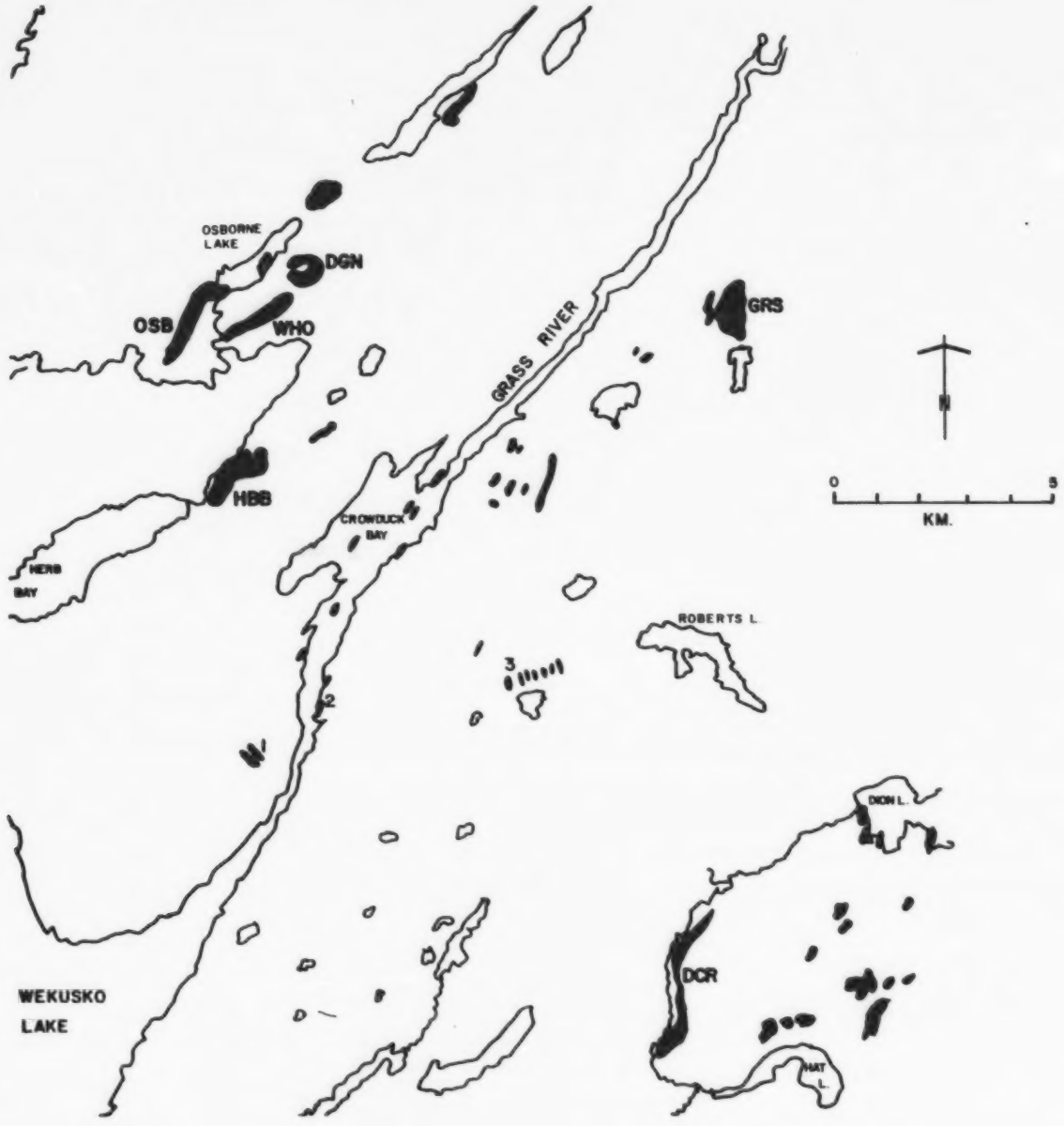

Figure 147: *Location of pegmatitic granites and lithium pegmatite deposits in the Wekusko Lake pegmatite field. Important pegmatitic granite bodies: OSB - Osborne Lake, WHO - White Owl, DGN - Doughnut, HBB - Herb Bay, GRS - Grass River, DCR - Dion Creek. Lithium pegmatites: 1 - Sherritt Gordon (SG), 2 - Violet-Thompson (VT), 3 - Green Bay (GB)*

PEGMATITIC GRANITES

Structural location and intrusive style

The structural setting and fabric of the pegmatitic granites varies with the size of individual intrusions.

Large bodies (up to 1 x 1.5 km in size) have intruded previously foliated host rocks largely by shouldering them aside and thus disrupting the regional metamorphic structure in the immediate vicinity of the contacts. Some incorporation of country rocks by stoping is also evident but not extensive. At Osborne Lake, foliations were deflected around the Doughnut body (Map 4) to a position subparallel to the contacts but not completely conformable. These deformational features imposed by the pegmatitic granites indicate forcible emplacement. The pegmatitic granites located northeast of Grass River intrude largely metabasaltic rocks, without a noticeable effect on their fabric; however, the contacts are poorly exposed. Inclusions of country rocks are rare. In the Dion-Hat Lakes area, pegmatitic granites form subconcordant pods and crosscutting fracture-filling dykes.

Internally, the large pegmatitic granite bodies are massive with local discontinuous layering of two types: (i) biotite ± garnet schlieren residual after digestion of (and transitional into) screens of metasediments, and (ii) bands of fine grained leucogranitic to aplitic material alternating with coarse potassic pegmatite. This localized internal layering shows no evident relationship to the margins of the bodies or external structural features. This is also true of biotite and/or muscovite in the fine grained leucogranites which usually show preferred orientation parallel to contacts, mafic schlieren, and pegmatite/leucogranite banding, with sporadic indepentent swirling. However, near the larger bodies at Osborne Lake a number of small outcrops XO m across, consisting of fine- to medium-grained leucogranite, exhibit moderately developed biotite foliation which consistently strikes northeast throughout each of the outcrops (Figs. 148-150).

The shapes of small bodies of pegmatitic granite are consistent with injection into dilation fractures; no evidence of replacement processes was observed (using criteria of Kretz 1968). Matching indentations in contacts (Fig. 151), and schist bridges enclosed in pegmatite bodies are both considered evidence for the dilational mechanism (Farmin 1941; Fig. 152). In contrast to the large bodies of pegmatitic granites which can easily withstand post-consolidation stresses, the small intrusions commonly show moderate to well-developed boudinage (Figs. 153 and 154).

Internal composition

As in the Cat Lake-Winnipeg River field, the pegmatitic granites consist of several compositional and textural phases. Pegmatitic leucogranites (graphic K-feldspar + quartz phenocrysts 5-100 cm in size, in a quartz + albitic plagioclase ± muscovite ± garnet, apatite, and/or tourmaline groundmass) are predominant. Equigranular fine grained leucogranites (K-feldspar + albitic plagioclase + quartz ± muscovite (±biotite) ± garnet) constitute patches in, and bands alternating with, the pegmatitic leucogranites; they sporadically show a tendency to develop

Figure 148: Inclusions of metasediments (dark subhorizontal bands) in fine grained leucogranite of the Osborne Lake pegmatitic granite

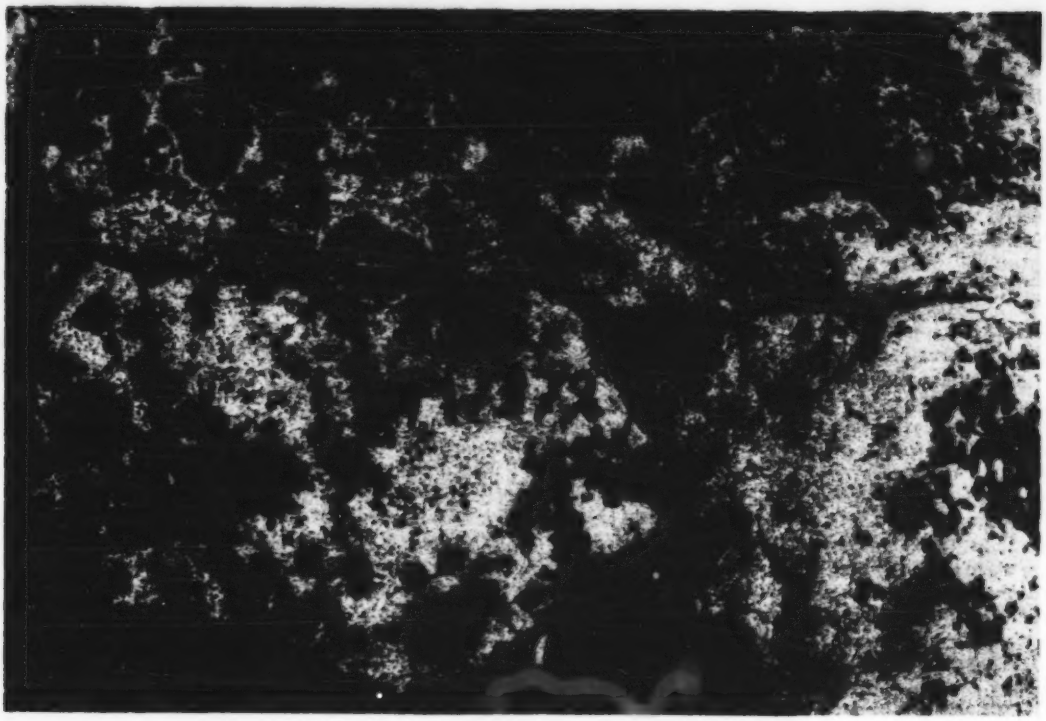

Figure 149: Schlieren-type layering by digested metasedimentary screens in the fine grained leucogranite phase of the Osborne Lake pegmatitic granite

Figure 150: Layered alternation of fine grained leucogranite and pegmatitic leucogranite; Osborne Lake pegmatitic granite intrusion

Figure 151: A fracture-filling pegmatite vein in a dilation structure in the gneissic Dion-Hat Lakes terrain; slight mismatch of fracture walls due to an oblique angle between the vein and surface

Figure 152: A schist screen in a lenticular pegmatitic granite body, in Crowduck Bay

Figure 153: Incipient boudinage of a pegmatite dyke, west of Godkin Lake

Figure 154: Advanced boudinage of a pegmatite sill in Crowduck Bay

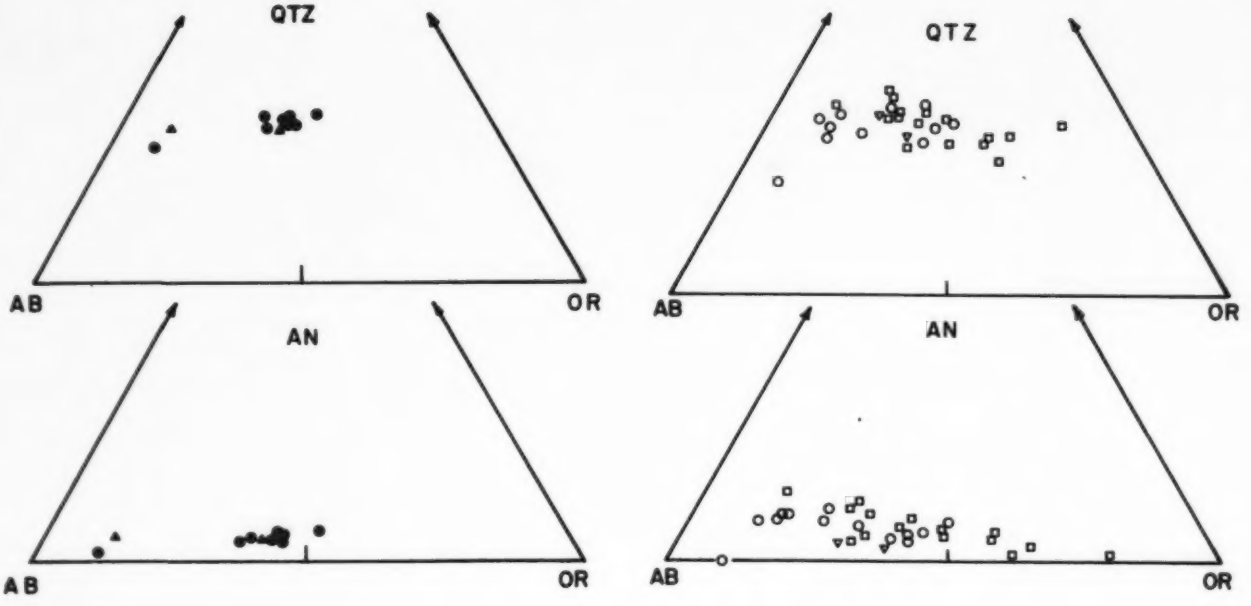

Figure 155: Proportions of normative felsic components of fine grained leucogranite phase (left, solid symbols) and of the pegmatitic leucogranite phase (right, open symbols) of pegmatitic granites: Osborne Lake area (circles), Grass River body (inverted triangles), Crowduck Bay area (triangles), and Dion Lake area (squares)

sodic aplitic compositions (with increasing plagioclase and decreasing K-feldspar contents). A potassic pegmatite phase (graphic to blocky K-feldspars with quartz blebs, with minor albite and coarse muscovite) is locally developed by a gradational change in texture and mineralogy from both pegmatitic and fine grained leucogranites; potassic pegmatite forms mostly small patches and bands (up to 5 m in length) in these host rocks.

All phases of the pegmatitic granites are represented in the Osborne Lake, northwest of Grass River, and Dion-Hat Lakes areas. The Crowduck Bay occurrences consist of small lenticular bodies composed predominantly of pegmatitic leucogranite (with subgraphic groundmass) which locally grades into potassic pegmatite assemblages. In this area, extensive greisen-like, muscovite + quartz (±garnet) contact zones are developed in bodies which intrude pelitic metasediments.

Accessory minerals

The assemblage of accessory minerals in the Herb Lake pegmatitic granites is restricted to a few species. Garnet is most widespread in aplitic and pegmatitic phases, as is apatite. Tourmaline is abundant in the Crowduck Bay bodies but scarce elsewhere. A patch of curvilamellar lithian muscovite was found in only a single pegmatitic pod in the White Owl body, and arsenopyrite occurs sporadically in the small lenticular intrusions along the Crowduck Bay.

The sparse accessory mineralization of the pegmatitic granites is in agreement with their modest degree of fractionation as discussed below.

Reaction with wall rocks

Reaction of the pegmatitic granites with the enclosing schists could not be studied because of the deep erosion along the intrusive margins and consequent burial under glacial drift and vegetation.

Petrochemistry

Table 78 contains representative chemical analyses of fine grained leucogranites and pegmatitic leucogranites. Normative Or-Ab-An plots put most of the analyzed fine grained leucogranites into the Ca-poor end of the low-temperature trough; only two of the analyzed samples show sodic compositions (Fig. 155). In contrast, the pegmatitic leucogranites display an almost continuous variation from potassic to sodic composition, with the Dion-Hat Lakes samples slightly more calcic than those from other areas (Fig 155). This is due, in part, to the coarse grain size and considerable inhomogeneity of the pegmatitic leucogranites, and also to the relatively small size (4-6 kg) of the analyzed samples. However, a certain degree of the scatter can be considered real in view of a similar spread obtained on much larger samples from the Cat Lake-Winnipeg River field, and of the $Na_2O>K_2O$ compositions of pegmatitic leucogranites reported from other regions (Orville 1960, Proctor and El-Etr 1968, and others). The restriction of potassic compositions to the Dion-Hat Lakes area may be explained by a different petrogenesis. The potassic samples come from small bodies enriched in K-feldspar, but with a relatively low degree of fractionation. These may represent early low-percentage partial melts derived from moderately calcic gneisses.

The pegmatitic granites represent the most fractionated major rock units in the Herb Lake field, in terms of low Ti, Zr, Ba, Sr, and high Li, Rb, Cs, Be, Ga, and Sn values. However, this is

TABLE 78. REPRESENTATIVE CHEMICAL ANALYSES OF THE PEGMATITIC GRANITES (W)

	Osborne L. f.g. leucogranite			Grass R. pegmatitic	Osborne L. leucogranites	
	244-1	2112-1B	379-1D	143-1A	72-1	2118-1
SiO_2, wt. %	75.10	74.60	75.95	74.70	74.70	75.30
Al_2O_3	13.64	13.48	13.62	14.74	14.72	14.58
TiO_2	0.11	0.18	0.01	0.00	0.00	0.00
Fe_2O_3	0.25	0.40	0.44	0.45	0.30	0.63
FeO	0.92	0.84	0.20	0.32	0.38	0.18
MnO	0.02	0.01	0.06	0.04	0.01	0.01
MgO	0.15	0.29	0.06	0.06	0.05	0.07
CaO	0.73	0.70	0.62	0.44	0.59	1.19
Na_2O	4.25	3.60	4.28	4.30	4.10	5.58
K_2O	4.22	4.52	3.96	4.30	4.78	1.82
P_2O_5	0.05	0.04	0.03	0.10	0.03	0.02
CO_2	0.14	0.18	0.06	0.06	0.03	0.04
H_2O	0.34	0.70	0.43	0.57	0.35	0.58
	99.92	99.74	99.72	100.08	100.24	100.00
Li, ppm	95	25	37	82	23	28
Rb	177	93	157	171	233	51
Cs	2.4	0.5	0.9	11.7	3.7	1.8
Be	2.0	0.3	1.7	2.9	1.3	1.1
Sr	51	48	39	46	36	53
Ba	617	448	123	3	39	nd*
Pb	18	21	20	15	22	22
Ga	25		34	20	45	36
U	7	nd				
Th	nd	1				
Zr	108	139	41	10	27	40
Hf	2.6					
Sn	4	nd	4	9	12	4
K/Rb	198	403	210	209	170	296
K/(Cs x 100)	146	750	366	30	107	84
K/Ba	57	84	267	11900	1018	-
Ba/Rb	3.5	4.8	0.8	0.02	0.2	-
Ba/Sr	12	9.3	3.2	0.06	1.1	-
Rb/Sr	3.5	1.9	4	3.7	6.5	0.96
Mg/Li	10	68	11	5	13	14
Zr/Sn	27		10	1	2.3	10
Zr/Hf	41.5					
Al/Ga	2888		2118	3900	1731	2142
La, ppm	16.7	18.9				
Ce	23.0	32.0				
Nd	15.0	19.0				
Sm	2.31	3.17				
Eu	0.21	0.25				
Dy	2.20	2.65				
Yb	0.75	0.85				
Lu	0.07	0.11				

* not detected

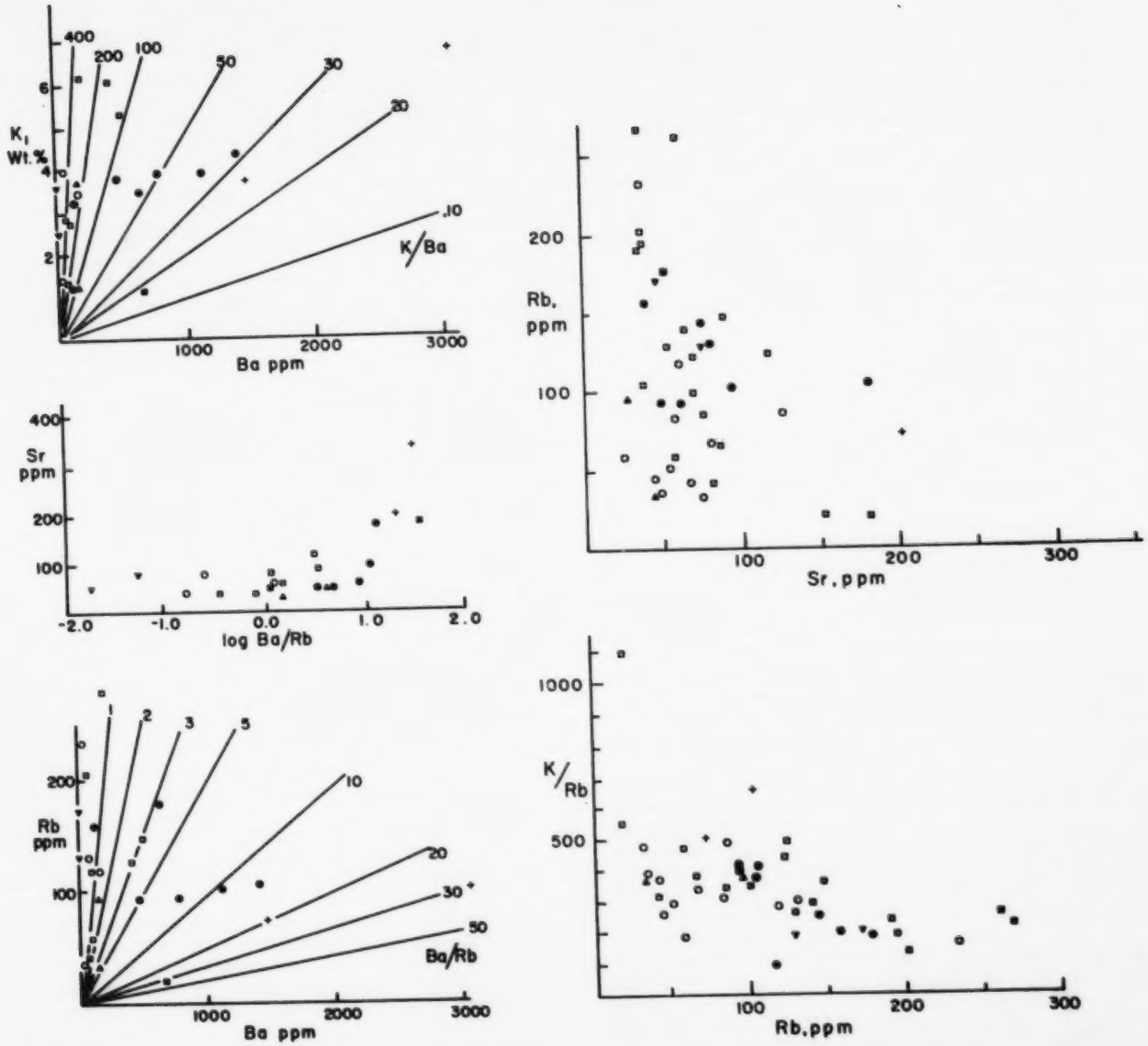

Figure 156: Selected major and trace-element characteristics of the fine grained leucogranites and pegmatitic leucogranites. Symbols as in Figure 155

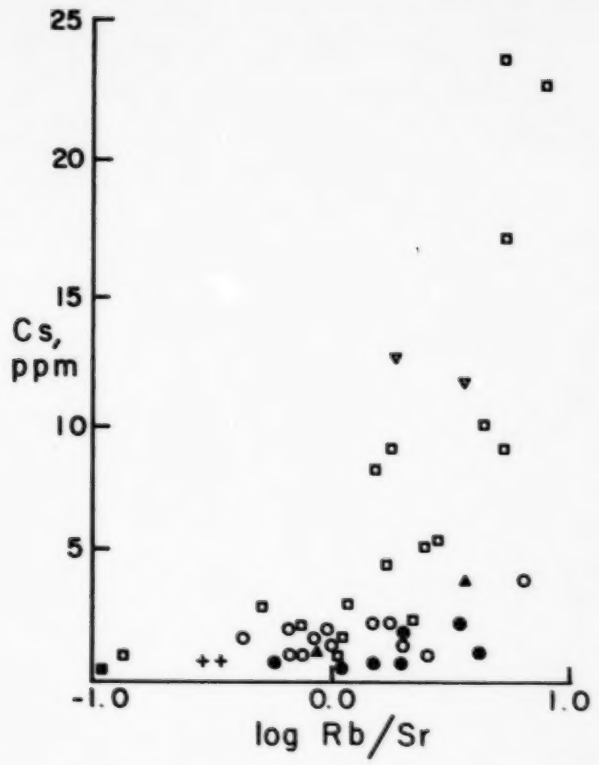

Figure 157: Cs vs. Rb/Sr in the fine grained leucogranites and pegmatitic granites. Symbols as in Figure 155. Note the Cs enrichment in the pegmatitic phase relative to the fine grained leucogranites

true only in a very relative sense, in comparison with other metamorphic and igneous units of the host area; e.g., about three-quarters of the analyzed samples have K/Rb ratios higher than the igneous average of 230, and very few samples show values lower than 200; about half of the data lie between 300 and 500.

Within the group of pegmatitic granites themselves, decreasing Ba/Rb and increasing Rb/Sr are accompanied by increasing Li, Cs, Be, Ga, Sn, and Pb, and by decreasing Ba, Zr, Ti, Al/Ga, Mg/Li, K/Rb, and K/Cs. Among the phases constituting them, the pegmatitic leucogranites are Ba-poor and Rb-, Cs-, (Sr-) enriched in comparison to the fine grained leucogranites (Figs. 156-157).

In terms of individual intrusions, the Herb Bay, Grass River and Dion Creek bodies show a degree of fractionation much higher than the other pegmatitic granites.

The general shape of the REE distibution in the fine grained leucogranitic phase is, at first glance, similar to that found for the Wekusko and Tramping Lake granites (Fig. 158). However, the overall abundances are lower, the Eu anomaly is more pronounced, and the heaviest REEs are more depleted, extending the slope set by the light REEs through the whole pattern.

Mineral compositions

Blocky potassium feldspar was the only mineral available in all pegmatic granite intrusions for systematic geochemical study. The enrichment of these feldspars in rare alkalis, illustrated in Figure 159, confirms the Herb Bay, Grass River, and Dion Creek bodies as the most fractionated in the district.

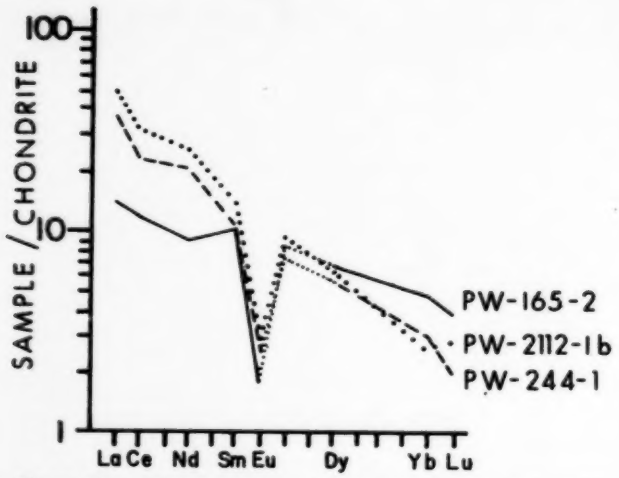

Figure 158: REE abundances in the fine grained leucogranite phase of the pegmatitic granites from Crowduck Bay (solid line) and from the Osborne Lake body (dashed and dotted lines)

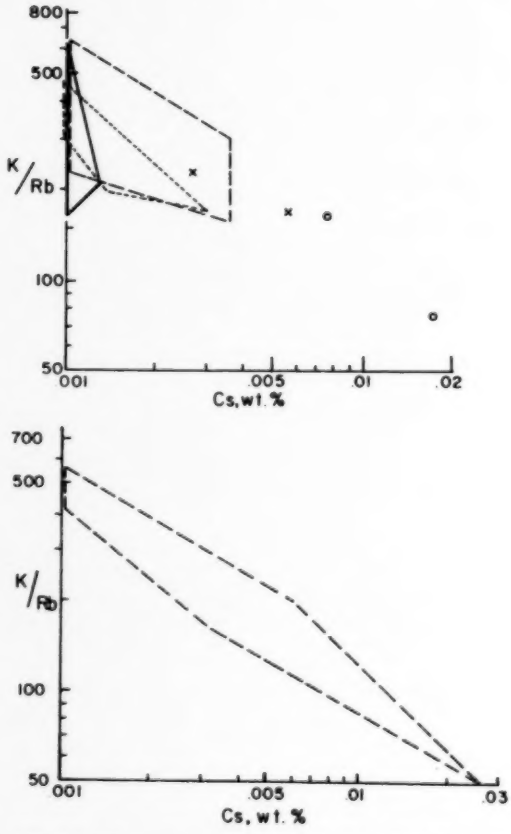

Figure 159: K/Rb ratio vs. Cs in blocky K-feldspars of pegmatitic granites (top) and small pegmatites east of Crowduck Bay (bottom). In pegmatitic granites: Osborne Lake (solid outline), Crowduck Bay (dotted outline), Grass River body (x), Herb Bay (circles), Dion-Hat Lakes area (dashed outline)

PEGMATITES

Pegmatites with significant mineralization belong to the three groups quoted above. The general characteristics of each group will be discussed separately, and will be followed by a section on their combined mineralogy and geochemistry. Pegmatite occurrences which do not belong to the three main groups will be briefly discussed in the final section.

The Sherritt-Gordon group (SG)

Figures 160 and 161 show the surface extent of the two main pegmatites which intrude gabbroic rocks of the Rex Lake plutonic complex, west of the Grass River outlet (location 1, Fig. 147). The eastern dyke has been traced for 500 metres, striking 300-315° and dipping steeply to the southwest. The dyke ranges from 10 cm to 5 metres in width, and splits into 3 subparallel veinlets at the southeast end. The western dyke has been traced for almost 400 metres, striking parallel to the eastern dyke at a distance of about 70 metres, and dipping 50°-70° to the southwest; its width varies between 1.5 and 10 metres. A third dyke reported approximately 1 km to the south was not observed.

Both dykes display some pinch and swell structures along strike as well as slight changes in strike. Abrupt termination of the dykes was observed against gabbro, with re-appearance farther along strike. These features suggest that the pegmatites intruded parallel fractures which were subsequently slightly deformed and locally displaced. This observation is supported by local post-crystallization deformation of early minerals in the dykes.

The orientation of the fractures occupied by the Sherritt dyke is sub-parallel to the D_3 joint system observed by Bailes (1975) in the area to the north (perhaps coincidentally).

The poor exposure of the dykes does not permit a detailed study of internal structure but a safe generalization can be made from the few outcrops revealing complete cross sections. The eastern dyke seems to be homogeneous in mineral distribution, and it shows only some coarsening of grain size inwards. The western dyke is asymmetric with the grain size increasing to the hanging-wall contact, and some accumulation of the spodumene, quartz and blocky K-feldspar along this contact. Occurrences of cleavelandite, saccharoidal albite, garnet, apatite, and beryl are rather sporadic and patchy; muscovite seems to be dispersed rather regularly throughout the whole dyke. No Nb-Ta oxide minerals were observed which would be visible in hand specimen.

The Violet-Thompson pegmatite (VT)

This dyke is located on the east shore of Grass River (Crowduck Bay) northeast of the Sherritt-Gordon property (location 2 on Fig. 147). It intrudes a series of Missi pebble to cobble conglomerates and is subparallel to parallel to their north east-trending foliation; it strikes appoximately 030°-038° with vertical dip (Fig. 162). The dyke is up to 20 metres wide, exposed over 130 metres along strike at its southern end, and it was traced by drilling for over 500 metres to the north. A lense-shaped outcrop of spodumene-bearing pegmatite 10 x 22 metres in size was discovered at the northern extension during the present field work, with the pegmatite pinching out on its southern end and open to the north.

The main exposure of the dyke near its southern end reveals a number of metasedimentary slabs and rudimentary bridges within the pegmatite, suggestive of pegmatite emplacement into a dilational structure. This is supported by the peculiar internal structure of the body, typical of vein fillings crystallizing in the course of gradually and continuously opening fractures: the dyke is homogeneous both texturally and compositionally, with an oblique ladder-like orientation of columnar (1-35 cm long) spodumene and K-feldspar plunging 10-25° at 320-340° (Fig. 163). This represents inclination of these crystals up to 30° from the perpendicular to the contacts with the host rock. Changes in attitude of the crystals occur along planes roughly parallel with the dyke contacts. This fabric of the mutually parallel columnar crystals, subperpendicular to the dyke contact, is fundamentally different from the near-perpendicular but divergent growth of crystals governed by geometric selection in basically static open fractures (cf. Jahns 1953). All the structural features of the Violet-Thompson dyke (similar to, e.g., certain types of chrysotile veins in serpentinites) strongly suggest continuous crystallization in a tension field of a slowly opening fracture, with steady influx of homogeneous parent material, and with the oblique angle of wall separation abruptly changing during the process. A complex but consistent pattern of K/Rb and K/Cs fractionation in K-feldspar observed in two complete cross sections of the dyke suggest that the eastern contact could have been the substrate and the growth possibly proceeded westwards.

Local fracture fillings parallel to the main dyke can be observed inside the pegmatite, with mineral assemblages identical to those of the main dyke but mostly lacking its fabric. Bending and fracturing of spodumene and K-feldspar healed by albite and quartz also indicate that the host fracture was active during and after the bulk of crystallization.

In addition to spodumene (which ranges between 10 and 20% by volume) and K-feldspar, the dyke contains mainly albite, quartz, and muscovite which constitute the medium- to coarse-grained matrix separating the columnar crystals. Garnet, apatite, and beryl are very subordinate. No Nb, Ta-oxide minerals have been observed.

The Green Bay group (GB)

This group is located about 4.5 km east-northeast of the Violet-Thompson dyke (location 3 on Fig. 147). It consists of 7 dykes intruding metabasalts of the Amisk Group, in a 2 km zone trending approximately 55° from the westernmost, and largest, pegmatite (Mulligan 1965). The individual dykes strike northwest to north-northwest with subvertical dips, mostly crosscutting the northeast regional foliation of the metabasalts. The pegmatite group is located inside two divergent faults striking east-northeast and north-northeast. If they are interpreted as conjugate horizontal shears, the attitude of the pegmatites would correspond to the theoretical orientation of associated tension fractures (Mulligan 1965).

Out of the seven pegmatites present, the westernmost (GB) and largest was examined in detail, and two minor dykes neighbouring to the east (GBB and GBC) have been sampled for geochemical characterization.

The GBA dyke is largely drift-covered and poorly exposed in trenches over 250 metres along strike which is approximately 350° with vertical dip. The width varies between 3 and 20 metres (Fig. 164). The pegmatite contacts crosscut the regional schistosity at a low, and variable, angle.

The dyke is roughly concentric in internal structure. Coarsening of grain size of the main constituents - K-feldspar, quartz, spodumene, and black tourmaline-towards the centre of the body is only locally interrupted by patches of saccharoidal albite, larger aggregates of muscovite, and by coarser albite stringers carrying garnet and beryl. Spodumene is concentrated in, but not confined to, the core. Sicklerite, most probably an alteration product of triphylite, is exceptional.

The GBB and GBC dykes show similar internal structure and composition, but they are much more influenced by post-consolidation tectonic activity which is very sporadic in the GBA dyke. They split into several subparallel veins, and they generally show much more active structural evolution than the main dyke. Spodumene occurs in them only in centrally located patches.

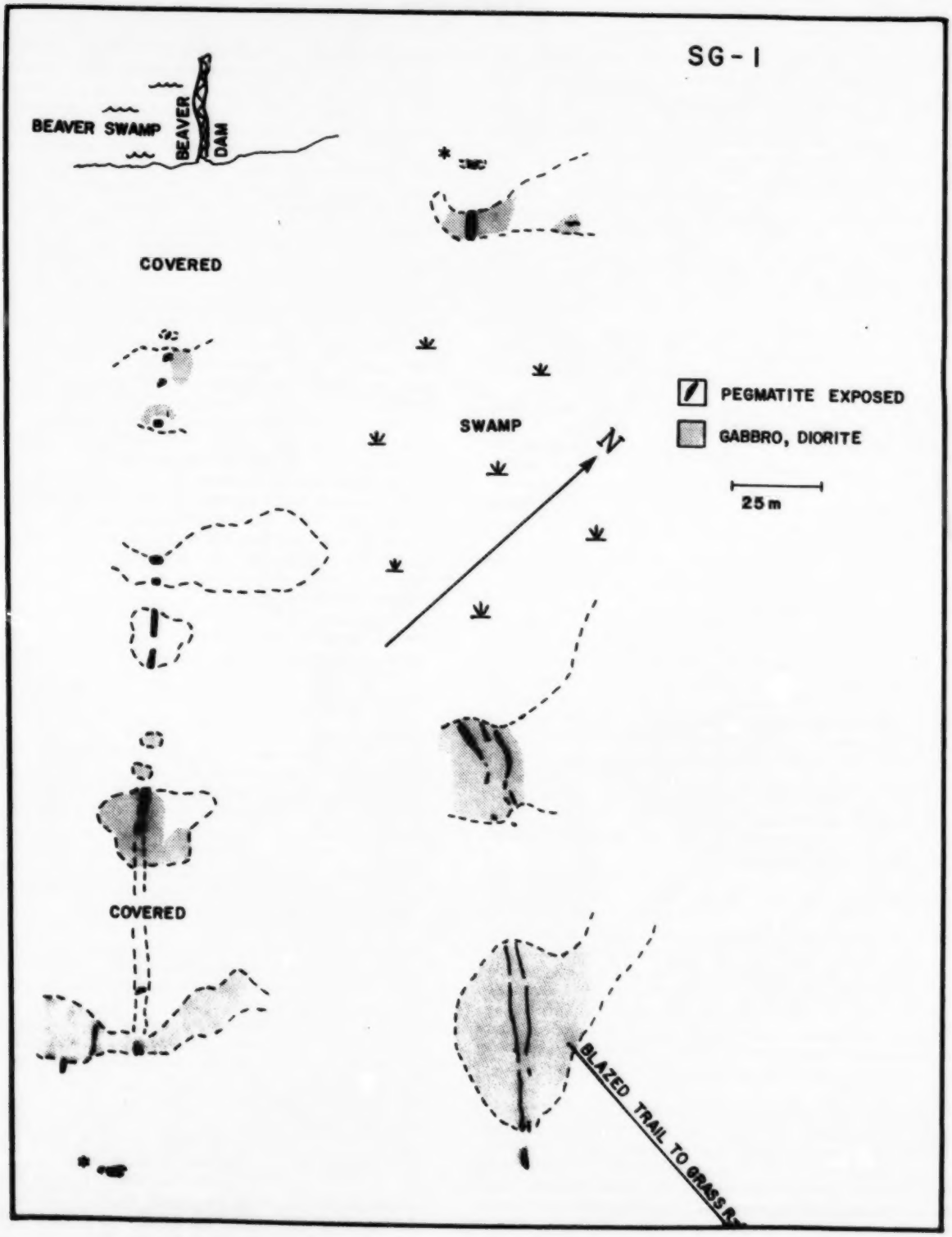

Figure 160: The Sherritt Gordon eastern dyke SG-1. Asterisks designate point of continuation of the two segments

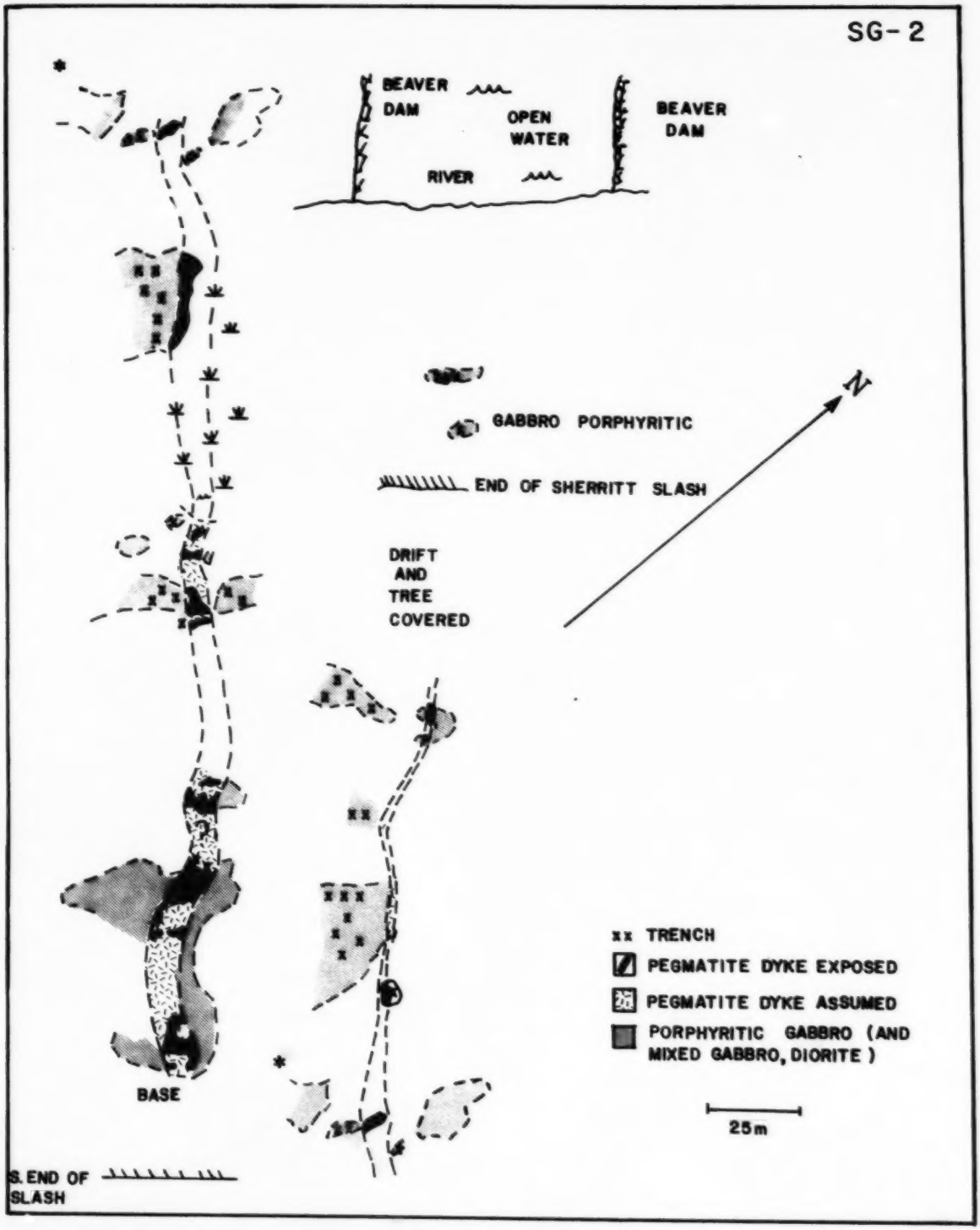

Figure 161: The Sherritt Gordon western dyke SG-2. Asterisks designate point of continuation of the two segments

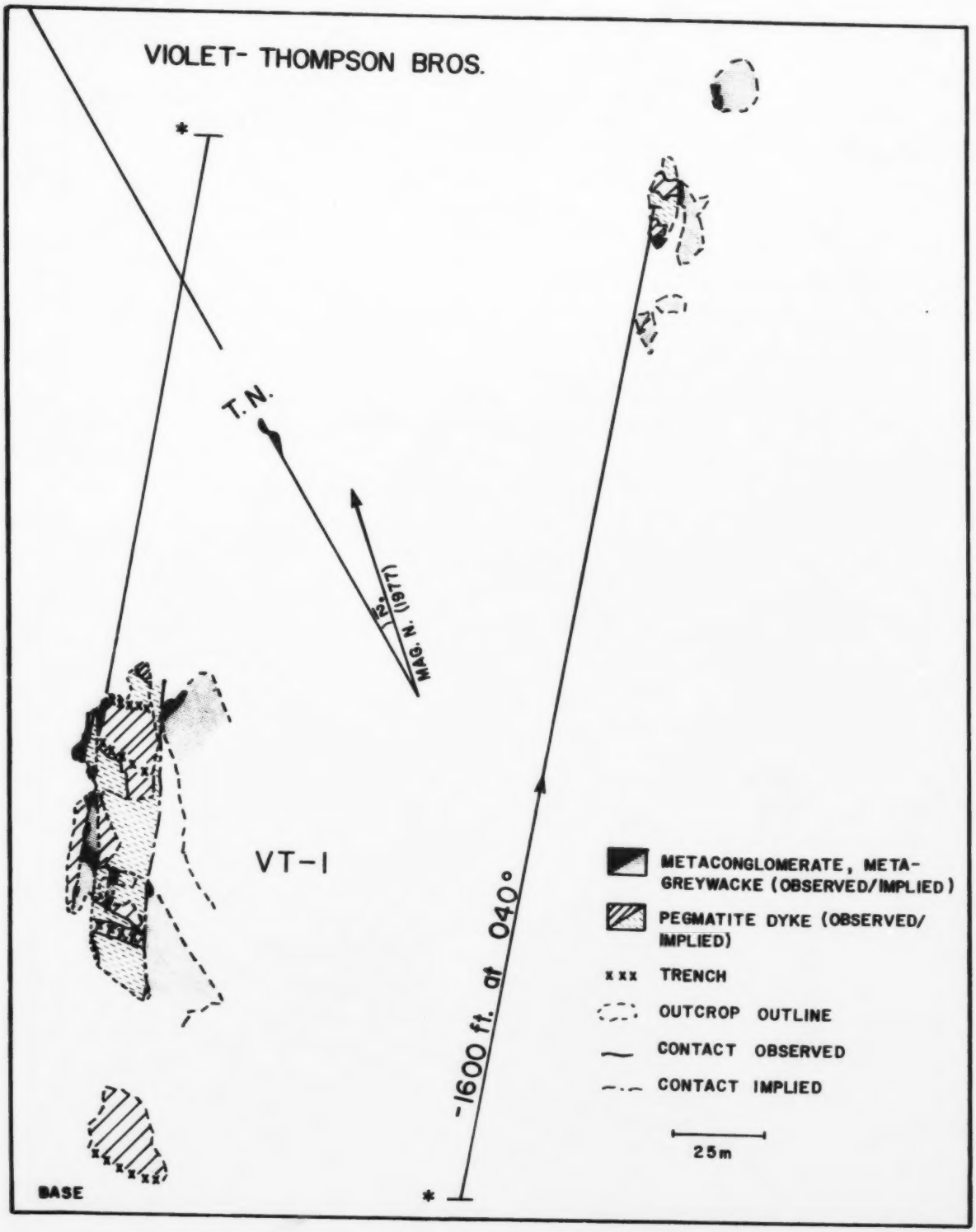

Figure 162: The Violet-Thompson pegmatite. Asterisks designate point of continuation of the two segments

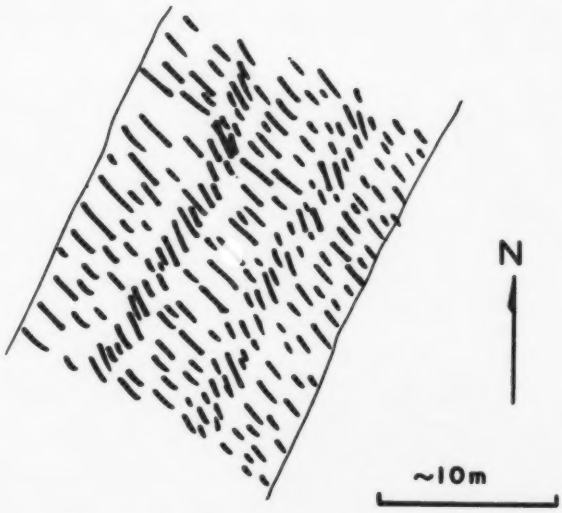

Figure 163: Schematic illustration of the preferred orientation of spodumene (and K-feldspar) in the Violet-Thompson pegmatite dyke

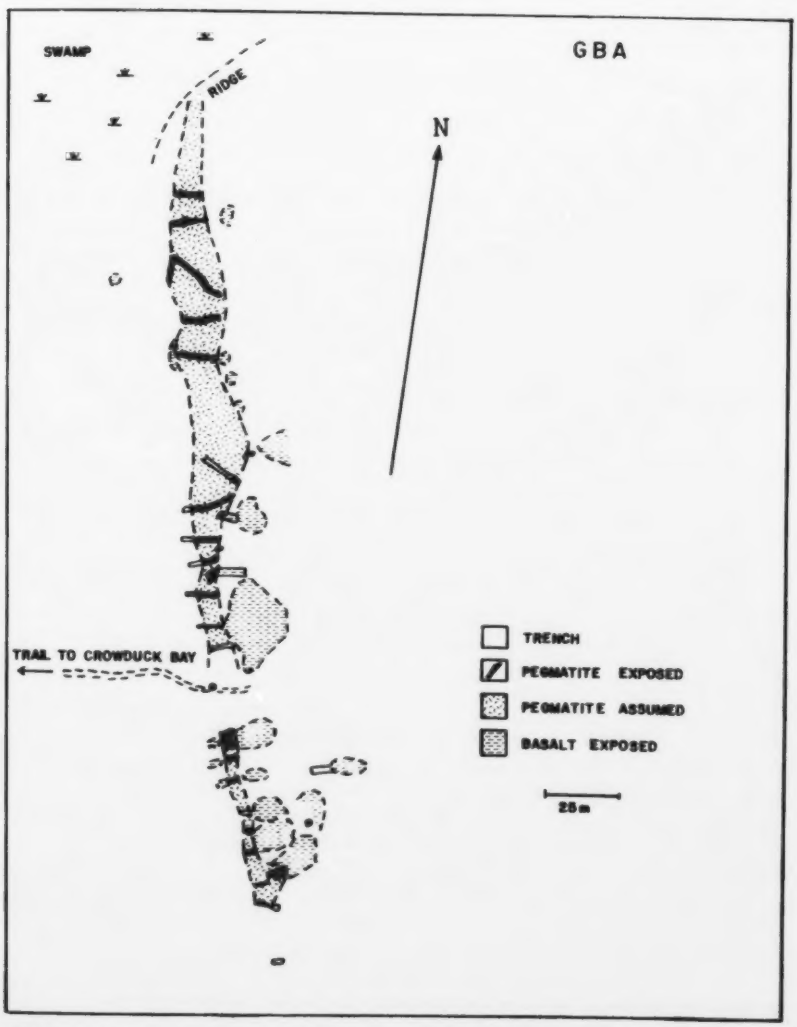

Figure 164: The westernmost Green Bay pegmatite dyke, GBA

TABLE 79 PARAGENESIS OF PEGMATITES IN THE WEKUSKO LAKE FIELD

	SG		VT	GB		
	SG-1	SG-2	VT	GBA	GBB	GBC
Microcline	●	●	●	●	●	●
Oligoclase	•	•	•	•	•	•
Albite	●	●	●	●	●	●
Quartz	●	●	●	●	●	●
Holmquistite						
Biotite	•		•	•	•	•
Muscovite	X	X	X	X	X	X
Li-muscovite						
Lepidolite						
Spodumene	X	O	●	●	O	O
Petalite						
Eucryptite						
Pollucite						
Epidote						
Chlorite						
Cordierite						
Garnet	•	•	•	•	•	•
Schorl	•	•	•	X	•	•
Elbaites						
Topaz						
Gahnite						
Beryl	?	•	•	•	•	?
Titanite						
Allanite						
Gadolinite						
Zircon						
Thorite						
Uraninite						
Magnetite						
Ilmenite						
Niobian rutile						
Aeschynite						
Fersmite						
Euxenite						
Yttrotantalite						
Cassiterite						
Columbite-tantalite						
Pseudo-ixiolite						
Microlite						
Tapiolite						
Wodginite						
Simpsonite						
Stibiotantalite						
Apatite	•	•	•	•	•	
Monazite						
Xenotime						
Triphylite-lithiophilite		•				
Amblygonite-montebrasite						
Sulphides of Fe, Cu						
As						
Mo						
Zn, Cd						
Bi						
Sb						
Pb, Ag						

Hydrothermal alteration causes, locally, sericitization of feldspars and tourmaline; surface weathering oxidizes triphylite- lithiophilite.

Symbols as in Table 20.

Mineralogy

As evident from the preceding descriptions, the mineralogy of all three pegmatite groups is practically identical (Tables 79-82) despite the widely separated locations, different attitudes, and individualized internal structures. The only difference observed in the field lies in the distinct enrichment of the GBA dyke in tourmaline and beryl, particularly towards its northern end; in the other pegmatites these two minerals are much less abundant.

Geochemical characteristics show a close relationship between the Sherritt-Gordon and Violet-Thompson groups, and a much more advanced fractionation in the Green Bay pegmatites. This is shown repeatedly by the plots of K/Rb vs. Cs in K-feldspars and muscovites, and by the Na/Li vs. Cs plot of beryls (Fig. 165). In the Green Bay group, the highest degree of fractionation is attained in the small dykes GBB and GBC.

The trend of the Green Bay beryls shown in Figure 165 is exceptional, showing an increase in Cs with increasing Na/Li ratio. No such relationship has been observed to date (Černý 1975, and unpublished data). However, the trend is based on 9 data sets and it is unlikely that additional analyses would substantially change its orientation.

Partial analyses of spodumene (Fig. 165) from all three pegmatite groups show increased Na_2O, and particularly Fe_2O_3, conforming to the characteristics of primary, relatively high-P spodumene of Heinrich's (1975) type 1, phenocrystic variety.

Other occurrences

Finally, two other groups of pegmatites will be briefly mentioned because of their significance in assessing the economic potential of the Herb Lake field.

K-feldspars were sampled from a series of minor pegmatites outcropping in the Missi metasediments on the eastern side of Crowduck Bay, northeast of the Violet-Thompson claim. The K/Rb vs. Cs field shown in Figure 158 is considerably elongate, with several values reaching the fractionation level of the SG and VT dykes, and one feldspar reaching the GBA fractionation level.

Another series of samples was taken from small bodies of pegmatitic granites grading into pegmatite veins south of Dion Lake. All of these are characterized by small size, concordant attitude in migmatitic gneiss host, lenticular shape, and discontinuity along strike; late alteration is widespread, affecting mainly plagioclase. The fractionation of rare alkalis in the K-feldspars is very poor (Fig. 158). Microscopic checks of some highly sericitized columnar minerals (mostly albite) revealed fragments of a spodumene-like mineral which could not be reliably identified by other methods. In view of the overall character of the pegmatites, and of their otherwise barren nature, the presence of spodumene is unlikely.

TABLE 80. COMPOSITIONAL CHARACTERISTICS OF SELECTED MINERALS FROM THE SHERRITT GORDON PEGMATITES

Blocky K-feldspar (16 samples)	arith. mean, wt.%	Rb 0.126	K/Rb 95.1	Cs 0.0084	
	std. deviation	±0.03	±22.1	±0.0050	
	range	0.088-0.187	61.5-132	0.0037-0.0185	
Core muscovite (3)	Li 0.11	Rb 0.255	K/Rb 34.7	Cs 0.0067	Be 0.0022
	±0.035	±0.024	±3.3	±0.0042	±0.0002
	0.074-0.144	0.236-0.282	31.1-37.5	0.0043-0.0115	0.0020-0.0024
Late beryl (4)	Li 0.346	Na 1.070	Na/Li 3.09	Cs 0.175	
	±0.044	±0.184	±0.18	±0.056	
	0.292-0.390	0.831-1.22	2.85-3.28	0.108-0.228	
Spodumene (4)	Na_2O 0.257	Fe as Fe_2O_3 1.178			
	±0.069	±0.225			
	0.158-0.306	0.96-1.40			
Garnet (7)	FeO 26.08	MnO 16.25	(MnO x 100)/(MnO + FeO) 38.27	CaO 0.73	MgO 0.34
	±4.50	±4.67	±10.91	±0.18	±0.05
	20.99-31.74	10.99-21.52	25.72-50.43	0.43-0.92	0.25-0.42

TABLE 81. COMPOSITIONAL CHARACTERISTICS OF SELECTED MINERALS FROM THE VIOLET-THOMPSON PEGMATITE

Blocky K-feldspar		Rb	K/Rb	Cs	
(31 samples)	arith. mean, wt.%	0.10	115.9	0.0040	
	std. deviation	±0.04	±29.3	±0.0022	
	range	0.061-0.240	43.6-161	0.0019-0.0131	
	Li	Rb	K/Rb	Cs	Be
Core muscovite	0.067	0.214	42.4	0.0030	0.0019
(4)	±0.008	±0.060	±8.9	±0.0020	±0.0009
	0.056-0.073	0.178-0.303	29.3-47.9	0.0017-0.0060	0.0013-0.0032
	Li	Na	Na/Li	Cs	
Late beryl	0.407	1.35	3.33	0.10	
(2)	±0.009	±0.18	±0.53	±0.015	
	0.400-0.413	1.22-1.48	2.95-3.70	0.089-1.10	
	Na_2O	Fe as Fe_2O_3			
Spodumene	0.198	1.237			
(3)	±0.038	±0.012			
	0.166-0.240	1.23-1.25			
Garnet	FeO	MnO	(MnO x 100)/(MnO + FeO)	CaO	MgO
(5)	24.85	17.50	41.28	0.94	0.31
	±6.11	±6.24	±14.38	±0.34	±0.09
	14.60-30.19	13.04-28.40	30.16-66.05	0.46-1.40	0.19-0.41

TABLE 82. COMPOSITIONAL CHARACTERISTICS OF SELECTED MINERALS FROM THE GREEN BAY PEGMATITE GROUP

Blocky K-feldspar		Rb	K/Rb	Cs	
(19 samples)	arith. mean, wt.%	0.392	33.7	0.0603	
	std. deviation	±.144	±15.1	± 0.0383	
	range	0.183-0.668	17.1-62.8	0.0158-0.1404	
	Li	Rb	K/Rb	Cs	Be
Core muscovite	0.171	0.792	12.5	0.0702	0.0021
(4)	±0.122	±0.432	±5.1	±0.0497	±0.0003
	0.025-0.314	0.473-1.42	5.9-17.7	0.025-0.123	0.0017-0.0023
	Li	Na	Na/Li	Cs	
Late beryl	0.331	0.903	2.83	0.939	
(9)	±0.080	±0.101	±0.50	±0.452	
	0.202-0.460	0.720-1.01	2.00-3.56	0.334-1.67	
	Na_2O	Fe as Fe_2O_3			
Spodumene	0.230	0.943			
(3)	±0.104	±0.446			
	0.16-0.35	0.428-1.21			
Garnet	FeO	Mno	(Mno x 100)/(MnO + FeO)	CaO	MgO
(1)	24.80	17.10	40.81	0.46	0.49

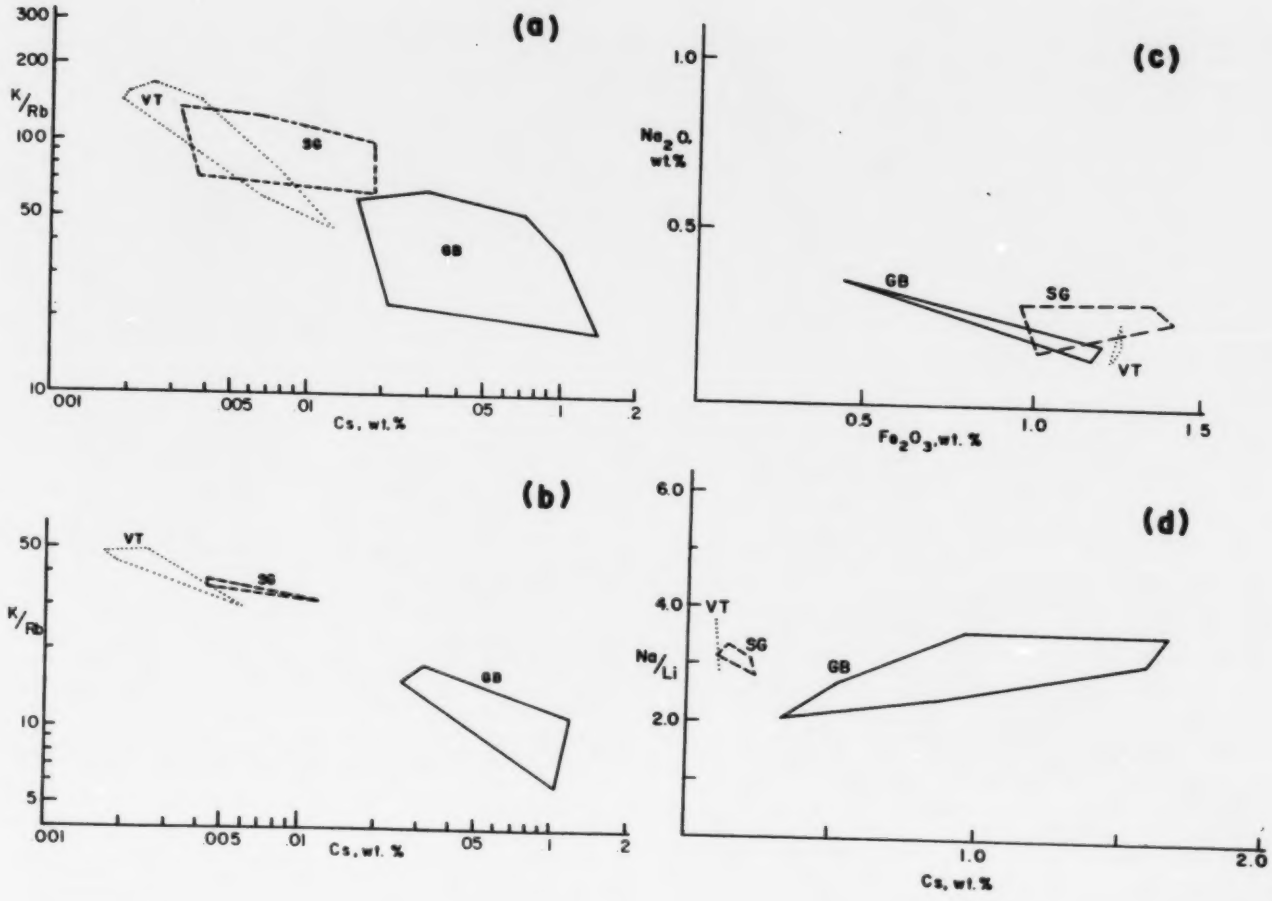

Figure 165: Compositional characteristics of pegmatite minerals from the SG, VT, and GB groups : (a) blocky K-feldspar, (b) muscovite, (c) spodumene, (d) beryl

STRUCTURAL GEOLOGY

INTRODUCTION

Structural studies along the northern edge of the Flin Flon Volcanic Belt and the adjacent southern edge of the Kisseynew Sedimentary Gneiss Belt by Bailes (1975) indicate that as many as 5 deformational events have affected rocks in the area.

Bailes (1975) demonstrates the close relationship between folding and metamorphic events across the metamorphic gradient which now best marks the boundary of the Kisseynew and Flin Flon-Snow Lake belts (Moore and Froese 1972). As a result, early northeast-folding events well preserved in the Herb Lake area were obliterated by the ensuing E-W deformation in the higher grade Kisseynew belt to the north (Bailes 1975). The same E-W fold axial traces so well defined on the Kisseynew side of the metamorphic gradient are only weakly displayed in the Wekusko Lake region. The recognition of variable effects of deformation under different degrees of mobility across a metamorphic gradient is the key to understanding the overall deformational history of the Kisseynew front.

The structural studies performed during the present pegmatite study were not of a regional nature, but rather restricted to the structural setting of the pegmatites and units possibly significant in pegmatite generation. Thus the present structural treatise attempts to place the pegmatite intrusions and their host rocks into the established structural history of the region; reconstructing a regional structural history from the localized mapping done during this study would be tenuous at best and superfluous in any case.

INTERPRETATION OF REGIONAL STRUCTURAL HISTORY

The regional structural history of the Wekusko Lake area as compiled from Bailes (1975) is as follows:

D_1 - This event developed early isoclinal folds (F_1), flattening minerals and fragments parallel to S_1 schistosity. This event is proposed by Bailes (1975) to have formed recumbent nappe structures of Missi metasediments which moved towards the south and were infolded into underlying Amisk metasediments.

D_2 - This event developed major north-northeast-trending folds (F_2) with axes plunging shallowly to the north-northeast. These structures deform earlier D_1 structures and have locally developed axial planar schistosity.

D_3 - This event developed east-trending open folds (F_3) (well developed in the Kisseynew belt but poorly developed in the Wekusko Lake region). Emplacement of the Herblet Lake complex (of which the Crowduck Bay gneiss dome is a part) may be associated with this folding.

D_4 - This event produced northeast-trending flexural folds (F_4) in the Kisseynew rocks to the north (Bailes 1975, Moore and Froese 1972). The present study demonstrates that they also occur south of the Kisseynew Belt, in the Flin Flon Volcanic Belt.

D_5 - This event comprises late, north-northwest-trending fractures and faults which Bailes attributes to a stress system with a northwest-trending principal compression axis.

DEFORMATION OBSERVED IN THE WEKUSKO LAKE AREA RELATABLE TO THE REGIONAL STRUCTURE

D_1 - This early deformational event is possibly best expressed southwest of Crowduck Bay, where pebbles in Missi metasediments are elongate in northwest-trending direction. Froese and Moore (pers. comm. 1978) define northwest-trending isoclinal folds along the west shore of Wekusko Lake in the Berry-Taylor Bays area (also noted by Russell 1957) as F_1 folds. In general, however, the presence of D_1 in the examined area is questionable.

D_2 - This deformational event resulted in the development of northeast-trending large scale F_2 folds (Map 4). It produced open folding of both Missi and Amisk strata about northeast-trending axial planes with axis plunging shallowly to the northeast. Southeast of Crowduck Bay, pebbles in Missi conglomerates flattened during D_1 are folded about an F_2 axis which is parallel to D_1 schistosity. Strong D_2 schistosity developed parallel to axial planes of the folded pebbles. The mineral and pebble lineations plunge to the northeast, probably reflecting axial plunges of F_2 folds.

D_3 - This east-trending open folding is exemplified by the doubly plunging F_3 folds in the Missi conglomerates, northeast of Lost Frog Lake (see Frarey 1950). Changes in plunge of mineral lineations along the length of the northeast elongate Crowduck Bay gneiss dome (Map 4) reflect undulational folding about approximately west-northwest-trending axial planes, possibly related to F_3 folding. The Crowduck Bay gneiss dome is interpreted as emplaced during F_3, controlled by F_2 and F_3 fold structure interference (Bailes 1975). Another probable expression of F_3 folding is evident south-southeast of Dion Lake, where a patch of unit F biotite gneiss dips shallowly to the north and south, away from a minor dome structure. This exposure of unit F may be due to upwarping in an F_3 fold to expose gneisses of possibly Amisk affiliation underlying Amisk volcanics.

D_4 - This late, north-northeast-folding event identified in the Kisseynew belt had not been recognized in the Flin Flon-Snow Lake belt to the south (Moore and Froese 1972, Bailes 1975). However, within the Crowduck Bay gneiss dome, mafic bands and stringers which generally trend northeast have been observed tightly folded about a later northeast axial plane with a moderately developed biotite axial planar schistosity (Fig. 166). Although they lack the concentric flexural style of the F_4 folds (Bailes 1975) and are more flow-fold in style, they may be F_4 features, or may simply be flow folds developed during dome emplacement.

D_5 - The major set of north-northwest-trending faults observed in the Kisseynew belt are not abundant in the Wekusko Lake area.

Instead, brittle deformation consists of two major fault systems. One is a set of northeast-trending faults parallel or sub-parallel to the major F_2 fold axis. This northeast fault system is offset by relative dextral movement, up to several hundred metres along an east-northeast-trending fault set (Map 4).

The majority of pegmatite dykes (such as those in Crowduck Bay) occur in northeast-trending orientation in much the same way as felsic pegmatites inject north-northwest-trending fractures in the Guay-Wimapedi area. If the generation of pegmatites occurred during the same event, the northeast faulting at Wekusko Lake may be of similar relative age as the north-northwest faulting in the Guay-Wimapedi area.

PLUTONIC AND ASSOCIATED ROCKS IN THE STRUCTURAL DEVELOPMENT AT WEKUSKO LAKE

Syntectonic units

In the Broad Bay granodiorite, igneous plagioclase crystals formed during early crystallization show progressive breakage during crystal transport, grading into protoclastic and re-crystallization shear textures in various outcrops. This variable textural development was accompanied by deuteric alteration during shearing and final crystallization. The crystallization, apparently simultaneous with strong to moderate tectonic foliation development, classifies this body as a syntectonic intrusion. The fabric orientation conforms with fabrics in adjacent metavolcanic units to the north, which were apparently foliated during F_1 deformation as their fabric wraps around the noses of F_2 folds. Thus unit L appears to be an early tectonic intrusion, possibly accompanying F_1 deformation.

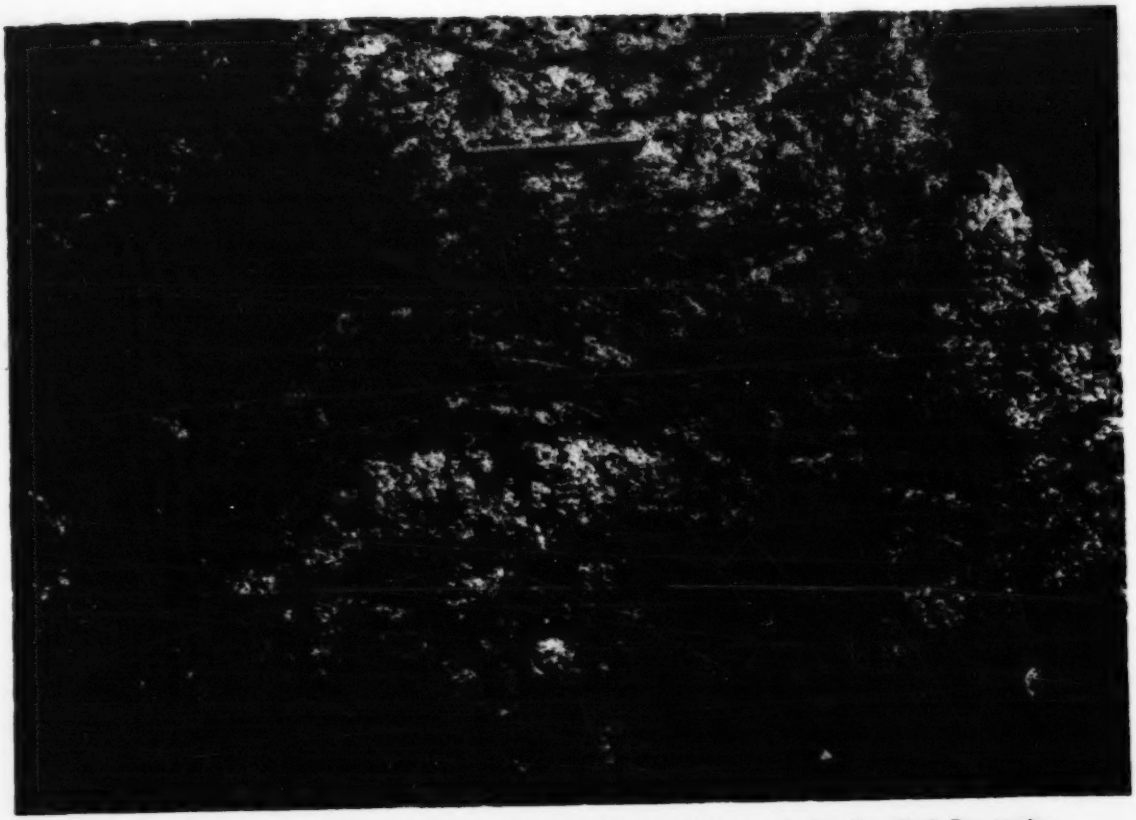

Figure 166: Folds of the F4 event, with NE-striking axial planes, in the Crowduck Bay gneiss dome

The strong northeast-trending foliation and alignment of amphibole and metasedimentary inclusions in the gneissic quartz diorites (M) suggests that intrusion and crystallization occurred under the influence of the main northeast-trending deformation D_3. The fact that the rock is recrystallized, probably during the main metamorphic event which followed D_3, further supports this interpretation.

The high degree of mobilization in the Crowduck Bay gneiss dome (see metamorphism), conformable fabrics and contacts, together with the outward dipping gneissosity and foliation, suggest diapiric emplacement. To mobilize this paragneiss in this manner a high metamorphic grade is required. The metamorphism reached the initial anatectic stage at the end of D_2 (Bailes 1975). Thus the Crowduck Bay gneiss dome must have been emplaced between the D_2 and D_3 events. Evidence that the gneiss dome was partially mobile during D_3 is provided by open folds in D_3 gneissosity with northwest axial traces, and by changes in plunges of the D_3 mineral lineations.

Late-tectonic intrusions

The Rex Lake plutonic complex is located southwest of the Crowduck Bay gneiss dome, in a northeast-trending belt of plutons apparently intruding a zone of weakness, possibly related to D_3 deformation.

Internally the gabbroic, dioritic, granodioritic and granitic phases that comprise the complex exhibit fabrics that range from weak to strong in foliation, and locally pass into irregular shear zones. Mineral lineations, generally quartz or biotite smears, are common near contacts between the batholith and surrounding Amisk metasediments. The usual tendency for marginal batholithic fabrics to occur parallel to contacts with the country rocks is not the dominant structural feature in the Rex Lake pluton. Instead, the foliations and the majority of lineation plunges are aligned with the regional northeast structural fabric (Map 4). In outcrop these fabrics do not appear to be secondary, but in thin section strain and recrystallization of quartz is clearly evident. This suggests that the Rex Lake plutonic complex was under the influence of northeast tectonic forces prior to complete solidification. However, the massive character of the unit R along the northwest edge of the batholith suggests that the resultant northeast strain was not influential over the entire batholith during all intrusive phases. Thus the Rex Lake pluton is classified as a syn- to late-tectonic intrusion possibly emplaced during the late, mild D_4 event. However, the possibility that it was intruded earlier under the waning influence of the much stronger D_3-northeast deformation cannot be ruled out.

The gabbroic rim of the Stuart Lake pluton (T) appears massive in outcrop. Internally the only fabric observed was apparent biotite flow foliations trending northeast in the granodiorite core. While evidence is not conclusive, the Stuart Lake pluton seems similar to the Rex Lake pluton in relative age, gross composition, and degree of structural fabric development. Thus it is considered a late-tectonic intrusion crystallized under some northeast-directed stress similar to the Rex Lake pluton.

The Wekusko porphyritic granite (U) is the third plutonic body in the northeast-trending belt of intrusions, located in the

extreme southwestern part of the studied area. This unit is mainly massive with no foliated contact zones, and only a trace of weakly developed flow foliation. The lack of foliated contacts and the euhedral to subhedral granular texture suggests that this igneous body crystallized in a relatively unstressed environment. Thin section study reveals early transport of plagioclase crystals with later static crystallization of quartz and K-feldspar.

Similarly the Tramping Lake granite (V) is a massive hypidiomorphic granular rock which apparently crystallized under largely static conditions.

Thus units U and V are considered the youngest major intrusions in the Wekusko Lake area, intruded into a relatively inert tectonic environment which did not conspicuously affect their fabric.

Large pegmatitic granites (W) do not show any indications of syn- or post-crystallization effects but some small bodies of fine-grained leucogranites at Osborne Lake display preferred northeast orientation of micas, suggesting crystallization under the regionally predominant stress.

Virtually all types of small pegmatitic granites and pegmatites show signs of deformation, but its intensity is highly variable. This may suggest several ages of pegmatite injection. However, systematic change in deformation among pegmatite types of possibly different relative ages was not observed. Thus a more favoured explanation is that of locally variable intensity of strain during the waning stages of a late tectonic event. Such a variable late deformation is evident in the host rocks, e.g. the Missi metasediments, across their strike. Also, the most intense deformation in pegmatitic rocks (including the spodumene-bearing localities) occurs along the Grass River lineament marked by frequent shear zones, which is suspected by Shanks and Bailes (1977) to represent a major fault zone.

As indicated earlier, the pegmatitic rocks in the Wekusko Lake field are located in the fracture systems produced by the latest D_3 event. The deformation suffered by the pegmatites is related to the late stages of the same event as no later deformation could be recognized in the area.

METAMORPHISM

REGIONAL METAMORPHIC SETTING

The boundary of the Flin Flon Volcanic Belt and the Kisseynew gneiss belt to the north is coincident with an increase in metamorphic grade from greenschist facies in the volcanic belt to the south, to upper amphibolite facies and the onset of anatexis at the Kisseynew boundary to the north (Froese and Gasparrini 1975, Bailes 1975). The isograds defining this increase in metamorphic grade from south to north have been established by Froese and Gasparrini (1975) from pelitic rocks in the Snow Lake area west of Wekusko Lake and are reproduced on Map 4. These isograds were extended into the Wekusko study area by Bailes (1975) as shown on the same map.

METAMORPHIC ISOGRADS

The mineralogy and reactions used by Froese and Gasparrini (1975) and Bailes (1975) to define the metamorphic isograds are as follows (after Bailes 1975):

(A) staurolite "in" isograd: chlorite + almandine + muscovite ⇌ biotite + staurolite + quartz + H_2O

(B) sillimanite "in" isograd: chlorite + staurolite + muscovite + quartz ⇌ biotite + sillimanite + H_2O

(C) staurolite "out" isograd: staurolite + muscovite + quartz ⇌ biotite + sillimanite + almandine + H_2O

(D) muscovite "out" isograd: muscovite + quartz ⇌ sillimanite + potassium feldspar + H_2O

Froese and Gasparrini (1973) plotted their isograd reactions on a PT diagram to determine that the reactions occurred at a pressur of 5 to 6 kilobars with a temperature increasing from 500° to 650°C from south to north. Bailes (1975) similarly determined that metamorphic conditions reached 4-6 kilobars and temperatures between 700° and 800°C in the Guay-Wimapedi area north of the present field of study. The temperature and pressure determined by Bailes (1975) is consistent with conditions prevalent at the onset of anatexis (Winkler 1976).

ISOGRAD IRREGULARITIES

The east-west metamorphic isograds as established by Froese and Gasparrini at Snow Lake and extended into the Wekusko Lake area by Bailes (1975) appear to be deflected in the Herb Lake region as evident from observations made during this study. Shanks and Bailes (1977) indicate that a major fault follows the southeast shore of Crowduck Bay, and that a smooth continuation of isograds cannot be expected across this fault. Deviations from the east-trending isograds may be significant in relation to the pegmatite occurrences.

The establishment of metamorphic reactions from existing mineralogy in the Wekusko Lake region, especially east of the Grass River, is hampered by the abundance of quartzofeldspathic Missi metasediments and by a general lack of aluminous pelitic metasediments. The general increase in maturity of sediments from north to south, noted in an earlier section further hinders development of metamorphic indicators to the south.

In certain outcrops where sediments are of favourable composition, mineralogy suggests that metamorphic grades are higher to the east and south than implied by the isograds on Map 4. For example, immediately south of Dion Lake a quartzofeldspathic gneiss (PW353, Map 5) is composed of plagioclase + quartz + sillimanite + biotite + garnet, indicating that metamorphism there has reached the biotite-sillimanite–almandine grade. On the northwest side of the lake (PW302, Map 5), mineralogy of arkosic metasediments consists of K-feldspar + quartz + biotite + hornblende + muscovite + chlorite + carbonate, and it suggests an amphibolite facies peak prior to retrogression. However, the presence of muscovite with quartz suggests a lower grade (Winkler 1976) than occurred south of Dion Lake.

Farther east of Dion Lake quartzofeldspathic gneisses possibly derived from arkosic metasediments are migmatized with the mobilizate retained in situ. These rocks display a mineralogy comprised of quartz + orthoclase + hornblende + and chlorite + magnetite. This suggests that metamorphism reached upper amphibolite facies prior to a retrograde greenschist event. This tendency for increased grade from northwest to south and east was also noted by Bailes(1976) working in the Saw lake area east of Dion Lake.

Shanks (pers. comm.) noticed an abrupt increase in metamorphic grade on the east shore of Wekusko Lake from greenschist facies on Lucky Island near Herb Lake townsite to middle amphibolite grade to the east. Also, near the Violet-Thompson pegmatite dyke, east of Grass River and south of the proposed staurolite "in" isograd, poikilitic hornblende occurs in the matrix of the Missi conglomerate. Shanks and Bailes (1977) propose a fault paralleling the east shore of Wekusko Lake and northward along Grass River, to account for the abrupt increase in grade on the east side of Wekusko Lake.

The most pelitic rocks north of Herb Lake townsite and east of Grass River (PW221, PW398, PW136) are typified by assemblages of feldspar + quartz + biotite + muscovite + magnetite + chlorite with no aluminous metamorphic mineral observed. North of Crowduck Bay and east along Grass River metasedimentary features such as crossbedding are increasingly obliterated to produce the quartzofeldspathic gneiss observed at PW136. Thus a general increase in metamorphic grade does occur north and east of Crowduck Bay, despite a general lack of indicators.

Thus the area east of Grass River appears to have increasing metamorphic grade both to the north and east. This suggests a more complicated isograd configuration for the area east of Wekusko Lake than for the Snow Lake area. This apparent deflection of the east-west isograd trend may be the result of two factors: (1) the isograds of Froese and Gasparrini (1973) may be parallel to the Kisseynew-Flin Flon-Snow Lake belt contact which swings southward at Dion Lake (McRitchie 1977), or, (2) a late Aphebian orogenic event along the Superior-Churchill boundary, which lies approximately 30 km east of Dion Lake, may be affecting metamorphic isograds in the Dion Lake area (Bailes 1976).

METAMORPHIC HISTORY AND DEFORMATION

Petrography of metamorphic rocks generally shows evidence of two metamorphic events.

The earlier and more intense event is the regional metamorphism of Missi and Amisk rocks resulting in the mineralogy described by Froese and Gasparrini (1973) where composition is suitable, and resulting in general increased recrystallization to the north, and to the east (and south) of Dion Lake, in more psammitic rocks.

A later retrograde event is also evident in Missi and Amisk rocks throughout the area resulting in the production of chlorite, carbonate, saussurite, and the addition of minor sulphides.

The main metamorphic event at Wekusko Lake occurred near the end of the major northeast-folding event D_2 (Bailes 1975). This is evident from the fact that large euhedral staurolite prophyroblasts (up to 6 cm long), formed in pelitic metasediments on islands at the southern end of Crowduck Bay, are not well aligned parallel to the strongly developed F_2 foliation, but have grown after the main F_2 deformation, gently deflecting F_2 foliations around the porphyroblasts. Accompanying euhedral garnets show no evidence of deformation by the D_2 event.

The mobilization and emplacement of the Crowduck Bay gneiss dome probably occurred as a consequence of heating during the main metamorphic event. This dome occupies a northeast-trending D_2 structure and has been weakly folded by

ensuing D_3 deformation. This also suggests that the main metamorphism reached maximum temperature after F_3 and prior to F_3. However, a metamorphic event of this magnitude may have overlapped several periods of deformation.

Late retrograde greenschist facies metamorphism has produced chlorite, carbonate, saussurite, sericite, reddish-colored biotite and introduced minor sulphide in most rock types. The greatest development of retrograde greenschist assemblages occurs in strongly foliated rocks, (units A, J, and N), sporadically in strongly gneissic rocks (units F, G, and H), and along shear zones in units S, T, and U. The greatest hydothermal effects are visible near shear zones which may be quartz-filled and often sulphide- and/or gold-bearing. This retrograde event may be synchrous with the introduction of gold into the Wekusko Lake area as identical assemblages typified by red biotite occur locally throughout the area and in the gold showings in the Rex Lake pluton. Quartz vein deposits in the Herb Lake townsite area have not been investigated in this regard.

Other minor retrograde development of chlorite occurs in patches in rock types devoid of strong fabrics, and in these cases such alteration may have occurred during slow cooling after the peak of the main metamorphism. However, where retrograde greenschist assemblages occur in more deformed rocks, the introduction of late solutions is evident. These solutions have invaded zones of weakness and introduced quartz, carbonate and sulphides, in addition to producing retrograde chlorite, saussurite and sericite.

The exact timing of this possible regional introduction of hydrothermal fluids, responsible for the retrograde process evident over the entire area, is somewhat problematic, as it may not represent a single event. Localized late migration of fluids within each separate plutonic rock is also a possibility. However, the fact that it has affected the main metamorphic asseblages in all rock types including metasediments and metavolcanics, and is most evident in northeast structural trends, suggests that it may have been synchronous with the late northeast deformation, D_4.

The development of greenschist metamorphism during D_4 is in agreement with Bailes' (1975) proposal of low to moderate pressure and temperature during D_4 for the Guay-Wimapedi area. The lack of D_4 folding in the Wekusko Lake area but the abundance of northeast-trending, commonly quartz-filled shear zones, may reflect the lower temperature and more brittle conditions existing to the south in the Wekusko Lake area during D_4. The shear zones and fractures may have provided paths for hydrothermal fluids (of unknown origin) to reach the present level and promote the retrogression.

POSITON OF INTRUSIVE ROCKS IN METAMORPHIC FRAMEWORK

Syntectonic Intrusions

The heterogeneous felsic intrusion of the Broad Bay granitoids (L) displays crush texture with much apparent milling during emplacement accompanied by extensive hydrothemal alteration. The original igneous texture was almost obliterated by saussuritization, sericitization, chloritization and carbonatization. The placement of this unit as a syntectonic intrusion due to what may be an F_3 foliation, implies that it was present during both later metamorphic events. The location of unit L at the south end of Wekusko Lake places it in the greenschist regional metamorphic zone. Thus it may have undergone two mild metamorphic events. Evidence of at least one post-emplacement metamorphic event is the presence of 345° trending sulphide-bearing shear zones, similar to the late, greenschist-retrograde sulphide-bearing shear zones present elsewhere in the area.

The Crowduck Bay and Herb Bay gneissic quartz-diorites (M) have been placed as intruding near the end of D_3 deformation. This suggests that it was present during the main metamorphism. The quartz diorite composition precludes development of aluminous metamorphic indicators; however, the recrystallization of quartz and some plagioclase (An content greater than An_{25}), and the amphibolitization of small inclusions suggest that it was present during amphibolite grade metamorphism.

Retrograde chlorite was observed in a single sample suggesting that this unit was not greatly affected by an ensuing retrograde metamorphic event.

The original composition of the Crowduck Bay gneiss dome (N,O) has locally suffered partial anatexis and remobilization due to upper amphibolite regional metamorphism. In addition retrograde greenschist metamorphic chlorite, saussurite and carbonate are present in many localities.

Late tectonic Intrusions

The Rex Lake plutonic complex (P, Q, R, S) has crystallized under the influence of a northeast-oriented strain such as occurred during D_3 or D_4 (see structure section).

The phases that display the most alteration are the dioritic unit Q and the granodioritic unit R. In these units, especially near contacts, secondary epidote, chlorite and carbonate are developed, and some ragged poikilitic hornblende that contains tiny plagioclase and quartz inclusions. In addition, some recrystallization of quartz, growth of albite on earlier-formed plagioclase crystals, and saussuritization of plagioclase occurs. The mafic gabbro, unit P, displays much evidence of hydrothermal alteration and silicification with many thin quartz veinlets and quartz blebs visible in outcrop. Alteration consists of uralitization of pyroxene (tremolite, biotite, and chlorite) and moderate saussuritization of plagioclase cores (albite, epidote, muscovite).

The patchy occurrences of the greenschist-like alteration, mainly near the borders of the batholith and near internal shear zones, suggests that rather than representing a metamorphism, this late event was caused by hydrous solutions migrating through the pluton prior to complete crystallization. The source for these solutions is uncertain but may have been the batholith itself.

Thus the Rex Lake pluton is proposed to be a late tectonic intrusion emplaced after the main metamorphic event, and crystallized under the influence of D_4 deformation, although the possibility that it may be earlier (post-D_3) cannot be ruled out.

The Stuart Lake pluton (T) which displays a northeast fabric probably related to D_4, shows alteration along northeast fractures and shear zones in the form of chlorite, carbonate, saussurite, hematite and minor sulphides. This late greenschist-like assemblage may be related to the late greenschist metamorphic event which accompanied D_4 deformation; alternatively it may represent an autometamorphic effect, as suspected in the Rex Lake pluton.

The massive granitic plutons of the Wekusko and Tramping Lake granites (U, V) have been established earlier as the last main plutons to intrude the Wekusko Lake area. This conclusion is supported by the lack of evidence for the main regional metamorphic event within the units. The only metamorphic effects within the plutons are traces of chlorite fringing biotite flakes in a few samples. This can be considered a late deuteric effect, unrelated to the regional greenschist-type retrogression.

Metamorphic effects on pegmatitic granites (W) are minor; however, local chloritization and carbonatization were observed in leucogranites near Osborne Lake.

Metamorphic effects on the spodumene-bearing pegmatite dykes are generally negligible. Those that are observed in most localities are of deuteric, autometasomatic character, involving components and reactions from within the pegmatites themselves. No chloritization or sulphide development was observed which would require material introduction from outside the bodies. Thus it seems likely that the mineralized pegmatites were not affected by the retrograde processes.

GENETIC RELATIONSHIPS

Introduction

Defining the process generating the mineralized pegmatites in the Wekusko Lake field is a difficult task for several reasons: the Li, Be-B-bearing pegmatites are scarce, similar, and spread over a sizeable area; plutonic bodies which may have played a role outcrop only at large distances from the pegmatite localities; pegmatitic granites which may be parental to the mineralized pegmatites show a different regional distribution pattern and a different intrusion style; and last but not least deep erosional gouges filled by glacial drift and swamps cover several contact zones, obscuring some of the most important features of the region. Thus the following discussion leans considerably on the geochemical evidence, regional structure and distribution of late granitoids within its framework, and on possible analogy with the Cat Lake-Winnipeg River pegmatite field and other districts of similar character.

The batholiths

As discussed earlier, the Crowduck Bay gneissic dome is a diapiric body of partly mobilized gneisses of a probable rhyolitic volcanoclastic composition. Its recrystallized and molten parts are not more fractionated than the source material, and they show, within the limits of available evidence, no relationship to plutonic or pegmatitic granites of the region.

The Rex Lake complex, together with the Stewart Lake intrusion and other analogs, is derived from at least the lower crust but the data at hand are not sufficient for more detailed discussion. In view of its complex fractionation patterns it deserves a more thorough study.

Unambiguous evidence is not available to specify the origin of the plutonic granites of the Wekusko and Tramping Lake granites. Both plutons have negligible normative corundum and low fractionation levels, and they exhibit extreme compositional homogeneity suggestive of deep-seated juvenile origin. A direct differentiation link to igneous sequences of the Rex Lake complex type seems to be excluded by side-shifted parallelism of pluton as a result of amphibole fractionation (Fig. 167a). Differentiation from an igneous precursor of granitoid composition, by means of predominant plagioclase fractionation seems to be the most plausible possibility. This is in agreement with the Ab-Or-Qtz plots which reflect neither crystallization conditions nor initial anatectic melt compositions (Fig. 168). The pressures indicated are too low in both cases, considering the PT conditions of regional metamorphism; thus this line of evidence, although not contradicting the interpretation reached above, remains per se inconclusive.

Of the plutonic bodies disclosed in the pegmatite field, none seems to be capable of generating Li, Be, F-rich granitic pegmatites. The degree of melting attained by the Crowduck Bay gneiss dome and by the Dion-Hat Lakes gneisses is too low to break down substantial amounts of biotite and other mafic minerals which are the carriers of Li in metamorphic suites (Holland and Lambert 1972). The Rex Lake and Stewart Lake plutonic complexes are excessively mafic to intermediate in their bulk compositions, and too primitive in the trace element fractionation levels attained by their most acid differentiates, to generate mineralized granitic pegmatites. The same can be said about the granitic plutons that show insufficient fractionation in all geochemical indicators examined (Table 83), and that occur in areas remote from the mineralized pegmatites.

The pegmatitic granites

The mode of distribution of the pegmatitic granites, enveloping the Crowduck Bay gneissic dome and penetrating the Dion-Hat Lakes gneisses, does not indicate a genetic link with the granitic plutons exposed in the southwest. The forcible intrusive character of the bodies surrounding the gneissic dome suggests that generation of their parent melts occurred at a level considerably lower than the present erosional surface. The contrast between the geochemical signature of the gneissic dome and that of the pegmatitic granites makes the anatexis of lower parts of the gneissic dome an unlikely source. In the

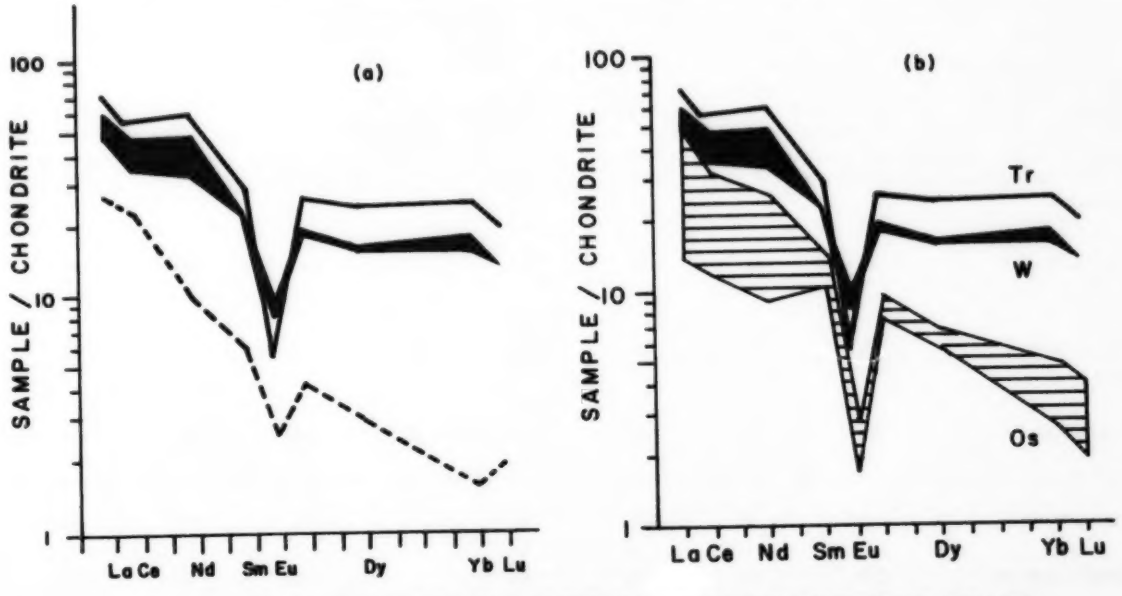

Figure 167: REE abundance relationships: (a) Wekusko and Tramping Lake granites vs. Rex Lake complex granite; (b) Wekusko and Tramping Lake granites vs. Osborne Lake pegmatitic granite

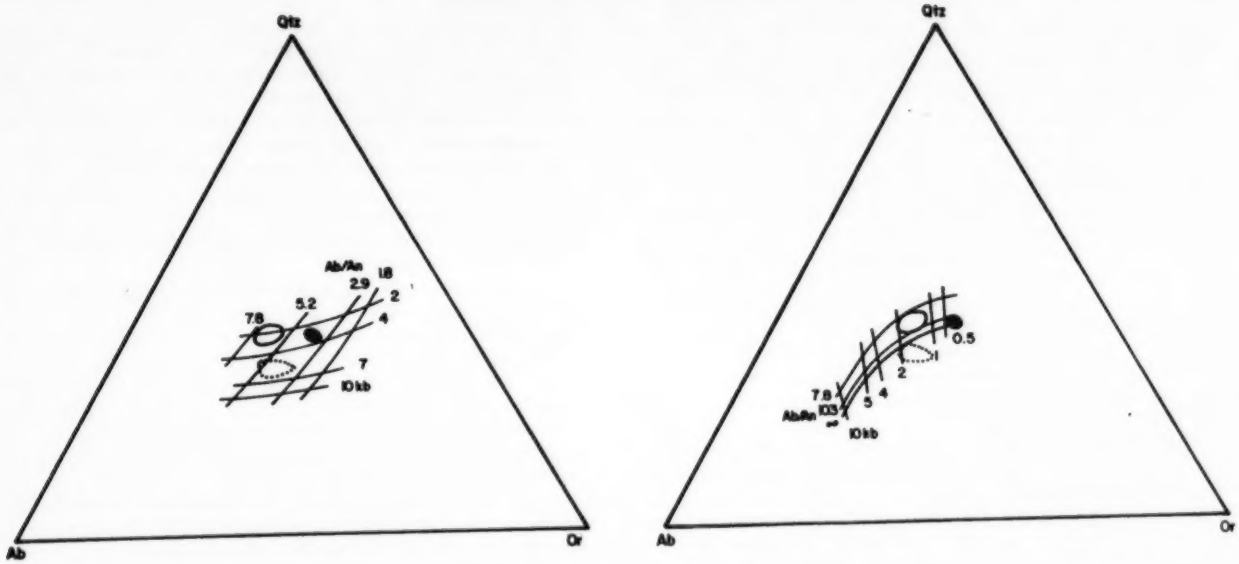

Figure 168: Ab-Or-Qtz mesonormative compositions in the Anderson and Cullers (1978) grids: Wekusko granite (solid outline), Tramping Lake granite (black field) and the main cluster of the fine grained leucogranites of the pegmatitic granite intrusions (dotted outline)

TABLE 83. GEOCHEMICAL INDICATORS OF BEUS AND SITNIN (1968) AND BEUS ET AL. (1968) COMPARED TO THE CHARACTERISTICS OF GRANITIC ROCKS OF THE WEKUSKO LAKE PEGMATITE FIELD. FIGURES IN BRACKETS ARE BASED ON LESS THAN 10 SAMPLES

	Li, ppm		Rb, ppm	Sn, ppm	V, ppm	Mg/Li		Zr/Sn	
Intrusion type	<25	>100	<150	>20	>4	<30	>100	<30	>100
Parental to Ta-bearing apogranites	<1%	64%	<1%	28%	1%	100%	<0.1%	83%	<0.1
Parental to Ta-bearing pegmatites	<1	41	5	26	1	39	0.4	93	14
Parental to Ta-poor pegmatites	26	27	24	16	1	27	30	87	5
Parental to Ta-free greisens	26	23	30	21	14	44	12	46	70
Barren granites	54	2	43	1	30	<<0.1	98	7	48
Wekusko granite	5.5	0	100	0	-	0	11	60	0
Tramping L. granite	(50)	(0)	(100)	(0)	-	(0)	(0)	(67)	(0)
Herb L. leucogranites	18	0	82	(0)	-	45.5	9	(87.5)	(12.5)

Dion-Hat Lakes gneissec terrane, mobilization of the pegmatitic granites from the gneisses in observed but only for bodies with very low fractionation levels; those relatively enriched in rare alkalis, Be, Sn, etc., are invariably intrusive. Thus the fractionated pegmatitic granites seem to have been generated by processes undisclosed at the surface. Their differentiation from deeper-seated intrusions of the Tramping Lake granite type is highly improbable in view of unrelated REE abundances (Fig. 167b); the decrease in HREE in the pegmatitic granites cannot be derived from the plutonic granites.

On the other side of the genetic linkage, a fractionation gap exists also between the pegmatitic granites and the Li, Be, B-bearing pegmatites. The collective compositional and mineralogical characteristics of the pegmatitic granites does not support the parent-product relation (Table 83). Of the three bodies which show above-average enrichment in rare elements (Herb Bay, Grass River, and Dion Creek), two are well outside the pegmatite area and the closest, the Grass River body, is located far beyond the northeastern extremity of the pegmatite group alignment. The styles of emplacement also contrast markedly from the forcibly intruded short-lenticular and plug-shaped bodies of the pegmatitic granites, to the passive fracture-filling injection of mineralized pegmatites. This is in sharp contrast with the rather uniform intrusive style of cogenetic pegmatitic granites and pegmatites in the Winnipeg River district.

Another factor bearing on the genesis of the pegmatites may be worth mentioning. In Heinrich's (1978) classification, lithium-rich pegmatites (containing close to 2 wt.% Li_2O) characteristic of the Herb Lake field, belong to the class 1 of Li-rich (1.1 - 2.4 wt.% Li_2O in bulk composition) unzoned bodies with "phenocrystic" Fe-rich spodumene. This pegmatite type seems to be separated from pegmatitic granites even in districts where both rock types are abundant and well exposed (e.g., Georgia Lake district, Černý and Trueman 1978). On the other hand, pegmatites typically generated from pegmatitic granites belong to Heinrich's class 2, zoned or complex pegmatites with LiO_2 contents of about 1 wt.%. It must be stressed, however, that this type of pegmatite classification is still *in statu nascendi*, and because of the difficulty of obtaining reliable quantitative data, the final form of this classification and its genetic significance are uncertain.

Despite all of the above considerations indicating a lack of link between the Wekusko Lake pegmatitic granites and the lithium-rich pegmatites, a qualifying statement may be in place: if a pegmatite source is to be sought among the outcropping igneous bodies, hidden analogs of the exposed pegmatitic granites would be the only likely source.

The pegmatites

The three groups of Li, Be, B-enriched pegmatites have much in common although they intrude different host-rock formations and occupy joint sets with different orientations over a distance of 6 km.

Despite the slightly different levels of rare-alkali fractionation attained in their bulk compositon, they are closely clustered and aligned on pertinent geochemical diagrams, and their accessory mineral assemblages are virtually identical. They penetrate late subvertical dilation fractures and extend to considerable depth along them. Most of the dykes show post-consolidation transverse offsets. All three groups are also situated within the lower amphibolite facies zone of a steep regional metamorphic gradient.

In view of the above observations it would appear that all three groups shared the same origin and were derived from the same type of source.

The plutonic bodies exposed in the pegmatite field and their hidden equivalents have been disqualified as possible sources, and the pegmatitic granites have been also dismissed, with a moderate reservation, on geochemical and structural grounds. Direct derivation of Li-rich pegmatites by partial anatexis is also improbable, for reasons mentioned earlier. Thus the pegmatites can only be related to a probably igneous source concealed at depth. In view of the evidence divorcing the pegmatites from any outcropping body which could be even remotely parental, the above statement carries much more weight than in its widespread usage as a convenient evasion of admitting ignorance.

Conclusions

The only igneous activity that may have generated mineralized pegmatites in the Wekusko Lake field is concentrated along, and between, the two north-northeast-trending fault lineaments through the Osborne Lake-Bart Lake-Kormans Lake-Anderson Bay and Berry Creek, and through Crowduck Bay and Grass River. Repeated and diverse magmatic activity, from upwarped migmatitic gneiss domes through differentiated gabbroic complexes and plutonic granites to forcible intrusions of pegmatitic granite stocks, is evidenced between these fault lineaments, the eastern of which is populated by the Li, Be, B-bearing pegmatites that are the last intrusive bodies in the regional evolution. These pegmatites cannot be safely linked to any outcropping intrusion; the parental body (or bodies) is evidently hidden beneath the present erosion surface but probably hosted by the same fault lineament.

ECONOMIC CONSIDERATIONS

GEOCHEMICAL POTENTIAL OF THE FIELD

As shown in the preceding sections, the geochemistry of the metamorphic sequences and particularly of the late plutonic intrusions, pegmatitic granites, and pegmatites indicates that the whole field is considerably primitive in terms of rare-alkali fractionation and in enrichment in other rare elements characteristic of granitic pegmatites (Table 83). The rare element enrichment attained in the Green Bay pegmatite group seems to be maximal for the field at its present erosion level, and no reasonable hope can be held for higher fractionation at greater depth. There are no granitoids outcropping in the area which would be potentially parental to highly fractionated pegmatites with more diversified mineralization.

Thus the Wekusko Lake pegmatite field is promising for lithium-rich pegmatites of the type represented by the three known pegmatite groups (SG, VT, and GB), carrying primary Na/Fe-enriched spodumene as the only but potentially abundant ore mineral. The more fractionated pegmatites of this type, similar to the Green Bay group, may contain economically interesting quantities of beryl.

The chances of finding significant deposits of other rare elements, such as Cs, Ga, Sn, Zr-Hf, Nb-Ta, REE, U and Th seem to be extremely poor.

EXPLORATION TARGET AREAS

Without a firm understanding of the pegmatites mode of origin it is difficult to formulate recommendations in regards to prospecting targets. Factors which must be considered are (a) the possible link between the more fractionated pegmatitic granites and the lithium-rich pegmatite groups, (b) their structural setting, and (c) their relationship to the metamorphic isograds.

Based on these indicators, the following two areas can be proposed as the most promising exploration targets:

(1) The Missi and Amisk metasediments on the eastern side of the Grass River-Crowduck Bay lineament, including the southeastern margin of the Rex Lake plutonic complex on the western side: this belt contains two of the three major lithium-bearing pegmatite groups, the Crowduck Bay swarm of pegmatitic granites, and a group of small pegmatite bodies north-northeast of the Violet-Thompson dykes, some of which show promising geochemical characteristics.

(2) A belt in the Missi and Amisk metavolcanics between the pegmatitic granites northeast of Grass River and the Green Bay pegmatite group, extended farther south and southeast into the area of crosscutting north-northeast- and east-northeast-trending faults. The highly fractionated pegmatitic granites and the Green Bay pegmatites may be related to the major east-northeast fault on their western side, and a repetition of the fracture pattern hosting the Green Bay dykes may occur in the faulted area 3 to 5 km to south-southeast from their location.

The following two areas can be suggested as "second-order" targets:

(3) The northeastern half of the belt flanked on the northwest side by the Osborne Lake-Bart Lake-Kormans Lake-Anderson Bay-Berry Creek fault system, and on the east side by the northwest margins of the Crowduck Bay gneiss dome, Rex Lake plutonic complex, and the Wekusko granite. The possible general structural analogy with the Grass River-Crowduck Bay lineament, and the presence of numerous pegmatitic granites, particularly the highly fractionated Herb Bay body, suggest the possiblity of mineralized pegmatitic occurrences.

(4) The Dion-Hat Lake area, particularly in the broader vicinity of the highly fractionated Dion Creek pegmatitic granite. However, the potential of this area seems to be rather low, in view of the probable high metamorphic grade, gneissic character of the country rocks, and generally poor development of brittle deformation.

In conclusion it may be suggested that, on a broader regional scale, mineralized pegmatites may possibly occur west of the study area, in a similar metamorphic setting south of the boundary of the Kisseynew and Flin Flon Belts. Abundant occurrences of pegmatitic granites support this speculation.

CONCLUDING REMARKS

INTRODUCTION

Two points of interest are discussed briefly in the conclusion of this study. A brief note on exploration techniques applicable to granitic pegmatites is desirable as the methods are not widely known and the information is not readily accessible. Recommendations for future research into petrogenesis of granitic pegmatites in the Canadian Shield, based on the results of the present study, conclude this chapter.

EXPLORATION METHODS

The Cat Lake-Winnipeg River pegmatite field has been prospected for mineralized pegmatites intermittently since the beginning of this century. Nevertheless, recent experience indicates that the old-fashioned leg-borne outcrop examination may still lead to new discoveries. The same is true in the Herb Lake field where outcrop stripping led to finds of new spodumene-bearing pegmatites during the last three years. However, the main drift of exploration should be oriented towards hidden deposits which require utilization of indirect detection methods.

The search for hidden deposits is particularly important in pegmatite exploration for two reasons, both of which are general as well as specific for the pegmatite fields considered here: (1) some of the largest and most diversified pegmatite deposits of the world are subhorizontal bodies which may be completely hidden, despite their overall giant dimensions, even if just beneath the erosion level; the Tanco deposit in the Winnipeg River district and its incidental discovery is a textbook example; (2) in steeply inclined to subvertical bodies which exhibit prominent zoning, the rare-element mineralization is almost invariably concentrated in their apical parts; these pegmatites are vulnerable to erosion because the first portions eroded are the most mineralized ones; the HGD dyke in the Maskwa Lake series, and the Gullwing pegmatite in the Dryden area of northwestern Ontario, are prime examples of subvertical pegmatites with diversified and relatively abundant mineralization in surface outcrops that disappear rapidly downdip.

Thus the flat-lying pegmatites are hidden easily, and subvertical pegmatites retain their mineralization when not exposed; indirect exploration methods are required to discover most occurrences of both types. This becomes all the more important in drift- or swamp-covered terrains such as most of the Cat Lake-Maskwa Lake district.

Three principal tasks can be distinguished in pegmatite prospecting and exploration: identification of parental granitoids, geochemical exploration for dispersion aureoles of hidden pegmatites, and preliminary pegmatite evaluation. The sequence and necessity of these individual steps are dictated by the local geology and by the kind of information available from earlier activities in the examined area.

IDENTIFICATION OF PARENTAL GRANITOIDS

Geochemical indicators distinguishing "barren" granitoids from the "fertile" types, and suggesting the different mineralization to be expected in the diversity of the latter type, have been developed by Beus and Sitnin (1968) and Beus et al. (1968), mainly for tantalum exploration. They are based on the geochemistry of granites which have been recognized as parental to distinct pegmatite types on geological grounds, and which come from geological formations of widely different ages. The empirical values of individual elements and elemental ratios are given in Tables 69 and 83, in comparison with the different granitoids examined in this study. At least 20 rock analyses are recommended of a single granitoid phase to provide a meaningful statistical basis.

DISPERSION AUREOLES OF PEGMATITE BODIES

Hidden pegmatite bodies betray their subsurface location by wall rock dispersion aureoles of a variety of elements that migrated along concentration, thermal, P_{load} or P_{H_2O} gradients during and after pegmatite emplacement. Positive haloes are produced by elements typically enriched in granititc pegmatites and carried by pegmatitic emanations pervading host rocks (pegmatite exomorphism). Negative aureoles are displayed by "non-pegmatitic" elements which may be leached by the above fluids and either widely dispersed or (relatively) enriched in the pegmatites. These phenomena have been studied frequently to decipher material balance in contact reactions or the genesis of pegmatite bodies in their entirety (e.g., Reitan 1956-1959, Wright 1963, Kretz 1968). However, for the purpose of practical exploration, they have been developed only recently by Beus et al. (1968) and Ovchinnikov et al. (1976).

Table 84 provides a qualitative review of elements producing positive dispersion aureoles around pegmatite bodies of different types. Table 85 summarizes mobility of elements in positive and negative haloes, and indicators suitable for distinguishing hanging wall and footwall segments of the aureoles. The references quoted above should be consulted for details of aureole zoning (imparted by different mobilities of individual elements), aureole asymmetry (governed by pegmatite shape and orientation, and diastrophic and/or non-diastrophic fabric and its orientation in the host rocks), and of the necessity of establishing background values for each region and rock type. The first experience with prospecting for wall rock dispersion haloes in Canada is treated briefly by Trueman (1978).

The geochemical exploration methods described in the references quoted above have been well developed not only for primary haloes in bedrock but also for secondary aureoles in autochthonous and allochthonous weathering crusts of different climatic types (Beus et al. 1968). However, the understanding of background, anomalies, and their contrast in glacial drift and swamp terrains typical of most of the Canadian Shield is very poor, and should be developed by potential users of the method. The techniques developed for other element associations in glacial and swampy overburden may serve for general guidance (e.g., Bradshaw et al. 1975).

TABLE 84. PEGMATITE TYPES AND DIAGNOSTIC ELEMENTS IN THEIR POSITIVE PRIMARY DISPERSION AUREOLES
(after Beus et al. 1968 and Ovchinnikov et al. 1976)

Pegmatite type	Diagnostic Elements
Aplites and barren pegmatites	B
Beryl-columbite pegmatites	B, Li, Sn, Be
Tantalum-bearing pegmatites	B, Li, Sn, Be, Cs, Rb
Quartz veins with cassiterite	B, Li, Sn, Be, Cs, W, As, F

TABLE 85. ELEMENTS CHARACTERISTIC FOR PRIMARY GEOCHEMICAL DISPERSION AUREOLES AROUND PEGMATITE BODIES
(adjusted after Beus et al. 1968 and Ovchinnikov et al. 1976)

Positive aureoles	
high mobility (wide aureoles)	B,Li, Cs, As(Rb)
low mobility (narrow aureoles)	Nb, Ta, Be, Sn(P) (Rb)
no distinctive haloes	Ga,Ge,Tl (P)
Negative aureoles	
high mobility (wide aureoles)	Ni, Ba, Sr, Pb, Zr
low mobility (narrow aureoles)	Ti, Cu, Sc, V, Mo, Cr, Zr

Hanging wall vs. footwall segments of aureoles	**Hanging wall**	**Footwall**
Zn.Cu.Cr	low	high
Ba.Sr.Pb	high	low
Ba.Sr.Pb/Zn.Cu.Cr	high	low

PRELIMINARY PEGMATITE EVALUATION

After finding a pegmatite in outcrop or drill core, a preliminary but rapid general assessment of its mineralization potential is desirable. As the mineralization potential is usually correlatable with fractionation of rare elements in rock-forming minerals, several methods have been developed utilizing this feature.

Analysis of pure separates of (blocky) K-feldspar, (core) muscovite, and (late) beryl for major and rare alkalis may be used for this purpose, to be correlated with data tabulated for these species in the descriptions of individual pegmatite groups. General guidelines for this method of pegmatite evaluation have been published by Gordiyenko (1971 for K-feldspar and muscovite; 1973 for lepidolite; 1976 for K-feldspar) and Černý (1975 for beryl); a wide variety of data is collected in Solodov (1971).

It must be kept in mind that fractionation is usually very strong within individual pegmatites, particularly in well zoned types. If blocky or core generations of the minerals quoted above are not available, the same species from other parts of the pegmatites can be used but approximate correction should be introduced. The degree of fractionation attained in the border, wall, and intermediate zones may be, and mostly is, lower.

It must be also remembered that geochemical evaluation is mostly a qualitative measure, indicating the degree of fractionation attained in a given pegmatite but not the degree of quantitative accumulation of a rare element and its mineral carriers. In some cases, even the qualitative approach may fail (e.g., Knorring 1974).

RECOMMENDATIONS FOR FUTURE RESEARCH

Of the pegmatite areas investigated in the present study, the Winnipeg River District is the best exposed and the most instructive for examination of genetic problems. Limited follow-up studies are continuing in this district to complement the extant data and interpretations.

Deciphering the petrogenetic history of this district is the first step towards formulating a general genetic model for mineralized pegmatite fields in the Superior Province. Besides its scientific significance, such a model would also be useful for developing a large-scale strategy for pegmatite exploration. However, the line of evidence should be collected from more than a single district.

Investigations of other regions related to the problem are necessary to test the conclusions reached here, and to clarify the genesis of pegmatitic granites, using even broader spectrum of methods than that applied to the present study. The association of pegmatitic granites and more or less mineralized pegmatites is relatively widespread in the greenstone belts of the Superior Province (e.g. Separation Lake on the English River, Beakhouse pers. comm. 1977; Lilypad Lakes at Fort Hope, Wallace 1978, in the English River belt; Georgia Lake district in the Quetico belt, Pye 1965; Magill Lake west of Gods Lake in Manitoba, Clark and Cheung 1978, and Medicine Lake east of Kenora, Pryslak 1976). Metarhyolites are abundant in some greenstone belts which host pegmatite fields (e.g. Lilypad Lakes and Medicine Lake). Examination of granitoids in other pegmatite districts can be expected to reveal additional intrusive complexes involving pegmatitic granites (e.g. Red Cross Lake and Red Sucker Lake in northeastern Manitoba, Setting Lake in northwestern Ontario). Metarhyolites in greenstone belts which host pegmatitic granites should also be examined to test their possible roles of consanguineous differentiates or sources contributing to anatectic melts.

TABLE 84. PEGMATITE TYPES AND DIAGNOSTIC ELEMENTS IN THEIR POSITIVE PRIMARY DISPERSION AUREOLES (after Beus et al. 1968 and Ovchinnikov et al. 1976)

Pegmatite type	Diagnostic Elements
Aplites and barren pegmatites	B
Beryl-columbite pegmatites	B, Li, Sn, Be
Tantalum-bearing pegmatites	B, Li, Sn, Be, Cs, Rb
Quartz veins with cassiterite	B, Li, Sn, Be, Cs, W, As, F

TABLE 85. ELEMENTS CHARACTERISTIC FOR PRIMARY GEOCHEMICAL DISPERSION AUREOLES AROUND PEGMATITE BODIES (adjusted after Beus et al. 1968 and Ovchinnikov et al. 1976)

Positive aureoles	
high mobility (wide aureoles)	B,Li, Cs, As(Rb)
low mobility (narrow aureoles)	Nb, Ta, Be, Sn(P) (Rb)
no distinctive haloes	Ga,Ge,Tl (P)
Negative aureoles	
high mobility (wide aureoles)	Ni, Ba, Sr, Pb, Zr
low mobility (narrow aureoles)	Ti, Cu, Sc, V, Mo, Cr, Zr

Hanging wall vs. footwall segments of aureoles

	Hanging wall	Footwall
Zn.Cu.Cr	low	high
Ba.Sr.Pb	high	low
Ba.Sr.Pb/Zn.Cu.Cr	high	low

PRELIMINARY PEGMATITE EVALUATION

After finding a pegmatite in outcrop or drill core, a preliminary but rapid general assessment of its mineralization potential is desirable. As the mineralization potential is usually correlatable with fractionation of rare elements in rock-forming minerals, several methods have been developed utilizing this feature.

Analysis of pure separates of (blocky) K-feldspar, (core) muscovite, and (late) beryl for major and rare alkalis may be used for this purpose, to be correlated with data tabulated for these species in the descriptions of individual pegmatite groups. General guidelines for this method of pegmatite evaluation have been published by Gordiyenko (1971 for K-feldspar and muscovite; 1973 for lepidolite; 1976 for K-feldspar) and Černý (1975 for beryl); a wide variety of data is collected in Solodov (1971).

It must be kept in mind that fractionation is usually very strong within individual pegmatites, particularly in well zoned types. If blocky or core generations of the minerals quoted above are not available, the same species from other parts of the pegmatites can be used but approximate correction should be introduced. The degree of fractionation attained in the border, wall, and intermediate zones may be, and mostly is, lower.

It must be also remembered that geochemical evaluation is mostly a qualitative measure, indicating the degree of fractionation attained in a given pegmatite but not the degree of quantitative accumulation of a rare element and its mineral carriers. In some cases, even the qualitative approach may fail (e.g., Knorring 1974).

RECOMMENDATIONS FOR FUTURE RESEARCH

Of the pegmatite areas investigated in the present study, the Winnipeg River District is the best exposed and the most instructive for examination of genetic problems. Limited follow-up studies are continuing in this district to complement the extant data and interpretations.

Deciphering the petrogenetic history of this district is the first step towards formulating a general genetic model for mineralized pegmatite fields in the Superior Province. Besides its scientific significance, such a model would also be useful for developing a large-scale strategy for pegmatite exploration. However, the line of evidence should be collected from more than a single district.

Investigations of other regions related to the problem are necessary to test the conclusions reached here, and to clarify the genesis of pegmatitic granites, using even broader spectrum of methods than that applied to the present study. The association of pegmatitic granites and more or less mineralized pegmatites is relatively widespread in the greenstone belts of the Superior Province (e.g. Separation Lake on the English River, Beakhouse pers. comm. 1977; Lilypad Lakes at Fort Hope, Wallace 1978, in the English River belt; Georgia Lake district in the Quetico belt, Pye 1965; Magill Lake west of Gods Lake in Manitoba, Clark and Cheung 1978, and Medicine Lake east of Kenora, Pryslak 1976). Metarhyolites are abundant in some greenstone belts which host pegmatite fields (e.g. Lilypad Lakes and Medicine Lake). Examination of granitoids in other pegmatite districts can be expected to reveal additional intrusive complexes involving pegmatitic granites (e.g. Red Cross Lake and Red Sucker Lake in northeastern Manitoba, Setting Lake in northwestern Ontario). Metarhyolites in greenstone belts which host pegmatitic granites should also be examined to test their possible roles of consanguineous differentiates or sources contributing to anatectic melts.

REFERENCES

Albuquerque, C.A.R. de

1977: Geochemistry of the tonalitic and granitic rocks of the Nova Scotia southern plutons; *Geochimica et Cosmochimica Acta*, v. 41, p. 1-13.

Alcock, F.J.

1918: Wekusko Lake area, northern Manitoba; *Geological Survey of Canada*, Summary Report 1917, Pt. D, p. 8-17.

1920: Reed-Wekusko map area, northern Manitoba; *Geological Survey of Canada*, Memoir 119, 62 p.

Anderson, J.L. and Cullers, R.L.

1978: Geochemistry and evolution of the Wolf River batholith, a late Precambrian rapakivi massif in north Wisconsin, U.S.A.; *Precambrian Research*, v. 7, p. 287-324.

Anderson, R.K.

1974: Rubidium-strontium age determinations from the Churchill Province of northen Manitoba; unpublished M.Sc. thesis, *University of Manitoba*, 75 p.

Anhaeusser, C.R.

1971: The Barberton Mountain Land, South Africa - guide to the understanding of the Archean geology of western Australia; Special Publication, *Geological Society of Australia*, v. 3, p. 103-119.

1973: The evolution of the early Precambrian crust of Southern Africa; *Philosophical Transactions, Royal Society London* A273, p. 359-388.

Anhaeusser, C.R., Mason, R., Viljoen, M.J. and Viljoen, R.P.

1969: A reappraisal of some aspects of Precambrian shield geology; *Geological Society of America Bulletin*, v. 80, p. 2175-2200.

Armstrong, C.W.

1969: The role of replacement processes in the formation of complex lithium pegmatites; unpublished Ph.D. thesis, *Department of Geology, University of Western Ontario*, London, Ontario; 134 p.

Armstrong, J.E.

1941: Wekusko, Manitoba; *Geological Survey of Canada*, Map 665A, with descriptive notes.

Arth, J.G.

1976: A model for the origin of the early Precambrian greenstone-granite complex of northeastern Minnesota; in: The Early History of the Earth, ed. B.F. Windley, Wiley and Sons, p. 299-302.

1979: Some trace elements in trondhjemites - their implications to magma genesis and paleotectonic setting in: Trondhjemites, dacites, and related rocks, ed. F. Barker, *Developments in Petrology* 6, Elsevier, p. 123-132.

Arth, J.G., Barker, F., Peterman, Z.E. and Friedman, I.

1978: Geochemistry of the gabbro-diorite-tonalite-trondhjemite suite of southwest Finland and its implications for the origin of tonalitic and trondhjemitic magmas: *Journal of Petrology*, v. 19, p. 289-316.

Arth, J.G. and Hanson, G.N.

1975: Geochemistry and origin of the early Precambrian crust of north-eastern Minnesota; *Geochimica et Cosmochimica Acta*, v. 39, p. 325-362.

Ayres, L.D.

1978: Metamorphism in the Superior Province of northwestern Ontario and its relationship to crustal development; in: Metamorphism in the Canadian Shield, ed. J.A. Fraser and W.W. Heywood; *Geological Survey of Canada*, Paper 78-10, p. 25-36.

Bailes, A.H.

1971: Preliminary compilation of the geology of the Snow Lake-Flin Flon-Sherridon area; *Manitoba Mines Branch*, Geological Paper 1-71, 18. p.

1975: Geology of the Guay-Wimapedi Lake area; *Manitoba Mineral Resources Division, Geological Services Branch*, Publication 75-2, 104p.

1976: Saw Lake area (Grass River Project); *Manitoba Mineral Resources Division, Geological Survey*, Report of Field Activities, p. 18-23.

1980: Geology of the File Lake area; *Manitoba Mineral Resources Division, Geological Report* 78-1, in press.

Bailes, A.H. and Malyon, J.

1976: Saw Lake, *Manitoba Mineral Resources Division*, Preliminary map number 1976 B-1.

Bailes, A.H. and McRitchie, W.D.

1978: The transition from low to high grade metamorphism in the Kisseynew sedimentary gneiss belt, Manitoba; in: Metamorphism in the Canadian Shield, ed. J.A. Fraser and W.W. Heywood, *Geological Survey of Canada*, Paper 78-10, p. 155-178.

Bailey, J.C.

1977: Fluorine in granitic rocks and melts: a review; *Chemical Geology*, v. 19, p. 1-42.

Barker, F. and Arth, J.G.

1976: Generation of trondhjemitic-tonalitic liquids and Archean bimodal trondhjemite-basalt suites; *Geology*, v. 4, p. 596-600.

Bateman. P.C., Clark, L.D., Huber, N.K., Moore, J.G. and Rinehart, C.D.

1963: The Sierra Nevada batholith, a synthesis of recent work across the central part; *United States Geological Survey*, Professional Paper 414-D, 106 p.

Beakhouse, G.P.
1977: A subdivision of the Western English River subprovince; *Canadian Journal of Earth Sciences*, v. 14, p. 1481-1489.

in prep.: Evolution of the English River gneissic belt; *Centre for Precambrian Studies, University of Manitoba*.

Beus, A.A.
1951: On zoning in granitic pegmatites; *Izvestiya of the Academy of Sciences of the Union of Soviet Socialistic Republics*, Geological Ser. 6, p.318-324.

1960: Geochemistry of beryllium and genetic types of beryllium deposits; *Academy of Sciences of the Union of Soviet Socialistic Republics*, Moscow; English translation, Freeman and Co., 1966, 401 p.

Beus, A.A. and Oyzerman, M.T.
1965: Distribution of rubidium in igneous rocks and the correlation between rubidium and potassium; *Geokhimiya*, No. 11, p. 1318-1324.

Beus, A.A. et al.
1968: Geochemical exploration for endogenic deposits of rare elements; Nedra Moscow; English translation, *Geological Survey of Canada*, Library, Ottawa, 263 p.

Beus, A.A. and Sitnin, A.A.
1968: Geochemical specialization of magmatic complexes as criteria for the exploration of hidden deposits; *XXIII International Geological Congress*, Prague, Report 6, p. 101-105.

Bond, W.D.
1973: The ovoid anorthositic gabbro at Bernic Lake, Manitoba; unpublished M.Sc. thesis, *Department of Earth Sciences, University of Manitoba*, Winnipeg, 68 p.

Bradshaw, P.M.D., ed.
1975: Conceptual models in exploration geochemistry; *Association of Exploration Geochemists*, Special Publication 3, Elsevier, 223 p.

Breaks, F.W., Bond, W.D. and Stone, D.
1978: Preliminary geological synthesis of the English River subprovince, northwestern Ontario and its bearing upon mineral exploration; *Ontario Geological Survey*, Miscellaneous Paper 72, 55 p.

Brisbin, W.C.
1979: Report on a gravity profile across the Lac du Bonnet batholith, southeastern Manitoba; *Centre for Precambrian Studies, University of Manitoba*, unpublished report, 42 p.

Bristol, N.A.
1962: An X-ray powder examination of some pegmatite minerals from southeastern Manitoba; unpublished M.Sc. thesis, *University of Manitoba*, Winnipeg, 115 p.

Bruce, E.L.
1917: Molybdenite near Falcon Lake, Manitoba; *Geological Survey of Canada*, Summary Report, Pt. D, p. 22-25.

Bruhn, R.L., Stern, C.R. and DeWitt, M.J.
1978: Field and geochemical data bearing on the development of a Mesozoic volcano-tectonic rift zone and back-arc basin in southernmost South America; *Earth and Planetary Science Letters*, v. 14, p. 32-46.

Buma, G., Frey, F.A. and Wones, D.R.
1971: New England granites: trace elements evidence regarding their origin and differentiation; *Contributions to Mineralogy and Petrology*, v. 31, p. 300-320.

Butrenchuk, S.B.
1970: Metamorphic petrology of the Bird Lake area, southeastern Manitoba; unpublished M.Sc. thesis, *Department of Earth Sciences, University of Manitoba*, Winnipeg, 61 p.

Campbell, F.H.A.
1971: Sedimentation and stratigraphy of part of the Rice Lake group, Manitoba, unpublished Ph.D. thesis, *Department of Earth Sciences, University of Manitoba*, Winnipeg.

Cann, J.R.
1970: Upward movement of granitic magma; *Geological Magazine*, v. 107, p. 335- 340.

Carlson, H.D.
1958: Geology of the Werner Lake-Rex Lake area; *Ontario Department of Mines*, Paper 66, pt. 4, 18 p.

Carmichael, I.S.E., Turner, F.J. and Verhoogen, J.
1974: Igneous petrology; McGraw-Hill Book Co., New York, 482 p.

Castle, R.O. and Theodore, T.G.
1972: Some genetic implications of the phase composition of a simple New England pegmatite; *United States Geological Survey*, Professional Paper 800B, p. B105-B117.

Cawthorn, R.G. and Brown, P.A.
1976: A model for the formation and crystallization of corundum-normative calc-alkaline magmas through amphibole fractionation; *Journal of Geology*, v. 84, p. 467-476.

Cawthorn, R.G., Strong, D.F. and Brown, P.A.
1976: Origin of corundum-normative intrusive and extrusive calc-alkaline magmas; *Nature*, v. 259, p. 102-104.

Černá, I., Černý, P. and Ferguson, R.B.
1972: The Tanco pegmatite at Bernic Lake, Manitoba. III.

Amblygonite-montebrasite; *Canadian Mineralogist*, v. 11, p. 643-659.

Černý, P.
1972a: The Tanco pegmatite at Bernic Lake, Manitoba. VII, Eucryptite; *Canadian Mineralogist*, v. 11, p. 708-713.

1972b: The Tanco pegmatite at Bernic Lake, Manitoba. VIII, Secondary minerals from the spodumene-rich zones; *Canadian Mineralogist*, v. 11, p. 714-726.

1974: The present status of the analcime-pollucite series; *Canadian Mineralogist*, v. 12, p. 334-341.

1975: Alkali variations in pegmatitic beryl and their petrogenetic implications; *Neues Jahrbuch für Mineralogie*, Abhandlungen, v. 123, p. 198-212.

1978: Alteration of pollucite in some pegmatites of southeastern Manitoba; *Canadian Mineralogist*, v. 16, p. 89-95.

Černý, P. and Bristol, N.A.
1972: New mineral occurrences in pegmatites of southeastern Manitoba; *Canadian Mineralogist*, v. 11, p. 560-563.

Černý, P. and Ferguson, R.B.
1972: The Tanco pegmatite at Bernic Lake, Manitoba. IV, Petalite and spodumene relations; *Canadian Mineralogist*, v. 11, p. 660-678.

Černý, P. and Harris, D.C.
1973a: Tetrolite, stibiotantalite, and antimonian microlite from the Odd West pegmatite, southeastern Manitoba; *Canadian Mineralogist*, v. 12, p. 76-78.

1973b: Allemontite and its alteration products from the Odd West pegmatite, southeastern Manitoba; *Canadian Mineralogist*, v. 11, p. 978-984.

1978: The Tanco pegmatite at Bernic Lake, Manitoba. XI, Native elements, alloys, sulfides, and sulfosalts; *Canadian Mineralogist*, v. 16, p. 625-640.

Černý, P. and Hawthorne, F.C.
1976: Refractive indices versus alkali contents in beryl: general limitations and applications to some pegmatite types; *Canadian Mineralogist*, v. 14, p. 491-497.

Černý, P. and Macek, J.
1972: The Tanco pegmatite at Bernic Lake, Manitoba. V, Coloured potassium feldspars; *Canadian Mineralogist*, v. 11, p. 679-689.

Černý, P., Rieder, M. and Povondra, P.
1970: Three polytypes of lepidolite from Czechoslovakia; *Lithos*, v. 3, p. 319-325.

Černý, P. and Silvola, J.
1980: The Tanco pegmatite at Bernic Lake, Manitoba. XII, Hafnian zircon; *Canadian Mineralogist*, v. 18, 313-321.

Černý, P. and Simpson, F.M.
1977: The Tanco pegmatite at Bernic Lake, Manitoba. IX, Beryl; *Canadian Mineralogist*, v. 15, p. 489-499.

1978: The Tanco pegmatite at Bernic Lake, Manitoba. X, Pollucite; *Canadian Mineralogist*, v. 16, p. 325-333.

Černý, P. and Trueman, D.L.
1977: Petrogenesis of pegmatites in the Cat Lake-Winnipeg River area; *Centre for Precambrian Studies, University of Manitoba*, Annual Report, 1976, p. 26-32.

1978: The distribution and petrogenesis of lithium pegmatites in the Western Archean of Canada; *Energy*, v. 3, p. 365-377.

Černý, P. and Turnock, A.C.
1971a: Niobium-tantalum minerals from granitic pegmatites at Greer Lake, southeastern Manitoba; *Canadian Mineralogist*, v. 10, p. 755-772.

1971b: Pegmatites of southeastern Manitoba; *Geological Association of Canada*, Special Paper 9, p. 119-127.

1975a: Beryl from granitic pegmatites at Greer Lake, southeastern Manitoba; *Canadian Mineralogist*, v. 13, p. 55-61.

Chappell, B.W. and White, A.J.R.
1974: Two contrasting granite types; *Pacific Geology*, v. 8, p. 173-174.

Charlton, L.D. and Martin, R.F.
1978: The effect of boron on the granite solidus; *Canadian Mineralogist*, v. 16, p. 239-244.

Chou, C.-L.
1978: Trace element studies in the Geotraverse Region-eastern Lac Seul area; *Proceedings of the 1978 Archean Geochemical Conference*, University of Toronto Press, p. 151-159.

Chou, C.-L., Hamud, A.J., Harris, N.B.W. and Goodwin, A.M.
1977: Geochemistry and origin of the eastern Lac Seul area, English River gneiss belt; *Proceedings of the Geotraverse Conference , University of Toronto 1977*, p. 80-93.

Clark, G.S., Anderson, R. and McRitchie, W.D.
1974: Total rock Rb/Sr ages from the Burntwood Lake area; *Centre for Precambrian Studies, University of Manitoba*, Annual Report 1974, p. 51-52.

Clark, G.S. and Cheung, S.-P.
1978: Rubidium-strontium whole-rock ages from the Oxford Lake-Knee Lake greenstone belt, northeastern Manitoba; *Centre for Precambrian Studies, University of Manitoba*, Annual Report, 1977, P. 106-121.

Clayton, R.N. and Mayeda, T.D.
1963: The use of bromine pentafluoride in the extraction of oxygen from oxides and silicates for isotopic

analysis; *Geochimica et Cosmochimica Acta*, v. 27, p. 43-52.

Coats, C.J.A. and Buchan, R.
1979: Petrology of serpentinized metamorphic olivine, Bird River Sill, Manitoba; *Canadian Mineralogist*, v. 17, p. 847-855.

Coles, R.L.
1973: Relationships between measured rock magnetizations and interpretations of longer wavelength anomalies in the Superior Province of the Canadian Shield; unpublished Ph.D. thesis, *Department of Earth Sciences, University of Manitoba*, Winnipeg, 87 p.

Colony, R.J.
1920: A norite of the Sudbury type in Manitoba; *Canadian Mining Journal*, v. 41, No. 47, p. 20-24.

1921: A norite of the Sudbury type in Manitoba; *Transactions of the Canadian Institute of Mining and Metallurgy*, v. 24, p. 186-190.

Condie, K.C.
1976a: Trace-element geochemistry of Archean greenstone belts; *Earth Science Reviews*, v. 12, p. 393-417.

1976b: Trace-element models for the origin of Archean volcanic rocks; in: The Early History of the Earth, ed. B.F. Windley, 1976, Wiley and Sons, p. 419-426.

Condie, K.C. and Baragar, W.R.A.
1974: Rare-earth element distributions in volcanic rocks from Archean greenstone belts; *Contributions to Mineralogy and Petrology*, v. 45, p. 237-246.

Condie, K.C. and Hunter, D.R.
1976: Trace-element geochemistry of Archean granitic rocks from the Barberton region, South Africa; *Earth and Planetary Science Letters*, v. 29, p. 389-400.

Cooke, H.C.
1922: Geology and mineral resources of the Rice Lake and Oiseau River areas, Manitoba; *Geological Survey of Canada*, Summary Report 1921, part C, p. 120-142.

Crouse, R.A. and Černý, P.
1972: The Tanco pegmatite at Bernic Lake, Manitoba. I, Geology and paragenesis; *Canadian Mineralogist*, v. 11, p. 591-608.

Crouse, R.A., Černý, P., Trueman, D.L. and Burt, R.O.
1979: The Tanco pegmatite, southeastern Manitoba; *Canadian Institute of Mining and Metallurgy Bulletin*, 1979, No. 2, p. 1-10.

Davies, J.F.
1952: Geology of the Oiseau (Bird) River area, Lac du Bonnet Mining Division; *Manitoba Mines Branch*, Publication 51-3, 24 p.

1954: Geology of the West Hawk Lake-Falcon Lake area, Lac du Bonnet Mining Division; *Manitoba Mines Branch*, Publication 53-4, 28 p.

1955: Geology and mineral deposits of the Bird Lake area; *Manitoba Mines Branch*, Publication 54-1, 44 p.

1956a: Manitoba lithium deposits; *Canadian Mining Journal*, v. 77, April No. 4, p. 78-79.

1956b: Geology of the Booster Lake area, Lac du Bonnet Mining Division; *Manitoba Mines Branch*, Publication 55-1, 15 p.

1957: Geology of the Winnipeg River area (Shatford Lake-Ryerson Lake), Lac du Bonnet Mining Division, Manitoba; *Manitoba Mines Branch*, Publication 56-1, 27 p.

1958: The lithium and beryllium pegmatites of southeastern Manitoba; *Canadian Institute of Mining and Metallurgy Transactions*, v. 61, p. 230-236.

Davies, J.F., Bannatyne, B.B., Barry, G.S. and McCabe, H.R.
1962: Geology and mineral resources of Manitoba; *Manitoba Mines Branch*, 190 p.

DeLury, J.S.
1917: Molybdenite at Falcon Lake, Manitoba; *Canadian Mining Journal*, v. 28, p. 460-462.

1926: Pegmatites of southeastern Manitoba; *Canadian Mining Journal*, v.47, p. 695-697.

1930: Beryl in Manitoba; *Canadian Mining Journal*, v. 51, p. 1017.

DeLury, J.S. and Ellsworth, H.V.
1931: Uraninite from the Huron Claim, Winnipeg River area, southeastern Manitoba; *American Mineralogist*, v. 12, p. 569-575.

Derry, D.R.
1931a: Geology of the area from Minaki to Sydney Lake, District of Kenora; *Ontario Department of Mines*, Annual Report, v. 39, pt.3, p.1-18.

1931b: The genetic relationships of pegmatites, aplites, and tin veins; *Geological Magazine*, v. 68, p. 454-475.

DeSitter, L.V.
1956: Structural geology; McGraw-Hill Book Co., New York, 485 p.

Dickson, W.L.
1974: General geology and geochemistry of the granitoid rocks of the northern Gander Lake belt, Newfoundland; unpublished M.Sc. thesis, *Memorial University of Newfoundland*, St. John's 122 p.

Didier, J. and Lameyre, T.
1969: Les granites du Massif Central francais: étude comparée des leucogranites et granodiorites; *Contributions to Mineralogy and Petrology*, v. 24, p. 219-238.

Dostal, J.
1975: The origin of garnet-cordierite-sillimanite-bearing rocks from Chandos Township, Ontario; *Contributions to Mineralogy and Petrology*, v. 49, p. 163-175.

Drake, M.J. and Weill, D.F.
1972: New rare earth element standards for electron microprobe analysis; *Chemical Geology*, v. 10, p. 179-181.

Drury, S.A.
1979: Rare-earth and other trace element data bearing on the origin of Archaean granitic rocks from Yellowknife, Northwest Territories; *Canadian Journal of Earth Sciences*, v. 16, p. 809-815.

Eckelmann, F.D., Long, L.E. and Olsen, E.A.
1958: Origin and occurrence of extensively developed layered structures in leucogranite-granite pegmatite, Huron Claim, Johnston Lake area, southeast Manitoba, Canada; *GSA-MSA Annual Meeting, Program and Abstracts*, p. 48.

Ellsworth, H.V.
1932: Rare-element minerals of Canada; *Canadian Department of Mines, Geological Survey*, Economic Geology Series 11, 272 p.

Elphick, S.C.
1972: Geology of the Mynarski-Notigi Lakes area; *Manitoba Mines Branch*, Publication 71-2C, 23 p.

Emmerman, R., Daieva, L. and Schneider, J.
1975: Petrologic significance of rare earths distribution in granites; *Contributions to Mineralogy and Petrology*, v. 52, p. 267-283.

Emmons, R.C., et al.
1953: Selected petrogenic relationships of plagioclase; *Geological Society of America*, Memoir 52, 240 p.

Ermanovics, I.F., McRitchie, W.D. and Houston, W.N.
1979: Petrochemistry and tectonic setting of plutonic rocks of the Superior province in Manitoba; in: Trondhjemites, Dacites, and Related Rocks, ed. F. Barker, *Developments in Petrology*, v. 6, Elsevier, p. 323-362.

Evans, H.T. Jr., Appleman, D.E. and Handwerker, S.S.
1963: The least-squares refinement of crystal unit cells with powder diffraction data by an automatic computer indexing method; *Program and Abstracts, American Crystallographic Association Meeting*, Cambridge, Mass., 42 p.

Ewart, A., Oversby, V.M. and Mateen, A.
1977: Petrology and isotopic geochemistry of Tertiary lavas from the northern flank of the Tweed volcano-southeastern Queensland; *Journal of Petrology*, v. 18, p. 73-113.

Farmin, R.
1941: Host-rock inflation by veins and dikes at Faas Valley, Calif.; *Economic Geology*, v. 36, p. 143-174.

Farquharson, R.B.
1975: Revised Rb-Sr age of the Lac du Bonnet quartz monzonite, southeastern Manitoba; *Canadian Journal of Earth Sciences*, v. 12, p. 115-118.

Farquharson, R.B. and Clark, G.S.
1971: Rb-Sr geochronology of some granitic rocks in southeastern Manitoba; *Geological Association of Canada*, Special Paper 9, p. 111-117.

Fisher, R.V.
1966: Rocks composed of volcanic fragments and their classification; *Earth Science Reviews*, v. 1, p. 287-298.

Flood, R.H. and Shaw, S.E.
1975: A cordierite-bearing granite suite from the New England batholith, N.S.W., Australia; *Contributions to Mineralogy and Petrology*, v. 52, p. 157-164.

Foord, E.E. and Mrose, M.E.
1978: Rynersonite, $Ca(Ta,Nb)_2O_6$, a new mineral from San Diego County, California; *American Mineralogist*, v. 63, p. 709-714.

Franklin, T.M.
1978: Petrochemistry of the south Sturgeon Lake volcanic belt; *Archean Geochemistry Conference 1978, Proceedings*, University of Toronto Press, p. 161-180.

Frarey, M.J.
1949: Crowduck Bay, Manitoba; *Geological Survey of Canada*, Map 987A, with descriptive notes.

Freund, H.H. and Turnock, A.C.
1971: Petrology of the paragneiss at Quesnel Lake, Manitoba; *Manitoba Mines Branch*, Publication 71-1, Report 10, p. 227-234.

Froese, E. and Gasparrini, E.
1975: Metamorphic zones in the Snow Lake area, Manitoba; *Canadian Mineralogist*, v. 13, p. 162-167.

Fryer, B.J. and Jenner, G.A.
1978: Geochemistry and origin of the Archean Prince Albert group volcanics, western Melville Peninsula, Northwest Territories; *Geochimica et Cosmochimica Acta*, v. 42, p. 1645-1654.

Fyfe, W.S.
1973: The granulite facies, partial melting, and the Archean crust; *Philosophical Transactions of the Royal Society*, London, v. A273, p. 457-461.

Fyfe, W.S. and Brown, G.C.
1971: Granites past and present; *Journal of Earth Sciences* (Leeds), Special Issue, p. 116-123.

Fyfe, W.S., Price, N.J. and Thompson, A.B.
1978: Fluids in the earth's crust; *Developments in Geochemistry*, v. 1, Elsevier, 383 p.

Galt, R.H.

1964: The mineralogy of the chrome spinels of the Bird River Sill, Manitoba; unpublished M.Sc. thesis, *Department of Earth Sciences, University of Manitoba*, Winnipeg.

Glikson, A.Y.
1976: Stratigraphy and evolution of primary and secondary greenstones: significance of data from shields of the Southern Hemisphere; in: The Early History of the Earth, ed. B.F. Windley, Wiley and Sons, 1976, p. 257-276.

Goad, B.E.
in prep: Pegmatitic granites from the Winnipeg River district, southeastern Manitoba; *Department of Earth Sciences, University of Manitoba*, Winnipeg, M.Sc. thesis.

Goodwin, A.M.
1972: The Superior Province; *in* Variations in Tectonic Style in Canada, ed. R.A. Price and R.J.W. Douglas; *Geological Association of Canada*, Special Paper 11, p. 585-589.

Gordiyenko, V.V.
1971: Concentration of Li, Rb, and Cs in potash feldspar and muscovite as criteria for assessing the rare metal mineralization in granite pegmatites; *International Geology Review*, v. 13, p. 134-142.

1973: Cesium in lepidolite as indicator of the cesium content of granitic pegmatites; *Doklady of the Academy of Sciences*, Union of Soviet Socialistic Republics, v. 209, p. 193-196.

1976: Diagrams for prognostic evaluation of rare-element mineralization in granitic pegmatites utilizing compositional variations in potassium feldspars; *Doklady of the Academy of Sciences*, Union of Soviet Socialistic Repulics, v. 228, p. 442-444.

Gordiyenko, V.V., Syritso, L.F. and Krivovichev, V.G.
1975: A new type of rare-metal apobasite metasomatites and the regular distribution of Cs, Li and Rb in them; *Doklady of the Academy of Sciences*, Union of Soviet Socialistic Republics, v. 224, p. 198-200.

Green, D.C. and Baadsgaard, H.

1971: Temporal evolution and petrogenesis of an Archean crustal segment at Yellowknife, N.W.T., Canada; *Journal of Petrology*, v. 12, p. 177-217.

Green, T.H.
1976: Experimental generation of cordierite- or garnet-bearing granitic liquids from a pelitic compositon; *Geology*, v. 4, p. 85-88.

Grice, J.D., Černý, P. and Ferguson, R.B.
1972: The Tanco pegmatite at Bernic Lake, Manitoba. II. Wodginite, tantalite, pseudo-ixiolite and related minerals; *Canadian Mineralogist*, v. 11, p. 609-642.

Hall, D.H.
1974: Long wavelength aeromagnetic anomalies and deep crustal magnetization in Manitoba and northwestern Ontario, Canada; *Geophysics*, v. 40, p. 403-430.

Hall, D.H. and Hajnal, Z.
1973: Deep seismic crustal studies in Manitoba; *Bulletin of the Seismological Society of America*, v. 63, p. 885-910.

Hancock, R.G.V.
1976: Low flux multielement instrumental neutron activation analysis in archaeometry; *Analytical Chemistry*, v. 48, p. 1443-1445.

Hanson, G.N.
1978: The application of trace elements to the petrogenesis of igneous rocks of granitic composition; in: Trace Elements in Igneous Petrology, ed. C.J. Allegre and S.R. Hart, *Developments in Petrology*, v. 5, Esevier, p. 26-43.

Harris, N.B.W.
1974: The petrology and petrogenesis of some muscovite granite sills from the Barousse massif, Central Pyrenees; *Contributions to Mineralogy and Petrology*, v. 45, p. 215-230.

1976: The significance of garnet and cordierite from the Sioux Lookout region of the English River gneiss belt, northern Ontario; *Contributions to Mineralogy and Petrology*, v. 55, p. 91-104.

Harrison, J.M.
1949: Geology and Mineral Deposits of the File-Tramping Lake Area, Manitoba; *Geological Survey of Canada*, Bulletin 20, 125 p.

Hart, S.R. and Davis, G.L.
1969: Zircon U-Pb and whole rock Rb-Sr ages and early crustal development near Rainy Lake, Ontario; *Bulletin of the Geological Society of America*, v. 80, p. 595-616.

Hauseux, M.A.
1977: Mode of uranium occurrence in a migmatitic granite terrain, Baie Johan Beetz, Quebec; *Canadian Institute of Mining and Metallurgy Bulletin*, v. 70, p. 110-116.

Heinrich, E.W.
1975: Economic geology and mineralogy of petalite and spodumene pegmatites; *Indian Journal of Earth Sciences*, v. 2, p. 18-29.

1978: Mineralogy and structure of lithium pegmatites; *Jornal de Mineralogia, Recife*, v. 7, p. 59-65.

Hess, H.H.
1960: Stillwater igneous complex, Montana; *Geological Society of America*, Memoir 80, 185 p.

Holland, J.G. and Lambert, R.St.J.
1972: The geochemistry of lithium in the Mainland Lewisian of Scotland; *24th Session of the International Geological Congress*, Montreal, Reports Section 10, p. 169-178.

Huang, W.-L. and Wyllie, P.J.
1974: Melting relations of muscovite with quartz and sanidine in the K_2O-Al_2O_3-SiO_2-H_2O system to 30 kilobars and an outline of paragonite melting relations; *American Journal of Science*, v. 274, P. 378-395.

Hunter, D.R., Barker,F. and Millard, H.T.Jr.
1978: The geochemical nature of the Archean ancient gneiss complex and granodiorite suite, Swaziland: a preliminary study; *Precambrian Research*, v. 7, p. 105-127.

Hutchinson, R.W.
1955: Regional zonation of pegmatites near Ross Lake, District of Mackenzie, Northwest Territories; *Geological Survey of Canada*, Bulletin 34, 50 p.

1959: Geology of the Montgary pegmatite; *Economic Geology*, v. 54, p. 1525-1542.

Irvine, T.N. and Baragar, W.R.A.
1971: A guide to the chemical classification of the common volcanic rocks; *Canadian Journal of Earth Sciences*, v. 8, p. 523.

I.U.G.S. Subcommission on the systematics of igneous rocks
1973: Classification and nomenclature of plutonic rocks recommendations; in: *Neues Jahrbuch für Mineralogie*, Monatshefte, p. 48-75.

Jackson, E.D.
1967: Ultramafic cumulates in the Stillwater, Great Dyke and Bushveld intrusions; in: Ultramafic and Related Rocks, ed. P.J. Wyllie, Wiley and Sons, New York, 438 p.

Jahns, R.H.
1953: The genesis of pegmatites. I. Occurrence and origin of giant crystals; *American Mineralogist*, v. 38, p. 563-598.

Jahns, R.H. and Burnham, C.W.
1969: Experimental studies of pegmatite genesis: I. A model for the derivation and crystallization of granitic pegmatites; *Economic Geology*, v. 64, p. 843-864.

Janes, D.A.
1976: Southeastern Manitoba; in: *Manitoba Mineral Resources Division, Geological Survey*, Report on Field Activities 1976, p. 88-92.

1978: Southeastern Manitoba; in: *Manitoba Mineral Resources Division, Geological Survey*, Report on Field Activities 1978, p. 93-94.

in prep.: Southeastern Manitoba; *Manitoba Mineral Resources Division*, Geological Report.

Josse, G.
1974: Rubidium-strontium age determinations from the Flin-Morton-Woosey Lakes area of the Flin Flon volcanic belt, west central Manitoba; unpublished M.Sc. thesis, *Department of Earth Sciences, University of Manitoba*, 73 p.

Juhas, A.D.
1973: Geology and origin of copper-nickel sulphide deposits of the Bird River area of Manitoba; unpublished M.Sc. thesis, *Department of Earth Sciences, University of Manitoba*, 106 p.

Kesler, T.L.
1976: Occurrences, development, and long-range outlook of lithium-pegmatite ore in the Carolinas; *United States Geological Survey*, Professional Paper 1005, p. 45-50.

Kleeman, A.W.
1965: The origin of granitic magmas; *Journal of the Geological Society of Australia*, v. 12, p. 35-52.

Knorring, O.V.
1974: On tantalum mineralization in some pegmatites from equatorial and southern Africa; 20th Annual Report, *Research Institute for African Geology, University of Leeds*, p. 34-38.

Kolbe, P. and Taylor, S.R.
1966: Major and trace element relationships in granodiorites and granites from Australia and South Africa; *Contributions to Mineralogy and Petrology*, v. 12, p. 202-222.

Koljonen, T. and Rosenberg, R.J.
1974: Rare earth elements in granitic rocks; *Lithos*, v. 7, p. 249-261.

Komkov, A.I.
1970: Relationship between the X-ray constants of columbites and compositon; *Doklady of the Academy of Sciences*, Union of Soviet Socialistic Republics, v. 195, p. 434-436.

Koster van Groos, A.F. and Wyllie, P.J.
1968: Melting relationships in the system $NaAlSi_3O_8$-NaF-H_2O to 4 kilobars pressure; *Journal of Geology*, v. 76, p. 50-70.

Kovalenko, N.I.
1977: The reactions between granite and aqueous hydrofluoric acid in relation to the origin of fluorine-bearing granites; *Geokhimiya* 1977, p. 503-515.

Kretz, R.
1968: Study of pegmatite bodies and enclosing rocks, Yellowknife-Beaulieu Region, District of Mackenzie; *Geological Survey of Canada*, Bulletin 59, 81 p.

Lahti, S.I.
1975: Eräjärven seudun pegmatiittien mineraaleista; *Geologi*, v. 27, p. 83-85.

Lenton, P.G.
1979: Mineralogy and petrology of the Buck Claim lithium pegmatite, Bernic Lake, southeastern Manitoba; unpublished M.Sc. thesis, *Department of Earth Sciences, University of Manitoba*, 164 p.

Lima de Faria, J.
1964: Identification of metamict minerals by X-ray powder photographs;Lisabon, 212 p.

Longstaffe, F.J.
1978: Oxygen isotope relations of Archean granitoids and granitoid gneisses, Western Superior Province; *Proceedings of the 1978 Archean Geochemistry Conference*, University of Toronto Press, p. 355-356.

1979: The oxygen isotope geochemistry of Archean granitoids; in: Trondhjemites, Dacites and Related Rocks, ed. F. Barker, Elsevier, p. 363-389.

Longstaffe, F.J., Černý, P. and Muehlenbachs, K.
1980: Oxygen isotope geochemistry of the granitoids in the Winnipeg River pegmatite district, southeastern Manitoba; *Canadian Mineralogist*, v. 18, in press.

Longstaffe, F.J. and Schwarcz, H.P.
1977: $^{18}O/^{16}O$ of Archean clastic metasedimentary rocks: a petrogenetic indicator for Archean gneisses?; *Geochimica et Cosmochimica Acta*, v. 41, p. 1303-1312.

Luth, W.C. and Tuttle, O.F.
1969: The hydrous vapor phase in equilibrium with granite and granite magmas; *Geological Society of America*, Memoir 115, p. 513-548.

Mackie, B.W.
1978: Petrogenesis of the Lac Turgeon granite and uranium occurrences near Baie Johan Beetz, Quebec; unpublished M.Sc thesis, *Department of Earth Sciences, University of Manitoba*, 84 p.

Marshall, P.A.
1972: Selected partition ratios in feldspars and micas from the Bernic Lake (Chemalloy) pegmatite Manitoba; unpublished M.Sc. thesis, *Department of Geology, University of Western Ontario*, 97 p.

Mason, D.R.
1978: Archean gneissic granitoids and their metamorphic enclaves on Highway 17, near Ignace, northwestern Ontario; *Archean Geochemistry Conference 1978, Proceedings*, University of Toronto Press, p. 181-184.

Masuda, A.
1975: Abundances of monoisotopic REE, consistent with the Leedey chondrite values; *Geochemical Journal* v. 9, p. 183-184.

Masuda, A., Nakamura, N. and Tanaka, T.
1973: Fine structure of mutually normalized rare-earth patterns of chondrites; *Geochimica et Cosmochimica Acta*, v. 27, p. 239-248.

McCann, W.S.
1921: The Maskwa River copper-nickel deposit, S.E. Manitoba; *Geological Survey of Canada*, Summary Report 1920, Part C, p. 21-29.

McKenzie, C.B. and Clarke, D.B.
1975: Petrology of the South Mountain batholith; *Canadian Journal of Earth Sciences*, v. 12, p. 1209-1218.

McRitchie, W.D.
1971: The petrology and environment of the acidic plutonic rocks of the Wanipigow-Winnipeg Rivers region, southeastern Manitoba; *Manitoba Mines Branch*, Publication 71-1, Report 2, p. 7-61

1977: GS-2 Reindeer Lake-Southern Indian Lake (regional compilation Program); in: Report of Field Activities, 1977, *Manitoba Mineral Resources Division*, p. 13-18.

Moore, E.S.
1913: Region east of the south end of Lake Winnipeg; *Geological Survey of Canada*, Summary Report 1912, p. 31-43.

Moore, J.M. and Froese, E.
1972: Geological setting of the Snow Lake area; *Geological Survey of Canada*, Paper 72-1, pt. B, p. 78-81.

Moore, P.B.
1971: Crystal chemistry of the alluaudite structure type: contribution to the paragenesis of pegmatite phosphate giant crystals; *American Mineralogist*, v. 56, p. 1955-1975.

1973: Pegmatite phosphates: descriptive mineralogy and crystal chemistry; *Mineralogical Record*, v. 4, p. 103-130.

Morrice, M.G. and Wilson, H.D.B.
in prep.: Geochemistry of the Lake of the Woods-Kakagi Lake Archean greenstone belt, northwestern Ontario.

Mulligan, R.
1957: Lithium deposits of Manitoba, Ontario and Quebec, 1956; *Geological Survey of Canada*, Paper 57-3, 26 p.

1961: Pollucite (caesium) in Canada; *Geological Survey of Canada*, Paper 61-4, 4 p.

1965: Geology of Canadian lithium deposits; *Geological Survey of Canada*, Economic Geology Report 21, 131 p.

1968: Geology of Canadian beryllium deposits; *Geological Survey of Canada*, Economic Geology Report 23, 109 p.

1975: Geology of Canadian tin occurrences; *Geological Survey of Canada*, Economic Geology Report 28, 155 p.

Munoz, J.L.
1968: Physical properties of synthetic lepidolites; *American Mineralogist*, v. 53, p. 1490-1498.

Nagasawa, H. and Schnetzler, C.C.
1971: Partitioning of rare earth, alkali and alkaline earth elements between phenocrysts and acidic igneous magma; *Geochimica et Cosmochimica Acta*, v. 35, p. 953-968.

Nahnybida, C.
1979: The Central Claim pegmatite, southeastern Manitoba; unpublished undergraduate thesis, *Department of Earth Sciences, University of Manitoba*, 52 p.

Nickel, E.H.
1961: The mineralogy of the Bernic Lake pegmatite, southeastern Manitoba; *Department of Mines and Technical Services, Mines Branch*, Technical Bulletin, TB 20, 38 p.

Nickel, E.H., Rowland, J.F. and McAdam, R.C.
1963a: Wodginite - a new tin - manganese tantalite from Wodgina, Australia, and Bernic Lake, Manitoba; *Canadian Mineralogist*, v. 7, p. 390-402.

1963b: Ixiolite - a columbite substructure; *American Mineralogist*, v. 48, p. 961-979.

Nockolds, S.R.
1954: Average chemical compositions of some igneous rocks; *Bulletin of the Geological Society of America*, v. 65, p. 1007-1034.

Norton, J.J.
1973: Lithium, cesium, and rubidium - the rare alkali metals; in: D.A. Brobst and W.P. Pratt, United States Mineral Resources, *United States Geological Survey*, Professional Paper 820, p. 365-378.

1975: Pegmatite minerals; in: Mineral and Water Resources of South Dakota, *South Dakota Geological Survey*, Bulletin 16, p. 132-149.

O'Neil, J.R., Shaw, S.E. and Flood, R.H.
1977: Oxygen and hydrogen isotope compositions as indicators of granite genesis on the New England batholith, Australia; *Contributions to Mineralogy and Petrology*, v. 62, p. 313-328.

Orville, P.M.
1960: Petrology of several pegmatites in the Keystone district, Black Hills, South Dakota; *Geological Society of America Bulletin*, v. 71, p. 1467-1490.

Ovchinnikov, L.N. (ed.).
1976: Lithogeochemical methods for prospecting rare-metal pegmatites; *Academy of Sciences of the Union of Soviet Socialistic Republics*, Moscow, 79 p.

Paul, B.J.
in prep.: Mineralogy, geochemistry, and petrology of the Huron Claim pegmatite, southeastern Manitoba; *Department of Earth Sciences, University of Manitoba*, M.Sc. thesis.

Penner, A.P. and Clark, G.S.
1971: Rb-Sr age determinations from the Bird River area, southeastern Manitoba; in: Geoscience Studies in Manitoba, ed. A.C. Turnock, *Geological Association of Canada*, Special Paper 9, p. 105-109.

Peterman, Z.E., Hedge, C.E., Coleman, R.G. and Snavely, P.D. Jr.
1967: $^{87}Sr/^{86}Sr$ ratios in some eugeosynclinal sedimentary rocks and their bearing on the origin of granitic magma in orogenic belts; *Earth and Planetary Science Letters*, v. 2, p. 433-439.

Pettijohn, F.J.
1963: Chemical composition of sandstones - excluding carbonate and volcanic sands; *United States Geological Survey*, Professional Paper 440-S, 19 p.

Pettijohn, F.J., Potter, P.E. and Siever, R.
1972: Sand and sandstone; Springer-Verlag, 211 p.

Posehn, G.
1976: The metaconglomerate and metagreywacke at Booster Lake, Manitoba; unpublished M.Sc. thesis, *Department of Earth Sciences, University of Manitoba*, 106 p.

Presnall, D.C.
1969: The geometrical analysis of partial fusion; *American Journal of Science*, v. 267, p. 1178-1194.

Presnall, D.C. and Bateman, P.C.
1973: Fusion relations in the system $NaAlSi_3O_8$-$CaAl_2Si_2O_8$-$KAlSi_3O_8$-SiO_2-H_2O and generation of granitic magmas in the Sierra Nevada batholith; *Geological Society of America Bulletin*, v. 84, p. 3181-3202.

Proctor, P.D. and El-Etr, H.A.
1968: Layered pegmatites, southern Wind River Mountains, Fremont County, Wyoming; *Economic Geology*, v. 63, p. 595-611.

Pryslak, A.P.
1976: Geology of the Bruin Lake-Edison Lake area, District of Kenora: *Ontario Division of Mines*, Geoscience Report 120, 61 p.

Puchelt, H. and Emmerman, R.
1976: Bearing of rare earth patterns of apatites from igneous and metamorphic rocks; *Earth and Planetary Science Letters*, v. 31, p. 279-286.

Pye, E.G.
1965: Georgia Lake area; *Ontario Department of Mines*, Geological Report 31, 113 p.

Ramik, R.A., Sturman, B.D., Dunn, P.J. and Povarennykh, D.P.
1980: Tancoite, a new Li-Na-Al phosphate from the Tanco pegmatite, Bernic Lake Manitoba; *Canadian Mineralogist*, v. 18, p. 185-190.

Ramlal, K.
1979: The chemical analysis of silicate rocks; *Centre for Precambrian Studies, University of Manitoba*, Annual Report 1978, p. 56-59.

Ramsay, J.G.
1964: Folding and fracturing of rocks; McGraw-Hill Book

Co. New York, 276 p.

Reitan, P.
1956: Pegmatite veins and the surrounding rocks. I, Petrography and structure; *Norsk Geologisk Tiddskrift*, v. 36, p. 213-239.

1958: II. Changes in the olivine gabbro surrounding three pegmatite veins, Risör, Norway; *Norsk Geologisk Tiddskrift*, v. 38, p. 279-311.

1959a: III. Structural control of small pegmatites in amphibolite, Rytterholmen, Krageröfjord, Norway; *Norsk Geologisk Tiddskrift*, v. 39, p. 175-195.

1959b: IV. Genesis of a discordant pegmatite vein, St. Hansholmen, Risör, Norway; *Norsk Geologisk Tiddskrift*, v. 39, p. 197-229.

Rinaldi, R., Černý, P. and Ferguson, R.B.
1972: The Tanco pegmatite at Bernic Lake, Manitoba. VI. Lithium-rubidium-cesium micas; *Canadian Mineralogist*, v. 11, p. 690-707.

Rowe, R.B.
1956: Lithium deposits of Manitoba; *Geological Survey of Canada*, Paper 55-26, 23 p.

Rucklidge, J.C. and Gasparrini, E.L.
1969: EMPADR VII, a computer program for processing electron microprobe data; *University of Toronto*.

Russell, G.A.
1957: Structural studies; Snow Lake-Herb Lake area; *Manitoba Mines Branch*, Publication 55-3, 28 p.

Ruzicka, V.
1979: Uranium and thorium in Canada, 1978; Current Research, pt. A., *Geological Survey of Canada*, Paper 79-1A p. 139-155.

Sangster, D.F.
1978: Isotopic studies of ore-leads of the circum-Kisseynew volcanic belt of Manitoba and Saskatchewan; *Canadian Journal of Earth Sciences*, v. 15, No. 7.

Schledewitz, D.C.P.
1972: Geology of the Rat Lake area; *Manitoba Mines Branch*, Publication 71-2B, 18 p.

Schwerdtner, W.M., Stone, D., Osadetz, K., Morgan, J. and Stott, G.M.
1979: Granitoid complexes and the Archean tectonic record in the southern part of northwestern Ontario; *Canadian Journal of Earth Sciences*, v. 16, p. 1965-1977.

Shanks, R.J.
1979: Stratigraphy of the Missi Group rocks, Wekusko Lake area, Manitoba; unpublished M.Sc. thesis, *Department of Earth Sciences, University of Manitoba*, 120 p.

Shanks, R.J. and Bailes, A.H.
1977: Missi Group rocks, Wekusko Lake area; *Manitoba Mineral Resources Division*, Report of Field Activities 1977, p. 83-87.

Smith, I.E.M. and Williams, J.G.
1978: Geochemical and petrographic constraints on the petrogenesis of Archean granitoids, Superior Province, Canada; *Geological Association of Canada - Mineralogical Association of Canada*, Annual Meeting 1978 Toronto, Program and Abstracts, p. 494.

Solodov, N.A.
1971: Scientific principles of perspective evaluation of rare-element pegmatites; Publishing House Nauka Moscow, 591 p.

Springer, G.D.
1949a: Geology of the Cat Lake-Winnipeg River area; *Manitoba Mines Branch*, Preliminary Report 48-7, 28 p.

1949b: Geology and mineral deposits of a part of southeastern Mantioba; *Precambrian* (Winnipeg), v. 22, No. 8.

1950: Mineral deposits of the Cat Lake-Winnipeg River area, Lac du Bonnet Mining Division; *Manitoba Mines Branch*, Publication 49-7, 14 p.

1952: Geology of the Rennie-West Hawk Lake area; *Manitoba Mines Branch*, Publication 50-6, 24 p.

Stauffer, M.R.
1964: The geometry of conical folds; *New Zealand Journal of Geology and Geophysics*, v. I, p. 28-41.

Steiger, R. and Knorring, O.V.
1975: A lithium pegmatite belt in Ireland; *Journal of Earth Sciences* (Leeds), v. 8, p. 433-443.

Stewart, D.B.
1963: Petrogenesis and mineral assemblages of lithium-rich pegmatites; *Geological Society of America*, Program and Abstracts, p. 159A.

1978: Petrogenesis of lithium-rich pegmatites; *American Mineralogist*, v. 63, p. 970-980.

Stockwell, C.H.
1933a: Genesis of a lithium pegmatite on the Bear Mineral Claim, southeast Manitoba; *Transactions of the Royal Society of Canada*, v. 27, Section IV, p. 27-36.

1933b: The genesis of pegmatites of southeast Manitoba; *Transactions of the Royal Society of Canada*, v. 27, Section IV, p. 37-51.

1937: Gold deposits of Herb Lake area, northern Manitoba; *Geological Survey of Canada*, Memoir 206, 48 p.

Strong, D.F. and Hanmer, S.K.
1980: The leucogranites of the southern Brittany: origin by faulting, frictional heating, fluid flux, and fractional melting; *Canadian Mineralogist*, v. 18, in press.

Taylor, S.R., Ewart, A. and Capp, A.C.
1971: Leucogranite and rhyolite: trace element evidence for fractional crystallization and partial melting; *Lithos*, v. 1, p. 179-186.

Thornton, C.P. and Tuttle, O.F.
1960: Chemistry of igneous rocks. I. Differentiation index; *American Journal of Science*, v. 258, p. 726-743.

Thorpe, R.S., Potts, P.J. and Sarre, M.B.
1977: Rare earth evidence concerning the origin of granites of the Isle of Skye, northwest Scotland; *Earth and Planetary Science Letters*, v. 36, p. 111-120.

Trueman, D.L.
1971: Petrological, structural and magnetic studies of a layered basic intrusion, Bird River Sill, Manitoba; unpublished M.Sc. thesis, *Department of Earth Sciences, University of Manitoba*, 71 p.

1976: Evidence in support of a meteorite impact crater at Poplar Bay, Lac du Bonnet, southeastern Manitoba; *Canadian Journal of Earth Sciences*, v. 13, p. 1608-1612.

1978: Exploration methods in the Tanco mine area of southeastern Manitoba, Canada; *Energy*, v. 3, p. 293-298.

1980: Stratigraphic, structural and metamorphic petrology of the Archean greenstone belt at Bird River, Manitoba; Ph.D. thesis, *Department of Earth Sciences, University of Manitoba*, 155 p.

Trueman, D.L., Posehn, G.A. and Stoetterau, W.
1976: Metamorphism, structure, and stratigraphy in the Rice Lake-Manigotagan gneiss belt, Bird Lake area, of southeastern Manitoba and northwestern Ontario; *Centre for Precambrian Studies, University of Manitoba*, 1975 Annual Report, p. 67-84.

Turek, A.
1971: Geochronology of the Rice Lake-Beresford Lake area; *Manitoba Mines Branch*, Publication 71-1, p. 313-324.

Turek, A. and Peterman, Z.E.
1971: Advances in the geochronology of the Rice Lake-Beresford Lake area, southeastern Manitoba; *Canadian Journal of Earth Sciences*, v. 8, p. 572-579.

Tyrrell, J.B.
1900: East Shore, Lake Winnipeg; *Geological Survey of Canada*, Annual Report, v. 11, 1898, pt. G.

Walker, T.L.
1931: Rare minerals in pegmatite, Pointe du Bois, Manitoba; *Contributions to Canadian Mineralogy 1931, University of Toronto Studies*, Geological Series No. 30, P. 9-13.

Wallace, H.
1978: Geology of the Opikeigen Lake area, District of Kenora (Patricia portion); *Ontario Geological Survey*, Report 185, 58 p.

Wedepohl, K.H.
1968: Chemical fractionation in the sedimentary environment; in: Origin and distribution of the elements, *International Series, Monographs in Earth Science*, v. 30, Pergamon Press, p. 999-1016.

Whitney, J.A. and Stormer, J.C. Jr.
1977: The distribution of $NaAlSi_3O_8$ between coexisting microcline and plagioclase and its effect on geothermometric calculations; *American Mineralogist*, v. 62, 687-691.

Williams, J.G.
1978: Geology of the Crystal Lake area, Quetico subprovince; *1978 Archean Geochemistry Conference Proceedings*, University of Toronto Press, p. 193-207.

Wilson, H.D.B.
1971: The Superior Province in the Precambrian of Manitoba; in: Geoscience Studies in Manitoba, ed. A.C. Turnock, *Geological Association of Canada*, Special Paper 9, p. 41-49.

Wilson, H.D.B., Morrice, M.G. and Ziehlke, D.V.
1974: Archean continents; *Geoscience Canada*, v. 1, p. 12-20.

Wilson, H.D.B., Morrice, M.G., Ziehlke, D.V. and Beakhouse, G.P.
1977: Development of greenstone-granite and gneissic terrains in Archean shields; *Centre for Precambrian Studies, University of Manitoba*, 1976 Annual Report, p. 2-21.

Wilson, J.F.
1972: The Rhodesian Archean craton - an essay in cratonic evolution; *Philosophical Transactions of the Royal Society London*, v. A273, p. 389-411.

Wison, J.F., Bickle, M.J., Hawkesworth, C.J., Martin, A., Nisbet, E.G. and Orpen, T.L.
1978: Granite-greenstone terrains of the Rhodesian Archean craton; *Nature*, v. 271, p. 23-27.

Winkler, H.G.F.
1967: Petrogenesis of metamorphic rocks; 2nd edition, Springer-Verlag, New York, 334 p.

Winkler, H.G.F., Boese, M. and Marcopoulos, T.
1975: Low-temperature granitic melts; *Neues Jahrbuch für Mineralogie*, Monatshefte, p. 245-268.

Wright, C.M.
1963: Geology and origin of the pollucite-bearing Montgary pegmatite, Manitoba; *Geological Association of America Bulletin*, v. 74, p. 919-946.

Wright, J.F.
1926: Geology and mineral deposits of Oiseau River map area, Manitoba; *Geological Survey of Canada*, Summary Report, 1924, Part B, p. 74-138.

MAPS NOT

FILMED

CARTES

OMISES